Structural Aspects of Protein Synthesis

2nd Edition

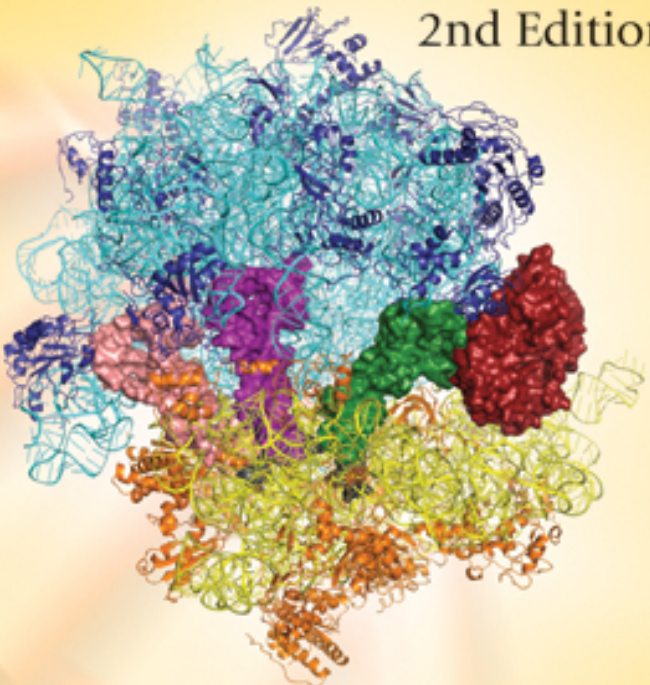

Anders Liljas • Måns Ehrenberg

World Scientific

Structural Aspects of Protein Synthesis

2nd Edition

This page intentionally left blank

Structural Aspects of Protein Synthesis

2nd Edition

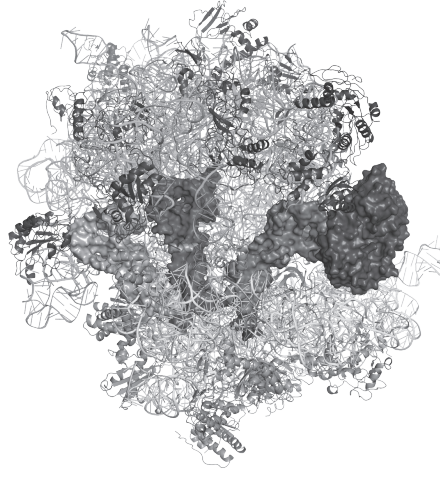

Anders Liljas
Lund University, Sweden

Måns Ehrenberg
Uppsala University, Sweden

World Scientific

NEW JERSEY • LONDON • SINGAPORE • BEIJING • SHANGHAI • HONG KONG • TAIPEI • CHENNAI

Published by

World Scientific Publishing Co. Pte. Ltd.

5 Toh Tuck Link, Singapore 596224

USA office: 27 Warren Street, Suite 401-402, Hackensack, NJ 07601

UK office: 57 Shelton Street, Covent Garden, London WC2H 9HE

Library of Congress Cataloging-in-Publication Data

Liljas, Anders.

Structural aspects of protein synthesis. -- 2nd edition / Anders Liljas, Lund University, Sweden, Måns Ehrenberg, Uppsala University, Sweden.

pages cm

Includes bibliographical references and index.

ISBN 978-9814313209 (hardcover : alk. paper) -- ISBN 978-9814313216 (pbk. : alk. paper)

1. Proteins--Synthesis. I. Ehrenberg, Måns. II. Title.

QP551.L4685 2013

572'.6--dc23

2013018180

British Library Cataloguing-in-Publication Data

A catalogue record for this book is available from the British Library.

Typeset by Stallion Press

Email: enquiries@stallionpress.com

Printed in Singapore

Dedication

To Charles G. Kurland
Teacher, supporter and friend

This page intentionally left blank

Preface

This is the first book in a new series covering fields where structural biology has made significant contributions. The books in the series will emphasize the advancements within these fields and how they have benefited from structural biology. In addition, selected scientists have been invited to contribute books within this series containing their most significant papers and their comments on the chosen directions of their research, scientific problems, selected approaches and achievements.

The first version of this book was published nine years ago. Given the great interest in the field of messenger RNA translation on ribosomes and the importance of structural biology for most fields of biology, the publisher suggested to us that we produce a second edition of the book. Much has happened in the last nine years and it has been a challenge to try to keep up with the many frontiers involved in the translation field. The Nobel Prize in Chemistry 2009 to Venki Ramakrishnan, Tom Steitz and Ada Yonath emphasized their significant contributions to this field. Their work, as well as the contributions from many other excellent scientists, is highlighted in this book.

In producing this book we have greatly benefited from the preprints and highly resolved illustrations that were generously made available to us by many of our colleagues. In the work on illustrations we have had tremendous help from Saraboji Kadhirvel and Andreas Ehnbom. We would also like to acknowledge financial support from The Royal Physiographic Society in Lund.

Anders Liljas and Måns Ehrenberg
Leksand and Uppsala
2013

Contents

This page intentionally left blank

1

The Basics of Translation

Protein synthesis is a remarkable process as indicated by its alternative name "translation." The genetic information, stored in the nucleic acids RNA and DNA of the cell, is encoded in sequences of three-letter "words" in a "language" with a four letter "alphabet." The three-letter words in the nucleic acid language are **TRANSLATED** into a protein language with a 20-letter alphabet. Long sequences of the four nucleic acid letters are first transcribed from DNA into messenger RNA (mRNA). Subsequently, sequences of the three letter mRNA words, written in the four nucleotide letters A, C, G, U are translated into the 20 amino acid letters that make up the proteins. For this translation, there are rules as for the translation of any written message. There is a dictionary for the translation, called the genetic code, and there are signals indicating where the reading should start and where it should end. This dictionary is virtually universal, a remarkable property that normally makes it possible for any organism to correctly translate any message from any other organism. The evolutionary aspects of this universality are fascinating. Not only does all life on earth appear to have a common origin, but there has also been extensive exchange of genetic material between different organisms over the billions of years of evolution. Thus, it is not to be excluded that a cow could "infect," or transfer genetic material to, a bacterium, as Brian Hartley once put it.

The translation machinery, found in different cellular compartments of all cells, is the ribosome. It is composed of a large and a small ribosomal subunit. The transfer RNAs (tRNAs), the universal adaptor molecules, are also fundamental for translation. Each tRNA is uniquely linked to, "charged with," a specific amino acid, and recognizes the nucleic acid word, the "codon," encoding this amino acid in the messenger RNA (mRNA).

Once an mRNA has been synthesized through transcription from DNA, it is targeted to the small ribosomal subunit. Here it binds in a specific manner with the start signal, the initiation codon, stabilized in the partial ribosomal P site of the small subunit by the initiator tRNA ($tRNA_i$) (Fig. 1.1). When the mRNA and the initiator tRNA are bound to the small subunit, it can dock to the large subunit to form a ribosome, ready for translation of the mRNA. The steps during initiation are assisted by initiation factors.

In the elongation phase when tRNAs, charged with their specific amino acids, recognize their codons through Watson-Crick base-pairing and complementary geometry, and they become bound to the ribosomal site for aminoacyl-tRNAs, the A site (Fig. 1.1). The accurate decoding of the message is essential for life, since frequent errors in protein synthesis would lead to junk proteins and cell death. To obtain a satisfactory fidelity of translation, an initial recognition is combined with an energy driven step called proofreading. When the decoding has been performed, the peptide bound to the tRNA in the P-site is transferred and covalently linked to the amino acid bound to the tRNA in the A site. The polypeptide chain is thus extended by one amino acid. Subsequently, the peptidyl-tRNA, now located to the A site, is translocated to the P site, which allows for a new cycle of elongation. Elongation factors catalyze two of the basic steps in translation: the binding of an aminoacyl-tRNA to the A site and the translocation of the peptidyl-tRNA from the A site to the P site. However, the central event in elongation, peptidyl transfer, is promoted by the ribosome itself without any auxiliary factor.

The translation of an mRNA is terminated when a stop codon has entered the A site. tRNAs do not recognize stop codons. These

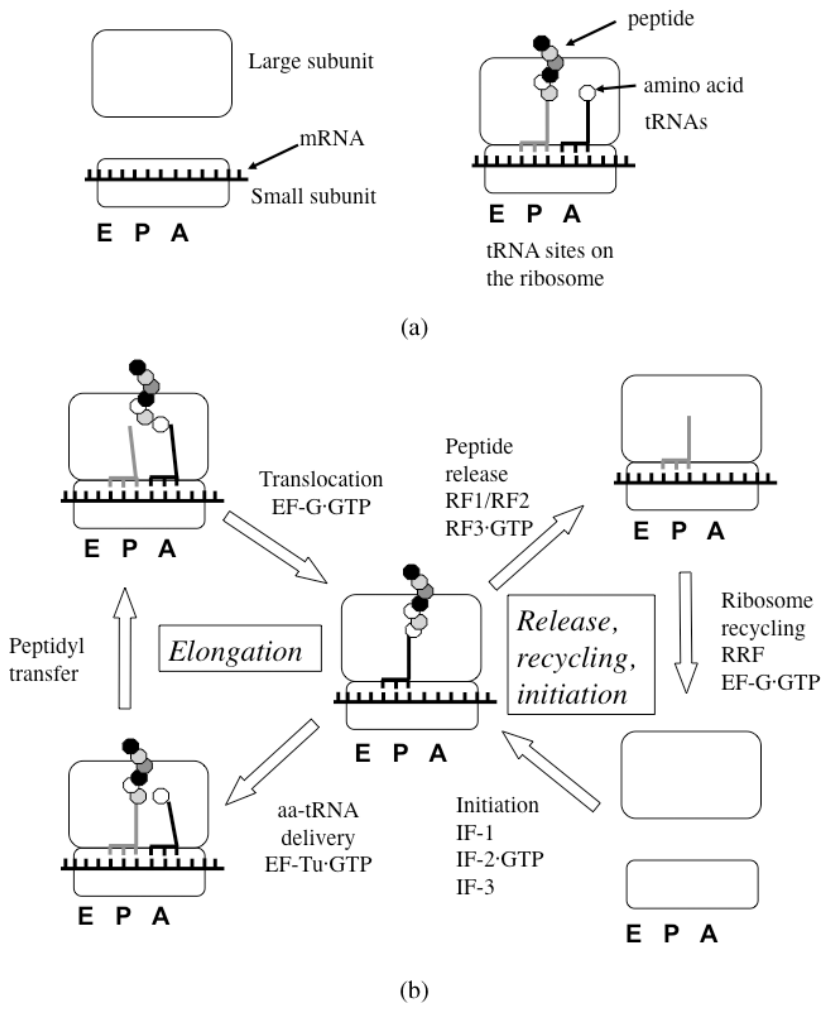

Fig. 1.1 **(a)** The symbols used in the drawing are explained. These symbols will be used repeatedly throughout the book. (**b**) A summary of translation on ribosomes. The start is on the lower right illustrating the initiation of protein synthesis from separated subunits, with the binding of the mRNA to the small subunit. In each round of the elongation cycle, one amino acid is incorporated. When a stop codon is exposed in the A-site, the peptide is released. Finally, the components of the system are recycled for a new initiation.

are recognized by proteins, which induce hydrolysis of the polypeptide from the P-site bound tRNA. These proteins, called class 1 termination factors or release factors, are subsequently released from the ribosome by a class 2 termination factor. After the termination of protein synthesis by the termination factors, the mRNA and the deacylated tRNA in the P site need to be removed from the ribosome and the subunits separated from each other. This will allow the small subunit to bind a new mRNA and together with a large subunit initiate a new round of translation. This phase of translation, following termination and preceding initiation, is called ribosomal recycling. It is carried out by a recycling factor together with one of the elongation factors. The whole process of translation is illustrated in Fig. 1.1.

The ribosome itself can carry out all the steps of mRNA translation and contributes fundamentally to the accuracy of mRNA decoding by tRNAs. At the same time, the translation factors greatly increase the kinetic efficiency of these steps. Of particular importance are the translational G-proteins IF2, EF-Tu and EF-G, which link the free energy of GTP hydrolysis to the translation process to drive it in a forward direction with high speed and great accuracy.

The structure of the translation machinery has always been of central importance since, as Watson expressed in 1964, "Unfortunately, we cannot accurately describe at the chemical level how a molecule functions unless we know first its structure." This need has been evident during the whole time translation has been studied and is one of the reasons why this book has been written.

In this treatise, we will focus on bacterial translation. Translation in archaea or eukaryotes will be mentioned when it provides deeper insight into bacterial translation or to emphasize the universal aspects of translation.

2

Historical Milestones

There are many striking accounts of historical developments related to protein synthesis (Perutz, 1962; Nomura, 1990; Spirin, 1999; Woese, 2001; Rich, 2001; Hoagland, 2003; Rheinberger, 2004).

A fundamental aspect of protein synthesis is that DNA provides the genetic blueprint for all proteins. How genetic information flows from DNA into proteins began to be revealed about half a century ago and in 1964, an interesting review of this genetic information flow was provided by Watson. In eukaryotic cells, the DNA is contained in one compartment, the nucleus, while proteins are synthesized in another compartment, the cytoplasm. Several types of observations made it clear that RNA had to be the missing link between DNA and proteins (Chamberlin & Berg, 1962). The genetic information contained in the DNA is transmitted to an intermediate, a messenger RNA (mRNA), which is subsequently translated into proteins (Crick, 1958). The double-helical structure of DNA (Watson & Crick, 1953) provided an insight into its fundamental importance for protein synthesis, in that it explained important interactions involved in replication of DNA as well as in transcription and translation. However, what is the machinery that could perform the remarkable process of translation?

Casperson (1941) was the first to observe the relationship between RNA and protein synthesis by identifying the very RNA-rich particles that were later to be called ribosomes. In subsequent

studies of *Escherichia coli* (*E. coli*), purified preparations of ribosomes led to the realization that proteins are synthesized on these particles (Tissières *et al*., 1960; Kurland, 1960). Ribosomes provide the machinery of translation. They contain RNA (rRNA) and proteins (r-proteins) and are composed of two subunits. In bacteria, their sedimentation constants are 30S for the small subunit and 50S for the large subunit, where S stands for Svedberg units. It was also observed that eukaryotic ribosomes are larger than bacterial ribosomes, sedimenting at 80S and 70S, respectively. However, the ribosomes of mammalian mitochondria, sometimes called mini-ribosomes, are noticeably smaller with significantly shorter rRNAs.

How can the RNA message be decoded so that a protein, a polypeptide with a well defined sequence is synthesized? Crick suggested that there had to be "adaptor" molecules that can read the message and incorporate the appropriate amino acids into the growing polypeptide according to the mRNA instructions. Each adaptor must be charged with its specific amino acid by a specific enzyme (Crick, 1958). The adaptor was suggested to be a small RNA molecule decoding the message through Watson-Crick base-pairing. Subsequently, the adaptors were identified as the tRNA molecules (then called sRNAs) and characterized (Hoagland *et al*., 1957), validating Crick's hypothesis (Fig. 2.1). Each one of these tRNA molecules could be uniquely charged with its specific amino acid to aminoacyl-tRNA (see Berg 1961 and references therein; Ibba and Söll, 2000; 2001).

One early question found a negative answer: the rRNA was not the message (Gros *et al*., 1961; Brenner *et al*., 1961; Jacob and Monod, 1961). The identification of the ribosomal subunits and the clarification of their separate roles were other important steps forward. It was established that the small ribosomal subunit is the site of decoding of the message (Okamoto & Takanami, 1963). Furthermore, it was shown that the ribosome protects about 25–30 nucleotides of the mRNA (Takanami & Zubay, 1964). The large subunit was found to be the site of incorporation of new amino acids through peptidyl transfer, but no covalent link was identified

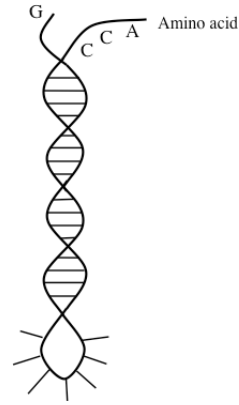

Fig. 2.1 An early "hairpin" model of the tRNA molecule (after Watson, 1964). The loop of unpaired bases at the lower end contains the anticodon. The length of the molecule was estimated to be 120 Å.

between the nascent polypeptide chain and the ribosome (Gilbert, 1963). It also became clear that there must be at least two sites for tRNA on the ribosome, one for a tRNA connected to the nascent peptide, the peptidyl-tRNA, and another for the incoming amino-acyl-tRNA (Warner & Rich, 1964; Watson, 1964). These sites would then have to contain elements from both subunits since the mRNA is bound on the small subunit and the nascent peptide on the large subunit. These tRNA sites were subsequently called the A (aminoacyl) and P (peptidyl) sites. In the early phase of research on translation, it was not clear why there is a need for two subunits that separate after termination of translation and reunite upon a new round of initiation of translation (Watson, 1964). The possibility that mRNA moves between the subunits and that the subunits move in relation to each other was first suggested by Spirin (1969).

Purified ribosomes, cellular fractions containing tRNAs and synthetic mRNAs allowed exploration of the genetic code (Nirenberg *et al*., 1966). Initially, not even the principle of design of the code was known. Code words consisting of only two of the four possible nucleotides (A; U; G; C) could not encode the 20 naturally occurring amino acids as they allowed for only 16 combinations ($4^2 = 16$). The code words would need to consist of at least three

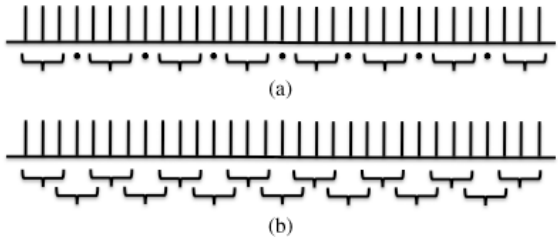

Fig. 2.2 A punctuated **(a)** or overlapping **(b)** reading of the mRNA.

nucleotides, allowing for 64 combinations ($4^3 = 64$). The code could either be punctuated or overlapping (Fig. 2.2). Neither of these possibilities turned out to be true. The genetic code is a three-letter code without code word overlap or punctuations between code words (Crick *et al*., 1961). Correct decoding requires that mRNA is read in its correct frame. In the 1960s, the complete genetic code was elucidated. The dictionary for the translation of the 64 three-letter code words or codons was established (Nirenberg & Leder, 1964; Söll *et al*., 1966; Crick, 1966a).

In the early phase of translation research, it was observed that the antibiotic streptomycin causes extensive misreading of the code so that proteins are made with erroneous peptide sequences even though the rate of protein synthesis remained the same (Davies *et al*., 1964). A large number of antibiotics, evolved by microorganisms to eliminate their competitors, were found to target different components and sites of the translation machinery (Cundliffe, 1980; 1990).

The ribosome not only contains RNA but also proteins. Initially, in comparing ribosomes with viruses that were better characterized, one could expect that the proteins would be few but occur in multiple copies. However, with the aid of gel electrophoresis and careful characterization, it became clear that there were a large number of different ribosomal proteins (Kaltschmidt *et al*., 1967; Kaltschmidt & Wittmann, 1970). The stoichiometry of almost all ribosomal proteins was subsequently found to be one per ribosome (Hardy, 1975).

Since proteins carry out most cellular functions, one would expect the ribosomal proteins to carry out the main functions of the ribosome and the rRNA to act as primarily a scaffold. An extensive effort was thus focused on characterizing the role of the proteins (see reviews by Kurland, 1972; Garrett & Wittmann, 1973; Wittmann, 1982). The amino acid sequences of the *E. coli* ribosomal proteins were determined at an early stage (see Giri *et al*., 1984 and references therein). The order of assembly for the proteins of the small subunit was established (Held *et al*., 1974). Furthermore, different attempts to associate ribosomal functions with the proteins were made (see Liljas 1982 for a review). Early indications that the ribosomal RNA had important functions came from the observation by Noller and Chaires (1972) that kethoxal modification of rRNA could inhibit tRNA binding. Furthermore, Shine and Dalgarno (1974) found that an mRNA would bind to the bacterial ribosome through base-pairing with the 3-end of the RNA of the small subunit. The elucidation of the nucleotide sequences of many rRNAs showed large regions of sequence conservation, hinting at important functions (Noller & Woese, 1981). Some investigators then began to explore if the RNA components constituted the main sites of ribosomal functions (Noller & Woese, 1981), and if the ribosome could be a ribozyme, i.e. an enzyme in which RNA and not protein carries out the catalytic action. Many ribosomal functions are now known to depend on the ribosomal RNA. In addition, several of the key partners in translation, mRNA and tRNA are also RNA molecules. The possibility of an early RNA world has been discussed (Gesteland *et al*., 1999). From biochemical experiments, it was suggested that the ribosome is a ribozyme (Noller *et al*., 1992; Noller, 1993). This will be further discussed in Chapters 8, 11 and 13 of this book.

The rate of protein synthesis on ribosomes is enhanced by different soluble protein factors (see an early review by Lipmann, 1969). They are grouped into initiation, elongation, termination and recycling factors. Our understanding of the role of the factor proteins has improved significantly in the last five years, but several questions remain unanswered (see Chapter 9). Two main

factors, discovered at an early stage, are the elongation factors Tu (EF-Tu) and G (EF-G), which are both involved in each cycle of elongation of the nascent polypeptide (see Lipmann, 1969 and Kaziro, 1978 for early reviews). Different but related versions of these two factors are found in cells from all organisms as well as in their organelles like mitochondria and chloroplasts (Pandit and Srinivasan, 2003).

The accuracy of translation was an enigma from early days. How can three base-pairs give a fidelity that is in the order of one error per 10,000 amino acids incorporated? It was yet a milestone in the understanding of translation when it was suggested (Hopfield, 1974; Ninio, 1975) and experimentally demonstrated (Thompson, 1977; Ruusala *et al*., 1982) that codon-anticodon recognition occurs in two steps, an initial recognition step and a proofreading step. The overall accuracy is the product of the accuracy in each of these two steps. Proofreading depends on the thermodynamic driving force provided by GTP hydrolysis (Kurland, 1978), making it possible to probe the same chemical difference between right and wrong substrate twice (Hopfield, 1974; Ninio, 1975) or several times (Freter & Savageau, 1980; Ehrenberg & Blomberg, 1980). While proofreading provides repeated tRNA selection in several steps, the ribosome itself contributes to the accuracy of each one of these steps (Ogle *et al*., 2003; Yoshisawa *et al*., 1999).

Protein synthesis is a complex process and the ribosome carries out several catalytic functions. For regular enzymes and ribosomes alike, structural insights along with high quality biochemical data are important to clarify function, and structural information about ribosomes has been in high demand over the decades. Numerous methods have been employed or developed to provide such structural insights. Initially, structural information was obtained with blunt tools like genetics, chemical crosslinking, chemical labeling, and enzymatic digestion of proteins or RNA. Such methods can give invaluable insights when combined with structural information at higher resolution. The interpretation of such results alone cannot give the accurate model that is needed for the functional

understanding of a complex enzyme system. Electron microscopy techniques were used from an early stage and have provided information of ever increasing detail (Palade, 1955; Hall & Slayter, 1959; Huxley & Zubay, 1960; Lubin, 1968). The identification of the shapes of the ribosome and its subunits was an important step in our familiarity with ribosome structures (Fig. 2.3; Stöffler & Stöffler-Meilicke, 1984; Gornicki *et al*., 1984; Lake, 1985; Spirin and Vasiliev, 1989). Furthermore, when different components could be placed within the envelope of the ribosome we obtained a structural framework for the ribosome that was easier to comprehend than featureless blobs. The modern technique of cryoelectron microscopy (cryo-EM) with ensemble averaging over large particle numbers and classification strategies (Frank *et al*., 1988; 1995) has given a rich harvest of structural insights at continuously improving resolution (Stark *et al*., 1997; Agrawal *et al*., 1998; Schuette *et al*., 2009). The old question of whether the two ribosomal subunits move with regard to each other during translation (Spirin, 1969) has been given a positive answer (Frank & Agrawal, 2000).

At an early phase, X-ray crystallography provided the structure of yeast phenylalanine tRNA (Robertus *et al*., 1974; Kim *et al*., 1974; Stout *et al*., 1976). The secondary structure of tRNA, with the

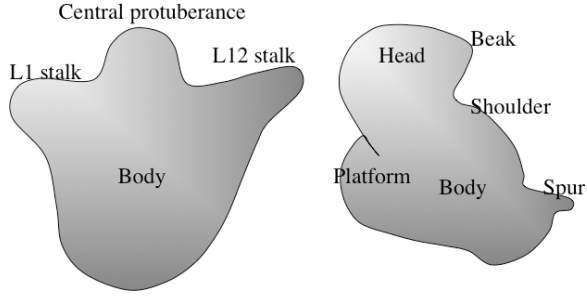

Fig. 2.3 The outline of the large (left) and small (right) subunits as observed by electron microscopy (Lake, 1976; 1985). This view of the large subunit is called the crown view. The two subunits are seen from the same side. To form the 70S ribosome, the small subunit is placed on top of the large in this orientation.

shape of a cloverleaf, was found to fold into a tertiary structure with the shape of an L. This clarified that the two functional parts of tRNA, the anticodon and the amino acid acceptor end of the molecule, are about 75 Å apart. Evidently, the sites on the ribosomal subunits interacting with each of the two ends of the tRNAs, the decoding site and the peptidyl transfer center, would also be expected to be this far apart.

Much crystallographic work has also been devoted to studying isolated ribosomal components (Ramakrishnan & White 1998; Al-Karadaghi *et al*., 2000a, b). Complete ribosomes or subunits initially seemed inaccessible to crystallography due to their flexibility and lack of homogeneity. Ada Yonath was the first to overcome these difficulties and has systematically explored possibilities to crystallize ribosomes and their subunits (Yonath *et al*., 1980, 1982, 1998). Improved crystallographic techniques have allowed the determination of structures of ribosomal subunits and whole ribosomes at resolutions allowing for determination of the positions of single atoms (Ban *et al*., 2000; Nissen *et al*., 2000; Wimberley *et al*., 2000; Schlünzen *et al*., 2000; Harms *et al*., 2001; Yusupov *et al*., 2001). The ribosome and its subunits remain the largest asymmetric objects so far studied by crystallography.

The crystallographic and cryo-EM studies of ribosomes have completely changed the field of protein synthesis and brought us into a new era. Now we can with certainty discuss the conformation of tRNA when bound to the ribosome (Selmer *et al*., 2006), or specific hydrogen bonds engaged in the discrimination of cognate and non-cognate anticodons of tRNAs in the decoding center of the small subunit (Ogle *et al*., 2002). Structural aspects of importance for our understanding of initial recognition and proofreading of tRNAs have been clarified (Ogle *et al*., 2003). We can also identify the atomic interactions in the peptidyl transfer center (PTC) of the large subunit (Ban *et al*., 2000; Schmeing *et al*., 2005) and determine how termination factors recognize stop codons and induce peptide release from the ribosome (Laurberg *et al*., 2008; Weixlbaumer *et al*., 2008; Korostelev *et al*., 2008). The initial observation that there is no protein

component in the vicinity of PTC has been challenged (Maguire *et al*., 2005; Selmer *et al*., 2006; Voorhees *et al*., 2009).

The revolution the structural insights have provided for the understanding of translation has been rewarded with the Nobel Prize in Chemistry 2009 awarded to Venkatraman Ramakrishnan, Thomas Steitz and Ada Yonath for "studies of the structure and function of the ribosome" (www.kva.se/en/pressroom/press-releases-2009/Nobel-Prize-in-Chemistry-2009/).

Further progress in ribosomal research will rely on high resolution crystal structures of the ribosome in functional complexes in combination with precise kinetic measurements and molecular computation approaches.

The ribosome is central for many cellular activities, primarily for the production of all proteins utilized in the cell or exported to other compartments. This makes it into a central locus for cellular control and inhibition (VanBogelen & Neidhardt, 1990). From many points of view, it is thus of fundamental interest to clarify its functional mechanisms in great detail, not the least since the ribosome is the target for about half of the existing antibiotic drugs. The rapidly developing resistance against clinically used drugs is a serious problem (Levy & Marshall, 2004). The combined structural and functional studies increase the possibilities of developing new and for medical reasons desperately needed antibiotics.

This page intentionally left blank

3

Methods of Studying Structure

For appreciation of the research presented in this book a brief summary of the most important structural methods may be helpful. The goal of structural research is generally to obtain a molecular model of a macromolecule or a macromolecular complex like the ribosome. For this one needs observations that relate to the molecular structure. In deriving a model from such observations, one cannot determine more parameters of the model than the number of independent observations. This means, in particular, that to obtain accurate coordinates of all the atoms of ribosomes or ribosomal subunits one needs hundreds of thousands of observations that relate to the positions of all the atoms.

During the long time that the structure of the ribosome has been studied, many of the methods of structure analysis have greatly improved. Some methods can only give a low-resolution picture. Thus, chemical cross-linking without the analysis of which groups are cross-linked is a low-resolution method. However, when the reacting components are identified at the amino acid residue or RNA base level or, even better, at the atomic level, cross-linking can provide valuable insights, particularly if combined with complementary high-resolution information. In general, low-resolution methods can give unique insights when combined with results from high-resolution methods. In many cases, they can by themselves give very valuable information

regarding large conformational features of the ribosome itself and its protein or RNA ligands.

The primary high-resolution method has been the crystallographic analysis of ribosomal subunits and whole ribosomes. Cryoelectron microscopy (cryo-EM) of functional ribosomal complexes has provided remarkable insights into important functional aspects of translation. Nuclear magnetic resonance (NMR) spectroscopy is a unique method for studies of dynamic aspects of molecular systems and, in particular, transient interactions. The translation system is rich in transient interactions, which could be further studied by NMR and fluorescence resonance energy transfer (FRET).

Some methods have been important in earlier phases of structural studies of ribosomes but have now become obsolete, and will not be described here.

3.1 LOW-RESOLUTION METHODS

Assembly

One of the early ways to explore the organization of the ribosomal subunits was to study their assembly from purified components into functional particles. This field was pioneered by Nomura (Mizushima & Nomura, 1970; Nomura, 1973; Held *et al.*, 1974) and Nierhaus (Röhl & Nierhaus, 1982), who determined the interdependence of the proteins of the small subunit of *E. coli* when associating with the 16S rRNA. It was found that certain proteins must first bind to the rRNA in order for subsequent proteins to follow. This suggested that the rRNA is not able to fold properly without the presence of specific proteins. A certain order of assembly was obtained for groups of proteins. It was later established by other methods, such as cross-linking and neutron scattering, that the interdependence of assembly is primarily related to the proximity between the proteins in the particles, even though there is little protein–protein contact within the ribosome (Capel *et al.*, 1987). A renewed interest in the complex process of assembly of ribosomes is based on the structural work on ribosomes and new methods such as mass spectrometry (Williamson, 2007).

Surface Accessibility to Enzymes and Chemical Modifications

There are numerous methods for exploring exposed surfaces of rRNA or proteins in the ribosome. One can expose them to modifying chemicals or hydrolytic enzymes. It is also possible to analyze protection against these modifications by binding different types of ligands to the ribosome. These methods have primarily been used for the studies of the rRNAs. Thus, in addition to the secondary and tertiary structures of the rRNAs, the binding sites for ribosomal proteins, tRNAs and translation factors have been investigated (Moazed & Noller, 1986, 1987, 1989; Moazed *et al.*, 1988). The protection against chemical modification of certain nucleotides is usually called "footprinting" (Stern *et al.*, 1988; Culver & Noller, 2000; Joseph & Noller, 2000). Footprinting has given valuable results, although these are not always easy to interpret. For instance, binding of a ribosomal protein, a tRNA or a factor to the surface of the ribosome normally makes the covered surface unavailable to footprinting. However, if the ribosome undergoes conformational changes upon such binding, the access to enzymes or reagents also at sites distant from the binding site may be changed.

In the method of mild proteolysis, low concentrations of proteolytic enzymes under natural conditions are used to give a record of flexible regions not involved in firm secondary structures (Gudkov & Bubunenko, 1989; Bubunenko & Gudkov, 1990). This approach has been used in the study of different conformations of elongation factors, but ribosomal proteins *in situ* can also give interesting and variable accessibility, depending on the state of the ribosome. For ribosomal proteins in isolation, it has been a method for studying their domain organization.

Proximity Information by Chemical Methods

Bifunctional cross-links and affinity labels of different lengths can be used to analyze structural proximity, whether permanent or transient. They have been used to explore the secondary structure of the rRNA and the proximity between different nucleotides or

different proteins within the ribosome. The ribosomal binding sites of tRNA and mRNA molecules or translation factors have also been examined this way. The method remains a very important tool for exploring structural and functional proximity on the ribosome.

Numerous cross-links with reactivity to different groups and with different lengths have been developed to explore the ribosome (see Baranov *et al*., 1998; 1999 for the ribosome cross-link database). Furthermore, the introduction of cysteines by site-directed mutagenesis into ribosomal proteins has been used to create binding sites for cross-linking or affinity labeling reagents.

Enzymatic and chemical modification and cleavage methods have also been very useful when combined with primer extension methods to identify rRNA structures and their changes (Stern *et al*., 1988). In particular, the Fe(II)-EDTA or hydroxyl radical methods provide extensive, valuable structural and functional insights (Culver & Noller, 2000; Joseph & Noller, 2000). By this method Fe-EDTA is bound to selected sites of the ribosome by cysteine mutagenesis. The hydroxyl radicals produced can react with sites on the ribosome within a range of about 20 Å.

Great care has to be exercised to avoid accidental and misleading covalent reactions between the reagent and components of the protein synthesis system. Sergiev *et al*. (2001) and Whirl-Carillo *et al*. (2002) have given critical evaluations of the correlation between chemical and crystallographic observations.

Fluorescence Methods

In fluorescence (or Förster) resonance energy transfer (FRET), the energy of an excited donor chromophore can excite an acceptor chromophore along a radiation-less pathway with an efficiency that decreases strongly with increasing distance between donor and acceptor (Förster, 1948, 1965), as validated experimentally (Haugland *et al*., 1969). In pioneering FRET studies, a number of groups on tRNAs and other components of the translation machinery were used to explore structural relationships (Huang *et al*.,

1975). Today, FRET is frequently used to obtain information about distances between donor and acceptor chromophores on the ribosome in the 20–80 Å range. Precise estimates of absolute distances by this method may be difficult to obtain, since the FRET efficiency depends also on other (generally unknown) parameters than interchromophore distances. One such parameter relates to the relative orientation of donor and acceptor, but this difficulty can be greatly reduced by the use of donors and acceptors coupled to the ribosome by flexible linkers.

More recently, single molecule FRET (smFRET) (Ha *et al*., 1996) has been used to explore dynamic aspects of transient complex formations and conformational changes of the ribosome, as reviewed by Blanchard (2009) and Aitken *et al.* (2010). smFRET is a method that can be used to study the kinetics of ribosome function from a new perspective. In smFRET kinetics the different functional states of the ribosome are seen as well-defined FRET signals. The kinetic information is obtained by extensive sampling of the lifetimes of these FRET states. Statistical analysis of how the system moves between its different FRET states provides kinetic models of ribosome function, and distance interpretation of the FRET signals can in favorable cases be used to relate the kinetic data to distinct conformations of the ribosome. smFRET is particularly valuable for detecting rapid kinetic events, which are hidden in classical relaxation techniques like quench flow and stopped flow due to averaging over large ensembles of molecules. Validation of ribosomal smFRET kinetics by careful comparison with classical, macroscopic kinetics performed with quench flow (Johansson *et al*., 2008) and stopped flow (Gromadski & Rodnina, 2004) techniques would greatly improve the interpretability of both approaches, but remains to be done.

Force Measurements

The forces underlying the movements of molecular systems can be studied using optical tweezers on the subnanometer and piconewton scale with a time resolution in the millisecond range

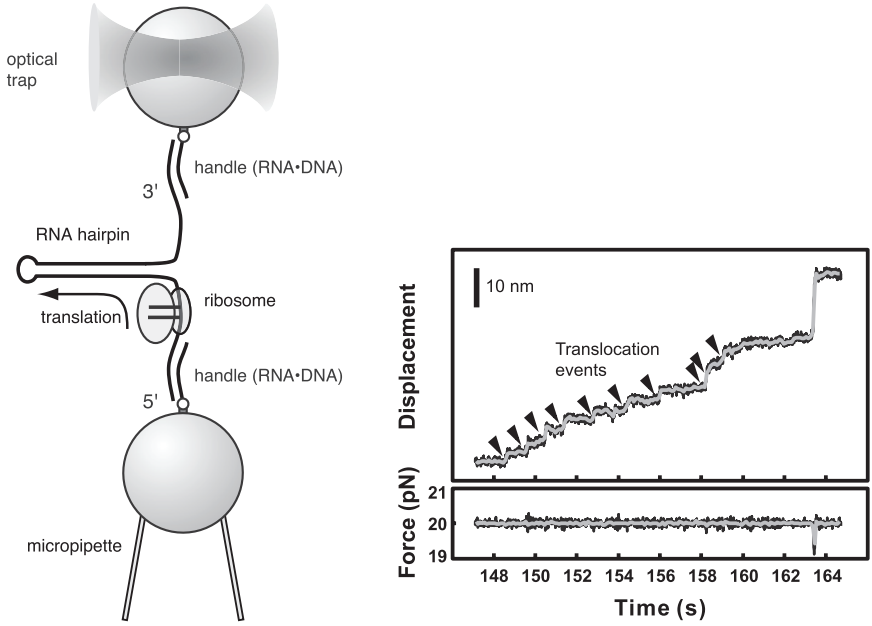

Fig. 3.1 Force measurements performed on a translating ribosome. Left: One end (the upstream end of the mRNA) is immobilized with a micropipette while the optical trap pulls on the other end (the downstream end of the mRNA). Right: When the ribosome translocates, the loop of the mRNA melts and the distance between the two ends increases. (Reproduced with permission from Aitken *et al.*, Single ribosome dynamics and the mechanism of translation, *Annu Rev Biophys* **39**:491–513. Copyright 2010, Annual Reviews Inc.)

(Greenleaf *et al.*, 2007; Aitken *et al.*, 2010). To perform force measurements there must be handles on the molecules involved. These handles can be very small polystyrene beads. The measurement can be done by immobilizing or trapping the handle of one component and trapping the handle of the other component in the focus of an infrared laser. The force on a molecular system can be deduced from the displacement of the bead from the center of the laser focus, since the optical trap has a restraining force proportional to the distance from the center of the focus, like a linear spring. The strength of the interaction can also be measured by pulling until the interaction ruptures.

Electron Microscopy

The identification of the shapes of the ribosome and its subunits was an important early step in our familiarization with ribosomes (Plate 2.1; Fig. 2.2). Electron microscopy (EM) was and is an important tool for studying the structure of particles as large as ribosomes (Hall & Slayter, 1959; Huxley & Zubay, 1960; Lubin, 1968). It has been applied in different forms and with increasing resolution. One early aim was to obtain the shapes of ribosomes and their subunits. Here several groups made seminal contributions to elucidate not only the shape but also the way ribosomal subunits associate (Stöffler & Stöffler-Meilicke, 1984; Gornicki *et al.*, 1984; Lake, 1985; Spirin & Vasiliev, 1989).

Subsequently the immune–EM technique was developed (Wabl, 1974; Tischendorf *et al.*, 1974; Lake *et al.*, 1974). Here antibodies were used to label selected entities on the ribosome (Stöffler & Stöffler-Meilicke, 1984; Lake, 1985). A distance relationship between epitopes could be established using ribosomes labeled with pairs of antibodies (Kastner *et al.*, 1981; Lake, 1982). Most of the results concerning the shapes of the ribosomal subunits and the locations of ribosomal proteins remain valid. The preliminary information about their elongated shapes was much later confirmed. However, immune–EM has a subjective component that sometimes led to doubtful interpretations and scientific controversy.

For the analysis of ribosomal shapes, improved methods have been employed. Electron diffraction from two-dimensional crystals is a useful way of analyzing structures, but few early attempts were made using this approach (Milligan & Unwin, 1986; Yonath *et al.*, 1987). Due to the difficulties in obtaining crystals and in analyzing them, methods focusing on single-particle averaging were developed.

Scattering Methods

Small angle neutron scattering (SANS) has provided valuable insight into the localization of ribosomal proteins before the time

of crystallography on whole ribosomes and subunits. The difference in scattering of neutrons by hydrogen and deuterium is used. Thus, the neutron scattering of deuterated pairs of proteins has been studied in a background of hydrogenated proteins. Distances between protein pairs as well as information about the shape of proteins have been obtained. From the pairwise distances of ribosomal proteins, a three-dimensional map of the 30S subunit from *E. coli* was constructed and related to the electron-microscopic shape (Capel *et al.*, 1987). In addition, a number of proteins from the 50S subunit have been located (May *et al.*, 1992; Willumeit *et al.*, 2001). Most of these results have turned out to be highly reliable even though they provide only low-resolution information. Contrary to the immune–EM technique the method does not suffer from subjective image interpretation.

Small angle X-ray scattering (SAXS) has gained a renewed interest as a valuable complement when it comes to questions of molecular shape. This method has a range of possibilities. The molecular weight of a molecular system can easily be estimated and possible aggregation can be detected. Likewise, the shape of a molecule can be obtained. SAXS offers the possibility of testing whether a molecular model, obtained for example by crystallography, is in agreement with the conformation in solution. Thus, release factors have been studied by X-ray scattering to compare their conformation in solution with the one on the ribosome and alone in crystals (Vestergaard *et al.*, 2005). Likewise, when highly flexible structures are concerned approximate shapes can be obtained (Grela *et al.*, 2007).

In fact, small angle scattering (SAS) is rapidly developing into a very useful tool for the analysis of macromolecules and their complexes, including *ab initio* estimates of their overall shapes (Petoukhov & Svergun, 2007).

Scattering of visible light can also be used. Here the wavelength is much larger than the molecular dimensions of the ribosome and its subunits. The scattered intensity from free ribosomal subunits is proportional to the sum of their squared molecular weights, $M_S^2 + M_L^2$, while the scattered intensity from the whole

ribosome is the square of its molecular weight, $(M_S + M_L)^2 = M_S^2 + M_L^2 + 2M_S M_L$. Since $M_S \approx 0.8$ megadalton (MDa) and $M_L \approx 1.5$ MDa, the scattered intensity from the whole ribosome ($I \sim 4.1$) is much larger than the intensity from its separate subunits ($I \sim 2.9$). Accordingly, visible light scattering is an ideal experimental tool for following the kinetics of subunit association and dissociation in real time (Grunberg-Manago *et al.*, 1975). More recently, stopped flow techniques in combination with monitoring of visible light scattering have been used in systematic studies of the roles of initiation factors in promoting subunit docking during initiation of protein synthesis (Antoun *et al.*, 2006a,b; Pavlov *et al.*, 2010) and the roles of EF-G and RRF during ribosome recycling after termination of protein synthesis to a new round of initiation of mRNA translation (Savelsbergh *et al.*, 2009).

Mass Spectrometry

A new and useful method for studying ribosomes and ribosomal states is electrospray mass spectrometry (MS). Not only can the full ribosomal particles and the individual components be identified, but under different solution conditions ribosomal states and different complexes can be seen. The ease with which ribosomal components dissociate from each other in the gas phase can give rich information (Benjamin *et al.*, 1998; Rostom *et al.*, 2000; Videler *et al.*, 2005). One example is the study of the stoichiometry and phosphorylation of the L12 stalk (Ilag *et al.*, 2005).

3.2 HIGH-RESOLUTION METHODS

Cryo-EM

In the study of ribosomes and functional ribosomal complexes, single-particle reconstruction using cryo-EM has been very valuable (Frank *et al.*, 1981; van Heel, 1987; Dubochet *et al.*, 1988; Frank *et al.*, 1996). Here large numbers of randomly oriented ribosomes in vitreous ice give different projections of the particle.

These can be combined into a three-dimensional picture of the ribosome. A rapidly growing number of functional complexes of ribosomes with tRNAs and factor proteins have been studied and will be discussed in later chapters. Particularly valuable are the complexes that have not been easy to crystallize, like the ribosome with its GTP hydrolyzing factors. Resolutions of better than 10 Å (Valle *et al*., 2003a,b) and now around 6 Å have been achieved (Connell *et al*., 2007; Schuette *et al*., 2009). Like all structural methods, EM is confronted with ensembles of conformations. However, powerful classification methods for identifying ribosomes with different occupancies of ligands and different conformations, essential for meaningful structures and for obtaining good resolution, have now been developed (Penczek *et al*., 2006a, b). In this way several states of a complex can often be studied from a single sample (Loerke *et al*., 2010). The spatial resolution has been defined in different ways. The method that has gained general acceptance is based on Fourier shell correlations calculated between two density maps using two independent sets of data (Boettcher *et al*., 1997; Frank, 2009).

Nuclear Magnetic Resonance

Nuclear magnetic resonance (NMR) can provide detailed structural information at the atomic level. One limitation, which is severe when it comes to the study of the ribosomes, is their large size. Molecular masses in excess of 40,000 Da are difficult to study by NMR. However, ribosomal proteins or fragments of rRNA have been studied by this method with excellent results. In particular, studies of well-chosen fragments of rRNA have given very good insights into ribosomal structure and function (Fourmy *et al*., 1996).

NMR is also a method well suited for characterizing the dynamics of molecules. It is remarkable that even complete ribosomes give an NMR spectrum despite a molecular mass of about 2.5 MDa. The observed spectrum is primarily due to the ribosomal protein L12, which is particularly flexible even though it is bound to the ribosome (Morrison *et al*., 1977; Tritton, 1980; Gudkov *et al*., 1982;

Cowgill *et al*., 1984, Mulder *et al*., 2004). The nascent peptide chain when inside the ribosome has also been studied by NMR (Hsu *et al*., 2007). The surface of L12 involved in transient interactions with translational factors has also been successfully investigated by NMR (Helgstrand *et al*., 2007).

X-Ray Diffraction

Crystallography on ribosomal components as well as ribosomal subunits or whole ribosomes has been performed for several decades. One prime limitation of this method is the absolute requirement for well-ordered crystals diffracting to a satisfactory resolution, while the size of the object is no limitation. Macromolecular crystals are sensitive to the energetic X-ray radiation. Cryocooling of the crystals to around 100 K has become a very important solution to this problem and has turned out to be essential for ribosomal crystallography (Hope *et al*., 1989). Despite the cooling, a number of crystals may be needed for a complete data set. This may require the inspection of numerous crystals, since not all diffract equally well. Furthermore, the crystals used for one data set need to be isomorphous with each other. This means that they should have the same unit cell dimensions and the same molecular orientations within the cells, which is not always the case.

In all crystallographic work, resolution is crucial. To claim a certain resolution, essentially all diffraction data to that Bragg spacing (the shortest distance between the planes that correspond to the diffracted beams) have to be accurately measured. No absolute criteria are used, but the data have to be measured with a good redundancy and repeated measurements of the same reflexion should agree ($R_{\text{merge}} = \sum |I_{\text{obs}} - \langle I \rangle| / \sum I_{\text{obs}}$, where I is one measurement of the intensity of a reflexion and $\langle I \rangle$ is the average of the different measurements of the reflexion, R_{merge} is the deviation of the individual measurements from their averages for all the diffraction data). The majority of the measurements in the highest resolution bin (a fraction of the data at the highest resolution)

should also have a significant intensity ($I/\sigma I$ taken as the average over all reflexions in a resolution bin, where I is the intensity of a reflexion and σI is the estimated standard deviation of the measurement). We note that the ultimate criterion for high-quality X-ray data is that the electron density map (see below) is well defined throughout the whole structure, which may not always be the case although the resolution average is high. The number of independent observations needed for the structure of the large ribosomal subunit at 2.4 Å resolution is more than 600,000.

Another problem is the need to obtain the phase angles in order to calculate the electron density maps. These phase angles cannot be directly measured experimentally; however, a number of methods can be employed to determine them. The classical method uses heavy atoms that scatter X-rays strongly, usually with compounds containing a single heavy atom. Due to the large size and the lack of symmetry of the ribosome, it has been advantageous to use large clusters of heavy atoms such as tungsten to obtain phase angles at low resolution (Yonath *et al.*, 1998; Ban *et al.*, 1998; Clemons *et al.*, 1999; Cate *et al.*, 1999). If the structure of a related molecule is known, one can computationally determine the orientation and position of the known molecule in the unknown crystal lattice, making it possible to calculate the phase angles. This method is called molecular replacement (Rossmann & Blow, 1962). In the case of ribosome crystallography, cryo-EM structures were used to obtain phase angles with molecular replacement at low resolution (Ban *et al.*, 1998; Weinstein *et al.*, 1999; Cate *et al.*, 1999). This approach has been valuable in identifying or verifying the positions of heavy atoms or heavy atom clusters. A different method takes advantage of the tunability of the X-ray wavelength at synchrotrons to record data across absorption edges for selected heavier atoms. This method is called multiple wavelength anomalous dispersion (MAD; Hendrickson, 1991). All these methods have been used to determine the structure of the ribosome.

Once the electron density has been calculated using the measured amplitudes and calculated phase angles in a Fourier summation, its interpretation demands great care. This is true not only for

crystallography but also for cryo-EM. Here it is important to be aware of the resolution (Table 3.1), the quality of the measurements and the phase angles obtained. In addition, some regions of the molecule may be more flexible than others, leading to poor or no density. In contrast to virus crystallography, where the high symmetry of the particles leads to high redundancy of the crystallographic information, ribosomes have no symmetry and thus the interpretability of maps at similar resolution will be very different.

Thus, an electron density map of whole ribosomes or ribosomal subunits at around 6 Å resolution can hardly be interpreted in

Table 3.1 Estimate of the Resolution Needed to Identify Some Molecular Features of Proteins and Nucleic Acids*

Protein	Nucleic Acid	Resolution (Å)
General shape	Distinguish nucleic acid from protein	20
	Double helix	12
α-helix	Single strand	9
β-sheet	Stacked base pairs, phosphate groups and sugar residues	4
Large side chains		3.5
Shaped bulbs of density for small side chains	Purines and pyrimidines distinguished	3.2
Conformation of side chains		2.9
Carbonyl groups, peptide planes	Individual bases	2.7
	Puckering of sugar	2.4
Puckering of Pro residues, holes in aromatic rings		2.0
Individual atoms	Individual atoms	1.5

* Adapted from Liljas *et al*. (2009) with permission.

terms of details of individual nucleotides or amino acids, particularly if they deviate from previously determined structures or well-known secondary structure arrangements. The RNA backbone, on the other hand, can easily be followed due to the heavier electron density of the phosphates and the clear helical paths (Ban *et al*., 1998, 1999; Cate *et al*., 1999; Harms *et al*., 1999; Clemons *et al*., 1999). Protein structures cannot be determined *de novo* at 6 Å resolution even though α-helices can be located. If a structure has been determined previously, deviations in structure due to conformational changes are easily identified.

At resolutions around 3 Å the RNA structures can be interpreted with much greater certainty, even though the hydrogen bonding may be difficult to identify. Protein structures might be interpreted without previous structural knowledge, but there is a risk of getting out of register along the polypeptide chain. If homologous structures are known, careful alignment of the multiple sequences will assist in the homology modeling needed to prevent wrong assignments.

At resolutions below 2.5 Å, there is usually no difficulty in determining the atomic structure of proteins and nucleic acids. The main uncertainty is the accuracy of the atomic positions and, as a consequence, the distances between atoms that are not covalently linked. In some instances, it may be difficult to determine the presence or absence of hydrogen bonds.

The whole ribosomal structure from *Thermus thermophilus* is now available at 2.8 Å resolution (Selmer *et al*., 2006) and the large subunit from *Haluarcula marismortui* is known at 2.4 Å resolution (Ban *et al*., 2000; Nissen *et al*., 2000). The separate small subunit and various complexes are known at lower resolution.

Once a crystal structure is known, it is relatively easy to investigate the binding of ligands. The simplest procedure is to soak the crystals in the ligand and collect the data. A difference electron density map should reveal the bound ligand and any conformational changes that have been caused. In the case of the ribosomes, numerous antibiotics have been studied when bound to subunits or whole ribosomes. A dynamic complex, like the ribosome where

substrates are moving through different channels, cannot be analyzed in a single fixed state. On the contrary, many states of the ribosome have to be studied. The antibiotics, like other inhibitors, may freeze the structure in different states and offer excellent opportunities for detailed analysis in distinct frozen functional states.

In the work on 70S ribosomes, protein L9 from one ribosome overlaps with the binding site for trGTPases such as elongation factor Tu (EF-Tu) or elongation factor G (EF-G). The removal of the part of L9 that overlaps has led to a new crystal form, which allows the binding of trGTPases (Gao *et al*., 2009).

The results from structural studies are generally accessible from databases such as the Protein Data Bank (PDB; http://www.rcsb.org/pdb).

3.3 COMPUTATIONAL METHODS

With an increasing number of relevant 3D structures — from both crystallography and cryo-EM — that provide information on the ribosome in different functional states, it is a major challenge to convert these structures to a quantitative description of protein synthesis. The main link between structure and function, in this respect, is to decipher the energetics of the processes involved and also to elucidate the dynamical pathways involved. Here, computational methods can play an invaluable role, as already indicated by several contributions (Trobro & Åqvist, 2005, 2007; Sund *et al*., 2010). However, the complexity of the translation process with key events ranging from rearrangements on the electronic level (peptidyl transfer, peptidyl-tRNA hydrolysis and GTP hydrolysis reactions) to large scale tRNA and ribosomal domain movements require that a broad arsenal of computational tools be employed. As far as the chemical reactions are concerned, these can be modeled both by detailed quantum-chemical electronic structure calculations, such as density functional theory (DFT) methods (Perdew *et al.*, 2009), of limited parts of the system (Wallin & Åqvist, 2010), and by more complete treatments of the QM/MM

type (quantum mechanics/molecular mechanics) that allow larger regions of the ribosome to be included and conformational sampling by molecular dynamics (MD) simulations. The empirical valence bond (EVB) method (Åqvist & Warshel, 1993) has proven particularly useful in the latter case, as it is sufficiently fast to allow extensive MD simulations and calculations of free energy profiles.

The available 3D structures may for various reasons sometimes be incomplete, for example in the sense that electron density is missing for key parts or that complexes with ligands of interest such as inhibitory compounds are lacking. In such cases, molecular docking methods may be useful for providing the missing structural information. One such case is the prediction of the interaction of the RF GGQ motif with the ribosomal A-site, where docking and MD methods were able to find the correct binding mode of the conserved RF motif (Trobro & Åqvist, 2007). A number of different docking algorithms and programs are available that can treat small molecule docking (Friesner *et al*., 2004), the usual case in drug design, up to more complex cases involving entire protein and RNA molecules as interaction partners (Chen *et al*., 2003). Both in the case of modeling chemical reactions and for evaluating binding affinities and equilibrium constants, it is critical to be able to obtain free energies from the computations. The most powerful method for this purpose is the so-called free energy perturbation (FEP) approach (Kollman, 1993), which is a rigorous statistical-mechanical technique for extracting free energies from MD simulations. This method, however, is rather time-consuming, which may sometimes be prohibitive. A faster but more approximate alternative is the linear interaction energy (LIE) method (Åqvist *et al*., 2002), which was used in an initial computational study of the energetics of codon–anticodon interactions in the decoding center (Almlöf *et al*., 2007). This method is also very powerful for ligand binding problems.

While MD simulation is a useful method for conformational sampling and exploration of the dynamics and thermal fluctuations around equilibrium conformations, it is computationally inefficient for studying large-scale motions in large systems. This

is mainly due to limitations in the timescales that can be reached, which are presently at most on the order of a microsecond for larger systems (such calculations are still computationally very expensive). There are, however, a number of more coarse-grained techniques that can be used to access motions occurring on longer timescales. In cases where the conformational endpoints of a slow process are known, one may speed up regular MD simulations by forcing the system to go from one state to the other using artificial restraints on the atomic coordinates. Such techniques have been named "steered" or "targeted" MD and they still correspond to an all-atom description of the system and its dynamics (Schlitter *et al*., 1993). A popular and potentially useful class of models is so-called coarse-grained ones where atoms are bunched together into larger units and their interactions described in a simplified way, for example based on statistical potentials (Warshel and Levitt, 1976). An even more drastic simplification is to consider a complex macromolecular structure as a network of simple harmonic interactions representing contacts between atoms or groups of atoms, for example at a resolution corresponding to protein and RNA backbones. The latter type is called Gaussian elastic network models (Tirion, 1996) and their normal modes around given stable conformational states can give information about dynamical pathways.

This page intentionally left blank

4

The Message — mRNA

The messenger RNA (mRNA) is a central molecule in translation of the genetic message from DNA into protein. Genomic DNA is transcribed into mRNA which can bind to the ribosome and be translated. In some RNA viruses, genetic information is stored in RNA that can be directly translated into protein on the ribosome.

4.1 THE GENETIC CODE

The genetic code (Fig. 4.1) is the universal dictionary by which the genetic information in DNA is translated into the functional workhorses of living organisms: the proteins. It is remarkable that the genetic code is virtually the same in all species. Although very minor deviations are found, it is evident that all life on earth has a common origin.

The code words or the "codons" of the genetic message are three nucleotides long (Crick *et al.*, 1961; Crick 1962, 1963). The three nucleotides in a codon specify the amino acid it encodes. The codons are read in a sequential manner from the 5'-end to the 3'-end of the mRNA. There are no overlaps or punctuations between the fixed starting (initiation) and termination (stop) codons (Fig. 2.2; Crick *et al.*, 1961). Since the four different nucleotides A, G, C, U are used in mRNAs, this leads to a dictionary of $4^3 = 64$

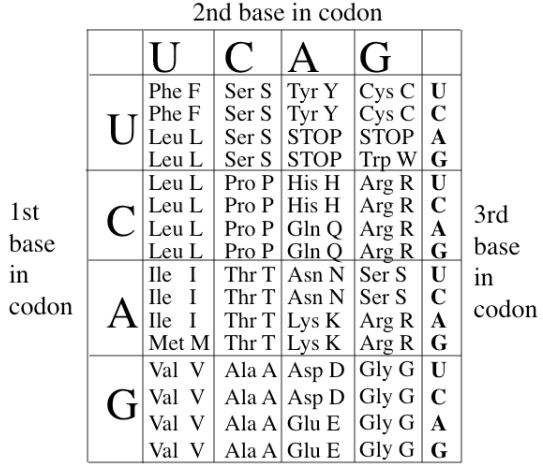

Fig. 4.1 The universal genetic code. The trinucleotide codons are translated to the 20 amino acids given with their three-and one-letter codes.

different words. Because there are 20 normally used (canonical) amino acids in proteins and 64 code words, the genetic code is said to be redundant.

Translation also needs a defined start codon and a defined stop codon. The start codon (generally AUG) defines the start of translation in the correct reading frame of the sequence of nucleotide triplets that is to be translated. The start or initiation codon is identical to the methionine codon (AUG). Special mechanisms are used to identify the proper initiation AUG codon, so that initiation does not occur on an internal methionine codon (see Secs. 8.1 and 11.3). In bacteria and archaea a GUG or UUG codon may sometimes function as the initiation codon.

There are three stop codons, UAA, UAG and UGA, leaving 61 codons for the 20 amino acids making the genetic code degenerate in the sense that there are often several, synonymous codons encoding the very same amino acid. For leucine, serine and arginine there are as many as six synonymous codons, whereas for methionine and tryptophan there is only one codon (Nirenberg

et al., 1966; Khorana *et al.*, 1966; Crick, 1966a). The first two nucleotides of synonymous codons are often, but not always, the same and then suffice to specify the identity of the amino acid. The genetic code has therefore been discussed as a 2 + 1 letter code with emphasis on the first two codon nucleotides (Hahn *et al.*, 2004).

Different organisms use the synonymous codons for the same amino acid at different frequencies; their 'codon usage' is different. The codon usage is correlated with the concentrations of the isoaccepting tRNAs, which together read the synonymous codons for a particular amino acid. Thus, the codon usage can differ to the extent that a gene transferred from one organism to another cannot be translated unless the new organism is supplemented with some missing isoacceptor tRNAs.

The universal genetic code deviates slightly from the one in vertebrate mitochondria. If a codon disappears from a genome there is no more any need for the corresponding anticodon and tRNA. If, however, this codon reappears, it can get a new amino acid assignment (Yokobori *et al.*, 2001). Mitochondrial genomes in metazoa are very short and the loss of a codon is more likely than in longer genomes. The most prevalent variants concern methionine and tryptophan, which have two codons instead of one (Knight *et al.*, 2001; Ambrogelly, Palioura & Söll, 2007). Each of the three stop codons in some mitochondria can be translated to amino acids. Furthermore, the arginine codons are often reassigned to another amino acid, in some cases to serine. A database with information about the genetic code and its variations is provided by Elzanowski and Ostell at http://www.ncbi.nlm.nih.gov/Taxonomy/Utils/wprintgc.cgi#SG1

4.2 TRANSCRIPTION

The genomic DNA cannot be directly translated. First, it must be 'copied' or transcribed into RNA by enzymes called RNA polymerases. This occurs by the classical mechanism discovered by Watson and Crick (1953): one template strand of the double-stranded DNA is copied in the 5′-to-3′ direction through

Watson–Crick base pairing into a complementary strand of RNA. The double-stranded DNA is opened up in a bubble that travels along the duplex during transcription, in which a DNA–mRNA hybrid is continuously formed and dissolved. Free energy variation of the transcription bubble is expected to modulate the rate of transcription (Yager and von Hippel, 1991). The process of transcription is strongly and dynamically regulated. Some genes are transcribed frequently, whereas others are transcribed only rarely. Again, some genes are transcribed during a brief period in the life of the cell, whereas others are copied more continuously. The regulation of transcription is controlled by a great number of gene-specific and general transcription factors, which inhibit or activate transcription of single genes or groups of genes. The RNA polymerase, guided by these transcription factors, perform the synthesis of an mRNA. Structures of RNA polymerases and transcription factors are known (Wang *et al*., 2006; Cramer *et al*., 2008).

In eukaryotes, transcription is performed in the cell nucleus and the transcripts are transported into the cytoplasm for ribosome binding and translation. Organelles like mitochondria and chloroplasts have their own genomes, which are transcribed to mRNA and translated to protein. However, some proteins are encoded by the nuclear DNA, synthesized in the cytoplasm and finally transported to the organelle (see Chap. 12; Frydman, 2001). In the case of bacteria and archaea, both transcription and translation take place in the cytoplasm. Bacterial mRNAs can be polycistronic, with information from more than one gene contained in one transcript.

4.3 PROCESSING OF THE TRANSCRIBED RNA

The primary transcript of an mRNA molecule frequently has to be processed to become an authentic mRNA. Several different processes are involved and those in eukaryotes differ from those in bacteria and archaea. The eukaryotic primary mRNA transcripts

normally contain longer or shorter regions, which are not translated. They form so-called introns, while the translated regions are called exons. The introns are removed from mRNA by the splicing machinery through cutting and ligation (Tarn & Steitz, 1997; Doudna & Cech, 2002; Patel & Steitz, 2003). Eukaryotic mRNAs are also modified by the addition of a poly(A) tail at the 3′ end of the message.

In eukaryotes the primary transcripts are also frequently edited to become mRNAs. This is sometimes done by changes of U to C or *vice versa* (Wedekind *et al*., 2003). More extensive editing occurs in mitochondria from trypanosomes, where the mRNAs are extensively modified by large enzymatic particles that use templates called guide RNAs (Estevez & Simpson, 1999).

Not only those mRNA molecules that are destined for translation are transcribed; nontranslated, functional tRNA, ribosomal RNA and small regulatory RNA molecules are also transcribed and processed.

4.4 TRANSLATIONAL REGULATION, READING FRAME AND USAGE OF THE GENETIC CODE

The control of gene expression in the form of protein synthesis occurs on both the levels of transcription and translation in various ways. Concerning the synthesis of ribosomes, ribosomal RNA is primarily controlled by the action of the global regulator molecule ppGpp (Dennis, Ehrenberg & Bremer, 2004). Synthesis of ribosomal proteins is regulated by feedback mechanisms in which the free concentrations of selected ribosomal proteins repress transcription of mRNAs for ribosomal proteins or translation of existing mRNAs for ribosomal proteins (Nomura *et al*., 1980, 1984). Some ribosomal proteins produced in excess over the rRNAs will bind the polycistronic mRNA and inhibit further translation (Romby & Springer, 2003). The action of small noncoding RNAs has created a revolution in our understanding of regulation of gene expression in eukaryotic cells. They also have a spectrum of tasks in bacteria, primarily in the regulation of translation. Thus, small

RNAs can repress translation by binding to the 5′-untranslated region aided by the protein Hfq or activate translation by melting inhibitory secondary structures (Gottesman, 2005; Urban & Vogel, 2007).

The initiation codon, AUG, not only defines the translation start but also the reading frame of an mRNA. Translation proceeds from the initiation codon in steps of three nucleotides (one codon) by successive binding of a cognate aminoacylated tRNA to each one of the open reading frame codons through base pairing between its anticodon and the mRNA codon. The frequent occurrence of termination codons out of frame interrupts translation in a wrong reading frame after just a few rounds of protein elongation. However, there are mRNAs whose correct translation *requires* frameshifting (Atkins & Gesteland, 2001; Baranov *et al*., 2002a). This is the case for termination or release factor 2 (RF2) from most bacteria (Baranov *et al*., 2002b). The stop codon (UGA) that is uniquely identified by RF2 occurs early in the correct reading frame of its mRNA. Thus, if there is enough RF2 in the cell, protein elongation will be stopped by RF2-dependent termination. However, if there is a shortage of RF2, protein elongation will not be terminated. Instead, there will be a + 1 frameshift and continued protein elongation until the whole RF2 molecule has been synthesized. This frameshift event, competing with the RF2-dependent termination, is aided by an internal so-called Shine–Dalgarno sequence.

A related phenomenon, known as ribosome hopping or bypassing, has been identified. In this case, when the ribosome pauses due to a shortage of aminoacyl tRNA cognate to its A-site codon, it may slide downstream along the open reading frame until it encounters a codon cognate to the peptidyl-tRNA, originally in the P-site of the pausing ribosome (Gallant *et al*., 2004). This means that the ribosome can slide along mRNAs without any contact between its P-site bound peptidyl-tRNA and the codons of the mRNA. When a codon matching the anticodon of the P-site tRNA occurs, be it in or out of the original reading frame, the sliding may stop and translation may be resumed. The functional significance of this mechanism has remained unclear, but it may be

related to the ability of ribosomes to resume translation of an open reading frame downstream from the stop codon of a previous operon reading frame in a multiopen reading frame mRNA.

Bacteria starved for an amino acid or some other essential nutrient may be regulated by stringent control. Some proteins (RelA and SpoT in gram-negative and Rel in gram-positive bacteria) respond to deacylated tRNA bound to the ribosomal A-site and increase the concentration of inhibitors (ppGpp and pppGpp) of RNA polymerase (see Sec. 9.6). As discussed above, an increasing concentration of the global regulator molecule ppGpp downregulates the synthesis of ribosomal RNA and ribosomal proteins (Dennis *et al.*, 2004).

A suppressor tRNA can read a stop (nonsense) codon and incorporate a specific amino acid and thereby prevent termination by a competing release factor. In addition, a few proteins in bacteria and eukaryotes contain seleno-cysteine (Se-Cys). Se-Cys incorporation is not achieved by a posttranslational modification as in the cases of other nonstandard amino acids. Instead, Se-Cys is incorporated during translation in response to the stop codon UGA. Se-Cys is the 21st amino acid incorporated into proteins according to the genetic information (Leinfelder *et al.*, 1989). The mechanism for this involves a special tRNA ($tRNA^{Sec}$), which can read the stop codon. A set of enzymes has specific functions in this system. $tRNA^{Sec}$ cannot bind to EF-Tu, due to an antideterminant sequence in its acceptor stem (Rudinger *et al.*, 1996). A special form of elongation factor Tu called SelB uniquely binds $tRNA^{Sec}$ (Forchhammer *et al.*, 1989). SelB has the property of identifying a specific secondary structure of the mRNA that precedes the stop codon that corresponds to Se-Cys. This leads to the suppression of the stop codon and the incorporation of Se-Cys (Thanbichler *et al.*, 2000).

Yet, another amino acid (the 22nd) incorporated into proteins according to the genetic information was found in a methylamine methyltransferase in some methanogenic archaea. The amino acid is named 'pyrrolysine' (Fig. 4.2) and is incorporated in response to the UAG stop codon (James *et al.*, 2001; Hao *et al.*, 2002; Srinivasan

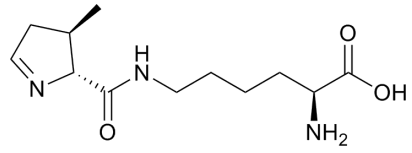

Fig. 4.2 The structure of the 22nd amino acid, pyrrolysine (kindly drawn by Andreas Ehnbom). It is encoded by the UAG stop codon.

et al., 2002; Ambrogelly, Palioura & Söll, 2007). Pyrrolysine is probably functionally important. The genome contains information for a $tRNA_{CUA}$ (or $tRNA^{Pyl}$) which reads the UAG codon and a special tRNA synthetase (PylS) which charges $tRNA^{Pyl}$. Genes for the biosynthesis of pyrrolysine have also been identified. $tRNA^{Pyl}$ can bind to EF-Tu, in contrast to $tRNA^{Sec}$. The Pyl genes have also been found in a few bacterial species (Zhang & Glayshev, 2007). The translation of UAG, instead of causing termination, is stimulated by a downstream pyrrolysine insertion sequence (PYLIS; Longstaff *et al.*, 2007).

5

The Adaptor — tRNA

The transfer RNAs (tRNAs) are central molecules in protein synthesis. Historically, when the structure of DNA and the basics of protein synthesis were clarified, the existence of tRNAs was still unknown. In 1956, Crick drew attention to the problem of assembling a polypeptide from an RNA template (Crick, 1958; Woese, 2001). A stereochemical complementarity between the mRNA codons and amino acids seemed impossible. He suggested that small RNA molecules could function as "adaptors." These could be charged with specific amino acids by enzymes, specifically recognizing both the RNA adaptor and its cognate amino acid. Subsequently, the adaptors would decode the mRNA by Watson–Crick base pairing, thereby ensuring that the amino acids were incorporated into polypeptide chains according to the prescription of the genetic code. Indeed, such adaptors were identified experimentally (Hoagland *et al.*, 1957; Hoagland, 2003). They were initially called soluble RNAs (sRNAs) but are now known as transfer RNA molecules, or tRNAs, normally containing about 75 nucleotides. Each tRNA is specific for one amino acid, but one amino acid can be specific for several tRNAs. The latter are often referred to as "isoacceptors," i.e. accepting the same amino acid in the reaction where tRNA is aminoacylated. For instance, there are six codons for the amino acid leucine. In *E. coli* these are read by

five leucine-specific tRNAs, all charged with leucine by the same aminoacyl-tRNA synthetase: LeuRS.

5.1 THE tRNAs

Noncoding RNA molecules, i.e. micro RNAs, which are not messenger RNAs, exist in all kingdoms of life. They are often involved in regulation of gene expression (Vogel & Wagner, 2007). The tRNAs have a different and well-understood role in translation and form the earliest known group of small noncoding RNAs. The tRNA genes are dispersed throughout the genomes and are frequently found in clusters. Some are associated with genes for ribosomal RNAs and there may be several genes for a certain tRNA (Komine *et al.,* 1990; Rudner *et al*., 1993; Marck & Grosjean, 2002). In addition to tRNAs cognate to the classical (canonical) 20 amino acids, there is a $tRNA^{Sec}$ for the 21st amino acid, selenocystein, and a $tRNA^{Pyl}$ for the 22nd amino acid, pyrrolysine, which in specific contexts can read stop codons, leading to the insertion of these amino acids in nascent proteins (see Chap. 4).

5.2 tRNA STRUCTURES

Primary and Secondary Structure

The tRNA molecules have several conserved features. The secondary structure of all known tRNAs is in a universal cloverleaf configuration (Holley *et al*., 1965). The 3′-end has an unpaired, conserved sequence, CCA, and the 2′-hydroxyl or 3′-hydroxyl of the terminal adenosine (A76) at the 3′-CCA end is the entity charged by the amino acid during aminoacylation of all tRNAs (Sec. 5.3). The 5′ and 3′-termini of the cloverleaf configuration are base-paired in the acceptor (aminoacyl) stem (AA stem) (Fig. 5.1). There are three cloverleaves, formed by three stem–loop structures: the dihydro-U arm (D arm), the anticodon arm (AC arm) with the anticodon in its loop and the TΨC arm (T arm). Their stems, composed of 4–7 base pairs, are the D stem, the AC stem and the T stem. Their

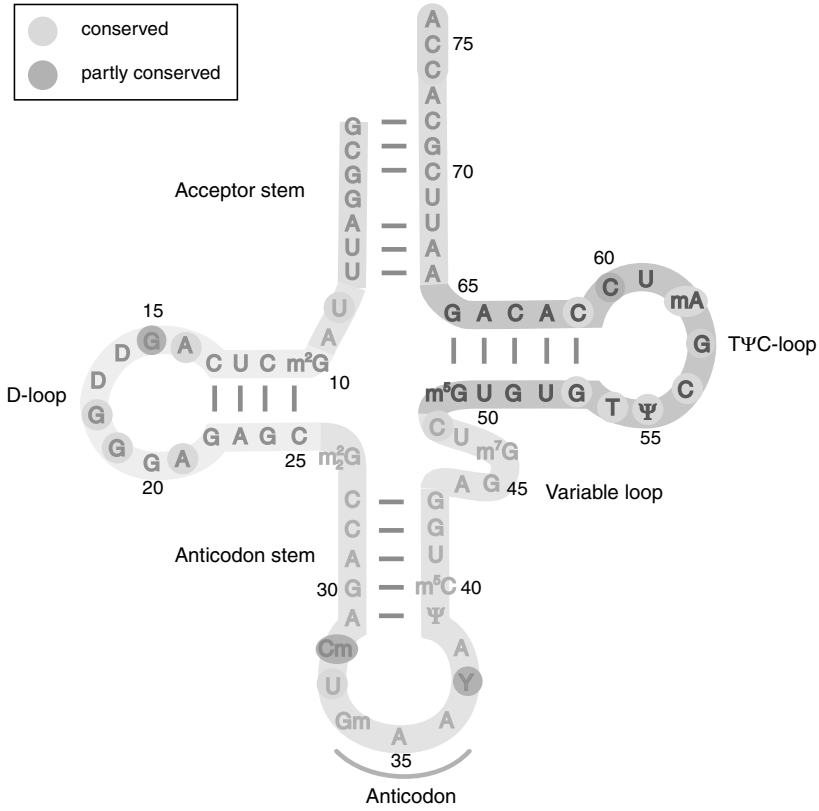

Fig. 5.1 The cloverleaf secondary structure of $tRNA^{Phe}$ from *Rhodospirillum rubrum*. The acceptor or the aminoacyl (AA) stem with the CCA sequence is at the 3′terminus. The D arm contains two dihydrouridines. The anticodon stem and loop (AC arm) contains the anticodon at the bottom (normally bases 34–36). The helix and loop to the right is called the TΨCG (in the figure called the TΨC loop) or T arm. Finally, there is an extra loop of variable length. (Copied with permission from Liljas *et al*., 2009, *Textbook of Structural Biology*.)

corresponding loops are the D, AC and T loops. There is also a variable arm, often short and lacking a base-paired stem (see below).

The initial tRNA gene transcripts contain sequences at both termini and in the anticodon area that are removed by special

tRNA-processing nucleases (Calvin & Li, 2008; Phizicky & Hopper, 2010) in 'maturation' steps leading to the native, functional tRNA molecules. A classical ribonuclease, trimming precursor tRNAs, is RNase P. This is normally a ribonucleoprotein complex, in which the RNA component often, but not always, retains residual catalytic activity in the absence of protein (Guerrier-Takada *et al.*, 1983; Kirsebom, 2007). In human mitochondria the RNase P function is carried out by protein only (Walker & Engelke, 2008). In most cases the 3′-terminal CCA residues of tRNAs are added, edited or repaired by a template-independent nucleotidyltransferase enzyme (Schürer *et al.*, 2001). The structures of several nucleotidyltransferases have been determined and a mechanism for their action has been proposed (Xiong & Steitz, 2004; Tomita *et al.*, 2006).

The mature tRNA molecules are extensively modified (see Björk, 1995; McCloskey & Crain, 1998; Byrne *et al.*, 2010, for reviews). Some modifications are so typical that they have given or influenced the names of the parts of the structure they belong to. For instance, the D loop is named after its 5,6-dihydrouridines (Fig. 5.1; Plate 5.1) and the T loop after the T (thymine) preceding a pseudouridine (Ψ). The anticodon loop is also frequently modified, with important consequences for translation of the mRNA code (see Chap. 11) (Ambrogelly *et al.*, 2007).

The 3D Structure

In 1973, the first three-dimensional structures of tRNA molecules were determined (Robertus *et al.*, 1974; Kim *et al.*, 1974). The cloverleaf secondary structure was confirmed but, surprisingly, it was found to be arranged in the shape of an L (Fig. 5.2). It is folded with the D and T loops forming the elbow region of the L through tertiary structure interactions. Furthermore, the anticodon was found at one end of the tRNA and the amino-acid-accepting CCA end, at the opposite end, approximately 75 Å away. This means that the

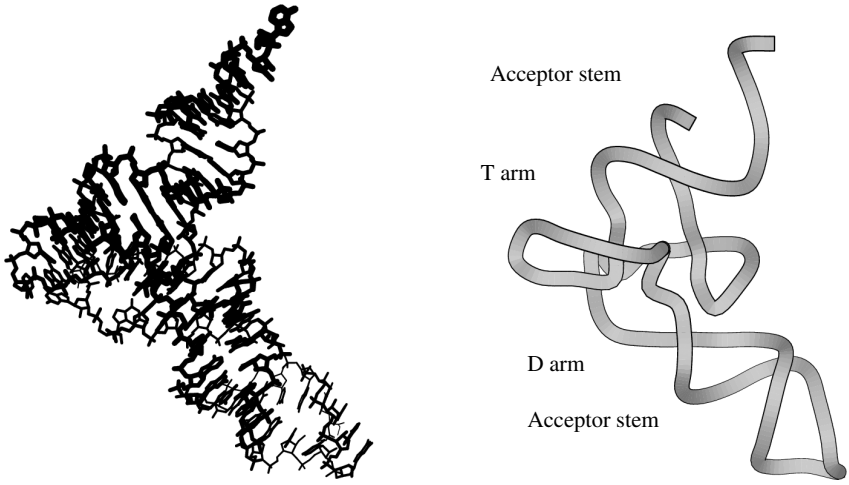

Fig. 5.2 The L-shaped three-dimensional structure of tRNA. The end of the acceptor stem, the single-stranded CCA end, where the amino acid is attached, is at one extreme end of the molecule about 75 Å from the anticodon in the opposite end. The D and T arms participate in forming the elbow of the molecule. [Figures kindly produced by Dr. M. Fodje, using the program MOLSCRIPT (Kraulis, 1991).]

anticodon cannot directly interact with the amino acid. It also means that when the tRNA incorporates the amino acid into the growing polypeptide on the ribosome, the mRNA and the decoding site are far from the site for peptidyl transfer — the peptidyl transfer center (PTC). This is consistent with the early notion that decoding is performed on the small ribosomal subunit, whereas peptidyl transfer is performed on the large subunit (Okamoto & Takanami, 1963).

The L shape of the tRNA molecule is universal and functionally essential. It is observed in crystal structures of tRNA alone or in complexes with tRNA synthetases, EF-Tu and, with minor rearrangements, in the ribosome itself, where the tRNAs have some conformational variability (see Sec. 8.2 and Chap. 11).

The variable loop, at the junction of the T stem and the AC stem, is often short and without base pairing, but for Leu, Ser,

Tyr and selenocystein (Se-Cys) it can be quite long and contain base pairs. In mitochondria from higher eukaryotes some tRNAs have evolved to greatly simplified structures by the removal of one of the stem–loop structures (Helm *et al.*, 2000), but the L shape of these tRNA variants is preserved.

A different tRNA conformation, the "λ-form," has been discovered (Ishitani *et al.*, 2003, 2008) for a tRNA in complex with an enzyme that modifies the tRNA nucleotide G15 in the D arm. This nucleotide is not accessible in an L shaped tRNA. G15 modification therefore requires a profound structural transformation that leads to the λ form via disruption of the base pairs and tertiary interactions of the D arm.

5.3 CHARGING — THE tRNA SYNTHETASES

The Charging Reaction

Peptide chains are mainly made from the 20 canonical amino acids. Commonly, one canonical amino acid is ester-bonded to all its cognate, isoaccepting tRNAs by one aminocyl-tRNA synthetase (aaRS) in the tRNA-charging reactions. Besides this set of charging enzymes, there exist two additional types of synthetases. That is to say, the 22nd amino acid, pyrrolysine, needs its specialized synthetase, PylRS (Srinivasan *et al.*, 2002; Nozawa *et al.*, 2009). In addition, some methanogenic archaea lack CysRS. They use a different path to incorporate cysteine. Here an unusual aaRS, SepRS, charges $tRNA^{Cys}$ with phosphoserine. Sep-$tRNA^{Cys}$ is subsequently converted to Cys-$tRNA^{Cys}$ (Sauerwald *et al.*, 2005; Ambrogelly *et al.*, 2007). Therefore, the total set of aaRSs has 22 members. Interestingly, the 21st amino acid, selenocysteine, does not require a special synthetase. Instead, $tRNA^{Sec}$ is serylated by SerRS (Leinfelder *et al.*, 1988). The serine is subsequently modified to selenocysteine (see Ibba & Söll, 2000, for a review).

The charging of an amino acid onto its cognate tRNA molecule is a two-step process. In the first major step, the amino acid is activated to aminoacyl-adenylate:

(1) Amino acid activation (Scheme 1)

$$\text{aaRS} + \text{aa} + \text{ATP} \rightleftarrows \text{aaRS}\cdot\text{aa}\cdot\text{ATP} \rightarrow \text{aaRS}\cdot\text{aa-AMP} + \text{pp}$$
$$\downarrow$$
$$\text{aaRS+aa+AMP}$$

In the second major step, the aminoacyl-adenylate reacts with the enzyme-bound tRNA in the formation of aminoacyl-tRNA on the enzyme:

(2) Aminoacylation (Scheme 2)

$$\text{aaRS}\cdot\text{aa-AMP} + \text{tRNA} \rightleftarrows \text{aaRS}\cdot\text{aa-AMP}\cdot\text{tRNA} \rightarrow$$
$$\rightarrow \text{aaRS}\cdot\text{aa-tRNA+AMP} \rightarrow \text{aaRS+aa-tRNA}$$
$$\downarrow$$
$$\text{aaRS+aa+tRNA}$$

Here, the 2′- or 3′-OH group of the terminal adenosine of the conserved CCA motif in the tRNAs directly attacks the high energy ester bond in aa-AMP, resulting in attachment of the amino acid to the ribose. After formation of aa-tRNA on the aaRS, aa-tRNA dissociates from the enzyme, forming free aa-tRNA and free aaRS (not shown). Accordingly, the net-reaction scheme catalyzed by the aaRS is (Scheme 3):

$$\text{aa} + \text{tRNA} + \text{ATP} \xleftrightarrow{\text{aaRS}} \text{aa} - \text{tRNA} + \text{AMP} + \text{pp}$$

That is to say, free amino acid and free tRNA react to form aa-tRNA at the expense of the hydrolysis of at least one molecule

of ATP to AMP and pyrophosphate. The aminoacylation reaction is "energy-coupled," in the sense that one energy-rich molecule, aa-tRNA, is formed, while another energy-rich molecule, ATP, is consumed. In this way the total reaction is 'energy-balanced' with respect to the participating molecules. This makes the coupled enzymatic reaction much more efficient than an uncoupled aminoacylation could have been. Furthermore, ATP is in the cell pumped far above its equilibrium with AMP and inorganic pyrophosphate (pp_i), which makes it possible to use the energy coupling to pump aa-tRNA far above its equilibrium with amino acid and tRNA. The displacement from equilibrium of ATP also allows great enhancement of the accuracy of the reaction by a proofreading or, equivalently, editing mechanism, as discussed further below in this chapter.

Classes and Subclasses of Aminoacyl-tRNA Synthetases

The molecular weights and oligomeric states of the aaRSs vary considerably (Vasil'eva & Moor, 2007; Guo *et al*., 2008). This originally led to some confusion regarding their evolutionary origins. However, in 1990, two classes of tRNA synthetases, class I and class II, were identified on the basis of their three-dimensional structures and sequences (Table 5.1). There are normally 10 aaRSs in each class (Table 5.2; Cusack *et al*., 1990; Eriani *et al*., 1990; Carter, 1993; Ibba & Söll, 2000). The division into the two classes is universal. In addition to the newly discovered SepRS (Fukunaga & Yokoyama, 2007) and PylRS (Lee *et al*., 2008; Nozawa *et al*., 2009) there are two versions of LysRS with distinct structures, one belonging to class I and the other to class II (Terada *et al*., 2002). Bacteria can have multiple synthetase genes; for example, *Deinococcus radiodurans* has two genes for TrpRS (Hausmann & Ibba, 2008).

Enzymes of the two classes have entirely different structures (Plates 5.2–5.4 and 5.7). Class I enzymes are mainly monomers but may also be homodimers. Class II enzymes are either dimers or

Table 5.1 Oligomeric States of Aminoacyl-tRNA Synthetases

Class I												
RS	L	I	V	C		M	R	E	Q	K	Y	W
Oligomeric state	α	α	α	α		α, α_2	α	α	α	α	α_2	α_2
Class II												
RS	S	T	G	A	P	H	D	N	K	F	Sep	Pyl
Oligomeric state	α_2	α_2	$\alpha_2 (\alpha\beta)_2$	$\alpha\,\alpha_4$	α_2	α_2	α_2	α_2	$\alpha_2\alpha_4$	$\alpha\,(\alpha\beta)_2$	α_4	α_2

Table 5.2 Characteristics of the aaRS Enzymes

	Class I	Class II
Sequence motif	HIGH	FRXE/D
	KMSKS	R/HXXXF
		GXGXGXER
Subclass a	L, I, V, C, M, R, K	S, T, G(α_2), P, H, A
b	E, Q, K	D, N, K
c	Y, W	G$(\alpha\beta)_2$, A, F, Sep, Pyl
Amino acylation	2′OH	3′OH
Fold of ATP domain	Rossmann (// β)	Antiparallel β
Amino acid binding	Deep pocket	Surface
tRNA acceptor end	Bent	Straight
Acceptor stem interaction	Minor groove	Major groove

tetramers. The aaRSs are modular and built of several domain modules (Fig. 5.3). While the ATP-binding or catalytic domain of class I aaRSs is a Rossmann fold with parallel β strands, the corresponding domain in the class II aaRSs consists of antiparallel β strands (Cusack *et al.*, 1990; Eriani *et al.*, 1990). Different consensus sequences, which are involved in the binding of ATP and the amino acid, characterize the two classes (Plate 5.3; Cusack, 1995). The aaRSs of the two classes recognize the acceptor stem of the

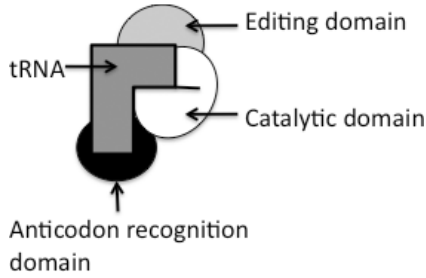

Fig 5.3 A common construction of tRNA synthetases. In this case the protein is illustrated by three domains. The white domain is the catalytic domain, performing both the activation and the transfer reactions. The black domain recognizes the anticodon of the tRNA. The light gray domain is an editing domain. The tRNA is represented by the dark gray outline.

tRNAs from opposite sides and charge the tRNA on the 2′-OH (class I) or the 3′-OH (class II) of the terminal riboses. This may have an interesting evolutionary background (see Chap. 13; Schimmel & Ribas de Pouplana, 2001). aaRSs often form complexes with accessory proteins and sometimes exist as high-molecular-weight multisynthetase complexes (Hausmann & Ibba, 2008).

Not only do the ATP-binding domains of the aaRSs display characteristic features (Plate 5.3), but also the other domains. Thus, the two classes of aaRSs can be divided into subclasses a, b and c based on sequence homology and domain architecture (Cusack, 1995). The aaRSs are built with modular domain arrangements where the very different ATP-binding domains define the class. The enzymes within each subclass have similar domain arrangements.

5.4 RECOGNITION OF AMINO ACIDS AND tRNAs BY AMINOACYL-tRNA SYNTHETASES

Aminoacyl-tRNA synthetases must couple amino acids to tRNAs both efficiently and accurately. The speed of the reaction is greatly facilitated by its energy coupling with ATP hydrolysis, as described above. Every aaRS must accurately recognize both

its cognate amino acid and its cognate set of isoaccepting tRNAs: if an erroneous aminoacyl-tRNA is created by a synthetase accepting either a noncognate tRNA or a noncognate amino acid, then it is likely that an erroneous amino acid will be incorporated in the nascent peptide determined by the anticodon of the tRNA. In aminoacylation, the functioning of the genetic code relies on *proteins* recognizing specific pairs of an amino acid and its cognate of tRNA, while transcription of DNA genes and codon reading by tRNAs depend to a large extent on Watson–Crick base pairing.

In aminoacylation the cognate nature of the amino acid is in many cases checked twice, before and after the transfer to the tRNA. However, the tRNA, being a larger and more variable molecule, is checked only once.

tRNA Recognition: Not a Simple Matter

The recognition of the different tRNAs by their aaRSs is sometimes, but not always, mediated by the anticodons (Plate 5.4). In many cases one aaRS has to recognize tRNA isoacceptors with different anticodons, making anticodon recognition less useful. Instead, the identification of a cognate tRNA among the different noncognate ones is due to a number of features of the individual tRNAs called the "identity set" (Giege *et al.*, 1998; Vasil'eva & Moor, 2007). Most elements of the identity set are localized in the anticodon and acceptor stems — the majority on the side of the tRNA that faces the aaRS (Fig. 5.4). For the tRNAs with a long variable arm, its orientation is another important feature for tRNA recognition (Tukalo *et al.*, 2005). A general observation is that several of these enzymes do not identify specific groups of the tRNAs but rather their unique detailed shapes (Tukalo *et al.*, 2005).

Amino acid Recognition: An Old Mystery

Very early, long before the basics of protein synthesis had been clarified, Pauling claimed that many amino acids with similar side

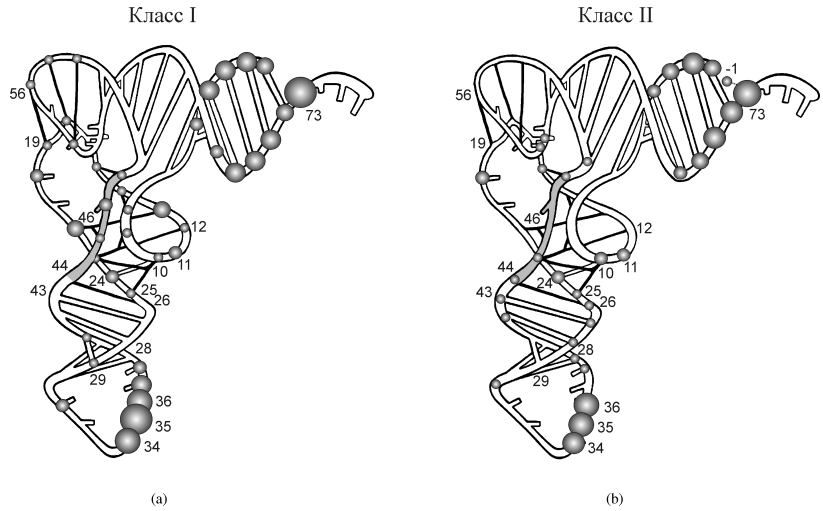

Fig. 5.4 The tRNA 'identity sets' for class I (a) and II (b) synthetases. [Reprinted with permission from Vasil'eva & Moor, 2007; Interaction of aminoacyl-tRNA synthetases with tRNA: General principles and distinguishing characteristics of the high-molecular-weight substrate recognition, *Biochemistry (Moscow)* **72**: 306–324. Copyright 2007, Pleiades.]

groups cannot be separated better than by factors of 10–100 by any conceivable protein (Pauling, 1958). From this he suggested that all proteins in living cells must be permeated with amino acid substitution error at levels between 1% and 10%, but his own as well as later experiments performed by others (Loftfield, 1963) showed that the level of amino acid substitution errors in the living cell must be smaller than 1/10,000 (10^{-4}).

This apparent discrepancy between prediction and experiment gained renewed interest by experiments probing IleRS-dependent aminoacylation of $tRNA^{Ile}$ with either cognate Ile or non cognate Val — two amino acids differing by a single methyl group. IleRS could activate Ile to Ile-AMP and Val toVal-AMP. Addition of $tRNA^{Ile}$ to Ile-AMP containing IleRS rapidly led to formation of Ile-$tRNA^{Ile}$, whereas addition of $tRNA^{Ile}$ Val-AMP containing IleRS led to hydrolysis of the aminoacyl-adenylate but no visible Val-$tRNA^{Ile}$

(Baldwin & Berg, 1966). It seemed therefore that this enzyme and perhaps other aaRSs have an editing facility: first, they discriminate between the cognate amino acid and its noncognate competitors in the amino-acid-activating step, and then, if the amino acid is noncognate, the aminoacyl-adenylate is hydrolyzed (pretransfer editing; see Scheme 1 above) or aminoacylation takes place, but the aminoacyl-tRNA is then rapidly hydrolyzed to amino acid and tRNA (posttransfer editing; see Scheme 2 above). It was then shown that misacylated Val-tRNA^{Ile} when added to IleRS in the absence of AMP and pp_i was rapidly deacylated, from which result it was suggested that the Baldwin– Berg (1966) experiment reflected a posttransfer editing mechanism (Eldred & Schimmel, 1972).

Shortly after, Hopfield (1974) and Ninio (1975) made seminal contributions to the conceptual basis of editing or 'proofreading' mechanisms. In essence, they showed that a given affinity difference between a cognate and a noncognate enzyme substrate complex can be used twice to enhance the accuracy of the reaction, provided that it is energy-coupled so that a cosubstrate like ATP or GTP is hydrolyzed upon product formation. This means that if the cognate substrate binds 100 times better to the enzyme than the noncognate one, then the selection accuracy can only be 100 in a single-step mechanism, but as much as 10,000 (100 x 100) if there is an additional editing step. Similar arguments can be applied to more complex schemes in which other kinetic parameters than just binding are involved in the editing mechanism.

Hopfield pointed out that the accuracy contribution to the aminoacylation reaction by editing (F) can be experimentally assessed by measuring the number of ATP molecules hydrolyzed per cognate (f_c) and noncognate (f_{nc}) aminoacyl-tRNA and forming the ratio $F = f_{nc}/f_c$. This relation between the hydrolysis of cosubstrates associated with cognate and noncognate reactions is universal and independent of the details of the mechanism, including the existence of multiple editing steps (Freter & Savageau, 1980; Ehrenberg & Blomberg, 1980). Yamane and Hopfield (1976) subsequently performed such an experiment and estimated the editing contribution to the accuracy by which IleRS chooses Ile rather than Val as about 200.

Using through rapid quench-flow experiments, Fersht showed that ValRS uses posttransfer editing (Scheme 2) to improve the accuracy by which Val is selected in relation to Thr in aminoacylation of $tRNA^{Val}$ (Kaethner & Fersht, 1976). He also used the same techniques to study the discrimination against Val in favor of Ile by IleRS. The experiments suggested pretransfer editing (Scheme 1), but he could not definitively rule out a posttransfer mechanism (Fersht, 1977). Inspired by the latter data set, Fersht formulated the double-sieve hypothesis, implying that a synthetase can efficiently discriminate against a noncognate amino acid, which is larger than the cognate one, making editing superfluous in such cases (Fig. 5.5). However, when the cognate amino acid (e.g. Ile) is larger than the noncognate one (e.g. Val), the initial discrimination is necessarily poor and subsequent editing must be used. He pointed out that in such cases the editing step could by the same argument be very precise by the existence of a hydrolytic site,

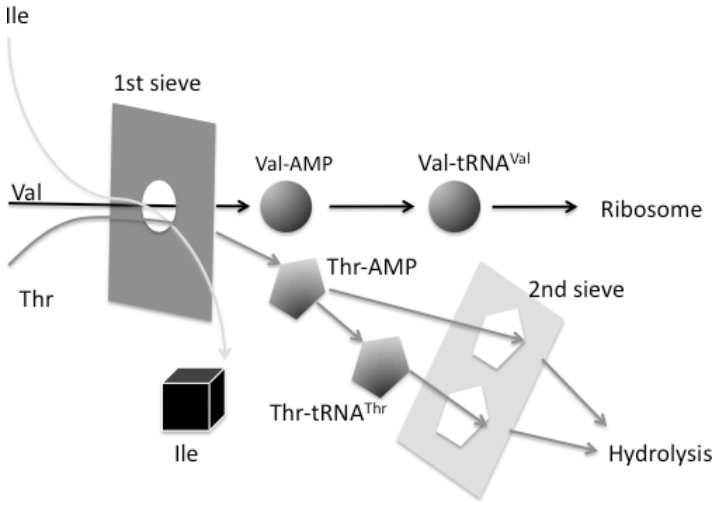

Fig. 5.5 The double-sieve mechanism, by which isoleucine is too big to be selected, but both valine and threonine pass the first sieve. However, due to the hydrophilic character of threonine it binds to the editing domain and is hydrolyzed off from the AMP or tRNA (Dock-Bregeon *et al*., 2004).

which accommodates the noncognate but not the larger cognate substrate. Since the double-sieve mechanism was suggested, a separate hydrolytic site for amino acid editing (proofreading) has been identified by biochemical and structural methods in about half of the known aaRSs (Mascarenhas *et al*., 2008).

The Structural Basis of Amino Acid Activation and Aminoacylation

An amino acid is first selected (Plate 5.5) for activation to be aminoacyl-adenylated by reacting with an ATP molecule, leading to the release of inorganic pyrophosphate (Scheme 1). The tRNA synthetases bind its cognate amino acid through specific hydrogen bonds as well as through a defined space where hydrophobic and van der Waals interactions play important roles.

In the subsequent step of aminoacylation of a tRNA, the aminoacyl-AMP is located next to the CCA end of the tRNA in such a manner that the 2′- or 3′-OH of A76 is juxtaposed with the amino acid. One example is ProRS (Plate 5.6).

The structural basis of amino acid editing

The functional significance of pretransfer editing (Scheme 1) has remained controversial due to the intrinsic instability of aminoacyl-AMP in solution and the technical difficulty of distinguishing this activity in the presence of posttransfer editing (Martinis & Boniecki, 2010). The posttransfer editing function is often associated with an editing domain of the aaRS (Fig. 5.6). The amino acid similarities are primarily found in subclasses Ia and IIa. The amino acids Val, Ile and Leu are closely related in structure and could easily be attached to a wrong tRNA. The selection has to depend on weak van der Waals interactions. The class Ia enzymes LeuRS, IleRS and ValRS all have homologous editing domains called CP1 which are conserved throughout evolution (Schimmel & Ribas de Pouplana, 2001). This domain is an insert of about 190 amino acid residues into the

catalytic domain. Structural information on the editing mechanism of IleRS and LeuRS shows the domain to adopt a number of different orientations due to flexible hinges connecting the CP1 domain to the main body of the aaRS (Plate 5.7; Nureki *et al.*, 1998; Silvian *et al.*, 1999; Tukalo *et al.*, 2005; Fukunaga & Yokoyama, 2005).

The editing domains of class IIa enzymes ThrRS and AlaRS are related but this is not the case for ProRS, which also belongs to subclass IIa. Furthermore, these editing domains are not related to the CP1 domain of subclass 1a. $tRNA^{Ala}$ can be misacylated by serine or glycine. An editing domain (cis-editing) can perform the editing, but in addition there are separate editing proteins (trans-editing) called AlaX. AlaX is homologous to the editing domain of AlaRS and ThrRS (Fig. 5.6). It is found in a

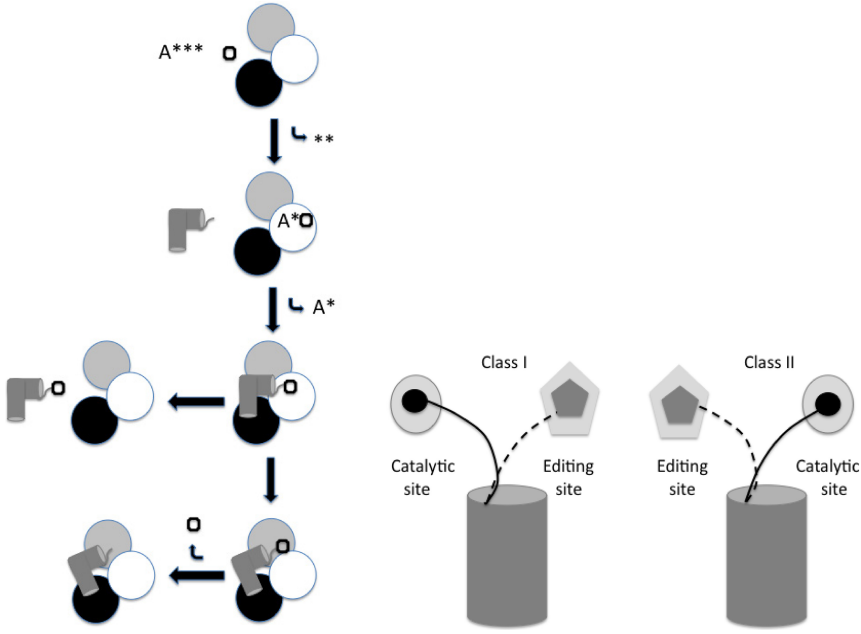

Fig. 5.6 *Left*: Aminoacylation and editing of a tRNA by an aaRS. The white domain is the aminoacylation domain and the gray domain is the editing domain. The black domain interacts with the anticodon. *Right*: The arrangement of the catalytic or transfer domain and the editing domain is different in aaRS of class I or II (Modified from: Dock-Bregeon *et al.*, 2000).

number of variants (AlaX-S, AlaX-M, AlaX-L) with different lengths and different functional characteristics. The AlaX proteins are widely dispersed in all three kingdoms of life but the simultaneous occurrence of all three in one species is rare. The structure of AlaX-M shows an N- and a C-terminal domain. The C-terminal domain has a bound zinc ion, which presumably is at the active site (Sokabe *et al*., 2005; Fukunaga & Yokoyama, 2007). However, the editing function remains even after removal of the zinc ion in AlaX-S (Sokabe *et al*., 2005). A conserved glycine-rich motif in the N-terminal domain is close to the active site and could be involved in substrate recognition. With the uncertainties

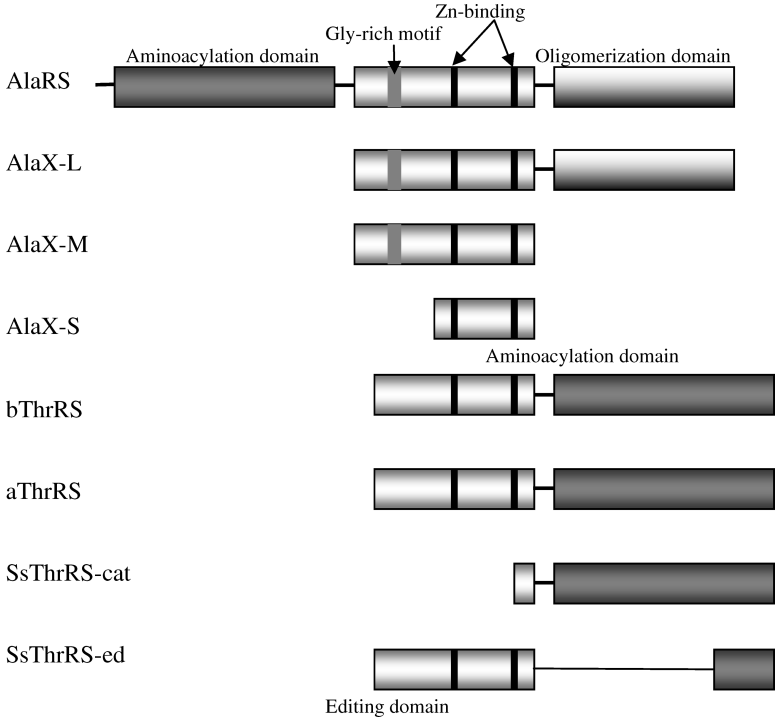

Fig. 5.7 Different domain arrangement in AlaRs and ThrRS. The aminoacylation and editing domains can be in the same peptide, but also in separate peptides. Different versions of AlaX and ThrRS illustrating the separated functions of catalysis and editing in some species. (Sokabe *et al*., 2005; Fukunaga & Yokoyama, 2007; Beebe *et al*., 2008.)

regarding the presence of zinc in substrate complexes, it is difficult to suggest detailed models of the editing mechanisms.

Structural information on the editing mechanism of ThrRS is also available (Dock-Bregeon *et al*., 2000, 2004). The editing domain of ThrRS is related to that of AlaRS in bacteria and eukaryotes. However, for most archaea there are separate genes for aminoacylation (Thr-cat) and editing (Thr-ed). The zinc-binding motif in the active site of ThrRS (Fig. 5.7; Plate 5.5) selects threonine but prevents valine from binding does not bind zinc in complex with substrate analogues. The editing site of ThrRS can bind AMP-Ser or tRNAThr wrongly charged with serine. Threonine cannot be accommodated into the editing site. A water molecule is suitably placed to hydrolyze the erroneous amino acid off (Dock-Bregron *et al*., 2004)

5.5 DEVIATIONS

Normally there are 20 types of aaRSs in an organism. However, whole genome analyses have revealed that there are deviations from this rule. The most dramatic deviation is found in methanogenic archaea. In *Methanococcus jannaschii* and *Methanothermobacter thermoautothropicus*, only 16 types of aaRSs are found (Bult *et al*., 1996; Smith *et al*., 1997). The apparently missing enzymes are AsnRS, CysRS, GlnRS and LysRS (see review by Stathopopoulos *et al*., 2001). This implies that there must be noncanonical mechanisms for the charging of tRNAs with asparagine, cysteine, glutamine and lysine, since the corresponding amino acid residues exist in the proteins of these archaea.

Even though these archaea lack normal lysyl-tRNA synthetases, they can charge $tRNA^{Lys}$ with lysine. When the charging enzyme was purified and its amino acid sequence determined, it turned out that this LysRS does not belong to class II, but to class I (Ibba *et al*., 1997). LysRS1, as the enzyme is denoted, is found in most archaea but also in some bacteria. One organism has both the class I and class II forms of the enzyme (Stathopopoulos *et al*., 2001).

Also, CysRS is missing in some archaea. Initially it was thought that $tRNA^{Cys}$ is charged with cysteine by ProRS (Stathopouplos *et al.*, 2000; Lipman *et al.*, 2000). However, as stated above, the charging is done through a different pathway using phosphoserine and SepRS (Sauerwald *et al.*, 2005; Ambrogelly *et al.*, 2007).

GlnRS or AsnRS are missing from all archaea and many bacteria. Here nondiscriminating GluRS misacylates $tRNA^{Gln}$ with Glu and subsequently a tRNA-dependent amidotransferase (AdT) converts Glu-$tRNA^{Gln}$ to Gln-$tRNA^{Gln}$ (Tumbula *et al.*, 2000). A similar mechanism can be ascribed to AspRS. This enzyme does not discriminate between $tRNA^{Asp}$ and $tRNA^{Asn}$ and charges both tRNAs with Asp. A transamidase then converts Asp-$tRNA^{Asn}$ to Asn-$tRNA^{Asn}$ (Curnow *et al.*, 1996). Two different AdT enzymes have been found: GatCAB and GatDE. GatCAB is heterotrimeric and can transamidate both Glu-$tRNA^{Gln}$ and Asp-$tRNA^{Asn}$ (Curnow *et al.*, 1998; Becker *et al.*, 2000; Tumbula *et al.*, 2000), while GatDE, which is heterodimeric, can produce only Gln-$tRNA^{Gln}$ (Tumbula *et al.*, 2000). Both enzymes require ATP for transamidation (Wilcox, 1969). The structure of $tRNA^{Gln}$ has been studied in complex with GluRS and GatCAB (Ito & Yokoyama, 2010). The acceptor arm of the tRNA points into the catalytic site ready to react with an analogue of Glu-AMP. GatCAB interacts primarily with the Gln-specific parts of the D arm of the tRNA but its active site is ready to receive the aminoacylated CCA end of the tRNA to perform the transamidation.

The misacylated Glu-$tRNA^{Gln}$ and Asp-$tRNA^{Asn}$ do not participate in protein synthesis, since they cannot bind to EF-Tu and incorporate wrong amino acids into the nascent polypeptide (Stanzel *et al.*, 1994; Cathopoulis *et al.*, 2008). The mechanism for this discrimination by EF-Tu is not known.

This page intentionally left blank

6

The Workbench — Ribosomes

6.1 THE COMPOSITION OF RIBOSOMES

The ribosome is built from two subunits: a large subunit and a small subunit. Depending on the species, the size of the ribosome and of its subunits differ (Table 6.1). The bacterial ribosome has been most extensively studied. It sediments at 70S, its small subunit at 30S and its large subunit at 50S; S stands for the Svedberg unit (Tissières & Watson, 1958; Tissières *et al*., 1959). The sedimentation coefficient is determined by the molecular weight of the particle, normalized to its friction coefficient. This normalization explains why association of the 30S with the 50S particle adds up to 70S, rather than 80S (30S + 50S particle). Eukaryotic ribosomes are normally larger — 80S, 40S and 60S, respectively (Chao & Schachman, 1956) — but some eukaryotic ribosomes and their subunits sediment like those of bacteria (Arisue *et al*., 2004). Mammalian mitochondrial ribosomes are smaller, with sedimentation coefficients 55S, 28S and 38S, respectively (O'Brien, 1971). Smallest ribosomes found so far, from trypanosomal mitochondria, sediment at 50S (Maslow *et al*., 2006, 2007). Here, the small subunits can co-sediment with protein-rich particles to get a sedimentation coefficient of 45S.

In bacterial ribosomes one large molecule of untranslated ribosomal RNA (rRNA) forms the core of each of the subunits

Table 6.1 Sedimentation Coefficients for Ribosomes and Ribosomal Subunits from Different Sources

Source	Ribosomes	Molecular Mass (MDa)	Small Subunit	Large Subunit
Bacteria	70S	2.4	30S	50S
Chloroplasts	70S		30S	50S
Archaea	70S	2.4	30S	50S
Mitochondria				
(plant)	78S		30S	50S
(yeast)	74S		37S	54S
(mammal)	55S	2.6	28S	39S
(protist)	50S		30S	40S
Eukarya	80S	4.0	40S	60S

(Kurland, 1960; Spirin, 1961). The subunits consist of many small protein molecules, normally with molecular masses of less than 20 kDa (Waller & Harris, 1961; Spitnik-Elson, 1962). In most ribosomes, the total mass of the rRNA is significantly larger than that of the proteins. It is then not surprising that the protein-RNA interactions are more extensive and the protein–protein interactions are more limited. The ribosomes from mammalian mitochondria have less rRNA and a larger complement of proteins (Table 6.2). Here, proteins replace and mimic parts of the deleted rRNA structurally and perhaps also functionally.

6.2 rRNA

The rRNAs form the core of ribosomes and provide the binding sites for the ribosomal proteins. These proteins stabilize the rRNA and organize its proper functional three-dimensional structure. Several ribosomal functions are closely associated with the rRNA, but all functions depend on the interplay between RNA and protein.

In bacteria, the single rRNA of the small ribosomal subunit has one rRNA molecule, and it is called 16S rRNA (1542

Table 6.2 Ribosomal RNA and Number of Ribosomal Proteins from Different Sources

	Small Subunit		Large Subunit	
Source	**RNA**	**Proteins**	**RNA**	**Proteins**
Bacteria	16S	23	23S, 5S	33
Chloroplasts	16S	25	23S, 5S, 4.5S	35
Archaea	16S	28	23S, 5S	40
Mitochondria				
(plant)	18S		26S, 5S	
(yeast)	15S	31	21S	46
(mammal)	12S	29	16S	50
(protist)	9S	77	12S	56
Eukarya	18S	33	5.8S, 25–28S, 5S	47

nucleotides in *E. coli*). In other organisms, the size of the corresponding RNA molecule varies among different organisms (see Table 6.2). In the large ribosomal subunit of bacteria, there is one small RNA molecule, called the 5S RNA (about 120 nucleotides). There is also a large RNA molecule called the 23S RNA (2904 nucleotides in *E. coli*). Also, the size of the RNA corresponding to the 23S RNA of bacteria depends on the species. Its occurrence may sometimes vary among different organisms, and it may even occur as a set of separate pieces (Table 6.2). Best-known are the 5.8S RNAs of eukaryotes and the 4.5S RNAs of chloroplasts. In some bacteria as well as eukaryotes, there can be additional fragments (Evguenleva-Hackenberg, 2005). Some eukaryotes have been mistakenly identified as bacteria due to their short rRNAs. The proteins of these ribosomes have made it certain that they are proper eukarya (Arisue *et al.*, 2004).

Gene expression of the genetic material through protein synthesis is essential for all life forms. Ribosomes are ubiquitous in all types of life. Since protein synthesis is performed on the ribosomes in the cells of all organisms, the nucleotide sequences of rRNA are therfore particularly suitable for phylogenetic analyses and have

been used entensively for studies of evolution as pioneered by Woese and Fox (1977). The first complete rRNA sequences were obtained from *E. coli* (Brosius *et al.*, 1978, 1980) and used to align oligonucleotide sequences available from hundreds of species (Noller & Woese, 1981). From these studies it could be established that archaea are not a subgroup of bacteria but form a unique kingdom of life (Woese & Fox, 1977; Woese *et al.*, 1990).

To obtain a unique scheme for the secondary structure of a large rRNA molecule from standard free energy considerations alone is not possible. Even for the much smaller tRNA molecule, this was initially difficult (see Chap. 5). However, since the base-pairing pattern of secondary structures normally is conserved, the sequences of a number of rRNA molecules could give a good consensus model of their secondary structures (Glotz & Brimacombe, 1980; Glotz *et al.*, 1981; Noller & Woese, 1981; Noller *et al.*, 1981). These early secondary structures identified the arrangement of the rRNAs into helices and domains (see Chap. 7). There was frequently less sequence conservation of the base-paired than of the single-stranded regions, suggesting that single-stranded rRNA could carry out essential functions which effectively slowed down the rate of sequence evolution.

The studies of the secondary structure of rRNA led to the conclusion that the 5S RNA has a secondary structure with the shape of a Y where the 5′-and 3′-termini form one of the five short helices of the molecule (Plate 6.1b; Ban *et al.*, 2000; Yusupov *et al.*, 2001). The 23S RNA has 101 helices denoted as H1–H101, according to Leffers *et al.* (1987). These form six domains (I–VI) extending from one central region of the 23S RNA (Plate 6.1b). A characteristic feature is central regions with extending helices. The 16S RNA of the small subunit has 45 helices denoted as h1–h45. These are organized into four different domains: the 5′-domain, the central domain, the 3′- major domain and the 3′-minor domain (Plate 6.1a). In the 16S RNA, the domains also extend from a central part of the structure. It is interesting that in essentially all of the RNA molecules, the 5′- and the 3′-ends are close in the secondary structure.

The organization of rRNAs from all species follows this general pattern of domain arrangements but the number of helices varies greatly. Despite the large variation in size of the rRNAs, the core of the secondary structure is preserved. The differences are found in the large variation in the size of the loops. Thus, the smaller rRNAs from mammalian mitochondria have either fewer or smaller helices (Koc *et al*., 2001a, b; Plate 6.2). In the case of rRNA from the large subunit of trypanosomal mitochondria, the entire domain II is absent (Sloof *et al*., 1985).

The organization of the rRNA in three dimensions has been explored by chemical methods (see Sec. 3.1; Sergiev *et al*., 2001; Green & Noller, 1997). RNA can be cleaved with enzymes or modified with chemicals and the positions of the cleavage or modification sites can be established with single-nucleotide precision. Bifunctional cross-linking can also be used for studies of RNA, and the cross-linked bases can be identified. In addition, chemical labeling of the rRNA from components of the protein synthesis system has been highly informative (Culver & Noller, 2000; Joseph & Noller, 2000). These methods give information about the proximity of RNA bases, e.g. regions, which are permanently or intermittently base-paired or proximal in tertiary structure. Furthermore, protection of RNA by ribosomal proteins or other components of the system against labeling or cleavage is informative.

The large rRNA of either ribosomal subunit folds into a fully functional particle with the aid of ribosomal proteins (see Sec. 6.4). A certain order of assembly has been identified (Held *et al*., 1974; Röhl & Nierhaus, 1982). The binding sites for the ribosomal proteins have been established by chemical and enzymatic methods, and have given further insights into the organization of the rRNAs (Stern *et al*., 1989; Powers & Noller, 1995; Mueller & Brimacombe, 1997; Mueller *et al*., 1997). The pattern of protein interaction with the rRNAs is sometimes very complex, with several domains of rRNA involved in the binding of a single protein.

Detailed information about the structure of fragments of the rRNAs has been obtained using NMR spectroscopy and X-ray crystallography (Fourmy *et al*., 1996; Yoshizawa *et al*., 1999; Wimberley

et al., 1999; Agalarov *et al.*, 2000). More recently, the crystal structures of complete ribosomal subunits from different species have provided extensive information about the organization of the rRNAs (Chap. 7). These studies show that the structures of the rRNAs are highly complex and the deviations from standard A-type RNA are numerous. On one hand, the hydrogen bonding between bases as well as between bases and ribose hydroxyls offers extensive possibilities for variation beyond the classical Watson–Crick interaction. On the other hand, bulges and loops in the secondary structures are frequently accommodated in the helical structures.

The rRNA molecules of *E. coli* have 35 modifications, with methyl groups mostly added to heterocyclic bases but also to riboses. Furthermore, some uridines are converted to pseudouridines. In yeast the rRNAs have over 100 modifications, and more than 200 are found in vertebrate rRNAs (Piekna-Przybylska *et al.*, 2008). In eukaryotes the main modifications are pseudouridylation and ribose methylation, often guided by small nucleolar RNAs (snoRNAs). The modifications are primarily concentrated to the functional center of the ribosome, such as the decoding center of the small subunit and the peptidyl transfer center of the large subunit. Information can be found at http://people.biochem.umass.edu/fournierlab/3dmodmap/

6.3 RIBOSOMAL PROTEINS

The Identification and Number of Ribosomal Proteins

A large number of normally small proteins are bound to the ribosomal RNAs. Precise enumeration of the ribosomal proteins has been difficult. When ribosomes are purified, different washing procedures lead to varying losses of proteins. Thus, several of the proteins are frequently present in substoichiometric amounts (Hardy, 1975). Nonribosomal proteins may also spuriously stick to the ribosome during purification. In addition, some of the authentic ribosomal proteins were initially not observed, since their limited size and high positive net charge made them

run out of the classical two-dimensional gel (Kaltschmidt & Wittmann, 1970).

E. coli is the reference organism for studies of translation. Here, the small ribosomal subunit has the proteins S1–S21 and the large subunit proteins L1–L36 (Table 6.2). However, L7 is a modified form of L12 that exists in *E. coli* but not in all species; L8 is a complex of L7/L12 and L10 (Pettersson *et al.*, 1976). Since L7 is idiosyncratic to a subgroup of bacteria, we will use L12 for the modified and unmodified versions of this protein. L26 was erroneously ascribed to the large subunit, but belongs to the small ribosomal subunit and is called S20. The exact number of proteins in some mitochondrial ribosomes remains unclear (Ziková *et al.*, 2008; Koc *et al.*, 2010). When the rRNAs are very small, the numbers of ribosomal proteins are often larger than in bacteria (see Table 6.2). In bacteria, the ribosomal proteins constitute about 33% of the ribosome mass, while in mammalian mitochondria the proteins constitute about 75% of the ribosome mass (Koc *et al.*, 2010). It is thus possible that ribosomal functions carried out by RNA in bacteria are carried out by ribosomal proteins in mammalian mitochondria.

In bacteria, many ribosomal proteins are encoded in polycistronic operons together with other ribosomal proteins. The existence of such operons rich in genes for ribosomal proteins has helped to verify the ribosomal nature of several proteins. In total, there are around 50–60 ribosomal proteins in bacteria and chloroplasts (Yamaguchi *et al.*, 2000; Yamaguchi & Subramanian, 2000), while there are between 70 and 80 in eukarya and even more in trypanosomal mitochondria (Table 6.2). Archaea have an intermediate number of proteins. Ribosome-based species assignment has been particularly difficult for some organisms, like the trichomonads. Here, the ribosomes sediment at 70S, but their rRNAs are shorter than their *E. coli* counterparts but the ribosomal proteins (approximately 80) are of the eukaryotic type. From the amino acid sequences of these proteins, it has been concluded that the trichomonads are eukaryotes (Arisue *et al.*, 2004).

A safe identification of the evolutionary relationship of a ribosomal protein to the ones in bacteria can be difficult due to

extensive divergence. The sequence identity may be below detection. However, the structure and location of a protein in the ribosome constitute a more safe and definite identification. With the limited species range of ribosomes studied by crystallography, many relationships may remain to be discovered.

When one is comparing the completely sequenced genomes, the few proteins that are universally conserved in all sequenced species are primarily ribosomal proteins (see App. 1; Lecompte *et al.*, 2002; Harris *et al.*, 2003; Mushegian, 2005) and translation factors (Pandit & Srinivasan, 2003). Evidently, a subgroup of these proteins is completely essential. Interestingly, a large number of ribosomal proteins, including some of the universally conserved ones, can be deleted from the *E. coli* ribosomes at retained cell viability without drastic effects on cell viability (Dabbs *et al.*, 1983; Dabbs, 1986; Tobin *et al.*, 2010). Even some of the totally conserved proteins have been deleted in these mutants.

Some ribosomal proteins contain posttranslational modifications, but their significance has often remained obscure. Mass spectrometry has been used to show that the *E. coli* proteins S11, L3, L11, L12, L16 and L33 are methylated at different types of residues (Polewoda & Sherman, 2007). It was shown early that L12 is acetylated at the amino terminus and, as mentioned above, its modified form has been called called L7 (Terhorst *et al.*, 1972). Ilag *et al.* (2005) observed that a fraction of L12 from *E. coli* is phosphorylated. The modified form binds more tightly to 70S. An extensive study of the phosphorylation of *E. coli* ribosomal proteins revealed that the proteins S3, S4, S5, S7, S9, S11, S12, S13, S18, S21, L2, L3, L4, L5, L9, L10, L11, L12, L13, L15, L16, L19, L20, L22, L23 and L24 are phosphorylated (Soung *et al.*, 2009). The sites of phosphorylation were identified and it was found that many of the proteins were multiply modified. It was also noticed that many proteins associated with mRNA binding were phosphorylated.

In eukaryotes, a broad range of modifications have been observed (Carroll *et al.*, 2008) and, furthermore, many of these

modifications are conserved among eukarya, suggesting that they are functionally relevant.

The Copy Number of Ribosomal Proteins

Ribosomal proteins are normally present in one copy per ribosome (Hardy, 1975). One exception is the acidic protein L12, which is found in four copies per *E. coli* ribosome. In certain bacteria, primarily the hyperthermophiles like *Thermus thermophilus*, there are six copies of L12 (Ilag *et al.*, 2005; Davydov *et al.*, 2008). In archaea, L12 is replaced by an acidic protein of the same size and unrelated sequence present in four copies per ribosome. In eukarya, different forms of proteins that are sequence-related to the acidic archaeal protein are also present in four copies per ribosome

In archaea, there are two very similar proteins, L15 and L18e. Their sequences, structures and RNA binding sites are similar due to a gene duplication (Klein *et al.*, 2004).

6.4 THE ASSEMBLY OF RIBOSOMES

It has been established that on one hand the ribosomal RNAs need some of the ribosomal proteins to be correctly folded; on the other hand, several of the ribosomal proteins cannot bind to their sites on the ribosome unless the RNA is correctly folded. Thus, there is a succession in the binding of ribosomal proteins to the rRNA. This has been explored for the ribosomal subunits. The proteins that participate in the early steps of assembly are marked in Appendix 1 (Held *et al.*, 1974; Röhl & Nierhaus, 1982). Only two proteins — S17 and L24 — of the early assembly proteins have been deleted in mutants (Dabbs *et al.*, 1983; Dabbs, 1986). All ribosomal proteins are assembled into the subunits before the latter can dock and form the 70S ribosome.

This page intentionally left blank

7

The Structure of the Ribosome

To determine the structure of the ribosome with its central role in the cell was for a long time a formidable challenge due to its large size and its lack of symmetry. Of primary interest have been the ribosomal binding sites for mRNA and tRNA molecules, the decoding site, the peptidyl transfer center, the binding sites of translation factor proteins and the large conformational transitions of the ribosome that underpin translocation of mRNA and tRNAs as well as ribosomal recycling after termination. Many different approaches have been taken to obtain detailed structures of the ribosome, its subunits and its functional complexes.

7.1 EARLY STUDIES OF THE STRUCTURE OF RIBOSOMAL SUBUNITS AND RIBOSOMES

It was early realized that in-depth understanding of mRNA translation on ribosomes would greatly benefit from detailed structural information (Watson, 1964). Ultracentrifugation studies had revealed the sedimentation behavior of the ribosome and its subunits (Petermann & Hamilton, 1952; Tissieres *et al*., 1959). Later, small angle x-ray scattering (SAXS; Serdyuk *et al*., 1970) and small angle neutron scattering (SANS) methods gave information about the radius of gyration of the ribosome and how its RNA and protein molecules are distributed in its structure (Engelman & Moore,

1972; Capel *et al*., 1987). It became evident that ribosomal RNA forms the core of the ribosomal particle (Rg = 65 Å), whereas the proteins are preferentially distributed on its surface (Rg = 102 Å).

Electron microscopy (EM) studies have provided initial outlines of the structure of the bacterial ribosome and its subunits (Lake *et al*., 1974; Lake, 1985; Tischendorf *et al*., 1974; Stöffler & Stöffler-Meilicke, 1984; Vasiliev *et al*., 1974; Spirin & Vasiliev, 1989). The small subunit has the shape of a right hand mitten (Fig. 2.3). It has features called the body, the thumb or the platform and the head, which correspond to the finger parts of the mitten. Regardless of species, this general shape seems to be universal (Lake, 1985). Subsequent cryoelectron microscopy (cryo-EM) studies using 3D reconstitution techniques have provided further structural details, some with illustrative names. Thus, the end of the ribosome's head is called the beak or the nose (Gabashvili *et al*., 2000). The upper part of the body on the side opposite to the platform is called the shoulder. The bottom part of the body has a minor protuberance called the toe or the spur. The interface side of the small subunit, i.e. the inner side of the mitten, interacts with the large subunit, whereas the opposite side is called the back or the solvent side of the small subunit.

The large subunit was early on observed to have a structure like a crown when seen from the side of the interface between the subunits. The three protuberances of the particle are called the central protuberance, the L12 stalk on the right hand side (Strycharz *et al*., 1978) and the L1 stalk on the left hand side (Lake & Strycharz, 1981; Dabbs *et al*., 1981). When seen in the perpendicular direction the particle has a hemispherical shape. The flatter surface is the interface side.

Attempts to identify the positions of individual proteins were made in the early EM studies using polyclonal antibodies specific to the different proteins (see Sec. 3.1; Lake, 1985; Stöffler & Stöffler-Meilicke, 1984). This technique is necessarily one of low resolution and the interpretation of the images has a subjective component. Nevertheless, a significant fraction of these early protein locations has subsequently been confirmed by the recent high-resolution crystal structures of the ribosome (see Table 7.1). Also at an early

Table 7.1 Selected Crystal Structures of Ribosomes or Ribosomal Subunits

Ribosome	Species	Resolution (Å)	Reference
50S	*H. marismortui*	2.4	Ban *et al.*, 2000
30S	*T. thermophilus*	3.1	Wimberley *et al.*, 2000
30S	*T. thermophilus*	3.3	Schlünzen *et al.*, 2000
70S	*T. thermophilus*	5.5	Yusupov *et al.*, 2001
50S	*D. radiodurans*	3.1	Harms *et al.*, 2001
70S	*E. coli*	3.5	Schuwirth *et al.*, 2005
70S	*T. thermophilus*	2.8	Selmer *et al.*, 2006
70S	*T. thermophilus*	3.7	Korostelev *et al.*, 2006
70S	*T. thermophilus*	3.5	Blaha *et al.*, 2009

stage, many of the ribosomal proteins appeared to be highly elongated. Even though this could not be safely established at such a low resolution, these overall shapes have more recently been validated by high-resolution crystallography.

A more objective technique used early on was based on the difference in neutron scattering between hydrogen and deuterium (see Sec. 3.1). Thus, distances between pairs of proteins, differently labeled from the rest of the small ribosomal subunit, were measured and a three-dimensional protein map of the subunit could be established (Capel *et al.*, 1987). Similar studies have been carried out on the large subunit (Willumeit *et al.*, 2001).

An early observation of specific interest is the EM identification of a tunnel penetrating the large subunit from the interface side to the external surface (Milligan & Unwin, 1986; Yonath *et al.*, 1987), which was later confirmed by cryo-EM (Frank *et al.*, 1995; Gabashvili *et al.*, 2001). This is the tunnel through which the nascent polypeptide exits the ribosome during mRNA translation (see Sec. 8.4), as further clarified by crystallographic investigations (Ban *et al.*, 2000; Schlünzen *et al.*, 2001; Voss *et al.*, 2006).

At the resolutions now achieved by cryo-EM (around 6 Å), individual rRNA helices and ribosomal proteins can be observed. Furthermore, the locations of tRNAs bound to the A, P and E sites

and translation factors have provided insights into the function and dynamics of the ribosome (see following chapters).

7.2 CRYSTAL STRUCTURES OF RIBOSOMES

Some Steps in the History of Ribosome Crystallography

Until recently, most structural work on ribosomes was carried out with blunt tools. Much of the so-gathered information was supported by other methods, but attempts to generate atomic models gave unreliable results. To crystallize whole ribosomes or even their subunits seemed like an impossible mission, not least due to the greatly heterogeneous material in the crystallization trials of the time. Thus, factors or proteins with uncertain roles in translation may adhere to the ribosomes. Furthermore, it is difficult to obtain subunits or ribosomes with a full complement of the ribosomal proteins (Hardy, 1975). In addition, translating ribosomes go through a number of conformational states, and different selections of these conformations may be trapped by different purification techniques. However, spontaneously ordered arrays of ribosomes were observed at an early stage (Morgan & Uzman, 1966; Kingsbury & Voelz, 1969; Unwin, 1977), and Milligan and Unwin (1986) were able to analyze two-dimensional ribosomal crystals of hibernating lizard oocytes.

Despite the low odds of success, Yonath started to explore the possibility of obtaining three-dimensional crystals of ribosomes or ribosomal subunits (Yonath *et al.*, 1980) from a broad range of species (Glotz *et al.*, 1987). Improvements in ribosome purification methods, crystal growth conditions and handling (Ban *et al.*, 1998; Clemons *et al.*, 2001; Gluehmann *et al.*, 2001), crystal freezing (Hope *et al.*, 1989), synchrotron equipment and methods (Hendrickson, 1991; Helliwell, 1998) have led to today's remarkably successful ribosome crystallography.

The crystallization experiments by Yonath's group initially concerned 50S subunits from a number of thermophilic bacterial species, like *Thermus thermophilus* or *Bacillus stearothermophilus*, and

the halophilic archaean *Haloarchula marismortui* (Yonath *et al*., 1980, 1982). Crystals of the 50S subunit from *H. marismortui*, prepared according to the original recipe (Shevack *et al*., 1985), eventually diffracted to a resolution of about 3 Å (von Böhlen *et al*., 1991). However, these crystals were thin and fragile, had variable cell parameters, were prone to X-ray radiation damage (Yonath *et al*., 1998; Harms *et al*., 1999) and were composed of crystallites with different orientations (twinning; Ban *et al*., 1999). All the same, this early crystallographic work was further developed to produce bigger crystals of higher quality (Ban *et al*., 2000). From these, the phase angles could be determined (see Sec. 3.2) and electron densities at resolutions of 9 Å (Ban *et al*., 1998), 5.5 Å (Ban *et al*., 1999) and finally 2.4 Å could be obtained (Ban *et al*., 2000). Already at 9 Å resolution the well-known overall shape of the large ribosomal subunit was identified along with detailed features such as double-helical RNA (Ban *et al*., 1998). Crystallographic analysis of the large subunit from *Deinococcus radiodurans* provided a structure of the 50S subunit also from a bacterial species (Harms *et al*., 2001).

Successful crystallization of 30S subunits and 70S ribosomes from *T. thermophilus* began in a Russian laboratory (Trakhanov *et al*., 1987) and was continued by the Yonath group (Glotz *et al*., 1987). The initially poor resolution was successively improved to around 3 Å (Table 7.1). One improvement was the inclusion of the heavy atom 'W-18' cluster (Tocilj *et al*., 1999). Ramakrishnan's group found that although the purified ribosomes contained protein S1, the crystals did not. Purification of S1-lacking ribosomes and introduction of the heavy atom compound osmium hexamine helped to improve the resolution (Clemons *et al*., 2001).

Crystals of the whole bacterial 70S ribosomes from *T. thermophilus* were initially at low resolution (Cate *et al*., 1999; Yusupov *et al*., 2001), but in subsequent studies of 70S ribosomes from *E. coli* and *T. thermophilus* crystals with close-to-atomic resolution have been obtained (Selmer *et al*., 2006).

The crystal structures of ribosomes and ribosomal subunits at high resolution (Table 7.1) have confirmed a number of previous hypotheses and refuted others. The information they provide has,

in conjunction with rapid kinetics techniques, molecular dynamics simulations and bioinformatics, led to a spectacular development in our understanding of the function, regulation and evolution of the ribosome.

The Small Subunit

The resolution of the structure of the small ribosomal subunit from *T. thermophilus* has increased step by step, from 5.5 Å (Clemons *et al.*, 1999) and 4.5 Å (Tocilj *et al.*, 1999) to around 3 Å (Wimberley *et al.*, 2000; Schlünzen *et al.*, 2000). The subunit structure confirms previous observations with EM and cryo-EM. All proteins in the small subunit except for ribosomal protein S1, absent in some species, have been located in the crystal structures. The location of S1 is, however, known from cryo-EM (Sengupta *et al.*, 2001). THX, a small basic polypeptide present in *T. thermophilus* but not in most other bacteria (Choli *et al.*, 1993), has also been observed in the crystal structure (Schlünzen *et al.*, 2000; Brodersen *et al.*, 2002).

The roughly globular domains of the 16S rRNA appear in separate regions of the small ribosomal subunit (Plate 6.1C). The 5′ domain is located in the body, the central domain in the platform and the 3′ major domain in the head of the small subunit (Plate 6.1C). The 3′ minor domain runs as a long helix (h44) from the region between the head and the body down to the bottom of the subunit. Helix h28 is the main contact link between the head and the body of the subunit. As observed also with other methods (Gabashvili *et al.*, 1999), this domain organization imparts a flexibility to the small subunit that is essential for its function (Ogle *et al.*, 2003).

The ribosomal proteins in the 30S subunit are clearly discerned in the electron density, and their structures have been determined. The interface side of the 30S subunit has few proteins, as previously deduced from tritium bombardment experiments (Yusupov & Spirin, 1986), and most proteins are located on the exterior side (Wimberley *et al.*, 2000; Schlünzen *et al.*, 2000). When comparisons have been made, the *in situ* structures of the 30S subunit proteins

are similar to those of the isolated proteins (Schlünzen *et al*., 2000; Brodersen *et al.,* 2002).

The small subunit binds to the mRNA and is actively engaged in its decoding by tRNAs. From structural and biochemical data, the binding sites for A- and P-site tRNAs have been characterized. Interestingly, a part of one subunit involved in the crystal packing (the spur or h6) mimics the anticodon of the P-site tRNA and interacts with the 3′ part of the 16S RNA as with an mRNA (Carter *et al*., 2000). The decoding site is closely associated with the top of the penultimate helix (h44) of the 16S RNA (Wimberley *et al*., 2000; Carter *et al*., 2000; Schlünzen *et al*., 2000).

The mechanism of decoding has been studied using fragments of the anticodon stem–loop (ASL) structure of a tRNA bound to the small subunit (Ogle *et al*., 2001, 2002). The ribosomal RNA interacts with the base pairing of tRNA and mRNA to distinguish cognate from near-cognate codons (see Chaps. 9 and 11). Furthermore, the presence of an ASL cognate to the mRNA triplet (codon) exposed in the A site induces a conformational closure of the small subunit (Ogle *et al*., 2002). It involves a rotation of the head of the small subunit toward the shoulder and subunit interface. The shoulder moves toward the subunit interface and h44. When, in contrast, the ASL–codon contact is near-cognate, i.e. one out of three base pairs is mismatched, the 30S subunit closure does not occur. However, in the presence of the antibiotic paramomycin also a near-cognate ASL–codon interaction induces the 30S subunit closure (see Chaps. 9–11).

The Large Subunit

The structure of the large (50S) ribosomal subunit has been clarified by crystallography (Ban *et al*., 2000; Harms *et al*., 2001; Klein *et al*., 2004). At low or moderate resolution the crystal structures (Ban *et al*., 1998, 1999) appeared similar to previous cryo-EM structures (Frank *et al*., 1995; Agrawal *et al*., 1996; Stark *et al*., 1997). At higher resolution, the low electron density of the two side protuberances, L1 and the L12 stalk, prevents unambiguous interpretation.

Subsequent studies have shed more light on these functionally important components (Yusupov *et al*., 2001; Diaconu *et al*., 2005; Selmer *et al*., 2006; Blaha *et al*., 2009; Jenner *et al*., 2010): they are stabilized by translational factors and can be seen in factor-containing functional complexes of the ribosome (see Chap. 9). Another flexible extension from the body of the large subunit is the A-site finger (ASF; Frank *et al*., 1995) composed of helix H38. Evidently, the two ribosomal subunits have different types of flexibility. The small subunit has interdomain flexibility, whereas in the large subunit the protuberances are mobile.

The six domains of the 23S RNA, identified from the analysis of its secondary structures, are thoroughly interwoven (Plate 6.1D; Ban *et al*., 2000; Harms *et al*., 2001). Therefore the core of the large subunit is stable, whereas the small subunit has a flexible core. The 5S RNA, located in the central protuberance of the large subunit, appears like a seventh domain of the 23S rRNA in the large subunit. On average, a large subunit protein contacts twice as many RNA domains as a small subunit protein (Klein *et al*., 2004). As in the small subunit, most of the proteins in the large subunit are located on the external surface while there are few proteins in the intersubunit interface (Ban *et al*., 2000; Harms *et al*., 2001). Two regions of the large subunit are particularly rich in proteins: the region binding the translational GTPase factors (trGTPases; L3, L6, L11, L10, L12, L13, L14) and the external side of the polypeptide exit tunnel (L19e; L22, L23, L24, L29, L31e; Klein *et al*., 2004).

Like in the small subunit, several proteins have small, globular and stable *in situ* structures similar to those of the corresponding proteins free in solution. However, a significant number of large subunit proteins have multiple domains or long extensions at their N or C termini, or sometimes long internal loops (see Sec. 7.3 and App. II; Ban *et al*., 2000; Harms *et al*., 2001; Klein *et al*., 2004).

The major function of the large subunit is to catalyze peptidyl transfer during protein elongation. This is done in the peptidyl transfer center (PTC). Here the acceptor ends of the tRNAs are stably bound close to each other, with the nascent peptide on the P-site tRNA and the incoming amino acid on the A-site tRNA.

The PTC was identified with the aid of previous biochemical observations (Ban *et al.*, 2000; Nissen *et al.*, 2000; Harms *et al.*, 2001; Schlünzen *et al.*, 2001). That is to say, nucleotides of the 23S RNA known to be important for binding of the A- and P-site tRNAs were identified in a groove across the interface side of the subunit. Furthermore, antibiotics, different types of tRNA fragments or other peptidyl transfer inhibitors contributed to the identification of the PTC in the crystal structure of the 50S subunit (Nissen *et al.*, 2000). The tunnel from the PTC at the interface side of the 50S subunit to the external side observed earlier now became distinct. The width of the tunnel is large enough to allow penetration of a nascent peptide from its entry near the PTC to its exit at the other end of the subunit. Some macrolide antibiotics, like erythromycin, bind near the peptide entry, thereby preventing synthesis of peptides longer than a few amino acid residues (see Sec. 10.5).

The 70S Ribosome

Structures of the complete bacterial ribosome provide functional insights that cannot be obtained from structures of the isolated ribosomal subunits. Ribosome function often requires a dynamic interplay between the subunits, and some subunit parts attain their proper structures only in the complete 70S ribosome. Early crystal structures of the bacterial ribosome (Cate *et al.*, 1999; Yusupov *et al.*, 2001; Schuwirth *et al.*, 2005; Korostelev *et al.*, 2006) have later been complemented with 70S structures of higher resolution and in functional complexes (Selmer *et al.*, 2006; Schmeing *et al.*, 2009, Gao *et al.*, 2009; Voorhees *et al.*, 2010; Jenner *et al.*, 2010). Resolution improvement has, for example, led to correct positioning of the unstructured protein L31 as an inter-subunit bridge and a new location of protein L28 (Selmer *et al.*, 2006). A remarkable finding is that the N terminus of protein L27 is very close to the acceptor ends of the A- and P-site tRNAs, suggesting a role for this protein in the peptidyl transfer reaction (Voorhees *et al.*, 2009; see further below), previously suggested to be catalyzed by RNA alone (Nissen *et al.*, 2000; Schmeing *et al.*, 2005).

It is essential for ribosome function that the two subunits can rotate in relation to each other in a ratchet-like movement (Chap. 8). The relative orientation of the two subunits in the unrotated conformation of the 70S ribosome (Gabashvili, 2000) has been clarified and the inter-subunit bridges localized (Fig. 7.1 and Plate 7.1).

The locations of the mRNA with the tRNA molecules in the A, P and the E sites are identified (Agrawal *et al.*, 1996; Stark *et al.*, 1997; Yusupova *et al.*, 2001; Jenner *et al.*, 2005; Yusupova *et al.*, 2006; Selmer *et al.*, 2006; Schmeing *et al.*, 2009; Gao *et al.*, 2009; Jenner *et al.*, 2010). The structure of the complete 70S ribosome reveals how the shape and length of the tRNA molecule precisely fit the distance between the decoding site on the small subunit and the PTC on the large subunit. Indeed, all the main activities of the ribosome occur at the subunit interface.

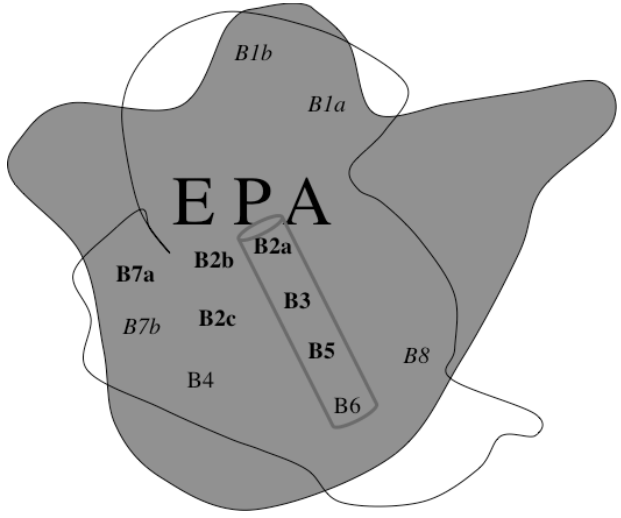

Fig. 7.1 The approximate locations of the inter-subunit bridges (see Plate 7.1 and Table 7.2). Helix h44 is shown as a cylinder. Bridges are maintained (shown in bold) or break (shown in italics) during the ratchet-like movement.

The RNA parts of the ribosome have many cavities that contain one or several water molecules (Voss *et al.*, 2006). Most of these water molecules can diffuse freely in and out of the ribosome, in contrast to water molecules trapped in a limited number of cavities in protein structures (Voss *et al.*, 2006). Although the grooves of the rRNA make the ribosome "wet," its stabilization by the secondary and tertiary structure of the rRNA prevents it from becoming spongelike and flexible.

7.3 THE INTER-SUBUNIT BRIDGES

The subunit interface, where inter-subunit bridges hold the subunits together, is essential for ribosome function. The subunits associate during initiation of protein synthesis and dissociate during ribosomal recycling after termination of peptide synthesis (Chap. 11). They also rotate in relation to each other in crucial steps of protein elongation. Since, furthermore, major functional sites are at the interface, essential dynamic properties of the ribosome depend on the formation, stability and breakage of inter-subunit bridges. These were first analyzed in the cryo-EM maps (Frank *et al.*, 1995; Gabashvili *et al.*, 2000) and subsequently in the crystallographic structures of the 70S ribosome (Cate *et al.*, 1999; Yusupov *et al.*, 2001; Selmer *et al.*, 2006; Jenner *et al.*, 2010; Dunkle *et al.*, 2011). Initially, the visible components of these bridges could not be identified. Currently, 14 inter-subunit bridges have been identified in *T. thermophilus* (Fig. 7.1; Plate 7.1). They were named B1–B8, but now we know that B1, B2, B6, B7 and B8 each contain several neighboring bridges (Table 7.2). Similar sets of bridges have been identified in *E. coli* and yeast (Gao *et al.*, 2003; Spahn *et al.*, 2001; Schuwirth *et al.*, 2005). A full consensus about the number of bridges and the residues involved has not yet been reached. Inter-subunit bridges provide a solvent-inaccessible area of more than 6000 $Å^2$ (Schuwirth *et al.*, 2005). Some of these bridges are mediated by ions, presumably Mg^{2+}, whereas water molecules mediate other bridges. Several of the bridge contacts are due to proteins in

Table 7.2 Inter-subunit Bridges as seen in *E. coli and T. thermophilus* 70S ribosomes (Yusupov *et al.*, 2001; Gao *et al.*, 2003; Schuwirth *et al.*, 2005; Korostelev *et al.*, 2006; Selmer et al., 2006; Agirrezabala *et al.*, 2008; Jenner *et al.*, 2010; Jin *et al.*, 2011; Zhou *et al.*, 2012). RNA helices from the small subunit are denoted "h" and those from the large subunit are denoted "H"

Bridge	Unrotated State				Rotated State				Comment
	30S Subunit		50S Subunit		30S Subunit		50S Subunit		
		Residues		Residues	Residues		Residues		
B1a	S13	92–94	H38	886–888	Bridge broken				A-site finger,
B1b	S13	2, 6, 8	L5	134, 141–3	Bridge altered				Weak contact that gets stronger.
					S19	63–71, 75–81	L5	109–114	
New	S13	50–73	L31	32–59					Flexible interactions.
	S19	6–9, 40–43, 64–68	L31	55–70					
B2a	h44	1492–1495	H69	1911–1918,	Bridge deformed				A1913 of H69 penetrates the
		1407–1410		1914–1917					minor grove of h44. A1492 and
	h45	1517		1919					A1493 of h44 interact with the codon-anticodon helix.
B2b	h24	794	H69	1922					
	h45	1516–1519	H69	1919–1920					
B2c	h24	770	H57	1468					Mg^{2+} mediated contact. Conserved.
	h24	770–771	H67	1832–1833					
	h27	899–900							
B3	h44	1417–1418	H71	1958–1959					Large minor groove surface complementarity.
		1482–1483		1947–1948					At the pivot point for subunit ratcheting, conserved.

(*Continued*)

Table 7.2 (*Continued*)

Bridge	Unrotated State				Rotated State		Comment
	30S Subunit		50S Subunit		30S Subunit	50S Subunit	
		Residues		Residues	Residues	Residues	
B4	S15	H53, L56, V60, R64	H34	715	Bridge deformed		H34 bends 12° at rotation.
	S15	R88, G89	H34	714, 716			Mg^{2+} mediated contact
B5	h44	1423	L14	R49			
	h44	1421	L14	E54			Mg^{2+} stabilised
			H71	1950, 1951			
	h44	1475	H62	1689			Mg^{2+} stabilized
			H64	1767			
B6	h44	1429–1430	H62	1703, 1704			Water-mediated
	h44	1432	L19	R108			
		1463	L19	R111			
New	h44	1442	L19	R118			Seen only in *T. thermophilus*
B7a	h23	702	H68	1846, 1848	h23 702	H68 1847 PO_4	Bridge is weakened
		698	H68	1849, 1896			A-minor motif.
B7b					h23 712–713	L2 162–164 172–174 177–178	
					713	Q164, Q168	
B7c					h24 773–776	L2 177–178, 198–202	
B8	h14	338–339	L14	R97	Bridge maintained		
	h14	345–347	L14	V115, S116, A118			Mg^{2+} stabilized
	h14		L19	K35, E36			Mg^{2+} stabilized

one subunit interacting with the rRNA of the other subunit (Table 7.2). The high degree of interspecies conservation among inter-subunit bridges highlights their functional importance (Gao *et al*., 2003; Schuwirth *et al*., 2005).

A 16S rRNA component of central importance for mRNA decoding by tRNA, helix h44, is at the subunit interface. It spans the whole body of the small subunit and makes several contacts with the large subunit as part of the bridges B2a, B3, B5 and B6 at subsequent turns of the double helix (Cate *et al*., 1999; Yusupov *et al*., 2001; Selmer *et al*., 2006).

In the ratchet-like motion of the subunits at translocation of mRNA and tRNA, class 1 release factor recycling by the GTPase RF3 (Gao *et al*., 2007) and ribosomal recycling by RRF and EF-G (Agirrezabala & Frank, 2009), the pivot point is situated close to bridge B3. Bridges close to the rotation axis (B2a–c, B3, B5 and B7a) are maintained at ribosomal ratcheting. Bridges at the periphery (B1a–b, B7b and B8) are rearranged or disrupted (Woese, 1970; Frank & Agrawal, 2000; Gao *et al*., 2003; Noller, 2008).

B1

The B1 bridges, connecting the head of the small subunit with the central protuberance of the large subunit in MSI, break during the ratchet-like motion. Bridge B1a is a contact between the A-site finger (ASF) or helix H38 and protein S13, and is situated above the A and P sites (Yusupov *et al*., 2001). B1a changes its interaction partner to S19 during the ratcheting process (Valle *et al*., 2003). Experiments with shortening of ASF suggest that B1a is not important for the stability of the 70S ribosome complex, but for attenuation of the frequency of +1 frame shifts in translocation. At rate-limiting concentration of EF-G, deletion of H38 increases the rate of translocation, suggesting that the accuracy and speed of translocation are negatively correlated (Komoda *et al*., 2006).

B1b/B1c, promoting a week inter-subunit contact, consists of proteins S13 and S19 in the head of the small subunit and protein L5 in the central protuberance of the large subunit (Yusupov *et al*.,

2001). Proteins S13 and S19 form a loose heterodimer that is engaged not only in bridge B1b/B1c with protein L5 but also in a newly observed bridge with protein L31 (Jenner *et al.*, 2010).

B2a

Bridge B2a connects the universally conserved helix H69 of the large subunit with helices h44 and h45 of the small subunit at the decoding site. It is located just below the D stems of the A- and P-site tRNAs (Plate 7.1; Gabashvili *et al.*, 2000; Yusupov *et al.*, 2001; Schuwirth *et al.*, 2005). A1913 of H69 extends into a pocket formed by h44 and A-site tRNA, and interacts with both A1492 of h44 and the ribose of nucleotide 37 of the A-site tRNA (Selmer *et al.*, 2006). A hydrogen bond is formed in the decoding center between N1 of A1913 and the 2′-OH of residue 37 of the A-site tRNA (Selmer *et al.*, 2006). In addition, a magnesium ion bridges the ribose of A1913 with the phosphate of residue 38 of the tRNA (Selmer *et al.*, 2006). This important bridge could provide a signaling pathway between the peptidyl transfer and decoding regions (Rodnina *et al.*, 2002; Bashan *et al.*, 2003; Spahn *et al.*, 2004; Cochella & Green, 2005; Frank *et al.*, 2005; Selmer *et al.*, 2006). Bridge B2a is flexible and is seen in different orientations in different structures (Harms *et al.*, 2001; Yusupov *et al.*, 2001; Shuwirth *et al.*, 2005; Selmer *et al.*, 2006; Agirrezabala *et al.*, 2008; Jenner *et al.*, 2010).

H69 is involved in the binding of RRF to the ribosome and moves upon binding of domain I of RRF (Lancaster *et al.*, 2002; Agrawal *et al.*, 2004; Wilson *et al.*, 2005; Pai *et al.*, 2008). In addition, domain IV of EF-G interacts with B2a (Gao *et al.*, 2007). Modification of nucleotides in the loop of H69 makes the subunit interaction weaker (Maivali & Remme, 2004; Gutsell *et al.*, 2005; Hirabayashi *et al.*, 2006). Deletion of H69 is dominantly lethal and greatly weakens the inter-subunit interaction, but ribosomes lacking H69 are surprisingly active *in vitro*. The H69 deletion greatly inhibits RF1-dependent peptide release and allows rapid ribosomal recycling also in the absence of the recycling factor RRF (Ali

et al., 2006). The latter observation suggests that during recycling RRF is required to break bridge B2a in the wild-type ribosome, but not in the H69 deletion mutant, where this bridge is absent.

7.4 THE STRUCTURES OF THE RIBOSOMAL RNA MOLECULES

The crystallographic structures of the ribosome (Table 7.1) have provided detailed information about the secondary, tertiary and quaternary structures of the ribosomal RNAs (rRNAs). They form the core of both ribosomal subunits and vary greatly in size, but they all have a common minimal structure (Gerbi, 1996; see also Plate 6.2). The idiosyncratic extensions of the minimal structures primarily occur on the external side, showing that the interface region is more highly conserved (Ban *et al.*, 2000). Likewise, the side with the platform is most conserved while the side with the shoulder is much less conserved (Kumar *et al.*, 2006).

The secondary structures are primarily based on double-stranded helices, but also on turns, bulges and kinks (Moore, 1999; Westhof & Fritsch, 2000). All previously known RNA motifs have been observed in the rRNAs (Moore & Steitz, 2003b), but they have also provided new motifs. One striking example is a new internal asymmetric loop called the kink-turn or K-turn (Klein *et al.*, 2001), often associated with binding of proteins (see below). Another example is the G-ribo motif (Steinberg & Boutorine, 2007), in which two RNA helices in side-by-side orientation are connected by a short unpaired region, where the ribose from one helix packs with the ribose and minor groove edge of a guanosine from the other helix. The eight G-ribo motifs found in ribosomes are highly conserved (Steinberg & Boutorine, 2007).

Of the 45 helices in the secondary structure of the 16S rRNA, 36 are coaxially stacked (Wimberley *et al.*, 2000). Helix h44 contains around 100 residues and spans the interface side of the body domain of the small subunit. A majority of the helices in this domain are approximately parallel with h44 and greatly elongated due to coaxial stacking.

The 23S rRNA of *H. marismortui* contains 2923 nucleotides. Of these, 1157 are in van der Waals contacts with proteins, and there are only 10 stretches of 23S rRNA extending beyond 20 nucleotides without protein contact. The longest such stretch has 47 nucleotides and forms the ridge of the peptidyl transfer cleft in domain IV of 23S rRNA cleft (Ban *et al*., 2000).

In the structure of the *H. marismortui* large subunit, two classes of conserved rRNA sequences were identified. One class is associated with binding sites for tRNAs and translational protein factors. In the other class, involved in tertiary or quaternary structure interactions within or between the domains of rRNA molecules, the adenosines are overrepresented (Ban *et al*., 2000) by the frequent occurrence of the 'A-minor motif.' Here, two or more stacked adenosines dock into the minor groove of adjacent RNA helices and make it wider than in their regular A form (Nissen *et al*., 2001; Moore & Steitz, 2003b). The adenines involved in these interactions participate in cross-strand base-stacking interactions stabilized by sugar and base-hydrogen bonds (Wimberley *et al*., 2000; Nissen *et al*., 2001). The A-minor motif is important for central functions of the ribosome. For instance, adenines 1492 and 1493 of the small subunit interact with the first two codon–anticodon base pairs in an A-minor motif (Ramakrishnan, 2002). Likewise, A76 of the A-site tRNA interacts through an A-minor motif with G2583 of the 23S RNA (Nissen *et al*., 2001; Voorhees *et al*., 2009).

7.5 THE STRUCTURES OF RIBOSOMAL PROTEINS

In the early attempts to obtain structural information about the ribosome, the focus was on the ribosomal proteins (r-proteins). These were more accessible than rRNA and it was generally believed that they carried out the main functions of the ribosome. Nuclear magnetic resonance (NMR) and X-ray diffraction were first used to obtain the structures of r-proteins in isolation, but the focus gradually shifted to r-proteins in complex with rRNA fragments.

One problem in these early studies was how to avoid denaturation during r-protein purification. Even when this difficulty was resolved (Liljas & Kurland, 1976; Liljas *et al.*, 1978; Dijk & Littlechild *et al.*, 1979), many proteins were unstable in the presence of proteolytic enzyme, at elevated temperatures, or lacked distinct secondary structure (Tumanova *et al.*, 1983). Proteins from thermophilic ribosomes and the possibility of heterologous protein expression improved the situation. Despite some success, ribosomal proteins in isolation have remained more difficult to handle and crystallize than normal globular proteins.

Free solution structures have been obtained with crystallography or NMR for less than half of the r-proteins. Most of these structures turned out to be globular with L9 (Hoffmann *et al.*, 1996) and L12 (Bocharov *et al.*, 2004), composed of several domains held together by flexible linkers, as exceptional cases.

Elucidation of the structures of the ribosomal subunits has now provided the structures of essentially all bacterial r-proteins and most archaeal r-proteins from the large subunit (Table 7.1). When proteins from the bacterium *T. thermophilus* are discussed, the letter T is put in front of the protein name (e.g. TS4). Likewise, the letters D, E and H represent proteins from the bacteria *D. radiodurans, E. coli* and the archaean *H. marismortui*, respectively.

The globular structures obtained from r-proteins in isolation could easily be fitted into the ribosomal subunit structures. It is now possible to understand why the other types of structures had been hard to determine for r-proteins in isolation. For these, the globular domains have long extensions or tails unlikely to have stable conformations in isolation (App. 2; Fig. 7.2; Ban *et al.*, 2000; Brodersen *et al.*, 2002; Klein *et al.*, 2004; Selmer *et al.*, 2006). Some of these proteins even lack any type of internal fold. Their organization is reminiscent of the protein–nucleic-acid interactions of histones or viral proteins (Liljas, 1986; Rossmann & Johnson, 1989; Luger & Richmond, 1998). From amino acid sequence and mild proteolysis, this type of proteins was predicted to be found also in the ribosome (Liljas, 1991).

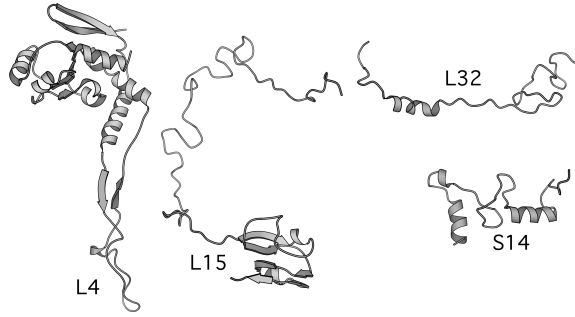

Fig. 7.2 Some ribosomal proteins with extended structures. (Reprinted with permission from Liljas *et al*., 2009, *Textbook of Structural Biology*.)

The r-proteins generally have their globular parts exposed on the outside of the ribosome, while their tails or long loops penetrate the interior subunit parts (Ramakrishnan & Moore, 2001). In addition, there is a dramatic charge separation of the r-proteins *in situ*. The surface parts are more acidic, while the inner parts are highly basic, neutralizing the negative charges of the RNA (Klein *et al*., 2004). The extensions are unusually rich in arginine, lysine and glycine, and are invariably in extensive contact with the RNA.

Relationships between Ribosomal Proteins

The relationship between r-proteins from the three domains (bacteria, archaea and eukarya) has been analyzed (see Appendix I). It is also continuously updated in a database (Bairoch; http://www.expasy.org/cgi-bin/lists?ribosomp.txt) and analyzed in the literature (Lecompte *et al*., 2002; Harris *et al*., 2003). With the structures of the *H. marismortui* and *D. radiodurans* 50S subunits, the relationship of L16 with L10e was identified from their fold and identity of position in the subunit (Harms *et al*., 2001, 2002). Other proteins, apparently replacing each other in the same location, have very different folds (Table 7.3).

A number of r-proteins were found to have related structures (Table 7.4). This is also the case for domains of translation factors

and may suggest evolutionary connections (Ramakrishnan & White, 1998; Draper & Reynaldo, 1999; Liljas *et al.*, 2000).

Klein *et al.* (2004) classified, the large subunit proteins into six groups: the antiparallel α+β group, the β barrel group, the α-helical group, the mixed α+β group, the zinc-containing group and the L15 group. This broad classification places proteins with similar motifs in the same group, but allows great overall structural variation among its members. It is expected that evolutionarily related proteins will appear in the same group. One example is the RNA recognition motif (RRM). This is composed of alternating β strands and α helices in a pattern called split β–α–β. Sometimes the motif

Table 7.3 Fold and Positional Relationship of Bacterial and Archaeal Proteins from the Large Subunit (Ban *et al.*, 2000; Harms *et al.*, 2001; Klein *et al.*, 2004; Mushegian, 2005; Selmer *et al.*, 2006; Korostelev & Noller, 2007; Roberts *et al.*, 2008; Rabl *et al.*, 2011)

Bacteria	Archaea/ Eukaryotes	Type of Relationship
Fold and position		
L15	L18e	Gene duplication. Related sequences, structure and similar binding sites on the 23S RNA. Archaea and eukaryotes have both proteins.
L16	L10e	Paralogues. Similar sequence, structure and position at A-site tRNA.
L33	L44e	Similar fold and position of the globular domain. Circularly permuted amino acid sequences?
	L28	Occupies part of the space of the extended part of L44e.

(*Continued*)

Table 7.3 (*Continued*)

Bacteria	Archaea/ Eukaryotes	Type of Relationship
Position only		
S4	S30e	Protein S4 is replaced by S30e.
S6, S18	S1e	C-terminal domain of S1e resembles S6 but is shifted in position.
S20	S4e, S6e, S8e	Three eukaryote proteins and RNA extension segments ES3 and ES6E fill part of the space of S20.
L17	L31e	Interact with the same parts of 23S RNA. At the end of the exit tunnel.
L19	L24e	Both form interprotein β sheets with L14 at inter-subunit bridge B6.
L20, L21	L32e	Loops of L20 and L21 occupy the same space as the loop of L32e. All interact with helix H46.
L23	L39e	L39e in *Hm* replaces the tail of bacterial L23.
L27	L21e	Interact with the same parts of 23S RNA. The tails have different orientations and interactions.
L28	L15e	Interact with the same parts of 23S RNA.
L34	L37e	Interact with the same parts of 23S RNA.
Similar structure		
L36	L40e	Similar structure. L40e would fit in an empty place in *Hm* where L36 is situated in *Dr*.
S12e	L7Ae	Similar structures.

Table 7.4 Classification of Ribosomal Proteins (Klein *et al.*, 2004; Selmer *et al.*, 2006; Wu *et al.*, 2008; Jenner *et al.*, 2010; Rabl *et al.*, 2011)

α-helical	S2, S4, S13, S14, S15, S18, S20, L12, L29, L19e, L39e
Antiparallel α+β, split β–α–β	S6, S8, S10, L1, L5, L6, L9, L12, L16, L22, L23, L30, L15e, L31e
Mixed α+β group	S3, S4, S5, S7, S9, S16, S19, L1, L3, L4, L5, L13, L7Ae, L32e
β meander	S3, S5, S11, L18
β barrel	L3, L14, L25
OB fold	S1, S12, S17, L2
SH3-like	L2, L24, L21e
Zinc-binding	S4, S26e, S27e, S29e, S31e, L31, L32, L36, L24e, L40e
Rubredoxin-like	L37Ae, L37e, L44e
L15 group	L15, L18e
Homeodomain	L11
Lack of tertiary structure	S14, THX

is repeated and becomes a double split β–α–β (Leijonmarck *et al.*, 1988; Orengo & Thornton, 1993; Brodersen *et al.*, 2002). This motif is found in the antiparallel α+β group, where quite a number of ribosomal proteins have a single or double split β–α–β (Table 7.4).

L2, L21e and L24 have similar folds, like the SH3 β barrel (Klein *et al.*, 2004). One domain of L3 is a β barrel similar to the conserved domain II in the trGTPase factors. The L15 group is in archaea composed of proteins L15 and L18e (Klein *et al.*, 2004), but in bacteria only of L15. Proteins L15 and L18e have sequence homology and are structurally related. They are neighbors and bind in similar ways to the 23S RNA. They have evolved after a gene duplication of L18e, which occurred before the separation of the three domains of life (Roberts *et al.*, 2008).

Another repeatedly occurring motif or fold is the oligonucleotide-binding or OB fold. This motif is composed of a five-stranded antiparallel β sheet (Murzin, 1993; Agrawal & Kishan, 2003). Protein S1 has six consecutive OB fold domains (see below).

One type of protein structure, often associated with nucleic acid interactions, is the zinc finger (Klug & Schwabe, 1995). The r-proteins provide several examples of such zinc fingers. Thus, somewhat unexpectedly, the ribosome is the binding site for a number of zinc ions in addition to magnesium and monovalent metal ions.

Protein–RNA Interactions

With few exceptions, all r-proteins interact with the ribosomal RNA. Except for the two protuberances of the large subunit, the r-proteins do not extend beyond the envelope defined by the rRNA (Ban *et al.*, 2000; Moore & Steitz, 2003b). Thus, ribosomes are very different from viruses, where proteins form a shell around the nucleic acid, and from nucleosomes, where the proteins form the core.

The kink-turn or K-turn is an RNA feature that is frequently associated with protein binding (Klein *et al.*, 2001; Plate 7.2). Here a so-called canonical stem, composed of two Watson–Crick base pairs, is followed by an internal loop and a noncanonical stem, typically starting with two non-Watson–Crick base pairs. The angle between the two stems is around 120°. The K-turn occurs six times in *H. marismortui* 23S rRNA and twice in *T. thermophilus* 16S rRNA. Nine proteins from the large subunit and two from the small subunit bind to RNA by such kinks. There is otherwise no systematic way that these proteins interact with the RNA, and their folds also differ significantly (Klein *et al.*, 2001).

Few general principles for the protein–RNA interaction have been identified except for charge neutralization, which is an essential component. There are distinct differences in the way that the globular domains and the tails or loops interact with the RNA (Moore & Steitz, 2003b; Klein *et al.*, 2004). The globular parts are normally located on the surface of the subunits, while the tails or loops bridge and fill the gaps between the different parts of the rRNA. The generally highly basic ribosomal proteins are frequently more acidic at the exterior of their globular domains, while the positive charges are located on the parts facing into the

ribosomal structure where they neutralize the negative charges of the rRNA. In fact, despite being a limited part of the protein component, the tails contribute in a major way to the interactions with the RNA.

Klein *et al.* (2004) thoroughly analyzed how ribosomal proteins from the large subunit of *H. marismortui* interact with its rRNA. The proteins that interact with the 5S RNA are L5, L18, L21e, L10e and L30. In bacteria, protein L25 with its three different versions (see below) should be added. In bacteria L10e corresponds to L16, and L21e in *H. marismortui* partly overlaps with L27 in bacteria. Whereas the tail of L27 interacts with A- and P-site tRNA in the PTC area, the tail of L21e has a different orientation (Harms *et al.*, 2001; Table 7.3). All other proteins except L12 interact with the 23S RNA.

There are at least four different main ways proteins interact with RNA: with the edges of bases exposed in the minor groove; in widened major grooves of RNA helices; with flipped-out bases or bulged nucleotides; with insertion of amino acid side chains into hydrophobic crevices between exposed nucleotide bases. Protein domains with similar structures can interact with the RNA in very different ways. Most of the interactions in the minor groove are with the 2-amino group of guanines in Watson–Crick base pairs. The interactions in widened regions of the normally narrow major groove are frequently with Watson–Crick, wobble or noncanonical base pairs. The extended tails are narrow enough to interact with such major grooves. Generally, extended portions of the proteins interact with the RNA.

The folding of the ribosomal subunits must occur in a complex assembly landscape (Talkington *et al.*, 2005). While magnesium ions can stabilize the secondary structure of RNA, proteins are needed for the long-range contacts (Moazed *et al.*, 1986). The proteins that bind early in the assembly of the ribosome must bind to and organize different pieces of the rRNA, maybe from different domains. A folded part of a protein can identify features of a contiguous piece of ribosomal RNA. Subsequently extended parts of the protein can associate with nearby or remote parts of the

rRNA. It is unlikely that an unfolded protein can interact specifically with unfolded RNA. Likewise, it is unlikely that a protein tail can thread itself into prefolded RNA (Moore & Steitz, 2003b; Klein *et al.*, 2004). Tails or loops or proteins without any tertiary structure would generally need to associate with partly folded parts of RNA and assist in bringing separated regions together.

The primary binders of the small subunit (S4, S7, S8, S15, S17, S20; Nomura, 1973) are globular proteins (Brodersen *et al.*, 2002). It seems intuitively evident that they, essentially being rRNA chaperones, must have a preformed structure to be able to do their job. Protein S15 has no flexible extension, whereas protein S14 has no tertiary structure (App. II). In agreement with the above description, S15 binds early, but S14 late in subunit assembly (Held *et al.*, 1974).

Many of the large subunit proteins interact with several domains of the 23S RNA (Moore & Steitz, 2003b). One extreme case is L22. It has a long extended loop that interacts with all six domains of the 23S RNA (Ban *et al.*, 2000; Schlünzen *et al.*, 2001). Several of the primary binders in the large subunit, like L2, L3, L4 and L31, have several long tails or loops (App. II; Klein *et al.*, 2004). The protein that may be most crucial for large subunit assembly is L24, which interacts only with domain I of 23S rRNA. The binding of L24 may prepare domain I for the binding of proteins L4, L22 and L29, which interact with other domains (Klein *et al.*, 2004). L3 is another protein important for the early assembly of the large subunit. Its globular domain interacts only with domain VI, while its extensions interact with all other domains except domain I. A number of additional proteins depend on the previous binding of L3.

Some Specific Proteins

S1

S1 is a protein that is present in almost all gram-negative bacteria and absent in many gram-positive bacteria (see App. 1). In *Bacillus subtilis* there is a truncated form of S1, unable to bind to the ribosome (Sorokin *et al.*, 1995). Its function is unknown. A smaller

version of S1 is also found in chloroplasts (Franzetti *et al*., 1992) but otherwise S1 is absent in eukaryotic cells. The function of S1 is to melt secondary structures at the 5′-end of mRNAs (Qu *et al*., 2012).

S1 is the largest protein in bacterial ribosomes, with a molecular weight of 61 kDa and high affinity for mRNA (Draper & von Hippel, 1978). It has a sixfold repeated domain structure, D1–D6, the OB fold, with about 70 amino acid residues in each domain (Subramanian, 1983). Repeated domain structures (D1–Dn) have been found as single or repeated domains in several RNA-binding proteins (Bycroft *et al*., 1997). One protein with a single S1 domain is bacterial initiation factor IF1 (see Fig. 9.8; Sette *et al*., 1997; Battiste *et al*., 2000). S1 is composed of two regions. The N-terminal region (D1–D2) promotes association of S1 with the small subunit, while domains D3–D6 promote mRNA binding with the small subunit.

S1 has been thought of as an elongated protein (Giri & Subramanian, 1977; Laughrea & Moore, 1977). The structural organization of the protein has been observed by cryo-EM (Sengupta *et al*., 2001). At 11.5 Å resolution, S1 has a central globular unit with two extensions and two holes. S1 from *T. thermophilus* in isolation appears compact and globular (Selivanova *et al*., 2003). NMR and SAXS experiments suggest that D4 and D5 stay attached to each other both with and without bound RNA whereas D3 is free or weakly binding to D4 (Aliprandi *et al*., 2008).

On the 30S subunit, S1 is located on the interface side and in the neck region between the head and the platform. This location coincides with the upstream part of the mRNA involved in the SD interaction. S1 is also one of the subunits of the Qβ replicase (Berestowskaya *et al*., 1988).

S4

Protein S4 has three properties, which have attracted attention since the early days of ribosome research: it controls translation of a specific polycistronic mRNA, participates in the first steps of small subunit assembly, and tunes the accuracy of tRNA recognition by the mRNA programmed ribosome.

S4 exists in all kingdoms of life, but has so far not been found in mitochondria (see App. II). It has a globular structure of three domains and lacks extended tails or loops (Davies *et al*., 1998; Markus *et al*., 1998). The N-terminal 40 residues form a zinc finger, where four cysteine residues bind a zinc ion (Brodersen *et al*., 2002).

S4 controls the expression of the α operon encoding S4, the α subunit of RNA polymerase and r-protein S17 in *E. coli* (Yates *et al*., 1980). The mRNA binding site of S4 resembles its 16S rRNA binding site (Nomura *et al*., 1980). When present in excess over 16S rRNA in the cell S4 autorepresses its own expression, thereby synchronizing the synthesis of S4 and S17 and, ultimately, of the 70S ribosome with the synthesis of the α subunit of RNA polymerase.

S4 is important for the assembly of the small ribosomal subunit (Held *et al*., 1974). Together with S7 it nucleates the folding of the 16S RNA by binding to five helices of the 5′ domain as well as to the central domain of the 16S RNA (Brodersen *et al*., 2002).

Proteins S4, S5 and S12 form a protein cluster at the shoulder and near the decoding center of the small subunit, which controls the accuracy of tRNA selection during mRNA translation. There is an interaction between S4 and S5 in this protein cluster, believed to be an integral part of its accuracy-tuning mechanism. Mutations in S4 and S5 often lead to *ram* mutations with enhanced codon misreading as their phenotype (Ogle *et al*., 2003), as further discussed in Chap. 11.

S12

S12 is a small ribosomal protein with a globular domain and an N-terminal tail. It can influence the fidelity of translation (Gorini, 1971; Kurland & Ehrenberg, 1987). S12 is unusual in that it binds on the interface side of the small subunit and at the decoding site of the small subunit (Wimberley *et al*., 2000; Carter *et al*., 2000; Schlünzen *et al*., 2000; Brodersen *et al*., 2002). The globular domain has an OB-fold and is at the interface side of the 30S subunit, while the N-terminal tail interacts with proteins on the external side of

the subunit. S12 interacts with helixes h3, h5, h18, h27 and h44 of the 16S RNA (Brodersen *et al*., 2002). It is close to the important adenines 1492 and 1493. Resistance to streptomycin, known to affect the accuracy of translation, is frequently conferred by mutations in S12 (see Sec. 10.3; Davies *et al*., 1964; Kurland, 1992). Streptomycin and protein S12 can both affect the balance between the two conformational states of the small subunit and thereby also the accuracy of translation (see Secs. 10.3 and 11.5). Residue Asp88 of S12 can be methylthiolated by RimO, a MiaB-like enzyme (Anton *et al*., 2008). Although Asp88 is universally conserved, the RimO-dependent modification is not. Mutations close to Asp88 can lead to streptomycin resistance.

Ribosome-bound S12 also interacts with EF-G (Girshovich *et al*., 1981; Valle *et al*., 2003b). Early studies have shown that S12 from *E. coli* is unusually rich in cysteinyl residues, and ribosomes with S12 modified with chloromercuribenzoate stimulate factor-free translocation (Gavrilova & Spirin, 1971; Southworth *et al*., 2002).

L1

L1 has given its name to the left protrusion of the large subunit when seen from the interface side. This protrusion is composed of L1 and helices H76–H78 of domain V of the 23S RNA (Zimmermann, 1980). The structure of L1 has been studied in isolation (Nikonov *et al*., 1996, Nevskaya *et al*., 2000) and in complex with a truncated fragment of the 23S RNA (Nikulin *et al*., 2003). The protein is composed of two domains that are separated by a short and, possibly, flexible hinge region (Unge *et al*., 1997). Mutant ribosomes lacking L1 are still functional (Subramanian & Dabbs, 1980).

The L1 stalk is flexible. It has been seen in different locations in different 50S structures and has been virtually invisible in others (Ban *et al*., 2000; Harms *et al*., 2001; Klein *et al*., 2004; Blaha *et al*., 2009). L1 and its binding site on the rRNA are more visible in structures of the 70S ribosome with bound tRNAs (Yusupov *et al*., 2001). The orientation of the L1 stalk in the structure of the isolated *D. radiodurans* 50S subunit differs by 30° from that in the structure

of the *T. thermophilus* 50S subunit in the 70S ribosome (Yusupov *et al.*, 2001). In extreme cases the L1 stalk can extend into solution or be quite close to the central protuberance of the large subunit.

The flexibility of the L1 stalk may control the movement of the deacylated tRNA into and out of the E site. With a tRNA in the E site L1 is located between the subunits and interacts with the elbow of the tRNA (Yusupov *et al.*, 2001; Valle *et al.*, 2003b; Penczek *et al.*, 2006; Frank, 2012). In this location, L1 and protein S7 from the small subunit prevent the deacylated tRNA from leaving the E site (Yusupov *et al.*, 2001; Valle *et al.*, 2003b). When the E site is empty, the L1 stalk is in an outer position. Thus, the L1 stalk acts as a gate for the exiting tRNA. Through its interaction with the deacylated tRNA, L1 may also participate actively in translocation (Valle *et al.*, 2003b). The two L1 conformations can be described as 'open' and 'closed', and exit of deacylated tRNA from the E site requires the open L1 conformation (see Sec. 11.5).

The largest movement of L1 occurs when EF-P binds to the ribosome (Blaha *et al.*, 2009). EF-P binds between the P and E sites and interacts with the initiator tRNA in the P site (see Sec. 9.2). L1 interacts with a negatively charged patch of EF-P. The observed flexibility of the L1 stalk suggests that it can establish contact with a deacylated tRNA in the P/E site and remain in contact until the tRNA dissociates from the ribosome (Blaha *et al.*, 2009).

L11

L10, L11 and L12 form a protein-rich region at the L12 stalk of the large subunit. They are part of the GTPase-associated center (GAC) and interact with the trGTPases IF2, EF-Tu, EF-G and RF3 (Wahl & Möller, 2002; Diaconu *et al.*, 2005; Kavran & Steitz, 2007; Gao *et al.*, 2009; Schmeing *et al.*, 2009). The r-proteins L11 and L10 are bound to domain II (H43 and H44) of the 23S RNA (Egebjerg *et al.*, 1990). L11 is composed of two domains (Wimberley *et al.*, 1999). The C-terminal domain (L11CTD) binds to the 23S RNA (residues 1051–1108), while a flexible linker connects the C-terminal with the

N-terminal domain of L11. The latter is important for stringent function (see Sec. 9.6). L11 is also important for the function of release factors 1 and 2 (Tate *et al*., 1984). Nevertheless, it can be deleted from the ribosome (Stark & Cundliffe, 1979). The protein is trimethylated at several sites by PrmA (Dognin & Wittmann-Liebold, 1980). Structures of complexes of the methylase and L11 engaged in modification of several sites have been determined (Demirci *et al*., 2008).

L10

L10, at the base of the L12 stalk, attaches the stalk to the 23S RNA and forms a strong complex with two or three dimers of L12 (see below). Even though the isolated L10:$L12_4$ complex is quite stable, some observations indicate that L12 easily dissociates from the ribosome (Subramanian & van Duin, 1977). In the classical extraction, ammonium chloride and ethanol are used to remove L12 exclusively from the ribosome (Hamel *et al*., 1972). Furthermore, L12 could easily be made to dissociate from the ribosome in the electrospray MS investigations (Hanson *et al*., 2003).

L10 is unstable in isolation and difficult to handle, but is stabilized by complex formation with L12 (Newcomer & Liljas, 1980). The L10–L12 complex is so strong that it does not dissociate but produces a unique spot, called L8, in the classical two-dimensional urea gels of *E. coli* ribosomal proteins (Kaltschmidt & Wittmann, 1970). This spot was identified as a complex of four copies of L12 bound to L10 (Pettersson *et al*., 1976; Österberg *et al*., 1977). L10 binds to H42–H44 of the 23S RNA via its N-terminal region (Gudkov *et al*., 1980).

Classically, the "L8"-complex contains two dimers of L12. Investigations by electrospray MS have shown that thermophilic bacteria can have three L12 dimers bound to L10 (Ilag *et al*., 2005; Nomura *et al*., 2008; Plate 7.3). The structure of L10 from *Termotoga maritima* with the N-terminal domains of three L12 dimers is known (Diakonu *et al*., 2005; Fig. 7.3). In addition, the structure of the L10 corresponding protein in the large subunit of *H. marismortui*

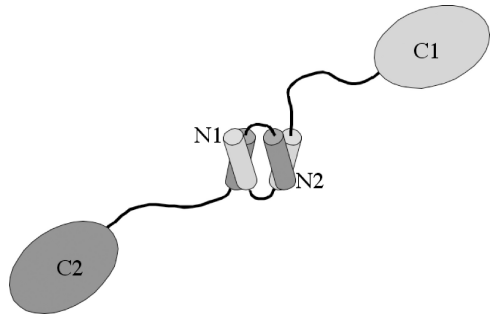

Fig. 7.3 A simplified illustration of the structure of the L12 dimer. The N-terminal domains have an antiparallel arrangement (Wahl *et al.*, 2000; Bocharov *et al.*, 2004). The hinge regions give the C-terminal a high flexibility.

could be interpreted, which elucidated the interaction of L10 with the ribosome and the 23S RNA. The L12 dimers bind to the C-terminal helix of L10 (Diaconu *et al.*, 2005). Each L12 dimer binds to 10 residues of the L10 helix. After deletion of the C-terminal 10 residues of *E. coli* L10, only one L12 dimer can bind (Griaznova & Traut, 2000). In *T. thermophilus* a triple repeat sequence in L10 illustrates the preferred peptide motif for L12 binding:

RAELVGVLQAP
MAELVGVLGGV
ARELVG I LEAY

L12

Protein L7/L12 was first characterized in *E. coli*, where its N-terminus can be acetylated (Terhorst *et al.*, 1972). The acetylated form of L12, often referred to as L7, is rarely seen in other species. Therefore L7/L12 is called L12 in this book. (For reviews see: Liljas, 1982, 1991; Gudkov, 1997; Wahl & Möller, 2002; Gonzalo & Reboud, 2003.)

Despite decades of work and determination of the structures of both ribosomes and ribosomal subunits, neither the structure nor

the functional role of L12 is well understood. While there is normally one version of L12 in bacteria, plant chloroplasts and mitochondria can have two and four different functional versions of L12, respectively (Delage *et al*., 2007). Yeast, mouse and human mitochondria have only one type of L12 molecule (Han *et al*., 2011). Human, bovine and three of the four plant mitochondrial L12 molecules (L12.1–L12.4) have N-terminal extensions of different lengths (Delage *et al*., 2007; Han *et al*., 2011). L12.4 has the longest extension, which is rich in acidic residues.

L12 forms the so-called L12 stalk on the right hand side of the large subunit viewed from the interface side (Fig. 2.2; Boublik *et al*., 1976; Strycharz *et al*., 1978). It is essential for the proper functioning of trGTPases (see Sec. 9.1). It is the only repeated protein in the ribosome and occurs as two or three strongly coupled dimers in the ribosome (Österberg *et al*., 1976, 1977; Ilag *et al*., 2005). L12 has two domains. The N-terminal domains of L12 (NTD) are involved in the strong dimer interaction (Gudkov & Behlke, 1978). The C-terminal domain (CTD) was the first part of the ribosome for which the structure was determined (Leijonmarck *et al*., 1980, 1987). By NMR methods the N-terminal domain of the L12 monomer was found to be composed of two α helices (α1 and α2; Bocharov *et al*., 1996, 1998). The two N-terminal helices in one subunit of the L12 dimer are antiparallel to each other and the two N-terminal helices of the other. The two pairs of N-terminal helices form hooks, which attach to each other in the dimer structure (Fig. 7.3; Wahl *et al*., 2000). Due to the large flexibility of L12 and L10, neither crystal structures of subunits nor of whole ribosomes have so far revealed the full *in situ* organization of proteins L12 and L10 in the ribosome.

The two domains of L12 from *E. coli* are connected by a flexible link or hinge, primarily involving residues 36–51 (Bushuev *et al*., 1989; Bocharov *et al*., 2004; Mulder *et al*., 2004). The hinge makes L12 highly flexible, as shown by different methods (Fig. 7.3; Table 7.5). The length and composition of the L12 hinge, rich in alanyl and glycyl resides, vary considerably between different organisms (Liljas *et al*., 1986; Bushuev *et al*., 1989).

Table 7.5 Domain Flexibility of L12

Method	Observation	Reference
Sequence	The hinge (*E. coli* residues 36–51) is difficult to align due to different lengths and composition. The region is rich in glycyl and alanyl residues.	
NMR	Spectra of ribosomes or 50S subunits show that L12 is highly flexible. The region 33–51 was identified as the source of flexibility.	Tritton, 1980; Gudkov *et al*., 1982 Cowgill *et al*., 1984 Bushuev *et al*, 1989 Mulder *et al*., 2004
Proteolysis	Spontaneous proteolysis of L12 occurred in the region 36–50 in crystallization attempts.	Liljas *et al*., 1978 Wahl *et al*., 2000
EM	The L12 stalk appears very variable in different states of the ribosome, if at all seen.	Agrawal *et al*., 1999 Valle *et al*., 2003a; b
	Nanogold-labeled C-termini were observed in four different locations in the subunit interface.	Montesano-Roditis *et al*., 2001
Crystallography	Subunit or ribosome structures rarely show L12 due to its mobility.	Ban *et al*., 2000 Yusupov *et al*., 2001 Harms *et al*., 2008
Crosslinking mutations	L12 can be crosslinked to proteins far away from the stalk.	Dey *et al*., 1998
	Decreasing the length of the hinge can lead to poor function.	Gudkov *et al*., 1991
	Changes of residues or increasing length have little effect.	Bubunenko *et al*., 1992

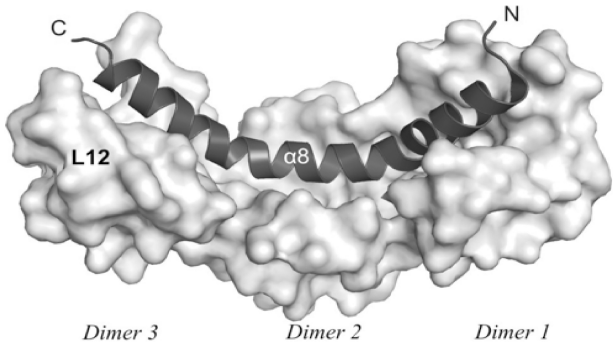

Fig. 7.4 The structure of the three dimers of N-terminal domains of L12 bound to α8 of L10 (blue). (Illustration by Saraboji Kadhirvel.)

The two or three NTD dimers of L12 are bound to the C-terminal helix (α8) of protein L10 (Fig. 7.4; Diaconu *et al.*, 2005). From investigations of the dimer (Bocharov *et al.,* 1996; Mulder *et al.*, 2004) or the pentameric L8 complex (Bocharov *et al.*, 1998), it is clear that the C-termini (CTD) interact neither with each other nor with the NTDs.

In the x-ray structure of L12 from *T. maritima* (Wahl *et al.*, 2000; Sanyal & Liljas, 2000), the crystallographic asymmetric unit contains two complete molecules and two N-terminal fragments. It is seen that the flexible hinge region can also adopt a helical conformation (α3; Fig. 7.5). From NMR studies it has been suggested that helix α3 in the N-terminal part of the hinge may exist transiently (Bocharov *et al.*, 2004). However, the α3 helix observed by crystallography is located over the twofold axis of the NTDs, which is where the C-terminal helix of L10 (α8) binds (Diaconu *et al.*, 2005). It remains, however, possible that the L12 hinge has helical conformation in another location.

NMR studies of L12 in 50S subunits or 70S ribosomes indicate that residues 40–51 of only two of these four hinge regions are greatly mobile (Mulder *et al.*, 2004). Whether the flexible L12 hinges belong to the same or separate dimers and whether the

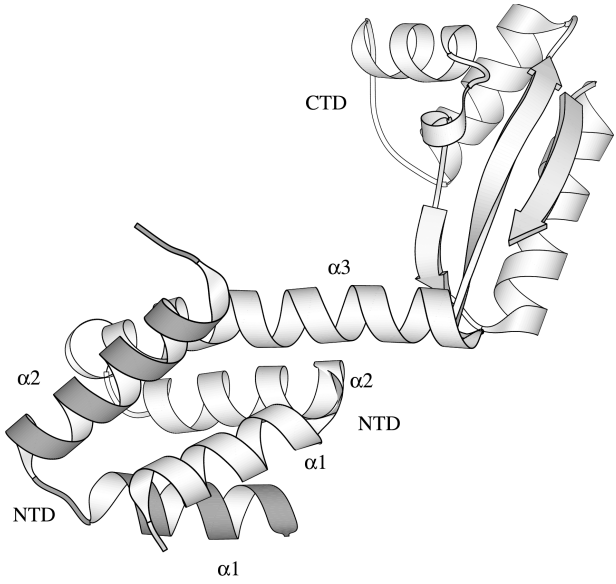

Fig. 7.5 The crystal structure of L12 (Wahl *et al*., 2000). The picture shows one full molecule (white) and one N-terminal fragment (gray). The dimer interaction between helices α1 and α2 is seen. In addition, the hinge of the complete monomer forms a helix, α3 located over the twofold axis of the dimer. This is the same location as for helix α8 of protein L10 in the larger complex. [Figure kindly provided by Dr. M. Fodje, using the program MOLSCRIPT (Kraulis, 1991).]

flexible forms of the four molecules alternate remain to be clarified (Fig. 7.6; Sanyal & Liljas, 2000).

Due to the flexible hinge, L12 can reach a large region of the large ribosomal subunit. Chemical crosslinking (Dey *et al*., 1998) and fluorescence spectroscopy (Zantema *et al*., 1982a, b) have shown a substantial part of the subunit interface to be accessible to L12 CTDs.

The removal or modification of L12 has detrimental effects on GTP hydrolysis in translational GTPases (Kischa *et al*., 1971; Hamel *et al*., 1972; Koteliansky *et al*., 1978; Pettersson & Kurland, 1980; Mohr *et al*., 2002), due to either impaired factor binding or impaired GTPase activity *per se*. The removal of the C-terminal

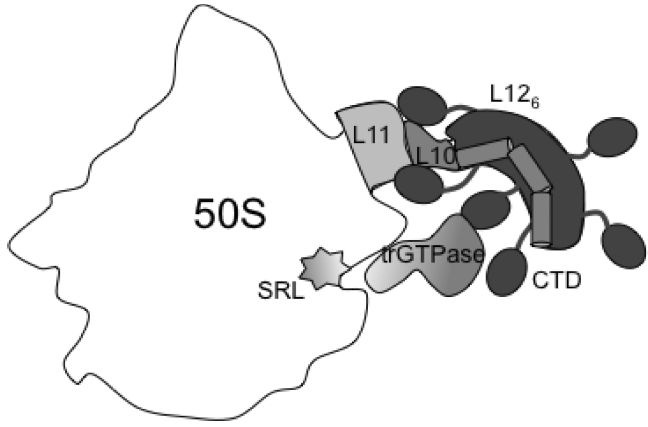

Fig. 7.6 The large subunit of ribosomes with three dimers of L12 bound to the three C-terminal helices of L10. The L12 C-terminal domains (CTD) extend from the stalk due to their hinge regions. A trGTPase is shown near its binding site, where the SRL is an important part.

domains has the same effect as removing the whole protein (Agthoven *et al.*, 1975; Koteliansky *et al.*, 1978). Thus, it is the CTD of L12 that interacts with the translational GTPases. Ribosomes with only one L12 dimer are still partially active (Griaznova & Traut, 2000). Ribosomes where one C-terminus of each L12 dimer was removed also retained activity (Oleinikov *et al.*, 1998). The removal of L12 delays the release of inorganic phosphate from EF-G after GTP hydrolysis (Mohr *et al.*, 2002). Spontaneous mutations in the hinge region (Kirsebom *et al.*, 1986) can lead to a decreased proofreading of aminoacyl-tRNAs in codon recognition (Ruusala *et al.*, 1982). If the hinge is significantly shortened, the ribosomes behave as if there was no CTD, but essentially doubling the length of the hinge has no effect (Gudkov *et al.*, 1991; Bubunenko *et al.*, 1992). We will return to the functional interactions between L12 and trGTPases in Chap. 9.

Two surprising observations concerning L12 have been made using electrospray MS (Ilag *et al.*, 2005). One is that in certain thermophiles three dimers can bind to L10 (see Section on L10). The other is that L12 molecules have the added molecular weight

of a phosphate moiety. The sites of phosphorylation are Ser15, Ser33, Thr52 and Ser89 (Soung *et al.*, 2009). The level of modification at these sites and the functional role of the phosphorylation remain unclear.

The P proteins

The proteins in eukarya and archaea corresponding to bacterial L12 and L10 can be phosphorylated and are therefore called the P proteins (Zinker & Warner, 1976). The P0 protein corresponds to L10 (Wool *et al.*, 1991), and is 100 amino acids longer than L10. Its N-terminal part is an orthologue of the whole bacterial L10 (Shimmin *et al.*, 1989). In eukarya there are two related proteins, P1 and P2, which functionally correspond to L12 in that they bind to P0 as two heterodimers (Tchorzewski *et al.*, 2000a, Ballesta *et al.*, 2000; Maki *et al.*, 2007) to form the right hand stalk of the large subunit (Uchiumi *et al.*, 1987; for reviews see Liljas, 1991; Ballesta *et al.*, 2000). P1/P2 have no sequence similarity with L12, but share the distinctly acidic nature of their bacterial counterparts. In archaea, there is only one L12 corresponding protein. In the literature, it has been called "archaeal L12" but, since it lacks sequence homology with L12 and is closely sequence-related to P1 and P2, we prefer the designation "archaeal P1/2." Like in bacteria, the archaeal P0 can bind three dimers of P1/2 to its C-terminal helix. The C-terminal region of P0 contains a sequence of about 30 residues identical with the C-terminal residues of P1, P2 and P1/2 (Santos & Ballesta, 1995).

P1 and P2 have N-terminal domains of about 70 residues followed by a flexible region of about 30 amino acid residues (Wool *et al.*, 1991; Bailey-Serres *et al.*, 1997; Tchorzewski, 2002). This hinge region is highly variable in length and amino acid sequence. It is rich in alanyl and glycyl residues. The highly charged C-terminal part of the hinge is dominated by acidic residues. The C-terminus of the protein has a conserved stretch of 10–13 residues. Several protein kinases can phosphorylate a conserved seryl residue in this region (Ballesta *et al.*, 1999). Like for bacterial L12, the C-terminal

region of the P1, P2 and P1/2 proteins interacts with translational GTPases (Bargis-Surgey *et al.*, 1999). The N-terminal domains of P1 and P2 are involved in the dimerization as well as binding to P0 (Ballesta & Remacha, 1996).

In yeast, where there are four different versions, P1A, P1B, P2A and P2B. P1A forms a heterodimer with P2B, and P2A forms a heterodimer with P1B (Tchorzewski *et al.*, 2000b; Guarinos *et al.*, 2001). The heterodimers are highly helical (Tchorzewski *et al.*, 2003). In plants, there is one additional P protein, P3 (Bailey-Serres *et al.*, 1997).

The stalk has been observed at low resolution by cryo-EM in ribosomes with a bound archaeal variant of EF-G — aEF2 (Gomez-Lorenzo *et al.*, 2000). However, in the crystallographic structure of the *H. marismortui* large subunit at high resolution, only parts of the P proteins have been seen due to high flexibility (Kavran & Steitz, 2007). The structures of the P0-related protein and stalk complexes from archaeal species have been determined (Kravchenko *et al.*, 2010; Naganuma *et al.*, 2010). The latter structure contains P0 with three dimers of the N-termini of P1/2. The structure of P0 is closely similar to that of L10. P1/2 is composed of four α helices in two layers. The dimer interface is formed by the two helices closest to the N-terminal (Fig. 7.7).

In all species this stalk is very long and flexible. The P0 C-terminal helix binds over the twofold axis of the dimer, as is also the case in the L10–L12 interaction. The first and the fourth helix of P1/2 interact almost orthogonally with the long helix of P0 (Fig. 7.8). So far the structures do not include the C-terminal parts of L12 or the P proteins, which would increase the length of the flexible stalk even further.

The possible arrangement of the P proteins in the ribosome will not be much different from the situation in the bacterial ribosome, as illustrated in Fig. 7.6. One difference is that the C-terminal domains of the P proteins are smaller and there is a C-terminal extension of P0 (L10 orthologue) of the same nature as the C-terminal domain of the P1 and P2 proteins.

If all P proteins are deleted, the ribosomes do not function. If only the P1 and P2 proteins are missing, the ribosome is still

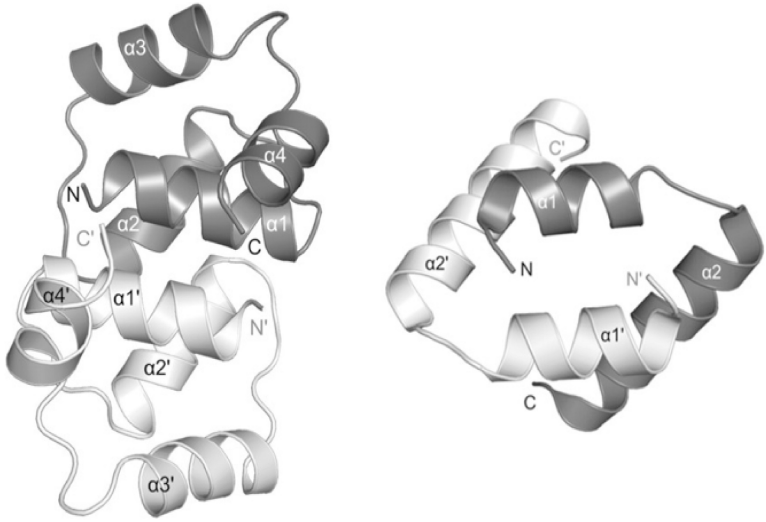

Fig. 7.7 The structure of the N-terminal part of a dimer of the archaeal protein P1/2 compared to bacterial L12. One monomer in white and the second one in gray. We are in both cases looking down the twofold axis of the dimer. Apart from the helical structure, it is difficult to identify a structural similarity. (Illustration by Saraboji Kadhirvel.)

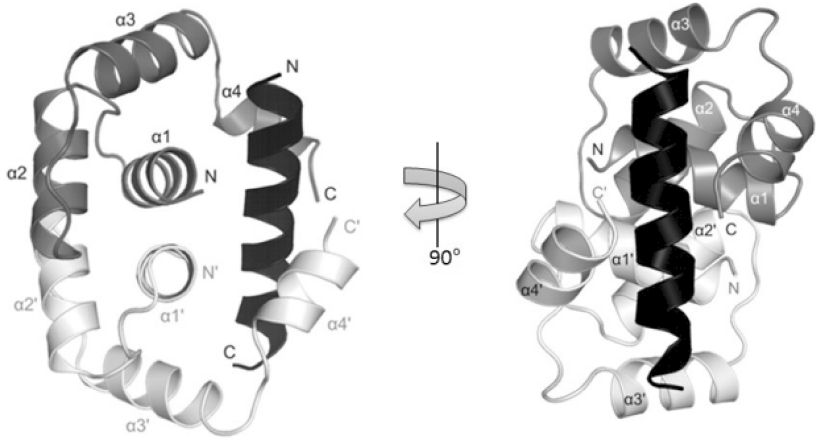

Fig. 7.8 Two orthogonal views of the P1/2 dimer binding to part of the C-terminal helix of the L10 (black) corresponding protein P0. (Illustration by Saraboji Kadhirvel.)

able to support protein synthesis with P0 alone (Santos & Ballesta, 1994; Remacha *et al*., 1995), but a different subset of mRNAs is translated. However, if the C-terminal conserved residues are also removed from P0, the ribosome is no more functional.

The yeast system offers a unique opportunity to study the individual roles of the four copies of P1 and P2. The four different yeast proteins have specific binding sites on P0 and can be mutated individually. The question is whether they have unique roles or their high flexibility enables them to substitute for each other. The fact that the C-terminus of P0 alone can induce GTP hydrolysis suggests that the proteins can substitute for each other.

There are pools of free ribosomal proteins in the cytoplasm, including the acidic stalk proteins (Ramagopal, 1976; van Agthoven *et al*., 1978; Zinker, 1980). A large fraction of patients with systemic lupus erythematosus develop autoantibodies against ribosomal P proteins (Elkon *et al*., 1985). The range of locations and functional aspects of the P proteins remain to be fully clarified.

L16 (L10e)

Ribosomal protein L16 has for a long time been associated with the function of the peptidyl transfer center (PTC). Thus, if L16 is added back to LiCl extracted 50S subunits, they regain peptidyl transfer activity (Moore *et al*., 1975; Maimets *et al*., 1984). L16 is universally conserved (App. I). In archaea and eukarya it is they called L10e. Structures of L16 from all domains of life are known and have been compared (Nishimura *et al*., 2004, 2008). As expected, L16/L10e is located in the vicinity of PTC (Nissen *et al*., 2000). However, the initial crystal structures of 50S subunits did not identify an immediate proximity of the protein with the acceptor ends of the A- and P-site tRNAs. The internal loop of L16 requires a 70S structure with stably bound tRNAs to become ordered (Voorhees *et al*., 2009; Jenner *et al*., 2010). The globular part of L16

binds above the elbow region of the A-site tRNA (Yusupov *et al*., 2001). Here arginines 51, 56 and 60 interact primarily with tRNA phosphates 53 and 54 (Voorhees *et al*., 2009). L16 is required for stable binding of the A-site tRNA. In archaea the internal loop is 11 amino acid residues longer than that in bacteria and may extend close to the acceptor ends and have a direct role in peptidyl transfer (Voorhees *et al*., 2009).

L22

L22 is one of the first proteins to bind to the 23S RNA in the assembly of the large subunit (Röhl & Nierhaus, 1982). Its role in assembly is obvious from the fact that it is in contact with all six domains of the 23S rRNA (Ban *et al*., 2000; Harms *et al*., 2001). In the large subunit it is bound with the globular domain to the exterior surface and the long β ribbon essentially along the exit tunnel (Ban *et al*., 2000). The structure of L22 was possible to determine in isolation despite its very extended shape (Unge *et al*., 1997). The β ribbon of the protein has been observed to adopt several different conformations in the ribosome. One of these conformations blocks the exit tunnel (Berisio *et al*., 2003b). The structure of an erythromycin-resistant mutant has also been determined (Davydova *et al*., 2002).

L27

Over the years there has been a long discussion on which, if any, proteins may participate in peptidyl transfer (see Sec. 8.3). Experiments by Noller *et al*. (1992) suggested that peptidyl transfer might be performed by ribosomal RNA alone. This was further strengthened by the crystallographic structure of the large subunit from the archaean *H. marismortui* (Ban *et al*., 2000; Nissen *et al*., 2000). From this structure, it was concluded that the closest distance between the PTC and any protein is 18 Å, and that the peptidyl transfer reaction is catalyzed by RNA alone and not by

protein (Harms *et al*., 2001). However, crosslinking studies have shown that protein L27 is close to the 3′ ends of both A- and P-site tRNAs in the bacterial ribosome. Deletion of L27 resulted in severe defects in cell growth and peptidyl transfer in particular (Maguire *et al*., 2005). The removal of the N-terminal three residues led to the same type of impairment of the peptidyl transfer reaction. With the high-resolution structure of *T. thermophilus* ribosomes, it became clear that the N-terminal residues of L27 are situated next to the P-site tRNA in PTC (Plate 7.4; Selmer *et al*., 2006; Jenner *et al*., 2010).

Computer simulations using *T. thermophilus* ribosomes show that when the N-terminal residues of L27 are removed peptidyl transfer becomes slower (Trobro & Åquist, 2008). These apparently conflicting data lead to the question whether archaeal ribosomes catalyze peptidyl transfer exclusively by RNA, while the reaction is catalyzed by both protein and RNA in bacteria (see Chap. 11 for a fuller discussion on this controversial point).

7.6 THE STRUCTURES OF EUKARYOTIC AND MITOCHONDRIAL RIBOSOMES

The eukaryotic 80S ribosome, and its 40S and 60S subunits, have been studied by cryo-EM and crystallography to the highest resolution of 3 Å (Klinge *et al*., 2001; Taylor *et al*., 2009; Armache *et al*., 2010a, b; Ben-Shem *et al*., 2010; Rabl *et al*., 2011; Ben-Shem *et al*., 2011). The main outlines of the ribosomes are very similar to those of bacteria. However, the larger rRNA molecules and the greater number of r-proteins make the eukaryal subunits larger than their bacterial counterparts. The structure of the additional RNA and the unique eukaryotic proteins have been clarified. The extra proteins and the extension segments of the 18S RNA are primarily located on the outer surface of the subunits, whereas the subunit interface is more conserved in the three kingdoms. More than half of the conserved proteins have extra extensions in eukarya. Furthermore, the ribosomal proteins

have more extensive contacts in eukarya than in bacteria (Voights-Hoffmann *et al*., 2012).

The structures of mitochondrial ribosomes (see Chap. 6) have been studied by cryo-EM. In the 55S bovine mitochondrial ribosome, helices of the 12S and 16S rRNA have been shortened compared to bacterial ribosomes. The trimmed RNA is covered with an outer layer of proteins (Sharma *et al*., 2009; Agrawal & Sharma, 2012). The interface between the subunits is more open. The additional proteins do not seem to replace specific parts of the rRNA, but just substitute for the lost volume. The mitochondrial large subunit is larger than the bacterial one despite the reduction of the rRNA. In particular, the 5S RNA is absent. However, the central protuberance, which is the location of the 5S RNA, is double in size due to the binding of proteins. The polypeptide exit tunnel seems considerably more open in mitochondrial ribosomes due to the reduced size of domains I and III in the large subunit RNA.

This page intentionally left blank

8

Ribosomal Sites and Ribosomal States

The basic functions of the ribosome are decoding, peptidyl transfer and translocation, a movement of the tRNAs and mRNA in relation to the ribosome. The peptidyl transfer center (PTC) and the decoding center (DC) of the ribosome are located on the large and small subunits respectively and at the interface between the ribosomal subunits (Fig. 8.1). The transport function of the ribosome requires the two subunits (Spirin, 1968, 1969; Bretscher, 1968; Spirin, 2002). In addition, the binding sites for the translation factors are also at the interface between the subunits. The ribosomal functions are to a large extent closely related to the rRNA. The binding of tRNAs and factors to the ribosome involves both the rRNAs and ribosomal proteins. Here we will focus on some of the main sites for ribosomal interactions with mRNA and tRNA as well as with translation factors and the nascent polypeptide.

The ribosome goes through a number of different states during protein synthesis. Some states are well characterized, while for others a fuller understanding is still in progress. The best-known states are the pre- and posttranslocation states of the ribosome. The main difference between them is the position whether the peptidyl tRNA is in the A or P site. A number of gross conformational differences have been observed and a ratchet-like rotation of the

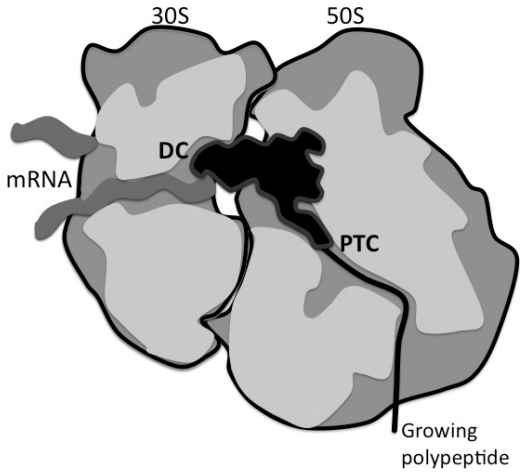

Fig. 8.1 A cross-section of a bacterial ribosome, showing the location of the functional centers at the interface of the small and large subunits. The mRNA binds around the neck of the small subunit and presents the codon to be read in the decoding center (DC). A tRNA (black) is bound with the anticodon at the DC and the aminoacyl acceptor end at the peptidyl transfer center (PTC). The growing polypeptide emerges from the PTC through the polypeptide exit channel.

subunits in relation to each other has been identified (see Chap. 7; Woese, 1970; Frank & Agrawal, 2000). It is evident from numerous observations that the ribosome is not a passive partner in the translation process, but actively responds to the ligands and participates in the process.

Some of the ribosomal states are known at close to atomic resolution, due to the crystallography and cryo-EM of the ribosomes and its subunits. The highly resolved structures form the basis for the interpretation of the different states studied by other methods.

8.1 THE BINDING OF mRNA

The Recognition of mRNA

During initiation an mRNA is bound around the neck of the small subunit, and the initiation codon, normally AUG, is placed in the

P-site. A primary component of the neck is a single helix of the 16S RNA, h28. Internal AUG methionine codons have to be avoided. The classic Shine–Dalgarno (SD; Shine & Dalgarno, 1974) model describes how this can be done in bacteria. It involves a nucleotide sequence rich in purines upstream of the initiator codon of the mRNAs that is complementary to the 3′ end of the 16S ribosomal RNA (Fig. 8.2a; Plate 8.1). This interacting region is variable in length and location in relation to the initiation codon (Fig. 8.2; Schulzaberger *et al.*, 2001). The SD interaction occurs in the cleft between the platform and the head of the subunit (Yusupova *et al.*, 2001). The regions of the ribosome in contact with the helix formed

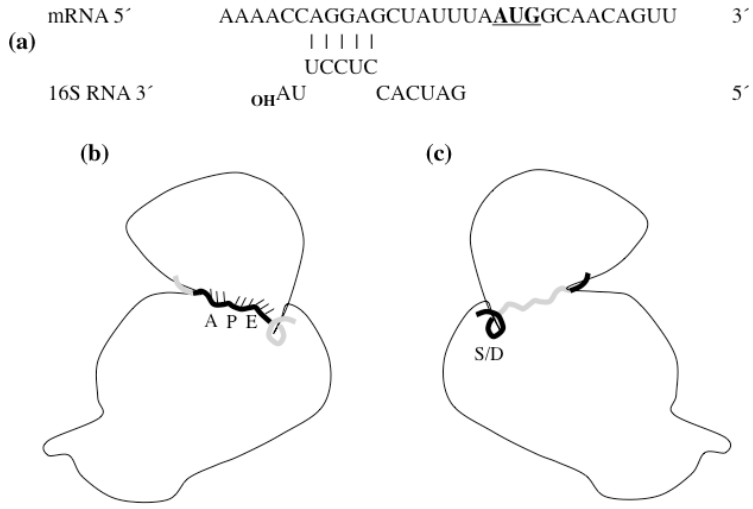

Fig. 8.2 The binding of the mRNA to the small subunit (Yusupova *et al.*, 2001). **(a)** One example of the base pairing between the 5′ end of the mRNA and the 3′ end of the 16S RNA. The initiator AUG codon is underlined. **(b)** The codons of the A, P and E sites are exposed on the interface side of the subunit. Only a few nucleotides in addition to the two codons of the mRNA are exposed, due to the narrow groove. **(c)** The mRNA crosses over from the interface side to the external side of the subunit in a narrow groove on the side of the shoulder. The SD base pairing between the 5′ end of the mRNA and the 3′ end of the 16S RNA is located in a groove between the head and the platform.

by the SD interaction are h20, h28 (the neck helix), h37 and proteins S11 and S18.

It has been realized that SD is a special case of a more general and complex mechanism (Boni, 2006; Nakamoto, 2009). In gram-positive bacteria the SD mechanism seems to be the dominating one, but in gram-negative bacteria, like *E. coli*, this sequence complementarity is more rarely used. Only a fraction of its genes have the purine-rich SD sequence. In some cases there is no leader sequence at all. A more general term for describing the interaction of the mRNA with the ribosome is 'ribosome-binding site' (RBS). Other terms used are 'translation initiation region' (TIR; Boni 2006) and 'cumulative specificity mechanism' (Nakamoto, 2009). The TIR of the mRNA can involve nucleotides −20 to +15 in relation to the first nucleotide of the initiation codon. A gene with a TIR lacking SD can be translated much more efficiently than a gene with an SD motif. Two features of the interaction between mRNA and ribosome in addition to SD are illustrated below.

Ribosomal protein S1, primarily found in gram-negative bacteria, is known to interact with mRNA (Draper & von Hippel, 1978). The two N-terminal domains of its repeat of six domains bind to the small subunit in the neck region, and the remaining four domains can interact with the mRNA upstream of the initiation codon. S1 is indispensable for translation of mRNAs in *E. coli*, especially those lacking the SD element (Sorensen *et al*., 1998).

It has long been realized that mRNAs can have intricate and stable secondary structure. These hairpins are able to bind to the ribosome without melting (Plate 8.1; Jenner *et al*., 2005). Obviously, the SD interaction is only part of the system for recognition and placement of the mRNA on the ribosome. In general terms, there is no specific sequence that signals initiation, but rather an ensemble of preferred bases and structures of the mRNA involved in multiple contacts of the small subunit. The SD and other interactions during initiation melt during the phase of elongation.

In eukaryotic systems, the binding site on the mRNA for the ribosome seems to be recognized differently. The eukaryotic mRNAs have an N^7-methylated GTP linked by a 5′–5′ pyrophosphate bond to

the terminal nucleotide, called a cap (Shatkin, 1976). The cap-binding proteins recognize this cap and mediate the binding of the mRNA to the small subunit. The cap is situated at a varying distance from the initiation codon, the first AUG. This AUG codon is part of a sequence [(gcc)gccRccAUGG; R stands for A or G]) called the Kozak sequence upstream of the initiator codon (Kozak, 1986, 1987). The apparent difference between the three kingdoms of life may be less than what has been thought. The initiation signals in eukaryotes are not unique but have complex properties. As a matter of fact, bacterial ribosomes can initiate from and translate eukaryotic mRNAs and vice versa. With the high conservation of other parts of the system, it is far from being ruled out that the more complex recognition of mRNA and initiation codons is common to all three kingdoms of life (Nakamoto, 2009).

The Binding Site for mRNA — The Decoding Site

The binding site for the mRNA has long been known to be located centrally on the small subunit (Shatsky *et al.*, 1991). The ribosome protects about 30 nucleotides of the mRNA by the binding (Steitz, 1969). Pieces of mRNA of different lengths bound to 70S ribosomes have been characterized crystallographically (Yusupova *et al.*, 2001; Jenner *et al.*, 2005; Selmer *et al.*, 2006; Yusupova *et al.*, 2006; Marzi *et al.*, 2007; Simonetti *et al.*, 2009). The mRNA binds as a necklace around the neck between the body and the head of the small subunit. In simple terms, the 5′ end of the mRNA contacts the back of the platform and wraps around the neck of the small subunit to place the codons to be read in the A and the P site respectively (Figs. 8.2b and 8.2c; Plate 8.1). The tunnel through which the mRNA has to move is so narrow that any secondary structure has to be unfolded. Ribosomal proteins S3–S5 surround the entrance to the tunnel. The mRNA tunnel entrance is 13 ± 2 nucleotides from the first nucleotide in the P site (Qu *et al.*, 2011). This means that at translocation of the mRNA the unwinding of secondary structure has to be done several codons before the mRNA is placed in

the A site. The rate of translocation depends on the GC content of the base-paired structures of the mRNA. The GTP hydrolysis by EF-G may be part of the energy to pull the strands of the mRNA apart (Qu *et al*., 2011).

It is evident that initiation has to start with the small subunit that binds the mRNA. When the small subunit is bound to the large subunit, there is no simple way to introduce an mRNA into the proper place through the tunnel between the subunits. Likewise, to dissociate an mRNA from the ribosome during ribosome recycling, the subunits need to be separated from each other.

The mRNA is threaded through two tunnels of the 30S subunit, and its ends protrude up- and downstream of the decoding region (Plate 8.1; Yusupova *et al*., 2001). The region of the mRNA in stable contact with the ribosome is nucleotides −5 to +12.

The decoding site has been defined by the crystallographic investigations both of the small subunit and of whole ribosomes (Carter *et al*., 2000; Schlünzen *et al*., 2000; Yusupov *et al*., 2001; Ogle *et al*., 2001, 2002; Korostelev *et al*., 2006; Selmer *et al*., 2006). It is situated on the interface side of the small subunit, close to the top of the penultimate helix or h44 of the 16S RNA. The mRNA makes a kink of about 45° between the codons in the A- and P-sites (Yusupov *et al*., 2001). The kink is stabilized by a magnesium ion that is bound to the phosphates of the first nucleotide of the A-site codon and the third nucleotide of the P-site codon (Plate 8.2). In addition, the magnesium binds to the phosphates of nucleotides 1401 and 1402 of the 16S RNA (Selmer *et al*., 2006). The downstream part of the mRNA has a variable structure, depending on whether the ribosome has the initiator tRNA in the P-site or not. The codon in the E-site also has a kink during the initation phase. Yusupova *et al*. (2006) refer to this state of the mRNA as tense. After the translation of one or several codons, the mRNA relaxes into a different conformation (see further under "The E site," Sec. 8.2).

8.2 THE tRNA BINDING SITES

The ribosome is a large enzyme, a polymerase, and the aminoacyl tRNAs are the substrates in the process of translation. Enzymes

need to distinguish correct from incorrect substrates and also bind the substrates in such a way that the chemical reaction can proceed at a physiological rate. The tRNAs and the ribosome have evolved together to make translation proceed with sufficient accuracy and speed.

The tRNA molecules are bound at the interface between the ribosomal subunits and form bridges between the decoding site on the small subunit and the PTC on the large subunit. The subunit arrangement fits the L-shaped structure of the tRNAs with the anticodon at one end and the amino acid at the opposite end (Fig. 8.1). Classically, two sites for tRNA molecules on the ribosome were discussed (Fig. 8.3; Plate 8.3; Warner & Rich, 1964; Watson, 1964). These are the A site (the site for the acceptor or aminoacyl tRNA) and the P site (the site for the donor or peptidyl tRNA). A third site has been identified. This is the E site, where the deacylated tRNA binds before it dissociates from the ribosome (Wettstein & Noll, 1965; Rheinberger *et al.*, 1981; Grajevskaja *et al.*, 1982; Kirillov *et al.*, 1983). A fourth site was also found: the entry or recognition site where aminoacyl-tRNA enters the ribosome when

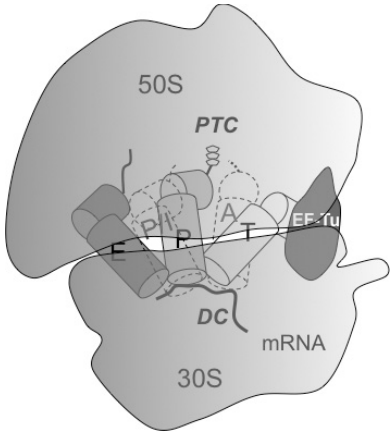

Fig 8.3 The T, A, P, P/I and E sites for tRNA bound to the ribosome. The P/I site is a hybrid site where fMet-tRNA has been observed (Allen *et al.*, 2005). When the tRNA is bound to EF-Tu, it is initially located in the T site. Subsequently the tRNA bends to interact with the mRNA. It is then in the A/T-site.

bound to EF-Tu (Hardesty *et al.*, 1969; Lake, 1977; Robin & Hardesty, 1983; Stark *et al.*, 1997). This site, the T site, is consistent with the observation that the aminoacyl residue cannot be engaged in peptide bond formation on the ribosome until it is released from EF-Tu (Fig. 8.3; Skogerson & Moldave, 1968).

Other modes of tRNA binding are called hybrid states (A/T, A/P and P/E), which are transition states (Plate 8.3; Fig. 8.4). Another such hybrid state is the way fMet-tRNA initially binds (Allen *et al.*, 2005). In the binding of initiator tRNA there is neither an E-site tRNA nor a nascent peptide that would stabilize the tRNA to the P site. This may explain its binding to the P/I site (Fig. 8.3).

The binding sites for tRNA were initially studied through their protection of rRNA from chemical modifications (Table 8.1; Moazed & Noller, 1989). The crystallographic and cryo-EM investigations of ribosomes have given an improved understanding of the tRNA sites and the dynamics involved in decoding, peptidyl transfer and translocation. Generally, there is good agreement between chemical and structural studies.

The tRNAs move through a tunnel between the subunits from the A/T and A sites on the side of the L12 stalk to the E site on the L1 side of the ribosome (Figs. 8.1 and 8.3). Throughout the process of

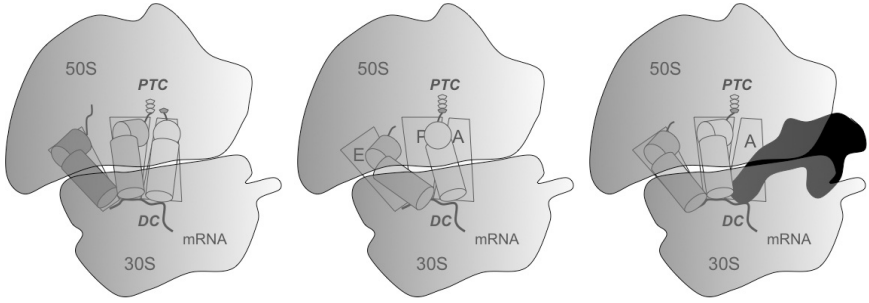

Fig. 8.4 The movement of the tRNA molecules between the A, P and E sites. Left: The aminoacyl-tRNA is accommodated in the A site. Middle: After peptidyl transfer the peptidyl-tRNA oscillates between the A site and the hybrid state A/P. This requires that the deacylated tRNA in the P site be in the hybrid P/E state. Right: EF-G (black) translocates the peptidyl-tRNA into the P site and the deacylated tRNA into the E-site.

Table 8.1 Protection of Specific Bases in *E. coli* 16S and 23S rRNA by tRNA*

		16S rRNA	23S rRNA
A site	Strong	**G530, A1492, A1493**	C2254, A2439, **A2451**, **G2553**, Ψ2555, A2602
	Weak	A1408, G1494	G1068, G1071, U2609
P site	Strong	G693, A794, C795 G926, G1401(N7)	**G2252**, **G2253**, A2439 **A2451**, U2506, U2584, U2585
	Weak	A532, G1338, A1339, G966	A1916, A1918, U1926, G2505
E site	Strong	—	C2394
	Weak	—	G2112, G2116

*After Moazed & Noller (1989). Some residues with important roles are shown in boldface.

translation, the anticodon stems of the tRNAs interact with the 30S subunit, and the D-stem, the elbow and the acceptor arm interact with the 50S subunit (Yusupov *et al*., 2001). The planes through the tRNAs in the A and E sites form angles of 26° and 46° respectively with the plane of the tRNA in the P site (Yusupov *et al*., 2001). The closest approach of the anticodons in the A and P sites is about 10 Å, due to the 45° angle between the A and P site codons in the mRNA (Yusupov *et al*., 2001; Selmer *et al*., 2006). Their acceptor ends are within 5 Å of each other. The closest approach between the anticodons of the P and E site tRNAs is about 6 Å. However, their elbows and 3′ ends are nearly 50 Å apart (Plate 8.1; Yusupov *et al*., 2001).

Most ribosome-interacting parts of the tRNAs are universally conserved. Not surprisingly, the binding sites for tRNA on the ribosome involve conserved parts of the ribosomal structure including both rRNA and proteins (Yusupov *et al*., 2001; Selmer *et al*., 2006; Jenner *et al*., 2010).

The T Site

The fact that the decoding of the mRNA by the tRNAs is done on the small subunit was established early on (Okamoto &

Takanami, 1963; Davies *et al*., 1964). The aminoacyl-tRNA binds to the ribosome as a ternary complex with elongation factor Tu and a bound GTP molecule (EF-Tu·GTP; see Chap. 9). The binding of such a ternary complex to the A site, with the structure it has as unbound (Nissen *et al*., 1995), would be incompatible with the size of the intersubunit cavity of the ribosome. EF-Tu would collide severely with the large subunit and in particular with the PTC. Rather, EF-Tu binds to the GTPase-associated region at the base of the L12 stalk of the large subunit (Schmeing *et al*., 2009). The aminoacyl-tRNA in the ternary complex binds initially to the T-site with the anticodon close to the decoding site, but with the acceptor end and its aminoacyl moiety far from the PTC (Fig. 8.3; Stark *et al*., 1997; Schmeing *et al*., 2009). For the anticodon to interact with the codon, a conformational change of the tRNA is needed. When the tRNA bends, the anticodon moves into the A site and the tRNA is in the hybrid A/T state (Plate 8.4). However, EF-Tu dominates in the binding of the ternary complex to the ribosome since the surface of the ribosome buried by the tRNA is only one-third of the area buried by EF-Tu (Schmeing *et al*., 2009).

The A/T site is a transition state during which correct (cognate) is distinguished from incorrect (noncognate or near-cognate) tRNAs. The difference in affinity between an isolated cognate and a near-cognate anticodon for their codons is not enough to explain the discrimination. Nevertheless, on the ribosome the cognate interaction is strongly favored (see Sec. 11.5). Incorrect matches between codon and anticodon make the ternary complex EF-Tu·GTP·aminoacyl-tRNA fall off from the ribosome. The ribosome plays an active role in the decoding. The cognate interactions are generally due to Watson–Crick base pairing. A significant part of the discrimination is due to residues of helix h44 of the 16S RNA that interact with the codon and the anticodon of the A-site bound tRNA (Valle *et al*., 2002; Stark *et al*., 2002). With cognate codons the affinity for the tRNA is increased through induced interactions with the ribosomal RNA. In particular, A1492, A1493 and G530 alter their conformations and recognize Watson–Crick base pairs

of cognate codon–anticodon complexes (see Chap. 11; Ogle & Ramakrishnan, 2005).

In addition to the interactions with EF-Tu, the aminoacyl-tRNA in the A/T site interacts with three regions of the ribosome, the shoulder domain of the 16S RNA, ribosomal protein S12 and the L11 region of 23S RNA (Valle *et al*., 2003a; Schmeing *et al*., 2009). C75 of the tRNA packs between A55 of the 16S RNA and residue 219 of EF-Tu. The highly conserved amino acid residues 74–76 of S12 interact at the junction between the acceptor arm and the D-stem with nucleotides 67 and 68. Nucleotide C56 in the conserved TΨCG sequence of the T-arm packs with A1067 of helix H43 of the 23S RNA in the GAR. Furthermore, helix H69 of the 23S RNA extends into the A site where nucleotide 1914 interacts through sugar packing with C25 of the D-arm (Stark *et al*., 2002; Valle *et al*., 2002, 2003a; Schmeing *et al*., 2009).

The A Site

When the anticodon of the aminoacyl-tRNA matches the codon in the decoding site, EF-Tu hydrolyzes its GTP molecule and dissociates. This permits the tRNA to accommodate into the A site with the anticodon bound to the codon on the small subunit and the acceptor stem with amino acyl moiety in the peptidyl transfer center on the large subunit. The shape of the tRNA when bound to the A site agrees with the classical structure of $tRNA^{Phe}$ (Robertus *et al*., 1974; Kim *et al*., 1974; Yusupov *et al*., 2001, 2005; Voorhees *et al*., 2009).

A summary of the most important contacts of the A site tRNA and the ribosome is found in Table 8.2 and Plate 8.5. In the A site the universal sequence PNSA of protein S12 (residues 44–47 in *E. coli*) is located between the 530 loop and the 1492–1493 region, and is involved in hydrogen bonding to the second base pair and to the wobble base pair of the codon-anticodon in the A site (Yusupov *et al*., 2001; Ogle *et al*., 2001, 2002). The elbow of the tRNA, between the D and T loops, is stabilized

Table 8.2 Interactions Between the Ribosome and a tRNA in the A Site

Interacting Component	Residues	tRNA Component	References
S19	C-terminal tail	Anticodon stem	Jenner *et al.*, 2010
L16	R51, R56, R60	G52, G53, U54	Voorhees *et al.*, 2009; Jenner *et al.*, 2010
L25	Q185	G53	Jenner *et al.*, 2010
L27	A2, H3	A76, C75	Voorhees *et al.*, 2009
h18	G530	A35	Ogle *et al.*, 2001
h34	C1054	G34	Ogle *et al.*, 2001
h44	A1493	A36	Ogle *et al.*, 2001
H38	G881, G882	G19	Jenner *et al.*, 2010
H38	A896	C56	Demeshkina *et al.*, 2010
	A2451	α-NH2	Nissen *et al.*, 2000
P-site tRNA	2′OH A76	α-NH2	Hansen *et al.*, 2002
H92	U2555	C74 (stacking)	Simonovic & Steitz, 2009
	G2553	C75	Kim & Green, 1999; Sharma *et al.*, 2004
	U2556–G2583	A76 (A-minor motif)	Nissen *et al.*, 2001

by protein L16 and the intersubunit bridge B1a (the A-site finger or H38; Yusupov *et al.*, 2001). The protein corresponding to L16 in archaea, L10e, has an internal loop that has not been localized, but could reach the acceptor ends of the tRNAs and participate in PTC (Voorhees *et al.*, 2009). H69, the bridge B2a, interacts with the inner side of the elbow of the L-shaped tRNA (Bashan *et al.*, 2003). Protein L25 in *E. coli* has longer variants in *T. thermophilus* and *D. radiodurans* (see Sec. 7.4). In these species, the protein reaches the A-site tRNA between the A-site finger and the L11 arm (Harms *et al.*, 2001; Jenner *et al.*, 2010). The CCA or acceptor part of the tRNA with its bound aminoacyl residue is in the PTC, close to the nascent peptide. Here C75 of the CCA end of the tRNA base-pairs with G2553 of the A loop (Green *et al.*, 1998; Yusupov *et al.*, 2001). Furthermore, A76 makes an A-minor interaction with the base pair U2506–G2583 of the 23S RNA (Hansen *et al.*, 2002b).

The P Site

The P site tRNA, just like the A-site tRNA, stretches across the tunnel between the subunits. It is centrally located at the subunit interface. During initiation the decoding is done in the P site. The P site is designed to hold the peptidyl-tRNA securely and make the peptide available for the next step of elongation. Thus, the P-site tRNA has extensive contacts with the ribosome (Plate 8.6). The P-site tRNA remains attached not only to the ribosome through the peptide in the PTC but also to the codon in the decoding site (Plate 8.5). 19% of its surface area is participating in ribosome contacts (Selmer *et al.*, 2006).

The tRNA in the P site is somewhat distorted compared to the classical crystal structure of $tRNA^{Phe}$ (Robertus *et al.*, 1974; Kim *et al.*, 1974). A kink occurs at the junction of the anticodon and the D-stems (Yusupov *et al.*, 2001; Selmer *et al.*, 2006). The distortion brings the acceptor stem closer to the amino acid in the A site. Releasing the strain, the acceptor stem would move toward the E site. The orientation of the P site tRNA is related to the A site tRNA by a 26° rotation (Yusupov *et al.*, 2001).

A detailed structural insight into how the anticodon stem loop (ASL) is bound to the P site initially came from studies of *T. thermophilus* 30S, where in the crystal packing helix h6 or the spur of one 30S subunit is bound like an ASL into the P site of another 30S subunit (Carter *et al.*, 2000). Other observations come from the crystallographic and cryo-EM studies of the 70S ribosomes from *T. thermophilus* and *E. coli* respectively (Yusupov *et al.*, 2001; Stark *et al.*, 2002; Valle *et al.*, 2002, 2003a, 2003b).

The tRNA in the P site has numerous contacts with the ribosome (Plate 8.6; Table 8.3). The earliest observation of a contact between the tRNA bound to the P site and the ribosome was the cross-link between the wobble base of the tRNA and C1400 of the 16S RNA (Ofengand & Liou, 1980). The bases G1338 and A1339 of h42 make A-minor interactions with base pairs G30:C40 and G29:C41 (Selmer *et al.*, 2006). Furthermore, the C-terminal tails of ribosomal proteins S9 and S13 interact with the ASL. Arg128 of S9, which interacts with phosphate 36 of the tRNA in the P site, is

Table 8.3 Interactions Between the Ribosome and a tRNA in the P Site

Ribosome Component	Residues	tRNA Residue	References
S9	R128	PO_4 36	Yusupov *et al.*, 2001
S13	C-terminal tail	Anticodon stem	Jenner *et al.*, 2010
L27	A2, G6, L7, R11	A77, C1, G2, G65	Voorhees *et al.*, 2009
16S RNA	C1400	C34	Prince *et al.*, 1982
	G1338	Base pair G30:C40	Selmer *et al.*, 2006
	A1339	Base pair G29:C41	Selmer *et al.*, 2006
23S RNA	G2252, G2251	C74, C75	Schmeing *et al.*, 2002; 2005
	A2450–C2501	A76 (A-minor motif)	Nissen *et al.*, 2001
	A2451	2′OH A76	Hansen *et al.*, 2002

universally conserved (Yusupov *et al.*, 2001). S13 is situated between the anticodon arms of the A and P site tRNAs, and is close to their anticodons (Stark *et al.*, 2002). Furthermore, protein L5 contacts the minor groove of H69 (subunit bridge B2a) which interacts with the T-loop and the minor groove of the D-stem of P-site tRNA (Yusupov *et al.*, 2001; Stark *et al.*, 2002).

C74 and C75 of the CCA end of the P-site tRNA form base pairs with G2252 and G2251 respectively, and A76 interacts with the P-loop (Samaha *et al.*, 1995; Green *et al.*, 1998; Nissen *et al.*, 2000; Yusupov *et al.*, 2001; Hansen *et al.*, 2002b). Furthermore, the acceptor end makes backbone–backbone contacts with the stem of the P-loop, and the CCA end is close to H93 (Yusupov *et al.*, 2001; Stark *et al.*, 2002).

The proximity of subunit bridge B2a (H69) to both the A and P sites as well as to both the decoding and the peptidyl transfer centers makes it a possible candidate for signal transmission between the decoding and the GTPase-associated region (Bashan *et al.*, 2003). Its inherent flexibility supports this possibility (Ban *et al.*, 2000).

The E site

The E site binds the deacylated tRNA molecule before it dissociates from the ribosome (Plate 8.7). It is at the end of the mRNA

and tRNA tunnel of the subunit interface on the L1 side. The E-site tRNA is related to the P-site tRNA by a rotation of 46° (Plate 8.3; Yusupov *et al*., 2001). In contrast to earlier findings (Moazed & Noller, 1989), it is clear that the E-site tRNA also interacts with both subunits (Yusupov *et al*., 2001; Yusupova *et al*., 2006; Selmer *et al*., 2006). The anticodon of the E-site tRNA is situated between the platform and the head of the small subunit (Yusupov *et al*., 2001; Selmer *et al*., 2006). Proteins S7 and S11 are the main 30S interactions with E-site tRNA. As mentioned above, the mRNA in the E site has two different conformations, depending on the number of bases, to the SD interaction. At initiation with a short distance between the SD region and the codon in the E site, the mRNA in the E site is in a tense and bent conformation, leading to there being no direct contact between codon and anticodon. However, during elongation, when the SD interaction is lost and a number of codons have been translated, the mRNA is relaxed and the first base of the codon in the E site interacts with base 36 of the anticodon of the tRNA (Yusupova *et al*., 2006; Demeshkina *et al*., 2010).

The tRNA acceptor end is far from the PTC. The binding of tRNAs to the 50S part of the E-site requires a free CCA end (Lill *et al*., 1986). A76 of the E-site tRNA is intercalated between G2421 and A2422 of the 23S RNA and hydrogen-bonded to the universally conserved C2394, leaving no room for an aminoacylated tRNA in the E-site (Schmeing *et al*., 2003; Selmer *et al*., 2006).

Proteins S7 and L1 can jointly block the exit of a deacylated tRNA from the E site. Protein L1 is deleted from the ribosome in some mutants, leading to ribosomes with a 50% activity that is restored upon addition of L1 (Subramanian & Dabbs, 1980; Sander, 1983). The L1 stalk, composed of H76–H78 and protein L1, has been observed in different conformations (Ban *et al*., 2000; Harms *et al*., 2001; Yusupov *et al*., 2001; Valle *et al*., 2003b; Schuwirth *et al*., 2005). The binding of a deacylated tRNA to the E site stabilizes the L1 stalk in a closed position (Yusupov *et al*., 2001; Valle *et al*., 2003b; Selmer *et al*., 2006). The most extreme position of the L1 stalk is when EF-P is bound on the E site side of an initiator tRNA in the

P site (Blaha *et al*., 2009). The open form of the L1 stalk would permit the dissociation of the deacylated tRNA from the E site.

Hybrid tRNA States

The chemical footprints of tRNAs bound to the different sites show characteristic patterns (Table 8.1). When the tRNA goes from the T site to the A site, through the P site and finally to the E site, it goes through several intermediate or hybrid states (Moazed & Noller, 1989). The A/T state is such a hybrid state, since it agrees with the A site for the ASL but the rest of the tRNA binds to EF-Tu as in the ternary complex.

A peptidyl-tRNA in the P site gives a characteristic protection pattern (Table 8.1). When a cognate aminoacyl-tRNA is added, peptidyl transfer occurs with interesting changes in the protection pattern. The nucleotide protections, characteristic for binding to the E site, appear (Moazed & Noller, 1989; Sharma *et al*., 2004). The P-site protections remain while the A-site protections are observed only for the 30S subunit. Addition of EF-G with GTP removes the A-site footprint. This suggests that a peptidyl-tRNA can be bound in a hybrid state, the A/P state, before translocation (Bretscher, 1968). While its ASL remains bound to the decoding part of the A site, the acceptor end has moved to the P-site part of the PTC (Fig. 8.4). This is natural, since the peptide in the exit tunnel is unlikely to shift its position depending on what tRNA it is bound to. However, it is more remarkable that the CCA end, upon peptidyl transfer, dissociates from the A-loop and associates with the P-loop. Likewise, after peptidyl transfer, the deacylated tRNA in the P-site moves according to the footprint to the P/E hybrid state. FRET and cryo-EM experiments suggest that the A/A and P/P tRNAs are in equilibrium with binding in the A/P and P/E states (Blanchard *et al*., 2004; Kim *et al*., 2007; Munro *et al*., 2007; Cornish *et al*., 2008; Korostelev *et al*., 2008; Agirrezeballa *et al*., 2008; Julian *et al*., 2008; Blanchard, 2009). The hybrid states could also be described as a translocation of the peptidyl-tRNA in relation to the 50S subunit (Ticu *et al*., 2009). The longer the peptide was, the more efficiently the hybrid state was

generated (Munro *et al.*, 2007). The hybrid state model will be further discussed in Secs. 8.6 and 11.4.

In going from the P/P state to the P/E state, the elbow of the tRNA moves by about 40 Å. However, the movement of the tRNA from the A/A to the A/P state is very marginal except for the CCA end (Plate 8.3; Agirrezabala *et al.*, 2008).

Yet one hybrid state has been identified — P/I (Allen *et al.*, 2007; Simonetti *et al.*, 2008). When the fMet is bound to the 70S ribosome with the anticodon at the AUG codon in the P site, it is supported neither by an E-site tRNA nor by a nascent peptide chain held in the exit tunnel. This causes the initiator tRNA to bind in the unique P/I hybrid state, where the tRNA is bound between the P and P/E states (Figs. 8.3 and 8.5). The translation factor EF-P may reorient the initiator tRNA, enabling it to bind into the proper P site and engage in the formation of the first peptide bond (Aoki *et al.*, 2008; Blaha *et al.*, 2008).

8.3 THE PEPTIDYL TRANSFER CENTER

The central function of the ribosome is to transfer a nascent peptide from the tRNA in the P site to the amino acid residue of the tRNA in the A site. These tRNAs are bound to subsequent codons of the mRNA in the decoding site. The peptidyl transfer center (PTC) is the site of this activity as well as the hydrolysis of

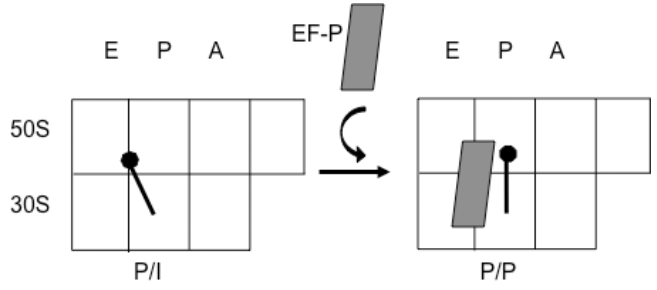

Fig. 8.5 Schematic representation of the ribosome with fMet-tRNA bound in the P/I state. It is moved into the proper P site aided by EF-P.

the peptide from a tRNA during termination. The nature of the PTC has been the subject of studies for a long time. It has long been clear that the large subunit is responsible for peptidyl transfer (Okamoto & Takanami, 1963; Monro *et al.*, 1968). A number of large subunit proteins affect peptidyl transfer but definite involvement has been lacking (Hampl *et al.*, 1981; Liljas, 1982). Kethoxal modification of guanine residues in the 16S RNA to inhibit the binding of tRNA has led to an increased interest in the rRNAs (Noller & Chaires, 1972). The identification of ribozymes with different catalytic activities (Cech *et al.*, 1981; Guerrier-Takada *et al.*, 1983) further suggested that the ribosome could belong to the family of ribozymes. Thus, assays representative of peptidyl transfer such as the puromycin reaction were performed with rRNA essentially devoid of ribosomal proteins, suggesting that the ribosome might be a ribozyme (Noller *et al.*, 1992; Noller, 1993).

A number of approaches have been used to identify the regions of the 23S RNA that are involved in peptidyl transfer (Sonenberg *et al.*, 1975). The central loop of domain V is of great importance (Barta *et al.*, 1984). Many nucleotides in this area are completely conserved; resistance against antibiotics that inhibit peptidyl transfer is found in this region; footprinting of nucleotides protected by tRNAs is found in this region; cross-linking from the acceptor ends of tRNAs, or from the amino acid and peptide attached to tRNA, is found in this domain; mutations in this region can severely affect peptidyl transfer (Eckerman & Symons, 1978; Hummel & Böck, 1987; Vester & Garrett, 1988; Mankin & Garrett, 1991; Moazed & Noller, 1991; Green & Noller, 1997).

Through crystallography the PTC has been identified as a cavity on the interface side of the large subunit (Nissen *et al.*, 2000). In the analyses of large subunits no protein was seen in the vicinity of the PTC (Ban *et al.*, 2000; Nissen *et al.*, 2000; Harms *et al.*, 2001). Thus, in the structure of the halophilic large subunit, no protein was observed within a radius of 18 Å from the PTC (Ban *et al.*, 2000; Nissen *et al.*, 2000). From more recent crystallography it is clear that a well-ordered PTC requires studies of 70S

ribosomes with stably bound tRNA molecules (Voorhees *et al.*, 2009; Jenner *et al.*, 2010). In such studies several proteins have regained interest (Plate 8.8).

The A- and P-site tRNAs bind with their CCA ends to the A and P loops respectively. Experiments to remove amino acid residues from the amino terminus of L27 have shown that the first three amino acids are important for high peptidyl transfer activity (Plate 7.5; Maguire *et al.*, 2005). Crystallographic studies of 70S ribosomes from *T. thermophilus* with A- and P-site tRNAs have shown that the N-terminal tail of L27 interacts with the 3′ ends of both A and P site tRNA (Plate 7.5; Selmer *et al.*, 2006; Voorhees *et al.*, 2009). L27 is not found in archaea (Ban *et al.*, 2000). An archaeal protein that is bound in a similar location on the interface side of the large subunit just below the central protuberance is L21e. However, its tail folds backward toward the interior of the subunit (Ban *et al.*, 2000; Harms *et al.*, 2001). Protein L16, on the other hand, interacts with the elbow regions of both tRNAs and has a loop of 11 residues in archaeal species, which is invisible in the structure of *H. marismortui*. Model building suggests that this loop could reach and interact with the acceptor ends of both A and P site tRNAs (Voorhees *et al.*, 2009).

The PTC has an approximate twofold symmetry. The CCA ends are related by an approximate 180° rotation (Nissen *et al.*, 2000; Yusupov *et al.*, 2001; Schmeing *et al.*, 2002; Hansen *et al.*, 2002b; Bashan *et al.*, 2003; Agmon *et al.*, 2003). Nucleotides 73–76 constitute the rotating moiety (Bashan *et al.*, 2003). In fact, much of the PTC has the same twofold rotational symmetry (Nissen *et al.*, 2000; Bashan *et al.*, 2003). The twofold symmetry includes the A and P loops. Around 90 nucleotides of the A-site part of the PTC are related by a 180° rotation to 110 nucleotides of the P-site part (Bashan *et al.*, 2003; Agmon *et al.*, 2003; Bokov & Stenberg, 2009; see Chap. 13). These two symmetrically related parts of the PTC are two halves of the central part of domain V of the 23S RNA.

The functional aspects of the PTC are further discussed in Sec. 11.4.

8.4 THE POLYPEPTIDE EXIT TUNNEL

It has long been known that ribosomes protect a number of amino acids of the nascent polypeptide from digestion by proteolytic enzymes (Malkin & Rich, 1967; Blobel & Sabatini, 1970). It was suggested that there could be a tunnel in the large subunit through which the polypeptide exits. From an early stage, it was clear that ribosomes interacted with microsomal membranes through the large subunit (Sabatini *et al.*, 1966). A tunnel was indirectly inferred from early EM studies in which ribosomes associated through the back of the large subunit when a dimeric protein was synthesized. Evidently, the nascent peptide appeared from the back side of the large ribosomal subunit (Bernabeau & Lake, 1982).

Subsequently, a tunnel through the large subunit was directly observed by electron microscopy at very low resolution (Milligan & Unwin, 1986; Yonath *et al.*, 1987). In more recent cryo-EM studies, a branched tunnel system was identified (Frank *et al.*, 1995; Gabashvili *et al.*, 2001). The crystallographic investigations (Ban *et al.*, 2000; Nissen *et al.*, 2000; Harms *et al.*, 2001) have made it clear that this tunnel originates at the PTC and leads to the outer surface of the large subunit (Plate 8.9). The tunnel length is 80–100 Å and the width varies between 10 Å and 20 Å, with walls mainly composed of RNA (82%), the remainder being protein (Voss *et al.*, 2006). In yeast, the tunnel is continuous with the translocon tunnel (Beckmann *et al.*, 1997; Menetret *et al.*, 2000). This is the tunnel through which the nascent peptide exits from the ribosome and can be further transported through the cytoplasmic membrane. A tunnel of this type is a necessity for the transport of proteins from the cytoplasm to other compartments (see Chap. 12). The transport needs a stable tunnel that can contact a receptor structure. Such a stable tunnel could only be generated in the body of the large subunit, since the subunit interface is highly dynamic. Thus, the stable organization of the large subunit corresponds to the need for a tunnel that remains open during the different stages of translation.

The most narrow passage of the peptide exit tunnel is composed of parts of the 23S RNA and two ribosomal proteins, L4 and

L22 (Nissen *et al.*, 2000; Berisio *et al.*, 2003b). Both L4 and L22 are built of globular bodies with a long protruding loop or β-ribbon (Worbs *et al.*, 2000; Unge *et al.*, 1999). The globular parts of the proteins are located on the outer surface of the large subunit stretching their tips, forming the most constricted part of the tunnel (Nissen *et al.*, 2000; Harms *et al.*, 2001; Berisio *et al.*, 2003b). Macrolide antibiotics (see Sec. 10.5), such as erythromycin, bind at the constriction of the tunnel not far from the PTC (Schlünzen *et al.*, 2001; Hansen *et al.*, 2002a).

With the knowledge of the exit tunnel, the conformation of the nascent peptide becomes an interesting topic, which has been thoroughly studied. Is the nascent chain straight or does it have secondary structure? Can the ribosome allow a partial folding (become pregnant) with a growing polypeptide? Lim and Spirin (1986) made a stereochemical analysis and suggested that the nascent polypeptide may form an α-helix when passing through the tunnel. Using labeled N-termini of nascent polypeptides, the emergence of the labels was observed after different lengths of nascent polypeptide had been synthesized for different proteins (Tsalkova *et al.*, 1998; Hardesty & Kramer, 2001). Between 44 and 72 amino acid residues could be hidden in the tunnel. An α-helix of 72 amino acids would have a length of 108 Å. It was found that the N-termini of proteins with large amounts of helical conformation emerged later than proteins with large amounts of β-structure. Studies using FRET suggest that transmembrane (TM) proteins can adopt helical conformations throughout the exit tunnel (Woolhead *et al.*, 2004).

Studies by cryo-EM and other methods — reviewed by Wilson & Beckmann (2011) — describe the tunnel as being divided into three parts: the upper part, above the constriction; the central part; the lower tunnel and the vestibule, which forms a wider opening. The upper and the central part of the tunnel have a joint length of about 50 Å, while the lower part is about 30 Å long. The depth of the vestibule is around 20 Å. These investigations show first of all that it is highly unlikely that any part of the tertiary structure of the nascent chain could fold inside the tunnel. Furthermore, some nascent polypeptides, despite high helical propensity, do not fold to

helical conformation in the central part of the tunnel. However, in the upper or lower part of the tunnel, the studies suggest that the nascent polypeptide can form an α-helix. In addition, it has been observed that β-hairpins can form in the vestibule part of the tunnel (Kosolapov & Deutsch, 2009).

Certain peptides can get stalled in the exit tunnel. This can cause a regulation of downstream genes (see reviews by Tenson & Ehrenberg, 2002; Wilson & Beckmann, 2011). Generally, the stalling is due to specific interactions between residues in the nascent chain with tunnel components. This is characterized for the secretion monitor polypeptide (SecM; Nakatogawa & Ito, 2001; Bhushan *et al.*, 2011). SecM bound in the tunnel leads to a shifted position of the ester linkage between the tRNA and the nascent peptide by about 2 Å. This would reduce the efficiency of peptidyl transfer and cause the stalling.

The polypeptide FXXXXWIXXXXGIRAGP also gets stalled (Nakatogawa & Ito, 2002). Mutations in the constriction part of the tunnel can avoid the arrest of translation (Nakatogawa & Ito, 2002). Peptides with a C-terminal prolyl residue can also induce a stalling of the ribosome (Gong & Yanofsky, 2002).

Two proteins in the archaeal ribosome are associated with the opening of the tunnel on the solvent side of the large subunit. They are L23 and L39e (Nissen *et al.*, 2000). In bacteria, there is only one protein, L23. L39e is a small and extended protein that in archaea replaces the tail of bacterial L23 (Harms *et al.*, 2001). L23 is part of the contact to the protein folding and transport machinery that docks at the opening of the exit site (Kramer *et al.*, 2002b; Pool *et al.*, 2002). This will be further discussed in Chap. 12.

8.5 THE GTPase BINDING SITE

One group of translation factors binds and hydrolyzes GTP (see Sec. 9.1). They are part of the large family of G-proteins (Bourne *et al.*, 1990, 1991). The translational GTPases (trGTPases) all bind to the same site of the ribosome and their GTPase activity is probably induced in similar ways (see Chaps. 9 and 11).

Elongation factor Tu (EF-Tu or EF-1α in eukaryotes) binds to the ribosome as a ternary complex with an aminoacyl tRNA and GTP molecule (Kaziro, 1979). It binds at the base of the L12 stalk of the large subunit, while the opposite end of the ternary complex, the anticodon of the tRNA, can interact with the decoding site of the small subunit (Stark *et al*., 1997, 2002; Valle *et al*., 2002, 2003a; Schuette *et al*., 2009; Villa *et al*., 2009, Schmeing *et al*., 2009; Voorhees *et al*., 2010).

Structural studies of EF-G bound to the ribosome have also been performed (Agrawal *et al*., 1998, 1999; Stark *et al*., 2000; Valle *et al*., 2003b; Connell *et al*., 2007, Gao *et al*., 2009). The overall shape of EF-G is very similar to that of the ternary complex of EF-Tu with tRNA (see Sec. 9.3; Nissen *et al*., 1995). When EF-G binds to the ribosome, it overlaps with the binding site of the ternary complex of EF-Tu and tRNA (Agrawal *et al*., 1998, 1999). Thus, domain IV of EF-G corresponds structurally to the ASL of the tRNA and interacts with the decoding region of the small subunit. The trGTPases IF2 and RF3 interact with the ribosome in related ways (see Chap. 9).

The conserved domain II of all trGTPases interacts with the small subunit in the region of helix h5 of the 16S RNA and protein S4 (Stark *et al*., 1997; Agrawal *et al*., 1988; Wilson & Noller, 1998; Valle *et al*., 2003a,b). The binding site for the G-domain of trGTPases on the large subunit has important contributions of rRNA, the α-sarcin/ricin loop (SRL) and GAR. The latter is composed of H43, H44 and ribosomal proteins L11 and the L10–L12 complex (Ban *et al*., 2000; Harms *et al*., 2001). EF-G makes a footprint at 1067 of domain II of the 23S RNA (Moazed *et al*., 1988). At an early stage, a cross-link was also identified between EF-G and nucleotide A1067 of the 23S RNA (Sköld, 1983). This interaction is distant from the GTP binding site of the factors. The G-domain interaction with GAR is described by Agrawal *et al*., 1998, 1999; Valle *et al*., 2003a, b; Connell *et al*., 2007; Gao *et al*., 2009; and Tourigny *et al*., 2013.

The SRL of the 23S RNA is formed by H95, which contains residues 2653–2667 (Endo *et al*., 1987). The loop got its name from the inhibiting modifications by a number of plant enzymes, among

others α-sarcin and ricin, on this region in eukaryotes (Wool *et al.*, 1992). SRL interacts with both elongation factors, as seen from protection of the rRNA to chemical reagents (Moazed *et al.*, 1988). It interacts specifically with the G-domains of the factors (Hausner *et al.*, 1987; Moazed *et al.*, 1988; La Teana *et al.*, 2001; Valle *et al.*, 2002, 2003a). Isolated EF-G can bind a 12-nucleotide fragment of the SRL (Munishkin & Wool, 1997).

8.6 THE RIBOSOMAL STATES

In early studies of the ribosomes, different states have been discussed, and also reversible conformational changes (Spirin, 1968; Spirin, 1985; Burma *et al.*, 1985; Noller 1991; Agrawal *et al.*, 1999b; Frank & Agrawal, 2000). Detailed insights into such states have been gained through structural studies. The nomenclature of the ribosomal states may be somewhat confusing. The number of states may be smaller than the number of names used. On the other hand, many intermediates are too short-lived to be detected with current experimental techniques (Frank, 2012).

Free Subunits and Translating Ribosomes, Initiation

During initiation, separated 30S and 50S subunits form 70S ribosomes and can bind an mRNA to the 30S subunit and an fMet-tRNA to the P site. This initiator-tRNA and the inter-subunit bridges are highly relevant to the association of the subunits (Zavialov & Ehrenberg, 2003). For example, intersubunit bridge B2a is next to the P-site, the binding site for the initiator-tRNA.

The Pre- and Posttranslocation States

In the elongation cycle, when an aminoacyl-tRNA is bound to the A site, peptidyl transfer can occur spontaneously. This is the ribosomal pretranslocation state. The ribosome then alternates between two main states with the peptidyl-tRNA bound to the A/A or the A/P site. Correspondingly, the deacylated tRNA is

bound to either the P/P or the P/E site (Plate 8.3; Moazed & Noller, 1989; Cornish *et al*., 2008). This also leads to a rotation of the small subunit in the counterclockwise direction with regard to the large subunit. Agirrezabala *et al*. (2008) found that about two-thirds of the ribosomes have undergone this rotation from the state called MSI to MSII. Translocation of the two tRNAs to the P and E sites respectively, and the movement of the mRNA to expose the next codon in the A site, are catalyzed by EF-G in complex with GTP. EF-G·GTP has a preference to bind to the MSII conformation of the ribosome. After GTP hydrolysis and completed translocation of the tRNAs, the ribosome returns to MSI. This is the posttranslocation state.

These two states can be identified in different ways. A classical method is to use puromycin (see Sec. 10.4). As long as a tRNA is in the A/A site, puromycin cannot bind to the PTC and react with and subsequently release the nascent peptide. However, after translocation to the post-translocation state, this is possible. A difficulty here is that if the peptidyl-tRNA is bound at the A/P site, puromycin is nevertheless able to bind and slowly react with the nascent chain (Sharma *et al*., 2004). A simple feature that identifies the posttranslocation ribosome is that when the peptidyl-tRNA is translocated to the P site an aminoacyl-tRNA can bind to the A site. The location of the peptidyl-tRNA also dictates which elongation factor should bind (Valle *et al*., 2003b; Zavialov & Ehrenberg, 2003).

The MSI and MSII States

The intersubunit bridges allow a certain rotational flexibility in the subunit interactions. The bridge B3 is at the pivot point of the rotation. Two main states have been observed (Agrawal *et al*., 1999b; Frank & Agrawal, 2000, 2001; Gao *et al*., 2003). Rotation occurs during all stages of translation and is associated with the movement of tRNAs between the different sites on the ribosome (Table 8.4). In the canonical state (MSI), the tRNAs are bound to the classical positions, A/A and P/P. In MSII the small subunit has

Table 8.4. Subunit Orientation and tRNA Location with Different Ribosome Ligands

A site	P site*	E site*	trGTPase Factor	30S/head Rotation	State of tRNAs	Resol. (Å)†	Reference‡
+	+	+	−	0°	A, P, E	5.5	Yusupov, 2001
IF1	fMet-tRNA	IF3	IF2·GDPNP	4°	P/I	13.8/8.6	Allen, 2005
−	fMet-tRNA	−	IF2·GDPCP	5°	P/P	14.3/9.5	Myasnikov, 2005
−	fMet-tRNA	−	IF2·GDP	0°	P/P	13.1/9.3	Myasnikov, 2005
−	fMet-tRNA	EF-P	−	0°	P/P	3.5	Blaha, 2009
Trp-tRNA	Phe-tRNA	tRNA	EF-Tu·GDPCP	0°	A/T, P, E	3.2	Voorhees, 2010
Thr-tRNA	Phe-tRNA	tRNA	EF-Tu·GDP+kir	0°	A/T, P, E	3.6	Schmeing, 2009
fMet-Trp-tRNA	tRNA	−	−	6°	A/P, P/E	8.9	Agirrezabala, 2008
−	tRNA	−	EF-G·GDPNP	6°	P/E	10.8	Valle, 2003b
−	tRNA	−	EF-G·GDPCP	9°/3°	P/E	3.1	Tourigny, 2013
−	MFTI-tRNA	tRNA	EF-G·GDP+FA	0°	P/P, E/E	13.1	Valle, 2003b
−	fMet-tRNA	tRNA	EF-G·GDP+FA	0°	P/P, E/E	3.6	Gao, 2009
−	fMet-tRNA	−	TetO·GTP-γS	0°	P/P	16/12	Spahn, 2001

(*Continued*)

Table 8.4. (*Continued*)

A site	P site*	E site*	trGTPase factor	30S/head rotation	State of tRNAs	Resol. (Å)†	Reference‡
RF1	tRNA	tRNA	–	0°	P/P, E/E	3.2	Laurberg, 2008
RF1	$tRNA^{fMet}$	–	–	0°	P/P	3.6	Korostelev, 2010
RF2	tRNA	tRNA	–	0°	P/P, E/E	3.5	Weixlbaumer, 2008
RF1	fMet-tRNA		RF3·GDP	0°	P/P	11.2	Pallesen, 2013
RF1	tRNA		RF3·GDPNP	10°	P/E	15.5/9.7	Gao, 2007a
–	tRNA		RF3·GDPCP	9°/3°	P/E	3.8	Jin, 2011
–	–	–	RF3·GDPNP	7°/14°	–	3.3	Zhou, 2012
RRF	tRNA	–	–	6°	P/E	14.1	Gao, 2005
RRF	$tRNA^{Phe}$	–	–	9°/4°	P/E	3.2	Dunkle, 2011
RRF	ASL^{Phe}	$tRNA^{fMet}$	–	0°	P, E	3.5	Weixlbaumer, 2007
RRF	–	–	EF-G·GDPNP	–	–	9.1/5.7	Gao, 2007b (50S)

*tRNA without any prefix means deacylated tRNA.

† The resolution for cryo-EM is presented by the 0.5 Fourier shell coefficient/3σ conventions.

‡ Only the name of the first author is shown.

rotated in the anti-clockwise direction by about 6° in relation to the large subunit, while the tRNAs move into the hybrid states, A/P and P/E. MSII can be in equilibrium with MSI (Cornish *et al*., 2008; Agirrezabala *et al*., 2008). There is a significant variation in the range of subunit rotation (Ratje *et al*., 2010). There are also a number of substates.

The binding of trGTPases in complex with GTP analogs is almost always associated with MSII. This is true of IF2, EF-G and RF3. On the contrary, EF-Tu, in complex with a GTP analog binds to MSI. However, after EF-Tu has dissociated from the ribosome and peptidyl transfer has occurred, the ribosome can spontaneously adopt the MSII state. EF-G·GTP binds to MSII and translocation induces a ratchet-like motion back to the MSI state (Fig. 8.6; Agrawal *et al*., 1999b; Frank & Agrawal, 2000, 2001; Gao *et al*., 2003; Valle *et al*., 2003b; Tourigny *et al*., 2013). However, the crystal structure of EF-G bound to 70S ribosomes in complex with GDP and FA shows the subunits in their canonical, MSI, state (Gao *et al*., 2009). Interestingly, EF-Tu and EF-G bind to opposite states of the ribosome. Furthermore, MSII is invariably associated with tRNAs in hybrid states and MSI is associated with the canonical states of the tRNAs if we disregard the A/T state.

An orthogonal and also variable rotation or swivel of up to 14° of the head of the small subunit is associated with the subunit rotation (Schuwirth *et al*., 2005). The movements between canonical and hybrid states of the head and shoulder of the small subunit are also closely associated with the interaction between a tRNA and its cognate codon (see Sect. 11.4). In addition, protein L1 moves 20 Å toward the E site through a rearrangement of H76 (Agirrezabala *et al*., 2008; Ratje *et al*., 2010).

The subunit rotation of about 6° corresponds to movements of about 20 Å at the edge of the small subunit (Valle *et al*., 2003b). The angle reported differs somewhat, partly depending on the resolution and method of structure alignment. The largest relative movement occurs between the head of the small subunit and the central protuberance of the large subunit. The axis of rotation is

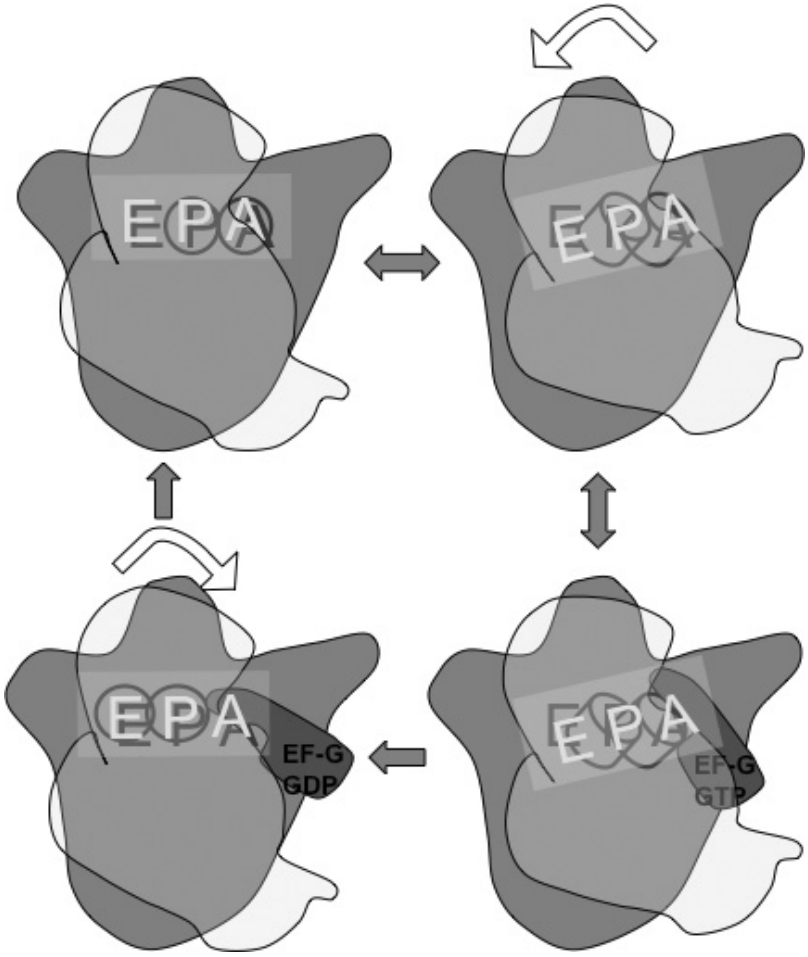

Fig. 8.6 After peptidyl transfer the tRNAs and the mRNA on the ribosome undergo translocation. Above, left: The tRNAs in the A/A and P/P sites participate in peptidyl transfer. Above, right: After peptidyl transfer the tRNAs can rotate into their hybrid states, A/P and P/E. Coupled to this, the small subunit rotates anticlockwise about 6° with regard to the large subunit. Below: After interaction with EF-G·GTP the ribosome returns to the canonical subunit orientation. As a result the peptidyl-tRNA and the deacylated tRNA move into the P and E sites respectively. Simultaneously, the mRNA moves to expose the next codon in the A site.

more or less perpendicular to the subunit interface and passes through h44 between the bridges B3 and B5 just above h27 (see Sec. 7.3; Gabashvili *et al.*, 2000; Yusupov *et al.*, 2001; Gao *et al.*, 2003; Zhang *et al.*, 2009). In this movement, three of the intersubunit bridges (B1a–B1c) change significantly. For bridges B1b and B1c, protein L5 finds alternate interactions with S13. H38 of bridge B1a moves from an interaction with protein S13 to one with protein S19 (Valle *et al.*, 2003b; Agirrezabala *et al.*, 2008).

Single-molecule studies using FRET (see Chap. 3) have given us new insights into the rotation of ribosomal subunits. The method has the potential to study the oscillations of the ribosome and the possible intermediate states.

The Locked and Unlocked States

Locked and unlocked states of the ribosome were discussed at an early stage (Spirin, 1968) and have gained renewed interest. The rotation of the small ribosomal subunit in relation to the large subunit is induced in the anticlockwise direction by peptidyl transfer (MSII) and in the opposite direction by EF-G·GTP (MSI; Frank & Agrawal, 2001; Zhang *et al.*, 2009). The rotation can also be induced in empty ribosomes (Agrawal *et al.*, 1999; Zhang *et al.*, 2009) or when a deacylated tRNA is situated in the P site (Valle *et al.*, 2003b). However, if a peptidyl-tRNA is located in the P site the ratchet-like movement is not possible. In this state EF-G·GDP is able to bind in the presence of fusidic acid (FA) but not EF-G·GTP (Valle *et al.*, 2003b). MSI is apparently a locked state with the stable position of the peptidyl-tRNA in the P-site (Zavialov & Ehrenberg, 2003; Valle *et al.*, 2003b; Aitken & Puglisi, 2010). The locked state can be unlocked (MSII) by binding an aminoacyl-tRNA to the A site, which leads to continued peptide transfer, or by removing the peptide from the P-site tRNA with puromycin (Valle *et al.*, 2003b; Aitken & Puglisi, 2010). Interestingly, L1 in the locked state is in an open position, but in the unlocked MSII state it interacts with the E-site tRNA.

The Restrictive and *Ram* States

During translation, the small subunit can also oscillate between two different states (Schuwirth *et al*., 2005), which are related to the fidelity of translation (see Sec. 11.4). In the restrictive state, the ribosome will stabilize the binding of cognate tRNA, but it has a reduced affinity for near-cognate aminoacyl-tRNA (Pape *et al*., 1998–2000). In the ribosome ambiguity state (ram), the affinity for tRNA in the A-site, cognate as well as noncognate, is higher. The fidelity of translation is naturally affected if one state becomes stabilized over the other (Allen & Noller, 1989; Lodmell & Dahlberg, 1997).

These two states correspond to two conformations of the small subunit (Ogle *et al*., 2003; Zaher & Green, 2009). When the A site is empty, the subunit is in an open or restrictive conformation (see Table 8.2). When the ASL of a cognate tRNA interacts with the mRNA in the decoding site, the small subunit adopts the closed or ram conformation (Ogle *et al*., 2003). The conformational change, due to the strong cognate interaction, is composed of rotational movements of the head and the shoulder of the small subunit toward the subunit center (Ogle *et al*., 2002, 2003). One element of the closed state is the change in conformation and the participation of G530, A1492 and A1493 in the decoding mechanism between the codon and the anticodon (Carter *et al*., 2000; Ogle *et al*., 2001–2003). A near-cognate tRNA-ASL associates weakly with the decoding site and does not induce the closed form of the subunit (Ogle *et al*., 2002).

The ribosome can also adopt the ram state in complex with error-inducing antibiotics (see Sec. 10.3). Thus, paromomycin makes the small subunit adopt its closed conformation even when a near-cognate tRNA is bound to the decoding site. In particular, the bases A1492 and A1493 are swung out of their normal positions as if they would identify a cognate interaction of mRNA and tRNA (Ogle *et al*., 2002).

Streptomycin is another error-inducing antibiotic (see Sec. 10.3). When bound, it leads to the closed conformation by interaction with well-separated parts of the small subunit (Table 8.5; Carter

Table 8.5 Induction of the Ram and Restrictive Conformations of the Small Subunit

Ribosomal State	Ram		Restrictive
Conformation of 30S subunit	Closed		Open
Empty A-site			X
Cognate tRNA in A-site	X		
Mutations in h27 of 16S RNA	X	or	X
Paromomycin	X		
Streptomycin	X		
Str resistance, S12 mutants			X
Revertants from *Str* resistance (mutants of S4 and S5)	X		

et al., 2000; Ogle *et al.*, 2003). Resistance to streptomycin is primarily due to mutations in ribosomal protein S12, which is located on the shoulder of the small subunit near the A-site and near the binding site of streptomycin (Kurland *et al.*, 1996; Wimberley *et al.*, 2000, Carter *et al.*, 2000). The S12 mutants are restrictive. Many of them disfavor the closed conformation (Ogle *et al.*, 2003). Some S12 mutants are hyperaccurate. To get a balanced level of fidelity and rate of translation, the bacterium can become streptomycin-dependent (Bilgin *et al.*, 1992). Revertants from streptomycin dependence are primarily found as mutants of ribosomal proteins S4 and S5 (Kurland *et al.*, 1996). These are ram mutants and are located on the opposite side of the subunit from S12 and on each side of the interface between the shoulder and the body of the subunit where the conformational alteration occurs (Wimberley *et al.*, 2000; Ogle *et al.*, 2003). The ram mutants decrease the number of bonds that need to be broken to allow closure of the domain (Ogle *et al.*, 2003).

Another component close to S12 that has been identified as important is helix h27, where mutations can both increase and decrease fidelity (Lodmell & Dahlberg, 1997). It was suggested that this helix has two different modes of base pairing and that mutants

would affect the balance. It now appears that these mutations affect the interface of the shoulder and the environment around h44 (Ogle *et al*., 2003).

The restrictive and ram conformations are related to the pre- and posttranslocational conformations. The open or restrictive state, which normally has no tRNA bound to the A-site, corresponds to the posttranslocational ribosome. The closed state, normally induced by the cognate tRNA, leads to a number of subsequent steps.

This page intentionally left blank

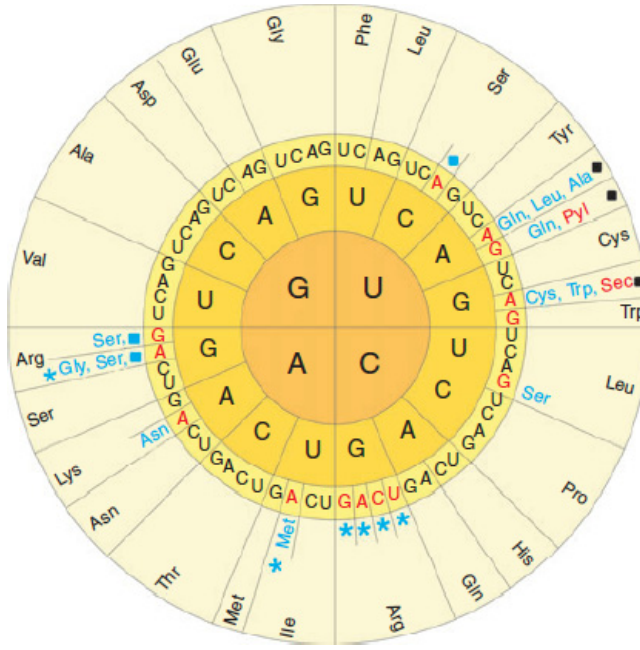

Plate 4.1 Changes of the genetic code, which has been seen in some species or organelles. Canonical codons and amino acids that are not changed are shown in black. Codons marked in red are changed to the amino acids shown in blue. Amino acids in red are noncanonical amino acids in addition to the 20 canonical ones. Filled squares denote stop codons. Blue asterisks indicate codons that can be unassigned in some species. (Reprinted with permission from Ambrogelly, Palioura and Söll, Natural expansion of the genetic code, *Nat Chem Biol* 3: 29–35. Copyright 2007, Nature Publishing Group.)

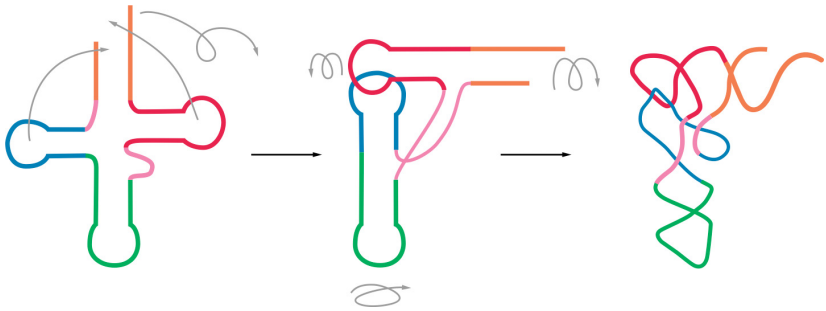

Plate 5.1 A schematic representation of the way the cloverleaf structure is organized in three dimensions. (Copied with permission from Liljas *et al*., 2009, *Textbook of Structural Biology*.)

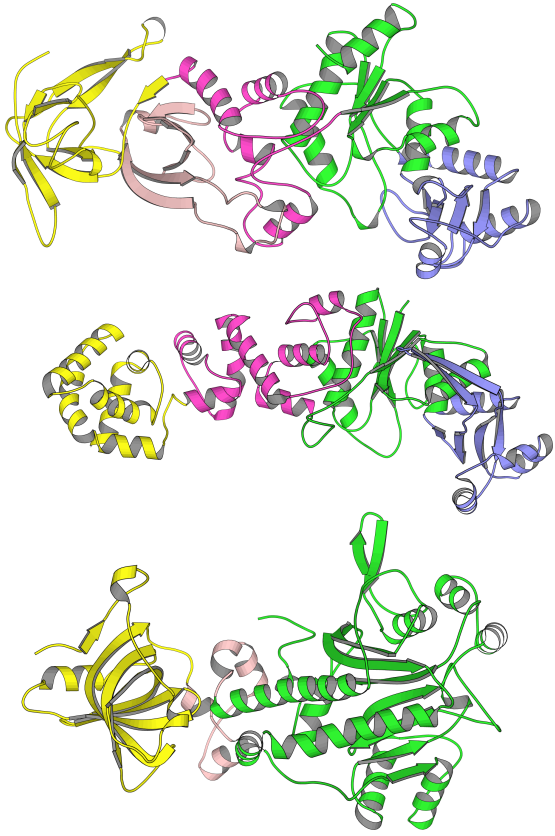

Plate 5.2 Gln, Glu (both class I, subclass b) and Asp (class II, subclass b) aaRS. The catalytic domains for GlnRS and GluRS (green) have an insert (blue), which is the editing domain. GluRS belongs to the same class and subclass as GlnRS but has a quite different structure. (Courtesy of Lars Liljas.)

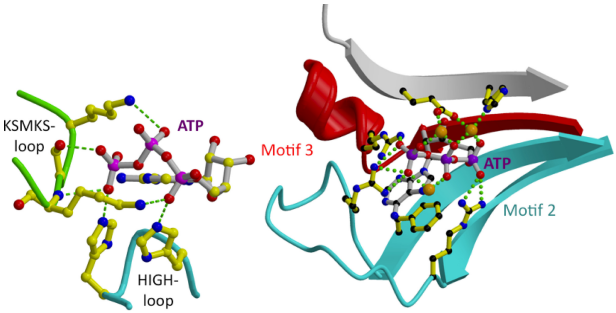

Plate 5.3 The binding of ATP to tRNA synthetases. *Left*: TyrRS (class Ic) with conserved residues of the KMSKS loop (green) and HIGH loop (blue) interacting with the ATP. *Right*: ProRS (class IIa). Residues of motifs 2 (blue) and 3 (red) interact with the ATP. The brown bolls represent magnesium ions. (Courtesy of Stephen Cusack.)

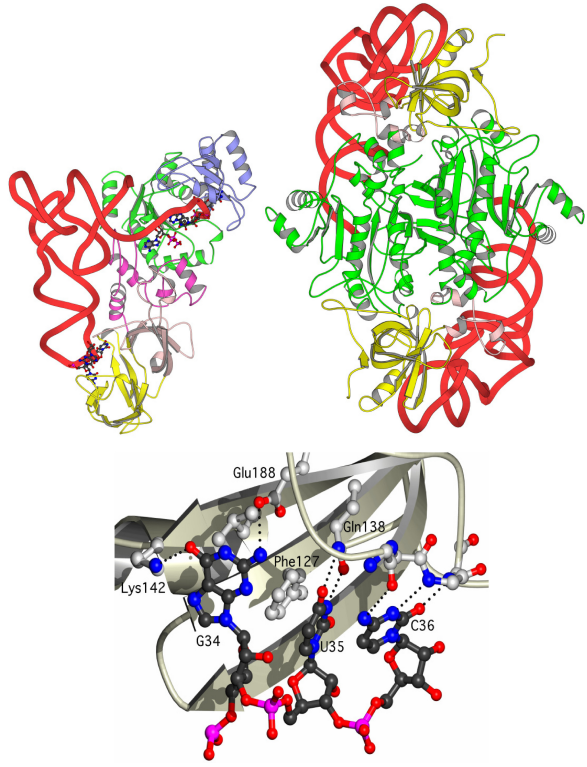

Plate 5.4 *Top left*: Gln-tRNA with GlnRS (class I). *Top right*: AspRS dimer with Asp-tRNA (class II). In both cases the anticodon is in contact with the RS. *Bottom*: Details of interaction of the anticodon with the RS in the case of AspRS. (Courtesy of Lars Liljas.)

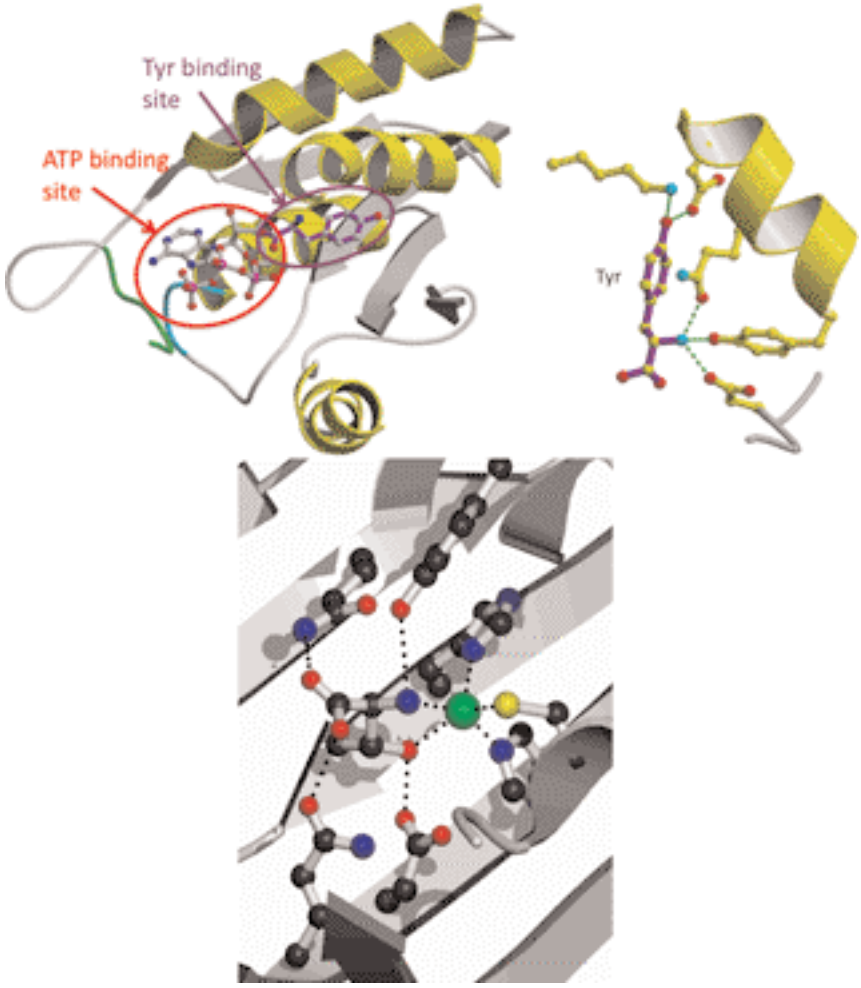

Plate 5.5 *Above left*: The catalytic domain of TyrRS (class Ic) with a bound ATP molecule and a tyrosine ready to react (courtesy of Stephen Cusack). *Above right*: The interactions of TyrRS with the tyrosine, which is specifically recognized by the hydrogen bonds to the OH group. *Below*: The specific binding of threonine to ThrRS (class IIa). A zinc ion (green) prevents valine from binding. (Courtesy of Lars Liljas.)

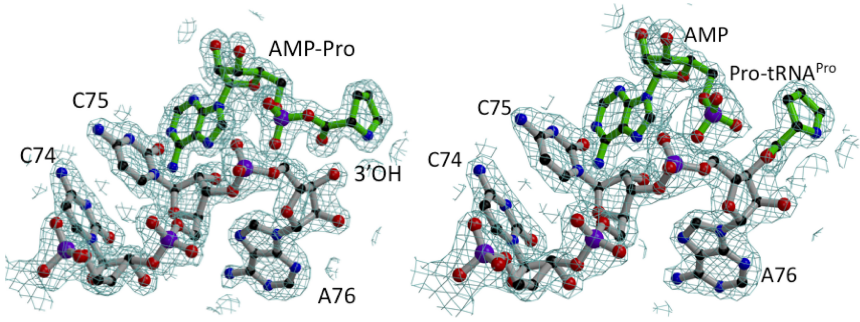

Plate 5.6 Crystal structures in the case of ProRS (class IIa). *Left*: The activated Pro residue is placed next to the CCA end of tRNAPro. *Right*: The aminoacylation is complete and the Pro residue is attached to the 3′ end of the tRNA, with the resulting AMP molecule still attached. (Courtesy of S. Cusack.)

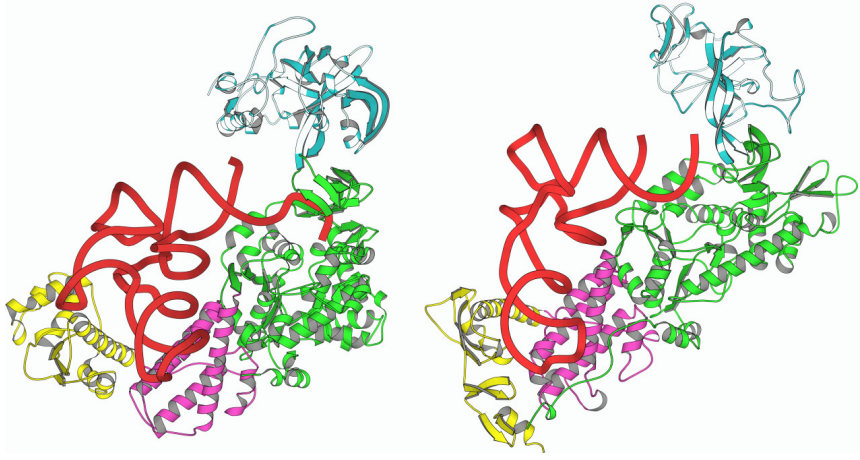

Plate 5.7 *Left*: LeuRS has no contact with the anticodon of the bound tRNA. However, the long variable loop (left part of the tRNA) is part of the tRNA recognition. The CCA end and the amino acid are in contact with the catalytic domain (green). The editing domain is in cyan. *Right*: IleRS with Ile-tRNA. The anticodon is recognized by the synthetase. Here the CCA end and the amino acid are close to the editing domain. (Courtesy of Lars Liljas.)

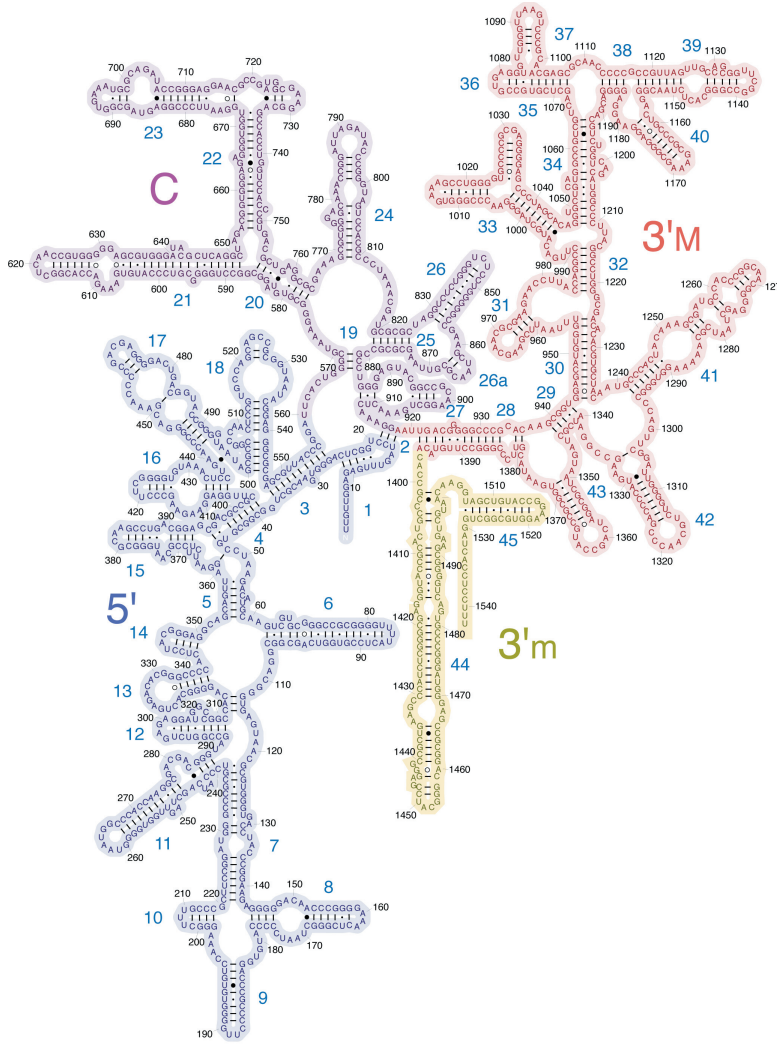

(a)

Plate 6.1 The secondary structure and domain organization of the ribosomal RNAs from *T. thermophilus*. **(a)** 16S RNA. The four domains are shown in different colors: the 5′ domain in blue, the central domain in purple, the 3′ major domain in red and the 3′ minor domain in yellow. (Courtesy of Harry Noller, UCSC.)

(*Continued*)

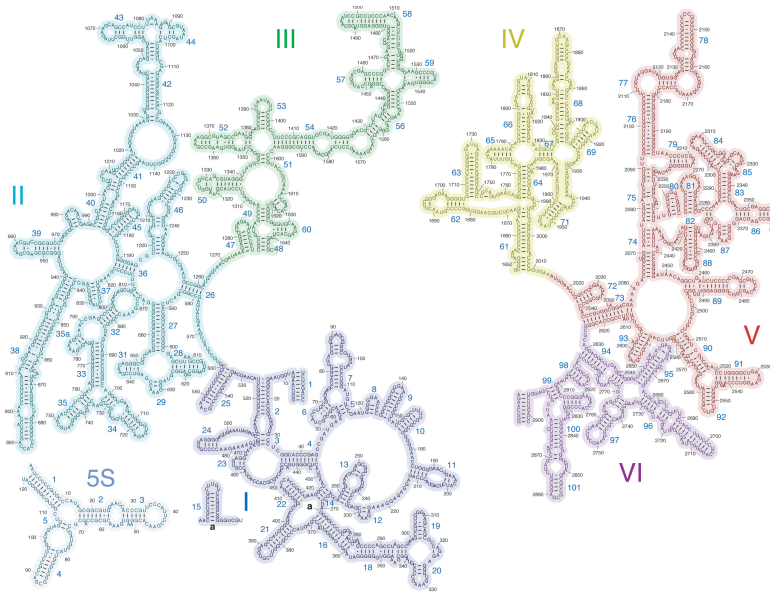

(b)

(c) (d)

Plate 6.1 (*Continued*) The helices are numbered from 1 to 45. **(b)** 23S RNA and 5S RNA. The six domains (I–VI) are shown in different colors. The helices are numbered 1–101. (Courtesy of Harry Noller, UCSC.) **(c, d)** The three-dimensional structures of the rRNAs of the small and large subunits, respectively. The coloring scheme is the same as in **(a)** and **(b)**. Notice in particular the long blue helix — the penultimate helix (h44) of the small subunit. While the RNA domains in the small subunit are separate folding units, the domains of the large subunit are interwoven. (Reprinted with permission from Yusupov *et al*., Crystal structure of the ribosome at 5.5 Å resolution, *Science* **292**: 883–896; copyright 2001, AAAS.)

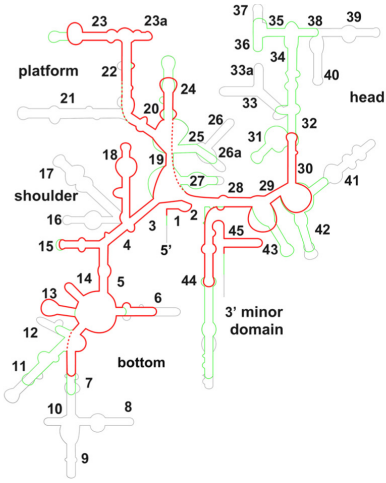

(a)

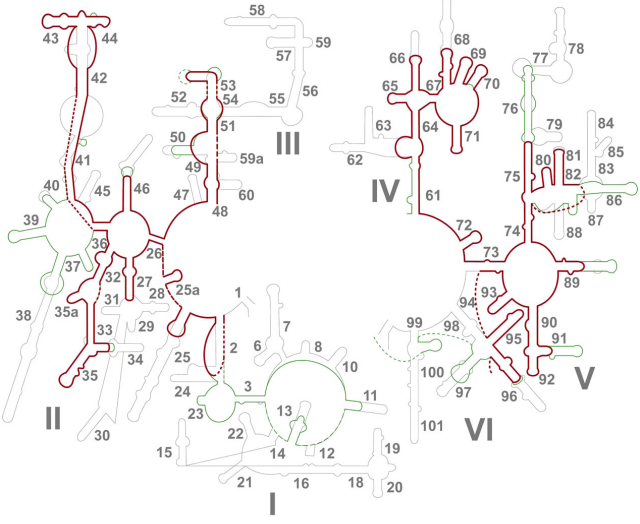

(b)

Plate 6.2 **(a)** A comparison of the organization of the 16S RNA from *T. thermophilus* with the 12S RNA of bovine mitochondria. **(b)** A comparison of the 23S RNA from *H. marismortui* with the 16S RNA of human mitochondria. The pieces that are lacking in mitochondria are shown in black. (Reprinted from Spremulli, 2003.)

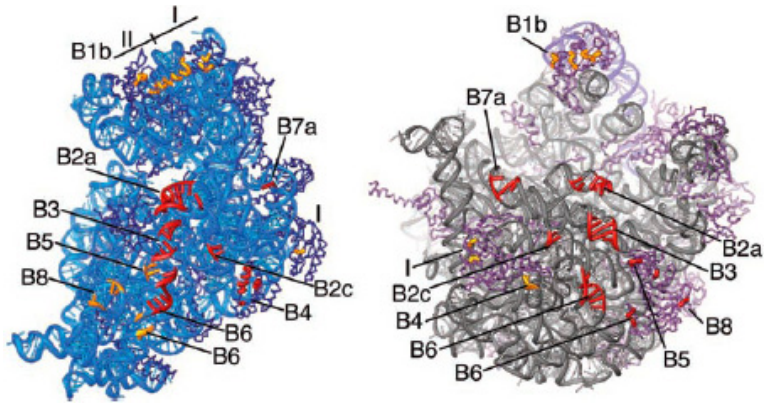

Plate 7.1 The inter-subunit bridges shown from the subunit interface sides. RNA components are illustrated in red and proteins in orange. (Reprinted from: Schuwirth *et al.*, 2005.)

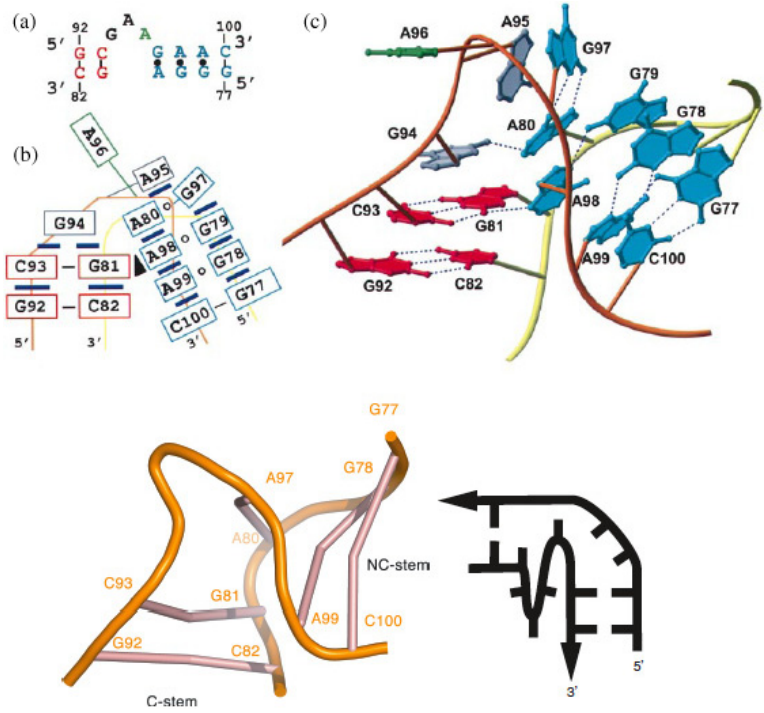

Plate 7.2 The kink-turn motif. (Bottom illustration reprinted with permission from Liljas *et al.*, 2009, *Textbook of Structural Biology*.)

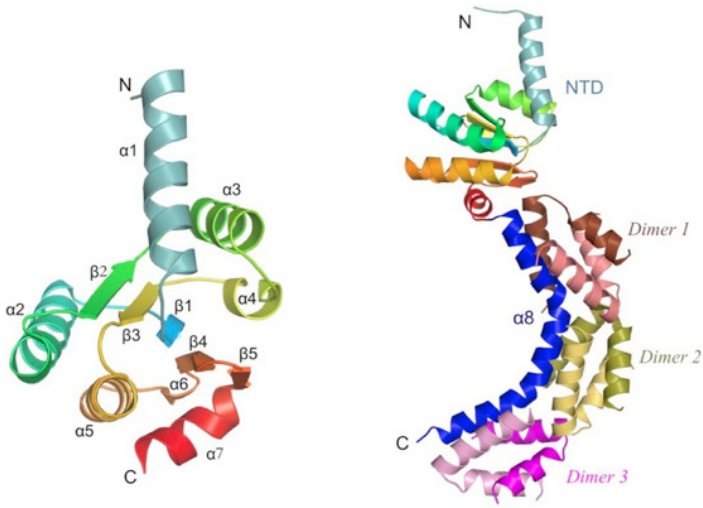

Plate 7.3 *Left*: The structure of the globular part of L10 from *T. maritima* (Diakonu *et al*., 2005). *Right*: The L10 structure including the C-terminal α helix (α8) to which three dimers of L12 bind. (Illustration by Saraboji Kadhirvel.)

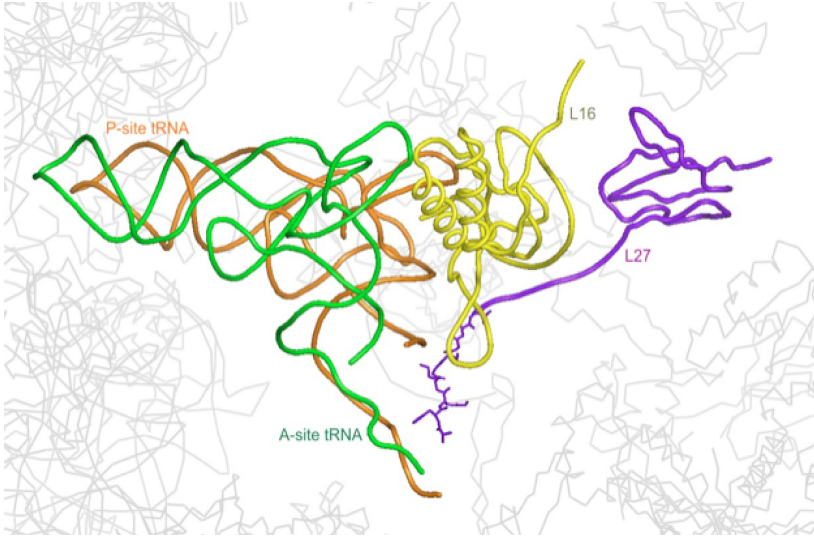

Plate 7.4 The N-terminal tail of L27 and an internal loop of L16 at the peptidyl transfer center next to the P-site tRNA. In archaea the loop of L16 (eL10) extends further by 11 amino acids and could reach the peptidyl transfer region. (Illustration by Saraboji Kadhirvel.)

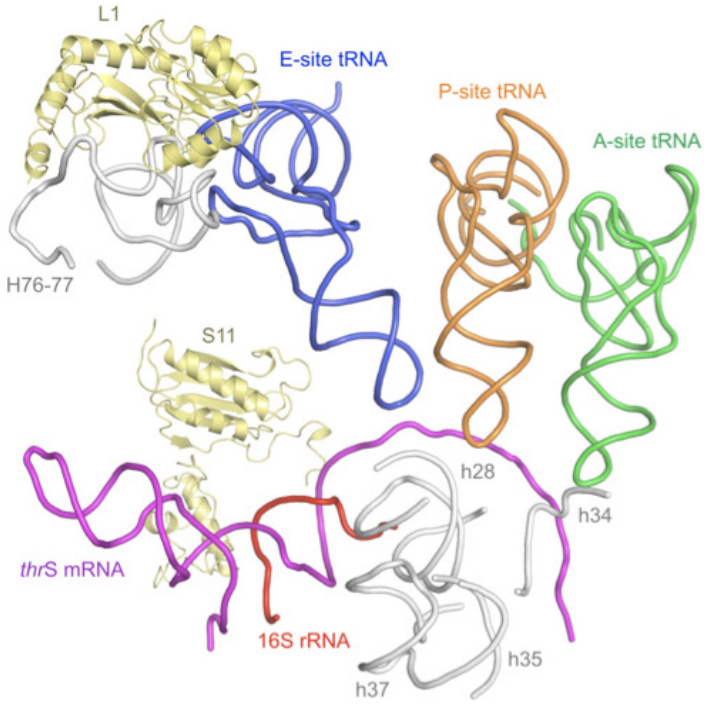

Plate 8.1 The binding of an mRNA (purple) with a hairpin loop. The 3′ end of the 16S RNA which participates in the Shine–Dalgarno interaction is seen in red. The A, P and E site tRNAs are shown, as well as the ribosomal protein S11 in contact with the mRNA (Jenner *et al*., 2005). (Illustration by Saraboji Kadhirvel.)

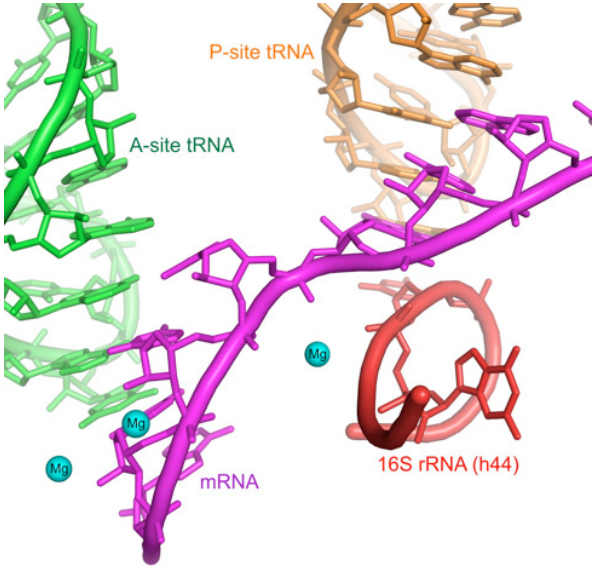

Plate 8.2 The organization of the mRNA (purple) and the A (green) and the P site (yellow) tRNA. A kink between the two codons is stabilized by a magnesium ion (cyan) that is bound to two phosphates in h44 (orange) and two successive phosphates of the mRNA (Selmer *et al.*, 2006). (Illustration by Saraboji Kadhirvel.)

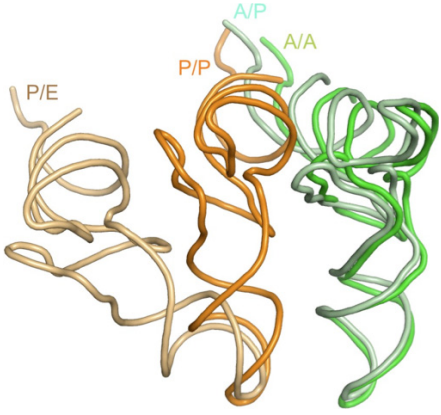

Plate 8.3 The hybrid states in relation to the classical sites (Agirrezabala *et al.*, 2008). The movement of the tRNA from the P/P site to the P/E site is a significant change that has to precede the movement of the tRNA from the A/A site to the A/P site, which involves essentially only the CCA end. (Illustration by Saraboji Kadhirvel.)

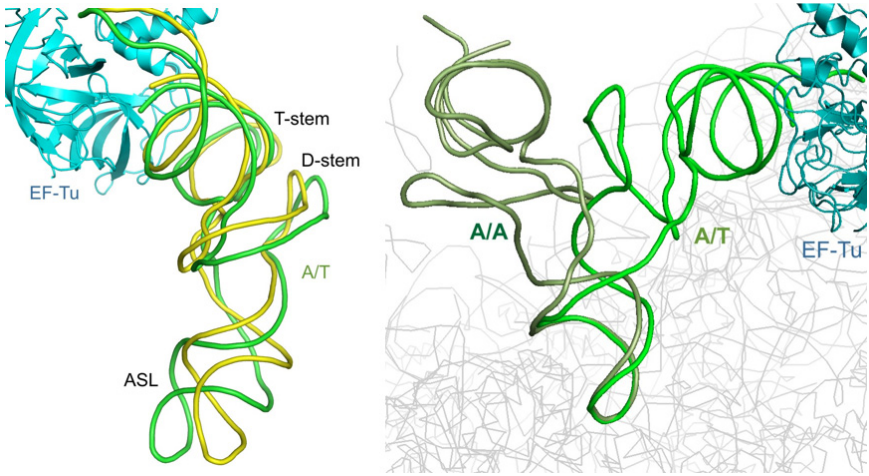

Plate 8.4 Left: The conformational difference between the tRNA in the ternary complex (T state; yellow) and the A/T state (green). Right: The difference between the tRNA in the A/T state and the A-site. (Illustration by Saraboji Kadhirvel.)

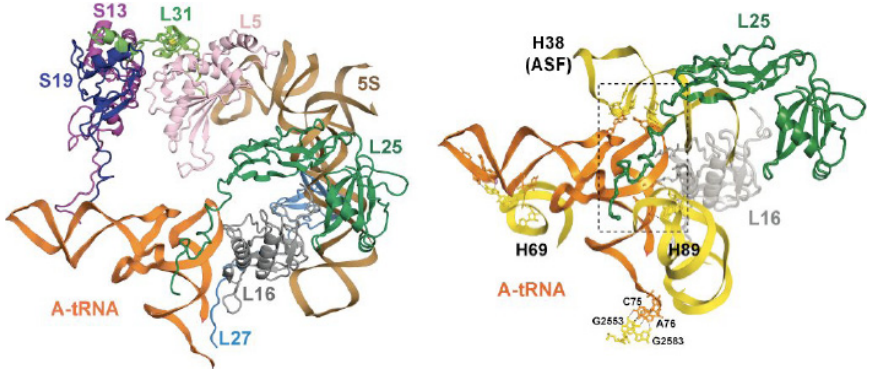

Plate 8.5 The tRNA in the A site. Left: Proteins in the vicinity of the A-site tRNA. Right: Helices of the 23S RNA close to the A-site tRNA. (Reprinted with permission from Jenner *et al.*, Structural rearrangements of the ribosome at the tRNA proofreading step, *Nat Struct Mol Biol* **9**: 1072–1079. Copyright 2010, Nature America Inc.)

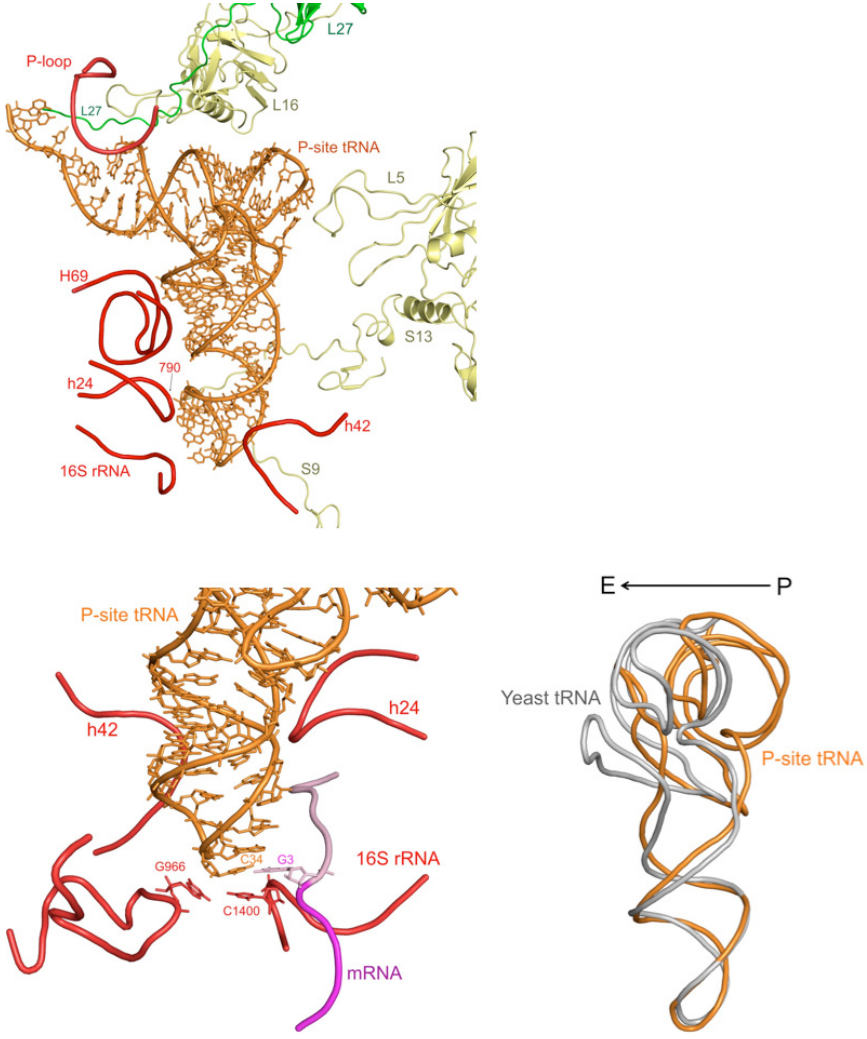

Plate 8.6 P-site tRNA (Selmer *et al.*, 2006). Above, The P-site tRNA in interaction with rRNA and proteins. Below, left: The interaction of the anticodon loop with mRNA and ribosome. Right: The conformational differences of the tRNA bound at the P site with the crystal structure of yeast $tRNA^{Phe}$ alone. The tRNA is slightly bent toward the A site. (Illustrations by Saraboji Kadhirvel.)

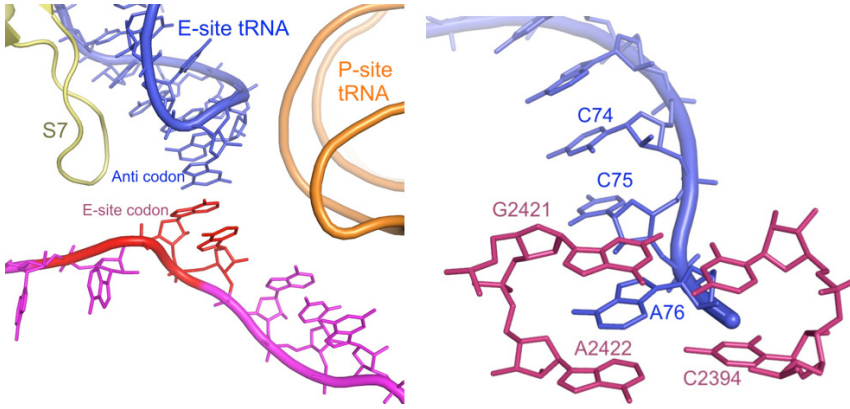

Plate 8.7 The E-site tRNA (Selmer *et al.*, 2006). In the tense conformation the anticodon is not in contact with its codon (left) and the acceptor end is in a pocket that does not permit the presence of an amino acid. (Illustration by Saraboji Kadhirvel.)

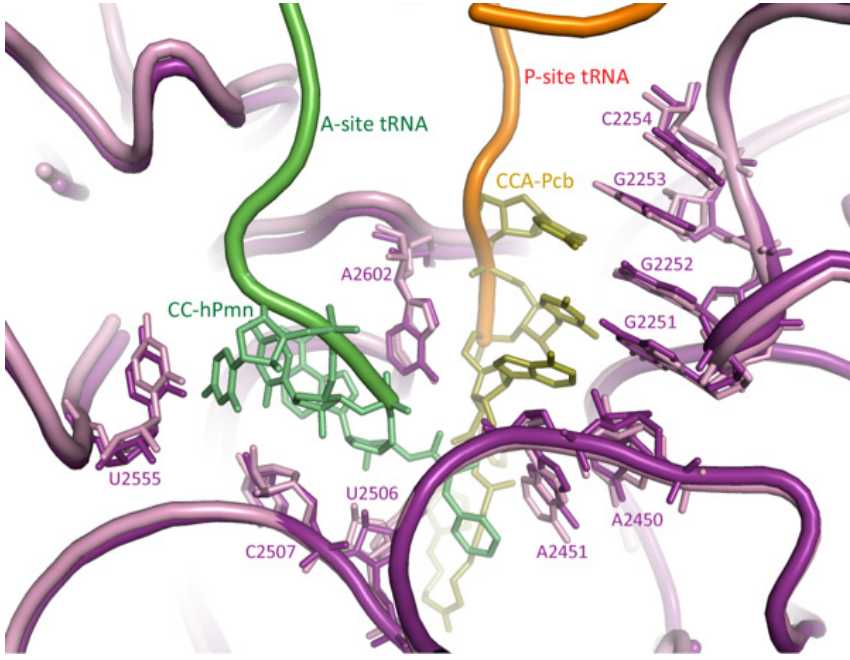

Plate 8.8 The structure of the PTC from Hm 50S subunits and from Tt 70S ribosomes are very similar (Voorhees *et al.*, 2009). (Drawing by Saraboji Kadhirvel.)

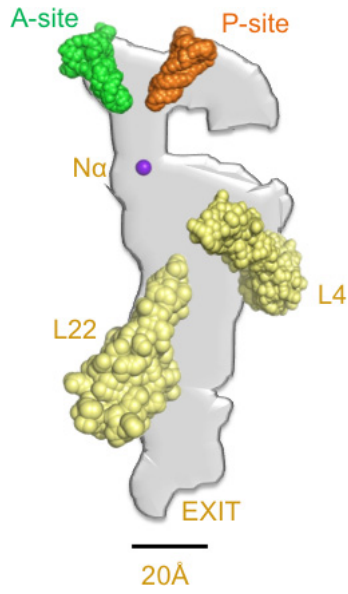

Plate 8.9 The exit tunnel as defined by a spherical probe of radius 3 Å. The locations of the ends of A- and P-site tRNAs, the N-terminal amino acid in the active site, and the tips of proteins L4 and L22 forming a constriction are marked (Voss *et al*., 2006). (Illustration by Saraboji Kadhirvel.)

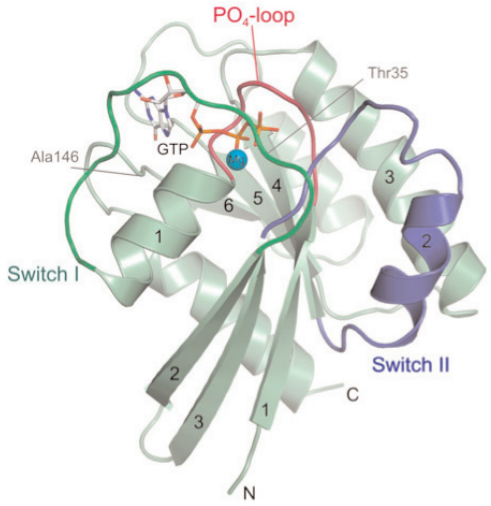

Plate 9.1 The structure of a G-protein with a bound GTP analog. The three important loops for GTP binding and GTPase function, the phosphate-binding loop (PO_4 loop; purple), switch I (green) and switch II (blue) are indicated (see also Fig. 9.5). (Illustration by Saraboji Kadhirvel.)

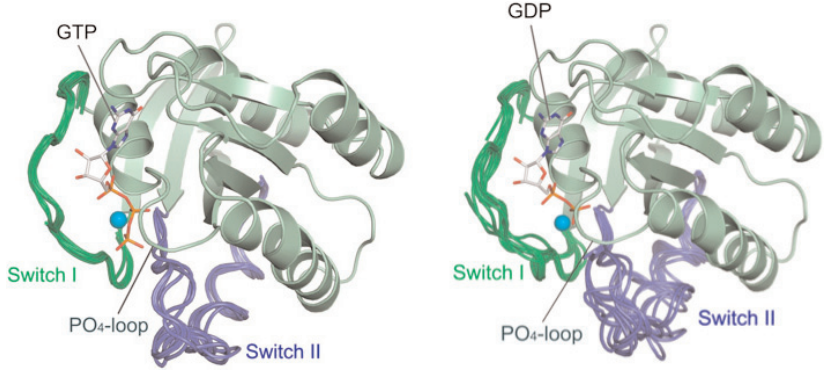

Plate 9.2 Comparison of the structure of the G-domains for trGTPases in the GTP and GDP conformations. In the GTP form the switch I and switch II loops from all proteins have very similar conformations, whereas in the GDP form they differ substantially. (Illustration by Saraboji Kadhirvel.)

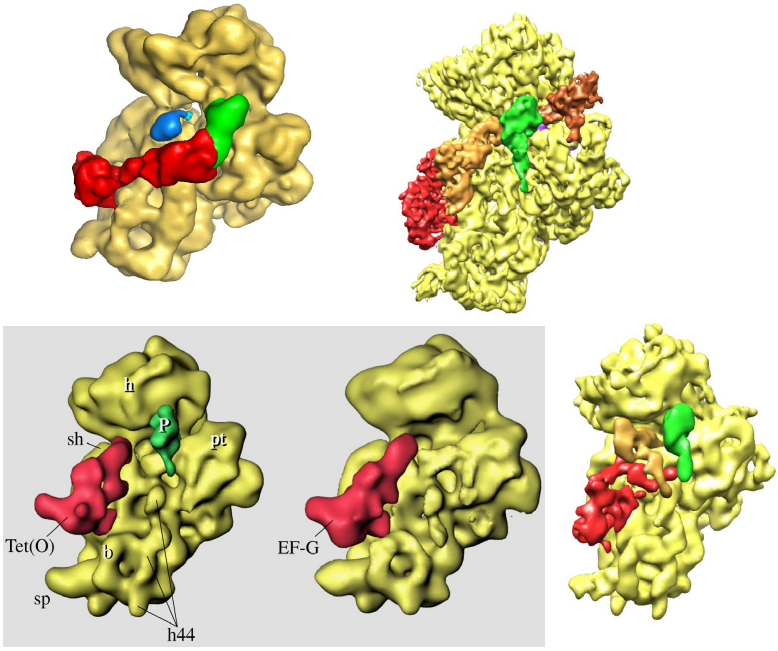

Plate 9.3 Some trGTPases bound to the small subunit, showing their similarity in binding. In order they are IF2 (kindly provided by Bruno Klaholz), EF-Tu (kindly provided by Christian Spahn), Tet O and EF-G (kindly provided by Joachinm Frank) and LepA (kindly provided by Christian Spahn). The trGTPases are red, IF1 is blue, P site tRNA is green, E site tRNA is brown and a tRNA in the A or A/T site is orange. (The figure with TetO and EF-G is reprinted with permission from Spahn *et al.*, Localization of the ribosomal protection protein TetO on the ribosome and the mechanism of tetracycline resistance, *Mol Cell* **7**: 1037–1045. Copyright 2001, Elsevier.)

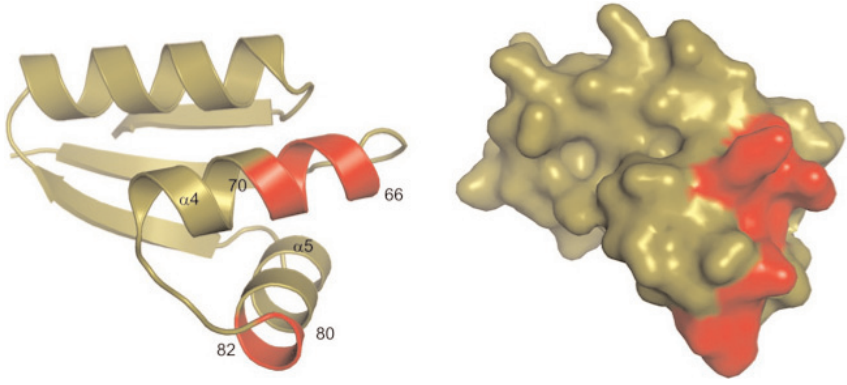

Plate 9.4 The surface of L12CTD that interacts with EF-G (Helgstrand *et al.*, 2007). (Illustration by Saraboji Kadhirvel.)

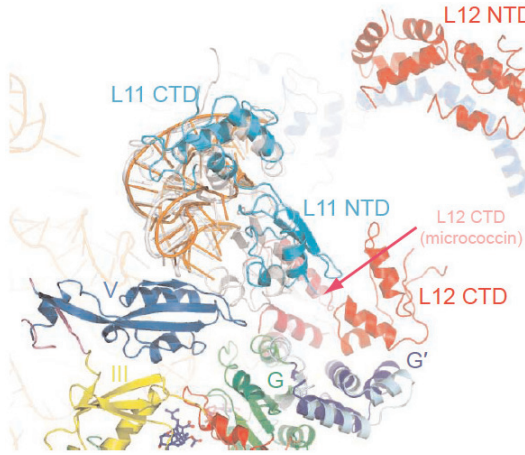

Plate 9.5 The interaction of the G′ and G domains of EF-G with L12CTD (red) and L11 (cyan) in studies of *T. thermophilus* 70S ribosomes (Gao *et al*., 2009). When EF-G is in complex 50S subunits (*D. radiodurans*) in the presence of micrococcin, L12CTD (pink) makes a tighter contact. (Illustration kindly provided by Venki Ramakrishnan.)

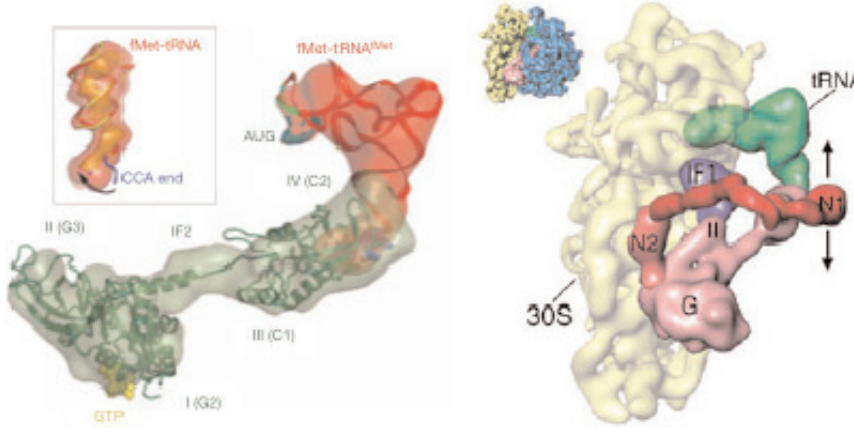

Plate 9.6 Left: IF2, when bound to 30S subunits, domain III swings into the proximity of domain IV, making a different part of the protein a flexible connecting region. (Reprinted with permission from Simonetti *et al*., Structure of the 30S initiation complex, *Nature* **455**: 416–421. Copyright 2008, Nature.) Right: IF1 (blue), IF2 (pink) and initiator tRNA (green) bound to 70S ribosomes. The N-terminal domains (red) of IF2 are seen. (Reprinted with permission from Allen & Frank, Structural insights on the translation initiation complex: ghosts of a universal initiation complex, *Mol Microbiol* **63**: 941–950. Copyright 2007, Wiley–Blackwell.)

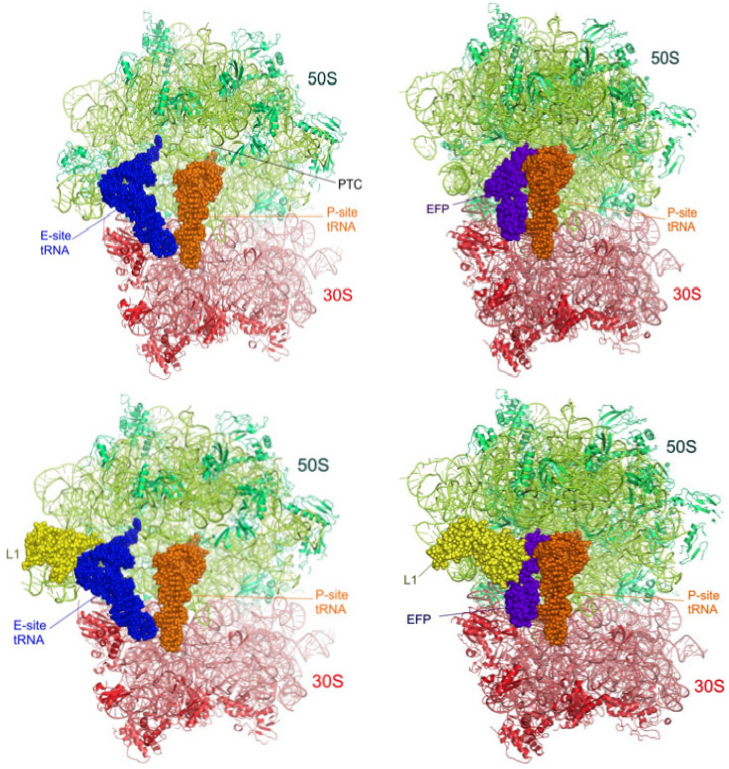

Plate 9.7 The 70S ribosome with and without EF-P bound in a position between the P and E sites that prevents slippage of fMet-tRNA into the P/I-site and facilitates proper positioning of fMet for the formation of the first peptide bond (Blaha *et al.,* 2009). The lower figures show the positions and interactions of protein L1 with E-site tRNA and EF-P. (Illustration by Saraboji Kadhirvel.)

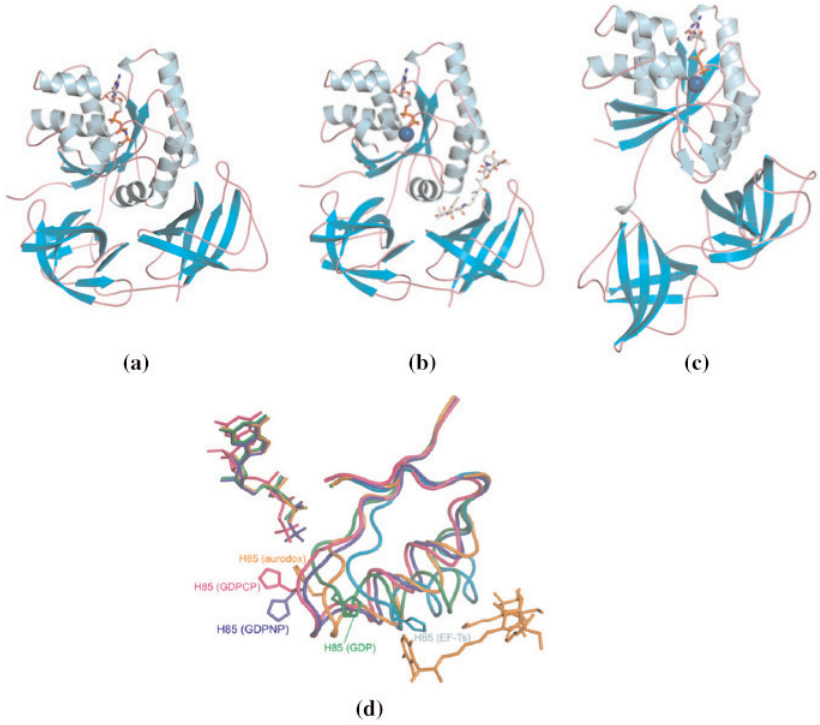

Plate 9.8 Three conformations of EF-Tu: **(a)** with GTP, **(b)** with GDP and the antibiotic aurodox, and **(c)** with GDP alone. **(d)** The dynamics of switch II and His84 in different conformations of EF-Tu. The aurodox inhibitor is seen at the lower right. His84 is important for the activation of the water that attacks the γ-phosphate. (Illustrations by Saraboji Kadhirvel.)

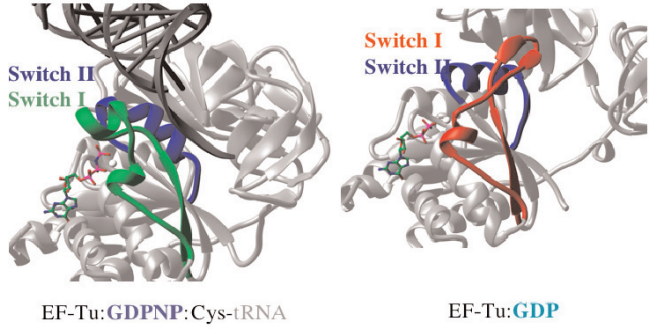

Plate 9.9 Left: The conformation of switches I and II in EF-Tu in the GTP conformation. Right: The conformation of switches I and II in EF-Tu in the GDP conformation. (Illustration kindly provided by M. Laurberg.)

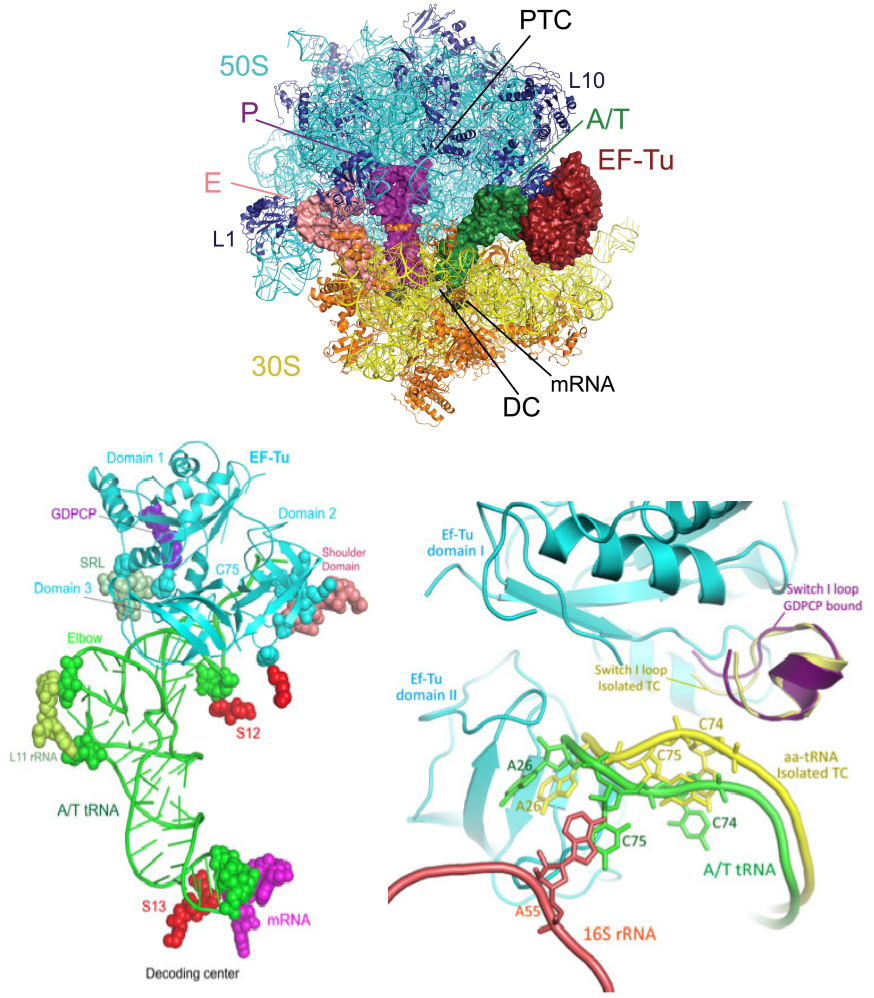

Plate 9.10 Above: EF-Tu with tRNA bound to the ribosome in complex with kirromycin. (Illustration kindly provided by Martin Schmeing.) Below, left: The ternary complex of Trp-tRNA and EF-Tu on the ribosome at the A/T site. Some ribosomal interactions with EF-Tu and the tRNA are indicated. Below, right: A comparison of the CCA end bound in the A/T site (green) and in the isolated ternary complex (yellow). The CCA end of the tRNA undergoes a conformational change when binding to the ribosome. (Illustrations by Saraboji Kadhirvel.)

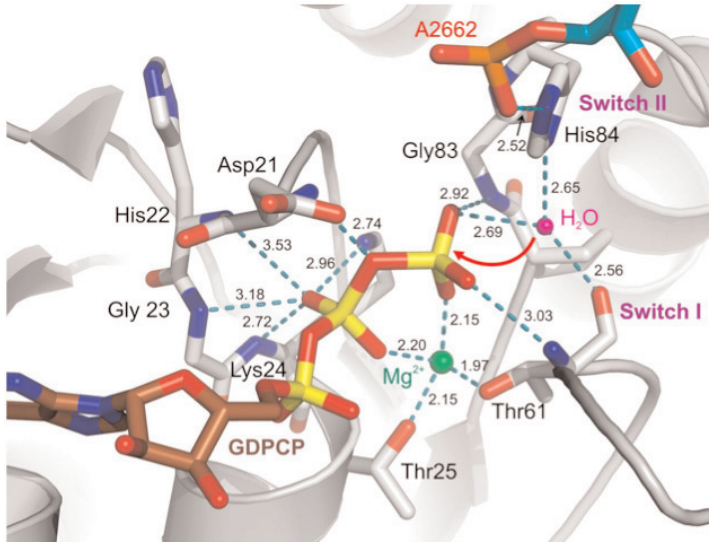

Plate 9.11 A GTP molecule placed as the GDPCP molecule in EF-Tu, when bound to the ribosome (Voorhees *et al*., 2010). In this conformation the water molecule donates hydrogen bonds to the carbonyl oxygen of Thr61 in switch I and to the γ-phosphate of GTP. The water molecule has therefore exhausted its potential to act as a donor of hydrogen bonds. The phosphate of A2662 in the SRL of the 23S RNA accepts a hydrogen bond from His84 of switch II and positions it next to the water molecule at the γ-phosphate. His84, which is in a negatively charged environment, must then be protonated to be able to hydrogen-bond to the water molecule. The histidine therefore does not activate the water molecule but positions it at the γ-phosphate to donate a proton to it in association with the in-line attack. (Reprinted with permission from Liljas *et al*., (comments on 'The mechanism for activation of GTP hydrolysis on the ribosome,' *Science* **333**: 37. Copyright 2011, AAAS.)

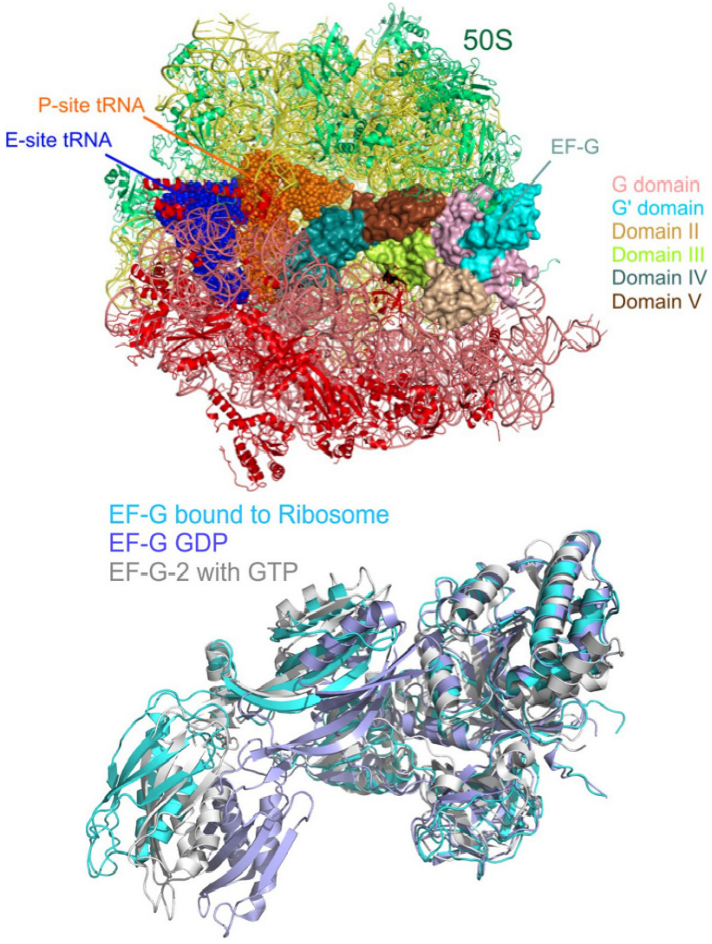

Plate 9.12 Above: EF-G bound to the ribosome (cf. EF-Tu in Plate 9.10). The small subunit RNA (yellow) and proteins (green) and the large subunit RNA (pink) and proteins (red). The P-site tRNA is orange and the E-site tRNA blue. The colors of the EF-G domains are shown in the illustration. (Gao *et al*., 2009). Below: A comparison between two conformations of EF-G off the ribosome (gray GDP, Hansson *et al*., 2005; blue EF-G-2 with GTP, Connell *et al*., 2007) and EF-G bound to the ribosome (light blue, Gao *et al*., 2009). (Illustrations by Saraboji Kadhirvel.)

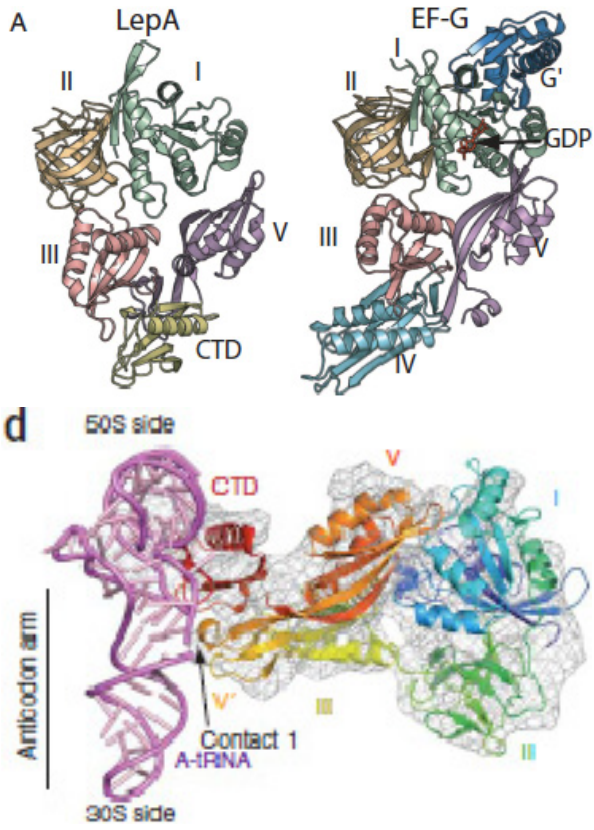

Plate 9.13 Above: The structure of LepA compared to its closest relative, EF-G (Evans *et al*., 2008). Two domains of EF-G, G' and IV, are absent in LepA. Instead of domain IV, LepA has a contact between domains III and V called V'. The C-terminus of LepA is a unique domain called CTD, approximately in the place of domain IV of EF-G. (Reprinted with permission from Evans *et al*., The structure of LepA, the ribosomal back translocase. *Proc Natl Acad Sci USA*. Copyright (2008) National Academy of Sciences.) Below: LepA binds to the trGTPase-binding site of the posttranslocational ribosome. Domains V' and CTD of LepA interact with the tRNA in the A site. The interaction of the CTD with the acceptor arm seems particularly interesting. (Reprinted with permission from Connell *et al*., A tRNA intermediate revealed on the ribosome during EF4-mediated back-translocation, *Nat Struct Mol Biol* **15**: 910–915 Copyright 2008, Nature.)

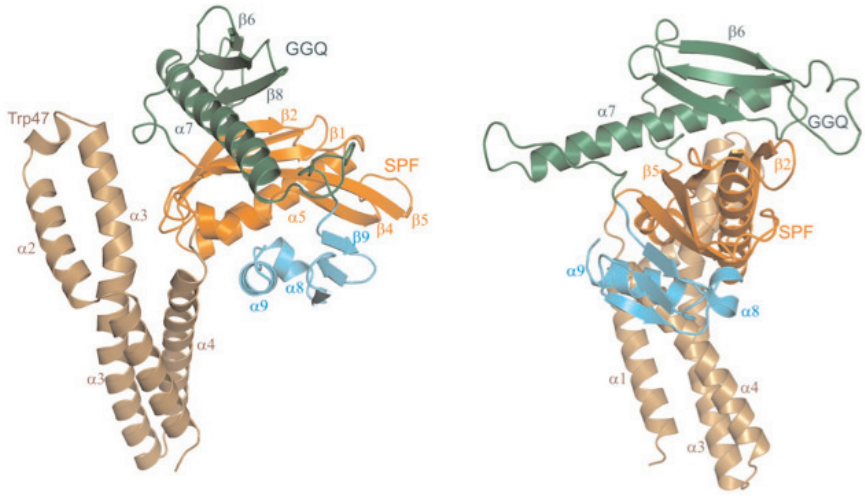

Plate 9.14 The structure of RF2. The domains are shown in brown (I), blue (II), purple (III) and green (IV). The distance between the GGQ and SPF motifs is much shorter than predicted from function. (Illustration by Saraboji Kadhirvel.)

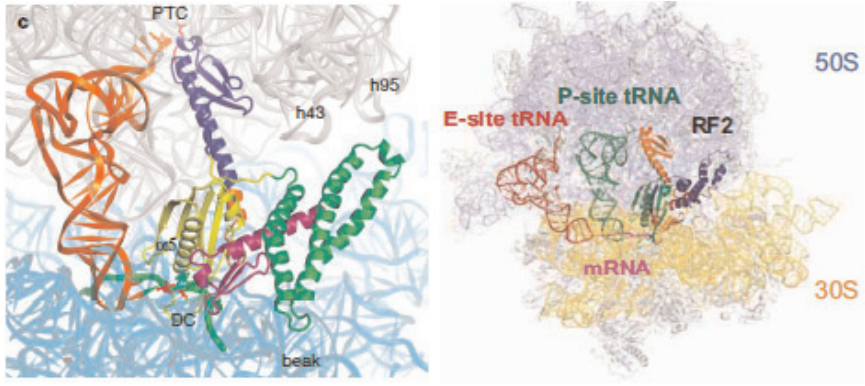

Plate 9.15 Left: RF1 bound to the ribosome. Domain I (green) is close to the factor-binding site, while the GGQ region (dark blue) reaches into the PTC area. (Reprinted with permission from Laurberg *et al.*, Structural basis for translation termination on the ribosome, *Nature* **454**: 852–857. Copyright 2008, Nature.) Right: RF2 bound to the ribosome. (Reprinted with permission from Weixlbaumer *et al.*, Insights into translational termination from the structure of RF2 bound to the ribosome, *Science* **322**: 953–956. Copyright 2008, AAAS.)

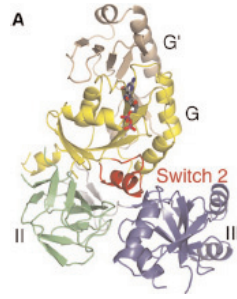

Plate 9.16 The structure of RF3. (Reprinted with permission from Gao *et al.*, RF3 induces ribosomal conformational changes responsible for dissociation of class I release factors, *Cell* **129**: 929–941. Copyright 2007, Elsevier Inc.)

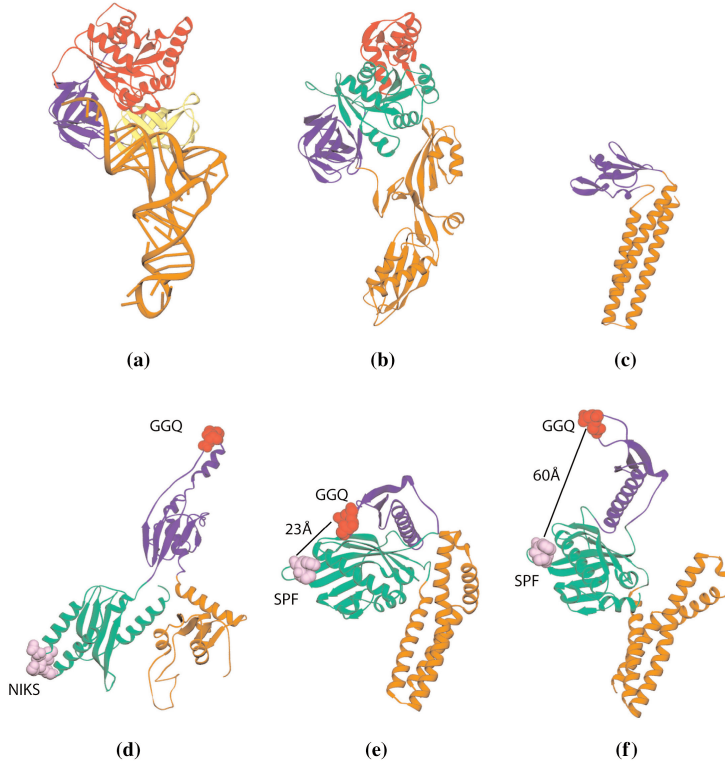

Plate 9.17 Some examples of tRNA mimicry. Not all of them correspond with a functional relationship. **(a)** The ternary complex of EF-Tu·GTP and aminoacyl-tRNA. **(b)** EF-G. **(c)** RRF. (**d**) eRF1. **(e)** RF2 as observed in the crystal structure. **(f)** RF2 as interpreted from the cryo-EM. (Reprinted with permission from Brodersen & Ramakrishnan, Shape can be seductive, *Nat Struct Biol* **10**: 78–80. Copyright 2003, Nature.)

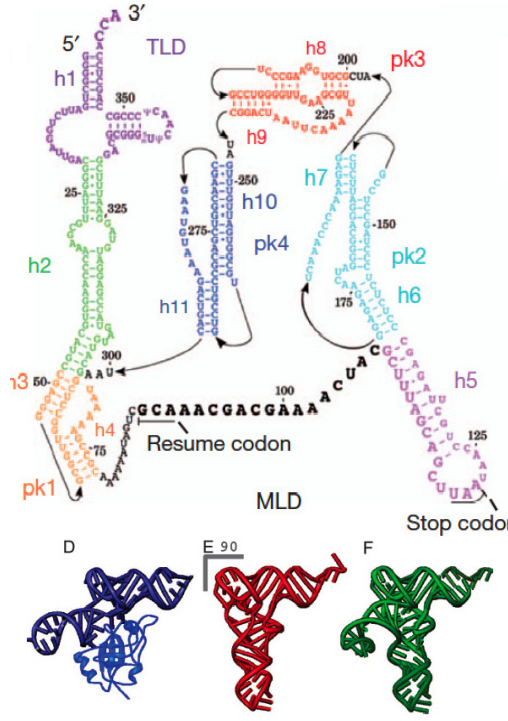

Plate 9.18 Top: The secondary structure of tmRNA. (Reprinted with permission from Ramrath *et al.*, The complex of tmRNA–SmpB and EF-G on translocating ribosomes, *Nature* **485**: 526–530. Copyright 2012, Nature.) Bottom: The structure of the TLD of tmRNA together with SmpB compared with a normal tRNA and a tRNA with a long variable arm. (Reprinted with permission from Bessho *et al.*, Structural basis for functional mimicry of long-variable-arm tRNA by transfer-messenger RNA, *Proc Natl Acad Sci USA* **104**: 8293–8298. Copyright 2007, The National Academy of Sciences of the USA.)

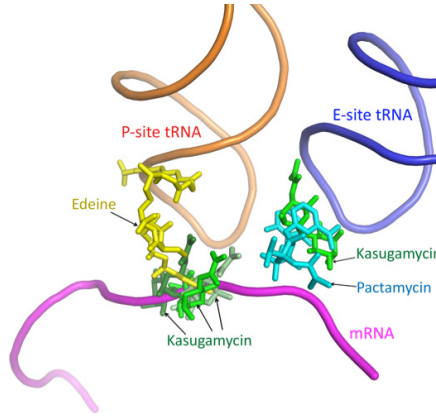

Plate 10.1 Edeine and pactamycin are located between the codon and anticodon of the P- and E-sites respectively. The binding of initiator tRNA is prevented by edeine (Pioletti *et al*., 2001; Dinos *et al*., 2004). In *E. coli* two binding sites for kasugamycin are observed, where on partly overlapps the binding site for edeine (Schuwirth *et al*., 2006). It also overlaps the binding of mRNA between the P-site and E-site codons. In *T. thermophilus* a second binding site for kasugamycin is seen. It overlaps with the binding site for pactamycin (Schluentzen *et al*., 2006; Drawn by Saraboji Kadhirvel.)

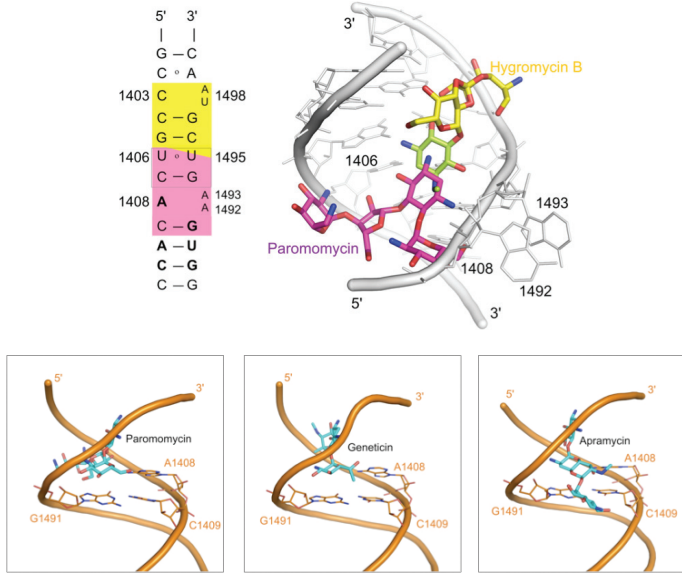

Plate 10.2 Above left. The secondary structure of part of h44. Right. A comparison of the binding of streptomycin and hygromycin B in relation to their binding sites on the secondary structure (Sutcliffe, 2005;). Below. The binding of some aminoglycosides to h44 (Hermann, 2005). Drawn by Saraboji Kadhirvel.

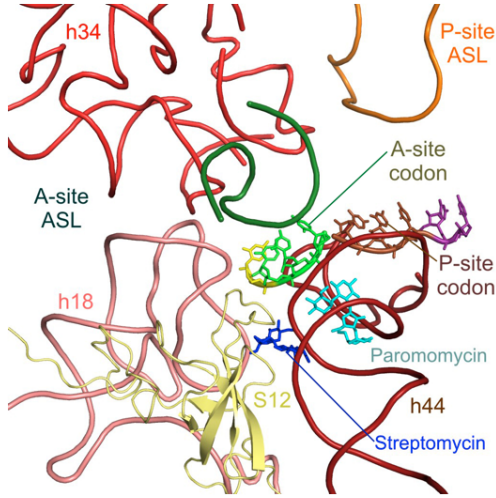

Plate 10.3 The binding of paromomycin (Carter *et al.*, 2000; Ogle *et al.*, 2001; 2002; 2003) and streptomycin. The anticodon stem loops (ASL) of the A- and P-site tRNAS are shown in green and brown respectively. (Drawn by Saraboji Kadhirvel.)

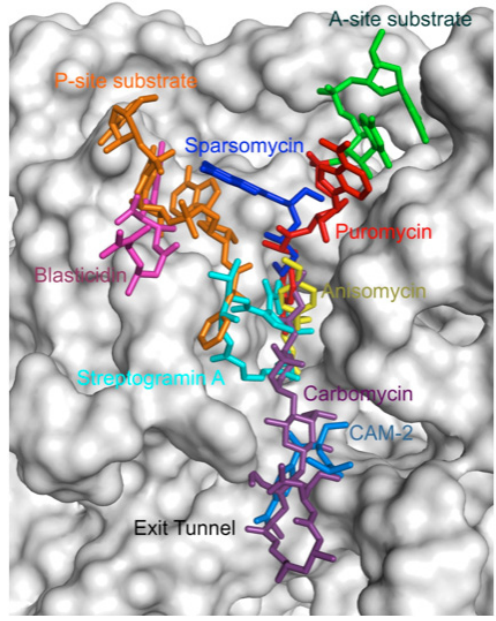

Plate 10.4 A number of antibiotics at their binding sites at the PTC. In bacteria chloramphenicol binds at a site overlapping with the site for anisomycin (CAM-1) and a second site (CAM-2) as observed in archaea (Drawn by Saraboji Kadhirvel.)

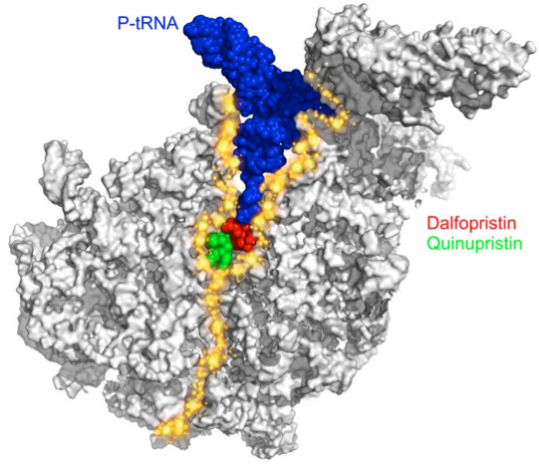

Plate 10.5 Dalfopristin and quinupristin bind to the peptide exit channel of the large subunit (Drawn by Saraboji Kadhirvel).

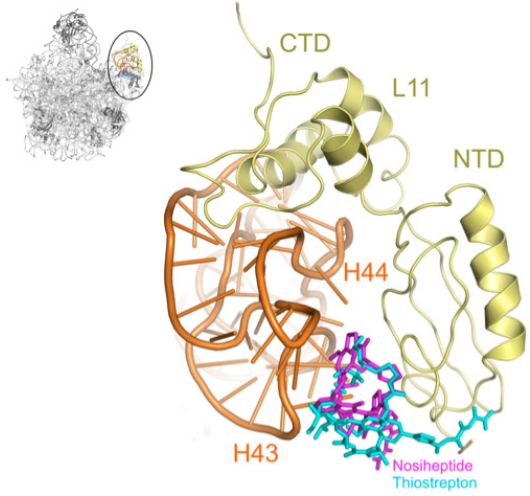

Plate 10.6 The binding of nosiheptide and thiostrepton to their overlapping binding sites at the base of the L12 stalk where the N-terminal domain of L11 binds to H43 and H44 (Harms *et al.*, 2008; Drawn by Saraboji Kadhirvel).

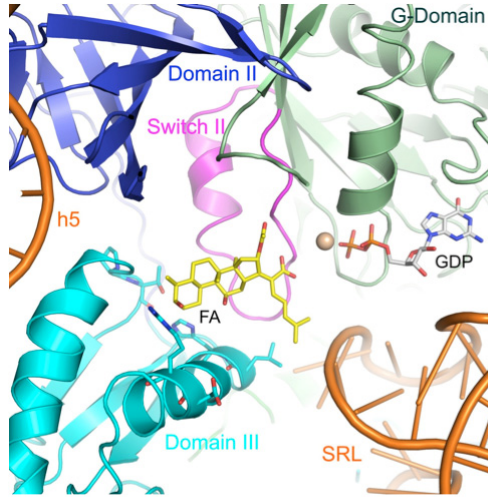

Plate 10.7 The binding of fusidic acid to EF-G in the crystal structure of the ribosome with a bound EF-G·GDP. The binding site between the G-domain and domain III is close to the GDP and switches I and II (Gao *et al*., 2009; Drawn by Saraboji Kadhirvel).

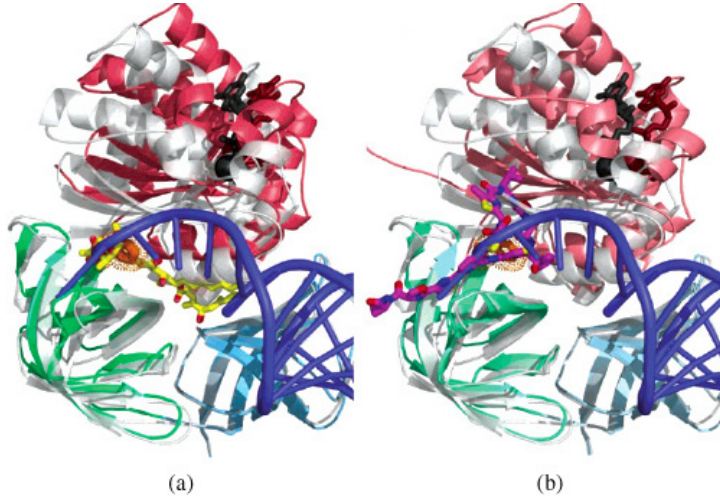

Plate 10.8 The complexes of EF-Tu with pulvomycin (A, yellow) and GE2270A (B, purple) show that the CCA end with the amino acid of the bound tRNA overlaps with the binding site for the antibiotics (Parmeggiani *et al*., 2006; Drawn by Saraboji Kadhirvel).

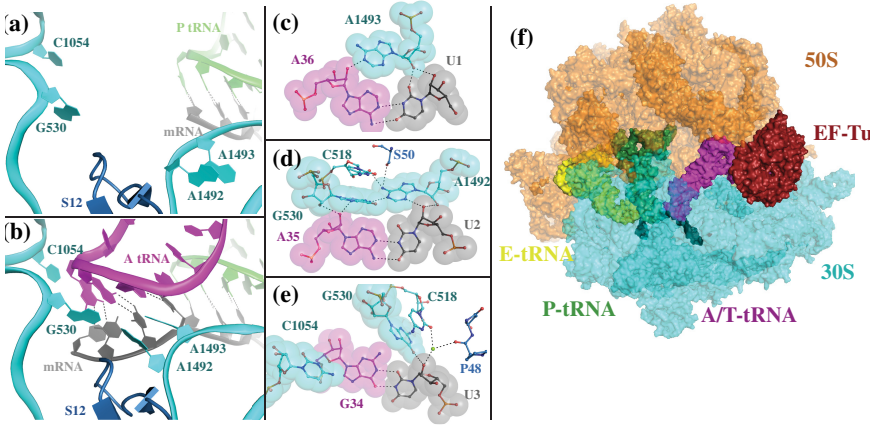

Plate 11.1 The discrimination between cognate and noncognate interactions in the decoding site is done with the aid of nucleotides from the 16S RNA (Ramakrishnan, 2009). Above: The mRNA codon (gray) and the anticodon of the tRNA (purple) interact with nucleotides of the 16S RNA. Below: The specific interactions between the base pairs of the codon–anticodon interaction and nucleotides A1493, A1492 and G530 of the 16S RNA. (Reprinted with permission from Schmeing & Ramakrishnan, What recent ribosome structures have revealed about the mechanism of translation, *Nature* **461**: 1234–1242. Copyright 2009, Nature.)

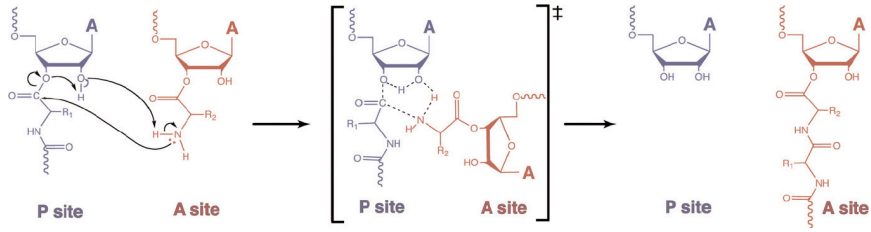

Plate 11.2 The possible mechanism of peptide transfer by the ribosome. The acceptor ends of the tRNAs in the P site (left) and A site (right). The 2′OH of A76 of the P site tRNA hydrogen-bonds to the α-amino group of the aminoacyl residue bound to the A-site tRNA and extracts a proton from the amino group to enable it to form a tetrahedral intermediate with the carbonyl carbon between the nascent polypeptide and the P site tRNA. After peptidyl transfer the peptide is bound to the A site tRNA and the proton transfer is completed with both the 2′ and 3′ OHs of A76 in the P site being protonated. (Reprinted with permission from Simonovic & Steitz, A structural view on the mechanism of the ribosome-catalyzed peptide bond formation, *Biochim Biophys Acta* **1789**: 612–623. Copyright 2009, Elsevier.)

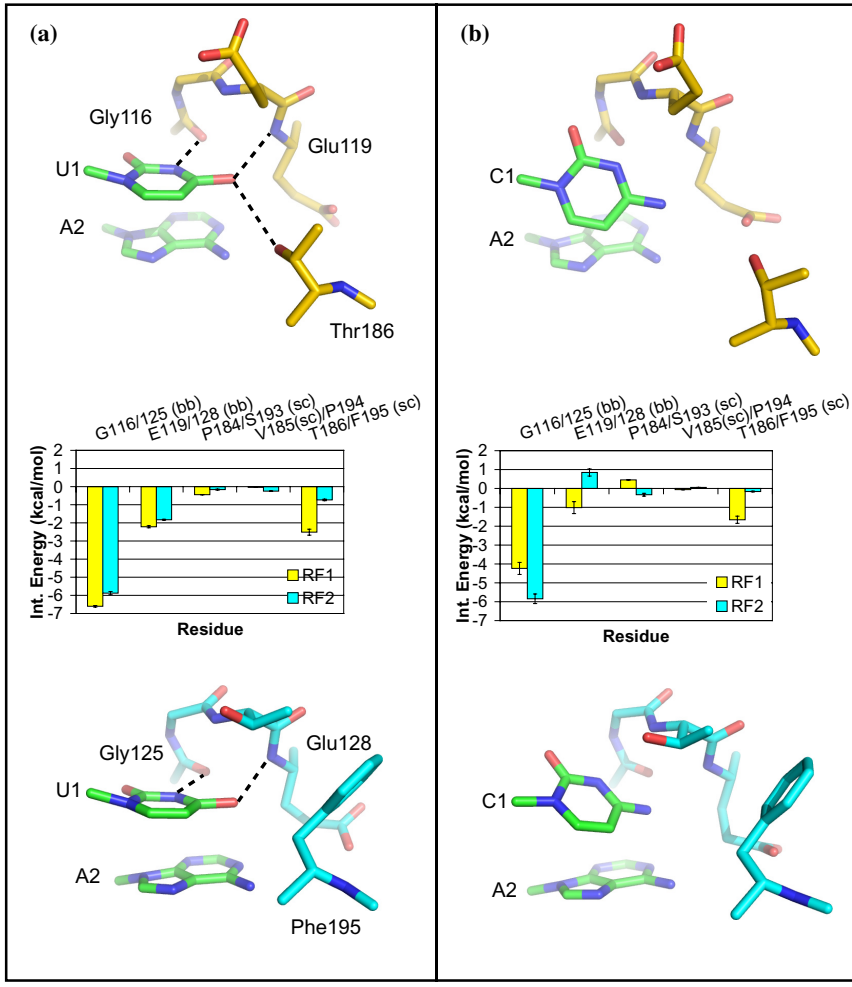

Plate 11.3 Reading of the first position of a step codon. U is recognized (**a**) and C is discriminated against (**b**) by RF1 (*yellow*, *top*) and RF2 (*cyan*, *bottom*). Hydrogen bonds are indicated by dashed lines. The interaction energies between release factor residues (sidechains sc; backbone bb) and the base in the first codon position. (Reprinted with permission from Sund *et al.*, Principles of stop-codon reading on he ribosome. *Nature* **465**: 947–951. Copyright 2010, Nature Publishing Group.)

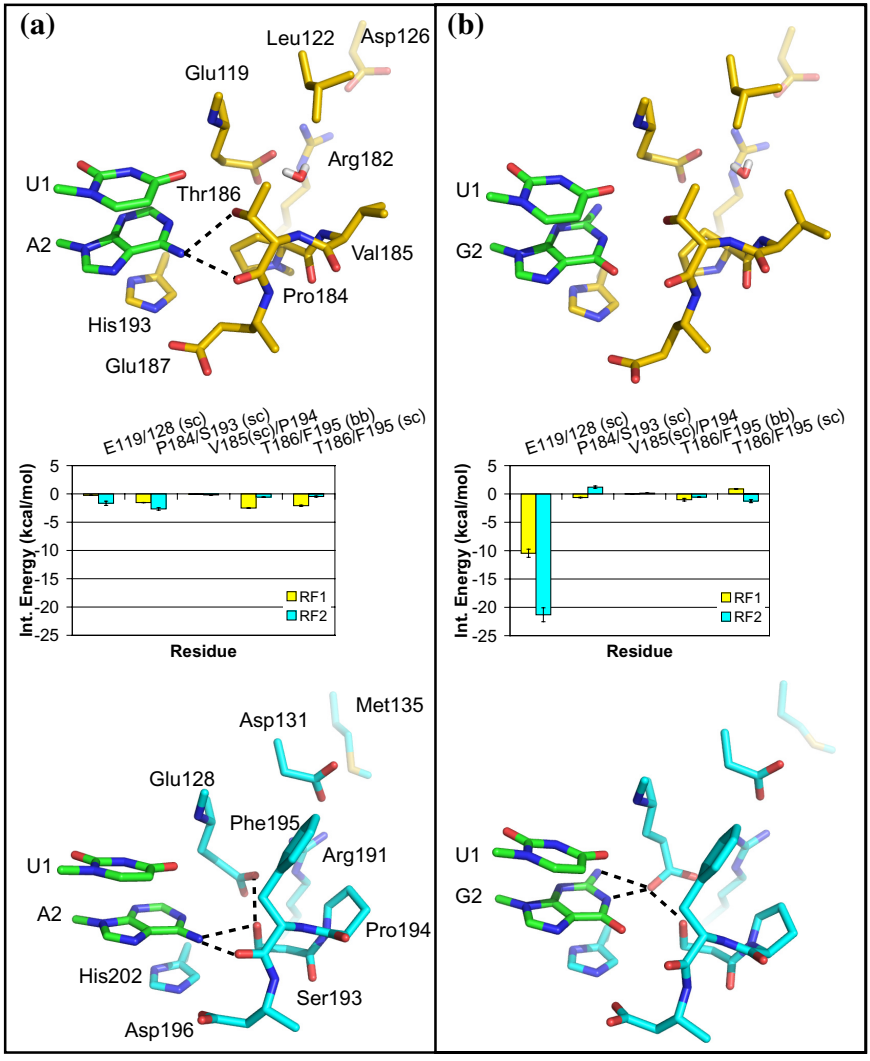

Plate 11.4 Reading of the second position of a stop codon. Average molecular dynamics structures of UAA (**a**) and UGA (**b**). RF1 discriminates against a G, while RF2 has dual specificity. (Reprinted with permission from Sund *et al.*, Principles of stop-codon reading on he ribosome. *Nature* **465**: 947–951. Copyright 2010, Nature Publishing Group.)

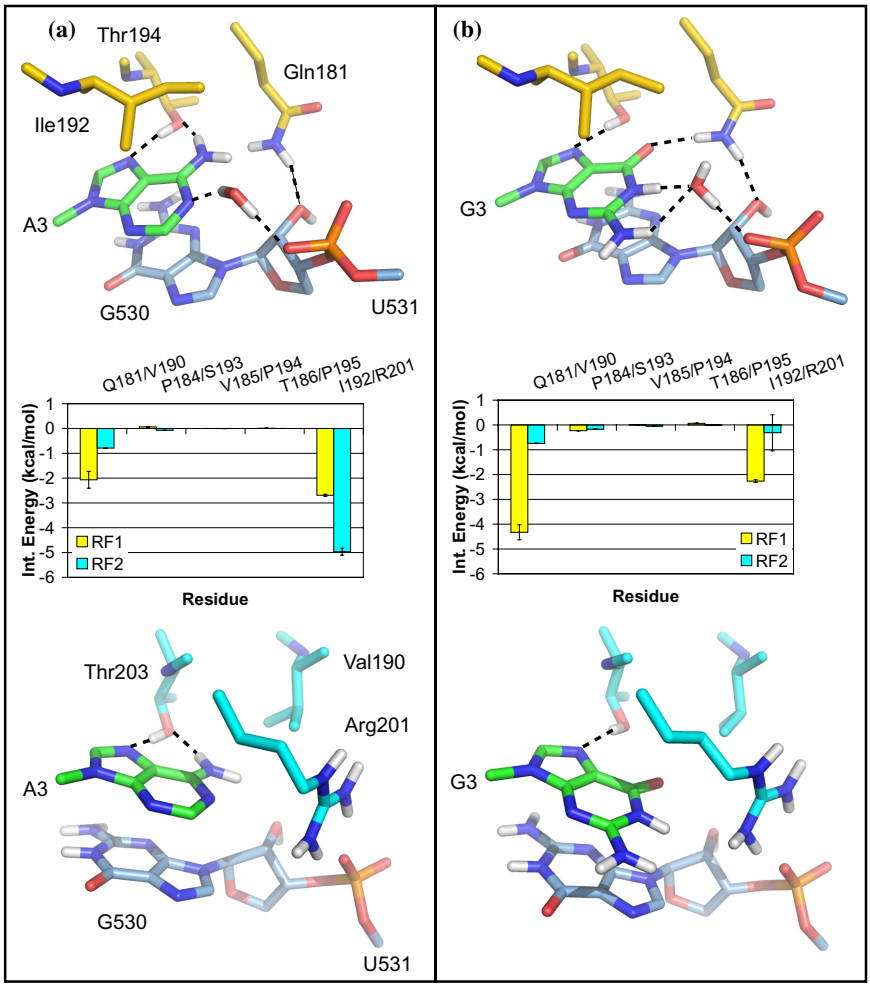

Plate 11.5 Reading of the third position of the stop codon. Average molecular dynamics structures of UAA (**a**) and UAG (**b**). RF1 reads both A and G while RF2 reads only the A. (Reprinted with permission from Sund *et al.*, Principles of stop-codon reading on he ribosome. *Nature* **465**: 947–951. Copyright 2010, Nature Publishing Group.)

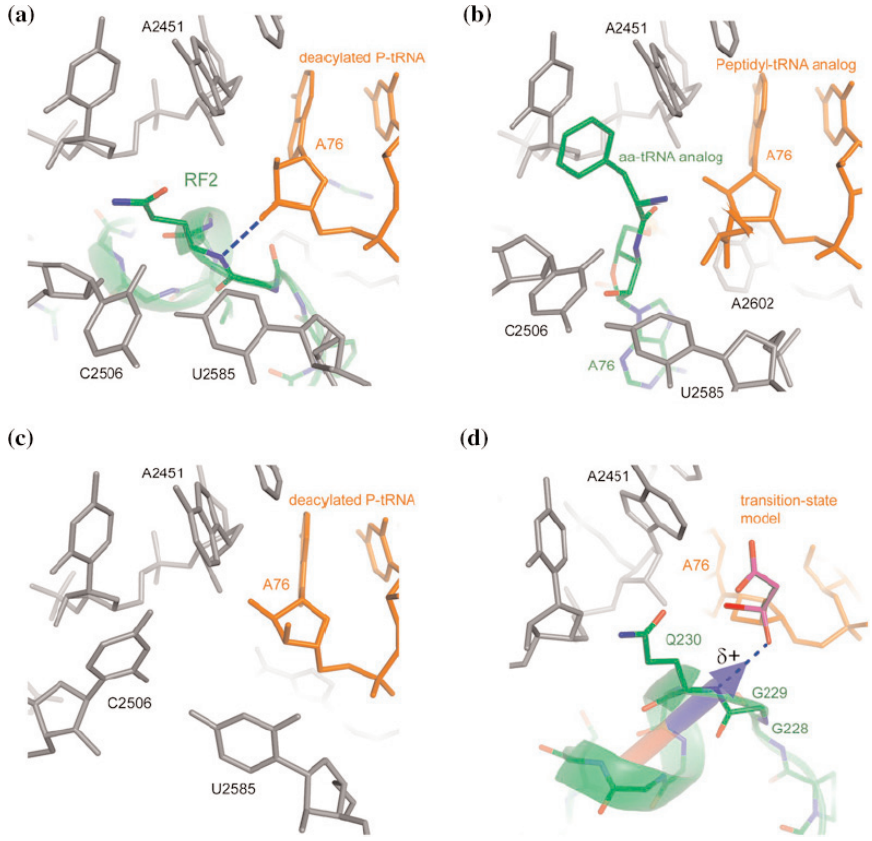

Plate 11.6 The GGQ motif interacts with the CCA end of the P-site tRNA, inducing hydrolysis of the nascent peptide. (**a**) The PTC with a deacylated tRNA in the P site and RF2 in the A site. (**b**) The A site with an aminoacyl-tRNA. (**c**) An empty A site with different conformations of C2506 and U2585. (**d**) Superposition of RF2 and peptidyl transfer transition state analog. (Reprinted with permission from Korostelev, Structural aspects of translation termination on the ribosome, *RNA* **17**: 1409–1421. Copyright 2011, Cold Spring Harbor Laboratory Press.)

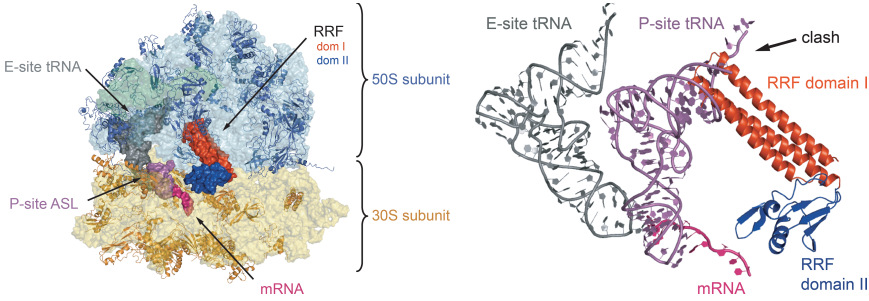

Plate 11.7 The binding site for the RRF on the ribosome and its relation to the tRNA sites. (Reprinted with permission from Weixlbaumer *et al.*, Crystal structure of the ribosome recycling factor bound to the ribosome, *Nat Struct Mol Biol* **14**: 733–737. Copyright 2007, Nature.)

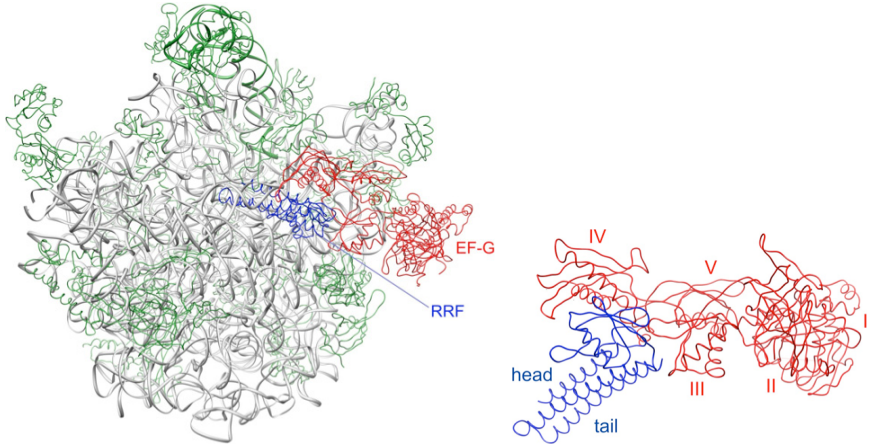

Plate 11.8 The RRF and EF-G*GDPNP bound to the 50S subunit (Gao *et al.*, 2007). (Illustration by Saraboji Kadhirvel.)

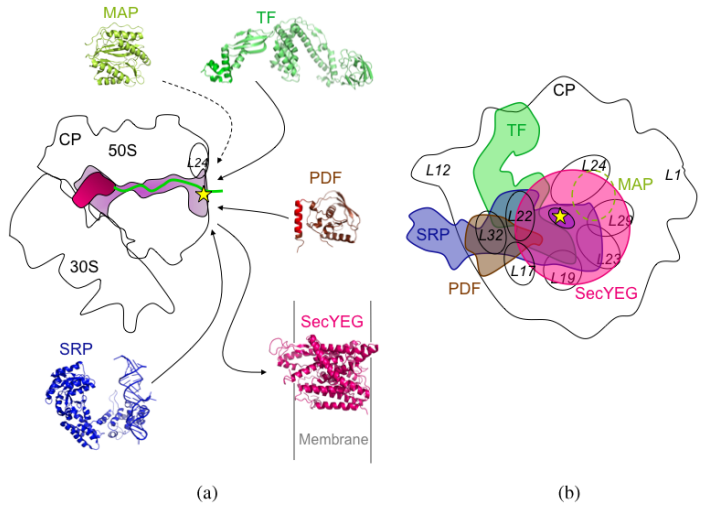

Plate 12.1 A. A cross-section of the 70S ribosome showing the P-site tRNA (purple) and the exit channel. B. The exit site of the 50S subunit. The proteins that will act upon the nascent polypeptide (NC) at the exit site of the large subunit: Peptide deformylase (PDF, brown), methionine amino-peptidase (MAP, no experimental data, dashed lime green), trigger factor (TF, green), signal recognition particle (SRP, blue) and the translocon (SecYEG or PCC, hotpink). The ribosomal proteins surrounding the exit site are labeled. Reprinted with permission from Selmer & Liljas. Exit biology: Battle for the nascent chain. *Structure* **16**: 498–500. Copyright (2008) Elsevier.

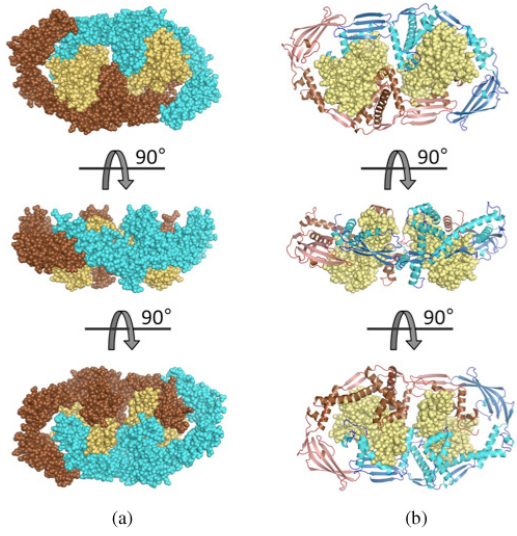

Plate 12.2 A. The structure of two molecules (blue and brown) of trigger factor (TF) with two molecules of ribosomal protein S7 (yellow). B. The structure of TF is shown as a ribbon (Martinez-Hackert & Hendrickson 2009). Illustration made by Saraboji Kadhirvel.

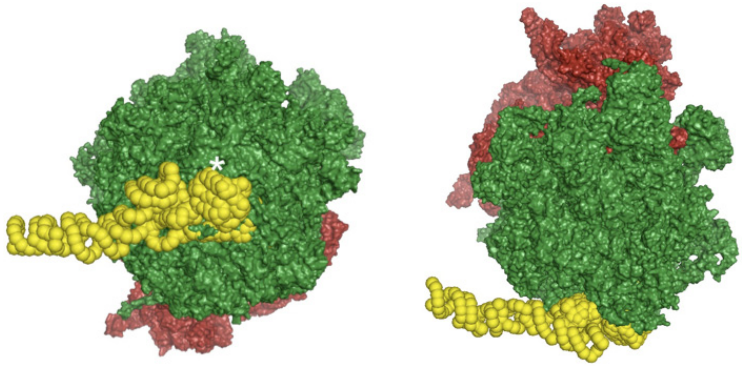

Plate 12.3 The complex between *E. coli* SRP (yellow) and the ribosome (large subunit green small subunit brown). The interaction at the exit site for the NC is illustrated by a star (Schaffitzel *et al.*, 2006). Illustration made by Saraboji Kadhirvel.

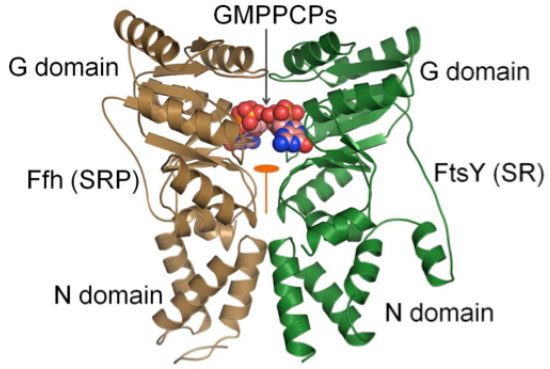

Plate 12.4 The pseudo-symmetric complex between Ffh (SRP; brown) and FtsY (SR; green). The 2-fold axis is marked by an axis. Only the N and G-domains are shown. The GDPNP molecules (atomic structures) are at the interface between SRP and SR (Egea *et al.*, 2004, 2005). Illustration made by Saraboji Kadhirvel.

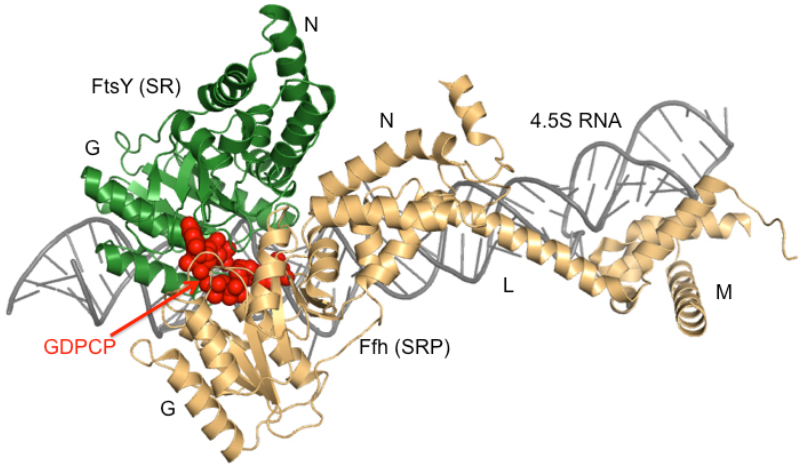

Plate 12.5 The structure of the complex between SRP and SR (Ataide *et al.*, 2011). The 4.5S RNA is shown in black, Ffh in blue and FtsY in green. The M-domain binds to the tetraloop side of the RNA while the NG domains bind to the distal end. Illustration made by Saraboji Kadhirvel.

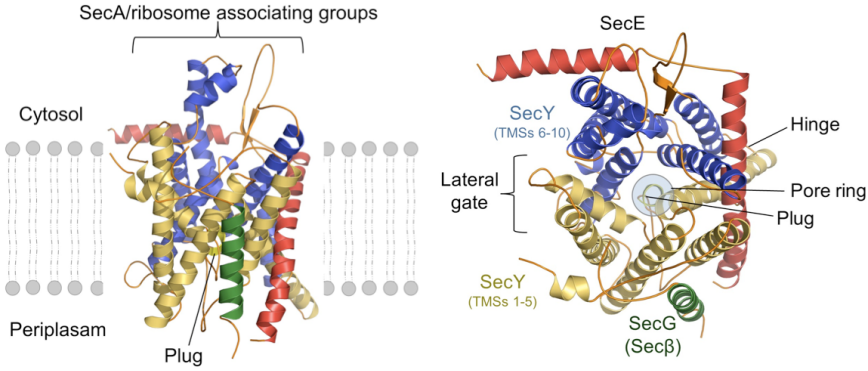

Plate 12.6 The translocon, or PCC, SecYEG from M. jannaschii forming a pore for the translocation of newly synthesized proteins out of the cytoplasm into the membrane (van den Berg *et al.*, 2004). The first five TM-helices of SecY are beige and the last five are blue. SecE is red and SecG is green. (Illustration made by Saraboji Kadhirvel).

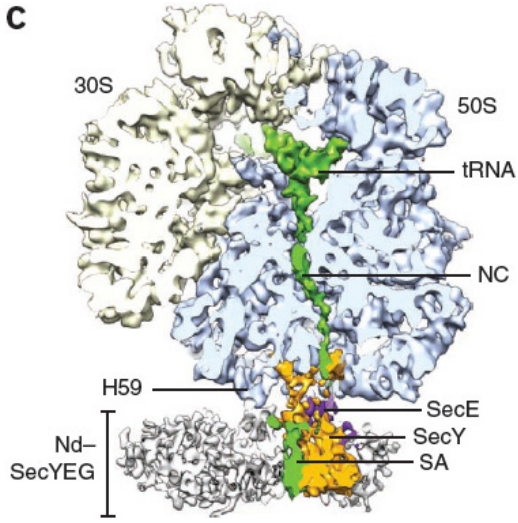

Plate 12.7 *E. coli* ribosomes in complex with SecYEG within a nanodisc (Nd; Fraunfeld *et al*., 2011). A P-site tRNA is bound to NC (green). SecY is shown in yellow and SecE in purple. The signal anchor part of NC is seen on the left side of SecY. Reprinted with permission from MacMillan Publishers Ltd: Frauenfeld *et al*., Cryo-EM structure of the ribosome-SecEY complex in the membrane environment. *Nature Struct. & Mo.l Biol.* **18**: 614–622. Copyright (2011) Nature.

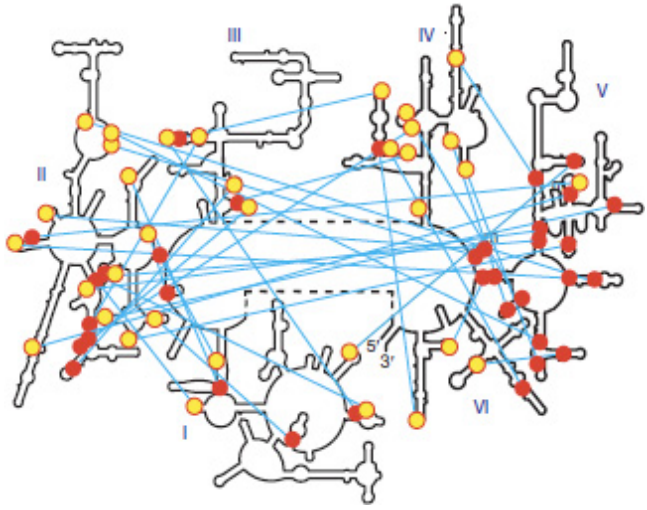

Plate 13.1 The distribution of A-minor motifs in the 23S RNA. The red dots correspond to the double helix part of an A-minor motif and the yellow dots to the loop part. The blue lines indicate the connections between helices and loops. It is noteworthy that domain V has almost only the helical parts of the A-minor motifs (Reprinted with permission from Bokov & Steinberg, A hierarchial model for evolution of 235 ribosomal RNA, *Nature* **457**: 977–980; 2009 Copyright, Macmillan Publishers Limited.)

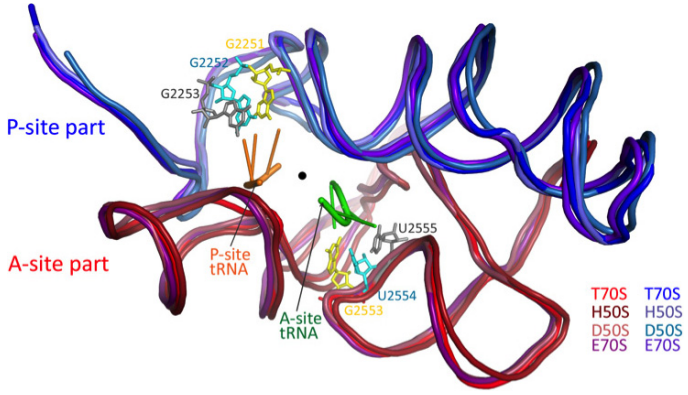

Plate 13.2 The symmetry of the PTC. The A-site part is shown in red and the P-site part in blue. The structures from Dr50S, Tt70S, Ec70S and Hm50S are superimposed. The CCA ends of A site (green) and P site (orange) tRNAs and their interacting regions of the A and P loops are also shown. (Illustration by Saraboji Kadhirvel.)

9

The Catalysts — Translation Factors

Protein synthesis is promoted (catalyzed) by a number of translation factors, which bind transiently to the ribosome during the different phases of translation (see the reviews by Lipmann, 1969; Kaziro, 1978). Is protein synthesis a spontaneous process or is an extra input of free energy needed? Certainly, it can be performed without translation factors with poly(U) as a messenger (see the review by Spirin, 1978), but the rates are many orders of magnitude below the ones for the full system. Slight impurities of translation factors could have supported the activity, but since different agents that inhibit elongation factors did not inhibit the factor-free translation, this possibility could be excluded. Thus, GTP was not needed for factor-free protein synthesis and no GTP hydrolysis was observed. Furthermore, noncleavable GTP analogs did not inhibit the process. Recent observations support the view that both forward and reverse translocation can be performed spontaneously (Shoji *et al.*, 2006; Konvega *et al.*, 2007). However, without the catalytic translation factors protein synthesis is very slow and error-prone.

Most bacterial translation factors have been extensively studied. This has led to proposals for detailed mechanisms of their roles in bacterial translation. However, there are many additional archaeal and eukaryotic translation factors that have only been partly investigated and therefore a detailed description of protein

Table 9.1 Bacterial Translation Factors

Protein	Universally Conserved*	GTPase	Role
Initiation			
IF1	X		Assists IF2 in initiation.
IF2	X	X	Binds 50S subunit to initiation complex (30S subunits, mRNA and fMet-tRNA).
IF3			Assists in dissociation of subunits.
EF-P	X		Homologous to eIF5A. Could be classified as an initiation factor.
Elongation			
EF-Tu	X	X	Binds aatRNA to A-site.
SelB	X	X	Binds SeCys-tRNA to A-site.
EF-Ts			Nucleotide exchange factor for EF-Tu.
EF-G	X	X	Catalyzes translocation of peptidyl tRNA from A- to P-site.
LepA (EF4)		X	Unknown function.
Termination			
RF1, RF2			Recognizes termination codons and releases peptide from P-site tRNA.
RF3	X		Releases RF1, RF2 from ribosome.
Recycling			
RRF			Dissociates the terminated ribosomes into subunits assisted by EF-G.

*Pandit & Srinivasan, 2003.

synthesis in these organisms is lacking. Table 9.1 gives a summary of the key bacterial translation factors. In addition, there are ribosome rescue proteins (see Sec. 9.6) that interact with the ribosome. Furthermore, there are chaperones and signal recognition proteins,

which also interact with the ribosome and participate in the folding and export of proteins (see Chap. 12).

9.1 THE TrGTPases

Several of the translation factors bind and hydrolyze GTP. They belong to the family of GTPases or G-proteins with several characteristic sequence motifs (Bourne *et al.*, 1990, 1991; Vetter & Wittinghofer, 2001). This family of proteins is structurally and functionally related to a large family of ATP-hydrolyzing enzymes (Leipe *et al.*, 2002). The translation factors that belong to the family are IF2, EF-Tu, SelB, EF-G, TetO and related variants, BipA/TypA and RF3. As a group, they can be called the translation GTPases (trGTPases). Some organisms do not have all the genes for these trGTPases (Fig. 9.1; Table 9.2; Pandit & Srinivasan, 2003; Margus, Remme & Tenson, 2007). Thus, RF3, SelB, TypA and Tet seem to be dispensable. For EF-Tu and EF-G there can be two or three genes.

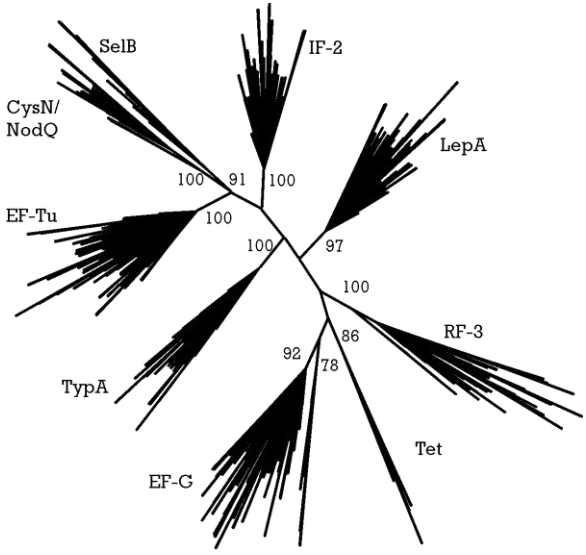

Fig. 9.1 Unrooted consensus tree of trGTPases. (Reproduced from Margus, Remm & Tenson, *BMC Genomics* **8**: 15, 2007.)

Table 9.2 Number of Genes for trGTPases in Archaea and Bacteria*

	IF2	EF-Tu	SelB	EF-G	RF3	LepA	TypA/BipA
Archaea	2†	1–2	0–1	1	—	—	—
Bacteria	1	1–2	0–1	1–3	0–1	1	0–1

* Margus, Remm & Tenson, 2007. 191 genomes were searched.
† In archaea there is one protein, eIF2γ, related to EF-Tu, and one, eIF5B, related to IF2.

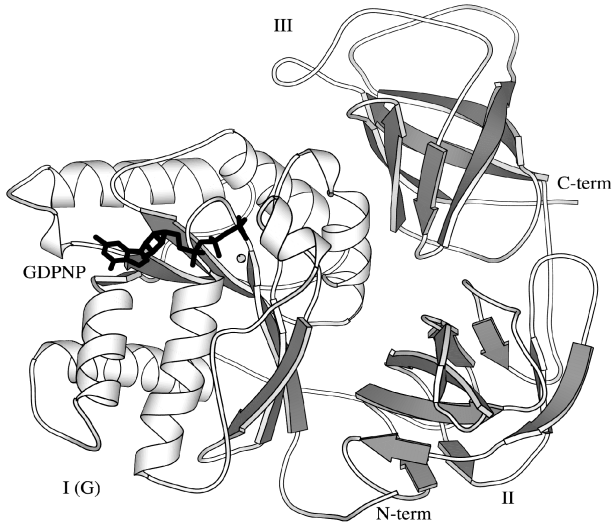

Fig. 9.2 The structure of EF-Tu, the first G-protein to be characterized (Kjeldgaard *et al.*, 1993). The domains are denoted I (the G-domain), II and III. In its complex with a GTP analog like GDPNP, it adopts a closed conformation. A magnesium ion is seen as a small gray circle between the β- and γ-phosphates. (Figure kindly provided by Dr. M. Fodje.)

G-proteins bind GTP or GDP and have a G-domain of 160–200 amino acid residues (Plate 9.1; Vetter & Wittinghofer, 2001). They have a special version of the Rossmann fold, with a large central parallel β-sheet surrounded by α-helices.

There are G-proteins composed only of one domain, but many are multidomain proteins (Fig. 9.2; Kjeldgaard & Nyborg, 1992).

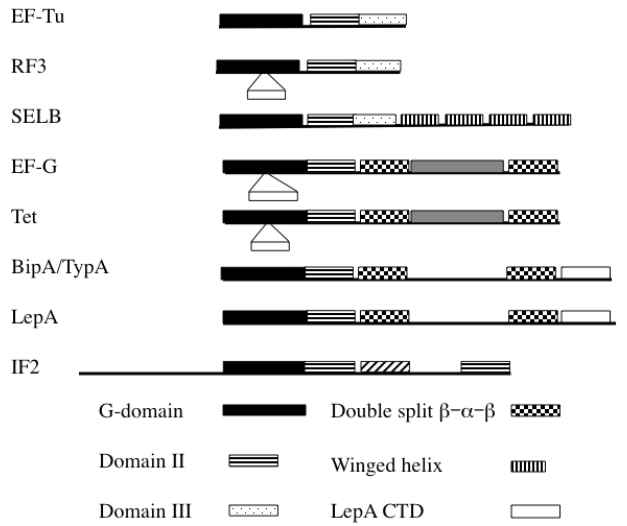

Fig. 9.3 The domain arrangement of trGTPases. The common domains for all trGTPases are the G-domain and domain II. EF-Tu, RF3 and SelB can be classified as the EF-Tu-like family, whereas EF-G, Tet, BipA/TypA and LepA belong to the EF-G family. IF2 is different from these two families. Normally the domains G and II occur at the N-terminus, but IF2 has an N-terminal extension. The G-domain of RF3, EF-G and the Tet family have an insert called G′.

All trGTPases are multidomain proteins with at least two domains in common; the G-domain and the subsequent domain, usually called domain II, a unique β-barrel (Fig. 9.3; Ævarsson, 1995).

A central event for the trGTPases is the GTP hydrolysis on the ribosome. All G-proteins undergo conformational changes associated with GTP hydrolysis (Plate 9.2). The conformational changes of the trGTPases catalyze different steps of protein synthesis, primarily through their interactions with tRNA and the ribosome.

G-proteins have an active *on* state in complex with GTP (Bourne *et al.*, 1990; Wittinghofer & Pai, 1991; Vetter & Wittinghofer, 2001). In this state they can bind to their receptor. The binding of the trGTPases catalyzes some functional steps. After hydrolysis of the GTP to GDP and inorganic phosphate (Pi), they adopt the *off* state

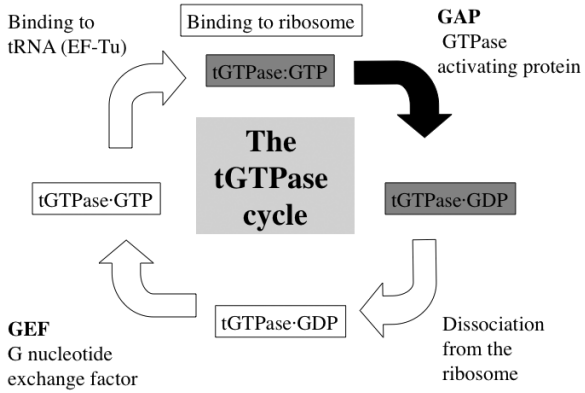

Fig. 9.4 The common elements of the functional cycle for the trGTPases. Two of the four steps are on the ribosome (dark background) and two are off the ribosome (white background). In the case of RF3 the nucleotide exchange also occurs on the ribosome (Zavialov *et al.*, 2001).

and fall off the receptor. The steps catalyzed by the G-proteins are virtually irreversible, due to GTP hydrolysis in the presence of a high concentration of GTP and a low concentration of GDP in the cell. The normal functional cycle for trGTPases is shown in Fig. 9.4.

Isolated G-proteins have low intrinsic GTPase activity (Kaziro, 1978). In the presence of ribosomes but without other components of the system, some of the trGTPases can also hydrolyze GTP in a manner that is uncoupled from protein synthesis (Arai & Kaziro, 1975).

A GTPase needs to interact with the appropriate component of the cell (GTPase-activating protein — GAP) to induce GTPase activity. Obviously, there are multiple possibilities of controlling this activity (Bourne *et al.*, 1990, 1991). The binding of a G-protein to the receptor may lead to an interaction with GAP (Bourne *et al.*, 1990, 1991). After GTP hydrolysis, the conformation of the G-protein changes in such a way that it dissociates from the effector.

Among the numerous GTPases that interact with ribosomes, a large group is needed for ribosome assembly, and this will not be further dealt with here (Caldon *et al.*, 2001; Britton, 2009). Another group of GTPases, the FtsY/Ffh family, is part of the signal recognition particle with its associated proteins and is involved

in transport of the nascent protein to a different compartment (see Chap. 12). BipA/TypA, on the other hand, seems to be a genuine trGTPase, albeit with as-yet-obscure function (Wang *et al*., 2008; deLivron *et al*., 2008).

Whereas many ATPases are motor proteins, most G-proteins act as molecular switches. The energy from ATP hydrolysis is used to drive different mechanochemical molecular processes (Goody & Hoffmann-Goody, 2002). A classical motor protein hydrolyzes its ATP molecule before the conformational change and before the work is done. The ATP hydrolysis leads to a conformational change of the ATPase, which leads to the mechanochemical work. However, a molecular switch induces a process which, when completed, sees the nucleotide become hydrolyzed. This then leads to a loss of affinity of the molecular switch for its receptor (Spirin, 2002). Thus, a characteristic difference between a motor protein and a molecular switch is when the nucleotide is hydrolyzed. Whether EF-G is a molecular switch or a motor protein is discussed (Cross, 1997; Myong & Ha, 2010).

The Consensus Elements, Nucleotide and Mg^{2+}-Binding

Five loops of the G-domains contain highly conserved sequences — the so-called consensus elements (G1–G5; Walker *et al*., 1982; Saraste *et al*., 1990; Bourne, 1990, 1991; Table 9.3). Amino acid residues of the consensus sequences are primarily involved in the binding of GTP or GDP and a magnesium ion. In addition, they sense whether the bound nucleotide is a di- or triphosphate. The consensus sequences connect the C-terminal side of a β-strand to the subsequent α-helix (Table 9.3; Figs. 9.5–9.7). The role of some of the individual residues can also be identified from Fig. 9.6. The first consensus element is the PO_4 loop (normally called the P-loop), interacting with the phosphate groups. Switches I and II interact with the GTP and GDP phosphates and the magnesium ion. The last two consensus elements provide the selection of G-nucleotides (Table 9.3; Fig. 9.6). The magnesium ion is an essential cofactor for GTP hydrolysis (Kjeldgaard *et al*., 1996).

Table 9.3 Consensus Elements of the trGTPases*

Element Alt. Name*	PO_4 loop G1	Switch I G2	Switch II G3	G4	G5
Sequence	GXXXXGKS/ TS/T	RGITI	DXXGH	NKXD	GSAL/K
Role	Interacts with α- and β-phosphates	Binding of γ- phosphate and Mg^{2+}	Indirect Mg^{2+} binding	Recognition of G- nucleotide	Binding of G- nucleotide
IF2	398–406	422–426	444–449	498–501	533–536
EF-Tu	18–26	58–62	80–85	135–138	172–175
SelB	7–15	34–38	57–62	112–115	146–149
EF-G	19–27	61–65	83–88	137–140	261–264
TetO	10–18	52–56	74–79	128–131	219–222
LepA	11–19	50–54	77–82	131–134	161–164
BipA/TypA	12–20	52–56	74–79	128–131	165–168
RF3	20–28	66–70	88–93	142–145	174–177

* All sequence numbers correspond to the *E. coli* proteins.
† Bourne, 1990.

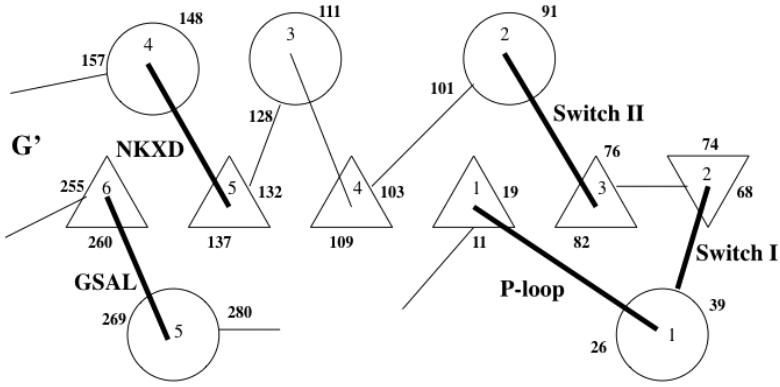

Fig. 9.5 The organization of the G-domain (EF-G). The circles represent α-helices and the triangles β-strands. The numbers on the secondary elements indicate the order number of helices and strands respectively. The numbers on the side represent the amino acid sequence number entering and exiting from that secondary structure element. The five loops with the consensus elements are highlighted. The PO_4 loop and switches I and II are essential for interaction with phosphates and recognition of γ-phosphate. The NKXD and GSAL loops identify the G-nucleotides.

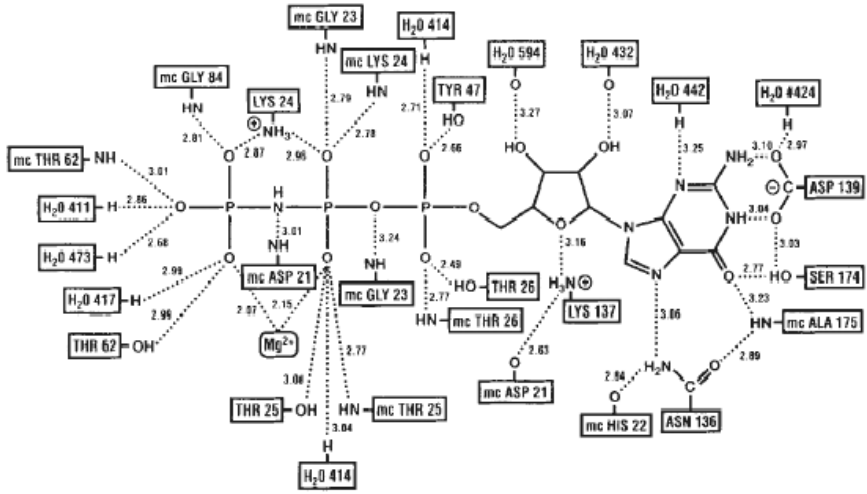

Fig. 9.6 The interactions between the GDPNP and *T. thermophilus* EF-Tu. (Reprinted with permission from Berchtold *et al.*, Crystal structure of active elongation factor Tu reveals major domain rearrangements. *Nature* **365**: 126–132. Copyright 1993, Nature.)

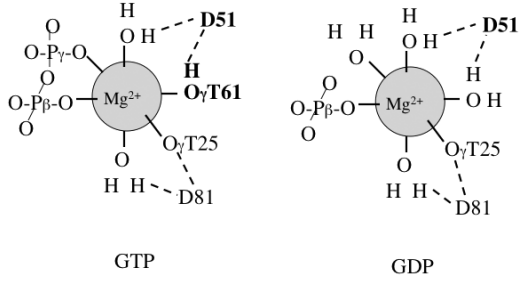

Fig. 9.7 The coordination around the magnesium ion in the GTP and GDP states of EF-Tu. The γ- and β-phosphates of the nucleotide bind to the magnesium ion. Thr25 of the PO_4 loop is a constant ligand to the magnesium ion, and Asp51 of switch I and Asp81 of switch II always interact with the magnesium ligands. Thr61 of switch I binds to the magnesium only in the GTP state.

The first loop, the phosphate binding or PO_4 loop (G1; residues 19–27 in EF-G), folds around the α- and β-phosphate moieties of the G-nucleotide. Residues 21–26 of EF-Tu all make hydrogen bonds to the GDP phosphates (Fig. 9.6; Berchtold *et al.*, 1993). Switch I, the effector region (G2; residues 38–68 in EF-G, and switch II (G3; residues 83–101 in EF-G) are loops that interact with the β- and γ-phosphates of the nucleotide directly (Fig. 9.6) or through the magnesium ion (Fig. 9.7). Their conformations respond to whether GTP or GDP is bound or whether the nucleotide-binding site is empty. The effector loop (switch I) is involved in receptor binding and switches conformation drastically between the GDP and GTP states (Plate 9.2). Switch II relays the state of the bound nucleotide to the conformation of the multidomain trGTPase. The local conformational changes drive global changes of the trGTPases and affect the state of the ribosome.

Ribosome Binding

The trGTPases in complex with GTP bind to overlapping binding sites on the ribosome (Heimark *et al.*, 1976; see Sec. 8.5; Plate 9.3), and the two domains (G and II) that are common to these proteins in all cases interact with the ribosome in similar ways. These interactions have been identified by cryo-EM and crystallography. These studies show that the G-domain interacts primarily with the sarcin–ricin loop (SRL) and the GAR of the large subunit at the base of the L12 stalk (see Sec. 8.5). Domain II interacts with the small subunit in the area of the shoulder and helix h5 of the 16S RNA (Wilson & Noller, 1998). The ASL of the tRNA in the ternary complex, EF-Tu·GTP·aa-tRNA, interacts with the decoding region of the small subunit, and so does domain IV of EF-G. Initially IF2 interacts only with the 30S subunit.

The 'Fly Trap'

L11 and the L12 stalk are bound to the same element of 23S RNA — H42-H44. L11 is not essential, but its absence causes thiostrepton

resistance in living bacteria (Chap. 10; Highland *et al.*, 1975). However, removal of L12 leads to a significantly reduced GTPase activity of both EF-Tu and EF-G (Kischa *et al.*, 1971; Fakunding *et al.*, 1973; Wahl & Möller, 2002; Mohr *et al.*, 2002; Diaconu *et al.*, 2005).

The N-terminal domain of L12 is involved in dimerization and binding to the C-terminal helix of L10 (Chap. 7.4). The C-terminal domain (L12CTD) is the functional part interacting with factors (Leijonmarck *et al.*, 1980). The ribosome contains two or three dimers of L12. The protein is highly flexible, depending on the hinge between its N- and C-terminal domains (Chap. 7.4; Bushuev *et al.*, 1989). The number of flexible L12 monomers varies, depending on whether the ribosomes are free from factors or whether EF-Tu or EF-G is bound to the ribosome with GDPNP or with the antibiotics kirromycin, fusidic acid or viomycin, respectively (Sec. 11.4; Gudkov *et al.*, 1982; Gudkov & Bubunenko, 1989; Gudkov, 1997; Ermolenko *et al.*, 2007). A variation in stalk structure is observable for ribosomes in various states (Stark *et al.*, 1997; Agrawal *et al.*, 1998, 1999; Diaconu *et al.*, 2005; Gao *et al.*, 2009).

Which part of L12CTD interacts with the factors? Mutations of V66, I69, K70 and R73 of L12 have little effect on GTP hydrolysis, but lead to an increased K_M for the binding of EF-G, indicating that these residues are involved in the binding of EF-G to the ribosome. Furthermore, these mutations inhibit the release of inorganic phosphate after GTP hydrolysis by EF-G (Savelsbergh *et al.*, 2005). Likewise, mutations of K65, V66, I69, K70, R73 and K84 have significant effects on ribosome binding of EF-Tu and as a consequence on GTP hydrolysis (Diaconu *et al.*, 2005).

The mutational studies generally agree with NMR experiments, suggesting that IF2, EF-Tu, EF-G and RF3 interact with one and the same helical surface of L12CTD (residues V66, A67, V68, K70, G79, L80, E82; Helgstrand *et al.*, 2007; Plate 9.4). This surface corresponds very well with the conserved surface area of L12CTD (Leijonmarck & Liljas, 1987; Wahl *et al.*, 2000; Wieden *et al.*, 2001). In studies of EF-G binding to the large subunit in complex with micrococcin, L12CTD interacts through these helices with EF-G (Harms *et al.*, 2008).

From studies of the interplay of L12 with IF2 it was concluded that L12 is needed for rapid factor-dependent subunit association (Huang *et al.*, 2010). The interaction between L12 and IF2·GTP accelerates the subunit association, but is not needed for subsequent GTP hydrolysis and Pi release. Mutations of V400 and H448 in the G-domain of IF2 can completely abolish GTP hydrolysis, while subunit association is retained (Huang *et al.*, 2009). Thus, the main role of L12 may be to recruit trGTPases to their specific activities on the ribosome. The effect on GTP hydrolysis is probably a secondary consequence of the binding to the ribosome.

How the trGTPases interact with the four or six copies of L12CTD is still unclear. The L12 stalk including H43–H44 of the 23S RNA (GAR) appears to go between an open and a closed state, depending on the state of the ribosome. With an empty or filled A site the L12 stalk is open, but when the ternary complex is bound to the A/T site it is closed (Valle *et al.*, 2003a). Also, when EF-G binds, the stalk is closed and bent toward EF-G (Gao *et al.*, 2009). L12CTD has been observed interacting with the G′-domain of EF-G both by cross-linking, cryo-EM and crystallography (Plate 9.5; Nechifor & Wilson, 2007; Datta *et al.*, 2005; Gao *et al.*, 2009). However, when EF-G binds to the ribosome in the presence of micrococcin, a position closer to the G-domain is observed (Harms *et al.*, 2008). For EF-Tu (Stark *et al.*, 1997) and IF2 (Allen *et al.*, 2005), interactions with the G-domain have been observed.

In summary, L12 is important for factor function, but not for GTP hydrolysis. The multiple copies of L12 and its CTD seem to participate in the recruitment of trGTPases and guide them to their binding site.

What trGTPase Should Bind?

With a common binding site for trGTPases on the ribosome, how is the right trGTPase selected to bind at a specific state? Without proper control the GTPases would idle and waste GTP. Apparently, the state of the ribosome and in particular the presence and position

Table 9.4 Ribosomal States That Lead to the Binding and GTP Hydrolysis by the trGTPases*

Factor	IF2	EF-Tu	EF-G	RF3
Ribosomal state	30S	Posttranslocation	Pretranslocation	Pretranslocation
Subunit orientation		MSI	MSII	MSII
A-site	IF1	—	pp-tRNA (A/P)	RF1/2
P-site	fMet-tRNA	pp-tRNA	tRNA (P/E)	tRNA
E-site	IF3-NTD	tRNA	—	—

*From Zavialov & Ehrenberg, 2003; Valle *et al.*, 2003b; see also Table 8.4.

of the peptidyl-tRNA control which trGTPase will bind (Valle *et al.*, 2003b; Zavialov & Ehrenberg, 2003). The corresponding two main conformations of the ribosome, pre- and posttranslocation or MSI and MSII, then also contribute to distinguishing which factor should bind.

IF2 binds to the 30S subunit with an mRNA and an fMet-tRNA bound (Table 9.4). After initiation the initiation factors must dissociate to allow EF-Tu to bind the first aminoacyl-tRNA to the A site. If a peptidyl-tRNA is bound to the P site, only EF-Tu can bind to the ribosome while the other trGTPases cannot bind (Zavialov & Ehrenberg, 2003). However, EF-Tu does not discriminate in binding between when a deacylated or peptidyl-tRNA is in the P site (Zavialov & Ehrenberg, 2003). The binding is controlled only by the codon in the A-site.

EF-G does not bind to ribosomes and hydrolyze its GTP if the peptidyl-tRNA is already in the P-site. However, it is not understood how EF-G can discriminate between a peptidyl-tRNA and a deacylated tRNA in the P site since it does bind to the latter (Zavialov & Ehrenberg, 2003; Valle *et al.*, 2003b). Possibly, a deacylated tRNA is not correctly positioned in the P site. Finally, RF3 binds and hydrolyzes its GTP if RF1/2 is bound at a stop codon and the nascent peptide is hydrolyzed and released from the tRNA in the P site (Table 9.4).

Binding Conformation of trGTPases

The trGTPases bind to a common binding site on the ribosome. They function with an on/off mechanism. With a bound GTP molecule they can bind and with GDP they will dissociate from the ribosome. With a common binding site the factors must have a common structure for the interaction.

Switch I is the effector loop that binds to the ribosome and is a key part of this process (Ticu *et al*., 2009). It becomes ordered, interacting with the GTP molecule or its analogs when the factors are free in solution. With GDP switch I is either disordered or pointing away from the nucleotide-binding cavity. When the factor binds to the ribosome in complex with GTP analogs, switch I interacts with the ribosome and remains ordered. When the factors are bound in complex with GDP and antibiotics, which stabilizes the ribosome-binding, switch I is disordered. Table 9.5 summarizes observations of the behavior of switch I in different trGTPases.

When the GTP molecule is hydrolyzed, the phosphate can dissociate and the contacts with the switch loops are lost. The factors change conformation.

The Induction of GTP Hydrolysis — The Ribosomal GAP

The GTPases have low intrinsic activity but can be activated to hydrolyze their bound GTP. This is generally done by a GTPase-activating protein (GAP) when the GTPase is bound to its effector and in response to specific states of their effectors. An arginine of the GAP (trans), called an Arg-finger, interacts with the phosphates to stabilize the transition state. In some cases the Arg-finger is part of the GTPase itself (cis). Some GAPs operate without Arg-fingers (Wittinghofer, 2006). So far no Arg-finger has been identified and it may be absent in trGTPases (Kubarenko *et al*., 2005).

The trGTPases have a histidine in place of the essential glutamine in switch II found in other GTPases (Bourne *et al*., 1991). One would expect that all trGTPases function in a similar manner and are activated on the ribosome by the same GAP. All components

Table 9.5 Conformation of Effector Loop (Switch I) in trGTPases

Factor	State	GTP	GDP	Empty	References
IF2 (eIF5B)	Free	GDPNP, partly disordered	Partly disordered	Partly disordered	Roll-Mecak *et al*., 2000
	Ribosome	GDPNP			Allen *et al*., 2005
EF-Tu (41–62)	Free	GDPNP, ordered, α-helix	Ordered, β-hairpin GDP+kir, partly ordered	Disordered	Nissen *et al*., 1995 Parmeggiani & Nissen, 2006
	Ribosome	GDPCP, ordered, α-helix	GDP+kir, disordered		Schmeing *et al*., 2009 Voorhees *et al*., 2010
EF-G (40–66)	Free	EF-G-2*GTP, ordered, α-helix T84A*GDPNP, partly ordered	GDP, disordered G16V, partly ordered	Disordered	Connell *et al*., 2007 Hansson *et al*., 2005 Czworkowski *et al*., 1994 Aevarsson *et al*., 1994
	Ribosome	GDPCP, ordered, α-helix GDPNP, ordered	GDP+fus, disordered GDP+vio, disordered		Gao *et al*., 2009 Valle *et al*., 2003b Tourigny *et al*., 2013
RF3	Free		GDP, disordered (Ec) or partly ordered (Vg; α-helix) ppGpp, ordered, α-helix		Gao *et al*., 2007a Kihira *et al*., 2012
	Ribosome	GDPNP, ordered GDPCP, weak density			Zhou *et al*., 2012 Jin *et al*., 2011

needed for GTP hydrolysis must be available in EF-Tu itself, since the reaction is induced in the presence of the antibiotic kirromycin in the absence of ribosomes (see Sec. 10.7; Wolf *et al.*, 1977). Thus, kirromycin may induce a conformation in EF-Tu similar to the active GTPase conformation caused by the ribosome. A structure of EF-Tu in complex with aurodox (methyl-kirromycin) shows the histidyl residue (His84) close to the γ-phosphate (Vogeley *et al.*, 2001), but a similar investigation using enacyloxin or kirromycin shows His84 in a different conformation (Parmeggiani *et al.*, 2006). However, in a crystal structure of EF-Tu in complex with GDPCP bound to the ribosome, the histidine is in contact with the water molecule close to the γ-phosphate (Voorhees *et al.*, 2010). EF-G does not hydrolyze its bound GTP off the ribosome. Just like for EF-Tu, EF-G when bound to GDPCP is in a state which is close to the hydrolysis step, with the histidine in contact with the water molecule (Tourigny *et al.*, 2013).

The GTPase-Activating Region

The identification of the ribosomal GAP has probably reached a final conclusion. A GTPase-activating region (GAR; see Sec. 8.5) has been identified, where the G-domains of the trGTPases bind to the ribosome at the base of the L12 stalk (Valle *et al.*, 2003a). Two molecular features could possibly be engaged in activating GTP hydrolysis: either the L12 stalk with protein L11 and its binding region of the 23S RNA (GAR) or the sarcin–ricin loop (SRL). Crystallographic studies of EF-Tu and EF-G with GDPCP bound to the ribosome have shown that L12CTD cannot interact near the GTP binding site since there is not enough space (Voorhees *et al.*, 2010; Tourigny *et al.*, 2013).

SRL is a conserved loop of H95 of the 23S RNA including residues 2659–2662. It is the closest ribosomal element to the GTP bound to the trGTPases (Chan *et al.*, 2004; Connell *et al.*, 2007; Schmeing *et al.*, 2009; Gao *et al*, 2009). Cleaving this region with α-sarcin inhibits trGTPases in the activation step (Blanchard *et al.*, 2004). His19 and His84 of EF-Tu, when bound to

the ribosome in the presence of kirromycin, interact with G2661. If this nucleotide is mutated to C2661, the ribosomes become hyper-accurate, probably due to weaker binding of near-cognate tRNA (Schmeing *et al*., 2009). When EF-Tu (or EF-G) is bound with the noncleavable analog GDPCP, His84 (His87) interacts with the phosphate of A2662 and is placed in its catalytic position next to the water molecule at the γ-phosphate of GDPCP (Voorhees *et al*., 2010; Tourigny *et al*., 2013). It is clear that the ribosomal GAP that induces conformational changes of the trGTPase and stabilizes their transition states is the ribosomal sarcin–ricin loop (Voorhees *et al*., 2010). The ribosome does not have a GTPase-activating protein but a GTPase-activating RNA — GAR! On the other hand, SRL does not undergo any conformational changes upon binding of EF-Tu or EF-G (Schmeing *et al*., 2009; Gao *et al*., 2009).

GTP Hydrolysis by trGTPases

The role of the ribosomal GAR is to activate the trGTPases by inducing conformational changes in the enzymes. The GTPase induction may be similar for all trGTPases.

A water molecule, placed near the γ-phosphate, opposite the β-phosphate, is needed for the GTP hydrolysis (Fig. 9.8). The three requirements for the activation of a GTPase are:

Stabilization of the Transition State

Activation of the water molecule by removing a proton so that the hydroxyl ion can make an associative in-line sn^2 attack on the γ-phosphate and hydrolyze the GTP to GDP and inorganic phosphate.

The critical residues inducing GTP hydrolysis in G-proteins have been identified (see the reviews by Vetter & Wittinghofer, 2001; Vetter & Wittinghofer, 2001 and references therein). In some cases a different residue is found (Wittinghofer, 2006). In the corresponding position in switch II of the trGTPases, there is no glutamine but a conserved histidyl residue (His87 in EF-G, His84 in EF-Tu, residue

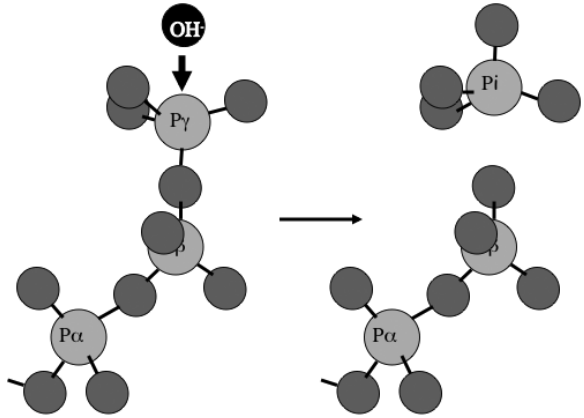

Fig. 9.8 GTP hydrolysis. An activated water molecule makes a linear attack on the γ-phosphate. Whether the reaction is associative, going over a pentavalent phosphor atom, or dissociative is debated (Wittinghofer, 2005).

numbers correspond to *T. thermophilus*). Histidine is a better base for the water activation than glutamine. However, all GTPases probably hydrolyze GTP by the same mechanism and use the same groups for the critical steps in the process. Thus, it is unlikely that trGTPases use histidine for water activation while other GTPases use the poor base glutamine or other residues. Now, there seems to be a consensus for small G-proteins that the γ-phosphate of the GTP molecule acts as a general base by removing a proton from the water molecule, enabling it to attack the γ-phosphate and hydrolyze the phosphate ester (Schweins *et al*., 1995; Pascualato & Cherflis, 2005; Kötting *et al*., 2006; Adamczyk & Warshel, 2011; Wallin *et al*., 2012).

In the case of EF-Tu and EF-G, the histidyl residue is stabilized in a new position by the phosphate of A2662 of SRL (Fig. 9.9). This places the water molecule suitably for activation and hydrolysis. The water molecule can transfer one of its protons to the γ-phosphate and attack the phosphate. This mechanism is very likely the one that operates in the case of all trGTPases. (See further the discussion in Sec. 9.3.)

The trGTPases have two common domains: the G-domain and domain II. It is interesting to note that the homologous domains in

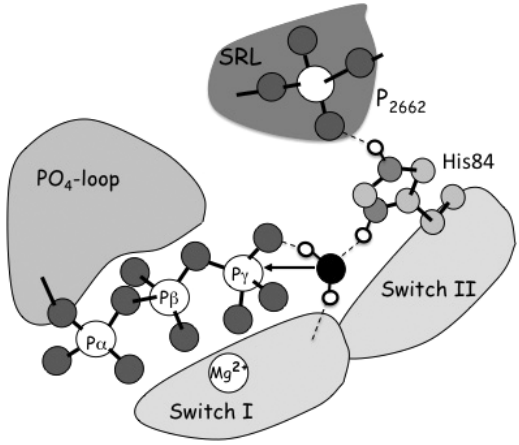

Fig. 9.9 The likely mechanism for GTP hydrolysis by the trGTPases. The phosphate of A2662 of SRL accepts a hydrogen bond from His84 (EF-Tu) and thereby positions it next to the water molecule close to the γ-phosphate, which is unprotonated. The water molecule donates its hydrogen bonds to Thr61 (EF-Tu) of switch I and to the γ-phosphate of GTP. His84 (EF-Tu) is in a negatively charged environment and therefore likely to be protonated. To be able to hydrogen-bond to the water molecule, the histidine has to donate a proton to the γ-phosphate, leading to the in-line attack by the hydroxyl ion on the γ-phosphate (Liljas *et al*., 2011).

EF-Tu, IF2 (eIF5B), EF-G and RF3 behave differently. In the conformational changes between the GTP and GDP conformations, domains G and II of EF-G basically retain their interaction (Laurberg *et al*., 2000; Gao *et al*., 2009), whereas for EF-Tu (Kjeldgaard *et al*., 1993), eIF5B (Roll-Mecak *et al*., 2000) and RF3 (Gao *et al*., 2007) domains II and III move dramatically in relation to the G-domain. This may be related to the conformational changes which these factors induce in the ribosomal subunits (see Sec. 8.5).

Phosphate Release

One step in ATP as well as GTP hydrolysis is the release of phosphate from the enzyme after the hydrolysis step. This can be done at different rates and can be coupled to other functional events due

to conformational changes that it may induce. In the case of IF2, release of the factor from the ribosome requires GTP hydrolysis. Whether phosphate release occurred before or after the dissociation of the factor is unclear (Huang *et al.*, 2009). For EF-G, GTP hydrolysis is very rapid upon binding of the factor to the ribosome. However, the phosphate is only slowly released (Seo *et al.*, 2006). Certain mutations of L12CTD (Val66, Ile69, Lys70 and Arg73) strongly inhibit phosphate release without affecting single round GTP hydrolysis or translocation. This becomes rate-limiting for EF-G turnover (Savelsberg *et al.*, 2005). Thus, L12 is sometimes important for Pi release.

Nucleotide Exchange

After GTP hydrolysis, G-proteins need to release the GDP molecule and be recharged with GTP. This is frequently done through the interaction with a G-nucleotide exchange factor (GEF; Bourne *et al.*, 1990, 1991). The GEF proteins normally work by removing the magnesium ion bound at the phosphates of the nucleotide (Vetter & Wittinghofer, 2001). The complexes between a number of G-proteins and GEFs have been characterized (Vetter & Wittinghofer, 2001).

The affinities for GTP and GDP differ greatly between the trGTPases (Table 9.6). Depending on the relative affinities for GTP and GDP, the GTPases may require GEFs. The best-known GEF in translation is EF-Ts catalyzing the exchange of GDP for GTP in EF-Tu. For IF2 and EF-G, exchange factors are not known and do not seem to be needed. RF3 uses the ribosome for the exchange of GDP for GTP (Zavialov *et al.*, 2001; Zavialov & Ehrenberg, 2003). Further details will be discussed below for each individual factor. A general observation is that the GEFs interact with switches I and II to reduce the affinity of the Mg^{2+} ion and the PO_4 loop which interacts with the α- and β-phosphates (Vetter & Wittinghofer, 2001).

9.2 INITIATION FACTORS

Initiation of protein synthesis is performed on the small subunit. To be able to bind the mRNA, the small and large subunits need to

Table 9.6 Functional Properties of trGTPases

	IF2	EF-Tu	SelB	EF-G	RF3
K_dGTP μM	10.6	0.36	0.74	2.7	2.5
K_dGDP μM	4.5	0.0049	13.4	1.8	0.0055
Affinity ratio GTP/GDP	0.42	0.014	18	0.67	0.0022
Reference	Hauryliuk *et al.*, 2009	Kaziro, 1978	Thanbichler *et al.*, 2000	Mitkevich *et al.*, 2012	Zavialov *et al.*, 2001
GEF		EF-Ts			Ribosome
GTPase trigger	50S binding	Codon recognition	Codon recognition	Ribosome binding	Ribosome binding
Role of GTP hydrolysis	Release of IF2 from 70S	Release of EF-Tu leads to tRNA release into PTC	Release of SelB leads to tRNA release into PTC	Translocation	Factor recycling

be separated since the mRNA passes between them and is wrapped around the neck of the small subunit (Yusupova *et al.*, 2001). The placement of the correct methionine codon (AUG) of the mRNA for the start of translation in bacteria is generally done with the aid of the ribosome-binding site or translation initiation region including the Shine–Dalgarno interaction (see Sec. 8.1). No translation factor is required for these interactions in bacteria. Three bacterial initiation factors, IF1–IF3, subsequently assist in the placement of the fMet-tRNA at the AUG start codon in the P-site. The 30S subunit with mRNA, fMet-tRNA and the three initiation factors form the 30S preinitiation complex (30S PIC). The initiation of translation is further discussed in Sec. 11.3.

Eukaryotic initiation is performed with the aid of 13 initiation factors, including over 30 protein subunits (see the reviews by Pestova & Hellen, 2000; Nyborg *et al.*, 2003; Voigts-Hoffmann *et al.*, 2012). The analysis of complete genomes has shown that the bacterial initiation factors IF1 and IF2 have homologs in the other domains of life. Thus, these initiation factors have been present since the universal ancestor stage of evolution (Kyrpides & Woese, 1998a). All eukaryotic and archaeal genomes also contain sequences

encoding factors called eIF1 (SUI1) and eIF5A. The eIF1 sequence is found in some but far from all bacterial genomes, and eIF5A has a bacterial homolog called EF-P (Kyrpides & Woese, 1998a). A complete understanding of initiation of bacterial translation would need to include the roles of these additional factors.

The eukaryotic factor eIF2 has no counterpart in bacteria. It binds the initiator tRNA and carries it to the small subunit and is released after GTP hydrolysis (see the review by Hinnebusch, 2000). eIF2 is a three-subunit protein where one of the subunits is related to EF-Tu or, even more closely, to SelB (Keeling & Doolittle, 1995; Keeling *et al.*, 1998). The close relationship was confirmed by the determination of the structure of the subunit e/aIF2γ (Schmitt *et al.*, 2002). The dissociation of eIF2 from the initiator tRNA and the ribosome is associated with GTP hydrolysis (Lee *et al.*, 2002). This GTP hydrolysis is induced differently than the regular trGTPases, since the large subunit with the SRL is absent.

Bacterial IF2 catalyzes the association of the two subunits. In archaea and eukaryotes, eIF5B catalyzes this activity and is an ortholog of IF2 in bacteria. Its structure and function are well characterized. Thus, two GTP molecules are hydrolyzed during archaeal and eukaryotic initiation (Lee *et al.*, 2002).

IF1

IF1 has been identified as a factor that stimulates the dissociation of the ribosomal subunits and the binding of IF2 (Grunberg-Manago *et al.*, 1975; Pavlov *et al.*, 2008). The structures of IF1 and eIF1A are known (Sette *et al.*, 1997; Battiste *et al.*, 2000). This small globular protein has an OB fold like ribosomal proteins S1, S12, S17, L2 (Table 7.4) or several cold shock proteins (Fig. 9.10). It binds to the decoding part of the A-site, as has been shown in different ways, including a crystal structure of the complex of the small subunit with IF1 (Moazed *et al.*, 1995; Dahlquist & Puglisi, 2000; Carter *et al.*, 2001; Plate 9.3). By this binding, it prevents tRNA molecules from binding here, in particular the initiator tRNA, and also assists in directing fMet-tRNA into the P-site.

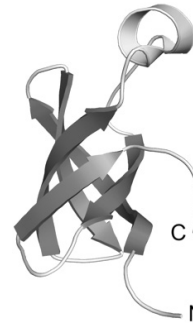

Fig. 9.10 The structure of IF1 (Sette *et al.*, 1997; Battiste *et al.*, 2000). The protein has a version of the OB fold. (Illustration by Saraboji Kadhirvel.)

IF1 interacts with IF2 on the ribosome (Moreno *et al.*, 1999; Allen *et al.*, 2005), which may explain why the two proteins are conserved throughout evolution (Stringer *et al.*, 1977; Choi *et al.*, 2000). No IF1 has been found in mitochondria (Koc & Spremulli, 2002). An insert in IF2 may substitute for the missing IF1. The structural location of the insert agrees with the relative positions of IF1 and IF2 (Gaur *et al.*, 2008).

IF2

IF2 is the largest of the bacterial translation factors and is a GTPase (Grunberg-Manago *et al.*, 1975; Gualerzi & Pon, 1990). In archaea and eukaryotes, eIF5B replaces bacterial IF2 (Myasnikov *et al.*, 2009). IF2/eIF5B is found in all organisms (Lee *et al.*, 1999; Choi *et al.*, 2000) and catalyzes the joining of the ribosomal subunits in a GTP-dependent manner (Pestova *et al.*, 2000; Shin *et al.*, 2002; Antoun *et al.*, 2003). However, eukaryotic eIF2, for which there is no corresponding factor in bacteria, catalyzes the binding of initiator tRNA to the small subunit. Bacterial IF2 can bind fMet-tRNA^{fMet}, but in the kinetically dominating pathway IF2·GTP binds by itself to the small subunit (Pavlov *et al.*, 2010; Milon *et al.*, 2010).

IF2/eIF5B has variable structure. *E. coli* IF2 has an N-terminal extension, of about 390 residues (Sacerdot *et al.*, 1992;

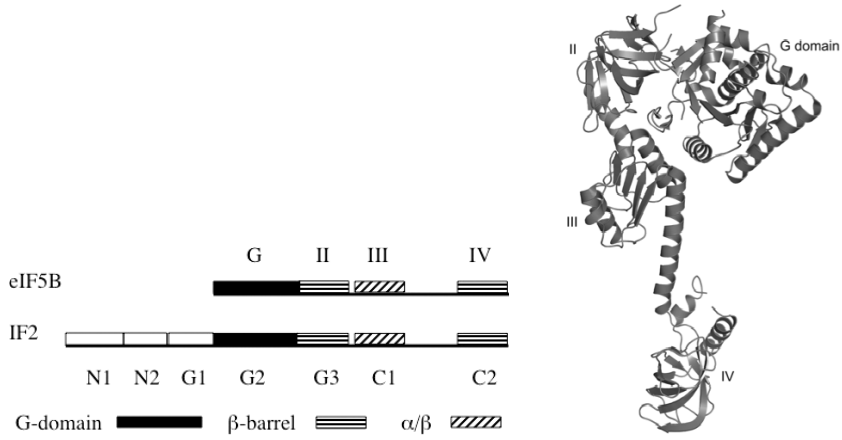

Fig. 9.11 Left: The domains of *Methanobacterium thermoautotrophicum* eIF5B are compared with terminology used for *E. coli* IF2. Right: The structure of *M. therm*. eIF5B (Roll-Mecak *et al*., 2000). The G-domain and domains II and III interact with each other, which is followed by the long α-helix and domain IV. (Illustration by Saraboji Kadhirvel.)

Tiennault-Desbordes *et al.*, 2001; Laursen *et al*., 2005; Caserta *et al*., 2006; Margus *et al*., 2007). Furthermore, it can be expressed in two main forms, IF2α and IF2β. The latter is produced from a downstream in-frame GUG codon and lacks the first N-terminal region (Plumbridge *et al*., 1985). *E. coli* IF2α has three domains in this N-terminal region (Fig. 9.11; Moreno *et al*., 1999) Two globular domains have been identified within the N-terminal extension (Allen & Frank 2007). The structure of the first 50 amino acids has been determined and shows similarities to DNA-binding proteins and some tRNA synthetases (Laursen *et al*., 2004). The N-terminal region contributes to the binding of IF2 to the small subunit (Moreno *et al*., 1998; Allen *et al*., 2005; Allen & Frank, 2007).

The crystal structure of an archaeal eIF5B has been determined for the empty form, with GDP and with GDPNP (Roll-Mecak *et al.*, 2000). The protein is highly extended (about 110 Å) and has the shape of a chalice (Fig. 9.11). The G-domain is situated at the N-terminus, followed by the classical domain II, as

in all trGTPases (Ævarsson, 1995). Domain III has a α/β fold reminiscent of a four-stranded Rossmann fold protein like domain II of ribosomal protein L1. Domain IV has the same antiparallel β-barrel fold as domain II, present in all trGTPases. The protein is remarkable, in that domain IV, the base of the chalice, is situated far away from the main body of the molecule due to a 40-Å-long α-helix that extends from the three N-terminal domains. One part of the helix, solvent-exposed on all sides, has the unusual amino acid sequence EEEKKKK. Switch I is disorganized in all crystal structures. Switch II is situated at the heart of eIF5B, between domains I, II and III (like in EF-Tu and EF-G; Sec. 9.3). The differences between the three structures of the protein primarily concern switch II, which undergoes distinct conformational changes, but not as dramatic as for EF-Tu (Roll-Mecak *et al.*, 2000). In the conformational changes from the GDP to the GTP state, domains II and III move as a block in relation to the G-domain like in EF-Tu. The small changes induced by the nucleotide, transmitted through switch II to the interdomain helix, lead to a significant movement of domain IV.

A number of mutants in switches I and II of IF2 have been analyzed in relation to the structures of eIF5B. Mutations that block GTP hydrolysis can nevertheless stimulate the joining of the subunits and stabilize initiator tRNA binding. However, they do not function in translation, since IF2 remains bound to the ribosome (Shin *et al.*, 2002; Antoun *et al.*, 2006a, b; Huang *et al.*, 2009). A suppressor mutation, in the G-domain of eIF5B, caused weaker binding to the ribosome and permitted release of the factor even without GTP hydrolysis (Shin *et al.*, 2002).

Cryo-EM studies have provided views of IF2 bound to 30S subunits (Simonetti *et al.*, 2008; Julián *et al.*, 2011; preinitiation complex, 30S PIC) as well as to the full 70S initiation complex (Allen & Frank, 2007; 70S IC). Plate 9.3 shows IF2 bound to the small subunit in a manner very similar to that of the other trGTPases.

IF2 and fMet-tRNA^{fMet} are anchored at one point each of the 30S subunit: the anticodon interacts with the initiator codon of the mRNA, and domain II of IF2 interacts with helices h5 and h14 of

16S RNA (Plate 9.6). In *E. coli*, domain N2 also interacts with the 30S subunit (Allen & Frank, 2007). Domain IV of IF2 interacts strongly with the CAACCA 3′ end of the tRNA. While IF2 does not carry fMet-tRNA^{fMet} to the ribosome, it anchors the initiator tRNA to the small subunit through these stabilizing interaction. A surprising difference is identified between the structure of eIF5B alone, and bacterial IF2 bound to the 70S IC or to the 30S PIC. In one case domains III (C1) and IV (C2) are closely associated (Julián *et al*., 2011). In the latter case domain III of IF2 is associated with domain IV instead of interacting with domain II (Simonetti *et al*., 2008). This relates in an interesting way to mutants that compensate for a deficiency to formylate the methionine of the fMet-tRNA. Some of these mutations are located on the surface of domain III, which can contact domain IV but seems to have no direct interaction with the initiator tRNA (Pavlov *et al*., 2011). If this is the case, the contact between the initiator tRNA and domain IV differs whether the tRNA is formylated or not. However, details of the structural interpretations remain uncertain, since there is no crystal structure of IF2 alone or when bound to the ribosome (Myasnikov *et al*., 2009).

When IF2•GTP and fMet-tRNA^{fMet} are bound to the small subunit forming the 30S PIC, the large subunit can attach. Indeed, the main task of IF2 is subunit association. A 2600 Å^2 surface of the 50S subunit becomes inaccessible upon association with IF2 (Allen *et al*., 2005; Antoun *et al*., 2006a). In this 70S IC the 30S subunit is oriented about 4° counterclockwise from the orientation in the postinitiation complex. This rotation is similar to the ratcheting (Table 8.4). The cryo-EM densities also reveal a number of additional features (Plate 9.6). The N-terminal extension of IF2 is seen close to domain II. Densities that fit nicely with IF1 and IF3 surround fMet-tRNA^{fMet} on each side. In addition, a density at the G-domain of IF2 and close to L11 could be a C-terminal domain (CTD) of L12 (Allen *et al*., 2005).

The GTP molecule bound to the G-domain gets into close contact with the SRL upon interaction of the 50S subunit (Allen & Frank, 2007). IF2 will rapidly hydrolyze its GTP, as soon

as the 50S subunit attaches. Normally, IF2 with GDP will dissociate. Mitkevich *et al*. (2012) have studied the interaction of IF2 with a 27-nucleotide fragment of SRL. Here it is evident that the binding of IF2 to GDP and SRL is mutually exclusive. However, IF2 binds strongly to SRL both without nucleotide and with GTP. Evidently, the GDP conformation of IF2 is not compatible with binding to SRL.

IF3

IF3 has multiple functions during initiation. It promotes dissociation of 70S ribosomes (Subramanian & Davis, 1970), and prevents association between the two ribosomal subunits before proper initiation has been achieved (Kaempfer, 1972). In addition, it directs the initiator tRNA to the P-site, accelerates binding of fMet-tRNA and influences the kinetics and fidelity of codon–anticodon recognition of the fMet-tRNA (Meinnel *et al*., 1999; O´Connor *et al*., 2001; Antoun *et al*., 2006b).

The structure of IF3 has been investigated (Biou *et al*., 1995; Garcia *et al*., 1995a, b). The protein has a dumbbell shape with two domains separated by an α-helix (Fig. 9.12). The location of the two domains on the ribosome has been investigated by crystallography, cryo-EM and chemical labeling studies (Moazed *et al*., 1995; McCutcheon *et al*., 1999; Pioletti *et al*., 2001; Dallas & Noller, 2001; Fabbretti *et al*., 2007; Myasnikov *et al*., 2009; Julián *et al*., 2011). Labeling studies and cryo-EM suggest a location of IF3C on the small subunit at the interface side of the platform (Fig 9.13). This binding site prevents H69 of the large subunit from interacting with the small subunit through intersubunit bridge B2b. It was not accessible for binding for packing reasons in the crystals (Pioletti *et al*., 2001). IF3N interacts with the knee region of the initiator tRNA (Julián *et al*., 2011).

The functional properties, at least *in vitro*, seem primarily to be associated with the C-terminal domain (Petrelli *et al*., 2003). IF3 dissociates spontaneously from the small subunit upon formation of the 70S ribosome (Antoun *et al*., 2006a).

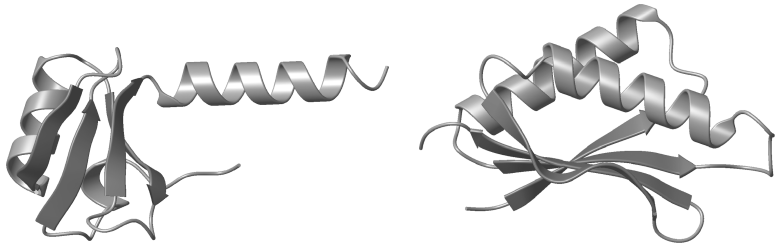

Fig. 9.12 The dumbbell structure of IF3 (Biou *et al*., 1995). The N-terminal domain (IF3N) and the connecting α-helix (left) are followed by the C-terminal domain (IF3C; right). (Illustration taken from Selmer, 2002 with kind permission.)

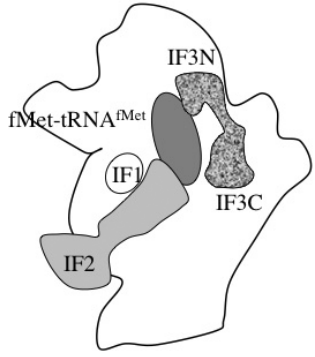

Fig. 9.13 The factors IF1 and IF3 occupy parts of the E and A sites respectively, surrounding and guiding the initiator tRNA. The C-terminal domain of IF2 interacts with the acceptor end of the tRNA. IF3N interacts with the knee of the initiator tRNA, while IF3C is at subunit bridge B2b (Myasnikov *et al*., 2009; Julián *et al*., 2011).

EF-P

With an increasing number of completely sequenced genomes, it is clear that a protein identified as an initiation factor in archaea and eukarya (a/eIF5A) is also present in bacteria (Kyrpides & Woese, 1998a, b). Thus, the protein is universal (Harris *et al*., 2003). In bacteria this protein, called EF-P, is essential for viability (Aoki *et al*., 1997, 2004). It has long been discussed as a possible elongation

factor (Glick *et al*., 1979). The protein has to a large extent been ignored as being not needed for normal translation.

The structure of EF-P/eIF5A is determined both from eukaryotes and archaea and from bacteria (Kim *et al*., 1998; Park *et al*., 2010). The latter have three domains with the shape of an L, reminiscent of the shape of a tRNA (Benson *et al*., 2000). The N-terminal domain is unique in structure, whereas the two following domains have similar folds. The archaeal and eukaryotic factors lack the third domain.

In archaea and eukaryotes a lysine of the protein is uniquely modified to a hypusine, which is essential for function (Park *et al*., 2010). The corresponding lysine in bacterial EF-P is located at the tip of a loop and also modified, to a hydroxylated lysyllysine by three enzymes in *E. coli* called YjeA, YjeK and YfcM (Yanagisawa *et al*., 2010; Park *et al*., 2012; Peil, *et al*., 2012). The modified form is the functional version of the protein. Thus, EF-P, a tRNA mimic, is aminoacylated by YjeA, a paralog of an aminoacyl synthetase (RS) lacking RS activity (Yanagisawa *et al*., 2010; Navarre *et al*., 2010).

A crystal structure of *T. thermophilus* 70S ribosomes in complex with EF-P (Plate 9.7) shows the factor bound between the P and E sites and positioning the initiator tRNA in the P site (Blaha *et al*., 2009). The modified residue is close to the CCA end of the initiator tRNA and interacts with C75 and the 23S RNA (Blaha *et al*., 2009). As shown by Allen *et al*. (2005) and Simonetti *et al*. (2008), the initial binding of fMet-tRNA is to the P/I site between the P and E sites (Fig. 8.4). This could be due to the absence of both an E-site tRNA and a nascent peptide, both of which would direct the tRNA to the P-site. Thus, the task of EF-P may be to move the acceptor end and the acyl moiety of the initiator tRNA into the peptidyl transfer site (Fig. 8.4; Blaha *et al*., 2009). This may clarifiy the role of EF-P as a factor operating in the transition from initiation to elongation. This explains why in eukaryotes it is classified as an initiation factor. The binding sites for EF-P and IF3 overlap. Therefore IF3 has to dissociate before EF-P can bind.

9.3 ELONGATION FACTORS

EF-Tu

The tRNA charged with amino acid needs to be protected from hydrolysis, which would otherwise easily occur in the cytoplasm. The role of elongation factor Tu (EF-Tu) is to bind and protect charged tRNAs and bind cognate tRNA to the ribosomal A-site (see the review by Krab & Parmeggiani, 1998). EF-Tu does not bind uncharged tRNAs. It is very abundant in the bacterial cell and can thus protect charged tRNAs from hydrolysis. In eukaryotes and archaea, its paralog is called elongation factor 1 (EF1) and is composed of several subunits.

EF-Tu is a trGTPase. Only when EF-Tu is activated with a GTP molecule can it bind the aminoacyl-tRNA. The complex between EF-Tu, GTP and aminoacyl-tRNA is called the ternary complex (TC). This complex binds to the ribosome. If the anticodon of the aminoacyl-tRNA bound to EF-Tu matches the codon of the mRNA in the decoding part of the A-site on the small subunit, EF-Tu is induced to hydrolyze its GTP to GDP. This has the effect that EF-Tu undergoes a large conformational change that leads to its dissociation from the tRNA and the ribosome. To be able to engage in a new elongation cycle, the GDP needs to be exchanged for GTP. This exchange is catalyzed by EF-Ts (Fig. 9.14).

EF-Tu recognizes the aminoacyl ester moiety of tRNAs but does not discriminate between different amino acids or tRNAs, with some exceptions. It does not bind fMet-tRNA or Se-Cys-tRNA^{Sec} (see below). Obviously, specific features of these special amino acids and tRNAs are recognized.

Structure

EF-Tu was the first G-protein to be characterized (Miller & Weissbach, 1977). Thus, the structure of the protein has had significant interest for comparisons with numerous other GTPases (Vetter & Wittinghofer, 2001). Initially the structure of the factor was characterized in complex with GDP

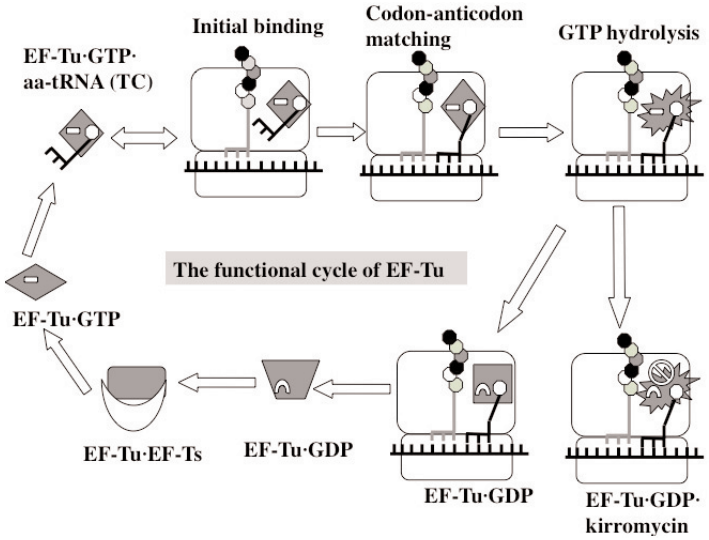

Fig. 9.14 The functional cycle of EF-Tu starts at the left, where EF-Tu in complex with GTP is in the *on* state and can bind any aminoacyl-tRNA. The ternary complex (TC) formed binds to the ribosome initially without contact between codon and anticodon. Subsequently a bend of the tRNA allows the anticodon to be checked against the codon. In the case of a cognate fit, the GTP is hydrolyzed to GDP and GTP hydrolysis changes the conformation of EF-Tu to the *off* state, and it dissociates from the tRNA and the ribosome. The aminoacyl-tRNA is then accommodated into the A site and EF-Tu will be recharged with a new GTP molecule by EF-Ts.

(Plate 9.8c; Kjeldgaard & Nyborg, 1992). The factor is composed of three domains: the G-domain at the N-terminus and domains II and III (see Fig. 9.2). Other crystal forms have allowed the examination of EF-Tu in complex with GDP, GDPNP, GDPNP and aminoacyl-tRNA (Berchtold *et al.*, 1993; Kjeldgaard *et al.*, 1993, Nissen *et al.*, 1995). The structure of EF-Tu in complex with antibiotics or EF-Ts is also described below.

The conformation of the GDP complex is an open structure with a hole between the three domains. In the effector loop (switch I), 14 residues were lost by proteolysis. After dissociation of GDP, assisted by EF-Ts, EF-Tu is able to bind a molecule of GTP

(Ruusala *et al*., 1982; Schümmer *et al*., 2007). EF-Tu in complex with GTP or its analogs has a significantly different and more closed structure (Plate 9.8; Berchtold *et al*., 1993; Kjeldgaard *et al*., 1993). GTP analogs such as GDPNP are used for the structural studies since GTP would be hydrolyzed during the time of the experiment. Domains II and III move as a block with regard to the G-domain. The largest movement of atoms on the surface is about 40 Å and can be described as a rotation of the G-domain in relation to domains II and III by 90° (Plate 9.8). The loss of the γ-phosphate after hydrolysis of the GTP is transmitted through the PO_4 loop to switch I, the effector loop, and switch II to affect the whole molecule. In particular, switch I undergoes a dramatic change (Polekhina *et al*., 1996). A β-ribbon in the GDP form (residues 56–66; *T. thermophilus* numbering) is converted to a short α-helix and a loop in the GTP form (Plate 9.9).

Ternary Complexes

Crystallographic structures of the complexes between EF-Tu and $tRNA^{Phe}$ and $tRNA^{Cys}$ have been determined (Nissen *et al*., 1995, 1999; Nielsen *et al*., 2004). GTP analogs were used in these experiments. The structures of the two complexes are highly similar. The conformation of the protein is marginally changed from the GTP-binding closed conformation. Likewise, the tRNA has the normal L-shaped structure. In the case of the complex with $tRNA^{Cys}$, the angle of the L is somewhat larger than normal, about 100° (Nissen *et al*., 1999).

All three domains of EF-Tu are engaged in the binding of tRNA, but only the aminoacylated CCA end, the acceptor stem and the T-stem and loop of the tRNA participate in the binding (Fig. 9.15c). Thus, the acceptor stem and the CCA end interact with specific pockets on domain II of EF-Tu while the amino acid binds in a large cavity between domains I and II (Nissen *et al*., 1995, 1999). The conserved residue Glu271 is stacked over the A76 and makes a hydrogen bond with the 2′OH of the ribose. The amino group of the aminoacyl residue forms hydrogen bonds to

the main chain carbonyl of Asn285 and the main chain NH of His273. The side chain of the aminoacyl moiety (Phe or Cys) is in van der Waals contact with the side chains of Asn285 and His67. The phosphorylated 5′ end binds between all three domains of EF-Tu and interacts with the conserved residues Lys90 and Arg300. The T-stem has a large interface with domain III. This interaction may be an important part of the selection of tRNAs (Nissen *et al.*, 1995).

EF-Tu should not form ternary complexes with initiator tRNA or $tRNA^{Sec}$. The formyl group of fMet prevents the specific recognition of the amino group by EF-Tu. Also, the missing base pair at positions 1–72 of $tRNA^{fMet}$ could be important for the discrimination. Three base pairs inducing a special structure at the joining of the acceptor and T-stems may be responsible for the discrimination of $tRNA^{Sec}$ (Rudinger *et al.*, 1996). Domain III of EF-Tu interacts with these nucleotides. Normally, specific hydrogen bonds are formed between G63 and G64 of the tRNA with Glu390 and Gly391 of EF-Tu (Nissen *et al.*, 1999). The ternary complex is in the ribosome-binding conformation. An overview of the conformations of EF-Tu is shown in Fig. 9.15.

Antibiotics Targeting EF-Tu

Four classes of antibiotics inhibit the function of EF-Tu (Krab & Parmeggiani, 1998, 2002). They fall into two functional groups. Pulvomycin and GE2270A lock EF-Tu in the ‘off’ state by preventing EF-Tu from adopting the active conformation and forming the ternary complex. Kirromycin and enacyloxin IIa lock EF-Tu in the ‘on’ conformation and prevent the release of EF-Tu from the ribosome after GTP hydrolysis (Fig. 9.15).

The best-characterized inhibitor, kirromycin, binds to EF-Tu·GTP or to the ternary complex (Parmeggiani & Swart, 1985). It inhibits the structural rearrangement of EF-Tu after GTP hydrolysis and Pi release. Thus, EF-Tu will not fall off the ribosome (Wolf *et al.*, 1977). The structures of EF-Tu·GDP with kirromycin, aurodox (N-methyl-kirromycin) or enacyloxin IIa

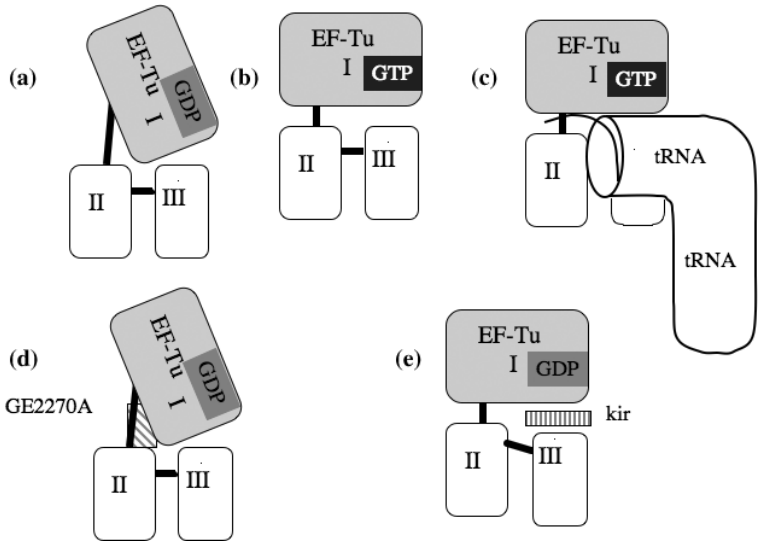

Fig. 9.15 Schematic representation of different active and inhibited conformations of EF-Tu. **(a)** The GDP conformation is open, without contact between domains I and II. **(b)** The GTP conformation has a closed arrangement of the domains. **(c)** A tRNA binds to the domain interface region of the closed GTP conformation of EF-Tu with the CCA-aminoacyl part between domains I and II. **(d)** EF-Tu, inhibited by GE2270A, is in the GDP conformation with the inhibitor bound between domains I and II (Heffron & Jurnak, 2000). The binding sites for the terminal A and the aminoacyl moiety are occupied, which prevents the formation of the ternary complex. **(e)** The kirromycin-inhibited form of EF-Tu is close to the GTP conformation (Vogeley *et al.*, 2001). The inhibitor is bound between domains I and III, locking EF-Tu in a closed conformation that cannot dissociate from the ribosome even though the GTP hydrolysis has taken place. This conformation also binds aminoacyl-tRNA.

have been investigated, as well as ternary complexes with kirromycin and enacyloxin (Vogeley *et al.*, 2001; Parmeggiani *et al.*, 2006a). Here EF-Tu is close to the GTP conformation (Fig. 9.15), explaining why the complex is retained on the ribosome despite the fact that the GTP molecule is hydrolyzed. These antibiotics act like glue between the G-domain and domain III.

To allow kirromycin to bind, the tight interaction between these domains is opened up somewhat (Plate 9.8b, d).

Crystal structures of EF-Tu with GE2270A and pulvomycin have also been determined (Heffron & Jurnak, 2000; Parmeggiani *et al.*, 2006b). Even though these antibiotics are quite different chemically, they bind to partially overlapping sites. Primarily they bind to domain II of EF-Tu and prevent the G-domain from adopting the active conformation even if the GTP analog GDPNP is bound (Fig. 9.15).

Binding of EF-Tu to the Ribosome

The ternary complex of EF-Tu with tRNA bound to the GTPase binding site of the ribosome (see Sec. 8.5) was initially analyzed by cryo-EM techniques (Stark *et al.*, 1997, 2002; Valle *et al.*, 2002, 2003a, Villa *et al.*, 2009; Schuette *et al.*, 2009). To make a stable complex with the ribosome, GDP and kirromycin were used. Kirromycin locks the ternary complex on the ribosome despite the fact that GTP hydrolysis has occurred. The best resolved cryo-EM studies are at 7 Å resolution or better (Villa *et al.*, 2009; Schuette *et al.*, 2009). However, it was a big step forward when crystals of 70S ribosomes with a ternary complex were obtained and a structure at 3.6 Å could be analyzed (Schmeing *et al.*, 2009). Subsequently, a complex using GDPCP was studied at 3.2 Å resolution (Voorhees *et al.*, 2010).

In the crystal structure of the ribosome with EF-Tu bound in complex with both kirromycin and paromomycin (Schmeing *et al.*, 2009), the E and P sites are occupied by $tRNA^{Phe}$ and the ternary complex contains a Thr-$tRNA^{Thr}$ (Plate 8.3). Here, the ribosome is in the classical (MSI) state (Table 8.4; Frank & Agrawal, 2000), with the 30S subunit in the closed state (Ogle *et al.*, 2002), which moves the 16S RNA toward EF-Tu (Sec. 8.2; Schmeing *et al.*, 2009). The L12 stalk is also in the closed state (see above). The bases in the small subunit that participate in identifying the cognate anticodon (G530, A1492 and A1493) are flipped out. The tRNA primarily interacts with EF-Tu through the same contacts as in the ternary

complex alone. Here the buried surface area is 1540 Å^2. On the other hand, the tRNA has few contacts with the ribosome and buries only 482 Å^2. The size of the buried surface relates to the strength of binding.

The structure of EF-Tu bound to the ribosome (Schmeing *et al.*, 2009) is essentially as in the crystal structures of the ternary complex with aurodox (Vogeley *et al.*, 2001; Nissen *et al.*, 1995, 1999; Parmeggiani *et al.*, 2006). The GTP-binding site of EF-Tu interacts with the SRL (Plate 9.10; Stark *et al.*, 2002; Valle *et al.*, 2002, 2003a; Schmeing *et al.*, 2009). Switch I of EF-Tu is invisible, probably due to multiple conformations (Valle *et al.*, 2003a; Schmeing *et al.*, 2009). No contact between EF-Tu and the L12 stalk could be observed (Schmeing *et al.*, 2009). Domain II of EF-Tu interacts with helix h5 of the 30S subunit (Valle *et al.*, 2003a). Two loops of EF-Tu change conformation to interact with the shoulder of the 30S subunit. In particular, this involves EF-Tu residues 219–226 and U368, which are highly conserved in all species (Schmeing *et al.*, 2009). If Gly222 is mutated to Asp, GTP hydrolysis is prevented. The codon–anticodon recognition is evidently not transmitted properly to the GTPase center due to improper interactions with the 16S RNA (Vorstenbosch *et al.*, 1996). In this conformation EF-Tu must be close to its transition state. The GTP molecule has been hydrolyzed, but the factor has not dissociated from the ribosome due to the presence of kirromycin.

The cognate tRNA is bound to the A/T-site (Plate 8.4; see also Sec. 11.4). The anticodon contacts the mRNA in the decoding area while the acceptor arm is bound to EF-Tu far from the PTC. This makes the anticodon stem of the tRNA bend by about 30°, which is necessary for the tRNA to interact with both the codon and EF-Tu. The 3′ end of the tRNA is also distorted. Protein S12 interacts with both the acceptor arm/D-stem junction and EF-Tu. The RNA of the GAR and the L12 stalk (A1067) both stack on C56 of the tRNA at the elbow (Schmeing *et al.*, 2009).

In the structure of EF-Tu with Trp-tRNA^{Trp} bound to the ribosome with GDPCP and paromomycin, switch I is ordered, suggesting that this state is on the functional path. The G-domain

is shifted about 7 Å in position to interact properly with the ribosome (Voorhees *et al.*, 2010).

Switch 1

The consensus sequence of switch I (RGITI) has several important roles in conformational changes associated with GTP binding, ribosome binding and GTP hydrolysis (Table 9.3; Ticu *et al.*, 2009). Thr61 binds to the magnesium ion, interacting with the phosphates (Berchtold *et al.*, 1993; Kjeldgaard *et al.*, 1993). The Arg-finger, frequently the arginyl residue of the switch I consensus sequence, stabilizes the transition state by electrostatic interactions. However, mutations of Arg58 have little effect on the GTP hydrolysis (Knudsen & Clark, 1995; Zeidler *et al.*, 1996). It is 8 Å away from the phosphates in the GTP conformation or in the ternary complexes (Berchtold *et al.*, 1993; Nissen *et al.*, 1995). In the structure of the EF-Tu complex with aurodox, Arg58 is flexible and invisible (Vogeley *et al.*, 2001), as in the structure of the ternary complex bound to the ribosome (Schmeing *et al.*, 2009). However, in the GDPCP structure Arg58 is stable, but not in contact with the phosphates (Voorhees *et al.*, 2010).

GTP Hydrolysis by EF-Tu

Since EF-Tu has a low intrinsic GTPase activity, it needs to be activated at the right moment on the ribosome. The activation mechanism is most likely a substrate-induced catalysis (see Sec. 9.1). EF-Tu is able to hydrolyze its bound GTP when a cognate anticodon of a tRNA base pairs with the codon of the mRNA. A signal is then passed from the decoding center (DC) on the small subunit to the G-domain and the GAR on the large subunit (Yusupov *et al.*, 2001; Stark *et al.*, 2002; Bashan *et al.*, 2003; Valle *et al.*, 2003a; Gregory *et al.*, 2009; Villa *et al.*, 2009; Schmeing *et al.*, 2009). Here helix H69 and protein S12 may have important roles in communicating to the GAR that the anticodon is cognate and that GTP should be hydrolyzed. As a consequence residues important

for the GTP hydrolysis are induced to adopt different conformations (see Sec. 9.1).

In the GTP conformation of EF-Tu, His84 is at a distance of 5 Å from a water molecule in the vicinity of the γ-phosphate (Kjeldgaard *et al.*, 1993). This is too far to have any role in activating the water molecule. The histidyl residue is furthermore shielded from close interaction with the water molecule by two hydrophobic residues, Val20 and Ile61. These residues have been called the hydrophobic gate (Berchtold *et al.*, 1993). Their role has been analyzed by mutations. V20G and I61A did not lead to any increase in intrinsic or ribosome-induced GTP hydrolysis (Jacquet & Parmeggiani, 1988; Krab & Parmeggiani, 1999). In the crystallographic study of EF-Tu bound to the ribosome with GDPCP, the histidine is in hydrogen bond contact with the water molecule, without any significant movement of the hydrophobic gate (Plate 9.11). Thus, the importance of the hydrophobic gate is limited.

Mutations of His84 reduce the GTPase activity of EF-Tu drastically (Cool & Parmeggiani, 1991; Zeidler *et al.*, 1995). However, variations of pH lead to the conclusion that the histidyl residue may not act as a general base (Daviter *et al.*, 2003).

Kirromycin and aurodox induce EF-Tu to hydrolyze GTP in the absence of ribosomes (Wolf *et al.*, 1974). The structure of the complex of EF-Tu with aurodox illustrates that His84 is capable of approaching the water molecule at the γ-phosphate (Vogeley *et al.*, 2001; Plate 9.8). In the kirromycin complex of EF-Tu with the ribosome His84 of EF-Tu is pointing away from the γ-phosphate (Schmeing *et al.*, 2009), but in the GDPNP complex His84 is within hydrogen bond distance of the water molecule (Voorhees *et al.*, 2010). The water molecule donates hydrogen bonds to the γ-phosphate and the carbonyl oxygen of Thr61. His84 is hydrogen-bonded to the phosphate of G2662 and is in a negatively charged environment, which suggests that it is already protonated and unable to receive a proton from the water molecule (Fig. 9.9; Plate 9.11). As discussed above, the GTP hydrolysis is most likely due to a substrate-induced catalysis mechanism (Schweins *et al.*, 1995; Liljas *et al.*, 2011; Wallin *et al.*, 2012). This mechanism is

probably the same for all trGTPases. The Arg-finger may be replaced by the positively charged histidine, which is in an ideal position to stabilize the transitions state in GTP hydrolysis.

In a study by Shi *et al*. (2012), the base pair U2653–C2667 was deleted without any dramatic effect on GTP hydrolysis by EF-Tu. In this case it is important to recognize that it is a phosphate of the RNA that has the catalytic role. Removing one base pair will certainly move A2662 by a significant distance, but another phosphate (probably of G2661) will more or less take the place of the catalytically active phosphate.

GTP hydrolysis induces a large conformational change in EF-Tu. In this conformational change, EF-Tu reverts to the GDP conformation where the G-domain moves with regard to domains II and III. In this way, the interaction between the G-domain and domain III is broken.

EF-Ts

EF-Ts is the G-nucleotide exchange factor (GEF) for EF-Tu. When EF-Tu is released from the ribosome in complex with GDP, EF-Ts binds to the complex to release the GDP molecule. EF-Ts structures are known from *T. thermophilus* (Jiang *et al*., 1996) and in complex with EF-Tu from *E. coli*, *T. thermophilus* and bovine mitochondria (Fig. 9.16; Kawashima *et al*., 1996; Wang *et al*., 1997; Jeppesen *et al*., 2005). The structure of the corresponding complex from yeast, eEF1A·eEF1Bα, has also been determined (Andersen *et al*., 2000). The structure of Qβ replicase is known too. It contains the complex between *E. coli* EF-Tu and EF-Ts (Kidmose *et al*., 2010). Even though the structures of the complexes are quite different, the functional principles are the same.

In the crystal structure, EF-Ts from *E. coli* forms a tight dimer where each of the EF-Ts monomers binds one EF-Tu molecule (Kawashima *et al*., 1996). *E. coli* EF-Ts is an elongated protein with four structural modules. The core module of the protein (residues 55–179) has a structural repeat where the N-terminal region (residues 55–140) is related to the C-terminal region (residues

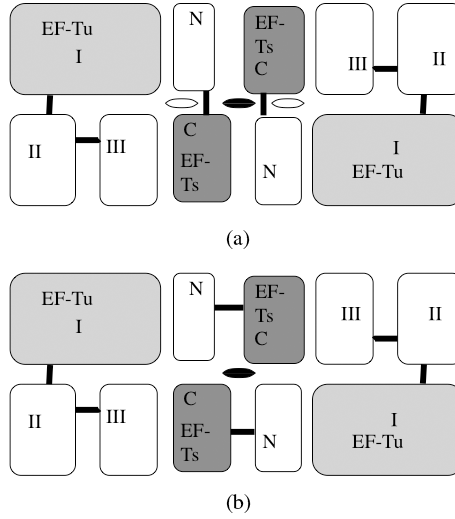

Fig. 9.16 The interaction between EF-Tu and EF-Ts in the crystal structures of **(a)** *E. coli* (Kawashima *et al*., 1996) and **(b)** *T. thermophilus*. In both cases the N-terminal region (N) interacts with the G-domain of EF-Tu and the C-terminal region (C) interacts with domain III of EF-Tu (Wang *et al*., 1997). The structures of EF-Ts that interact with EF-Tu are related, even though they belong to one molecule in the case of *E. coli* and to two molecules in the case of *T. thermophilus*. The filled symbol between the subunits signifies a molecular twofold axis, and the open symbol represents a local pseudo-twofold symmetry axis.

141–179) through an approximate twofold symmetry axis (Fig. 9.16a; Kawashima *et al*., 1996). The N-terminal region interacts with the G-domain of EF-Tu, whereas the C-terminal region interacts with domain III of the same molecule of EF-Tu (Fig. 9.16a). Thus, in *E. coli,* there is an interaction between one molecule of EF-Ts with one molecule of EF-Tu (Kawashima *et al*., 1996).

EF-Ts from *T. thermophilus* is considerably shorter than EF-Ts from *E. coli*. It also forms a dimeric structure (Jiang *et al*., 1996; Wang *et al*., 1997). Here, each monomer of EF-Ts interacts with two molecules of EF-Tu (Fig. 9.16b; Wang *et al*., 1997). One monomer of EF-Ts interacts with the G-domain through its N-terminal region, and the other monomer of EF-Ts interacts with domain III of the

same molecule of EF-Tu through its C-terminal region (Fig. 9.16b). Thus, the two forms of EF-Ts are very differently organized. The twofold axis observed between two heterodimers of *E. coli* EF-Ts·EF-Tu (Kawashima *et al.*, 1996) also corresponds to a twofold axis of the heterotetramer of *T. thermophilus* EF-Ts·EF-Tu (Wang *et al.*, 1997). Despite the differences in organization, the structures and amino acid sequences of the surfaces of EF-Ts interacting with EF-Tu are very similar (Wang *et al.*, 1997). Evidently, the two structures of EF-Ts are related and have an interesting evolutionary background. The conformation of EF-Tu in both complexes is closest to the GDP conformation even though no nucleotide is present. EF-Ts can also remove GTP from EF-Tu, but since the conformation required for complex formation differs much from the one with GTP, the kinetics is unfavorable (Wang *et al.*, 1997).

The structure of the mitochondrial complex of EF-Tu and EF-Ts (Jeppesen *et al.*, 2005) suggests that this EF-Ts is most closely related to EF-Ts from *E. coli* despite significant differences.

The removal of the magnesium ion from EF-Tu by EDTA leads to a loss in affinity for the nucleotide (Arai *et al.*, 1972). Thus, it was expected that EF-Ts would act in a similar way. The crystal structures show that the most important interaction of EF-Ts is with the PO_4 loop and switch II of EF-Tu. Asp80 and Phe 81 of the conserved sequence element TDFV in EF-Ts induce structural changes in EF-Tu. Asp80 causes a shift in position of helix B of switch II. Residues involved in the binding of the magnesium ion get moved from their binding positions. This leads to loss of the magnesium and therefore also of GDP (Kawashima *et al.*, 1996; Wang *et al.*, 1997). Phe81 of EF-Ts binds to a hydrophobic pocket of EF-Tu and causes a series of conformational changes through side chains of residues His119, Gln115 and His19 of EF-Tu. This leads to a flip of the peptide between Val20 and Asp21, which causes the loss of the hydrogen bond donor, the peptide nitrogen, and a replacement with a hydrogen bond acceptor, the carbonyl oxygen (see Fig. 9.6). This becomes highly unfavorable for the interaction with the GDP (Wang *et al.*, 1997). Distortions of the binding site of the ribose and guanine base are also induced. A kinetic analysis shows that all

these changes and distortions are needed to explain the efficiency of the release of the GDP (Wieden *et al*., 2001; Schümmer *et al*., 2007).

The structures of GEFs are generally not related to each other (Vetter & Wittinghofer, 2001). This is also true of the structure and interaction of the yeast factor eEF1Bα, which functions as a GEF for the factor corresponding to EF-Tu in eukarya, eEF1A (Andersen *et al*., 2000). eEF1Bα is not structurally related to the bacterial EF-Ts and does not bind to the corresponding region. However, the main effect of EF-Ts and eEF1Bα, as of all GEFs (Vetter & Wittinghofer, 2001), is to remove the magnesium ion from its position near the GDP phosphates and to induce a peptide flip in the PO_4 loop. This reduces the binding affinity for GDP. Since the concentration of GTP in the cytoplasm is much higher than the concentration of GDP, GTP will compete favorably for an empty nucleotide site in EF-Tu.

SelB

Some proteins involved in oxidation/reduction need selenium in the form of selenocysteine (Se-Cys) for function (Forchhammer *et al*., 1989). This residue is not among the 20 normal amino acid residues for which there are genetic code words. Rather, Se-Cys is incorporated through the translation of a stop codon, UGA. A hairpin loop of the mRNA following the UGA, the selenocysteine-inserting sequence (SECIS), distinguishes a true stop codon from a UGA codon which should be translated as Se-Cys (Fig. 9.17). The distance between the UGA codon and the hairpin loop is about 20 nucleotides. SelB is essential for incorporating this 21st amino acid, selenocysteine, into a number of proteins (Forchhammer *et al*., 1989). The protein functions as an EF-Tu for aminoacylated SeCys-tRNA (Baron *et al*., 1993).

SelB·GTP binds $tRNA^{Sec}$, which EF-Tu cannot (Suppmann *et al*., 1999). In addition, SelB recognizes and binds to the SECIS hairpin loop, of the mRNA (Fourmy *et al*., 2002). When the UGA codon reaches the A site, the likelihood that RF2 will bind and terminate

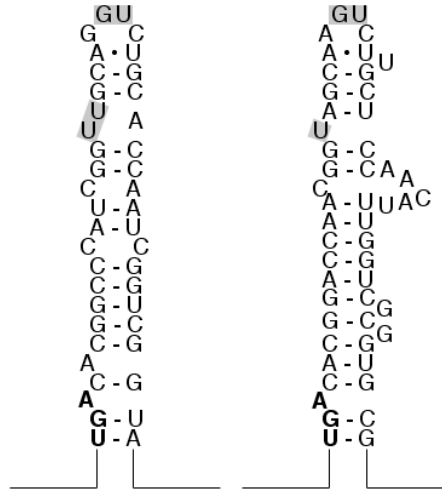

Fig. 9.17 mRNA hairpin structures of *E. coli fdhF* and *fdnG* directing the insertion of Se-Cys into corresponding proteins (SECIS elements). The UGA codon is shown at the base of the hairpin, and the nucleotides protected against chemical modification by SelB are shaded (Hüttenhofer *et al*., 1996). [With kind permission from Selmer (2002).]

protein synthesis is decreased. Instead, SeCys is incorporated into the nascent peptide, due to the ternary complex of SeCys-tRNA (anticodon UCA), SelB and GTP which is bound to the mRNA hairpin (Suppmann *et al*., 1999).

The N-terminal half of bacterial SelB (SelB-N) corresponds to the three domains of EF-Tu (Kromayer *et al*., 1996). The structure of the C-terminal half (SelB-C), the mRNA-binding part of SelB from *Moorella thermoacetica*, was found to be composed of four closely similar domains (winged helix fold; WH1–WH4) arranged in the form of an 'L' (Fig. 9.18; Selmer & Su, 2002; Ganichkin & Wahl, 2007). The kink is between WH2 and WH3. A number of structures have also been determined between the SECIS element and the whole of SelB-C or parts of it from different species (Yoshizawa *et al*., 2005; Soler *et al*., 2007; Beribisky *et al*., 2007; Ose *et al*., 2007).

In addition, the structure of an archaeal variant of SelB has been determined (Leibundgut *et al*., 2005). The shape of the

Fig. 9.18 Left: The crystal structure of SelB from the archeon *Methanococcus maripaludis* (Leibundgut *et al*., 2005). Domains I–III are similar to EF-Tu in the GTP conformation. Domain IV interacts with the SECIS hairpin element. (Illustration by Saraboji Kadhirvel.) Right: The structure of the C-terminal half of bacterial SelB (Selmer & Su, 2002). The four structurally similar domains (winged helix motifs) form the shape of an 'L'. The very last domain contains highly conserved residues. Mutations in this domain can lead to a changed specificity for the hairpin loop of the mRNA. (Courtesy of Maria Selmer.)

molecule is similar to that of IF2. Here the C-terminal extension is only one domain of a different fold from the winged helix found in bacteria. In eukaryotes and probably also in archaea, an adaptor protein connects SelB to the SECIS element (Copeland *et al*., 2000).

From the location of the conserved residues of the long bacterial C-terminal extension and from studying functional mutants, it is evident that the main interactions with the stem-loop of the mRNA are due to the seventh or the C-terminal domain (Kromayer *et al*., 1999; Li *et al*., 2000). The ternary complex of

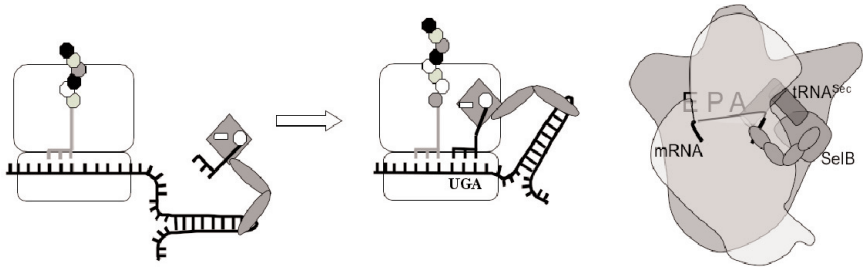

Fig. 9.19 Left: SelB in complex with Se-Cys-tRNA^{Sec} binds to the SECIS loop structure of the mRNA and travels with the mRNA. Middle: When the UGA stop codon is exposed in the DC, the anticodon of tRNA^{Sec} interacts with the codon. The result is that Se-Cys is incorporated in response to a stop codon. Right: A schematic illustration of the way SelB can place tRNA^{Sec} in the A/T site while interacting with the SECIS structure of the mRNA on the other side of the shoulder of the small subunit.

SeCys-tRNA, GTP and SelB obviously can interact with two points on the mRNA. The anticodon of SeCys-tRNA interacts with the UGA codon, and the stem-loop structure of the mRNA will interact with the C-terminal domain of SelB. Since the EF-Tu-related parts of SelB bind to the T site, and since the anticodon of the tRNA extends far from the factor protein, it is evident that an elongated structure of the C-terminal domains of SelB is needed (Fig. 9.19) to reach the stem-loop structure of the mRNA (Selmer & Su, 2002). The approximate position of the stem-loop was estimated from structural examination of the path of the mRNA on the 30S subunit (Yusupova *et al.*, 2001).

EF-G

Elongation factor G (EF-G) is the translocase of translation and is a large trGTPase with a molecular weight of around 80 kDa (Ovchinnikov *et al.*, 1982). Many bacteria have two or even three variants of EF-G. A variant EF-G from *T. thermophilus* is called EF-G-2. Its amino acid sequence is significantly different. It is not known whether the different versions have different physiological

roles. The archaeal and eukaryotic factors corresponding to EF-G are called EF2.

After peptidyl transfer, a peptidyl tRNA is located in the A site and a deacylated tRNA in the P site. The tRNAs move into the hybrid sites A/P and P/E spontaneously (Aggirezebala *et al.*, 2008). Then they need to be translocated to the P and E sites, respectively. The mRNA is also translocated with the peptidyl-tRNA to make a new codon exposed in the A site. The deacylated tRNA in the E site will subsequently fall off the ribosome. This process can occur spontaneously, but very slowly (Spirin, 1985). Normally, it is catalyzed by EF-G (Kaziro, 1978; Spirin, 1985). When EF-G has dissociated, the ribosome is ready for a new cycle of elongation.

Structure

When the amino acid sequence of EF-G was first determined (Ovchinnikov *et al.*, 1982), it was obvious that its N-terminal region is homologous to the N-terminus of EF-Tu (Laursen *et al.*, 1981). Part of the G-domain was identified this way.

The structure of EF-G (Fig. 9.20) is highly elongated, about 120 Å, and composed of six domains where an insertion in a loop of domain I (residues 1–280), called G′ (residues 158–253), could be considered as a separate domain (Czworkowski *et al.*, 1994; Ævarsson *et al.*, 1994). EF2 from yeast has a related insert from a neighboring loop (Fig. 9.21; Ævarsson *et al.*, 1994, Jørgensen *et al.*, 2003). Archaeal EF2 has smaller extensions in both these loops (Fig. 9.21; Ævarsson *et al.*, 1994). Domain II is composed of residues 288–400, domain III residues 405–482, and domain IV residues 483–605 and 674–691. Finally, domain V is composed of residues 606–673.

The G-domain and domain II have corresponding domains in EF-Tu and all trGTPases. Furthermore, EF-G with GDP mimics the ternary complex (Nissen *et al.*, 1995). Protein domains III–V of EF-G mimic a tRNA molecule (see also Sec. 9.6). Thus, the ‘off’ (GDP) conformation of EF-G mimics the ‘on’ (GTP) conformation of the ternary complex (Plate 9.12).

Fig. 9.20 The structure of EF-G from *T. thermophilus* (Ævarsson *et al.*, 1994; Czworkowski *et al.*, 1994; Al-Karadaghi *et al.*, 1996; Laurberg *et al.*, 2000). The five domains I (G), II, III, IV, V and the subdomain G′ form an elongated molecule. (Illustration kindly provided by Lars Liljas.)

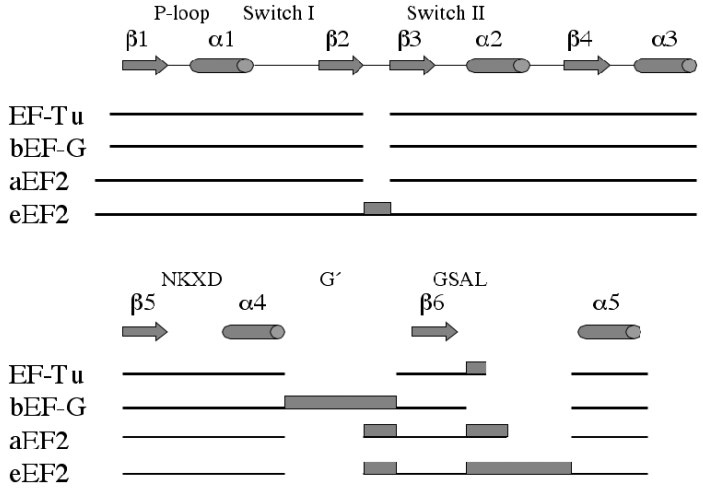

Fig. 9.21 Different inserts into domain I of EF-G and EF2 from bacteria, archaea and eukaryotes compared to EF-Tu. While bacterial EF-G has a long insert called G′ before β-strand 6, eukaryal EF2 has a short insert here and a longer one after β6. Archaeal EF2 has short inserts in both places (Ævarsson, 1995).

The conformation of EF-G with a bound GDP molecule (Czworkowski *et al.*, 1994; Al-Karadaghi *et al.*, 1996) is similar to the one without any bound nucleotide (Ævarsson *et al.*, 1994). The structure of a mutant, H573A, provides a picture of a different GDP structure, in this case with a bound magnesium ion at the β-phosphate (Laurberg *et al.*, 2000). A structure of EF-G with a GTP analog (Hansson *et al.*, 2005) and a structure of the EF-G-2 variant in complex with GTP have also been determined (Connell *et al.*, 2007). Apparently, the inherent GTP hydrolysis is extremely low for this form of the factor. The latter structure is less bent than the normal form with GDP bound. The structure of EF-G from *Staphylococcus aureus*, the target species and protein for the antibiotic fusidic acid, has also been determined (Chen *et al.*, 2010). Here the orientation of domains III–V with regard to domains G and II is again different from the one in *T. thermophilus*. This is probably partly due to the crystal packing, where there is a β-sheet that extends from domain II in one molecule to subdomain G′ in another molecule.

The conformational changes start at the nucleotide-binding site and extend across the interface between the two blocks that are mobile with regard to each other (Laurberg *et al.*, 2000). The bound nucleotide affects residues of the PO_4 loop, which in turn affect residues of switch II to adopt different conformations like a domino effect (Laurberg *et al.*, 2000). In this way, the state of the nucleotide-binding site in the G-domain is communicated to domain III, which is highly flexible and probably critical for the different states of EF-G. In fact an EF-G where domain III was deleted could not hydrolyze GTP (Martemyanov & Gudkov, 2000). Two residues that seem central to this interaction are Phe90 and Leu457. Mutations of most residues along this path of conformational changes can cause FA resistance (Laurberg *et al.*, 2000). Due to its flexibility, switch I of EF-G is not seen in structures of free EF-G except for the case of EF-G-2 with GTP (Table 9.5). Here the GTP molecule is shielded from interaction with water by the two switch loops (Connell *et al.*, 2007).

The amino acid sequences of switch I of EF-Tu and EF-G are highly similar. For two molecules with clearly related structures

and binding to overlapping binding sites on the ribosome, one could expect that the effector loops undergo related conformational changes (Laurberg *et al.*, 2000). Kolesnikov and Gudkov (2002) tested this possibility and concluded that these effector loops are designed for different functions or different ribosomal states since a hybrid of EF-G with the effector loop of EF-Tu does not function properly on the ribosome.

The conformational changes of EF-G (Fig. 9.22), which are central to efficient translocation, depend on a communication between the nucleotide-binding site and the domain interfaces. One experiment that illustrates this is the introduction of an intramolecular

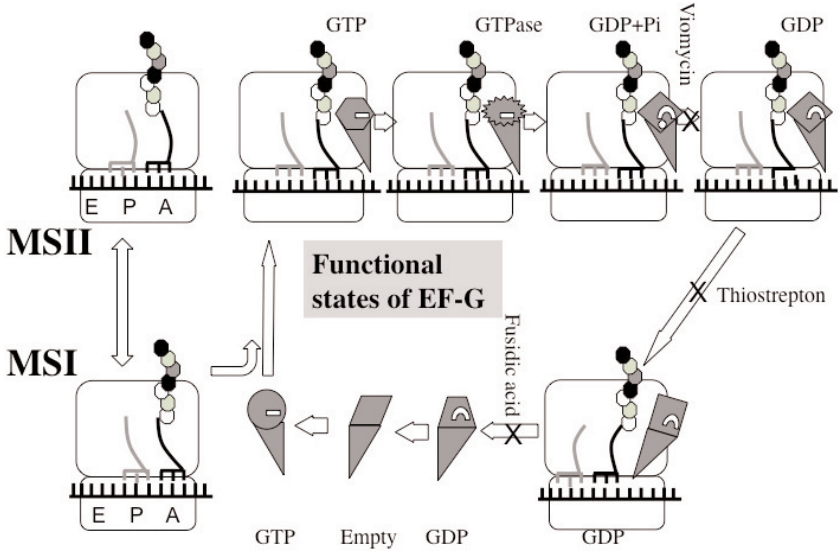

Fig. 9.22 The functional states of EF-G. EF-G binds to ribosomes where the peptidyl-tRNA is in the A/P. The figures on the left illustrate the transitions of the peptidyl-tRNA and the deacylated tRNA between classical and hybrid states of the ribosome. GTP hydrolysis precedes translocation (Rodnina *et al.*, 1997). The white little strip symbolizes the GTP molecule and the little semicircle represents GDP. Viomycin inhibits between GTP hydolysis and translocation, and thiostrepton inhibits EF-G from moving into the A site. Fusidic acid (FA) inhibits the dissociation of EF-G from the ribosome after translocation.

disulfide cross-link between the G-domain and domain V (Peske *et al*., 2000). The resulting EF-G retains some capacity of single round GTP hydrolysis but cannot translocate and cannot be released from the ribosome. If the disulfide is reduced, the mutant EF-G functions normally. Translocation needs a movement of domains IV and V in relation to the G-domain (Valle *et al*., 2003b; Gao *et al*., 2009). These observations further support the concept that GTP hydrolysis precedes translocation (Peske *et al*., 2000).

EF-G Bound to the Ribosome

After peptidyl transfer the deacylated tRNA in the P site and the peptidyl tRNA in the A site are in equilibrium with their movements to the P/E and A/P sites respectively. EF-G with GTP or GTP analogs preferrably binds to pretranslocational ribosomes where the peptidyl-tRNA is in the A/P site and the ribosome is in the rotated MSII state (Table 8.4; Agrawal *et al*., 1999; Valle *et al*., 2003b), while EG-G with GDP and FA binds to the MSI conformation of the ribosome (Valle *et al*., 2003b; Connell *et al*., 2006; Gao *et al*., 2009). The structure of EF-G when bound to the ribosome is significantly more extended than the crystal structures of isolated EF-G (Plate 9.12). Furthermore, EF-G binds to the ribosome much in the same way as the ternary complex of EF-Tu·GTP and aa-tRNA.

The binding of trGTPases to ribosomes in crystals was impossible until 2009 because of a crystal packing effect where one domain of protein L9 bound to the binding site of the GTPases of a neighbor ribosome. After a mutation removing the extending part of L9, a new crystal form could be produced where trGTPases can bind (Gao *et al*., 2009). In this structure EF-G is bound to the ribosome in complex with GDP and FA. Here switch I is disordered, but EF-G remains bound to the ribosome since it is in complex with FA and remains in the binding conformation. In the GDP state of EF-G off the ribosome, switch II is in a different and more open conformation, allowing for efficient exchange of the nucleotide (Gao *et al*., 2009).

Table 9.7 Interaction of EF-G with the Ribosome*

Region of EF-G	30S	50S
G-domain		GAR at base of L12 stalk
GTP-binding site		SRL (of H95)
G′-domain		L11 NTD, one L12 CTD
Domain II	Shoulder; h5, h15, S4 region	
Domain III	h5, S12	SRL
Domain IV	Decoding center, h44, P-site codon and ASL	H69
Domain V		H43/44, H89, L11, L6

*Nechifor & Wilson, 2007; Gao *et al*., 2009.

EF-G is bound between the two subunits, stretching from L11 at the base of the L12 stalk into the decoding part of the A site. Domain IV of EF-G is located in the DC, with its tip close to the top of h44 of the small subunit interacting with the anticodon of the tRNA in the P site (Table 9.7). While domains G and II retain their normal interactions with the 50S and 30S subunits respectively, domains III–V are stretched out in such a way that the tip of domain IV is about 37 Å from its position in the crystal structure of the mutant H573A of EF-G (Laurberg *et al*., 2000). The structural results agree with studies by chemical methods (Wilson & Noller, 1998; Ticu *et al*., 2009).

The nucleotide does not directly interact with the ribosome. However, the surface signal that GTP is bound is the effector loop of the G-domain (switch I). Thr64 in switch I interacts with the γ-phosphate and adopts a conformation that allows EF-G to bind to the ribosome. This conformation may be best represented by the structure of EF-G-2 with a bound GTP (Fig. 9.22; Plate 9.12). Furthermore, the conformation where the released phosphate remains bound to EF-G is not known. The final conformation is the one that will fall off the ribosome and could be close to the GDP structure observed in several crystal structures of the isolated factor. This structure is strongly related to the ternary

complex, which is in turn to bind to the ribosome. Some type of imprinting may be in operation (Liljas, 1996).

The order of the functional steps remains being discussed. In the classical view translocation precedes GTP hydrolysis (Inoue-Yokosawa *et al.*, 1974; Belitsina *et al.*, 1975; Modollel *et al.*, 1975; Spirin, 1985, 2002). However, from the rates of the different steps of translocation it appears that GTP hydrolysis must precede translocation (Rodnina *et al.*, 1997). In such a case, the function of EF-G may be more closely related to the motor proteins than to the molecular switches to which the other trGTPases belong (Cross, 1997). However, it should be remembered that translocation can occur spontaneously and does not need the GTP hydrolysis that EF-G uses to perform its function.

Release of Inorganic Phosphate

One of the functional steps after GTP hydrolysis is the release of the inorganic phosphate (Pi). Kinetic analysis using a fluorescent-labeled phosphate-binding protein (Brune *et al.*, 1994) has shown that the Pi release is significantly delayed after GTP hydrolysis (Wintermeyer *et al.*, 2001; Savelsbergh *et al*. 2002). Some rearrangement of the complex of ribosomes with EF-G·GDP·Pi has to occur before the release of the phosphate. No structural insight has yet been gained.

Antibiotics Targeting EF-G and EF2

One antibiotic that affects the function of EF-G is fusidic acid (FA; see Sec. 10.7 and Fig. 9.22). FA traps EF-G on the ribosome after GTP hydrolysis and translocation (Willie *et al.*, 1975). This inhibition of protein synthesis is a parallel to the inhibition by kirromycin that locks EF-Tu on the ribosome. Contrary to EF-Tu, which can bind kirromycin off the ribosome, FA binds only when EF-G·GTP binds to the ribosome (Baca *et al.*, 1976). Obviously, then, FA cannot induce EF-G to hydrolyze its GTP off the ribosome as the EF-Tu·kirromycin complex does.

A crystal structure of EF-G on the ribosome was determined in the presence of FA (Gao *et al*., 2009). FA is bound between switch II of the G-domain and its bound GDP molecule and domain III (Plate 10.7). Resistance to FA is obtained by mutations of amino acid residues in several regions of EF-G (Johansson & Hughes, 1994). These mutations occur primarily in the interface between domains G, III and V. Only some of these mutations are at the FA-binding site of EF-G (Johansson *et al*., 1996; Gao *et al*., 2009). At least three mechanisms could be involved in obtaining FA resistance. In addition to interfering with the binding site, a mutation could lower the energy barrier that prevents the factor from changing its conformation to allow EF-G·GDP to dissociate from the ribosome. Furthermore, a different group of mutations could lower the affinity of EF-G·GDP·FA for the ribosome, thus avoiding the blockage of protein synthesis that occurs when EF-G remains bound on the ribosome.

Mutant EF-Gs, which are more sensitive to FA than wild-type EF-G are also known (Martemyanov *et al*., 2001). These FA-sensitive mutants are revertants from FA resistance where the original mutation has been removed (Johanson *et al*., 1996). The sensitivity to FA is coupled to a higher affinity for GTP, whereas FA resistance is related to a lower affinity for GTP (Martemyanov *et al*., 2001). A high affinity for GTP may be the primary fact that leads to a higher or lower affinity for the ribosome and thus would increase the chance for FA to bind to EF-G on the ribosome.

GTP Hydrolysis and Translocation

GTP hydrolysis of EF-G precedes translocation (Rodnina *et al*., 1997). In GTPases an Arg-finger, possibly in switch I, is generally involved. In EF-G this would be Arg59, but this cannot be the Arg-finger since mutations of it have a limited effect (Mohr *et al*., 2000). Mutants of the conserved Arg29 have more dramatic effects on GTP hydrolysis and it seems essential (Mohr *et al*., 2000). However, Arg29 is about 11 Å from the β-phosphate of GTP. Its role in GTP hydrolysis is probably indirect.

L12 is important for the GTP hydrolysis by EF-G (see Secs. 7.4 and 9.1). The G′-domain as well as the G-domain can interact with one copy of L12CTD (Sec. 9.1; Plate 9.5). Helix A of the G′-domain has been cross-linked to L12 (Nechifor & Wilson, 2007). Furthermore, mutations of two acidic residues of this helix to lysines reduce both GTP hydrolysis and translocation dramatically (Table 9.7; Nechifor *et al*., 2007). As described in Sec. 9.1, these effects on GTP hydrolysis may not be direct, but related to the role of L12 in bringing the trGTPases to their binding site.

Crystallographic results show that EF-G binds to the ribosome in the same manner as EF-Tu (Voorhees *et al*., 2010) with His87 hydrogen-bonding to the phosphate of A2662 (Tourigny *et al*., 2013). This places a water molecule close to the γ-phosphate to catalyze hydrolysis. Like for EF-Tu, a substrate-induced catalysis is the likely mechanism (Liljas *et al*., 2011; Wallin *et al*., 2012). The γ-phosphate removes one proton from the water molecule, which activates it for an in-line sn^2 attack.

Experiments using a 27-nucleotide fragment of SRL have shown that EF-G with GTP or without bound nucleotides can bind to SRL (Munishkin & Wool, 1997; Mitkevich *et al*., 2012). However, in complex with GDP EF-G cannot bind. On the other hand, if EF-G was bound to SRL the binding of GDP was inhibited. Both in the case of IF2 and EF-G, the binding to GDP and to SRL are mutually exclusive (Mitkevich *et al*., 2012).

In association with GTP hydrolysis, EF-G undergoes a conformational change that leads to translocation. Compared to the conformations of the factor alone, translocation needs a more extended EF-G to reach the anticodon of the tRNA in the P site. Such extended conformations have been observed when EF-G is bound to the ribosome (Valle *et al*., 2003b; Gao *et al*., 2009; Tourigny *et al*., 2013).

In studies of translocation with different nucleotides, Zavialov and Ehrenberg (2003) came to conclusions different from those of Rodnina *et al.* (1997). The former investigators used puromycin or RF2 to analyze to what extent translocation had occurred with EF-G in complex with GDP, GDPNP and

GTP. One major difference is that puromycin binds only to the A site part of the PTC, whereas RF2 needs an A site that is empty in both the DC and the PTC. They made the observation that translocation with GDP is insignificant but with GTP efficient. Since RF2 needs to bind to the A site to hydrolyze the nascent peptide from the P site tRNA, EF-G has to translocate the tRNAs and dissociate before this can happen. As soon as the CCA end of the A site tRNA is moved into the A/P site, puromycin can bind and react (Sharma *et al.*, 2004). A slow increase in the accessibility of both puromycin and RF2 to react with the nascent peptide must be interpreted as a slow translocation and dissociation of EF-G.

EF-G mutants

The role of domains, functional groups and sites of EF-G have been investigated by mutational analysis (Table 9.8). The functional properties investigated are the ability to perform GTP hydrolysis and translocation as well as the coupling between these two properties. In addition, several mutants were investigated as to whether they after interaction with the ribosome would permit puromycin to react with the nascent peptide as an early step of translocation.

In some experiments, whole domains were deleted. Domain G' was deleted but the resulting mutant aggregated and could not be purified (Nechifor *et al.*, 2007). Deletion of domain IV and/or domain V had no effect on GTP hydrolysis. However, such truncated factors could not translocate (Rodnina *et al.*, 1997; Martemyanov & Gudkov, 1999; Savelsbergh *et al.*, 2000a). This agrees with the placement of domain IV in the DC during translocation. EF-G without domain III could neither hydrolyze GTP nor translocate (Martemyanov & Gudkov, 2000). However, this truncated factor bound quite well to ribosomes in the presence of GDP and FA. We do not yet understand why this truncated factor cannot hydrolyze GTP, but it is evident that domain III is a central element in the factor.

Table 9.8 Some Mutants in EF-G Affecting Function

Mutation	GTPase	Trans-Location*	Puromycin Reactivity†	Reference
Wild type	+	+	+	
Domain deletions				
ΔI	−	−	Low	Borowski *et al*., 1996
ΔIII	−	−	−	Martemyanov & Gudkov, 2000
ΔIV	+	Low	Low	Rodnina *et al*., 1997
	+	−	−	Martemyanov & Gudkov, 1999
ΔIV+V	+		Low	Savelsbergh *et al*., 2000a
ΔV	+		Low	Savelsbergh *et al*., 2000a
Local mutations				
F95A (I, Sw2)	See text	Low		Ticu *et al*., 2011
E224K (G′)	−	−		Nechifor *et al*., 2007
E228K (G′)	−	−		Nechifor *et al*., 2007
D442A (III)	Low	Low		Ticu *et al*., 2011
L464A (III)	ND	Low		Ticu *et al*., 2011
H465A (III)	Low	+		Ticu *et al*., 2011
I468A (III)	ND	Low		Ticu *et al*., 2011
R472A (III)	ND	Low		Ticu *et al*., 2011
K503I (IV)	+	Low		Kovtun *et al*., 2006
508, 4 aa insert	+	Low	Low	Kolesnikov & Gudkov, 2003
H583K/R (IV)	+	−		Savelsbergh *et al*., 2000a
586, 6 aa insert	+	Low	−	Martemyanov & Gudkov, 1998
G162SC-T649C	+	−		Peske *et al*., 2000

* Translocation was identified by the release of deacylated tRNA from the E-site.
† Puromycin reactivity with peptidyl-tRNA after treatment with the mutant factor.
Residue numbers refer to *E. coli*.
ND means 'not determined,' Low means 'reduced activity,' − means 'almost absent activity,' and + means 'close to normal.'

The mutation Phe95Ala (*E. coli* numbering) gives unexpected results (Ticu *et al*., 2011). The mutant protein hydrolyzes GTP already in isolation and the addition of ribosomes only marginally further stimulates GTPase activity. Phe95 is located in a critical area between switch II and domain III, and is also one of the residues that when mutated can lead to strong fusidic acid resistance (FA^R; Johansson & Hughes, 1994). Gao *et al*. (2009) found it to be located at the binding site for FA. Furthermore, it is near His92, which is directly involved in the placing of the water molecule next to the γ-phosphate during GTP hydrolysis (Ticu *et al*., 2011). The corresponding phenylalanine in *S. aureus* has also been mutated (F88L; Koripella *et al*., 2012). Here it was observed that the peptidyl dropoff was increased by the mutation. Since such a dropoff generally occurs from the A site, it was evident that the mutated EF-G was deficient in translocation.

Domain IV has two loops at the tip of the domain 503–516 (loop I) and 577–589 (loop II). Loop I with two conserved glycines forms a tight turn, which is inserted into the minor groove between P site tRNA and codon. The conserved residues Gln507 and His583 of the two loops form hydrogen bonds to phosphate oxygens of U37 and A38 of the P site tRNA, respectively (Gao *et al*., 2009). Kolesnikov & Gudkov (2003) analyzed the effect of mutations in both loops and came to the conclusion that an intact conformation is needed for efficient translocation. Mutations of the loops at the opposite side of domain IV had little effect (Kovtun *et al*., 2006). The mutation that is locked by a disulfide bridge (Table 9.7) cannot translocate, but can hydrolyze GTP despite the fact that the identification of the residue proximity comes from the GDP conformation (Peske *et al*., 2000).

LepA — EF4

Early on it was discovered that the amino acid sequence of the amino-terminal domain of the protein LepA is related to the G-domain of trGTPases (March & Inouye, 1985). With the aid of the structures of EF-Tu and EF-G, it was possible to extend this

similarity to include the whole G-domain as well as domain II. Since the family of trGTPases all have these two domains and no other GTPase has the domain II structure, it seemed increasingly likely that LepA had to be a trGTPase of unknown function (Ævarsson, 1995).

The protein is highly conserved, but is found only in bacterial systems. In some papers it has been called EF4 (Connell *et al*., 2008). It is normally expressed at a low level, since there are numerous rare codons in its sequence (March & Inouye, 1985). However, in certain conditions of growth stress the level of expression is significantly increased (Pech *et al*., 2011). The presence of LepA increases the fidelity of translation. Qin *et al*. (2006) suggested that LepA performs an unexpected function, to back-translocate the ribosome. The binding of LepA to the ribosome is preferentially done in the posttranslocational state (Connell *et al*., 2008). However, a study by Liu *et al*. (2011) has shown it to be more likely that LepA is one of the ribosome rescue factors. It competes with EF-G for the binding to the pretranslocated ribosome and forms a complex that inhibits elongation transiently. LepA·GTP induces a new conformation, different from the posttranslocated ribosome, but where the peptidyl-tRNA is readily accessible to react with puromycin. The binding of EF-G·GTP can rapidly release the inhibited ribosome. The conditions for which this inhibition will be a benefit are not yet identified.

The structure of LepA has been determined (Evans *et al*., 2008). The protein is most similar to EF-G, but nevertheless quite unique. The G′-domain is absent in LepA as well as domain IV, the domain interacting with the DC. The connection in LepA between domains III and V is due to two β-strands (Evans *et al*., 2008). This element is called domain V′ (Connell *et al*., 2008). LepA has a unique C-terminal domain, CTD, to some extent replacing the lacking domain IV at the extreme end of the molecule (Evans *et al*., 2008).

The structure of LepA when bound to the ribosome is known from cryo-EM work (Connell *et al*., 2008). The factor is clearly bound to the trGTPase-binding site. Contrary to EF-G, when

bound to the ribosome, LepA does not overlap with the A site. However, the tRNA in contact with LepA is not in the normal A site. The elbow with the T loop has moved up. This binding mode, called the A/L site, leads to displacements of H38 and H69. This further has the effect that the A site finger (H38) in the intersubunit bridge B1a changes its conformation to interact with the T loop of the tRNA. The regions of interaction between LepA and the tRNA involve subdomain V′ and the CTD (Plate 9.13). The CTD interacts with the acceptor arm of the A-site tRNA. The CCA end seems to be displaced from its site in the PTC. This may explain the puromycin reactivity of the peptide.

9.4 RELEASE FACTORS

RF1 and RF2

The termination or release factors RF1 and RF2 hydrolyze and release the completed polypeptide from the P site tRNA in response to a stop codon exposed in the A site (Ganoza, 1966; Kisselev *et al.*, 2003). The termination factors compete with the tRNAs for decoding the mRNA. Normally, there is no tRNA for the stop codons. Two exceptions are the tRNAs coding for Se-Cys and pyrrolysine (see Sec. 4.4).

RF1 and RF2 in bacteria are paralogs (Craigen *et al.*, 1985). RF1 recognizes the stop codons UAA and UAG, whereas RF2 responds to UAA and UGA (Scolnick *et al.*, 1968). The expression of RF2 in most bacteria needs a shift in reading frame (see Sec. 4.4). In eukaryotes, there is only one factor, eRF1, which recognizes all three stop codons (Zouravleva *et al.*, 1995). These release factors are of class I. RF3 is a class II release factor (Zouravleva *et al.*, 1995) and a trGTPase. It catalyzes the removal of release factors RF1 and RF2 from the ribosome (Caskey *et al.*, 1969; Capecchi & Klein, 1969; Freistroffer *et al.*, 1997). RF3 is lacking in some bacterial species, among them *T. thermophilus*, and is not found in archaea (Kisselev & Buckingham, 2000). Thus, it could not be essential. The corresponding molecule in eukaryotes is called eRF3 (for a review see

Inge-Vechtomov *et al.*, 2003). Whether a different protein can substitute for RF3 in species lacking the protein is not known.

Swapping conserved amino acid sequences between RF1 and RF2 led to the identification of a region that switches the recognition of stop codons (Ito *et al.*, 2000). This so-called anticodon mimicry motif was found to be the tripeptide PxT for RF1 and SPF for RF2 (Ito *et al.*, 2000; Nakamura & Ito, 2003). It was surprising that a peptide as short as three residues could identify and discriminate between the stop codons. The side chains of three consecutive amino acid residues rarely point in the same direction. It was also surprising that nonpolar residues like alanyl, prolyl and phenylalanyl could be used for selective interactions. A conserved sequence in eRF1 (NIKS) was suggested to have the corresponding function in eukaryotes (Frolova *et al.*, 2002).

The sequence GGQ is universally conserved in the class I release factors (Frolova *et al.*, 1999). Mutants of class I release factors where this conserved motif is changed are slow in hydrolyzing the peptide (Frolova *et al.*, 1999; Seit-Nebi *et al.*, 2001; Zavialov *et al.*, 2002). Furthermore, the glutamine residue of the GGQ motif is methylated to N^5-methylglutamine, which is important for function (Dinçbas-Renqvist *et al.*, 2000; Heurgué-Hamard *et al.*, 2005). A gene called prmC codes for the methylating enzyme. In bacteria this gene is normally located downstream of the gene for RF1 (Heurgué-Hamard *et al.*, 2002).

Structures

Due to the similarity in function, it has been thought that release factors of class I would mimic tRNA (Smrt *et al.*, 1970; Brown & Tate, 1994; Ito *et al.*, 2000). Regardless of the assumed mimicry, DC on the small subunit and the PTC on the large subunit are 75 Å apart. Song *et al.* (2000) obtained the first experimental insight into the structures of release factors by determining the structure of human eRF1. The protein is composed of three domains with the shape of a 'Y.' Some spatial relationship to tRNA was suggested. Here the peptide, GGQ, is located at one extreme of the molecule. The part that probably

decodes the mRNA is located at the end of a different domain. Whether the conformation of eRF1 is the same when bound to the ribosome as in the crystal structure remains to be elucidated.

The structure of *E. coli* RF2 (Plate 9.14; Vestergaard *et al.*, 2001) has no structural similarity to eRF1 (Song *et al.*, 2000). Only the tripeptide GGQ is common to bacteria and eukarya (Frolova *et al.*, 1999). In the crystal structure of *E. coli* RF2, the two functional regions, the GGQ and SPF sequences, are no more than 23 Å apart, much shorter than the distance between the DC and the PTC (Vestergaard *et al.*, 2002). The observed conformation is not a packing artefact, since RF1 has the same conformation when bound to its methylation enzyme, PrmC (Graille *et al.*, 2005).

Structures of RF1 and RF2 bound to ribosomes show that the factors undergo large conformational changes where the two functional sites of the molecule can reach the distant sites (Laurberg *et al.*, 2008; Weixlbaumer *et al.*, 2008; Korostelev *et al.*, 2010; Zhou *et al.*, 2012). Such drastic conformational changes, where even the structures of the domains are rearranged, are rare, and the inter- and intramolecular interactions allowing this flexibility are of significant interest. The conformational change may be related to the need to safely identify the stop codon before the peptide can be hydrolyzed (Laurberg *et al.*, 2008). The PxT and SPF sequences directly contact the stop codons. Domain I of the factors binds close to the factor-binding site, while the GGQ region of domain III reaches into the PTC after the conformational change (Plate 9.15; Fig. 9.23).

Release Factor Interactions with Stop Codons

Crystal structures of *T. thermophilus* RF1 and RF2 when bound to 70S ribosomes have been determined in complex with their respective stop codons (for reviews see Liljas, 2008; Korostelev, 2011; Klaholz, 2011). Class I release factors bind to the MSI conformation of the ribosome (Table 8.4). The two characteristic sequence motifs of RF1 and RF2 interact with their codons but are not solely responsible for the identification of them. The motifs interact through

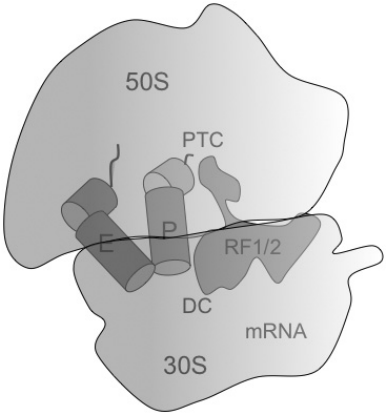

Fig. 9.23 The ribosome with release factor RF1 or RF2 bound. One domain binds in the DC and one in the PTC, where the GGQ motif participates in hydrolyzing the nascent peptide off from the P-site tRNA.

hydrogen bonds with the first two bases of the stop codons. The distinction of RF1 from RF2 is due to specific hydrogen-bonding patterns between the second nucleotide and the identified protein motifs (Klaholz, 2011; Korostelev, 2011). For further discussion of the functional aspects, see Sec. 11.5.

RF3

After the hydrolysis of the peptide from the tRNA in the P site, RF1/2 needs to be released from the ribosome. RF3 is a trGTPase that binds to terminated ribosomes and performs this function (Freistroffer *et al.*, 1997). Not all bacteria, including *T. thermophilus*, have an RF3. The structures of both eRF3 and bacterial RF3 are known and are related (Plate 9.16). Domains G and II are homologs to all trGTPases (Ævarsson, 1995). The structure of eRF3 is very closely related to that of EF-Tu (Kong *et al.*, 2004). Bacterial RF3 is somewhat different, in that the G-domain has an inserted subdomain, G', like in EF-G. In addition, domain III has a unique fold with a central β-sheet flanked by two α-helices (Gao *et al.*, 2007).

9.5 RIBOSOME-RECYCLING FACTOR

Once the release factors have terminated the synthesis of a protein, the ribosome is in a posttermination state. The mRNA remains bound to the 70S ribosome as well as a deacylated tRNA in the P site. Normally, the ribosomes are part of a polysome. Observations of random reinitiation of protein synthesis have been made (Janosi *et al.*, 1998). The ribosome-recycling factor (RRF) prevents such random reinitiation by recycling the posttermination ribosomes that are bound to the mRNA (Janosi *et al.*, 1996; Kaji *et al.*, 2001). The RRF functions together with EF-G and is a conserved protein in bacteria and chloroplasts (Hirashima & Kaji, 1973). There are different views on what the RRF does. One line of observation is that it dissociates polysomes into monosomes and releases the mRNA and tRNA (Hirashima & Kaji, 1972). The other focuses on the fact that the RRF only separates the two ribosomal subunits, without releasing the mRNA or the deacylated tRNA (Karimi *et al.*, 1999).

The structure of the RRF has been determined for a number of species (Selmer *et al.*, 1999; see Vesper & Wilson, 2006, for a review). The protein has two domains with the shape of an 'L' (Fig. 9.24) and can nicely be superimposed nicely on a tRNA

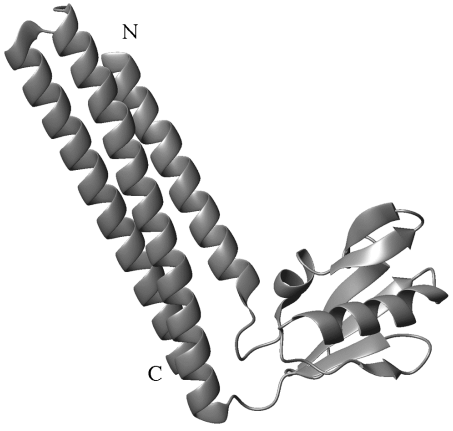

Fig. 9.24 The structure of the RRF (Selmer *et al.*, 1999)

molecule (Selmer *et al.*, 1999). Domain I (the tail domain) is composed of three long α-helices, and domain II (the head domain) is composed of β-strands as well as some shorter helices. The hinge between the two domains allows a fair amount of flexibility, as is seen when one is comparing the structures (Vesper & Wilson, 2006).

9.6 tRNA MIMICRY

Many proteins that participate in protein biosynthesis interact with the ribosomal sites for tRNA (Table 9.9). The structures of several of them have been unraveled (see Nyborg *et al.*, 2000; Kristensen *et al.*, 2001; Brodersen & Ramakrishnan, 2003, for reviews).

The first clear observation of a protein mimicking tRNA was for EF-G, where domains III–V mimic the tRNA part of the ternary complex EF-Tu·GDPNP·aminoacyl-tRNA (Nissen *et al.*, 1995). During translocation, the tRNA mimicry part binds to the A/T site and specifically to the decoding part of the A site (Agrawal *et al.*, 1997; Valle *et al.*, 2003b; Gao *et al.*, 2009). As expected, the structure of yeast EF2 has essentially the same tRNA mimicking structure. However, domain IV is considerably broader (Jørgensen *et al.*, 2003).

The next case was the RRF, which is an excellent mimic of a tRNA, judging from its structure (Selmer *et al.*, 1999). However, it does not bind to the ribosomal A site in a tRNA-like manner (see Sec. 9.5). The termination factors of class I, which cause the hydrolysis of the peptide when a stop codon is encountered in the A site, could be expected to mimic tRNA. To some extent they have structures that mimic tRNA (Song *et al.*, 2000; Vestergaard *et al.*, 2002). However, in the case of the bacterial factor, a large conformational change is necessary to bring it from the state in the crystals to the state when binding to ribosomes. Here the tRNA mimicry is less obvious (Laurberg *et al.*, 2008; Weixlbaumer *et al.*, 2008). As Brodersen and Ramakrishnan (2003) phrased it, shape can be seductive (Plate 9.17).

Several other proteins that participate in protein synthesis also mimic tRNA, in different ways. Thus, EF-P has a structure with the

Table 9.9 Binding of tRNA and Proteins to the tRNA Sites During Translocation

	Translation State			Sites			
	GTPase	**A/T**	**A**	**A/P**	**P**	**E/P**	**E**
Initiation	IF2		IF1		f-Met-tRNA		IF3-NTD
Elongation							
aa binding	EF-Tu	aa-tRNA			pp-tRNA		tRNA
Peptidyl transfer	—		aa-tRNA		pp-tRNA		
Translocation	EF-G	EF-G		pp-tRNA		tRNA	
			RelE		pp-tRNA		
Termination			RF1/2		pp-tRNA		
	RF3					tRNA	
Recycling	EF-G	EF-G	RRF		RRF	tRNA	
Proteins that bind to the A or A/T site: IF1, EF-G, RelE, RF1/2, RRF, SmpB, Stringent factor, RaiA							

shape of an 'L' and the same dimensions as a tRNA molecule (Benson *et al*., 2000; Blaha *et al*., 2009). It does not bind like a tRNA but binds close to the initiator tRNA on the E site side (Blaha *et al*., 2009) to position fMet-tRNA properly in the P site (Aioki *et al*., 2004). The C-terminal four domains of SelB also have a tRNA mimicry structure but have nothing to do with the tRNA-binding sites (Selmer & Su, 2002). A ribosomal protein from *T. thermophilus*, TL5, also has the classical tRNA shape (see Sec. 7.4; Fedorov *et al*., 2001). This protein is also a general stress protein, called CTC, that is expressed in high quantities in *B. subtilis* if the bacteria are exposed to stress conditions (Völker *et al*., 1994; Korobeinikova *et al*., 2008). It is not known whether the receptor for this tRNA-like stress protein requires a tRNA-like shape.

The factor IF1 is too small to mimic a tRNA. However, it binds to the decoding part of the A site on the small subunit (Carter *et al*., 2001). The N-terminal domain of IF3 binds to the part of the E site which is located on the small subunit (see Sec. 9.2; Moazed *et al*., 1995; Dallas & Noller, 2001). Even if these proteins do not mimic a tRNA in shape, they bind to sites for tRNA on the ribosome. A summary of the proteins that mimic tRNA or bind to tRNA sites is provided in Table 9.10. It is remarkable that in all steps of protein synthesis except during tRNA binding and peptidyl transfer, specific proteins occupy the A site (Kristensen *et al*., 2001). Furthermore, the bacterial translation factors can essentially be divided into two main categories. One group of factors bind to tRNA-binding sites and the others are trGTPases (Kristensen *et al*., 2001). EF-G belongs to both categories.

9.7 RIBOSOME RESCUE FACTORS/RIBOSOMAL PROTECTION PROTEINS

A multitude of proteins that interact with ribosomes under different conditions have been identified (Table 9.11). They are more or less well characterized in their binding and function. A number of them are clearly ribosome rescue factors with a role in different physiological situations and problems. A selection of such proteins are briefly described here.

Table 9.10 GTPases and tRNA Mimics in the Translation System

Protein	GTPase	tRNA Shape	tRNA Binding Site	Comments
IF1			A	Anticodon stem-loop
IF2	+			Binds 50S to preinitiation complex
IF3			E	Antiassociation
EF-P		+	'E'	Homologous to eIF5A
EF-Tu	+			Binds aa-tRNA to ribosome
SelB	+	+		mRNA-binding part has L-shape
EF-G	+	+	A/T	Translocase
RF1,2			A	Peptide release
RF3	+			RF1/2 release
RRF		+	A+P	Recycling of ribosomal subunits
SmpB			A	Anticodon stem-loop
TL5		+		Ribosomal protein of variable size, shock factor

Table 9.11 Ribosome Rescue Factors

Protein	Role	Binding Site
TetO/TetM	Tetracycline removal, GTPase	GAR
BipA/TypA	Unknown, GTPase	70S, 30S
RelA/SpoT	Regulation during amino acid starvation	A site
RelE	Fragments mRNA during nutritional stress	A site
tmRNA	Recovery of stalled ribosomes with a fragmented mRNA	A site
YaeJ	Peptide hydrolysis from stalled ribosomes	70S, 100S
RaiA	Prevents ribosome dissociation during environmental stress	30S subunit
RMF	Formation of inactive 100S ribosome dimers during environmental stress	30S subunit
HPF, YfiA, YbhB	Regulate ribosomal dimer formation	30S subunit
SRA	Unknown function	30S subunit

TetO/TetM

A number of mechanisms lead to resistance to tetracyclines (Thaker *et al.*, 2010). One of them includes a range of ribosomal protection proteins (RPPs), the best-characterized of which may be TetM and TetO (Burdett, 1996; Trieber *et al.*, 1998; Dantley *et al.*, 1998). These proteins eliminate the antibiotic inhibitor tetracycline from the ribosome in a GTP-dependent manner (Burdett, 1996; Trieber *et al.*, 1998). The primary binding site for tetracycline is located in the region between the shoulder and the head of the small subunit, near the decoding part of the A site (see Sec. 10.2).

TetO and TetM have masses of 70 kDa and about 50% sequence similarity to EF-G (Sanchez-Pescador *et al.*, 1988). All six domains of EF-G have corresponding parts in TetO, but the G′-domain is quite small. With this similarity, one would expect a similarity to EF-G in binding to the ribosome. Spahn *et al.* (2001) reported a cryo-EM investigation of the binding of TetO in complex with GTP-γS to the ribosome. Indeed, the protein binds essentially like EF-G, with one clear difference, domain IV, which mimics the anticodon part of the tRNA in a ternary complex, does not extend to contact the anticodon in the P site, but rather interacts with the junction between the head and the shoulder of the small subunit, where the binding site for tetracycline is located (Brodersen *et al.*, 2000; Pioletti *et al.*, 2001). There is yet another important difference. EF-G, when bound to the ribosome with GTP analogs, binds to the MSII state (Agrawal *et al.*, 1999; Frank & Agrawal, 2000), However, TetO in complex with GTP-γS binds to MSI (Table 8.4; Spahn *et al.*, 2001). Tetracyclin inhibits the accommodation of aminoacyl-tRNA into the A site. The ribosome must then be in the MSI state.

The mechanism of binding and dissociation of TetO seems to be similar to that of EF-G. The protein binds to the ribosome with GTP and, after tetracycline removal and GTP hydrolysis, it dissociates from the ribosome (Connell *et al.*, 2003). It is unlikely that TetO makes a steric clash with tetracycline. It is more probable that it induces conformational changes in h34 and h18 of the 16S RNA, which leads to the dissociation of tetracycline (Spahn *et al.*, 2001).

When TetO is bound to the ribosome, its domain III is close to protein S12 (Spahn *et al*., 2001). Mutations in S12, whether causing streptomycin resistance or streptomycin dependence, result in decreased TetO activity. One mutation of S12 (K42Q) abolishes the TetO activity totally (Taylor *et al*., 1998).

BipA/TypA

BipA, also called TypA, is a trGTPase very similar to EF-G, TetO and LepA. It has some of the domains of EF-G, but the G′-domain is very much truncated (Farris *et al*., 1998). Further it, is more related to LepA in lacking domain IV of EF-G and having a distinct C-terminal domain (CTD; deLivron *et al*., 2009). Normally, BipA binds to 70S ribosomes in a GTP-dependent manner. Under conditions of stress it can bind to the 30S subunit. Most likely, it binds to the same site of 70S ribosomes as other trGTPases, but how it interacts with the 30S subunit remains to be clarified. An investigation of the association with 30S subunits and 70S ribosomes identified the CTD as an essential ingredient (deLivron *et al*., 2009). So far the role of BipA remains obscure, but it is most certainly related to some form of translational stress.

Stringent Response

When *E. coli* experiences starvation of an amino acid or other nutrients, the level of uncharged tRNA goes up significantly (Yegian *et al*., 1966). This can lead to a situation where a deacylated tRNA occupies the A site. Stringent factor, ppGpp synthase I (PSI) or RelA is expressed by the gene *relA*. As a response to starvation or heat shock, RelA produces what is called magic spot II (MSII), guanine nucleotide pentaphosphate (pppGpp). This nucleotide is produced from ATP and GTP (Fig. 9.25; Haseltine & Block, 1973; Sy & Lipman, 1973). A separate enzyme, guanine pentaphosphate phosphohydrolase (GPPA), can convert pppGpp to ppGpp, guanine nucleotide tetraphosphate (Keasling *et al*., 1993; Kuroda *et al*., 1997). ppGpp acts as an alarmone and binds to RNA polymerase and causes what is

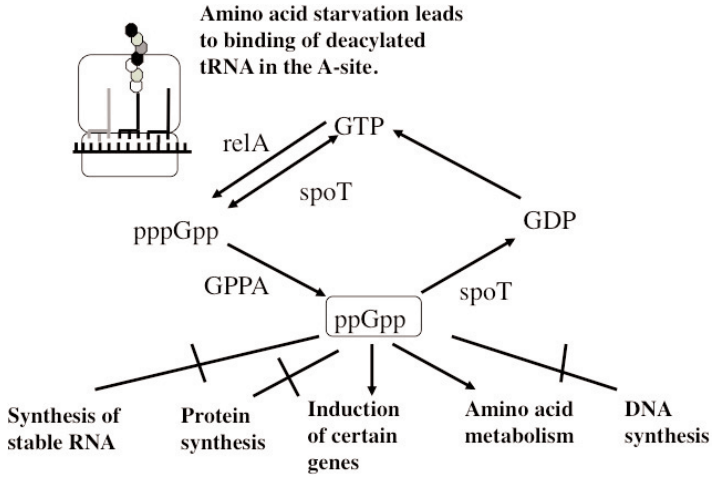

Fig. 9.25 The synthesis, degradation and role of (p)ppGpp, which is dependent on amino acid starvation (after Izutsu *et al*., 2001). RelA and SpoT control the synthesis and breakdown of the nucleotide, which can inhibit the synthesis of DNA, rRNA, tRNA and proteins but induce some genes related to amino acid metabolism.

called stringent control of transcription, i.e. transcription is immediately inhibited (Stent & Brenner, 1961; Artisimovitch *et al*., 2004).

Recent analysis shows that the classical description of the function of RelA is wrong. It does not produce MSII when it encounters a deacylated tRNA on the ribosome. Rather, the limited number of RelA molecules are all bound to ribosomes under normal conditions (English *et al*., 2011). If a ribosome with a bound RelA molecule encounters a deacylated tRNA in the A site, RelA falls off and becomes active and synthesizes MSII until it rebinds to a ribosome.

Stringent control is relieved by mutations of RelA or a protein produced by the gene *relC*. The product of *relC* is ribosomal protein L11 (Friesen *et al*., 1974; Parker *et al*., 1976). Ribosomes devoid of L11 are inactive in the synthesis of pppGpp (Wendrich *et al*., 2002). However, L11-deficient ribosomes are viable and still bind RelA. Evidently, ribosomes lacking L11 will bind RelA more strongly. The flexible linker of L11 is important, as well as the

proline-rich helix of the NTD of L11 (Kasai *et al*., 2004; Jenvert & Holmberg Schiavone, 2007).

When sufficient amounts of the missing amino acid are again available, the corresponding tRNAs will be charged and the ternary complex formed will compete with the bound deacylated tRNA for the A site (Schilling-Bartetzko *et al*., 1992; Wendrich *et al*., 2002). ppGpp production inhibits transcription of genes involved in the translational apparatus (Lazzarine & Dahlberg, 1971; Dennis & Nomura, 1974) but upregulates genes encoding enzymes involved in amino acid biosynthesis (Cashel *et al*., 1996; Zhou & Jin, 1998).

In gram-negative bacteria there is a second protein related to RelA. This protein, produced by the *spoT* gene, is called SpoT or PSII (Laffler & Gallant, 1974). While RelA and SpoT are guanosine 3′,5′-bis(diphosphate) synthetases, SpoT is also a guanosine 3′,5′-bis-(diphosphate) 3′-phosphohydrolase (ppGppase; Heinemeyer & Richter, 1977; Sy, 1977). In a strain where the PSII activity was deleted, the contribution of RelA was responsible for the initial burst of (p)ppGpp synthesis during glucose and amino acid starvation, but that RelA was inactive when amino acids were available (Gentry & Cashel, 1996). Gram-positive bacteria have only one protein, called Rel, which like SpoT has both synthetase and hydrolase activities (Wendrich & Marahiel, 1997; Mittenhuber, 2001). SpoT does not interact with the ribosome but with the central cofactor of lipid synthesis, the acyl carrier protein (ACP; Battesti & Bouveret, 2006).

An examination of the *E. coli* spoT protein of 702 amino acid residues showed that the ppGpp-ase activity was contained in the first 203 residues and that the PSII activity was contained in the region 67–374 (Gentry & Cashel, 1996). A further study indicated that Asp 293 was indispensable for ppGpp synthesis in *E. coli* SpoT (Fujita *et al*., 2002).

Structural information on these enzymes is available. The structure of the N-terminal half of the Rel protein from *Streptococcus dysgalactiae equisimilis*, a gram-positive bacterium, has been determined (Hogg *et al*., 2004). Residues 5–159 contain the hydrolase

domain, and residues 176–371 the synthetase domain. A central three-helix bundle connects the two domains. The hydrolase domain is α-helical and is structurally homologous with the catalytic domain of cyclic nucleotide phosphodiesterases (PDEs; Xu *et al*., 2000; Huai *et al*., 2003). PDEs all have a conserved His-Asp sequence and are metallophosphohydrolases (Aravind & Koonin, 1998). In the case of Rel, a manganese ion is bound at these conserved residues. The synthetase domain is a mixed α/β protein with a fold related to the palm domain of mammalian DNA polymerase β (Sawaya *et al*., 1997). The two active sites are located about 30 Å apart (Hogg *et al*., 2004).

The crystals of Rel contain two conformations of the N-terminal half of the protein. In both there is a GDP molecule bound to the synthetase active site. In one molecule, the synthetase active site seems to be in an active conformation. Here the hydrolase is in an inactive conformation. In the other molecule with the inactive conformation of the synthetase active site, there is an unusual GDP derivative seen at the hydrolase active site. This nucleotide is best interpreted as a guanosine 5′-diphosphate-2′:3′-cyclic monophosphate (ppG2′:3′p; Hogg *et al*., 2004). It seems evident that the two sites with opposing activities control each other. Most likely, the C-terminal, ribosome-binding domain also affects the activities of the two active sites.

The management of suitable levels of (p)ppGpp in bacteria (Table 9.12) involves two more proteins, called GPPA and PPX. PPX is a protein involved in polyphosphate metabolism and, more specifically, the breakdown of inorganic polyphosphate (Rangarajan *et al*., 2006). GPPA is produced from the *gppA* gene, which is important for

Table 9.12 Proteins Involved in Synthesis, Conversion of pppGpp to ppGpp and Breakdown of (p)ppGpp

Bacteria	Synthesis	Conversion	Degradation
Gram-negative	RelA (SpoT)	GPPA	SpoT
Gram-positive	Rel		Rel

the conversion of the pentaphosphate to the tetraphosphate (Keasling *et al*., 1993). The structure is available for a combined PPX/GPPA from *A. aeolicus* (Kristensen *et al*., 2004, 2008). The most recent structure includes the alarmone ppGpp bound in a cleft between the two domains of the enzyme. The structure reveals the position of the product and the substrate position, and catalysis can be envisioned.

RelBE

Two proteins related to nutritional stress are RelB and RelE. They form a toxin–antitoxin pair (Gotfredsen & Gerdes, 1998; Grønlund & Gerdes, 1999). RelE is a toxin by being a global inhibitor of translation, while RelB can neutralize its effect by forming a protein–protein complex. RelE binds to the ribosome (Galvani *et al*., 2001).

The toxic action of RelE is to hydrolyze the mRNA — not free mRNA but mRNA exposed in the ribosomal A site (Pedersen *et al*., 2003). The structure of the archaeal RelB–RelE complex is known (Takagi *et al*., 2005; Francuski & Sanger, 2009). The proteins form a heterotetramer. The structure of RelE bound to the 70S ribosome is also known before and after cleavage of the mRNA (Neubauer *et al*., 2009). RelE binds to the decoding part of the A site. Its basic nature gives it a strong affinity for nucleic acids.

RelB is an autorepressor of RelBE transcription and RelE is a corepressor. Normally, the proteins are not expressed. During amino acid starvation, the level of RelB decreases and, as a consequence, the expression of RelBE increases significantly (Christensen *et al*., 2001). The protease Lon specifically degrades RelB and thereby activates RelE as an inhibitor of translation (Christensen *et al*., 2001).

tmRNA

Bacterial ribosomes can get stalled at the 3′ end of a degraded or defective mRNA. A factor that can recover the ribosomes is an

RNA molecule of between 260 and 430 nucleotides called 10Sa RNA, SsrA or tmRNA (for reviews, see Karzai *et al*., 2000; Moore & Sauer, 2007). As the third name indicates, this RNA molecule functions both as messenger and tRNA in a process called trans-translation (Keiler *et al*., 1996). The tmRNA functions in complex with small protein B (SmpB).

The 5′ and 3′ ends of tmRNA fold into the tRNA-like domain (TLD), which can be charged at its 3′ CCA end with alanine by AlaRS and delivered to the stalled ribosome in complex with EF-Tu and GTP (Plate 9.18; Kazai *et al*., 2000). Once the alanyl residue is added to the nascent peptide and the TLD is translocated to the ribosomal P site, an open reading frame of the tmRNA — mRNA-like domain (MLD) — will be translated. Ten amino acids are incorporated up to the stop codon of the tmRNA. In this way, the ribosome is rescued and the released peptide can be recognized and eliminated by degrading systems of the cell (Fig. 9.26).

Crystal structures of part of the complex are available (Gutmann *et al*., 2003; Bessho *et al*., 2007). SmpB is associated with the TLD of tmRNA (Karzai *et al*., 2000). The TLD in complex with SmpB corresponds to a long-variable-arm tRNA (Plate 9.18; Bessho *et al*., 2007). SmpB, which has an OB fold, corresponds to the anticodon and D-stems of a tRNA (Bessho *et al*., 2007). IF1 is another protein with an OB-fold that binds to the DC (see Sec. 9.2). Both could thus be described as mimics of part of a tRNA (Gutmann *et al*., 2003; Bessho *et al*., 2007; Table 9.9).

The structure of tmRNA when bound to the ribosome in complex with SmpB, EF-Tu·GDP and kirromycin has been characterized by cryo-EM (Valle *et al*., 2003c; Kaur *et al*., 2006; Gillet *et al*., 2007). The antibiotic inhibits the release of EF-Tu and the TLD cannot be accommodated to extend the nascent peptide. With the secondary structure of tmRNA and since EF-Tu has been studied bound to the ribosome, the density could be interpreted (Plate 9.18). Part of the tmRNA forms a loop around the beak of the 30S subunit. A crystal structure of the ribosome with EF-Tu·kirromycin, TLD and SmpB is also available (Neubauer *et al*., 2012). SmpB is essential for this

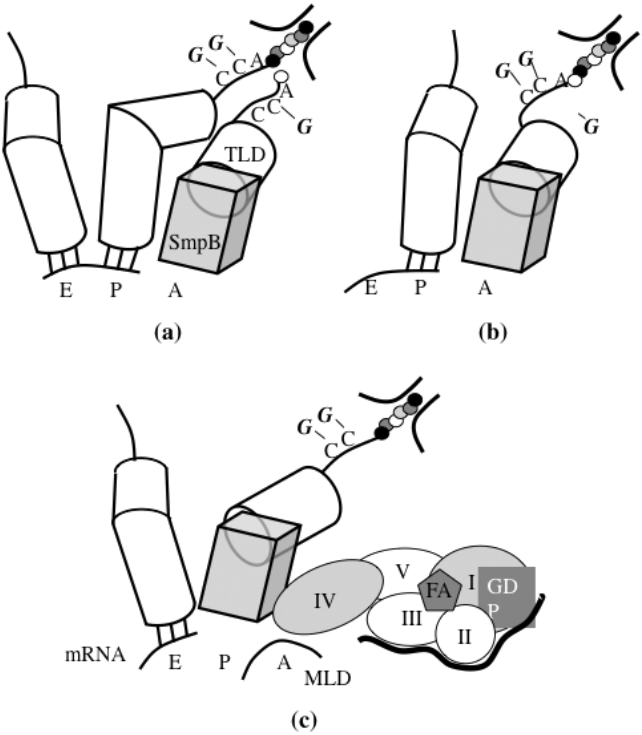

Fig. 9.26 The process in which tmRNA and SmpB interact with a stalled ribosome where the mRNA is truncated. **(a)** The aminoacylated TLD is accommodated with SmpB in the A site. **(b)** Peptidyl transfer has occurred from the P site tRNA to the TLD. **(c)** EF-G translocates the complex of the TLD and SmpB from the A/P site to the P site. At the same time, the mRNA part of tmRNA is brought into the decoding part of the A site.

process and is placed in the decoding center of the ribosome (Fig. 9.27; Karzai *et al*., 1999; Hallier *et al*., 2004; Gillet *et al*., 2007; Cheng *et al*., 2010; Neubauer *et al*., 2012). SmpB is also needed for the GTP hydrolysis by EF-Tu (Shimizu & Ueda, 2006). In this preaccommodated state a second SmpB molecule binds to the TLD and contacts the 50S subunit close to GAC (Gillet *et al*., 2007).

After GTP hydrolysis and dissociation of EF-Tu, the TLD accommodates into the A site and the peptidyl transfer center to engage in peptidyl transfer to the alanyl residue bound to the TLD. In this

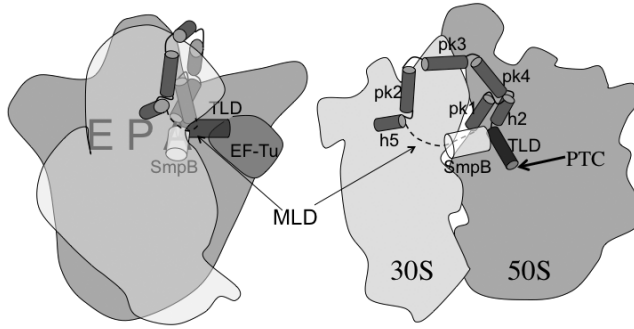

Fig. 9.27 A schematic illustration of the binding of tmRNA and SmpB to the ribosome. On the left is the initial stage, when the TLD binds with EF-Tu to the A/T site. SmpB binds to the decoding site. On the right is a schematic view of the accommodated TLD after EF-Tu has hydrolyzed its GTP molecule and dissociated. The different regions of the tmRNA are bound around the beak of the small subunit. The MLD is shown by a dashed line.

accommodated state the acceptor end of the TLD is bound at the peptidyl transfer center and the SmpB at the decoding part of the A site remains while the second SmpB molecule has dissociated (Shpanchenko *et al*., 2005; Hallier *et al*., 2006; Cheng *et al*., 2010).

Subsequently, EF-G translocates the complex into the P site and the MLD will act as the messenger to label the defective protein for destruction (Fig. 9.26; Ramrath *et al*., 2012). Finally, the TLD with SmpB will be translocated into the E site.

YaeJ

Trans-translation by tmRNA is a complex process and in *E. coli* strains with defective tmRNA mRNAs without stop codons will anyway be translated efficiently. However, stalled ribosomes can be released from their mRNAs. One small protein that is involved is YaeJ, a peptidyl-tRNA hydrolase (PTH) that is found in many gram-negative bacteria and is completely conserved in eukaryotic genomes (Handa *et al*., 2011a). Like class I release factors, it has the typical GGQ motif. In addition, the structure of the protein is related to the structure of domain 3 of class I release factors

containing the motif (Singarapu *et al*., 2008; Handa *et al*., 2011b). YaeJ is associated with both 70S and 100S dimeric ribosomes and has a long basic C-terminus used for the ribosome binding. The most likely role of YaeJ is to cleave the nascent peptide off stalled ribosomes in a codon-independent manner (Handa *et al*., 2011a).

The structure of YaeJ bound to the 70S ribosome shows the N-terminal domain in the 50S part of the A site and the GGQ motif at the PTC (Fig. 9.28). The C-terminal tail is located downstream of the A-site part of the mRNA path (Gagnon *et al*., 2012). The tail partly adopts the structure of an α-helix and interacts with the phosphate backbone of the rRNA. Stalled ribosomes frequently have their mRNAs cleaved. Thus, the tail may function as a sensor for ribosomes not active in translation.

Ribosome Rescue Factors Operating in the Stationary Phase

In the stationary phase, *E. coli* becomes highly resistant to a number of environmental stresses, including antimicrobial agents.

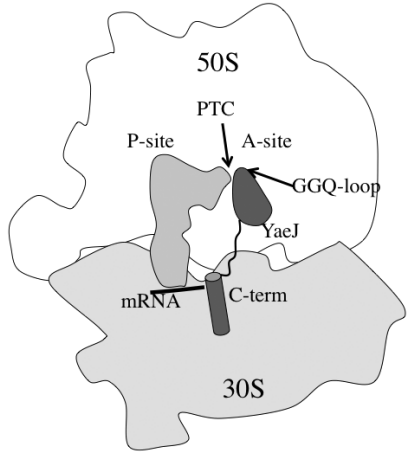

Fig. 9.28 A schematic illustration of the binding to the ribosome of YaeJ (Gagnon *et al*., 2012). The C-terminal α-helix binds across the mRNA-binding grove in stalled ribosomes where the mRNA lacks a stop codon. The N-terminal domain binds with its GGQ motif in the PTC able to hydrolyze the ester bond between tRNA and nascent peptide.

This change occurs simultaneously with the expression of a large number of genes. Among these genes are a number of ribosome-associated genes encoding proteins such as RMF (ribosome modulation factor), SRA (stationary-phase-induced ribosome-associated protein), protein Y (RaiA or YfiA), protein G (YhbH) and HPF (hibernation-promoting factor) (Izutsu *et al*., 2001; Sato *et al*., 2009). Furthermore, in *E. coli* the 70S ribosomes can be induced to dimerize and form 100S ribosomes, which have no translational activity, and this is a state referred to as ribosomal hibernation (Yoshida *et al*., 2002; Sato *et al*., 2009). This is one way to prevent ribosomal degradation.

RMF

RMF (55 aa) transcription is induced by the global regulator ppGpp under starvation or stress conditions (Izutsu *et al*., 2001). RMF binds to the mRNA channel and prevents the SD/anti-SD interaction in the small subunit. The binding of RMF inhibits the binding of mRNA to the small subunit and prevents initiation. This also has the effect that 70S ribosomes dimerize and form inactive 100S particles (Wada *et al*., 1990; Polikanov *et al*., 2012).

RMF induces a conformational change of the small subunit that makes the ribosomes dimerize into a particle with twofold symmetry. The main interactions are through the head and protein S2. RMF is not bound at the dimer interface, but the conformational change moves the head of the small subunit away from the central protuberance to facilitate a more extensive interaction between the two heads in the dimer.

HPF, YfiA and YhbH

HPF (94 aa) binds to the small subunit, but only one copy binds per ribosome dimer. The structure of the small protein was determined by NMR (Sato *et al*., 2009). A cryo-EM structure of the factor bound to the ribosome is also available (Fig. 9.29; Kato *et al*., 2010). The factor promotes the dimerization of ribosomes to 100S

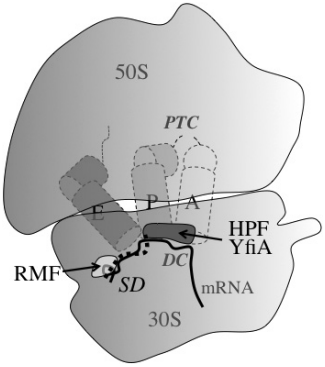

Fig. 9.29 Schematic illustration of the binding sites of RMF, HPF and YfiA to the ribosome. RMF binds to the SD region, preventing initiation, with the effect that the ribosome dimerizes. HPF and YfiA bind in the decoding area for the tRNAs. YfiA has a negatively charged tail (dotted), which may distort the binding of RMF.

particles. The ribosomal dimers form due to contacts between the 30S subunits. RMF and HPF can bind simultaneously to interfere with initiation of protein synthesis (Ueta *et al*., 2005). The binding of HPF interferes with all tRNA-binding sites but also with initiation factors IF1 and IF3 as well as EF-G. Since IF3 prevents the association of the subunits into full ribosomes and EF-G together with RRF stimulates the dissociation of the ribosomes, the binding of HPF prevents the dissociation of 100S particles into subunits.

YfiA (113 aa) and YhbH (95 aa) are HPF paralogs with antagonistic roles (Ueta *et al*., 2005). YfiA has a long flexible C-terminal tail that inhibits ribosomal dimer formation. It inhibits translation during cold shock, probably by stabilizing the 70S ribosome and preventing new initiation. YhbH, on the other hand, binds exclusively to 100S ribosomes and probably only one copy per 100S ribosome (Ueta *et al*., 2005). The structure of YfiA bound to the 30S subunit is known (Fig. 9.29). The binding site is at the decoding part of the P and A sites, near the site for IF1, and partly overlapping with the mRNA (Vila-Sanjurjo *et al*., 2004). The close relative of YfiA, YhbH, is expected to bind to the same surface of the

ribosome. It is then interesting that it has the opposite effect (Ueta *et al.*, 2005). The negatively charged tail of YfiA may distort the binding of RMF to the ribosome. The binding of these factors on the mRNA and tRNA binding sites on the small subunit can obviously not occur on translating ribosomes, but function under starvation or stress.

SRA

SRA is another small protein that binds tightly to the 30S subunit. For some time it was considered to be a ribosomal protein (S22). However, its stoichiometry is only 0.1–0.4 copies per ribosome (Izutsu *et al.*, 2001).

10

Inhibitors of Protein Synthesis — Antibiotics, Resistance

Numerous compounds inhibit protein synthesis (Vazquez, 1974). Many of them are known to bind to the ribosome. The inhibitors are to a large extent natural products isolated from different microorganisms, which excrete these antibiotics in their fight for living space. The antibiotics can kill bacteria and are then bacteriocidal, but most antibiotics inhibit bacterial reproduction and are therefore bacteriostatic. A number of antibiotics, which target the protein synthesis machinery, are clinically used since they selectively inhibit certain bacteria.

Normally, an organism is resistant to the antibiotics it produces. Thus, the resistance mechanism must have coevolved with the antibiotics with the potential of spreading to other organisms. The microbial resistance to antibiotics has become a serious and growing health problem (Chopra, 2000; Woodford & Livermore, 2009). The search for new synthetic or semi-synthetic inhibitors and antibiotics for which there are no resistance mechanisms is therefore a major effort (Knowles *et al*., 2002; Franceschi & Duffy, 2006; Skripkin *et al*., 2008).

An inhibitor acts like a 'spanner in the works' (Spahn & Prescott, 1996). In the ribosome, an antibiotic may inhibit a functional process by binding to an essential binding site or by changing the functional

dynamics of the machinery in such a way that the transition to the next state is blocked (Table 10.1; Fig. 10.1). Thus, like in the studies of other enzymes, the analyses of inhibitors and the resistance against them provide good means of understanding the underlying function (Blaha *et al.*, 2012).

Since the functional sites of the ribosome are primarily composed of rRNA, it is not surprising that antibiotic binding sites are generally located on the rRNA (Cundliffe, 1987, 1990). As there usually are multiple genomic copies of the rRNAs, mutations of the rRNAs rarely lead to resistance. However, antibiotic resistance is frequently due to enzymes that can modify the antibiotic or the rRNA, but resistance can also be caused by mutations in ribosomal proteins, which are usually encoded by only one gene each.

It is remarkable that antibiotics that inhibit the ribosome with a filled or blocked A site induce a cold-shock response and antibiotics that inhibit the ribosome when the A site is empty induce heat shock (VanBogelen & Neidhardt, 1990). Evidently, the ribosome also acts as a sensor of the state of the cell.

The ribosomal antibiotics inhibit a range of different steps of protein synthesis. We will describe only some for which the binding sites are identified by crystallography, in most cases on subunits or complete ribosomes, but in other cases only in complex with segments of the rRNA (see also Wilson 2004, 2009, 2011).

10.1 INHIBITORS OF INITIATION

Edeine and pactamycin inhibit protein synthesis in all domains of life (Odom *et al.*, 1978). Thus, it is not surprising that they bind to conserved regions of the ribosome. Edeine protects 16S RNA at a site that overlaps with protection by kasugamycin and pactamycin (Woodcock *et al.*, 1991; Mankin, 1997). Despite very different structures, edeine and pactamycin bind to nearby regions, between the P- and E-sites (Brodersen *et al.*, 2000; Pioletti *et al.*, 2001). Edeine and pactamycin seem to act antagonistically (Dinos *et al.*, 2004). Edeine induces a base pairing between G693 and C795 (Brodersen *et al.*, 2000), while pactamycin breaks it (Pioletti *et al.*, 2001).

Table 10.1 Some Translational Inhibitors Mapped by Structural Methods.

Inhibitor	Bound to	Binding Site	References
Inhibitors of initiation, 30S			
Edeine	T30S	P-site, h24, h28, h44, h45	Pioletti *et al*., 2001
Kasugamycin	E70S	mRNA site, at P- and E-site codons	Schuwirth *et al*., 2006
	T30S	Two sites, at P- and E-sites	Schluenzen *et al*., 2006
Pactamycin	T30S	E-site, h23b, h24a	Brodersen *et al*., 2000
Inhibitors of aminoacyl-tRNA binding, 30S			
Tetracycline	T30S	h18, h31, h34, h44	Brodersen *et al*., 2000; Pioletti *et al*., 2001
Decoding site inhibitors, 30S			
Apramycin	h44 fragment		Han *et al*., 2005
Gentamycin	h44 fragment		Yoshizawa *et al*., 1998
Geneticin	h44 fragment		Vicens & Westhof, 2003
Tobramycin	h44 fragment		Vicens & Westhof, 2002
Paromomycin	T30S	h44	Fourmy *et al*., 1996, 1998; Carter *et al*., 2000
Streptomycin	T30S	h18, h27, h44, S12	Carter *et al*., 2000

(*Continued*)

Table 10.1 *(Continued)*

Inhibitor	Bound to	Binding Site	References
Peptidyl transfer inhibitors, 50S			
Anisomycin	H50S	C2452, U2504	Hansen *et al*., 2003; Blaha *et al*., 2008
Blasticidin S	H50S	Two sites: G2251 or G2252	Hansen *et al*., 2003
Chloramphenicol	D50S, E70S, T70S	1st site: G2061; C2452, U2504	Schlünzen *et al*., 2001; Dunkle *et al*., 2010 Bulkley *et al*., 2010
	H50S	2nd site: A2058, A2059	Hansen *et al*., 2003
Linezolid	H50S, D50S		Ippolito *et al*., 2008; Wilson *et al*., 2008
Puromycin	H50S, D50S		Nissen *et al*., 2000b; Schmeing *et al*., 2002; Bashan *et al*., 2003
Sparsomycin	H50S, D50S	P-site CCA end, U2585, A2602	Schlünzen *et al*., 2001; Hansen *et al*., 2002b, 2003; Bashan *et al*., 2003
Exit tunnel inhibitors, 50S			
Macrolides/ketolides			
ABT-773	D50S		Schlünzen *et al*., 2003
Azithromycin	D50S, H50S, T70S		Schlünzen *et al*., 2003, Tu *et al*., 2005; Bulkley *et al*., 2010
Carbomycin A	D50S, H50S		Hansen *et al*., 2002a; Pyetan *et al*., 2007
Claritromycin	D50S		Schlüntzen *et al*., 2001
Erythromycin	D50S, E70S, H50S, T70S		Schlünzen *et al*., 2001, Tu *et al*., 2005; Bulkley *et al*., 2010; Dunkle *et al*., 2010

(*Continued*)

Table 10.1 *(Continued)*

Inhibitor	Bound to	Binding site	References
Roxithromycin	D50S		Schlünzen *et al*., 2001
Spiramycin	H50S		Hansen *et al*., 2002a
Telithromycin	D50S, E70S, H50S, T70S		Berisio *et al*., 2003a; Tu *et al*., 2005; Bulkley *et al*., 2010; Dunkle *et al*., 2010
Troleandromycin	D50S		Berisio *et al*., 2003b
Tylosin	H50S		Hansen *et al*., 2002a
Lincosamides			
Clindamycin	D50S, H50S, E70S		Schlüntzen *et al*., 2001; Hansen *et al*., 2002; Tu *et al*., 2005; Dunkle *et al*., 2010
Streptogramins A			
Dalfopristine	D50S		Harms *et al*., 2004
Virginiamycin M	H50S		Hansen *et al*., 2003; Tu *et al*., 2005
Streptogramins B			
Quinupristin	D50S, H50S		Harms *et al*., 2004; Tu *et al*., 2005
Virginiamycin M	H50S		Tu *et al*., 2005
Virginiamycin S	H50S		Tu *et al*., 2005

(*Continued*)

Table 10.1 *(Continued)*

Inhibitor	Bound to	Binding Site	References
Factor-related inhibitors			
EF-Tu			
Kirromycin	EF-Tu	Domain interface G-III	Vogeley *et al*., 2001
Aurodox	T 70S*EF-Tu		Schmeing *et al*., 2009
GE2270A	EF-Tu	Domain interface G-II	Heffron & Jurnak, 2000
Binding of EF-G (thiopeptides)			
Thiostrepton	D50S	A1067, A1095, L11NTD	Lenzen *et al*., 2003; Harms *et al*., 2008
Nosiheptide	D50S	A1067, A1095, L11NTD	Harms *et al*., 2008
Micrococcin	D50S	A1067, A1095, L11NTD	Harms *et al*., 2008
EF-G			
Fusidic acid	T 70S*EF-G	Domain interface G-III	Gao *et al*., 2009
Translocation			
Hygromycin B	T30S, E70S	P-site, h44	Brodersen *et al*., 2000; Borovinskaya *et al*., 2008
Pactamycin	T30S	E-site, h23b, h24a	Brodersen *et al*., 2000
Spectinomycin	T30S, E70S	h34, hinge head–body	Carter *et al*., 2000; Borovinskaya *et al*., 2007
EF2			
Sordarin	Yeast EF2	Interface between domains III, IV and V	Jørgensen *et al*., 2003

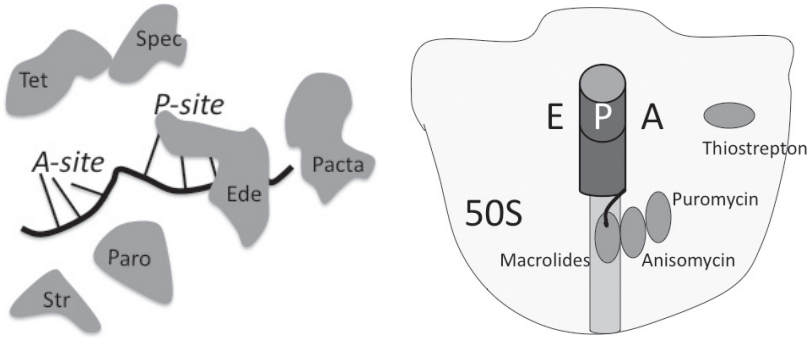

Fig. 10.1 The binding sites of some antibiotics on the ribosomal subunits. On the left are some binding sites on the small subunit and their relationship to the mRNA and decoding. On the right is the large subunit with some of its sites for antibiotics in relation to the P-site tRNA and the exit channel.

They have both been thought to affect initiation, but a more thorough analysis suggests that edeine inhibits initiation whereas pactamycin inhibits early translocation steps (Dinos *et al.*, 2004). Both inhibitors may affect the mobility of the 30S platform during subunit association or displace the mRNA in the E-site region (Carter *et al.*, 2000). This would disturb the binding of the mRNA, for example the SD interaction (see Sec. 8.1), which occurs just upstream of the E-site codon (Yusupova *et al.*, 2001). Furthermore, both antibiotics interact with bases that are protected by IF3 (Moazed *et al.*, 1995).

Edeine

Edeine (Ede) is a pentapeptide amide, spermidine-like compound (Fig. 10.2). It inhibits initiation by preventing the binding of fMet–tRNA to the small subunit (Dinos *et al.*, 2004). The inhibition is due to a disturbance of recognition of the AUG start codon in the P-site (Pioletti *et al.*, 2001; Dinos *et al.*, 2004). Ede also increases the level of misincorporation (Dinos *et al.*, 2004). It interacts with helices h24, h28, h44 and h45 (Plate 10.1; Pioletti *et al.*, 2001). The

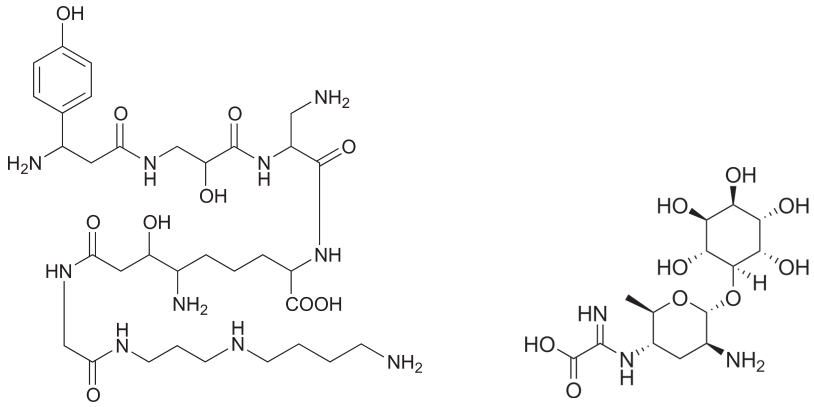

Fig. 10.2 Left: Edeine (drawn by Andreas Ehnbom). Right: Kasugamycin (from Wikipedia).

aromatic part of Ede makes hydrogen bonds with G926 in h28 like a regular base pair. A790–A792 in the loop of h24 interacts through their sugar residues with the hydrophobic part of Ede. This leads to a distortion of h24a that induces C795 to form a base pair with G693 of h23b. Addition of Ede after the formation of the initiation complex has no inhibitory effect, since part of the binding site is already occupied.

Kasugamycin

Kasugamycin (Ksg) is known to inhibit initiation on 30S subunits by blocking initiator tRNA from binding (Okuyama *et al.*, 1971). It has been employed clinically (Ishigami *et al.*, 1967) but is now primarily used to kill fungi in rice fields (Umezawa *et al.*, 1965). The binding site has been identified crystallographically in both *E. coli* 70S ribosomes (Schuwirth *et al.*, 2006) and *T. thermophilus* 30S subunits (Schlüntzen *et al.*, 2006). In *Thermus* there are two binding sites. The common binding site overlaps with the codons of the P- and E-sites of mRNA and partly with the binding site for edeine (Pioletti *et al.*, 2001). The second *Thermus* site overlaps with the binding site for pactamycin (Brodersen *et al.*, 2000). Low-level Ksg resistance can be

caused by the lack of a methylase, KsgA, which dimethylates adenines 1518 and 1519 (Helser *et al*., 1972). A bound Ksg is not in contact with these residues but the resistant form lacking these modifications has a different conformation (Demirci *et al*., 2010), which may explain why Ksg bound to the unmodified ribosome does not inhibit initiation (Schuwirth *et al*., 2006). Mutations of A794, G926 or A1519 also lead to resistance (Vila-Sanjuro *et al*., 1999).

10.2 INHIBITORS OF AMINOACYL-tRNA BINDING

Tetracycline

Tetracycline (Fig. 10.3) has been used extensively since the 1940s as a 'broad-spectrum' antibiotic, in both human and veterinary medicine (Chopra *et al*., 1992). This has lead to widespread resistance (Salyers *et al*., 1990; Taylor & Chau, 1996). Tetracycline has one strong binding site on the small ribosomal subunit in addition to several weaker ones (Epe *et al*., 1987; Kolesnikov *et al*., 1996). The strong binding site is between the head and shoulder of the small subunit near the position of the anticodon-stem-loop (ASL) of the A-site (Brodersen *et al*., 2000; Pioletti *et al*., 2001). Tetracycline binds to helix h34 (residues 1054–1056 and 1196–1200) and helix h31 (residues 964–967) at the A-site (Maxwell, 1967; Geigenmuller & Nierhaus, 1986). It inhibits neither the binding of the ternary complex with its tRNA to the A/T-site (see Sec. 9.3) nor the dissociation of EF-Tu after GTP hydrolysis (Gordon, 1969). However, it prevents aminoacyl-tRNA from accommodating into the A-site (Wilson, 2004). Since the aminoacyl-tRNA therefore dissociates, one effect of tetracycline binding to the ribosome is that the GTP pool of the cell gets depleted

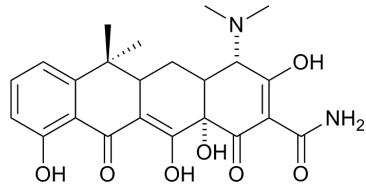

Fig. 10.3 Tetracycline (drawn by Andreas Ehnbom).

(Brodersen *et al.*, 2000). Tetracycline also inhibits the binding of release factors RF-1 and RF-2 to the ribosome (Brown *et al.*, 1993).

The secondary binding sites probably have no inhibitory effects, but it was noticed that one of them is close to h27, h44 and h11 (Brodersen *et al.*, 2000; Pioletti *et al.*, 2001). This location may affect accuracy (Lodmell & Dahlberg, 1997).

Resistance against tetracycline is gained by a mutation, G1058C, in the immediate proximity of the primary binding site for tetracycline on the 16S RNA (Ross *et al.*, 1998). Another type of resistance is due to ribosomal protection proteins, Tet(M) and Tet(O), which are homologues of EF-G (Burdett, 1996; Trieber *et al.*, 1998; Dantley *et al.*, 1998). These proteins eliminate the bound tetracycline by interacting with the A-site (see Sec. 9.6).

10.3 INTERFERENCE WITH DECODING; DISTORTION OF FIDELITY

A number of antibiotics disturb the decoding mechanism by binding to the small subunit (Davies *et al.*, 1964). They are not inhibitors, but they interfere with the correct reading of the message and increase the error frequency of translation. They permit binding of not only cognate but also near-cognate and probably noncognate tRNAs. Thus, they increase the incorporation of wrong amino acids by one or two orders of magnitude (Wilson, 2009). Since decoding is done in two major steps, both initial recognition and proofreading could be affected (see Sec. 11.6). The antibiotics that interfere with the decoding site are primarily the aminoglycosides (Fig. 10.4), which are bacteriocidal. Many reviews of their binding as well as mutations leading to resistance are available (Auerbach *et al.*, 2004; Wilson, 2004; Hermann 2005; Poehlsgaard & Douthwaite, 2005).

The structures of several related compounds bound to small RNA fragments related to part of h44 (Vicens & Westhof, 2001, 2002, 2003; Han *et al.*, 2005; Hermann, 2005) or to the small subunit or whole 70S ribosomes have been investigated (Carter *et al.*, 2000; Ogle *et al.*, 2001, 2002; Hermann, 2005; Selmer *et al.*, 2006). These

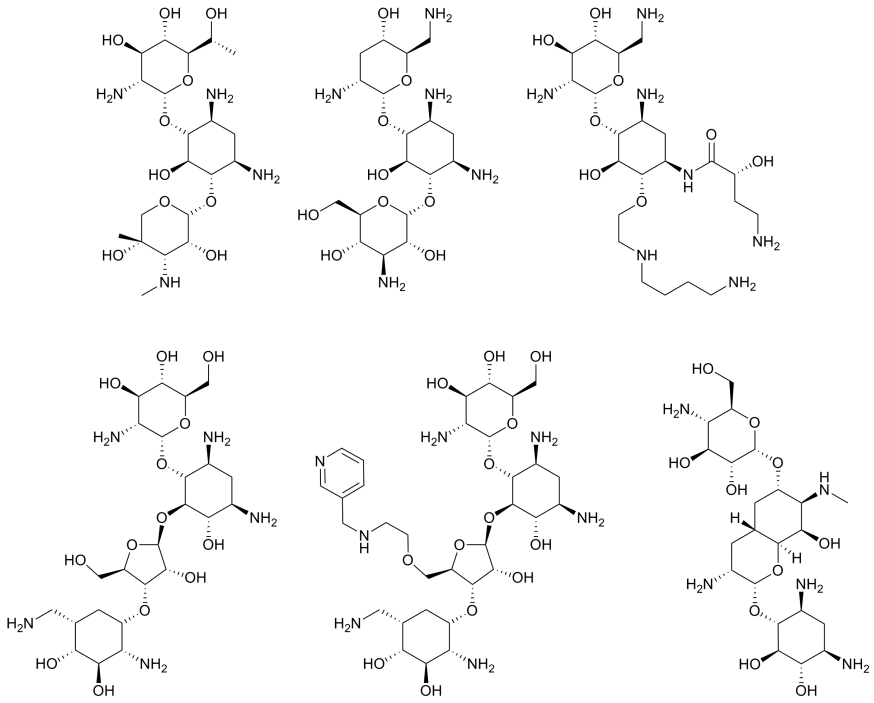

Fig. 10.4 From left to right: Geneticin, tobramycin, neomycin derivative, paromomycin, paromomycin derivative and apramycin (drawn by Andreas Ehnbom).

antibiotics primarily bind to the decoding center in the neck region of the small subunit at the top of h44 (Plate 10.2). The binding site is composed of base pairs 1409–1491 and 1406–1495. The bases between these residues are normally stacked on the base pairs within the helix. The aminoglycosides bind to the major grove and stack on nucleotide 1491, hydrogen-bond to A1408 and interact with the backbone structure of A1492 and A1493. This forces bases A1492 and A1493 out of the helix. As discussed in Sec. 8.6, they affect the balance of the small subunit between the restrictive state and the ribosome ambiguity (*ram*) state, or — in structural terms — between the open and closed conformations of the small subunit.

Paromomycin

Paromomycin is an antibiotic of the aminoglycoside family. The structural studies of paromomycin bound to the 30S subunit have given a leap in our insight of decoding (Fourmy *et al.*, 1996, 1998; Carter *et al.*, 2000; Ogle *et al.*, 2001, 2002, 2003). The ribosome identifies the cognate mRNA–tRNA interaction by a conformational change and specific hydrogen bonds of the conserved nucleotides G530, A1492 and A1493 (see Chaps. 9 and 11; Moazed & Noller, 1986; Ogle *et al.*, 2001, 2002). The binding of paromomycin induces this discriminating conformational change regardless of whether the tRNA is cognate or not (Ogle *et al.*, 2001, 2002). It forces A1492 and A1493 to flip out from the helix (Carter *et al.*, 2000; Ogle *et al.*, 2001, 2002, 2003). This facilitates the closure of the shoulder domain. In this way paromomycin induces misreading of the mRNA due to an increased affinity for near-cognate and noncognate tRNA (Karimi & Ehrenberg, 1994; Pape *et al.*, 2000; Zaher & Green, 2009). Paromomycin also forces the small subunit to adopt the *ram* or closed conformation of the small subunit (see Table 8.5). Apramycin, geneticin and many other aminoglycosides bind in a very similar manner to paromomycin (Plate 10.2). Interestingly, paromomycin and hygromycin B bind to adjacent sites, but the functional steps they inhibit are different (see below). Paromomycin can also bind to the 50S subunit in the vicinity of H69, restricting its dynamics and thereby stabilizing the subunit bridges (Borovinskaya, 2007).

Streptomycin

One of the most thoroughly characterized aminoglycoside antibiotics affecting decoding is streptomycin (Fig. 10.5; Kurland, 1992). The binding of streptomycin to the ribosome leads to an error-prone decoding of the message. This is due to disturbance of the initial selection step as well as the proofreading step (Karimi & Ehrenberg, 1994, 1996). Streptomycin binds to a single site, different from the site for paromomycin, and interacts with the

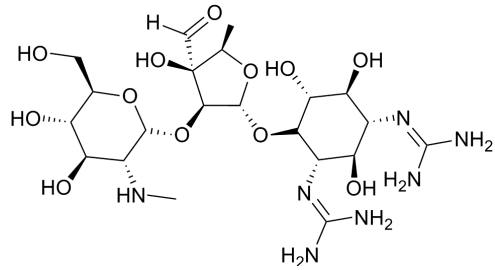

Fig. 10.5 Streptomycin (drawn by Andreas Ehnbom).

phosphate backbone at four different regions of the 16S RNA, primarily nucleotides U13, G526, A915 and C1490 as well as Lys45 of ribosomal protein S12 (Plate 10.3; Carter *et al.*, 2000). These residues were initially identified by analysis of streptomycin protection (Moazed & Noller, 1987), cross-linking (Gravel *et al.*, 1987) and mutagenesis (Montandon *et al.*, 1986; Melancon *et al.*, 1988; Pinard *et al.*, 1993).

The fidelity of translation is affected if the *ram* state gets stabilized over the restrictive state (Sec. 8.6; Allen & Noller, 1989; Lodmell & Dahlberg, 1997; Ogle *et al.*, 2003). Streptomycin, like paromomycin, stabilizes the *ram* state or closed conformation of the small subunit, which has increased affinity for noncognate aminoacyl-tRNA (see Table 8.2). Resistance to streptomycin is primarily due to mutations of ribosomal protein S12. Such mutations make the ribosomes restrictive and sometimes hyperaccurate (Kurland *et al.*, 1996). S12 stabilizes the same region of the small subunit as streptomycin. Thus, mutations affecting the loops of the protein that contact nucleotides 908–915, 524–527 and helix h44 can lead to streptomycin resistance (Carter *et al.*, 2000). In these mutants, the *ram* state is destabilized sufficiently that the balance between the two states can be maintained even in the presence of streptomycin. For some of these mutants, the balance is shifted to the extent that the ribosome gets streptomycin-dependent. In other words, the balance is shifted toward the restrictive state so much that streptomycin is needed for efficient translation, still with sufficient fidelity. Mutations of ribosomal

proteins S4 and S5 can revert the streptomycin dependence (Kurland *et al*., 1996; Ogle *et al*., 2001, 2002, 2003).

For hyperaccurate mutants, not only the initial recognition is affected but also the proofreading (Ruusala & Kurland, 1984; Ruusala *et al*., 1984). This means that even though a cognate tRNA is bound to the A-site, GTP hydrolysis has been induced and EF-Tu has dissociated, the cognate aminoacyl-tRNA has an increased likelihood to fall off before peptidyl transfer. Thus, S12 mutations can disturb the approach of the acceptor part of the tRNA with its aminoacyl moiety into the peptidyl transfer site.

10.4 INHIBITORS OF PEPTIDYL TRANSFER

The peptidyl transfer center (PTC) binds the acceptor ends of the tRNAs in the A- and P-sites (Plate 8.8). The center contains the A- and P-loops binding the CCA ends of the tRNAs as well as the site where peptidyl transfer occurs. In addition, there are two hydrophobic crevices: One at the PTC and the other at the entrance to the peptide exit tunnel. The former is where the amino acid of the aminoacyl-tRNA is bound and could be called the A-site cleft or crevice. Inhibitors of peptidyl transfer are bound to either of these sites. Several of these inhibitors have structures like aminoacylated nucleotides. Ligands to the A-site cleft of the 50S subunit make the cleft adopt an open conformation (Blaha *et al*., 2008, 2012).

Puromycin

A classical inhibitor that acts in the peptidyl transfer site is puromycin (Yarmolinsky & de la Haba, 1959). Puromycin is a mimic of the acceptor end of an aminoacyl-tRNA (Fig. 10.6). It is composed of the terminal adenosine of the tRNA with the amino acid tyrosine linked via an amide bridge instead of an ester bond. The adenine is in the form of dimethyl-adenine.

When bound to the A-site, puromycin acts as acceptor of the nascent peptide from the peptidyl-tRNA in the P-site. The small

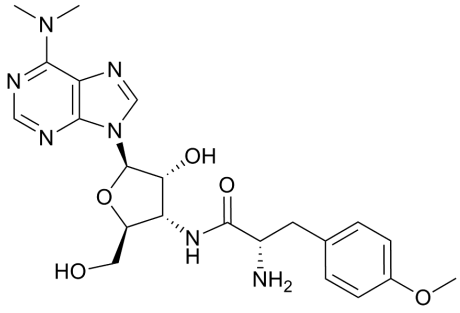

Fig. 10.6 Puromycin (drawn by Andreas Ehnbom).

puromycin molecule cannot participate in translocation but falls off the ribosome together with the peptide. Puromycin has been used to analyze whether translocation has occurred and the state at the PTC. However, since it can also slowly react with the peptide of a tRNA in the A/P-state, it may not reveal whether the peptidyl-tRNA is fully translocated or not (Zavialov & Ehrenberg, 2003; Sharma *et al.*, 2004). The interaction of the EF-G-like factor LepA with the ribosome also induces a state in which puromycin can react with the nascent polypeptide (see Sec. 9.3; Liu *et al.*, 2011).

A number of crystallographic studies of puromycin bound to the ribosome have been performed. The tyrosyl moiety binds to the A-site cleft. The dimethyl-adenine of puromycin is hydrogen-bonded to G2583 and the 2′-hydroxyl of the ribose is hydrogen-bonded to U2585 (Nissen *et al.*, 2000). Puromycin can also be incorporated into larger structures. One of these, the Yarus tetrahedral intermediate analogue (CCdA-p-Puro), has been characterized structurally (Welch *et al.*, 1995). Another puromycin derivative is a 13-base-pair minihelix terminated with CC-puromycin (Nissen *et al.*, 2000). In both cases, puromycin binds to the A-site (Plate 10.4). The adenines corresponding to position 76 of the A- and P-site tRNAs bind to the PTC in nearly identical ways, making A-minor interactions, and are part of the twofold symmetry of the PTC (Sec. 8.3; Nissen *et al.*, 2000; Nissen *et al.*, 2001; Bashan *et al.*, 2003).

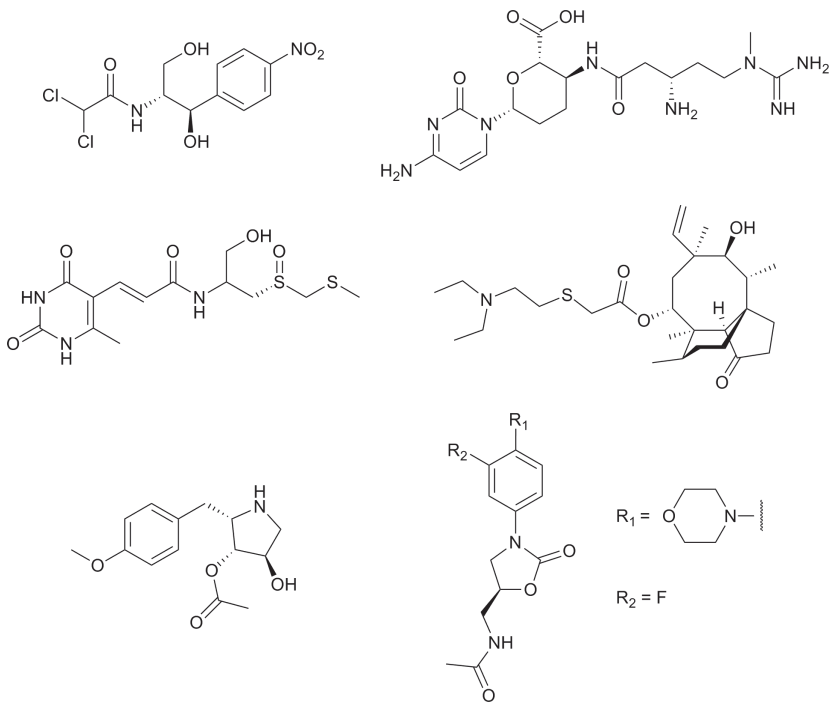

Fig. 10.7 Some of the inhibitors binding to PTC. From left to right, top to bottom: Chloramphenicol, blasticidin S, sparsomycin, thiamulin, anisomycin and oxazolidinone (drawn by Andreas Ehnbom).

The reaction with puromycin and the removal of the nascent peptide does not induce structural changes in the ribosome. The reaction leads to a deacylated tRNA in the P-site which in many respects is indistinguishable from a termination complex where RF1/2 has hydrolyzed the peptide from the peptidyl-tRNA in the P-site and RF3 has removed RF1/2 (see Sec. 9.4).

Anisomycin

Anisomycin (Fig. 10.7) inhibits archaeal, yeast and human ribosomes, but not bacterial ribosomes (Barbacid & Vazquez, 1974; Ioannou *et al*., 1997). Puromycin and chloramphenicol are related

to anisomycin, and their binding sites overlap with the site of linezolid (see below) and the amino acid attached to the A site tRNA, but details of the binding differ (Plate 10.4; Hansen *et al.*, 2003). Anisomycin also interferes with P-site substrates.

The structures of 11 mutants of *H. marismortui* 50S subunits resistant to anisomycin have been studied to understand the mechanism of resistance when the mutation is distant from the binding site (Blaha *et al.*, 2008). Such mutants propagate through the ribosome to stabilize the apo conformation of the A-site cleft (without a ligand) where the cleft is in its closed conformation.

Chloramphenicol

The binding of chloramphenicol (Fig. 10.6) has been studied on three bacterial species as well as on *H. marismortui* (Wilson, 2009, 2011). Two different binding sites have been observed, CAM-1 and CAM-2. In bacteria it binds to the PTC crevice (CAM-1), while in *H. marismortui* it binds in the crevice at the entrance to the exit tunnel (CAM-2; Plate 10.4; Hansen *et al.*, 2003). The binding to CAM-1 as described for *E. coli* and *T. thermophilus* is probably the best representation of the binding mode (Dunkle *et al.*, 2010; Bulkley *et al.*, 2010). The binding site overlaps with the aminoacyl group of the A-site tRNA. It also overlaps with the binding site for anisomycin and stacks with C2452. The methylene hydroxyl group binds to a potassium ion. Both binding sites for chloramphenicol are compatible with biochemical studies, and the crystallographic findings explain a number of apparently conflicting observations (Hansen *et al*, 2003, Wilson, 2011).

Linezolid

Linezolid is a synthetic antibiotic of the oxazolidinone class that binds to the A-site part of PTC and inhibits the accommodation of aminoacyl-tRNA (Ippolito *et al.*, 2008; Wilson *et al.*, 2008; Wilson,

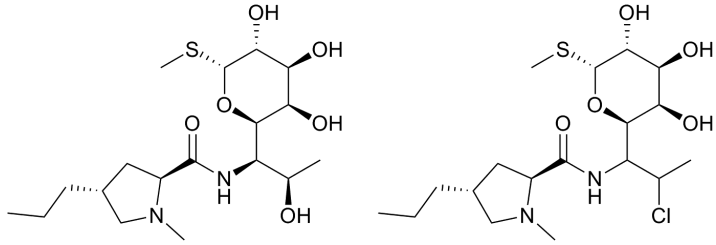

Fig. 10.8 Lincomycin and clindamycin (drawn by Andreas Ehnbom).

2009, 2011). It binds to the A-site cleft as anisomycin and chloramphenicol. Mutants resistant to linezolid are found at the binding site (A2451, C2452, U2504 and G2505) but also further away (G2576).

Lincosamides

Lincomycin and clindamycin (Fig. 10.8) are lincosamides. Clindamycin also binds to the 50S subunit with its propyl pyrrodinyl group in the A-site cleft, and the galactose group overlaps with the position of the desosamine sugar of the macrolides (Schlüntzen *et al*., 2001; Tu *et al*., 2005; Dunkle *et al*., 2010). The early studies on *Deinococcus radiodurans* 50S subunits (D50S) differ in details from the two subsequent investigations.

Blasticidin S

Two binding sites are observed for blasticidin S. The inhibitor has a cytosine base, which can interact with the two guanines of the P-loop (Fig. 10.6; Plate 10.4; Hansen *et al*., 2003). The stronger binding site is with G2251 and the weaker with G2252. These sites thus overlap with the CCA end of the P-site tRNA, which illustrates the mode of inhibition by blasticidin.

Sparsomycin

An antibiotic that has received considerable attention is sparsomycin (Fig. 10.6; Goldberg & Mitsugi, 1966; Vazquez, 1979;

Cundliffe, 1981). It binds with unusually high affinity only in the presence of a P-site substrate. It binds to the PTC and is found to stack with A2602 (Porse *et al*., 1999; Hansen *et al*., 2002b, 2003; Bashan *et al*., 2003; Schmeing *et al*., 2005). In the *H. marismortui* 50S subunit (H50S), sparsomycin interacts with the CCA end of the P-site tRNA and overlaps with the aminoacyl moiety in the A-site (Plate 10.4). In D50S the sparsomycin binding is different, possibly representing an early binding state (Wilson, 2011). Obviously the binding of sparsomycin is incompatible with peptidyl transfer. For ribosomes where both A- and P-sites are occupied, sparsomycin will induce translocation (Fredrick & Noller, 2003).

10.5 INHIBITORS OF THE EXIT TUNNEL

Several antibiotics inhibit the elongation of the nascent polypeptide by blocking the exit tunnel near the PTC (Fig. 10.9).

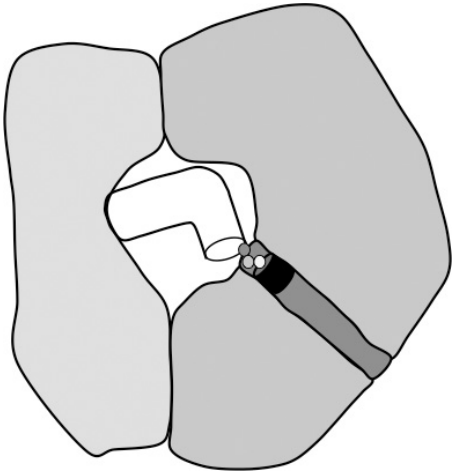

Fig. 10.9 A simplified cross-section of the ribosome, showing the peptidyl-tRNA and the exit tunnel. The macrolides inhibit protein synthesis by binding as a plug (black) in the exit tunnel. Only a limited number of amino acids can be incorporated into the nascent peptide. Different macrolides bind somewhat differently in the same general area.

As a group they are called MLS [sometimes MLS_BK — for macrolide (e.g. erythromycin), lincosamide (lincomycin), streptogramin B (dalfopristin) and ketolide] antibiotics. Ketolides (e.g. telithromycin) are derived from the macrolides and could be grouped with them, but have a broader spectrum. While macrolides and streptogramins have large rings, lincosamides have much simpler structures. These inhibitors bind to sites that are close or overlapping. Macrolides inhibit protein synthesis in bacteria, but not in archaea or eukaryotes (Poehlsgaard & Douthwhite, 2003; Mankin, 2008).

The macrolides are based on 14–16-membered lactone rings with different sugar substituents (Fig. 10.10). They do not normally inhibit peptidyl transfer (Pestka, 1972; Centreras & Vazquez, 1977; Andersson & Kurland, 1987). Ribosomes that are already engaged in elongation of nascent peptides are not inhibited by macrolides (Odom *et al.*, 1991). Ribosomes that are inhibited before they have a nascent peptide can synthesize only a few peptide bonds; the length depends on the nature of the

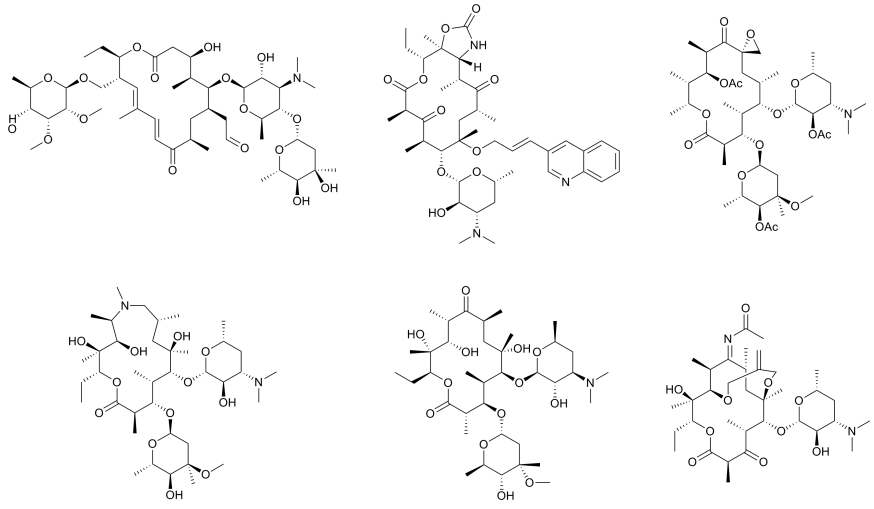

Fig. 10.10 Some macrolides with 14–16-memberred lactone rings. From left to right, top to bottom: Tylosin, cethromycin, troleandomycin, azithromycin, erythromycin and EP-001304 (drawn by Andreas Ehnbom).

inhibitor. The peptide synthesized in the presence of these inhibitors can sometimes be as long as five amino acid residues, but for the larger macrolide carbomycin A (Plate 10.4) not a single peptide bond can be formed (Mao & Robishaw, 1971; Poulsen *et al.*, 2000). The binding sites of a number of macrolides have been studied by crystallography, sometimes with ribosomes or subunits from four different species (Wilson, 2011). The binding area is in the narrow upper part of the exit tunnel, near proteins L4 and L22. Their binding sites partly superimpose the second binding site for chloramphenicol in H50S (CAM-2; Hansen *et al.*, 2003). All macrolides bind in a similar manner (Wilson, 2011). The length of the peptide synthesized primarily depends on the substituents in the C5 position of the lactone ring (Mao & Robishaw, 1971; Poulsen *et al.*, 2000; Hansen *et al.*, 2002a). The conformation of the macrolides is such that most polar groups of the lactone ring are located on one side, making the opposite side hydrophobic (Hermann *et al.*, 2005).

Macrolides — 16-Membered Lactone Rings

Carbomycin A, spiramycin and tylosin (Fig. 10.10) have 16-membered lactone rings. They bind adjacent to the PTC and their lactone rings superimpose almost exactly (Plate 10.4; Hansen *et al.*, 2002a). The main structural difference upon binding of these antibiotics is a movement of A2103 in the large subunit of *H. marismortui* (*E. coli* A2062). The same reorientation of this residue was also seen when a substrate was bound to the P-site (Hansen *et al.*, 2002a).

Unexpectedly, a covalent bond is formed between the C6 position of each 16-membered lactone ring and N6 of A2103 (*E. coli* A2062). This was observed as a continuous electron density between the antibiotics and the nucleotide. Any modification of the aldehyde group at position C6 of the lactone ring reduces the inhibitory strength very considerably (see references in Hansen *et al.*, 2002a). The binding of the hydrophobic side of the

lactone ring is against an essentially hydrophobic surface of the tunnel wall.

15-Membered Lactone Rings

One 15-membered lactone ring antibiotic, the azalide azithromycin (Fig. 10.10), has been studied by crystallography (Hansen *et al*., 2002a; Schlünzen *et al*., 2003; Tu *et al*., 2005). Azithromycin is a semisynthetic derivative of erythromycin (Bright *et al*., 1988). One major difference from the 16-memberered ring macrolides is the absence of the covalent bond to A2103 (Hansen *et al*., 2002a). The binding site in *D. radiodurans* is somewhat different and two molecules of azithromycin are bound close together. The second binding site is further down the tunnel, near proteins L4 and L22 (Schlünzen *et al*., 2003).

14-membered Lactone Rings

Some macrolide antibiotics with 14-membered lactone rings (clarithromycin, erythromycin, roxithromycin, telithromycin, troleandomycin, triacyloleandromycin and the ketolide ABT-773; Fig. 10.10) have been studied with crystallography for four different species (Schlünzen *et al*., 2001, 2003; Berisio *et al*., 2003a,b; Tu *et al*., 2005; Wilson *et al*., 2005; Gurel *et al*., 2009; Dunkle *et al*., 2010; Bulkley *et al*., 2010; Belousoff *et al*., 2011). Initially there were some discrepancies with regard to the binding site and the conformation of the inhibitor. These differences have subsequently been resolved (Wilson, 2011).

Streptogramins

Dalfopristin and quinupristin are streptogramins of types A and B, respectively (Fig. 10.11). They bind cooperatively to separate sites in the peptide exit channel (Plate 10.5; Harms *et al*., 2004; Tu *et al*., 2005). Virginiamycin M, a streptogramin A, has a 20-member ring and binds with virginiamycin S, a streptogramin B,

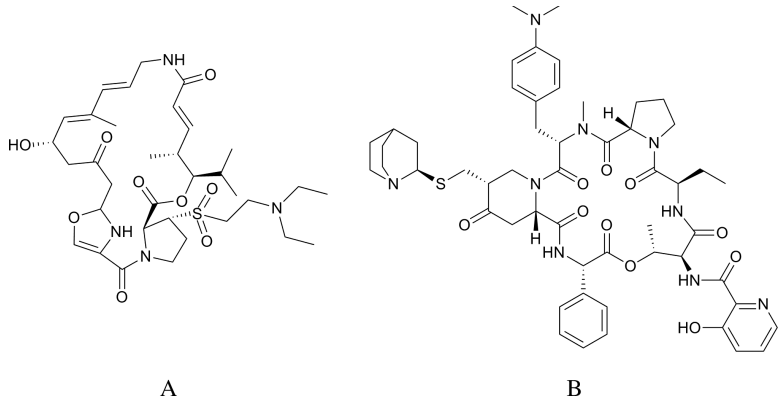

Fig. 10.11 Dalfopristin and quinupristin are streptogramins of types A and B, respectively (drawn by Andreas Ehnbom).

in the PTC crevice but extends into the P-site and causes conformational changes (Hansen *et al*., 2003; Tu *et al*., 2005). The cooperativity partly depends on the hydrophobic interactions of the two molecules and their joint interaction with A2062 (Harms *et al*., 2004).

Macrolide Resistance

The MLS antibiotics generally bind against a hydrophobic side of the wall of the exit channel. The hydrophilic group, N2 of G2099 in *H. marismortui* (2058 in *E. coli*), interrupts this hydrophobic surface, replacing the adenine frequently occurring in bacteria. The resistance to macrolides is much higher in organisms that have a G in this position than those that have an A (Retsema & Fu, 2001). A series of structural studies of complexes of MLS antibiotics have been performed on *H. marismortui* where the G has been mutated to A (Tu *et al*., 2005). The affinity is sometimes dramatically increased, but the locations of the inhibitors remain essentially the same. Another mechanism of resistance to macrolides is due to enzymes that methylate N6 of A2058 (Retsema & Fu, 2001; Vester & Douthwaite, 2001, Hansen *et al*., 2002a).

Resistance to the macrolides can also be associated with components of the constriction of the tunnel. Mutations of the extended parts of L4 and L22 in the narrow part of the tunnel can thus give resistance to macrolides. Mutations of L4 can prevent the binding of the antibiotics, while mutations of L22 can open the narrow part of the tunnel (Jenni & Ban, 2003). In both cases, the passage of the nascent peptide through the exit tunnel is enabled. A study of *H. marismortui* where three amino acids have been deleted in the tip of a loop opens the gap of the constriction of the tunnel (Tu *et al*., 2005).

The synthesis of certain peptides can be performed in the presence of MLS inhibitors (Tenson *et al*., 1997). Normally this is done by the ejection of the inhibitor, like with a bottlebrush (Lovmar *et al*., 2006). However, in the case of josamycin, with a 16-membered lactone ring, peptides with a certain sequence can pass the inhibitor in the peptide exit channel (Lovmar *et al*., 2009).

10.6 INHIBITORS OF TRANSSLOCATION

Hygromycin B

Hygromycin B (HygB; Fig. 10.12) is an aminoglycoside that has little effect on fidelity (Eustice & Wilhelm 1984a, b). It rather effectively inhibits translocation and spontaneous reverse translocation in bacteria as well as Eukarya (Cabanas *et al*., 1978; Gonzales *et al*., 1978; Eustice & Wilhelm, 1984b; Borovinskaya *et al*., 2008). The affinity of aminoacyl-tRNA for the A-site is increased in the presence of HygB (Eustice & Wilhelm, 1984a). HygB binds close to the A-site on the small subunit where other aminoglycosides bind, at the top of h44 (Plate 10.2; Moazed & Noller, 1987; Brodersen *et al*., 2000; Borovinskaya *et al*., 2008). It binds to the major groove of h44 and is close to the neck of the small subunit, and contacts the mRNA at the P-site where conformational changes occur during translocation (Frank & Agrawal, 2000). The analysis of the *E. coli* 70S complex with hygromycin B shows conformational changes not observed in the analysis of 30S subunits (Borovinskaya *et al*., 2008). A1492 and

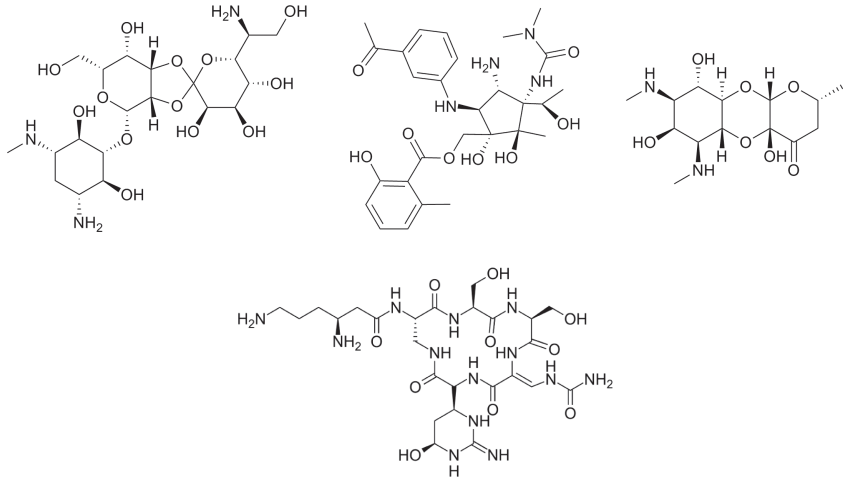

Fig. 10.12 The antibiotics (from left to right) hygromycin B, pactamycin and spectinomycin (drawn by Andreas Ehnbom). Viomycin (below) was taken from Wikipedia.

A1493 of the 16S RNA as well as A1913 of 23S RNA flip out of the normal positions and A1493 adopts a position between the A- and P-site tRNAs. This conformation together with the contact between the antibiotic and the mRNA may be sufficient to prevent forward or backward translocation (Borovinskaya *et al*., 2008).

Pactamycin

Pactamycin (Ptc; Fig. 10.12) has been considered to inhibit the release of initiation factors from the initiation complex (Cohen *et al*., 1969; Kappen & Goldberg, 1976). Recent findings suggest that the main effect of the inhibition is on translocation (Dinos *et al*., 2004). The antibiotic mimics two nucleotides that are stacked on each other and binds on top of G693 of h23b. The central ring of Ptc mimics the RNA backbone and interacts with C795 and C796 in h24a (Brodersen *et al*., 2000). It prevents the formation of the G693:C795 base pair (Dinos *et al*., 2004). This is the binding site for the E-site codon. The mRNA at the E-site will be displaced

very significantly, which prevents any possible interactions with an E-site tRNA. The antibiotic must also prevent the ratchet-like motions where the head of the small subunit moves with regard to the platform (Valle *et al*., 2003b). Resistance to Ptc is caused by the mutations A694G, C795U and C796U in good agreement with the binding site (Mankin 1997; Brodersen *et al*., 2000).

Spectinomycin

Spectinomycin (Fig. 10.12) inhibits the translocation of peptidyl-tRNA from the A- to the P-site catalyzed by EF-G (Bilgin *et al*., 1990). A crystallographic analysis has identified the binding site of the rigid spectinomycin molecule in the small subunit neck region at the tip of h34, where it primarily interacts with nucleotides G1064 and C1192 (Carter *et al*., 2000; Borovinskaya *et al*., 2007). Protein S5, in which mutations causing resistance to spectinomycin have been mapped (Wittmann-Liebold & Greuer, 1978), is in the vicinity but not immediately interacting. Translocation involves movements of the head region of the small subunit (Frank & Agrawal, 2000; Valle *et al*., 2003b; Ogle *et al*., 2003). h34 and the spectinomycin-binding site are close to the pivot point of such movements. The E70S structure with spectinomycin shows the head locked in an intermediate position (Borovinskaya *et al*., 2007). Furthermore, protein S5 is at the domain interface of the small subunit which has a significant role in controlling the open and closed conformations of the decoding site (Carter *et al*., 2000; Ogle *et al*., 2003).

Viomycin and Capreomycin

Viomycin (Fig. 10.12) and capreomycin are members of the tuberactinomycin family of antibiotics, and they inhibit both spontaneous and EF-G-catalyzed translocation (Modolell & Vasquez, 1977). Viomycin stabilizes the interaction between 30S and 50S subunits (Yamada & Nierhaus, 1978; Jerinic & Joseph, 2000). Chemical protection experiments suggest that it binds and stabilizes the MS11 conformation of the ribosome near subunit bridge B2a, where h44

and H69 interact (Ermolenko *et al*., 2007). The protected nucleotides are, as when EF-G binds with GDPNP to the ribosome, U913 and G914 of the 23S RNA and C912–A915 and A1408 of the 16S RNA (Moazed & Noller, 1987; Powers & Noller, 1994; Ermolenko *et al*., 2007). Studies using FRET suggest that the transition between the classical and ratcheted states of the ribosome has been slowed down significantly (Kim *et al*., 2007). The binding of viomycin and capreomycin has also been studied by crystallography (Stanley *et al*., 2010). The binding sites partly overlap with the sites for paromomycin and hygromycin B. In these studies the ribosome is in the classical nonrotated state. Like for hygromycin B, A1492 and A1493 are observed in flipped-out conformations, which stabilized the A-site tRNA significantly. Stanley *et al*. (2010) suggest that this strong interaction with the A-site tRNA may inhibit translocation.

10.7 INHIBITORS OF TRANSLATION FACTORS

There are inhibitors that bind to translation factors to inhibit some of their functional steps. There are also inhibitors that by binding to the ribosome prevent elongation factors from binding to the ribosome. The inhibitors that belong to this family, called thiopeptides, are thiostrepton, nosiheptide and micrococcin. Their structures have similarities (Fig. 10.13) but their effects are somewhat different.

Thiopeptides

Thiostrepton inhibits EF-G from catalyzing translocation (Bodley *et al*., 1970c; Cameron *et al*., 2002; Lenzen *et al*., 2003). EF-G binds weakly when thiostrepton is bound, but its conversion to a more stable complex is prevented (Rodnina *et al*., 1999; Cameron *et al*., 2002; Seo *et al*., 2004, 2006; Pan *et al*., 2007). Single-turnover GTP hydrolysis occurs, but both the release of inorganic phosphate and multiple-turnover GTP hydrolysis are prevented (Seo *et al*., 2006). In contrast, thiostrepton stimulates GTP hydrolysis by IF2

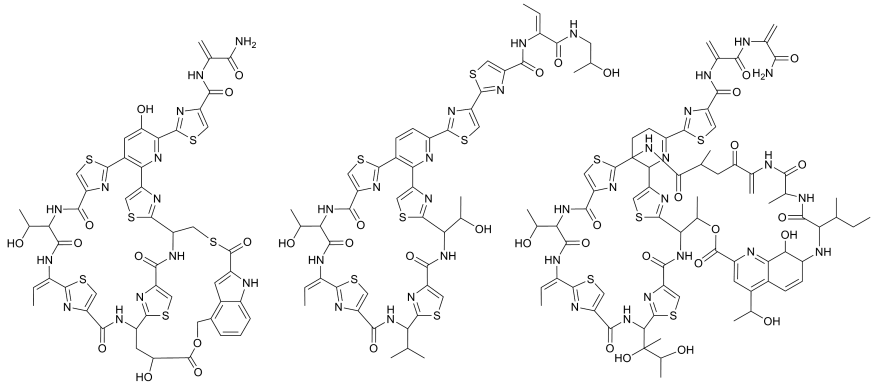

Fig. 10.13 The chemical formulae of nosiheptide, micrococcin and thiostrepton, which prevent EF-G from binding properly to the ribosome (drawn by Andreas Ehnbom).

(Cameron *et al.*, 2002; Grigoriadou *et al.*, 2007). Thus, the binding sites of EF-G and IF2 on the 50S subunit may not be completely overlapping.

The crystal structure of thiostrepton in complex with the RNA fragment 1051–1108 has been determined (Lenzen *et al.*, 2003). The binding site includes H43 and H44 in domain II of the 23S RNA. This part of the 23S RNA binds L11 as well as the complex of L10 and L12 (Dijk *et al.*, 1979; Beauclerk *et al.*, 1984; Wimberley *et al.*, 1999). This binding site is at GAC at the base of the L12 stalk of the large subunit (Harms *et al.*, 2008). Thiostrepton and nosiheptide bind similarly (Plate 10.6), while micrococcin binds at a slightly different position, as shown by crystallographic studies of *D. radiodurans* 50S subunits (Harms *et al.*, 2008). The inhibitors all bind in a cleft between the N-terminal domain of L11 (L11-NTD) and loops of H43 and H44. Thiostrepton rests on conserved nucleotides A1067 and A1095 (Harms *et al.*, 2008). A methylase that uniquely modifies A1067 leads to thiostrepton resistance (Thompson *et al.*, 1982). On the other hand, the binding of thiostrepton or micrococcin prevents the methylation of A1067 (Lenzen *et al.*, 2003; Harms *et al.*, 2008). Furthermore, mutations of nucleotides A1067 and

A1095 make ribosomes resistant to thiostrepton (Thompson *et al*., 1988; Rosendahl & Douthwhite, 1994).

L11 is needed for thiostrepton and micrococcin binding, and its absence leads to resistance (Highland *et al*., 1975; Cundliffe *et al*., 1979; Thompson *et al*., 1979; Wienen *et al*., 1979). This is due to the fact that the major surface contact with thiostrepton is due to L11NTD (314Å^2; Harms *et al*., 2008). Mutations of L11NTD can also confer resistance (Porse *et al*., 1998, 1999; Cameron *et al*., 2004).

The binding site for thiopeptides overlaps with the binding site for EF-G — more specifically, its domain V (Connell *et al*., 2007; Harms *et al*., 2008; Gao *et al*., 2009). In addition, the position of L11NTD is different in the structures of 50S subunits with thiopeptides and 70S ribosomes with bound EF-G (Harms *et al*., 2008; Gao *et al*., 2009).

Micrococcin, despite binding to the same region, stimulates uncoupled GTP hydrolysis by EF-G (Cameron *et al*., 2002; Lenzen *et al*., 2003). The antibiotic interacts fully with A1095 but less with A1067. L11NTD remains close to its native position (Harms *et al*., 2008). Furthermore, in this complex the CTD of one molecule of L12 interacts with L11NTD and conserved residues of L12CTD interact with domain G′ of EF-G. Harms *et al*. (2008) suggest from these differences in binding that the interactions with L12CTD in the complex with micrococcin may give hints about the intricacies of EF-G binding and GTP hydrolysis.

Inhibitors Binding to EF-G and EF2

Fusidic acid (FA; Fig. 10.14; Bodley *et al*., 1969) binds to EF-G only when the factor is bound with GTP to the ribosome (Baca *et al*., 1976). It is a slow inhibitor and permits several GTPase turnovers before the inhibition is complete (Seo *et al*., 2006). EF-G with FA then remains firmly attached to the ribosome after GTP hydrolysis. A large number of FA resistant mutations are known (Johanson & Hughes, 1994). They are found in three primary locations of the EF-G molecule, the G domain, the interfaces between domains G and III and between domains G and V (Johanson *et al*., 1996,

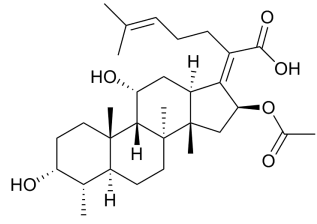

Fig. 10.14 Fusidic acid (drawn by Andreas Ehnbom).

Laurberg *et al*., 2000; Nagaev *et al*., 2001). A proposed site between the G domain and domain III (Laurberg *et al*., 2000; Hansson *et al*., 2005) has been confirmed by the crystal structure of EF-G in complex with FA bound to the ribosome (Gao *et al*., 2009; Plate 10.7). Thr84, Phe90 and L457 are at the binding site and when mutated confer FA resistance (Johansson & Hughes, 1994). The binding of FA prevents switch II from adopting the GDP conformation. This prevents domains III and IV from adopting the OFF conformation and EF-G remains bound to the ribosome (Gao *et al*., 2009).

Resistance to fusidic acid can be achieved in a number of ways other than mutations in EF-G. In *Streptococcus aureus* the protein FusB can give resistance. The structure of the protein is known as well as a likely way of interacting with EF-G (Guo *et al*., 2012).

For the fungal factor EF2, which corresponds to EF-G, there is an inhibitor that may be compared to FA (Capa *et al*., 1998; Justice *et al*., 1998; Dominguez *et al*., 1999). This inhibitor is called sordarin. By binding to yeast EF2, it locks the factor on the ribosome. The structure of EF2 with a bound sordarin molecule has been determined. The conformation of the complex is quite different from the unliganded molecule or the conformations of EF-G. The sordarin molecule binds to the interface between domains III, IV and V (Jørgensen *et al*., 2003) at a site where a number of mutations causing sordarin resistance are located. Even though the binding site is different from where FA binds to EF-G and kirromycin binds to EF-Tu, in all these cases the conformational changes that lead to release are prevented. Mutants in ribosomal protein P0 can induce resistance to sordarin (Gomez-Lorenzo & Garcia-Bustos, 1998; Justice *et al*., 1999).

Inhibitors Binding to EF-Tu

Like fusidic acid locks, EF-G on the ribosome kirromycin and enacyloxin IIa (Fig. 10.15) bind EF-Tu to the ribosome, even though the GTP molecule is hydrolyzed (Wolf *et al.*, 1977; Parmeggiani & Swart, 1985; Cetin *et al.*, 1996; Zuurmond *et al.*, 1999). The binding sites overlap and are between domains G and III (Plate 9.14B; see also Sec. 9.3; Vogeley *et al.*, 2001; Parmeggiani *et al.*, 2005). The antibiotics act like glue between these domains and do not permit the conformational change that leads to the dissociation of EF-Tu from the ribosome. An interesting aspect of kirromycin is that it can induce EF-Tu to hydrolyze its GTP even off the ribosome (Wolf *et al.*, 1974). This may suggest that EF-Tu and other trGTPases contain all residues needed for GTP hydrolysis.

Mutants of EF-Tu resistant to kirromycin have been characterized. From this a possible binding site for the antibiotic was suggested (Abdulkarim *et al.*, 1994; Mesters *et al.*, 1994). The predicted site generally agrees with the experimentally determined one. Most of the mutations occur close to the binding site for aurodox (methylkirromycin; Vogeley *et al.*, 2001). However, a number of mutations are located further away from the binding site. Q341H and E390K affect the binding of aa-tRNA, thus decreasing the likelihood that EF-Tu with aurodox will be firmly bound to the ribosome and preventing the reading of an mRNA (Vogeley *et al.*, 2001).

Another type of antibiotics, pulvomycin and GE2270A (Fig. 10.15), inhibit the formation of the ternary complex. GE2270A also inhibits the transition from the inactive GDP conformation to the active one with GTP. The structures of the complexes with EF-Tu are known (Heffron & Jurnak, 2000; Parmeggiani *et al.*, 2006). The inhibitors are bound at the interface between domains I and II. The pocket where the terminal A of the acceptor end of the tRNA binds is occupied by the inhibitor (Fig. 9.11; Plate 10.8). This then explains the mode of inhibition of these antibiotics.

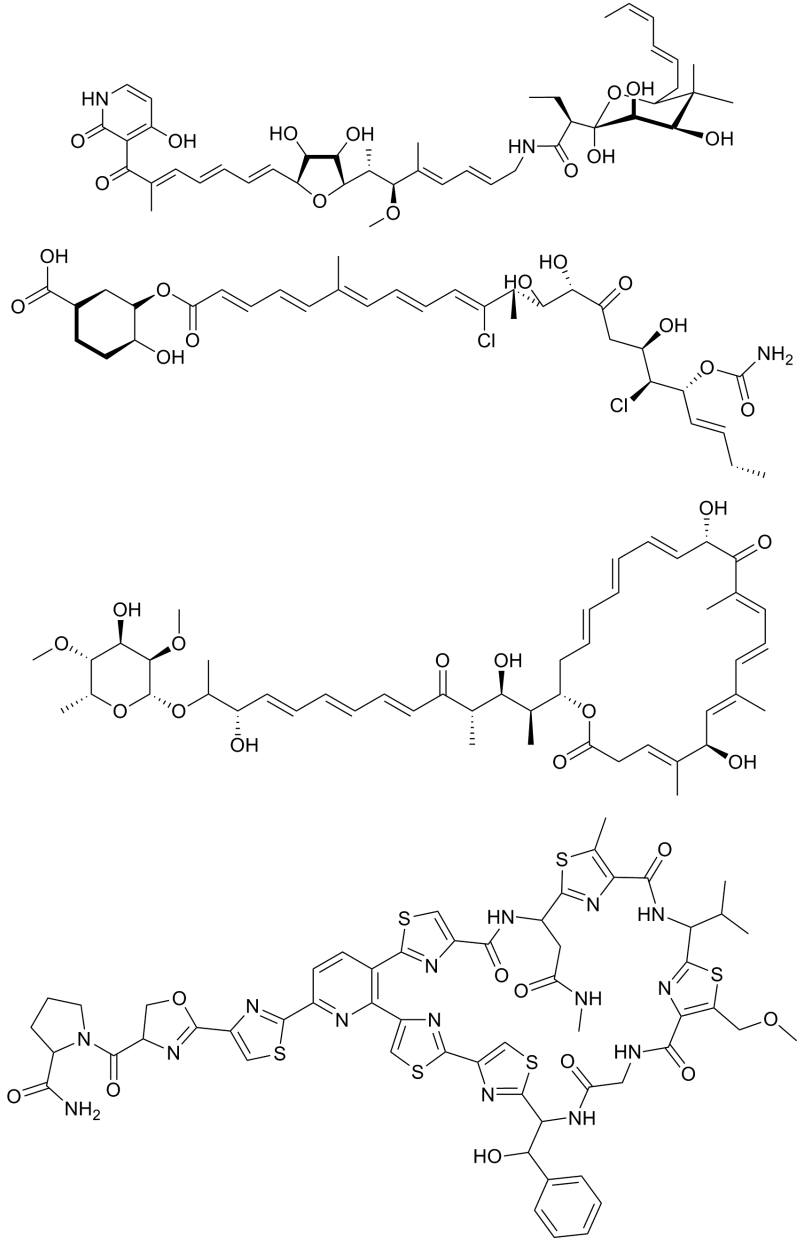

Fig. 10.15 Inhibitors binding to EF-Tu: Kirromycin, enacyloxin IIa, pulvomycin and GE2270A (drawn by Andreas Ehnbom).

11

The Process —Translation

Translation is the process by which the inherited genomic information is translated into functional proteins — a process that is essential for all cells and organisms. A genome may contain from less than 1000 to more than 30,000 translated genes, depending on the organism. In most genomes, the hereditary material is in the form of DNA, but in certain viruses, it is RNA instead. The process of translation is usually preceded by a transcription, and the actual product of translation, a protein, is frequently transported from where it was synthesized into some other compartment of the cell.

The process of translation occurs on the ribosome in the cytoplasm or in the cellular organelles, mitochondria and chloroplasts. Protein synthesis in bacteria is the most-explored system, and the process is the focus of this chapter.

11.1 THE DYNAMICS OF TRANSLATION AND THE RIBOSOME

Translation involves numerous RNA and protein molecules that bind to and dissociate from the ribosome. In addition to these highly dynamic interactions, the ribosome itself is a dynamic enzyme. Its two subunits can move with regard to each other. The

30S subunit has been observed to rotate by about 6° with regard to the 50S subunit after peptidyl transfer (Table 8.4; Frank & Agrawal, 2000; Agirrezabala *et al*. 2008; Noeske & Cate, 2012).

The subunits themselves are also dynamic. The small subunit is built from four structural units, domains, that move in relation to each other. The large subunit may be less flexible, since its six rRNA domains are thoroughly woven together. However, the two stalks on each side of the large subunit, which are related to the entry and exit of tRNA and factor proteins, are both highly flexible. Thus, the ribosome is a dynamic multicomponent enzyme that can respond to the binding of different ligands by entering different functional states (Spirin, 1969). In particular, the translocation step needs movements of the mRNA by one codon and the tRNAs from the A- to the P- and from the P- to the E-site (Plate 8.1; Yusupov *et al*., 2001).

The subunit bridges that hold the ribosome together have evidently evolved to allow the relative rotation of the subunits. They are either flexible or have alternate binding interactions. Such flexibility was observed for the subunit bridge B1a which is broken or B1b which changes its contact (see Sec. 7.3).

11.2 CENTRAL ASSAYS

In the exploration of the ribosomal functions, numerous assays *in vitro* have been developed. Even though many of these are far from the physiological situation, they aim at examining different steps of the ribosomal activity.

One of the classical assays is to use poly-U as messenger to synthesize poly-Phe. Ribosomes are combined with mRNA, mixed or purified tRNA, tRNA synthetases, and translation factors EF-Tu and EF-G. The rate and fidelity of poly-Phe production under varying conditions are measured. Later, natural mRNAs, with a mixture of codons representing different amino acids were used (Rodnina *et al*., 1995). Such mRNAs can be a few codons in length, with or without the SD region, or they may correspond to complete genes.

Depending on the ratios and nature of the components in *in vitro* experiments, one can measure a single round of a certain

step, e.g. translocation, or multiple turnover (Rodnina *et al*., 1997). When one component is present in much smaller amounts than the other components, one can analyze either a single round of reactions or, if the limiting component can be recycled, multiple-turnover events. Thus, if EF-G·GTP is present in larger amounts than pretranslocation ribosomes, one can study single-round GTP hydrolysis or translocation. On the other hand, if EF-G is limiting, but not GTP or pretranslocation ribosomes, multiple turnover of EF-G activity can be followed.

Studies of peptidyl transfer can not only be done with full tRNA molecules, but tRNA fragments can also be used. Different fragments of the acceptor CCA end of the tRNAs can be used in what is called the "fragment reaction" (Traut & Monro, 1964; Monro, 1967). Puromycin is a minimal fragment with only the A-part of the acceptor end. It binds only at the A-site part of the PTC and functions as an acceptor of the nascent peptide from the P site (see Sec. 10.4). This leads to termination of protein synthesis and dissociation of puromycin linked to the nascent peptide. This assay is used to explore the occupancy of the A and P sites, and can be used to establish whether translocation has occurred. Puromycin does not bind to ribosomes when the A site is occupied. Translocation will allow puromycin to bind and react with the nascent peptide. After peptidyl transfer, the acceptor end of the tRNA in the A site can spontaneously move to the hybrid A/P site, where the CCA end will base-pair with the P loop. This will also allow puromycin to react with the nascent peptide (Sharma *et al*., 2004). The fragment reaction is biologically relevant, since it occurs at the same site as the normal peptidyl transfer reaction and is inhibited by the same inhibitors (Moore & Steitz, 2003b).

11.3 INITIATION

The bacterial translation apparatus goes through a number of distinct steps during initiation:

(1) Binding of mRNA to 30S subunits;
(2) Binding of IF1, IF2·GTP and IF3 to their binding sites;

(3) Binding of fMet-tRNA to the P/I site; this forms the 30S preinitiation complex (30S PIC);
(4) Association of 50S subunits and formation of the 70S initiation complex (70S IC);
(5) GTP hydrolysis by IF2;
(6) Dissociation of factors and formation of the postinitiation complex;

Bacterial mRNAs are frequently polycistronic and can thus contain information for several proteins. Translation is initiated by the binding of an mRNA to free ribosomal small subunits. An mRNA can hardly bind to 70S ribosomes, since it binds to the interface side and in a narrow groove around the neck of the small subunit (see Sec. 8.1; Yusupova *et al.*, 2001; Jenner *et al.*, 2005; Selmer *et al.*, 2006; Simonetti *et al.*, 2009).

For correct initiation, the initiation codon (AUG or GUG) needs to be selected and placed at the ribosomal P site. In bacteria, the selection of the initiation methionine codon over elongation methionine codons or out-of-frame AUGs is done through specific interactions of a part of the mRNA preceding the AUG initiation codon with the small subunit RNA (Sec. 8.1). A classical description is the Shine–Dalgarno (SD) interaction. However, a range of alternatives has been identified. mRNAs without an SD sequence as well as poly(U) can also initiate. The ribosome has high affinity for both artificial and natural mRNAs to the proper binding site.

The binding of IF3 must be an initial step of initiation, since this factor prevents the formation of the 70S ribosome (Grunberg-Manago *et al.*, 1975) and may assist in the removal of deacylated tRNA from the small subunit (Karimi *et al.*, 1999). IF3C prevents the small subunit from interacting with the large subunit by binding to h24, part of the B2b subunit bridge where the A-site finger (H69) makes a contact from the large subunit (McCutcheon *et al.*, 1999; Dallas & Noller, 2001). IF3N binds to the knee region of initiator tRNA (Fig. 9.13; Julián *et al.*, 2011).

IF1 binds to the decoding part of the A site and prevents tRNAs from binding there (Fig. 9.13; Moazed *et al.*, 1995; Carter *et al.*,

2001). It interacts with the top of h44 and forces A1492 and A1493 out of their stacked positions, reminiscent of the way cognate tRNA does (Carter *et al*., 2001). Furthermore, IF1 induces a conformational change of the small subunit that may represent a transition state between subunit association and dissociation (Carter *et al*., 2001; Ramakrishnan, 2002). IF1 and IF3 bind on each side of the initiator tRNA (Fig. 9.13; Dallas & Noller 2001; Julián *et al*., 2011). For efficient binding of initiator tRNA to the 30S subunit, all initiation factors are required (Antoun *et al*., 2006a).

Previous models for initiation have suggested that IF2 carries fMet-tRNA^{fMet} to the ribosome. This would correspond to the situation in archaea and eukaryotes where eIF2 carries the initiator tRNA to the ribosome. However, eIF2 does not have a corresponding factor in bacteria. The task of IF2 and eIF5B is, rather, to stabilize the bound initiator tRNA and to catalyze the joining of the small with the large subunit (Pestova *et al*., 2000; Lee *et al*., 2002). Since one of the roles of IF3 is to prevent association of the subunits, it has to be partially or fully ejected before the large subunit can associate with the initiation complex.

Thus, the initiator tRNA binds to the P site, contrary to all other incoming tRNAs, which bind to the A site. IF2 is guided by IF1 in the A site and IF3 in the E site (Carter *et al*., 2001; Dallas & Noller, 2001). A remarkable finding is that the initiator tRNA does not bind to the P site, but to a site between the P site and the hybrid P/E site. This new site is called the P/I site (Figs. 8.3 and 8.4; Allen *et al*., 2005; Allen & Frank, 2007; Simonetti *et al*., 2008). In its P/I site the anticodon stem of fMet-tRNA^{fMet} is rotated and the elbow is closer to the E site. The aminoacyl moiety would need to move about 28 Å to get into the peptidyl transferase center (Allen *et al*., 2005).

The understanding of the role of IF2/eIF5B in subunit joining is only partial. Domain II of IF2/eIF5B interacts with the small subunit (see Sec. 9.1; Julián *et al*., 2011). In addition, IF2 interacts with IF1 in the A site (Fig. 11.1; Choi *et al*., 2000) and, due to the long helix, domain IV stretches across the IF1 in the A site to interact with the initiator tRNA in the P/I site (Roll-Mecak *et al*., 2001). In a properly formed 30S PIC, IF2/eIF5B will act like a trap where the G-domain

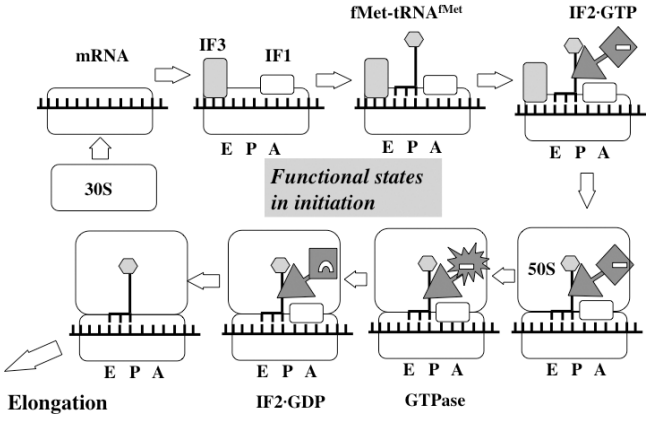

Fig. 11.1 Initiation of bacterial translation. The small subunit (left, middle) binds a messenger RNA and subsequently initiation factors IF1, IF2 and IF3. IF1 binds to the A site, and IF3 to the E site. The factors assist in the binding of fMet-tRNA^{fMet} to the P site. IF2·GTP catalyzes the joining of the large subunit after spontaneous release of IF3. The GTPase of IF2 is activated, and this factor and IF1 dissociate. The initiator tRNA is left in the P site of the 70S ribosome and can engage in elongation.

has affinity with the GTPase-associated region (GAR) of the large subunit at the base of the L12 stalk. The factor will bridge the ribosomal subunits and bring them together. In this procedure, only properly initiated small subunits with an initiator tRNA bound to the P site will be joined with a large subunit. The 30S subunit will not bind in the canonical orientation but is rotated by 4° anticlockwise in relation to the large subunit, like in the MSII state (Table 8.4; Allen *et al.*, 2005). The docking rate is determined by a conformational change in IF2 conferred by GTP, the formyl group and methionine of initiator tRNA, while the tRNA body has small influence. The presence of IF3 reduces the docking rate (Pavlov *et al.*, 2011)

Antoun *et al.* (2003) observed that GDP prevents fast association of the large subunit with the initiation complex as well as the start of elongation. GDPNP, on the other hand, allows fast association of the large subunit, but the start of elongation is very much slowed down due to the lack of dissociation of IF2. If IF2 remains

bound to the 70S ribosome in complex with GDPNP, fMet cannot form a peptide bond with puromycin (Antoun *et al.*, 2003). Since there is no reason to believe that IF2 blocks the PTC, the alternative is that fMet is not properly located in the P site part of the PTC until IF2 has dissociated. This is in agreement with the observations of the initiator tRNA being bound to a hybrid P/I site (Fig. 8.4; Allen *et al.*, 2007; Simonetti *et al.*, 2008). Like other tGTPases, GTP is needed for IF2 to permit rapid association of the subunits and release of the factor after GTP hydrolysis to allow the start of elongation (Blaha *et al.*, 2009).

With fMet-tRNA^{fMet} bound to a hybrid site of the ribosome (Allen *et al.*, 2007; Simonetti *et al.*, 2008), EF-P may help it to be properly placed for the start of elongation and the formation of the first peptide bond (Blaha *et al.*, 2009). The joining of the large subunit to the small subunit and the dissociation of initiation factors IF1 and IF2 conclude the initiation part of translation (Antoun *et al.*, 2003).

In eukaryotes translation is normally initiated by a mechanism that involves the m^{7}G cap at the 5′ end of the mRNA and a multitude of initiation factors. An alternative mechanism, used primarily by many eukaryotic viruses, depends on an RNA structure called the internal ribosome entry site (IRES). The IRES is a complex RNA structure composed of three domains where domain 3 binds to the P site like the ASL of a tRNA and placing the mRNA properly into the decoding part of the A site (Zhu *et al.*, 2011). Domain 3 is bent toward the E site to leave room for a new tRNA to enter the A/P site to become translocated into the P site for proper protein synthesis to begin.

11.4 ELONGATION

In each cycle of elongation, one amino acid is incorporated into the nascent peptide. The *in vivo* rate of translation is about 20 amino acids incorporated per second and ribosome (Kjeldgaard & Raussing, 1974; Liang *et al.*, 2000). This means that each complete

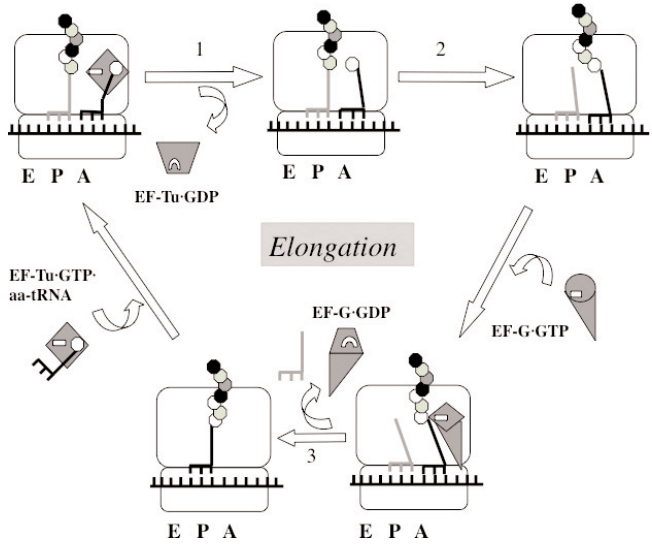

Fig. 11.2 A summary of elongation in protein synthesis. The cycle starts at the bottom left with a peptidyl-tRNA in the P site. EF-Tu brings in a new aminoacyl-tRNA in the A/T state and dissociates after GTP hydrolysis (transition state 1), allowing the tRNA to bind to the A site. In transition state 2, the acceptor end of the A site tRNA has moved into the PTC close to the P-site tRNA to participate in peptidyl transfer. The translocation of the peptidyl-tRNA from the A site to the P site is catalyzed by EF-G (transition state 3). The elongation cycle needs two catalysts, EF-Tu and EF-G. The peptidyl transfer step is spontaneous.

cycle of elongation is performed in 50 msek. Figure 11.2 shows a summary of the steps involved in elongation.

At the start of the elongation cycle, the ribosome is in the post-translocation state with fMet-tRNA or a peptidyl tRNA in the P site. This tRNA is bound with its anticodon to its codon at the neck of the 30S subunit, while the acceptor end is at the PTC of the large subunit. The nascent peptide is situated in the peptidyl exit tunnel (Sec. 8.4). In several crystallographic investigations of the 70S ribosome, tRNAs were bound simultaneously to all three sites — A, P and E (Cate *et al.*, 1999; Yusupov *et al.*, 2001; Schmeing *et al.*, 2009). The affinity of the E site with deacylated tRNA was found to be significant.

Binding of Aminoacyl-tRNA — Decoding

Codon–anticodon relationships

tRNA 'reads' the genetic code, with its 64 'words' or codons (see Sec. 4.1). Since the code is degenerate, the codon usage can be different in different organisms. The codons used are correlated with the set of tRNAs, expressed (Dong *et al.*, 1996). In some cases, the codon usage is limited to a small set of tRNAs, while in other species there are tRNAs corresponding to most codons.

The anticodon, normally at positions 34–36 of the anticodon stem and loop (ASL) of a tRNA, reads the codons of the mRNA primarily by Watson–Crick base-pairing (Fig. 11.3). However, the first base of an anticodon can base-pair with different bases in the third position of a codon. Thus, noncanonical base pairs occur in the third, so-called 'wobble' position of the codon (Crick, 1966b). This also includes modified bases of the tRNA. This allows some tRNA to read several codons. Thus, a limited set of tRNAs can read a larger set of codons.

Fidelity-related States of the Small Subunit

An important aspect of translation is fidelity. An incorrect translation of the mRNAs may lead to catastrophic consequences for the cell. Fidelity includes identification of the correct initiation codon,

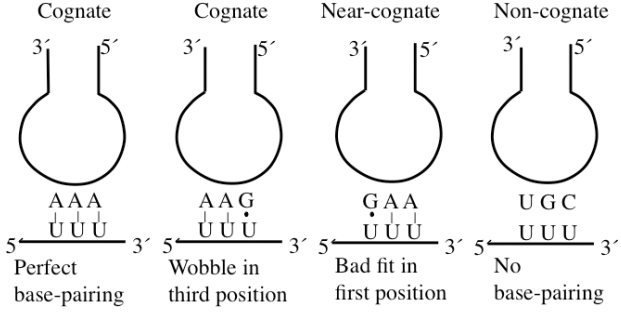

Fig. 11.3 Different types of interactions between anticodon of tRNA (*top*) and mRNA (*bottom*).

maintenance of the correct reading frame, and the correct translation of each codon and termination of protein synthesis at a stop codon.

The small subunit undergoes a conformational change from an open to a closed form when a codon of the mRNA binds a cognate tRNA in the A site (Sec. 8.6; Ogle *et al.*, 2002, 2003; Schmeing & Ramakrishnan, 2009). These conformational changes involve movement of the body of the small subunit with regard to the platform, a tilt of the head toward the subunit interface, opening/closing of the head relative to the shoulder and swiveling of the head (Agirrezabala *et al.*, 2011). Only cognate interactions induce this closing of the small subunit (Agirrezabala *et al.*, 2011).

Antibiotics, such as paromomycin or streptomycin, that stabilize the closed form will lead to error-prone reading (see Sec. 10.2; Carter *et al.*, 2000; Ogle *et al.*, 2002, 2003). On the other hand, mutations in S12 that cause streptomycin resistance or streptomycin dependence may lead to hyperaccurate ribosomes (Kurland *et al.*, 1996). Such mutations destabilize the closed form (Ogle *et al.*, 2002). Revertant mutations that lead to a fidelity close to normal are found in proteins S4 and S5 (Andersson *et al.*, 1986). The closed form of the small subunit leads to breakage of the interactions between S4 and S5. Obviously, then, mutations that break this interaction can stabilize the closed form and are of the ram (ribosome ambiguity) phenotype (Fig. 11.4; Clemons *et al.*, 1999; Carter *et al.*, 2000; Ogle *et al.*, 2002, 2003). However, experimental data showing that a combination of an S12 and an S4 mutant, both conferring hyperaccuracy, leading to wild type accuracy, suggest that accuracy tuning by ribosomal mutations is more complex than indicated by the crystallographic studies. Furthermore, another experimental study shows no correlation between reduced affinity of binding between mutated variants of S4 and S5 and increased translation errors.

The Mechanisms of Decoding

In the cell, aminoacylated tRNAs bind to EF-Tu·GTP. The elongation cycle begins with the binding of such a ternary complex,

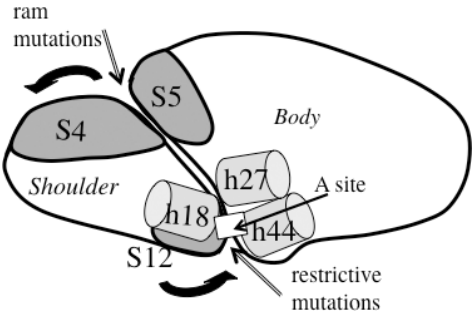

Fig. 11.4 Some of the conformational changes of the small subunit related to decoding (Ogle *et al.*, 2003). The shoulder can move with regard to the rest of the subunit. The decoding A site is located at the neck of the subunit. A cognate interaction of codon and anticodon causes a closing of the subunit, as indicated by the black arrows. The binding of streptomycin or paromomycin in this area also causes such a closing of the subunit. This leads to errors in decoding. Restrictive mutations in S12 shift the balance to a more open subunit and fewer decoding errors. Ram mutations in S4 and S5 on the external side of the subunit shift the balance toward a closed conformation of the subunit and a lower fidelity of translation. (After Ogle *et al.*, 2001.)

aminoacyl-tRNA·EF-Tu·GTP, to the T site of the ribosome (see Sec. 8.2; Moazed & Noller, 1989). This binding is dominated by the interaction between EF-Tu and the ribosome (Schmeing *et al.*, 2009). The next step involves the recognition of the codon by the anticodon of the tRNA, or the decoding. The error rate in translation is in the order of 10^{-3}–10^{-4} (Kurland *et al.*, 1996). The difference in affinity between cognate and near-cognate tRNAs is not enough to explain this low error frequency (Grosjean, *et al.*, 1978; Kurland, 1992). In fact, the base-pairing of an incorrect codon–anticodon pair can be more stable than a correct one. Thus, the cognate interaction between the UUU codon and the phenylalanine anticodon GAA is less stable than the noncognate interaction between the cysteine codon UGC and the arginine anticodon GCG (Ramakrishnan, 2002). Nevertheless, on the ribosome, the cognate interaction is greatly favored.

Two main types of mechanisms that can explain the high fidelity of translation have been discussed. The current understanding of the system suggests that the ribosome uses both. The two mechanisms are:

(1) *Geometric recognition*. The properties of the decoding site are such that the base-pairing is geometrically screened by the ribosome. This is possible if the correct codon–anticodon pairing leads to conformational changes of the decoding site (Ogle *et al*., 2001, 2003; Ramakrishnan, 2002).
(2) *Kinetic proofreading*. The accuracy, A, of the process is the product of the initial accuracy, I, and the proofreading accuracy, F: A = I·F. In addition to the initial selection of tRNAs in ternary complex selection (Hopfield, 1974; Ninio, 1975) with EF-Tu and GTP, there is proofreading after GTP hydrolysis (Thompson & Stone, 1977; Ruusala *et al*. 1982).

Initial Recognition

The functional significance of the three-dimensional L shape of the tRNA and the extension of the CCA end is gradually becoming understood with the insights into how this shape is utilized during protein synthesis on the ribosome. The most obvious point of flexibility in the tRNA is the elbow of the L-shaped molecule. Indeed, a range of angles has been observed in the elbow region in some tRNA structures (Moras *et al*., 1980) and in a complex between EF-Tu and $tRNA^{Cys}$ (Nissen *et al*., 1999).

In the initial selection, EF-Tu·GTP of a ternary complex binds to the ribosome regardless of whether the codon exposed in the A site is cognate or noncognate. This has been clarified by fluorescence spectroscopy (Rodnina *et al*., 1993, 1995a, b, 1996). In this initial binding, the anticodon does not interact with the codon (Fig. 11.5a).

To discriminate between a cognate and a noncognate tRNA, the ASL has to make a bend of about 30°. This bend occurs at nucleotides 25–30 and 40–48 (Valle *et al*., 2002, 2003a; Stark *et al*., 2002; Schmeing *et al*., 2009). As inferred already in the studies of the

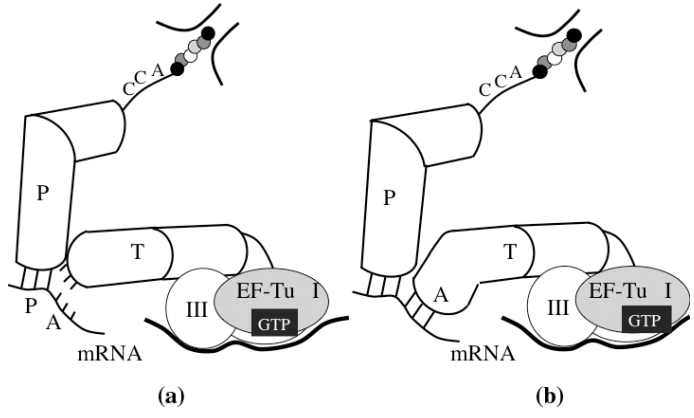

Fig. 11.5 A simplified representation of the binding of an aminoacyl-tRNA in complex with EF-Tu·GTP to the decoding site of the ribosome. (**a**) The initial binding to the T site, where the main interaction between EF-Tu and the ribosome takes place. The binding occurs regardless of the presence or absence of mRNA, or whether the codon is cognate or noncognate. (**b**) The anticodon stem makes a bend with regard to the D-stem to interact with the codon of the mRNA. The cognate codon–anticodon interaction leads to GTP hydrolysis.

first crystal structure of tRNA, this region could allow some flexibility (Robertus *et al.*, 1974; Valle *et al.*, 2003a). The bent conformation of the tRNA is most certainly due to the multiple interactions of the tRNA with EF-Tu, the mRNA and the ribosome. The ASL of a cognate tRNA in the A/T state binds in the same manner as the ASL of a tRNA in the A site (Yusupov *et al.*, 2001; Ogle *et al.*, 2003; Valle *et al.*, 2003a; Schmeing *et al.*, 2009; Voorhees *et al.*, 2010).

In case the codon does not match the anticodon, the binding affinity for the tRNA remains low and the ternary complex is likely to fall off. The number of ternary complexes tested in this way in each cycle of elongation must be significant. At the core of initial recognition and proofreading are the codon–anticodon interactions in the decoding site. Three universally conserved bases of the 16S RNA have been identified by footprinting experiments to be involved in the decoding site. They are G530, A1492 and A1493 (Moazed & Noller, 1986, 1990; Powers & Noller, 1990).

NMR experiments on a fragment of helix h44 have given structural insights (Fourmy *et al.*, 1996; Yoshizawa *et al.*, 1999). Crystallographic experiments on binding cognate and near-cognate ASLs to the small subunit have provided a very interesting picture of how the ribosome participates in the decoding. Thus, correct Watson–Crick base-pairing between the mRNA and the cognate tRNA induces conformational changes of A1492 and A1493 of h44 as well as of G530 of h18 (Plate 11.1; Carter *et al.*, 2000; Schlünzen *et al.*, 2000; Yusupov *et al.*, 2001; Ogle *et al.*, 2001–2003). The two adenines flip out from their normal configuration and insert into the minor groove of the codon–anticodon helix, forming A-minor motif interactions (Nissen *et al.*, 2001).

The three 16S RNA bases hydrogen-bond to the 2′ OH groups of both riboses of the first two base pairs of the short codon–anticodon helix (Plate 11.1). The analogy of a ruler has been made, where the unique distance between the 2′ OH groups of a Watson–Crick base pair is checked. A1493 checks the first base pair of the codon-anticodon helix in the A site, and the second base pair is checked by A1492 and G530. The wobble base pair does not have the same strict requirements for base-pairing, but here also the ribose of the codon nucleotide hydrogen-bonds to G530 (Ogle *et al.*, 2001, 2002). These interactions remain during initial recognition when EF-Tu has dissociated (Valle *et al.*, 2003a; Selmer *et al.*, 2006).

If the antibiotic paramomycin is bound at the decoding site, the fidelity is significantly reduced (Pape *et al.*, 2000). The antibiotic induces A1492 and A1493 to be oriented as if the codon–anticodon match was perfect (see Sec. 10.3; Ogle *et al.*, 2001–2003). The conformational changes of these three bases are associated with a closure of the 30S subunit (Ogle *et al.*, 2002, 2003).

The Hirsh suppressor is a mutant of $tRNA^{Trp}$ that can read UGA stop codons (Hirsh, 1970). Here G24, which is far from the anticodon, is mutated to an A. Similarly, the mutant A9C of $tRNA^{Trp}$ can read the UGA stop codon (Smith & Yarus, 1989). Structural analysis has suggested how the discrimination between U and A in the third or wobble position is done (Schmeing *et al.*,

2011). Two possibilities initially seemed likely. The mutations may increase the flexibility of the tRNA to more easily adopt the A/T conformation. Alternatively, the mutants may be additionally stabilized in the A/T-conformation. 70S complexes with wild-type and ternary complexes with kirromycin and mutant tRNAs bound to UGG or UGA codons were studied crystallographically. The mismatch in the wobble position in the codon–anticodon interaction is clearly seen in the mutants. This structural distortion involves both tRNA and mRNA, and propagates in the tRNA from residue 34 to residue 31 in the anticodon. In the G24A mutant an additional hydrogen bond to G44 is formed in the A/T-conformation, which is stabilized by the mutation. This then leads to miscoding. The A9C mutation destabilizes a base triple, which leads to a destabilization of the whole tRNA that would more readily allow it to adopt the A/T-state (Schmeing *et al.*, 2011).

GTP Hydrolysis

EF-Tu normally has a low intrinsic GTPase activity, but when the anticodon of its bound tRNA matches a codon of the mRNA on the ribosome the hydrolytic activity is induced. The GTP hydrolysis leads to dissociation of EF-Tu from the ribosome (Fig. 11.6). Apparently, EF-Tu needs to undergo some conformational changes to become an active GTPase. However, not only EF-Tu but also the tRNA and the ribosome undergo conformational changes upon binding of a cognate ternary complex (Schmeing *et al.*, 2009; Voorhees *et al.*, 2010). Comparing the two ternary complexes bound to the ribosome, there is a rotation of the G-domain of about 4° between the complex with GDP and kirromycin and the complex with GDPCP (Voorhees *et al.*, 2010). This prevents a collision between switch I and SRL, and leads to an ordered structure of switch I in the GDPCP case but not for the case of GDP and kirromycin. The correct binding of the ternary complex also induces conformational changes in switch II. His84 of switch II in EF-Tu, which is a crucial residue for GTP hydrolysis, is not normally in the vicinity of the γ-phosphate of the GTP (Plate 9.8; Nissen *et al.*,

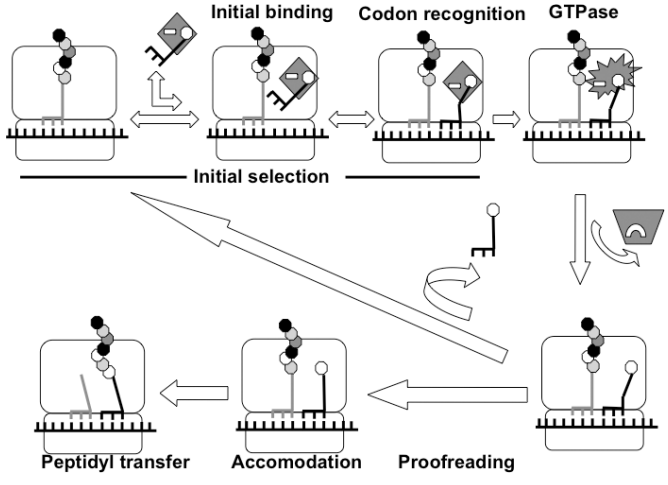

Fig. 11.6 A summary of aminoacyl-tRNA binding to the A site of the ribosome. The initial selection is composed of two steps: initial binding and accommodation. In the proofreading step, the tRNA can fall off the ribosome or proceed to peptidyl transfer.

1995). However, under correct conditions it is brought into the proximity of the water molecule which hydrolyzes the GTP to GDP and inorganic phosphate (Voorhees *et al.*, 2010).

The effect of these conformational changes is that His84 gets hydrogen-bonded to a phosphate oxygen of A2662 in SRL and thereby positioned to move the hydrolytic water molecule into contact with the γ-phosphate of the GTP (Voorhees *et al.*, 2010). The mechanism of hydrolysis has been discussed in Sec. 9.3.

Proofreading

When the GTP molecule has been hydrolyzed, the EF-Tu·GDP complex adopts a conformation with low affinity for the aminoacyl-tRNA and the ribosome and it dissociates (Yokosawa *et al.*, 1975). The acceptor stem and the aminoacyl moiety of the tRNA which were bound to EF-Tu in the A/T site can now be reoriented into the A site and into the PTC on the large subunit (Fig. 11.7;

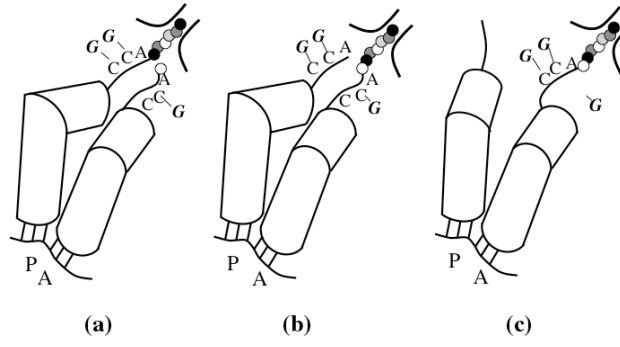

Fig. 11.7 The tRNAs in the A and P sites before and after peptidyl transfer. (**a**) The state after GTP hydrolysis and dissociation of EF-Tu·GDP. The bend between the ASL and the D-stem of the A site tRNA has closed and allows the tRNA to accommodate into the A site next to the peptidyl-tRNA in the P site. Even though the bodies of the tRNAs are related by a sideways movement, the CCA ends are related by a 180° rotation through interactions with the A and P loops, respectively. The nascent peptide of the P site tRNA is in the exit tunnel. C75 of the A site tRNA forms a base pair with G2553 of the 23S RNA. Similarly, C74 and C75 of the P-site tRNA interact with G2251 and G2252. (**b**) The state immediately after peptidyl transfer. (**c**) The 3′ ends of the tRNAs are relocated such that the tRNAs become bound in the P/E and A/P states.

Härävi Stark *et al.*, 1997; Valle *et al.*, 2003a). The tRNA acts like a spring where the strain in the bend between the anticodon stem and the D-stem is relieved and the tRNA regains its normal L shape (Valle *et al.*, 2003a). In this movement, the ASL maintains its position and interaction with the codon (Valle *et al.*, 2003a).

This process is called the proofreading step of binding the aminoacyl-tRNA to the A site (Fig. 11.6; Thompson & Stone, 1977; Ruusala *et al.*, 1982). An incorrect (noncognate) match of the anticodon to the codon renders high probability that the aminoacyl-tRNA will dissociate before its amino acid is properly located in the PTC of the ribosome, while a correct (cognate) match renders low probability of aminoacyl tRNA dissociation. The affinity for the cognate tRNA is considerably higher than for near- or noncognate tRNAs (Rodnina *et al.*, 2000). Furthermore, the peptidyl moiety in

the P site can react with the aminoacyl moiety in the A site only if it is properly located. If these steric requirements are not satisfied, maybe due to improper base-pairing in the decoding site (75 Å away), the reaction will be slowed down to the extent that the aminoacyl-tRNA may fall off long before peptidyl transfer can occur (Liljas, 1990).

The main steps of aminoacyl-tRNA binding and peptidyl transfer may be summarized in the following way (Fig. 11.6):

(1) Initial selection of aa-tRNA. A ternary complex of EF-Tu·GTP·aa-tRNA binds to the T site, in which EF-Tu interacts with the factor-binding region of the ribosome.
(2) A bend in the aa-tRNA between the anticodon and D-stems of the tRNA allows the anticodon of the EF-Tu bound tRNA, in the A/T state to interact with the A-site codon.
(3) When the aa-tRNA is cognate to the A-site codon, GTP is hydrolyzed on EF-Tu with high probability. When the aa-tRNA is non-cognate, the ternary complex dissociates from the ribosome with high probability in the initial selection step.
(4) After GTP hydrolysis, EF-Tu·GDP dissociates from the ribosome. When aa-tRNa is cognate, it accomodates with high probability in the A site, and transfer of the peptide on P-site tRNA to the A-site tRNA occurs with high probability. When the aa-tRNA is non-cognate, it dissociates with high probability in the proofreading step.
(5) Stabilization of the cognate, but not the non-cognate, codon-anticodon contact by 16S rRNA bases enhances the selectivity of both the initial and proofreading selection steps.
(6) There is a trade-off between rate and accuracy of the codon reading by ternary complex (Johansson *et al.*, 2012).
(7) The peptide is transferred from the tRNA in the P site to the aminoacyl moiety on the tRNA in the A site.

Peptidyl Transfer

The PTC is located in a pocket on the interface side of the large subunit at the entrance of the peptide exit tunnel which finishes on

the external side. For all enzymatic activities, proximity and correct orientation of the reactants are major factors. Furthermore, groups of the ribosome, coenzymes or metal ions that participate in the process are obviously of interest.

The ribosome enhances the rate of peptide bond formation in the order of 10^7 compared to the spontaneous reaction in water. Studies of *H. marismortui* large subunits in complex with different substrate analogs have nevertheless provided detailed insights into the arrangements of the PTC (Schmeing *et al*., 2005). The peptidyl transfer reaction is rapid for a cognate tRNA (can be as rapid as $160s^{-1}$; Johansson *et al*., 2008). PTC catalyzes peptidyl transfer after the substrates have been placed close to each other in the proper orientation, thereby lowering the entropy of activation (Sievers *et al*., 2004). In addition, water is excluded from the active site (Schmeing *et al*., 2005). Unlike serine proteases, there is no evidence of a covalent intermediate formed with the ribosome in this process, and neither is there any metal ion involved in the process (Schmeing *et al*., 2005).

Peptidyl transfer is essentially the reverse of breaking a peptide bond by a protease. The α-amino group on the aminoacyl-tRNA in the A site, in its neutral state, makes a nucleophilic attack on the carbonyl carbon of the ester linkage between the P-site tRNA and the nascent peptide (Plate 11.2). In the PTC the acceptor ends of the tRNAs are held in place by highly specific interactions with the 23S RNA (Fig. 11.7). In the case of the P-site tRNA, it is the P-loop (Table 8.3), whereas the A-site tRNA is held by the A-loop (Table 8.2). Furthermore, a number of conserved bases of the 23S RNA, A2451, U2506, U2585, C2452 and A2602 surround the active site (Bashan *et al*., 2003; Schmeing *et al*., 2005). The α-amino group of the amino acid bound to the A site tRNA is of particular interest, since it needs to be deprotonated to become activated (Johansson *et al*., 2011). Here hydrogen bonds could be formed to the 2′OH of A76 of the P site tRNA and to A2451 (Nissen *et al*., 2000; Hansen *et al*., 2002).

Initially, N3 of A2451 was suggested to function as a general base and deprotonate the α-amino group and subsequently stabilize the oxyanion of the substrate carbonyl group of the P site

tRNA (Nissen *et al*., 2000). However, later experiments suggested this to be a less likely role of the base (Polacek *et al*., 2001; Youngman *et al*., 2004; Behringer *et al*., 2005; Trobro & Åqvist, 2005; Åqvist *et al*., 2012). Furthermore, using a hydroxyl instead of the α-amino group made it highly unlikely that any general acid/base with a pKa around neutral was involved in peptidyl transfer (Bieling *et al*., 2006). Studies at higher resolution with various substrate analogs have shown that A2451 is not within hydrogen-bonding distance of the α-amino group (Schmeing *et al*., 2005). This leaves the 2′OH at the 3′ end of the P-site tRNA with the essential role of participating in proton transfer in the PTC (Dorner *et al*., 2003; Weinger *et al*., 2004).

The nucleophilic attack leads to a short-lived tetrahedral intermediate. For the reaction to become complete, the 3′ oxygen of the P site tRNA, to which the nascent peptide was bound, needs to be protonated. Furthermore, when the carbonyl carbon goes through the intermediate tetrahedral state, the carbonyl oxygen develops into an oxyanion that needs to be stabilized by something corresponding to the oxyanion hole in proteases.

The PTC is primarily composed of RNA (see Sec. 8.4; Noller *et al*., 1992; Ban *et al*., 2000; Nissen *et al*., 2000; Harms *et al*., 2001). In the work on *H. marismortui* large subunits, no protein was seen in the vicinity of the PTC (Ban *et al*., 2000; Nissen *et al*., 2000). However, the work on bacteria suggests that a protein has some role in peptidyl transfer. Thus, removing three amino acids from the N-terminus of *E. coli* L27 impairs the peptidyl transfer activity (Plate 7.5; Maguire *et al*., 2005). A cross-link between the N-terminus of L27 and A76 of the P site tRNA has also been observed (Wower *et al*., 1998; Harms *et al*., 2001; Kirillov *et al*., 2002). The amino terminus of L27 could contribute to the oxyanion hole (Maguire *et al*., 2005; Selmer *et al*., 2006). It was found that the amino terminal methionine was removed, but other parts of L27 were observed to interact with both tRNA molecules. The N-terminal amino group of Ala2 interacted with the phosphates of the A site C75 and C2452, but the distance from the amino group to the phosphate of A76 was about 5 Å (Voorhees *et al*., 2009). Furthermore, a

water molecule between the A site substrate carbonyl group also receives a hydrogen bond from this amino group. Thus, L27 does not seem to contribute to the oxyanion hole, but to stabilizing the acceptor ends of the A and P site tRNAs. This explains the reduced activity of variants of L27 with a shortened N-terminus (Maguire *et al*., 2005; Selmer *et al*., 2006; Trobro & Åqvist, 2008; Schmeing *et al*., 2009; Voorhees *et al*., 2009; Jenner *et al*., 2010). The oxyanion hole in both bacteria and archaea is most likely formed by a water molecule bound to A2602 and U2584 (Schmeing *et al*., 2005; Trobro & Åqvist, 2008; Simonovic & Steitz, 2009).

L16 is also required for peptidyl transferase activity (Moore *et al*., 1975). In bacteria it interacts with the elbow of A-site tRNA, but does not reach into the PTC. However, in the archeon *H. marismortui* the loop is longer and could stabilize the >CCA-ends of both tRNA substrates, thereby facilitating peptidyl transfer (Voorhees *et al*., 2009).

Thus, when the α-amino group of the aminoacyl-tRNA in the A site is suitably oriented close to the carbonyl carbon of the ester linking the peptide to the P site tRNA, the ribose 2′OH of A76 of the P site tRNA can deprotonate and stabilize the uncharged form of the α-amino group (Hansen *et al*., 2002b; Bashan *et al*., 2003). A tRNA with a terminal 2′ deoxyadenosine can be charged with an amino acid, is active as A site substrates, but cannot donate its nascent polypeptide to an A site tRNA (Quiggle *et al*., 1981). Furthermore, the 2′OH of A76 not only deprotonates the α-amino group but also transfers the proton to its neighboring 3′OH (Dorner *et al*., 2003; Moore & Steitz, 2003a, b). In conclusion, no group of the ribosome contributes any essential function to the PTC except to place the substrates appropriately in the right orientation next to each other with the aid of the A and P loops (Simonovic & Steitz, 2009).

The Acceptor Ends and Hybrid States

Before peptidyl transfer the CCA part of the A-site tRNA base-pairs with G2553 of the A-loop and the CCA part of the P-site

tRNA base-pairs with G2251 and G2252 of the P-loop (Green *et al*., 1998; Nissen *et al*., 2000; Bashan *et al*., 2003). Small acceptor end fragments of tRNA can bind to either the A or the P site. In case the fragment contains an amino acid with a free amino group, the A site is preferred, possibly because of lack of suitable interactions in the P site (Hansen *et al*., 2002b). Acceptor end fragments of peptidyl-tRNA bind to either site (Hansen *et al*., 2002b). Footprinting experiments on tRNA molecules interacting with 70S ribosomes suggest that after peptidyl transfer the CCA end of the P-site tRNA can move to the E site. In other words, the deacylated tRNA can move to the hybrid P/E site (Moazed & Noller, 1989; Green *et al*., 1998). Likewise, the CCA end of the peptidyl-tRNA in the A site can move into the hybrid A/P site and interact with the P-loop (G2251 and G2252; Fig. 11.7; Moazed & Noller, 1989; Samaha *et al*., 1995; Green *et al*., 1998). The hybrid states of tRNA binding, proposed by Bretscher already in 1968, are associated with the rotated state of the small subunit with regard to the large subunit (MSII; Fig. 8.6; Table 8.4; Frank & Agrawal, 2000; Valle *et al*., 2003b).

Crystals of *H. marismortui* 50S subunits are active in peptidyl transfer (Schmeing *et al*., 2002). In a crystallographic study where CCA-Phe-caproic acid-biotin (CCA-pcb) was bound to the P site and CC-puromycin was bound to the A site, the electron density showed CC-puromycin-pcb in the A site and a deacylated CCA in the P site. Thus, the structure reveals a state after peptidyl transfer. Interestingly, the CCA fragments of the products remain in essentially the same positions as the substrates (Schmeing *et al*., 2002; Hansen *et al*., 2002b). However, the deacylated tRNA fragment in the P site was seen only at low occupancy, suggesting that its affinity for the site was reduced. The short peptide remains in its normal position at the entrance to the peptide exit tunnel. These results suggest that movement into the hybrid states is not simultaneous with peptidyl transfer (Green *et al*., 1998; Schmeing *et al*., 2002). Cryo-EM studies also suggest that the peptidyl-tRNA remains in the A site after peptidyl transfer (Valle *et al*., 2003b). If the CCA end had moved from the A to the P site after peptidyl

transfer, one would have expected that puromycin could react with the peptidyl-tRNA, but this requires translocation by EF-G (Borowski *et al.*, 1996). Furthermore, Wower *et al.* (2000) have shown that the CCA end of the P site tRNA does not move spontaneously to the E site. However, in related crystallographic experiments it was found that a single peptidyl-CCA fragment would bind equally well to the A and P sites (Hansen *et al.*, 2002). These observations have developed into a dilemma: When do the tRNAs move into the hybrid sites and when does the small subunit rotate relative to the large subunit?

Kim *et al*. (2007) made the important observation in FRET experiments that the dynamics of the ribosome with regard to the classical and hybrid states was highly dependent on the magnesium concentration. Aggirezabala *et al*. (2008) reinvestigated by cryo-EM the pretranslocational ribosomes at low Mg^{2+} concentration and found that the tRNAs can spontaneously oscillate between A/A and P/P sites and the hybrid A/P and P/E sites. Related observations suggest that a deacylated tRNA in the P site stabilizes the rotated hybrid state (Julian *et al.*, 2008; Cornish *et al.*, 2008; Marshall *et al.*, 2008).

The tRNAs in the A and P sites are related by a sideway movement, but the CCA ends are related by an approximate 180° rotation (Sec. 8.3; Nissen *et al.*, 2000; Yusupov *et al.*, 2001; Schmeing *et al.*, 2002; Hansen *et al.*, 2002b; Bashan *et al.*, 2003; Agmon *et al.*, 2003). This rotation is related to the twofold symmetry of the A and P loops (Nissen *et al.*, 2000; Agmon *et al.*, 2003; Bashan *et al.*, 2003). When the peptidyl tRNA is in the A/P hybrid site, it is base-pairing to the P loop (Moazed & Noller, 1989). It is interesting to note that the Tyr and Phe residues of the product CC-puromycin-pcb when covalently linked also remain close to their substrate positions. The side chains are oriented in opposite directions and the peptide is in a β-type of configuration (Schmeing *et al.*, 2002). The peptide produced then also agrees with the 180° rotation of the PTC. There is limited interaction between these amino acids and the ribosome, but further into the exit tunnel the nascent peptide interacts with the ribosome.

Translocation

Translocation is a Spontaneous Process Inherent in the Ribosome

Translocation proceeds in several steps and results in the movement of a peptidyl-tRNA from the A to the P site and concomitantly, a deacylated tRNA from the P to the E site. At the same time, mRNA moves one codon in the ribosomal frame and expose a new codon in the empty A site of the post-translocation ribosome. The hybrid states A/P and P/E and the rotated MSII configuration of the two subunits are important intermediates in this translocation process. These hybrid states define the pre-translocation ribosome. After translocation the ribosome returns to the MSI configuration. In addition, the L1 stalk alternates between a closed and an open state. The closed state relates to a CCA end of a tRNA in the P/E site (Spahn *et al*., 2004).

Inoue-Yokosawa *et al.* (1974) presented a classical model of translocation. Normally, EF-G·GTP catalyzes this process connected with hydrolysis of GTP (Ishitsuka *et al*., 1970; Kaziro, 1978; Rodnina *et al*., 1997). However, a slow rate of translocation has been observed without factors (Pestka, 1969; Gavrilova & Spirin, 1971; Gavrilova *et al*., 1976; Southworth *et al*., 2002). These results have been questioned on the grounds that energy is normally required for similar activities. Small amounts of EF-G could possibly lead to the results observed. However, even in the presence of fusidic acid (see Sec. 10.7) translocation was observed (Spirin, 1978).

Furthermore, Gavrilova and Spirin (1971, 1972) found that p-chloromercuribenzoate stimulates the spontaneous translocation. Since this reagent modifies thiols, it could hardly have a role in the PTC, which has limited contribution of protein molecules. Protein S12, which has several thiols, was early on identified as the main site (Gavrilova *et al*., 1974). From its location in the decoding site of the small subunit and its potential to affect conformational changes of the small subunit, it may stimulate translocation.

The antibiotic sparsomycin also induces translocation in the absence of EF-G and GTP (Fredrick & Noller, 2003). It binds at the PTC and inhibits peptidyl transfer (see Sec. 10.4; Hansen *et al*.,

2002b; Bashan *et al.*, 2003). Several antibiotics that inhibit EF-G-dependent translocation also inhibit translocation by sparsomycin (Fredrick & Noller, 2003). They include viomycin, paramomycin, neomycin, streptomycin and spectinomycin (see Sec. 10.2). These inhibitors target the subunit interface. The fact that the same inhibitors inhibit translocation induced by EF-G and sparsomycin suggests that the mechanisms must be similar. Inhibitors like thiostrepton and fusidic acid specifically inhibit EF-G but are not related to the binding or action of sparsomycin. Other antibiotics with no effect on EF-G-dependent translocation inhibit translocation catalyzed by sparsomycin. They are lincomycin, spectinomycin, carbomycin A and chloramphenicol (Fredrick & Noller, 2003). These inhibitors prevent the interaction of sparsomycin with the peptidyl-tRNA in the PTC (Schlünzen *et al.*, 2001; Hansen *et al.*, 2002b).

In crystal structure analyses of large subunits, sparsomycin stabilizes the binding of peptidyl-tRNA but blocks the access of aminoacyl-tRNA to the peptidyl-tRNA by binding to part of the A site (Schlünzen *et al.*, 2001; Hansen *et al.*, 2002b). Sparsomycin interacts with the ribose-phosphate backbone of C75 and A76 of the P site tRNA, as well as with the nascent peptide, thereby stabilizing the acceptor end in the P site (Hansen *et al.*, 2002b). This apparently leads to a complete translocation of the peptidyl-tRNA into the P site (Fredrick & Noller, 2003). Some conformational changes of the ribosome upon binding of sparsomycin are known. A2602 undergoes a movement to stack with the aromatic ring of sparsomycin (Hansen *et al.*, 2002b). This movement could possibly be transmitted through the ribosome with the effect that the tRNA is translocated. However, it is also possible that the tRNA itself has a major role. Once the acceptor end is stabilized in the P site, the stacking interaction between the acceptor end and the rest of the tRNA may lower the activation energy to translocate the rest of the tRNA and the mRNA to the P site (Hansen *et al.*, 2002b; Fredrick & Noller, 2003). A structural analysis of 70S ribosomes with a peptidyl-tRNA and sparsomycin would be interesting.

It is remarkable that the binding of the small sparsomycin molecule to the large subunit can be transmitted over a large distance to the small subunit and lead to translocation of the mRNA (Southworth & Green, 2003). Likewise, it is remarkable that EF-G or modification of S12 can catalyze the same process by binding far from the PTC where sparsomycin is bound. Fredrick and Noller (2003) suggested that one of the universally conserved uridines, U2584 or U2585, could play the same role as sparsomycin in the case of the EF-G–catalyzed translocation. The binding of sparsomycin changes the balance between the restrictive and ram states of the ribosome (see Sec. 8.6). This may suggest that the finely tuned functional balance of the ribosome may have evolved from a slow and spontaneous translocation stimulated by the binding of specific small molecules to the situation where a translation factor efficiently catalyzes translocation once peptidyl transfer is performed. One major difference is that, once sparsomycin is bound, it remains bound and becomes an inhibitor, while EF-G·GDP is released, permitting further rounds of peptidyl transfer and translocation. However, it is evident that translocation is intrinsic to the ribosome, as was suggested long ago (Pestka, 1969; Gavrilova & Spirin, 1971; Gavrilova *et al.*, 1976).

EF-G–Catalyzed Translocation

The rate of ribosomal translocation is accelerated at least 1000-fold by the catalysis by EF-G (Katunin *et al.*, 2002). EF-G binds to the ribosome in complex with GTP (Nishizuka & Lipmann, 1966; Kaziro, 1978). The classical view of translocation is that EF-G acts as a molecular switch like other GTPases (Vetter & Wittinghofer, 2001). According to this mechanism, it binds to the ribosome with GTP, translocates the peptidyl-tRNA, the deacylated tRNA and the mRNA, hydrolyzes its GTP and subsequently falls off the ribosome in complex with GDP. Spirin (2002) has summarized the arguments for this view. According to an alternative view, EF-G, like several ATPases, may act like a mechanochemical or motor protein (Rodnina *et al.*, 1997; Cross, 1997). The main observation

supporting this mechanism is that EF-G hydrolyzes its GTP shortly after it has bound to the ribosome and that translocation was found to be slower than GTP hydrolysis (Rodnina *et al*., 1997).

It has been suggested that EF-G·GTP specifically identifies ribosomes in the unlocked, rotated pretranslocation state with a peptidyl-tRNA bound in the A/P state (MSII; Agirrezabala *et al*., 2008; Munro *et al*., 2010). When EF-G binds, then GTP-hydrolysis occurs very rapidly (Rodnina *et al*., 1997), followed by the last step of translocation catalyzed by EF-G·GDP. The alternative view is that when EF-G·GTD binds to the non-ratcheted ribosome (MSI), it drives the ribosome into the ratcheted state, where GTP hydrolysis occurs. The last step of translocation is then catalyzed by EF-G in the GDP form. Furthermore, EF-G dissociates from the ribosome correlated with the opening of the L1 stalk. The opening of the L1 stalk is related to the release of the E-site tRNA (Spiegel *et al*., 2007).

The crystallographic work on EF-G and EF2 off the ribosome has identified several different conformations. Details are discussed in Sec. 9.3. The three N-terminal domains, G, G' and II, form a block whose internal interactions remain (Laurberg *et al*., 2000; Jørgensen *et al*., 2003). However, the tRNA-mimicking domains (IV and V) go through distinct movements. Domain III, the most mobile domain, moves independently (Jørgensen *et al*., 2003). Cryo-EM and crystallographic studies of EF-G bound to the ribosome confirm and extend these observations. Two types of complexes have been studied: with GDPNP/GDPCP or with GDP and fusidic acid (FA; Agrawal *et al*., 1998, 1999; Frank & Agrawal, 2000, 2001; Frank, 2003; Gao *et al*, 2003; Valle *et al*., 2003b; Gao *et al*., 2009; Tourigny *et al*., 2013). In addition, yeast ribosomes have been studied by cryo-EM in complex with yeast EF2 and sordarin (Gomez-Lorenzo *et al*., 2000).

Ribosomes in complex with EF-G or EF-2 show the factor bound to essentially the same site as the ternary complex between EF-Tu·GTP and aminoacyl-tRNA (Stark *et al*., 2002; Valle *et al*., 2002, 2003b; Schmeing *et al*., 2009; Gao *et al*., 2009; Tourigny *et al*., 2013). This agrees with the structural mimicry between the ternary complex and EF-G (Nissen *et al*., 1995; see Secs. 9.3 and 9.6). EF-Tu binds

to the canonical conformation (MSI) of the ribosome, while EF-G stabilizes the rotated conformation (MSII) of the ribosome (Spiegel *et al*., 2007; Ermolenko & Noller, 2011). When EF-G binds to the pre-translocational ribosome (MSII), the rotation of the small subunit is further increased (Agirrezabala *et al*., 2008). The authors also identify why EF-G cannot easily bind to the classical MSI conformation of the ribosome; domain IV of EF-G will collide with helix h34 of the 30S subunit. In a crystal structure with EF-G·GDPCP bound to the ribosome the small subunit has rotated 9° (MSII) with a tRNA in the P/E state (Table 8.4; Tourigny *et al*., 2013).

Domain IV of EF-G and EF2 binds to the decoding part of the A site in the structures with GDPNP, with GDP and FA or with sordarin (Fig. 11.8). This means that translocation has occurred in all studied complexes, even with GDPNP, which means without GTP hydrolysis. In complex with FA, EF-G is not able to dissociate from the ribosome despite the fact that GTP hydrolysis has occurred.

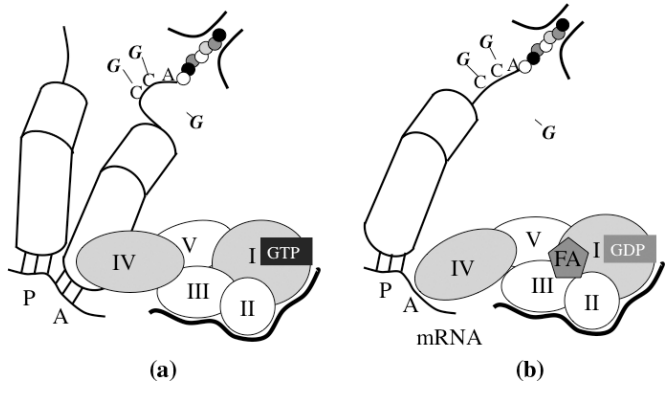

Fig. 11.8 A schematic representation of translocation. (**a**) EF-G in complex with GTP binds to the ribosome with the tRNAs in the A/P and P/E sites. (**b**) EF-G undergoes a conformational change and pushes the anticodon of the peptidyl-tRNA into the P site together with the mRNA. Domain IV occupies the decoding part of the A site. The figure illustrates the state after GTP hydrolysis. In this process the ribosome goes from the rotated MSII to the classical MSI state. In the presence of fusidic acid (FA) the factor remains bound for a long time.

These observations alone cannot discriminate between the two models for translocation. The classical model, where translocation precedes GTP hydrolysis (Spirin, 2002), agrees with the structural observations. However, in the alternative model, where GTP hydrolysis precedes translocation, even GDPNP is observed to slowly lead to translocation (Rodnina *et al*., 1997; Zavialov & Ehrenberg, 2003).

The changes in subunit orientation (MSII to MSI) and subunit structure during translocation are apparently inherent to the ribosome but can be catalyzed by the action of EF-G·GTP. The relative orientation of the two subunits changes by about 6°–9° (Table 8.4). Simultaneously, the structure of the small subunit is changed. The movements of the head domain and shoulder may be the most significant (see Sec. 8.6). The tip of domain IV of EF-G reaches the top part of h44, which undergoes a lateral movement of about 8 Å parallel to the path of the mRNA (VanLoock *et al*., 2000; Valle *et al*., 2003b; Gao *et al*., 2009). This leads to an opening and closing of the path for the mRNA in the structure of the 70S ribosome in a way that would simplify translocation of the mRNA. The translocation of the mRNA occurs during the clockwise rotation of the small subunit with regard to the large subunit from MSII to MSI (Ermolenko & Noller, 2011).

A full insight into the interplay between EF-G and the ribosome that leads to translocation is still lacking. However, a likely scenario is the following (Figs. 11.8 and 11.9):

(1) EF-G in complex with GTP binds to pretranslocation ribosomes (MSI or MSII) with the tRNAs in hybrid states. If in the MSI state, the ribosome is driven into the MSII state.
(2) Activation of the GTPase. Interactions and conformational changes of both ribosome and EF-G. His87 of switch II interacts with SRL. L12 CTD stabilizes the transition state.
(3) GTP hydrolysis (Rodnina *et al*., 1997). The mechanism is like the one for EF-Tu.
(4) Pi is released from EF-G·GDP. This step occurs simultaneously but independently of translocation. For certain mutants of L12 the Pi release is slow.

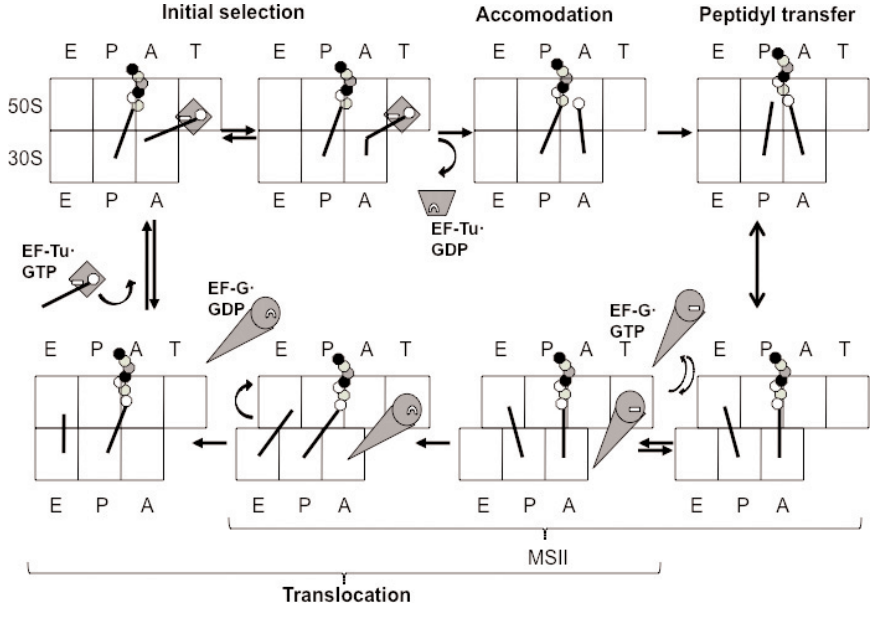

Fig. 11.9 A summary of the functional steps during elongation. The ribosome is in the MSI state except when indicated. The PTC is between the A and P sites on the large subunit.

(5) Translocation. During translocation, domain IV of EF-G moves into the decoding part of the A site. This stabilizes the tRNAs in standard states (P and E) and translocates the mRNA.
(6) The subunits return to normal orientation (MSII to MSI).
(7) EF-G·GDP dissociates from the ribosome.
(8) A new ternary complex (EF-Tu·GTP·aminoacyl-tRNA) can bind to the posttranslocation ribosomes and start a new cycle of elongation.

In the case of EF-G·GTP with FA, the process will halt, at step 7. EF-G with nonhydrolyzable analogs will also slowly proceed to this step, even though no GTP is hydrolyzed. In these cases EF-G remains bound to the ribosome and unable to dissociate.

The base-pairing of the tRNAs to the A and P loops guides the orientations of the CCA ends. When the CCA end of the peptidyl-tRNA

is rotated, the nascent peptide is also rotated, for the part nearest to the peptidyl-tRNA by 180°, and for the rest maybe less. It is also moved a slight distance into the exit tunnel (Bashan *et al.*, 2003). The rotation can be performed without sterical clashes. Two nucleotides close to the twofold rotation axis come into close contact with the rotating moiety. They are A2602 and U2585. The large conformational freedom of A2602 may be related to the rotational movement of the rotating moiety (Bashan *et al.*, 2003).

The Relationship between EF-Tu and EF-G

All trGTPases bind to overlapping sites, the GTPase site, of the ribosome. This is mirrored by the fact that they all have two domains in common — the G-domain and domain II, interacting with the 50S and 30S subunits, respectively. The mimicry between the ternary complex and EF-G is an extension of this similarity, and they can be regarded as twin molecules (Fig. 11.10). A number of observations are related to this fact:

- The factors bind to overlapping sites of the ribosome.
- EF-Tu binds to posttranslocation ribosomes (MSI), whereas EF-G binds to pretranslocation ribosomes (MSII).
- A correct match of codon and anticodon in the decoding site induces GTP hydrolysis for EF-Tu. For EF-G, GTP hydrolysis occurs directly upon binding. Translocation is achieved by domain IV of EF-G binding to the decoding part of the A site. The order of events for the two factors is reversed.
- EF-G·GDP dissociates from a site that fits for the ternary complex EF-Tu·aa-tRNA·GTP.
- The trypsin susceptibility of L12 is different when EF-Tu is bound to the ribosome with GDPNP or kirromycin. This trypsin sensitivity is opposite to what is found when EF-G is bound with GDPNP or FA (Gudkov & Gongadze, 1984; Gudkov & Bubunenko, 1989).

In the large family of GTPases, there is a considerable variation in the size and sequence of the effector loop. This is most certainly

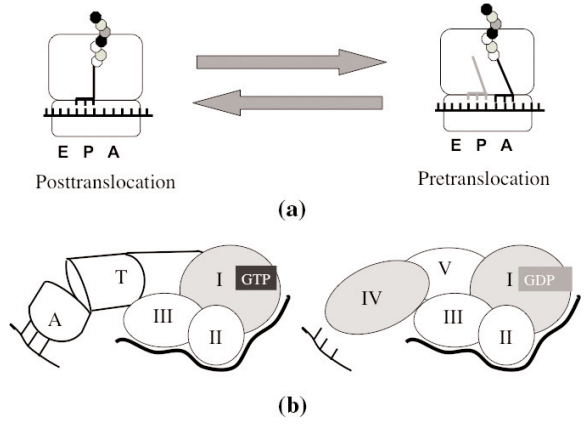

Fig. 11.10 (**a**) The ribosome oscillates between the pre- and posttranslocation states. EF-Tu and EF-G have reciprocal roles in binding to overlapping sites on the ribosome. (**b**) EF-Tu binds to the posttranslocated ribosome and hydrolyzes its GTP molecule when a cognate interaction has occurred between codon and anticodon in the decoding site. EF-G hydrolyzes its bound GTP immediately after it has bound to the pretranslocated ribosome. Subsequently, translocation occurs by moving domain IV of EF-G into the decoding region.

due to its interaction with very different receptors. However, the effector loops of EF-Tu and EF-G have a high degree of sequence identity. Thus, one could expect that this loop could be exchanged between the two proteins. This is, however, not possible. A hybrid EF-G with the effector loop of EF-Tu does not support protein synthesis despite the fact that it binds to the ribosome and can hydrolyze GTP (Kolesnikov & Gudkov, 2002). Presumably, despite the similarities, there are important differences between the effector loops, which enable EF-Tu to interact with posttranslational ribosomes and EF-G with pretranslocation ribosomes.

11.5 TERMINATION

Termination of protein synthesis depends on the exposure of one of the three stop codons UAA, UAG and UGA in the decoding part

of the A site. In bacteria, the class I release factor RF1 responds to the stop codons UAA and UAG while RF2 responds to UAA and UGA. The release factors decode the stop codons and hydrolyze the completed peptide from the P-site tRNA. The hydrolysis may be induced directly or indirectly (Nakamura & Ito, 2003). Eukarya have a single class I release factor, eRF1, without any structural relation to the bacterial release factors (see Sec. 9.4). The class II release factor RF3 in bacteria and eukarya catalyzes the dissociation of the class I release factors from the ribosome after hydrolysis of the ester bond connecting peptide and P-site tRNA (Zavialov *et al*., 2001, 2002; Freistroffer *et al*., 1997). This factor is lacking in some bacterial species (see Table 9.2).

RF3·GDP binds to termination complexes with ribosome-bound RF1/2 and a deacylated tRNA in the P site (Zavialov *et al*., 2001, 2002; Zavialov & Ehrenberg, 2003). If the peptide is not hydrolyzed, RF3 cannot exchange its GDP for GTP (Zavialov & Ehrenberg, 2003). When the peptide is hydrolyzed, RF3 can exchange its GDP for GTP, release RF1/2 from the ribosome, and subsequently hydrolyze its GTP to GDP and be released from the terminated ribosome. Evidently, when the peptide is released from the P-site tRNA, the ribosome undergoes a conformational change, allowing the nucleotide exchange (Gao *et al*., 2007). It is the class I RF bond to the ribosome that acts as nucleotide exchange factors.

Class I Release Factors

The structures of class I release factors were expected to resemble those of tRNAs. In eRF1, the location of GGQ (see Sec. 9.4) was at one extreme of the Y-shaped structure and the potential decoding region at the extreme end of another domain (Song *et al*., 2000). The structure of bacterial RF2 made it clear that the eukaryotic and bacterial release factors have no structural similarity (Plate 9.14). Secondly, the two supposed functional sites, corresponding to the extreme ends of a tRNA, were no more than 23 Å apart (Vestergaard *et al*., 2001).

Contrary to expectation, the class I release factors have no structural resemblance to tRNA molecules when bound to the ribosome,

either in shape or in the manner they are bound (Laurberg *et al*., 2008; Weixlbaumer *et al*., 2008; Korostelev *et al*., 2010). The crystal structures of the isolated proteins are different from their conformation in solution and when bound to the ribosome (Vestergaard *et al*., 2005). The domains become oriented so that they place the functional regions in their expected locations. The 'anticodon mimicry' motif (Ito *et al*., 2000) is in the decoding site of the small subunit. The common sequence GGQ is placed at the PTC. The release factors activate a water molecule in the PTC to hydrolyze the ester bond between the tRNA and the completed peptide.

The ribosomal conformation is the classical, nonrotated MSI. Evidently, the binding of class I release factors and peptide hydrolysis does not change the subunit orienation from the state after the terminal translocation step (Table 8.4).

The three stop codons all begin with a U. A and G in this position would collide with two conserved glycines of the tip of helix 5 of RF1, and a C could not hydrogen-bond properly. The U hydrogen bonds to the protein in a manner similar to an A:U base pair for both class I factors (Plate 11.3; Korostelev, 2011). In the presence of class I release factors, the third base of the stop codon swings away from its anticodon-recognizing position to interact with other residues of the factors. This is due to a loop of the codon-recognizing peptides of the factors that inserts between bases 2 and 3 of the stop codon. In both cases a histidine stacks on the second base (Plate 11.4). Furthermore, the third base of the stop codon stacks on G530, normally important in the recognition of cognate anticodons (Plate 11.5). The A or G in the third position hydrogen-bonds specifically with conserved side chains outside the anticodon mimicry motifs (Korostelev, 2011; Klaholz, 2011). Pyrimidines in the third position are discriminated against, due to their inferior stacking and hydrogen-bonding potential (Weixlbaumer *et al*., 2008). The universally conserved nucleotides A1492 and A1493 do not participate as they do in the recognition of sense codons, but stabilize the interaction with the factors.

The Thr and Ser of the PxT and the SPF motifs are engaged in specific hydrogen bonding, whereas the hydrophobic residues are involved in van der Waals interactions (Plate 11.3). For RF1 the threonine of the PxT motif and the protein backbone

hydrogen-bonds to U1. Both the proline and the threonine interact with A2 (Laurberg *et al*., 2008). In RF2 the serine of the SPF motif makes contact with the second base of the codon and can hydrogen-bond to A2 as well as G2. Neither RF1 nor RF2 can form hydrogen bonds to U or C in this position. Thus, the concept of 'tripeptide decoding' is not as simple as initially thought (Ito *et al*., 2000; Nakamura & Ito, 2002; Sund *et al*., 2010).

In the conformation of RF1 and RF2 when bound to the ribosome, interacting with their appropriate stop codons, there is a specific interaction of a switch loop of the release factor, protein S12. The conserved nucleotides A1913, A1492 and A1493 of the ribosome stabilize the catalytic conformation of the factors (Laurberg *et al*., 2008; Weixlbaumer *et al*., 2008; Korostelev *et al*., 2008, 2010; Korostelev, 2011; Klaholz, 2011).

Peptide Hydrolysis

Several crystal structures describe the state after the release of the peptide from the P site tRNAs (Laurberg *et al*., 2008; Weixlbaumer *et al*., 2008; Korostelev *et al*., 2010). However, one analyses the structure of a bound aminoacyl-NH-tRNA in the P site (Jin *et al*., 2010). Furthermore, in the crystal structures the glutamine of the GGQ motif does not seem to have the methylation modification (Sec. 9.4). This makes attempts to understand the mechanism of hydrolysis difficult. The completely conserved GGQ motif is part of a loop of domain 3 of the factors and is placed in the PTC of the ribosome. The two glycines have unique conformations that only glycines can adopt, which may explain why they are conserved (Weixlbaumer *et al*., 2008). They are placed next to the A76 of the CCA end of the P site tRNA. The GGQ loop displaces U2585, while U2506 leaves the ester bond of the peptidyl-tRNA open for hydrolytic attack, contrary to the situation during peptidyl transfer. The glutamine of the GGQ loop is in the same position as the ester and aminoacyl groups of an aminoacyl-tRNA bound to the A site (Plate 11.6; Korostelev, 2011). Mutations of the glutamine side chain have only minor effects (Seit-Nebi *et al*., 2000; Seit-Nebi *et al*., 2001; Shaw & Green, 2007). A major role for the glutamine side chain may

therefore be excluded. Furthermore, the role of the methylation of the side chain may be related to the binding of the factor rather than to hydrolysis (Korostelev, 2011). However, the peptide nitrogen of the GGQ glutamine is at a position where it can interact with and stabilize the transition state tetrahedral intermediate (Laurberg *et al*., 2008; Trobro & Åquist, 2009). Substitution of the glutamine with proline eliminates the hydrogen-bonding capacity of the NH group and the peptide relase activity (Korostelev *et al*., 2008). As for other functions of translation, one can expect that the ribosome participates actively in termination. Thus, mutations of A2602 in the PTC reduce the peptide release activity significantly, whereas mutations affecting other residues in this site (A2451 and U2585) have little effect (Polacek *et al*., 2003; Nakamura & Ito, 2003).

Hydrolysis of the peptide requires the activation of a water molecule appropriately placed (Fig. 11.11). Here the molecular dynamics

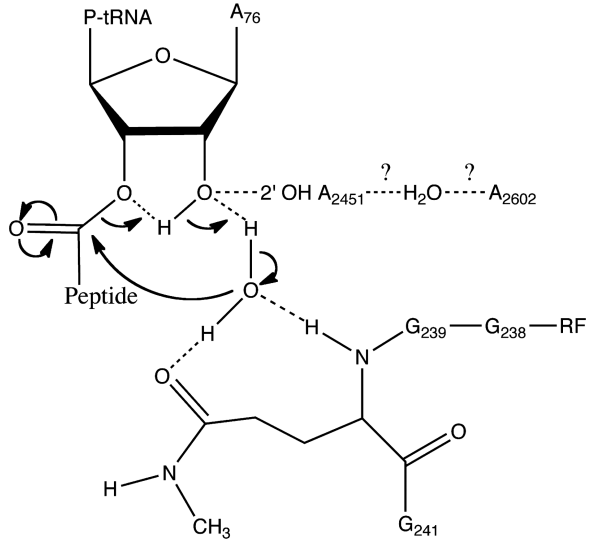

Fig. 11.11 The possible interactions in the PTC during peptide hydrolysis. (Reprinted with permission from Jin *et al*., Structure of the 70S ribosome bound to release factor 2 and a substrate analog provides insight into catalysis of peptide release. *Proc. Natl. Acad. Sci. USA* **107**: 8593–8598. Copyright 2010, National Academy of Sciences.)

calculations may bridge the gap between the crystal structures of the completed reaction and what happens during the reaction. The glutamine and the 2′OH of A76 can hydrogen-bond to the water molecule and position it for inline attack on the ester bond (Trobro & Åqvist, 2007, 2009; Laurberg *et al.*, 2008; Weixlbaumer *et al.*, 2008). It is worth noting that the terminal 2′OH of the P-site tRNA is involved in both peptidyl transfer and peptide hydrolysis.

Class II Release Factors

The role of RF3 is to release RF1 and RF2 from the post-termination ribosome (Fig. 11.12). RF3 is a tGTPase with the classical G-domain

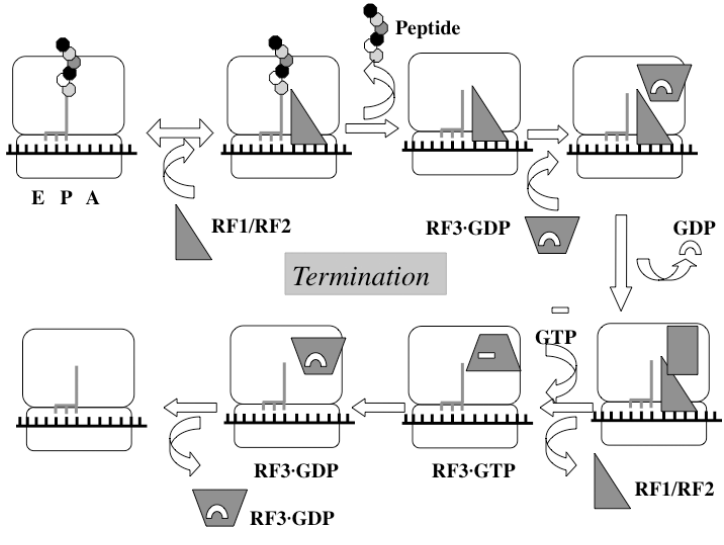

Fig. 11.12 The steps involved in termination of protein synthesis. The ribosome on the top left in the classic state (MSI) has a stop codon in the A site. RF1 or RF2, depending on the stop codon, binds to the A site and releases the peptide. To remove RF1/RF2, a tGTPase, RF3, is normally needed. It binds in complex with GDP to the ribosome which functions as a GEF and replaces GDP with GTP. The associated conformational change of the factor and the ribosome to MSII will cause RF1/RF2 to dissociate. Subsequently, RF3 hydrolyzes its GTP to GDP and dissociates from the ribosome.

and a domain II (Ævarsson, 1995). Its mode of action is somewhat unorthodox. It binds to the ribosome in complex with GDP (Zavialov *et al*., 2001). Then, the class I RF bound to the ribosome first acts like a GEF to replace GDP with GTP and subsequently, in the MSII state, as a GAP to induce GTP hydrolysis. This leads to the dissociation of the release factors from the ribosome (Zavialov *et al*., 2002).

RF3 has been studied when bound to the 70S ribosome by cryo-EM (Klaholz *et al*., 2004; Gao *et al*., 2007; Pallesen *et al*., 2012) and by crystallography (Jin *et al*., 2011; Zhou *et al*., 2012). A number of different conformations have been observed.

One of the crystal structures was with an mRNA composed of a start and stop codon and an fMet-tRNA in the P site, and RF3·GDPCP bound to the site for trGTPases (Jin *et al*., 2011). The RF1 added to the ribosome before crystallization could not be seen. The tRNA is seen in the P/E site with the CCA end of the deacylated fMet-tRNA in the E site. The 30S subunit has rotated in the counterclockwise orientation by 9.3° (MSII) and the head of the 30S subunit has rotated by 2.9° in relation to the body (Table 8.4). RF3 binds at the subunit interface much the same way as EF-G binds. The G-domain and the GTP analog are close to the SRL. Domain III of RF3 is rotated as much as 57° from its orientation in the structure of RF3·GDP in isolation. This places domain III near the shoulder of the 30S subunit and is probably due to the binding of a GTP analog with associated conformational changes of switches I and II. The intersubunit rotation leads to steric clashes between both subunits and release factors of class I that have to dissociate. However, there are no direct major clashes between the class I and II release factors.

The other crystal structure contains 70S ribosomes, an RF3 in complex with GDPNP and an mRNA (Zhou *et al*., 2012). A deacylated tRNA molecule was lost from the ribosome during crystallization. Here the 30S subunit is rotated by 7° with regard to the 50S subunit and a more dramatic rotation of the head of the small subunit by 14° (Table 8.4). Zhou *et al*. (2012) have provided a detailed list of the subunit bridges in both the MSI and MSII

conformations, which differ between the present structures. This may be due to slightly different states as well as the relatively low resolution of the investigations. H69 undergoes a rotation to preserve the B2a subunit bridge in MSII (Zhou *et al*., 2012). The C-terminal helix of L10 with four N-terminal domains of L12 is seen in a new orientation rotated about 60° from a previously identified orientation (Gao *et al*., 2009).

Here, RF3 binds in a somewhat different manner from EF-Tu and EF-G. RF3 has more contacts with proteins L6 than the L11 stalk and a different orientation of the G-domain by about 45° in relation to SRL (Zhou *et al*., 2012). Furthermore, switch I is ordered. The large rotation of domain III in relation to domains G and II is seen also in this investigation.

In addition, a cryo-EM study with both RF1 and RF3·GDP bound to the ribosome has been made (Pallesen *et al*., 2012). Two states were characterized. In one, RF1 and RF3, without nucleotide, are bound. This corresponds to the nucleotide-exchanging state of RF3 and is in the MSI conformation. In the other state, RF3 is bound with GDPNP. Here the ribosome is in the MSII conformation, which causes RF1 to clash with the ribosome and fall off.

Interestingly, a density is interpreted as the CTD of one L12 molecule (Pallesen *et al*., 2012). It may be involved in recruiting RF3 to the ribosome and keeps interacting with RF3 in both states, but with different orientation. When RF3 is bound with GDPNP, the CTD of L12 forms a bridge to the NTD of L11.

11.6 RIBOSOME RECYCLING

When the ribosome has reached a stop codon and the peptide is released, the extensive machinery of the ribosome has to be reused. For this, the mRNA and the deacylated tRNA have to be released. Since the mRNA is threaded through the tunnel between the subunits and in intimate contact with the neck region of the small subunit and the deacylated tRNA has tight interactions in the P site, the subunits would need to dissociate. Furthermore, for

a new initiation, they have to be separated, since the initiation starts with the small subunit alone. The ribosome-recycling factor (RRF) participates in this process together with EF-G (Karimi *et al.*, 1999; Zavialov & Ehrenberg, 2003). RRF is composed of two domains, with a fair amount of flexibility between them (Sec. 9.5; Vesper & Wilson, 2006).

The RRF, which mimics tRNA, does not bind like a tRNA to the ribosome. The footprinting of the RRF on the ribosome using the Fe-EDTA method suggested that RRF binds in an unexpected manner across both the A and P sites for tRNA (Lancaster *et al.*, 2002). A deacylated tRNA in the P site would have to move to the P/E hybrid site.

The *T. thermophilus* RRF (ttRRF) does not function in *E. coli* (Toyoda *et al.*, 2000). Mutants that would make it functional in *E. coli* are concentrated around the hinge between the two domains (Toyoda *et al.*, 2000; Ito *et al.*, 2002). In particular, a deletion of five C-terminal residues was part of this group of mutants (Fujiwara *et al.*, 1999). The mutations around the hinge region suggest that the flexibility of the molecule is functionally important.

The interaction with EF-G on the ribosome has been analyzed by various means. The RRF from *Mycobacterium tuberculosum* will not function in *E. coli*. However, if this factor is complemented by EF-G from the same species, function is regained (Rao & Varshney, 2001). This suggests a direct contact during the functional cycle. The same pairwise dependence exists for the *T. thermophilus* factors (Ito *et al.*, 2002). Mutants of *E. coli* EF-G that enable a functional interaction with ttRRF are localized to one side of domain IV, which is also essential for translocation. However, these mutations are distinct from mutations in domain IV, which lead to a low rate of translocation (see Table 9.7).

Cryo-EM studies have been made of RRF bound to the 70S ribosome (Agrawal *et al.*, 2004; Gao *et al.*, 2005) or to the 50S subunit together with EF-G (Gao *et al.*, 2007). Crystal structures have also been determined of the RRF bound to the 50S subunit or to the 70S ribosome (Wilson *et al.*, 2005; Borovinskaya *et al.*, 2007; Weixlbaumer *et al.*, 2007; Pai *et al.*, 2008; Dunkle, 2011). In one

crystal structure, the P site has only an ASL structure. In addition, there is a partially occupied tRNA in the E site, but in a new orientation (Plate 11.7; Weixlbaumer *et al*., 2007).

When bound to the ribosome, the RRF retains its L shape, as in the structure off the ribosome. Domain I of the RRF overlaps with the site of the acceptor ends of both P and A site tRNAs, and forces the tRNA into the P/E site (Plate 11.7). The ribosome then adopts the rotated MSII configuration (Plate 11.5; Lancaster *et al*., 2002; Wilson *et al*., 2005; Gao *et al*., 2005; Dunkle *et al*., 2011). The swivel rotation of the head toward the E site is associated with the P/E hybrid state of the tRNA. The mRNA and the ASL of the tRNA are shifted about 6 Å from their normal location. A kink between the ASL and the D-stem allows the tRNA to swing into the 50S part of the E site. Domain I of the RRF is important for the binding to the ribosome and interacts with several parts of 23S RNA as well as proteins S12, L16 and L27 (Weixlbaumer *et al*., 2007). The tip of domain I interacts with the P-loop of the 23S RNA, while domain II interacts with protein S12 (Dunkle *et al*., 2011).

The simultaneous binding of EF-G and the RRF to the 50S subunit studied by cryo-EM gives further insight into the recycling process (Plate 11.8; Gao *et al*., 2007). The subunit binds the RRF and EF-G*GDPNP cooperatively despite the fact that the binding of both to the 70S ribosome is incompatible (Gao *et al*., 2007; Dunkle *et al*., 2011). EF-G binds to the 50S subunit in its normal conformation. Here domains IV and V overlap with the position of domain II of the RRF. This causes a significant conformational change of the RRF. Domain II rotates by 60° from its initial orientation and forms a closed structure with domain I. The hinges between the two domains of RRF interact with domain III of EF-G. In particular, the conserved loops of domain III of EF-G interact with conserved residues in the hinge region of RRF. Domain II of the RRF has a large interface with domain IV of EF-G. Domain IV of EF-G may force the RRF by electrostatic repulsion to adopt this new conformation (Gao *et al*., 2007). The mutational studies of EF-G for residues of functional importance in relation to the RRF have identified this interface

(Ito *et al*., 2002). The new conformation of the RRF disrupts the subunit bridges B2a and B3 (Gao *et al*., 2007). After GTP hydrolysis the altered conformation of EF-G will clash with the RRF and separate the ribosomal subunits from each other.

The disassembly of the ribosomal subunits by the RRF and EF-G*GTP is inhibited by fusidic acid (FA), which inhibits the conformational change of EF-G and its release from the ribosome (Hirashima & Kaji, 1973; Hirokawa *et al*, 2002, 2005; Savelsbergh *et al*., 2009). Recycling is also inhibited by vanadate, an analog of phosphate (Savelsbergh *et al*., 2009). The interpretation is that at increasing concentration vanadate will bind to the phosphate-binding site on EF-G and prevent the important steps of the action on the RRF induced by phosphate release.

Ribosomal recycling begins with the binding of the RRF inducing the MSII state of the ribosome. This is recognized by EF-G·GTP, which binds and forces the RRF to change its conformation. After GTP hydrolysis EF-G changes its conformation and, together with the bound RRF, the subunit contacts will break (Zavialov & Ehrenberg, 2003).

12

Protein Processing, Folding and Targeting

When a nascent chain (NC) is emerging from the peptide exit channel, a number of activities will proceed to make the protein ready for its tasks, inside or outside the cell or perhaps located in a membrane. The exit site of the ribosome is unusually rich in ribosomal proteins and includes L17, L19, L22, L23, L24, L29 and L32. The enzymes peptide deformylase (PDF) and methionine aminopeptidase (MAP) bind at the exit site to process the exiting polypeptide, trigger factor (TF) engages in the folding of the peptide and the signal recognition particle (SRP) and the translocon (SecYEG) or protein-conducting channel (PCC) will identify the destination of the protein and bring it there. These different proteins or complexes cannot bind to the ribosome at the same time, since their binding sites are partly overlapping (Plate 12.1; Selmer & Liljas, 2008; Giglione *et al*., 2009; Kramer *et al*., 2009).

12.1 PROCESSING OF THE NASCENT PEPTIDE

Peptide Deformylase

Normally, the N-terminus of a polypeptide that is synthesized on the ribosome has a formylated methionine. This formyl moiety protects the amino group from unwanted side reactions and is

normally removed by PDF as soon as it emerges from the ribosomal exit site (Adams, 1968; Ball & Kaesberg, 1973). The structures of the enzyme from several species have been determined (Guilloteau *et al*., 2002; Escobar-Alvarez *et al*., 2009; Nam *et al*., 2009). The enzyme is essential in bacteria and therefore a target for antibiotics. PDF is a single-domain 20 kDa zinc enzyme. The binding of PDF to the ribosome has been studied (Bingel-Erlenmeyer *et al*., 2008). A C-terminal α-helix is the ribosome-binding module of PDF. Crystals of *E. coli* ribosomes were studied with the bound helix. It is located at the exit site, in a groove between ribosomal proteins L22 and L32. The known structure of PDF was placed according to the position of the C-terminal helix. This positions the active site of PDF toward the exit site. Thirteen amino acid residues in an extended conformation could span the distance.

Methionine Aminopeptidase

MAP removes the N-terminal methionine from the NC (Ball & Kaesberg, 1973). Structures of MAP are known to have a 'pita-bread' fold and an active site with two metal ions (Roderick & Matthews, 1993; Ye *et al*., 2006). MAP can loosely associate with the ribosome and perform the hydrolysis while the peptide chain emerges from the exit channel. The binding site is not well characterized. No known RNA or protein recognition motif has been identified in the catalytic domain of MAP. Therefore the N-terminal extension that has been characterized in the enzyme from *Mycobacterium tuberculosis* could contain the binding feature. This extension, lying on the surface of the enzyme, has a sequence, PxxP, with a poly-Pro II configuration. SH3 domains often recognize this type of structure (Zarrinpar *et al*., 2003). Ribosomal protein L24 has such an SH3 domain suitably placed to bind MAP near the peptide exit site (Plate 12.1; Addlagatta *et al*., 2005).

12.2 FOLDING OF THE NASCENT CHAIN

A newly synthesized protein is exposed to the crowded environment in the cell. The protein concentration is about 300 mg/ml and

the environment is hostile due to a large number of proteolytic enzymes. If the protein is not properly folded, it may aggregate or be degraded. Thus, proper folding of the NC is an important aspect of translation. It is also of significant interest whether it can fold inside the peptide exit channel.

The NC has to pass through the exit tunnel before it is exposed to the cytoplasmic environment. Between 30 and 70 amino acid residues of the NC can be contained in the tunnel, depending on the secondary structure of the polypeptide (Kramer *et al*., 2001). The tunnel is 80–100 Å long and 10–20 Å wide (Nissen *et al*., 2000; Harms *et al*., 2001; Gabaswili *et al*., 2001). It is for the most part hydrophobic and stably built but has some flexible zones (Berisio *et al*., 2003b; Voss *et al*., 2006; Fulle & Gohlke, 2009). The zone where proteins L4 and L22 form a constriction is the most rigid one. The construction of the large subunit, with six interwoven domains of 23S RNA, limits the flexibility of the inner part of the subunit and the tunnel. The lack of flexibility suggests that there cannot be enough space for the folding of tertiary protein structures.

The twofold symmetry of the PTC with the CCA ends of A site and P site tRNAs (see Chap. 8) requires that amino acid residues that have just been linked into a peptide have a twofold relation, i.e. they are fully extended as in a β-strand. It is unlikely that translocation can force the entire NC to obey the same twofold rotation. Therefore, at some distance from the PTC the growing peptide may adopt a different conformation.

Depending on the sequence and composition of a protein, both extended and helical conformations have been seen in the tunnel of eukaryotic ribosomes (Woolhead *et al*., 2004). Theoretical calculations suggest that helical conformations are stabilized in the tunnel (Ziv *et al*., 2005). By model building, an α-helix of 41 amino acids could be placed in the tunnel (Voss *et al*., 2006). Observations of the NC with a high propensity for an α-helix by cryo-EM on wheat germ ribosomes suggest that NC is unfolded in the upper part of the peptide exit tunnel, whereas it can be helical closer to the opening (see Chap. 8; Bhushan *et al*., 2010; Wilson & Beckmann, 2011). In a study of the folding of green fluorescent protein (GFP) and some of its relatives with a different color, the proteins were

extended at the C-terminus to establish when proper folding was achieved and fluorescence observed (Kelkar *et al*., 2012). The result was that 45 residues beyond the C-terminus were required for proper folding of the protein and expression of fluorescence. Obviously, no part of the protein could be trapped in the exit tunnel for the protein to be properly folded.

Protein folding may begin already as the peptide is passing through the lower part of the peptide exit tunnel of the ribosome and be completed spontaneously when it emerges from the exit tunnel. However, in many cases, chaperones are needed for the proper folding of the emerging polypeptide (Hartl & Hayer-Hartl, 2002). Several types of chaperones are induced by thermal stress. This has given them the name 'heat shock proteins' (Hsp). Some chaperones interact directly with the ribosome and the NC both in prokaryotic and eukaryotic systems (for a review see Frydman, 2001). The sites identified by the chaperones are exposed hydrophobic regions. In bacteria, the NC can primarily interact with small or "holding" chaperones that bind to ribosomes. TF and DnaK belong to this class (Deuerling *et al*., 1999; Teter *et al*., 1999; Hoffmann *et al*., 2010). These are proteins that primarily prevent the aggregation of the growing polypeptide. In many cases, the interactions with these chaperones are sufficient for the proper folding of the protein. In other cases, interactions with the more complex oligomeric ring-shaped chaperonins like GroES/Hsp60 are needed for the proper folding of the protein. These are not known to interact with the ribosome.

Trigger Factor

TF is a bifunctional protein. It is a chaperone and a peptidyl-prolyl-cis/trans isomerase (PPIase; Bang *et al*., 2000; Frydman, 2001). It binds to the ribosome and participates in the correct folding of the NC (Lill *et al*., 1988; Bukau *et al*., 2000). It is probably the first chaperone to interact with the NC and protects it from aggregation or misfolding as it emerges from the ribosome (Fig. 12.1; Kramer *et al*., 2002b; Hoffmann *et al*., 2006; Tomic *et al*., 2006). *In vitro* studies indicate that TF can bind to the ribosome waiting for peptides to

emerge. However, *in vivo* studies suggest that TF is not recruited until about 100 amino acid residues are translated (Oh *et al*., 2011).

TF copurifies with a large number of proteins of different sizes (8–120 kDa), including several ribosomal proteins (Martinez-Hackert & Hendrickson 2009; Hoffmann & Bukau, 2009). Most of the TF substrates are components of larger complexes such as the ribosomal subunits. The ribosomal proteins associating with TF have long N- or C-terminal tails or extended internal loops and belong to proteins that are late in the assembly of the small subunit (Martinez-Hackert & Hendrickson, 2009; Held *et al*., 1974). These extended features are frequently highly positively charged (Liljas, 1991). TF may function as a ribosome assembly factor, which binds and protects its substrates until they are assembled into their complexes. This would explain why TF is found in two- to three-fold molar excess over ribosomes (Lill *et al*., 1988). It has also been observed that TF seems to have a special role in the folding of β-barrel outer-membrane proteins (Oh *et al*., 2011).

The crystal structures of TF from *E. coli* (Ferbitz *et al*., 2004) bound to the large subunit of *H. marismortui* ribosomes and from *T. maritima* in complex with a substrate, ribosomal protein S7 (Martinez-Hackert & Hendrickson, 2009), have been determined. The elongated protein is composed of three domains. The N-terminal domain (NTD; residues 1–110) contains the ribosome-binding loop, the middle domain (residues 147–229) is the PPIase domain, with homology to FK506-binding proteins, and the C-terminal domain (CTD; 111–146 and 230–425) is related to the chaperone SurA (Bitto & McCay, 2002; Schultze-Gahmen *et al*., 2005). The PPIase domain is not needed for the chaperone activity (Li *et al*., 2001; Genevaux *et al*., 2004; Kramer *et al*., 2004).

The structure of TF-S7 is composed of two copies of TF, binding two copies of S7, but 1:1 complexes are also seen in solution. The dimerization is substrate-mediated. The orientation of the TF domains or segments is flexible, depending on its state (Martinez-Hackert & Hendrickson, 2009). The substrate, S7, binds in its native conformation through hydrophilic interactions with TF. CTD forms a concave structure that holds the substrate, and NTD

contributes to the binding in the dimer (Plate 12.2). A total surface area of 4520 Å^2 gets buried in the binding of S7, which is about three times bigger than a normal specific interface. However, the interface is poorly packed and the contact specificity is low. The same concave surface must also be used on the ribosome as a hydrophilic 'Anfinsen cage' (Martinez-Hackert & Hendrickson, 2009). However, TF also exposes hydrophobic residues in the concave cavity and the affinity of TF for different peptides has been investigated (Patzelt *et al.*, 2001; Rutkowska *et al.*, 2008). It was found that TF binds weakly to peptides with aromatic and positively charged amino acids. This agrees with the observation of both hydrophobic and hydrophilic binding surfaces (Martinez-Hackert & Hendrickson, 2009).

The structure of TF-NTD bound to the 50S subunit has also been studied (Ferbitz *et al.*, 2004; Baram *et al.*, 2005). The factor interacts with proteins L23 and L29, to which it also has been cross-linked at the opening of the exit tunnel on the external surface of the large subunit (Plate 12.1; Kramer *et al.*, 2002b). A mutation in L23 can destroy the interaction with TF (Kramer *et al.*, 2002b). Observations by neutron scattering indicate that TF also can bind to the ribosome as a homodimer (Blaha *et al.*, 2003).

In summary, TF deviates from classical chaperones in several ways. It binds the substrate not primarily through hydrophobic interaction but rather through hydrophilic interactions with the substrate in its native conformation. TF may have an important function in assembly of larger complexes such as the ribosomal subunits. The release of substrates does not need ATP. The complex with TF dissociates since the interaction with the complex to which the substrate belongs is more favorable than the binding to TF (Martinez-Hackert & Hendrickson, 2009).

Chaperones Involved in the Folding of the Nascent Polypeptide

When the NC is released from the ribosome, it may not be properly folded, but exposes hydrophobic surfaces. Chaperones, like

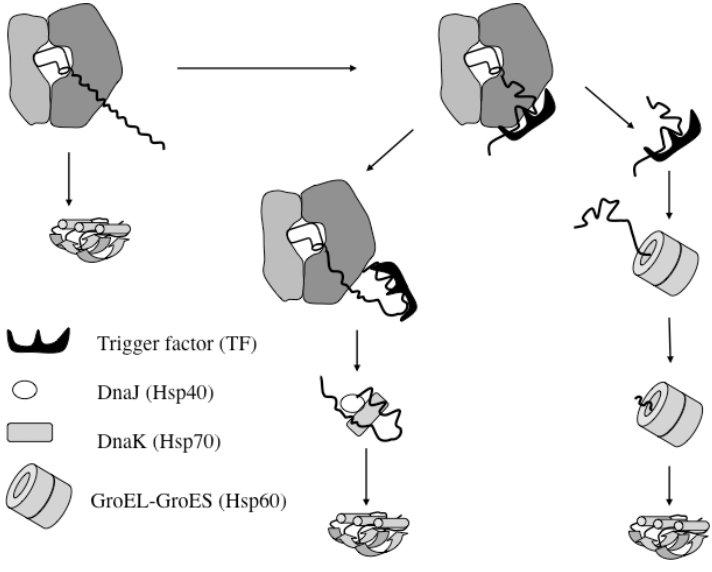

Fig. 12.1 Different folding pathways of the NC. The polypeptide may fold spontaneously, after interaction with trigger factor or after ATP-dependent folding assisted by chaperones DnaK/DnaJ (Hsp70/Hsp40) or GroEL/GroES.

DnaK/DnaJ and GroE in addition to TF, may then interact with the peptide (Fig. 12.1). Their structures and functions are studied in detail (see e.g. Liljas *et al.*, 2009), but the details are beyond the topics for this book.

DnaK belongs to the Hsp70 family of chaperones and is a very abundant ATPase (Herendeen *et al.*, 1979). Its role partly overlaps with that of TF (Teter *et al.*, 1999; Deuerling *et al.*, 1999). The simultaneous deletion of the genes for TF and DnaK is lethal (Teter *et al.*, 1999; Deuerling *et al.*, 1999). A nascent peptide that interacts with TF may also interact with DnaK (Albanese & Frydman, 2002). However, DnaK is not recruited to ribosomes that lack TF (Kramer *et al.*, 2002a). In bacteria, DnaJ (a member of the Hsp40 family of chaperones) is a cochaperone that assists DnaK and induces its ATPase activity, while GrpE catalyzes the nucleotide exchange of DnaK (Suh *et al.*, 1999). The J-domain of DnaJ induces the ATP

hydrolysis in DnaK that leads to high affinity for the polypeptide (Fig. 12.1). The nucleotide exchange assisted by GrpE leads to polypeptide release (Harrison *et al*, 1997). Both TF and DnaK can be cross-linked to nascent polypeptides (Schaffitzel *et al*., 2001).

GroE is a double-barreled chaperone composed of two rings of seven GroEL subunits (Xu *et al*., 1997; Harrison, 1997; Saibil & Ranson, 2002). Substrates for folding bind in the GroEL barrel on one side (Fig. 12.1). Associated with the binding of the seven GroES subunits as a lid of the barrel and ATP hydrolysis, the peptide is folding inside this Anfinsen cage and is subsequently released. During this process a second, unfolded peptide can bind in the opposite barrel. The GroE system works like a two-cylinder engine.

12.3 TRANSPORT OF THE NASCENT POLYPEPTIDE

About 25–30% of bacterial proteins function in membranes or outside the cell. Proteins are synthesized in the cytoplasm and then transported to their final destination by either of two complex transport systems (Fig. 12.2; Walter and Blobel, 1980, 1982; Driessen & Nouwen, 2008; Cross *et al*., 2009). In both pathways protein factors maintain the substrate in a transport-competent condition.

One transport system, where the ribosome does not interact, is due to proteins that initially interact with TF and where translation is completed. Here a tetrameric chaperone, SecB, picks up the unfolded protein. Through interactions with a clamp-formed ATPase, SecA and SecYEG, the protein is transported out of the cytoplasm (Zimmer *et al*., 2008; Driessen & Nouwen, 2008). Since the ribosome is not directly involved, we will not discuss this route further.

In the main transport system, the proteins are transported while they are synthesized. A protein to be secreted has a tag, an N-terminal extension, which is a signal sequence of 20–30, generally hydrophobic, amino acids (von Heine, 1990). This signal peptide contains information about the final destination of the protein and is initially recognized by the soluble signal recognition

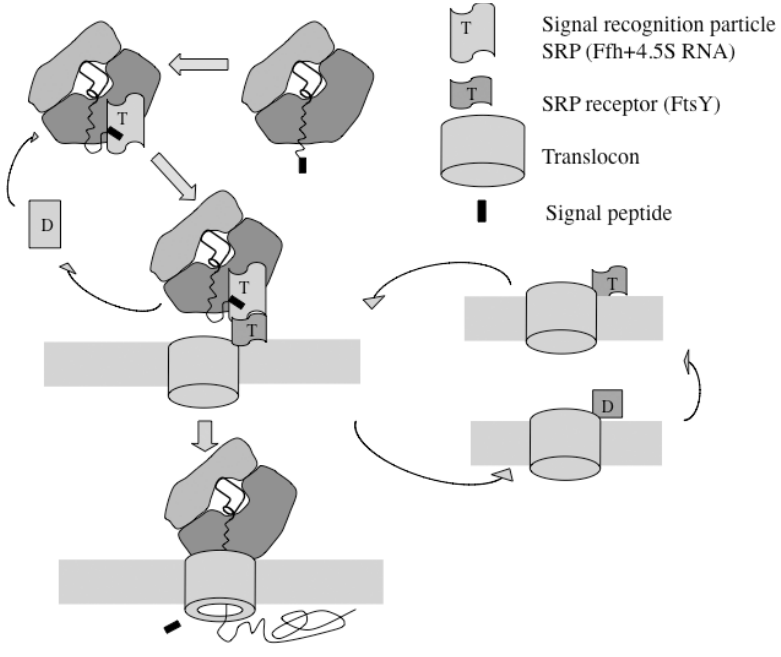

Fig. 12.2 SRP and SR participate to transport a protein out of the cytoplasm (after Bates *et al*., 2000; Keenan *et al*., 2001). The letters T and D on the symbols for the SRP and the SRP receptor represent GTP and GDP, respectively.

particle (SRP) in the cytoplasm. SRP makes a complex with the signal recognition particle receptor (SR; a membrane-associated protein) and the SecYEG, a protein-conducting channel (PCC) in the membrane that permits export of the protein to its final destination (Keenan *et al*., 2001; Calo & Eichler, 2011). The ribosome interacts with several components of this transport machinery.

Signal Recognition Particle

The signal peptide is recognized for both its α-helical structure and its hydrophobicity. It may adopt a helical conformation already during its passage through the exit channel (Woolhead *et al*., 2004; Bhushan *et al*., 2010). Proteins targeted for the cytoplasmic

membrane or for transport into the periplasm get bound to SRP through their signal peptide while they are emerging from the ribosome. SRP is composed of an RNA molecule and a variable number of proteins (Table 12.1; Keenan *et al*., 2001). In bacteria, the RNA component is called 4.5S RNA (120 nucleotides), whereas in archaea and eukarya it is 7S RNA (about 300 nucleotides). The 7S RNA is composed of two domains, the Alu-domain (absent in 4.5S RNA) and the S-domain, part of which corresponds to the 4.5S RNA (Poritz *et al*., 1988). Chloroplast SRP lacks the RNA component entirely (Schuenemann *et al*., 1998; Chandrasekhar *et al*., 2008).

The number of proteins of SRP varies from one to six, depending on the species (Table 12.1). One protein, SRP54/Ffh (fifty-four homologue), is conserved in all species and is the only SRP protein in bacteria. It is a GTPase and is composed of three domains, N, G and M, with the middle one being a classical G-domain (Freymann *et al*., 1997). The M-domain is connected to the N- and G-domains through a flexible linker (Keenan *et al*., 1998). The hydrophobic signal peptide associates with a deep hydrophobic groove of the methionine-rich M-domain. The M-domain also binds to helix 8 of 7S RNA or of 4.5S RNA (Keenan *et al*., 1998; Batey *et al*., 2000). The N-domain of Ffh initially interacts with ribosomal proteins L23 and L29 just outside the exit tunnel of the ribosome (Fig. 12.3 and Plates 12.1 and 12.3; Pool *et al*., 2002; Schaffitzel *et al*., 2006). This binding site partly overlaps with the site for TF. The two proteins compete for binding to the NC and the ribosome (Plate 12.1; Beck *et al*., 2000; Albanese & Frydman, 2002; Gu *et al*., 2003; Ullers *et al*., 2003; Schaffitzel *et al*., 2006).

In eukaryotes, the Alu-domain with proteins SRP9 and SRP14 reaches the binding site for trGTPases and competes with EF2 for binding (Halic *et al*., 2006). The distance between the polypeptide exit tunnel and the binding site for trGTPases is more than 150 Å, and eukaryotic SRP is therefore quite extended. This binding of the Alu-domain leads to translational arrest (Dudek *et al*., 2006). The translational arrest observed in eukaryotes at this state has not been seen in bacteria, which lack the Alu-domain.

Table 12.1 Components of SRP, SR and Sec Translocase in the Three Domains of Life.

	Bacteria	Archaea	Eukarya	Comments
SRP				
RNA	4.5S	7S	7S	7S RNA has Alu- and S-domains. 4.5S RNA from eubacteria corresponds to part of the S-domain from Eukarya.
Proteins			SRP9 SRP14	Heterodimers of SRP9:SRP14 bind to the Alu-domain.
		SRP19	SRP19	Binds to the S-domain.
	Ffh (P48)	SRP54	SRP54	GTPase. Binds to the S-domain. Depends on the binding of SRP19 in Eukarya and Archaea.
			SRP68 SRP72	Heterodimers of SRP68/SRP72 bind to the S-domain.
SR				
	FtsY	FtsY	SRα	GTPase.
			SRβ	GTPase, membrane-bound.
Translocon				
	SecYEG	SecYEβ	Sec61αβγ	A heterotrimeric pore-forming protein complex.

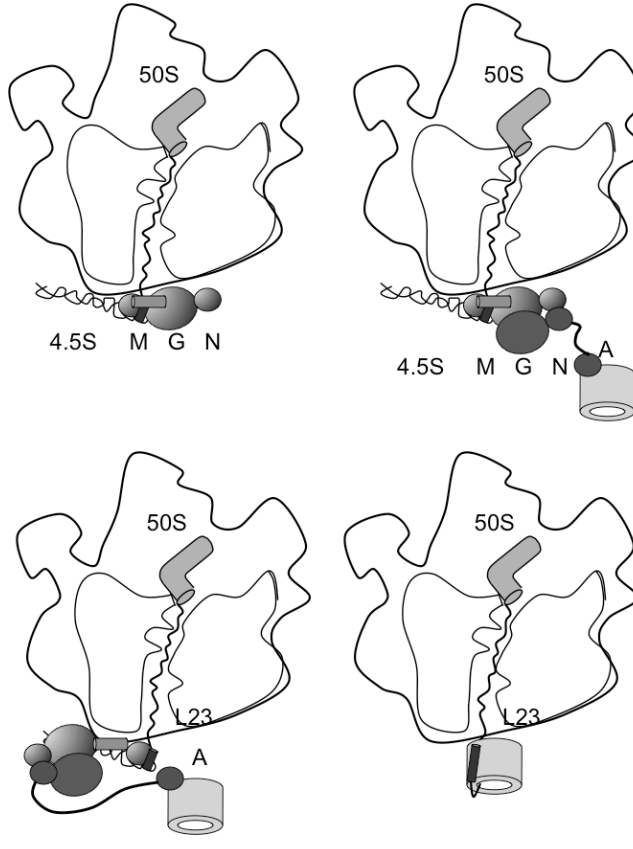

Fig. 12.3 *Upper left*: The interaction between the 4.5S RNA and protein Ffh with the 50S subunit is illustrated by a cross-section through the exit channel. The linker between the G- and the M-domain is shown as a gray cylinder. The peptidyl-tRNA with the signal recognition peptide (black) is shown. *Upper right*: The complex with FtsY (dark gray) is formed. *Lower left*: A conformational change makes the NG-domains of Ffh and FtsY interact with the distal end of the 4.5S RNA, where GTP hydrolysis can be induced. This conformational change exposes ribosomal proteins L23 and L29 at the peptide exit channel for the interaction with the translocon in the cytoplasmic membrane. *Lower right*: The SRP and SR have dissociated after GTP hydrolysis and the peptide exit tunnel of the ribosome can interact with the translocon.

Signal Recognition Particle Receptor

In bacteria, SR is a single soluble protein, FtsY. It is loosely attached to the membrane (Lurink *et al*., 1994). In eukaryotes, there are two proteins, SRα and SRβ (Keenan *et al*., 2001; Table 12.1). SRα corresponds to FtsY. All SR proteins are GTPases and FtsY of SR is a close homologue of Ffh of SRP, despite different functional roles (Keenan *et al*., 2001). Instead of the M-domain, FtsY has an A-domain that associates with the membrane and the translocon (Angelini *et al*., 2005).

The 4.5S RNA is essential for *in vivo* viability (Wood *et al*., 1992). Two roles have been identified: An increased rate of complex formation between the two GTPases and the subsequent stimulation of the GTPase activity (Peluso *et al*., 2001). The 4.5S RNA is an elongated molecule with a tetraloop at one end (helix 8) and two termini at the opposite, distal end (helix 5). Deletion of an increasing number of residues at the distal end first leads to the loss of GTP hydrolysis and subsequently to the loss of complex formation between SRP and FtsY (Ataide *et al*., 2011).

When the signal peptide of the NC emerges from the exit tunnel of bacterial ribosomes, it binds to the M-domain of Ffh in its GTP conformation (Keenan *et al*., 1998; Batey *et al*., 2000). Ffh and FtsY in their GTP conformations then form a complex with the ribosome (Montoya *et al*., 2000). This interaction is due to the N- and G-domains of both molecules (Montoya *et al*., 2000). The two homologous proteins form a symmetric heterodimer with the two GTP molecules located in a composite active site (Plate 12.4; Focia *et al*., 2004, Egea *et al*., 2004, 2005).

In an early step of the interaction of SRP and SR with the ribosome, Ffh and FtsY bind to the tetraloop side of the 4.5S RNA. An investigation by cryo-EM has shown this structure (Estrozi *et al*., 2011). Crystallographic studies of the complex of full-length 4.5S RNA and the two proteins with bound GDPCP show a later state where the M-domain binds near the tetraloop of 4.5S RNA, while the N- and G-domains after a large conformational change bind at the opposite end of the 4.5S RNA (Ataide *et al*., 2011). A linker of 30

amino acid residues forms a helix and a spacer between the two parts of Ffh. The interaction with the distal end of the 4.5S RNA is important for the induction of GTP hydrolysis.

The movement of the N- and G-domains of both proteins exposes the ribosomal surface near the peptide exit channel and ribosomal proteins L23 and L29. This leads to the binding to the PCC or translocon (Figs. 12.2 and 12.3; see Mori & Ito, 2001; Driessen & Nouwen, 2008, Cross *et al*., 2009 for reviews). The ribosome and the translocon jointly induce the two or three GTPases, to hydrolyze their GTP molecules. Subsequently the SRP and SR dissociate. The translational arrest in eukaryotes is relieved and the cotranslational transport can proceed.

The Translocon — SecYEG

The protein-conducting channel (PCC) or translocon is a membrane channel with a narrow pore composed of several proteins (van den Berg *et al*., 2004). It can translocate polar proteins out of the cytoplasm as well as insert hydrophobic proteins into the membrane. In eukaryotes, it is called Sec61 and composed of trimers of the Sec61 α, β and γ subunits (Rapoport *et al*., 1996). In bacteria and archaea the protein corresponding to the α- and γ-subunits are called SecY and SecE respectively. The β-subunit of eukaryotes and archaea shows no homology to the SecG subunit in bacteria. Crystallographic structures are available of the complex from the bacterium *Thermotga maritime* (Zimmer *et al*., 2008) and the archeons *M. jannashii* and *Pyrococcus furiosus* (Plate 12.6; van den Berg *et al*., 2004; Egea & Stroud, 2010). Cryo-EM structures are available from *E. coli* (Mitra *et al*., 2005; Frauenfeld *et al*., 2011). In the latter case one copy of the translocon is bound to a nanodisk where a lipid bilayer is contained within a ringlike protein structure (Plate 12.7). The nanodisk is 100–120 Å wide and 40–50 Å high (Frauenfeld *et al*., 2011).

SecY with 10 TM helices has a pseudosymmetry axis parallel with the membrane. Five helices in each symmetric part make the structure clamlike. The other two subunits have one or two TM helices. The pore is located between the two domains of the SecY subunit. The cytoplasmic side has a 20–25 Å-wide tapering funnel

down to a constriction. Six conserved isoleucines form the constriction. SecE stabilizes the interaction between the two domains of SecY. In the absence of SecE, SecY becomes unstable and can be degraded (Kihara *et al*., 1995). SecG is at the periphery of the complex with a single TM helix.

Obviously, the ion permeability barrier of the membrane must be maintained despite this channel. This is due to a short helix (the plug) connected to a loop on the periplasmic side and located in the constriction. The plug may be moved (van den Berg *et al*., 2004). The hydrophobic part of the signal peptide of the protein to be transported may form a helix, and a likely binding site has been identified in the funnel. The binding of the signal sequence triggers displacement of the plug and opening of the channel by a small rearrangement of the two SecY domains.

The contact between the nanodisk with the translocon and the ribosome leaves a gap on one side of between 15 and 25 Å (Frauenfeld *et al*., 2011). The cytoplasmic loops L6/7 (between TM helices 6 and 7) and L8/9 make contact with the ribosomal peptide exit tunnel and with RNA helices H50–H53–H59 and H6–H24–H50, respectively. Both loops also contact ribosomal protein L23. Furthermore, the C-terminus of SecY interacts with ribosomal components in the exit tunnel. SecE also interacts with the large subunit, particularly proteins L23 and L29 (see Plate 12.1).

Once the synthesis and transport of the protein is completed, the signal peptide is removed by a signal protease bound to the membrane (Dalbey & Wickner, 1985). The signal peptidase has a Lys-Ser catalytic center and the recognition site is at the C-terminal region of the signal peptide (Rawlings & Barrett, 1994).

Integral membrane proteins do not need a signal peptide. Instead, their first TM helix functions as a signal for membrane insertion. While the orientation of a signal sequence is with the N-terminus toward the cytoplasm, the first helix of membrane proteins can either face the cytoplasm or be translocated to face the periplasm. Here the positive inside rule applies (von Heijne, 1986). In order to insert a protein into the membrane, a lateral gate of the pore between the two domains of the translocon is used (Zimmer *et al*., 2008; Egea & Stroud, 2010; Frauenfeld *et al*., 2011).

This page intentionally left blank

13

Evolution of the Translation Apparatus

In the study of evolution, the currently living organisms give us a fragmented representation of the past. The translation apparatus is very ancient and most likely one of the first molecular systems that 'crystallized' at a very early stage, probably even before the emergence of cells (Woese & Fox, 1977; Woese, 2002; Roberts *et al.*, 2008). The rRNA molecules are universal and therefore they provide excellent material for studying evolutionary relationships between species. From sequence analysis of 16S RNA, Woese & Fox (1977) concluded that there are three main domains among living organisms: Bacteria, Archaea and Eukarya.

The genetic code is universal with minor variations, primarily in mitochondria of higher eukaryotes (Chap. 4). Furthermore, rRNAs, tRNAs, tRNA synthetases, many ribosomal proteins, some of the translation factors and part of the transport machinery are also universal (Chaps. 5, 9 and 12; Harris *et al.*, 2003). Thus, since the translation system contains elements of the very early biological world, it may even provide insights into RNA and protein molecules preceding the last universal common ancestor (LUCA). Part of the discussion in this chapter concerns the developments before the occurrence of LUCA, partly in the primordial soup before the first cells.

Key molecules of the translation apparatus are RNA molecules, mRNA and tRNA. The main functional sites of the ribosome are to a certain extent due to rRNA. This has led to the suggestion of an early world where RNA was the dominant biological polymer. Crick (1968) suggested that the original ribosome might have been composed of RNA alone. The multitude of chemical reactions needed to provide the building blocks for such a world could possibly be catalyzed by ribozymes (Joyce, 2002). However, due to the low catalytic efficiency of ribozymes, contributions of amino acids and peptides would enhance the rates and compete favorably with a biology purely based on RNA (Wong, 1991; Kurland, 2010). The further development of longer peptides and small proteins would seem like a winning concept. tRNAs, rRNAs and early ribosomal proteins may have coevolved in the primitive cells (Woese, 1998), but also small RNA molecules and antibiotic progenitors that could regulate translation (Davies, 1990; Dinos *et al*., 2004).

The sequence information and the structures of ribosomes prove that ribosomes from wildly different sources are closely related. This may suggest that some primitive ribosome already existed before LUCA. The inner parts of the ribosomal large subunit (LSU) show least differences and appear to be most ancient (Fox & Ashinikumar, 2004; Hsiao *et al*., 2009). It is interesting to note that these inner parts have less of well-structured RNA (A-form helices) and proteins (helices and β-structures). On the other hand, the frequency of magnesium ions in the inner part of LSU is considerably higher than in the outer regions (Hsiao *et al*., 2009). It is not excluded that the PTC and the decoding center have evolved separately and combined at a later stage (Fox & Naik, 2004; Noller, 2004; Polachek & Mankin, 2005). The PTC is contained within domain V of the 23S RNA and could be assumed to fold by itself. However, the decoding part of SSU has components of several domains and it is therefore difficult to identify any small structure capable of performing the decoding function (Smith *et al*., 2008).

13.1 EVOLUTION OF THE GENETIC CODE, tRNAs AND tRNA SYNTHETASES

Genetic Code

The genetic code is universal (see Chap. 4). It must have originated before the last universal common ancestor (Knight *et al*., 2001). There is no trace of alternative codes that might once have coexisted.

Three main models for the evolution of the genetic code have been proposed: the stereochemical theory, the adaptive theory and the coevolution theory (Koonin & Novozhilov, 2009). A stereochemical relationship between the different amino acids and the anticodons seemed unlikely already to Crick (1968). We now know that there is no physical interaction between the anticodon and the amino acid it codes for (see Chap. 5).

The coevolution theory postulates that the initial code had fewer than 20 amino acids. Which were the first ones and how were they coded (Moura *et al*., 2010)? Certain amino acids could be converted while bound to their tRNA, as is still done in some species (see Chap. 5; Wong *et al*., 2007). However, each such modification needs one or several specific enzymes.

The adaptive theory focuses on the need to prevent errors in decoding the message. Here it is an advantage that similar amino residues are coded by related codons (Woese, 1965; Epstein, 1966).

Whichever route the evolution of the genetic code proceeded along, any change of the code words would lead to the disruption of several established coded proteins. At this stage the code would be frozen; this has been named the 'frozen accident theory' (Crick, 1968).

tRNA

The evolution of tRNAs has been intensely discussed. Crick, in his adaptor hypothesis, suggested that small RNA molecules could decode the mRNA by carrying specific amino acids. The real tRNA adaptors were significantly larger than Crick had expected. The cloverleaf secondary structure is conserved and so is the L-shaped

three-dimensional structure (Chap. 5). The adaptor part of the tRNA, the CCA end, is also conserved.

The two arms of the L-shaped tRNA could have started as a simpler structure, possibly a single hairpin (Woese, 1968; Hopfield, 1978; Di Giulio, 2009a). This would correspond to a central cut through the cloverleaf in a diagonal direction. In metazoan mitochondria, the TΨC arm or D-arm of the tRNAs is replaced with a shorter loop (Anderson *et al*., 1981; Bruin & Klug, 1983; Wolstenholme *et al*., 1987). Many tRNA genes contain introns, which are removed by splicing. Many, but far from all such introns, are inserts in the anticodon loop, which means a different cut of the molecule. Along the same line, tRNAs in some archaeal species are split in their genomes in a 5′ half and a 3′ half structures forming hairpins, and subsequently fused into functional tRNAs (Randau *et al*., 2005; Di Guilio, 2009b). Whether this is an ancient feature revealing a more primordial tRNA is unclear.

aaRS

The aminoacyl-tRNA synthetases (aaRS) must have evolved jointly with the tRNAs and the genetic code. The two classes of aaRS are enzymes with evolutionary relationships within each class but not between the classes. The two families may have evolved from two single-domain enzymes with less specific charging of tRNAs (Schimmel *et al*., 1993). The class of aaRS to which a certain amino acid belongs is the same throughout evolution with one exception, namely lysine (see Table 5.2; Ribas de Pouplana & Schimmel, 2001). Each subclass is also likely to have had a common ancestor. If the current set of enzymes with their subclasses is arranged as in Table 13.1, pairs of relatively similar amino acid residues are grouped together.

As discussed (Chap. 5), enzymes of class I attach the amino acid on the 2′ hydroxyl whereas enzymes of class II charge the tRNA on the 3′ hydroxyl. X-ray structures of aaRS in complex with their tRNAs show that pairs of class I and II aaRS and of the same subclass could bind to opposite sides of the acceptor stem of their

Table 13.1 The Symmetry of the aaRS Subclasses*

Class	I	II	
Subclass			
a	M	P	Hydrophobic (mainly)
	V	T	
	L	A	
	I	G	
	C	S	
	R	H	
b	E	D	Charged and amidated
	Q	N	
	K	K	
c	Y	F	Aromatic
	W		

*From: Ribas de Pouplana & Schimmel, 2001.

tRNAs without a steric clash (Ribas de Pouplana & Schimmel, 2001). The synthetases may have evolved as pairs to protect the charged tRNA in hostile environments. This may further support an early genetic code with fewer amino acids and a higher ambiguity between related amino acids. The expansion to the present canonical genetic code must have occurred through duplication and mutations of genes for both tRNAs and synthetases. Such an evolution would lead to related codons for related amino acids (Ribas de Pouplana & Schimmel, 2001). Thus, the codons for the aromatic residues (subclasses Ic and IIc) all begin with U (Fig. 4.1). The codons for subclasses Ib and IIb (charged and amidated residues) all share A for the second base. Asn and Gln may have evolved at a late stage from their acidic origins, Asp and Glu respectively (Skoulobris *et al*., 2003). In Archaea and many bacterial species there is no synthetase for Asn and Gln (Chap. 5). Four of the six class Ia and four of the six class IIa synthetases have a common middle base in their codons, U and C respectively. They are differentiated primarily by their first base. A primitive genetic code with a smaller set of amino acids, with paired tRNA synthetases

and a low charging specificity, would depend on the availability of amino acids.

13.2 THE EVOLUTION OF RIBOSOMAL RNAs

With the large size of current ribosomal RNAs it is likely that in early ribosomes they were smaller. Furthermore, the conserved parts of the rRNAs are likely to be ancient, whereas later additions may be unique. The decoding and even more the peptidyl transferase site are responsible for the basic functions of the ribosome and are therefore expected to contain ancient elements.

Despite the large variations in size, the organization of the rRNAs is largely the same. The number of helices and loops varies greatly between the rRNAs from different species, but the organization into domains and features of the secondary structure remain. In the base-paired regions the sequences vary, whereas the most conserved regions of the rRNA are single-stranded (Noller & Woese, 1981). Since these single-stranded regions primarily interact with other RNA molecules through base pairing, the need for conservation is evident. These interactions involve the subunit interface, the decoding center, peptidyl transferase and sites of interaction with tRNA (Mushegian, 2005).

Thus, for the interplay between the tRNAs and the rRNA in the decoding site, the residues G530, A1492 and A1493 are conserved due to their essential function in maintaining high fidelity. In the ribosome, the conserved acceptor end of the tRNAs is paralleled by the conserved A and P loops that base-pair with the CCA ends of the tRNAs in the A and P sites.

When one is comparing ribosomal RNAs, it is evident that there are both sequence and structural signatures, which are characteristic of different domains of life (Roberts *et al*., 2008). If one includes the structural signatures in the analysis of the 23S RNAs, there is a deep separation between bacteria and Archaea. The structure of eukaryotic ribosomes has also provided insights into the organization of the extension segments of eukaryotic rRNA (Rabl *et al*., 2011; Klinge *et al*., 2011; Ben-Shem *et al*., 2011; Melnikov *et al*., 2012).

The six domains of the 23S RNA are interwoven in a complex way. This permits an analysis of the interconnectivity of different segments and their interdependence to form the structure of LSU. Hury *et al*. (2006) provide such an analysis and describe the possible sequential addition of domains starting with domain V, followed by domain IV. Domain III seems to be the most recent addition. One question has been discussed without any definite answer: When was the GTPase center in domain II added to the evolving ribosome? Without the catalyzing translational GTPases, protein synthesis must have been very slow.

The distribution of A-minor motifs (see Sec. 7.4) supports the hypothesis of a protoribosome consisting of the PTC (Bokov & Steinberg, 2009). The structure of an A-minor motif is based on a double helix with which a loop of unpaired adenines interacts (Chap. 7). The conformational integrity of the loop depends on the presence of the double helix. Therefore it seems likely that the helix must have preceded the adenine-rich loop. The distribution of the A-minor motifs is far from random (Plate 13.1). Domain V has essentially only the helical components of the motif, while all other domains contribute the matching loop parts. This supports the hypothesis that domain V is the most ancient part of LSU, the protoribosome, to which other parts have gradually been added (Bokov & Steinberg, 2009).

Domain V of LSU does not contribute any subunit bridges in the interaction with SSU (see Chap. 7). Thus, if domain V is the most ancient part of LSU, it seems unlikely that it would have interacted with a precursor of the SSU.

Evolution of the PTC

In the evolution of a large molecular complex like the ribosome, the distribution of parts between the interior and the surface is of interest. Features in the interior cannot be easily added or dramatically changed, whereas features on the surface with few interactions with other parts of the molecular system can more easily be changed (Hury *et al*., 2006). As discussed above, the PTC

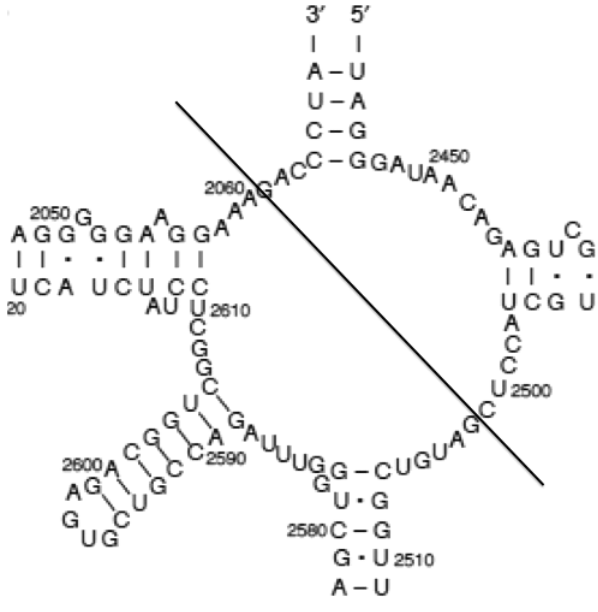

Fig. 13.1 The secondary structure of domain V with the symmetry between the A-site part (below the line representing the twofold axis) and the P-site part (above the line). The twofold symmetry axis is perpendicular to the drawing.

of domain V of LSU may be the most ancient functional center of the ribosome. A remarkable observation is that it has a twofold symmetry. Not only are parts of the two substrates, the CCA ends of the A- and P-site tRNAs and the A and P loops of the 23SRNA, related by an approximately 180° rotation (Nissen *et al.*, 2000), but a significant region of the surrounding ribosomal RNA obeys the same symmetry (Fig. 13.1, Plate 13.2; Agmon *et al.*, 2003). About 90 nucleotides on each side seem to obey this symmetry (Bashan *et al.*, 2003). This symmetric arrangement appears to be conserved for ribosomes from all domains of life (Agmon *et al.*, 2005). The symmetric arrangement of the tRNA molecules is necessary for efficient peptidyl transfer and of significant evolutionary interest. The symmetry of the PTC was further studied by Bokov and

Steinberg (2009). They support the previous observations and find that 110 nucleotides could be included in each half of the repeated structure.

A twofold symmetry within one polymer is highly unlikely to occur through a stepwise evolution. However, there are numerous examples of oligomeric proteins with twofold symmetry where some orthologs have evolved into a single polypeptide with two symmetrically related domains. This is the case for the acidic proteases, which sometimes are homodimers with twofold symmetry right through the active site. In other cases, they are monomers with two structurally similar domains with twofold symmetry and with the active site on the symmetry axis (Davies, 1990; Wlodawer & Gustchina, 2000). In these "dimeric" monomers it is evident that gene duplication and gene fusion have occurred.

The advantage of the gene duplication and gene fusion is that an initially symmetric dimer and catalytic site can evolve through mutations to fit two different substrates in a better way to optimize the catalytic task. The symmetry of the structure of domain V of the 23S RNA where the A site is related to one half of the central part of domain V and the P site to the other half (Fig. 13.1; Agmon *et al*., 2003; Bokov & Steinberg, 2009) matches the symmetry relationship between the two CCA ends of the tRNAs involved in peptidyl transfer are evidences for this early evolution (Nissen *et al*., 2000).

One may therefore suggest that the ribosome started as a simple peptidyl transfer enzyme, composed of two RNA molecules assisted by polyamines or some shorter peptides, perhaps like the N-terminal tail of L27 or the loop of L16 (Plate 7.5). The molecules corresponding to tRNAs could have been as short as the CCA trinucleotides binding the amino acid. Activated amino acids bound to such tRNA precursors could have been combined in a more or less random fashion lacking a guiding message. However, the charging process of the tRNA precursors could have been the selective step.

Evolution of the 5S RNA

The 5S RNA has, like the tRNA molecule and the PTC, an apparent symmetry, which has been analyzed from a large number of sequences (Fig. 6.1b; Branciamore & Di Giulio, 2011). Rather than gene duplication and gene fusion, they suggest inverse duplication, which means that the two halves of the molecule are complementary.

13.3 EVOLUTION OF PROTEINS IN TRANSLATION

Evolution of Ribosomal Proteins

The database of ribosomal protein sequences is rapidly growing, primarily due to the number of genomes that have been completely sequenced. From sequence comparisons, it is evident that more than 50% of the bacterial ribosomal proteins correspond to proteins in archebacteria as well as eukaryotes (Fig. 13.2; App. 1). Chloroplast (Yamaguchi *et al*., 2000; Yamaguchi & Subramanian, 2000; Tiller *et al*., 2012) and mitochondrial ribosomes (Koc *et al*., 2010; Desmond *et al*., 2011) have a set of ribosomal proteins that overlaps almost completely with the proteins in bacterial ribosomes. In addition, they contain several unique proteins. Ribosomes from trypanosomal mitochondria are extreme, with an exceptionally high number of proteins (Ziková *et al*., 2008).

Bairoch *et al*. provide a database of ribosomal proteins (http://www.expasy.org/cgi-bin/lists?ribosomp.txt). Comparisons have been made of the sequences of the ribosomal proteins found in completed genome sequences (Lecompte *et al*., 2002; Mears *et al*., 2002; Mushegian, 2005; Korobelnikova *et al*., 2012). A large fraction of the proteins are found in all three domains of life (Fig. 13.2). Furthermore, all proteins in archaeal ribosomes are found in Eukarya, but there are no additional proteins that are common to bacteria and Archaea. Protein L27 is common to bacteria and Eukarya but absent in Archaea.

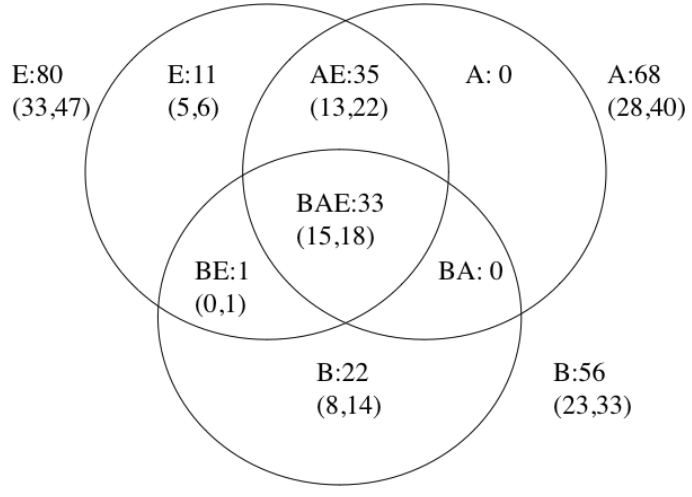

Fig. 13.2 Diagram showing the distribution of r-proteins between bacteria (B), Archaea (A) and Eukarya (E). The number of common proteins is given after the letters. The numbers related to the small and large subunits respectively are given within parentheses. Compare with App. 1.

While the amino acid sequences can suggest that proteins are related, they may have diverged so far that a possible homology is difficult to identify. However, proteins related by fold and location in the ribosomes can add to the number of homologous proteins. A clear case is L16, which is an ortholog of L10e (Harms *et al.*, 2002; see also Chap. 6). Thus, the list of conserved proteins may increase when complete structures of archaeal, mitochondrial and chloroplast ribosomes also become known.

Structural studies of ribosomal proteins show that several different ribosomal proteins have the same or closely related folds and may have a common origin (Table 7.3). The relationship of ribosomal proteins to proteins having other functions is also revealed by structural studies. More sequence and structural data may clarify whether this is due to a common evolutionary origin or not.

r-Protein Tails and Loops May be Ancient

The early ribosome may primarily have been composed of RNA, as discussed earlier. However, the negative charges of the phosphates were certainly neutralized by metal ions, mainly magnesium. Shorter peptides were probably also present to further stabilize the folded RNA but also to increase the catalytic efficiency.

In an extensive analysis of complete genomes, the evolution of the proteome has been analyzed with a particular focus on proteins involved in metabolism and proteins involved in translation (Caetano-Anollés *et al*., 2011). Here it seems evident that metabolic protein domains preceded the earliest proteins in translation, ribosomal proteins, elongation factors and tRNA synthetases. However, it is difficult to envision a system for synthesis of protein domains performed by other proteins whose origin remains obscure. In this discussion it seems essential to relate the emergence of proteins to the earliest simple RNA molecules and their role in early protein synthesis.

The ribosomal external surface contains the most variable parts of the rRNAs and is exposed to recent changes. One characteristic of many ribosomal proteins is the long unstructured N- or C-terminal tails or extended loops going into the interior, more conserved parts of the subunit structures (Fig. 7.2; App. 2). Out of the 33 universally conserved proteins (Fig. 13.2), 23 have tails or loops bridging between different parts of the rRNA. In addition, about half of the nonconserved proteins also have tails or loops. The globular parts of these proteins are all found on the surface with less conserved parts of the ribosome. It is interesting that some protein tails are found in very similar places in the interior even though they belong to different proteins in bacteria and Archaea (Table 7.3). In protoribosomes these tails may have been the only protein components, which during evolution may have been fused with different protein domains. Very few ribosomal proteins are engaged in the subunit bridges. This also supports the notion that the surface parts of the proteins are later additions. Proteins with this type of tails and loops are also found in viruses and in the histones. Again, their

function is to stabilize nucleic acid structure and could be very ancient.

Some of these tails and loops could have been elements of the primordial ribosome and could then be among the most ancient proteins, but would not be accessible for searches for conserved domain structures. A thorough evolutionary analysis of such tails and loops remains to be done. Protoribosomes based on some small RNA molecules, like the dimeric PTC structure with short unstructured peptides, could have been the synthetic apparatus for making simple metabolic proteins.

Evolution of Factors Involved in Translation

Harris *et al.* (2003) have investigated the universally conserved genes in all available genomes. No more than 80 such genes were found. Only 50 show the same phylogenetic relationship as the rRNAs. Of these, 37 encode proteins or factors associated with the ribosome in modern organisms such as ribosomal proteins. IF1, IF2, EF-P, EF-Tu, SelB and EF-G seem to be universally conserved (Table 9.1). The GTPases and in particular their G-domains are the earliest elements of translation factors (Caetano-Anollés *et al*., 2009). In the analysis of the evolution of protein domains, elements of the translation factors seem to have preceded the domains of ribosomal proteins (Caetano-Anollés *et al*., 2009). The use of translation factors without ribosomes seems odd. This would rather support an early ribosome lacking fully developed protein domains, but with shorter peptides stabilizing the rRNA.

Among the additional universally conserved proteins are methionine peptidase and three proteins (SecY, Ffh and FtsY) involved in protein insertion into membranes or protein export. These proteins also show a phylogenetic relationship to the rRNA and interact with the ribosome (see Chap. 12; Harris *et al*., 2003).

13.4 THE RNA WORLD OR RNA-DOMINATED WORLD

The hypothesis of an early RNA world (Gilbert, 1986; Gesteland *et al*., 1999, 2006) has been a tempting thought. A central aspect is

that several RNA molecules have evolved to produce proteins: the mRNA, the tRNAs and the rRNAs. Together they contain many of the functional components needed for translation. The observation that the peptidyl transfer site has twofold symmetry where half of domain V of the 23S RNA makes up the A-site and the other half the P-site suggests that an early peptidyl transferase may have contained a small dimerizing RNA molecule. The activated amino acid may have been bound to something of the size of a CCA molecule that would assist in orienting the amino acid properly with regard to another amino acid or a growing polypeptide.

Components of the translation system may have had a long evolution in the primordial soup: the genetic code, the earliest tRNAs, some early charging synthetases, the rRNA and some peptides or early ribosomal proteins. With the charges of the phosphates in the RNA, there must have been a need for charge neutralization and stabilization of the structures. As discussed, the positively charged tails of the ribosomal proteins may be remnants of the early ribosomes and many of the universally conserved r-proteins have such tails or loops penetrating into the rRNA. These unstructured peptides may later have gained their globular domains, which are all located on the surface of the ribosome.

Thus, the last common universal ancestor must have contained not only the RNA molecules but also a small number of universally conserved shorter peptides and proteins, with a major fraction of them participating in translation.

Appendix I. List of Ribosomal Proteins Classified on the Basis of Sequence Similarities

Family Name	Alt. Name[1]	Taxonomic Range[1,2]	Del. in Mutant[3]	Ribosomal Function/Comment
L1	L10a	A B E	BaD	L11 operon.[6] tRNA E site
L2	L2e	A B E		
L3	L3e	A B E		Assembly[4]
L4	L4e	A B E		Assembly.[4] S10 operon.[6] Exit tunnel
L5	L11e	A B E		
L6	L9e	A B E		
L9		B		
L10	P0	A B E		β operon.[6] At GAR
L11	L12e	A B E	BaD	At GAR
L12		B		At GAR Replaced by P1/P2 in archaea and eukarya
L13	L16e	A B E		Assembly[4]
L14	L23e	A B E		
L15	L28e	A B E	D	Has a structure related to L18e
L16	L10e	A B E		
L17		B		
L18	L5e	A B E		
L19		B	D	
L20		B		Assembly[4]
L21		B		
L22	L17e	A B E		Assembly.[4] Exit tunnel
L23	L25e	A B E		
L24	L26e	A B E	D	Assembly[4]

(*Continued*)

Appendix I. (*Continued*)

Family Name	Alt. Name[1]	Taxonomic Range[1,2]	Del. in Mutant[3]	Ribosomal Function/Comment
L25		B		CTC-type protein
L27		B E	D	
L28		B	D	
L29	L35e	A B E	D	
L30	L7e	A B E	D	
L31		B		
L32		B		
L33		B	BaD	
L34		B		
L35		B		
L36		B		
P1/P2		A E		
L6e		E		
L8e	L7a	A E		
L13e		A E		
L14e		A E		
L15e		A E		
L18e		A E		Has a structure related to L15
L19e		A E		
L20e		A E		
L21e		A E		
L22e		E		
L24e		A E		

(*Continued*)

Appendix I. (*Continued*)

Family Name	Alt. Name[1]	Taxonomic Range[1,2]	Del. in Mutant[3]	Ribosomal Function/Comment
L27e		E		
L28e		E		
L29e		E		
L30e		A E		
L31e		A E		
L32e		A E		
L33e		A E		
L34e		A E		
L36e		E		
L37e		A E		
L38e		A E		
L39e		A E		
L40e		A E		Fused to C-terminus of ubiquitin. Zn-finger
L41e		A E		
L42e	L44a	A E		
L43e	L37Ae	A E		
S1		B	D	Interacts with mRNA
S2	S0Ae	A B E		
S3	S3e	A B E		
S4	S9e	A B E		Assembly.[5] α operon[6]
S5	S2e	A B E		
S6		B	BaBuD	
S7	S5e	A B E		Assembly.[5] Str operon[6]

(*Continued*)

Appendix I. (*Continued*)

Family Name	Alt. Name[1]	Taxonomic Range[1,2]	Del. in Mutant[3]	Ribosomal Function/Comment
S8	S22e	A B E		Assembly.[5] Spc operon[6]
S9	S16e	A B E	BuD	
S10	S20e	A B E		
S11	S14e	A B E	D	
S12	S23e	A B E		At decoding site
S13	S18e	A B E	BuD	
S14	S29e	A B E		S29e is a zinc-finger protein
S15	S13e	A B E	Bu	Assembly[5]
S16		B		
S17	S11e	A B E	BuD	Assembly[5]
S18		B		
S19	S15e	A B E		
S20		B	BaBuD	S20 operon[6]
S21		B		
S22		B		Stationary phase
THX		B		Found in *Thermus* but few other bacteria
S1e		A E		Replaces S6 and S18. C-terminal domain resembles S6
S4e		A E		Replaces S16 and S20
S6e		A E		Replaces S20. Phosphorylated. Similar to L25
S7e		E		
S8e		A E		Replaces S20

(*Continued*)

Appendix I. (*Continued*)

Family Name	Alt. Name[1]	Taxonomic Range[1,2]	Del. in Mutant[3]	Ribosomal Function/Comment
S10e		E		Beak
S12e		E		Beak. Analogue of HmL7Ae
S17e		A E		
S19e		A E		
S21e		E		Ubiquitin-like
S24e		A E		
S25e		A E		
S26e		A E		mRNA interactions. Zinc-finger protein
S27e		A E		Fused to C-terminus of ubiquitin. Zinc-finger
S28e		A E		mRNA interactions
S30e		A E		Partly in the same location as S4
S31e		A E		Beak. Zinc finger. Ubiquitin-fusion protein
RACK1		E		Interacts with cellular proteins. Regulation. WD-repeats

(Large subunit L; Small subunit S.)

"A" = archaea; "B" = bacteria; "E" = eukaryotes. Information about eukaryotic proteins were obtained from Rabl *et al.*, 2011; Klinge *et al.*, 2011; Ben-Shem *et al.*, 2011; Jenner *et al.*, 2012.

L7 = L12; L8 = L10·$(L12)_n$ n = 4 or 6; L26 does not exist = S20.

[1]Bairoch; http://www.expasy.org/cgi-bin/lists?ribosomp.txt.

[2]Proteins found in BAE are universally conserved.

[3]D — (Dabbs *et al.*, 1983, Dabbs, 1986), Ba — (Baba *et al.*, 2006); Bu — (Bubunenko *et al.*, 2007).

[4]Röhl & Nierhaus, 1982.

[5]Held & Nomura, 1974.

[6]Translational control. See Nomura *et al.*, 1984.

This page intentionally left blank

The Domain Arrangement, Fold, Tails, Loops, Hinges, Location and Interactions of Ribosomal Proteins. Data on 30S Subunits from *T. Thermophilus* (Tt) by Carter *et al.* (2000); Brodersen *et al.* (2002) and Schlüntzen *et al.* (2000); on 50S Subunits from *H. marismortui* (Hm) by Ban *et al.* (2000) and Klein *et al.* (2004); on 50S subunits from *D. radiodurans* (Dr) by Harms *et al.* (2001); on *E. coli* 70S (Ec) (Schuwirth *et al.*, 2005); on *T. thermophilus* (T) 70S Ribosomes by Selmer *et al.* (2006) and Jenner *et al.* (2010).

Protein	Domain Arrangement	Domain Fold	Tails, Loops and Hinges	Location, Primary Interactions with Proteins and RNA Helices, Function
S1	1–185 6 repeats (1–6), 70 amino acids each	OB fold		Binding to 30S subunit. Repeats 3–6 interact with mRNA.
S2	(1–97, 160–240) 1 domain	α+β	(98–159) α-hairpin loop (241–256) Disordered	Back of 30S. At hinge head–body, h35–h37, h26.
S3			(1–20) Bound on CTD	
	NTD (21–106) CTD (107–207)	α+β sandwich α+β; β-meander		Back of head; 3′ major domain. S10, S14, h16, h34–35, h38.
			(208–239) Disordered	
S4	(1–40) I (41–98, 196–209) II (99–195)	Zn finger α-helical α+β		Back of shoulder. S5, five-way junction of h3, h4, h16, h17, h18.
S5	NTD (1–74) CTD (75–147)	βββα-meander α+β sandwich	(15–27) β-hairpin	Back of body. h1, h2, h26, h28, h34–h36.
S6	(1–92)	Double-split β-α-β		Platform. Tight complex with S18, h22, h23.
			(93–101) C-terminal tail	

(*Continued*)

Appendix II. (*Continued*)

Protein	Domain Arrangement	Domain Fold	Tails, Loops and Hinges	Location, Primary Interactions with Proteins and RNA Helices, Function
S7	(15–155)	α+β	(1–14) N-terminal tail	Head. h23b, h28, h43; junction of h29, h30, h41, h42.
S8	NTD (1–63) CTD (74–130)	Split β-α-β Double-split β-α-β, reversed	(63–81) Hairpin loop	Back of body. h20–h22, h25. (S2), S5.
S9	(1–105)	α+β sandwich	(106–128) C-terminal tail	Top of head. S7, h29–h31, h38–h39, h41, h43. S10, S13.
S10	(1–42, 68–105)	Double-split β-α-β	(43–67) β-ribbon	Top of head. h31, h34, h39, h41, h43.
S11	(1–111)	βββα-meander, like L18	(112–129) C-terminal tail	Top of platform. S18, h23, h23b, h23, h24, h45.
S12	(25–135)	OB fold	(1–24) N-terminal tail	S8, S17. 50 Å long. Goes across subunit. h3, h5, h18. Interface, at decoding center.
S13	(1–64)	α-helical	(67–126) α-helical tail	Head, interface. h41–h42. Bridge B1, L31. S19, h30–31. At ACL of P-site tRNA.
S14			(1–61) α-helical tail	Head. h31–h34, h38, h42, h43.
S15	(1–88)	Four-helix bundle		Base of platform. B4. Junction of h20–h24.

(*Continued*)

Appendix II. (*Continued*)

Protein	Domain Arrangement	Domain Fold	Tails, Loops and Hinges	Location, Primary Interactions with Proteins and RNA Helices, Function
S16	(1–79)	β+α	(80–88) C-terminal tail	Lower part of body. h4, h7, h12, h15, h17, h21.
S17	(1–85)	OB fold	(23–41) Extended β-ribbon (85–105) α-helical tail	Junction of 5′ and central domain below platform. h7, h11, h20–h21, h27.
S18	(21–82)	α-helical	(1–20) N-terminal tail (83–88) C-terminal tail	Platform. Complex with S6. h22, h23, h26. Extends β-sheet of S11.
S19	(8–80)	α+β	(1–10) N-terminal tail (77–93) C-terminal tail	Head. S13, h30–h33, h42. Bridge B1. L31. A-site tRNA.
S20	(11–76)	Three-helix bundle	(1–10) N-terminal tail 93–106 C-terminal tail	Bottom of 30S. h6, h11, h13, h44. h9.
S21				
THX	1–26	Folded around helix		Top of head. h30, h41–h43.
L1	I (1–66, 159–228) II (71–158)	Split β-α-β Rossmann fold		L1 protuberance. H76–H78.
L2	(62–130) (131–194)	OB fold β-barrel, SH3-like	(1–61) N-terminal tail (195–237) C-terminal tail	Interface, on L1 side. H66. Bridge B7b. Strong contact with L37ae.

(*Continued*)

Appendix II. (*Continued*)

Protein	Domain Arrangement	Domain Fold	Tails, Loops and Hinges	Location, Primary Interactions with Proteins and RNA Helices, Function
L3			(1–22)* N-terminal tail	Edge of interface. Below L6 on L12 side. L13, L14, H94, H96, H100–H101.
	NTD (25–163)	β-barrel, domain II of trGTPases	(206–260)* Internal loop	
	CTD (261–337)	Antiparallel α+β		
L4			(41–105)*	Exit tunnel. Pos. 62–67, close to macrolides. External side. L18e, L37e, H19–H20, H29, H46.
	1–235	Mixed α+β		
			(170–190)*	
L5	(1–176)	Double-split β-α-β		Central protuberance. H3 of 5S RNA. H84. L18. Bridge B1b, S13, S19.
L6	NTD (1–79)	Split β-α-β		Below L12 stalk. L13, H97.
	CTD (80–177)	Split β-α-β		
L9	NTD (1–40)	Split β-α-β		Below L1 stalk.
			Connecting helix (41–73)	
	CTD (75–149)	Mixed α+β		
L10	1–140	Split β-α-β		Base of L12 stalk. Binds 2 or 3 dimers of L12.
			141–178 Long α-helix	
L11	NTD (1–72)			Base of L12 stalk.
	CTD (75–141)	Homeodomain		
L12	NTD (1–37)	Helical hairpin		L12 stalk. 2 or 3 dimers bind to L10.
			Flexible hinge (37–52)	
	CTD (53–120)	Split β-α-β		

(*Continued*)

Appendix II. (*Continued*)

Protein	Domain Arrangement	Domain Fold	Tails, Loops and Hinges	Location, Primary Interactions with Proteins and RNA Helices, Function
L13	(1–145)	Mixed α+β		External side. L3, L6, H41.
L14	NTD (1–88) CTD (103–122)	β-barrel		L3. Interprotein β-sheet with L19 (HL24e). Interface side. Bridges B5 and B8. h14, h44.
L15	(61–150)	2 sheets, like L18e	(1–60)* N-terminal tail	External side below L1 stalk. L18e, L32e. H29, H31.
L16	(1–137)	Double-split β-α-β	75–91	H38, H89. Loop, interacts with elbow of P-site tRNA.
L17	(1–127)	OB fold		Back side of 50S.
L18	(21–186)	Mixed α+β, like S11	(1–21)* N-terminal tail	Central protuberance. L5, L21e. H1 of 5S. RNA.
L19	(1–146)		Very long hinge	Interprotein β-sheet with L14. Interface side. Bridges B6 and B8. h14, h44.
L20	(1–118)		Very long α-helical tail	H25.
L21	(1–101)	β-barrel	Extended loop	
L22	(1–113)	Split β-α-β	(80–100)* Long β-ribbon	Globular domain at external side. Ribbon at peptide exit tunnel. H26.

(*Continued*)

Appendix II. (*Continued*)

Protein	Domain Arrangement	Domain Fold	Tails, Loops and Hinges	Location, Primary Interactions with Proteins and RNA Helices, Function
L23	(1–96)	Split β-α-β	Tail in Dr	External side at peptide exit tunnel. L29, L39e, H50–H51.
L24	(17–110)	β-barrel, SH3-like	(1–16)* N-terminal tail	External side. H7, H19–H20.
Ec L25	(1–94)	β-barrel, 7 strands		Helix IV of 5S RNA.
L25 (= TtL5)	(1–91) (92–176)	β-barrel 2 antiparallel sheets	 (177–206) C-terminal tail	5S RNA, at central protuberance. Between 5S RNA and L11. A-site tRNA, L16, H38 (ASF).
L25 = DrCTC	(1–104) (105–189) (190–253)	β-barrel 2 antiparallel sheets Helical		5S RNA. Between 5S RNA and L11, H38 ASF. Interface, A-site tRNA.
L27	(9–85)		1–9? N-terminal tail	Acceptor end of P-site tRNA.
L28	(1–98)			
L29	(1–65)	α-helical		External side. L23, H5–H7.
L30	(1–60)	Split β-α-β		External side. H40–H41.
L31	(10–40)	Zinc finger motif	(1–9) N-terminal tail (41–71) C-terminal tail	Bridges between central protuberance of 50S (5S RNA, L5) and head of 30S (S13 and S19). At E-site tRNA.

(*Continued*)

Appendix II. (*Continued*)

Protein	Domain Arrangement	Domain Fold	Tails, Loops and Hinges	Location, Primary Interactions with Proteins and RNA Helices, Function
L32	(1–60)	Zinc finger motif	C-terminal tail	
L33	(1–54)	β-barrel		Near E-site tRNA.
L34	(1–49)			
L35	(1–65)			
L36	(1–37)	Zinc finger motif		No corresponding protein in *H. marismortui*.
L7Ae	(1–119)*	Mixed α+β. Like domain III of eRF1		Below L1 stalk. Strong contact with L15e. Sequence and structural homology to 15.5 kDa spliceosomal protein and L30e.
L15e	(1–67, 98–169)*	Split β-α-β	(68–97)* (170–194)* C-terminal tail	Edge of interface on L1 side. Strong contact with L7Ae. L44e, H10–H11, H15, H21.
L18e	(1–115)*	2 sheets, like L15		External surface. L4, L15, H27–H31. No corresponding protein in bacteria. The long H30 in *H. marismortui* is absent in *D. radiodurans*.
L19e	(1–51)* (91–143)*	α-helical	(52–90)*	Bottom of interface surface. H47–H48, H63. Replaced in bacteria by a longer H59.

(*Continued*)

Appendix II. (*Continued*)

Protein	Domain Arrangement	Domain Fold	Tails, Loops and Hinges	Location, Primary Interactions with Proteins and RNA Helices, Function
L21e	(24–95)*	β-barrel, SH3-like	(1–23)* N-terminal tail	External surface below central protuberance. L18, H86.
L24e	(4–56)*	Zinc finger motif		Interface side. Interprotein β-sheet with L14.
L31e	(7–88)*	Split β-α-β		Bottom of external surface.
L32e	(95–236)*	Mixed α+β	(109–179)*	External surface. L15, H46.
L37Ae	(1–72)*	Zinc finger motif		Interface side. Strong contact with L2.
L37e	(1–56)*	Zinc finger motif	(1–15) N-terminal tail (42–56)	Buried internally. L4, L39e.
L39e	(1–49)*	α-helical	Whole protein	External surface. L23, L37e.
L40e	(20–46)*	Zinc finger motif	1–19, 47–56	
L44e	(1–24, 62–92)*	Zinc finger motif	(25–61) Internal loop	L15e, H88.

* Residue numbers refer to *H. marismortui*.

References

Some Useful Addresses on the Internet

A database providing information on the genetic code and its variations is provided by Elzanowski & Ostell at:
http://www.ncbi.nlm.nih.gov/Taxonomy/Utils/wprintgc.cgi?mode=c
There is a database that is directly relevant to translation:
http://recode.genetics.utah.edu
A database of the sequences of ribosomal proteins by Bairoch *et al*. at:
http://www.expasy.org/cgi-bin/lists?ribosomp.txt)
Protein Data Bank, PDB; http://www.rcsb.org/pdb
A database of aligned ribosome complexes (Jarasch *et al*., 2012);
http://daresite.genzentrum.lmu.de

References

Abdulkarim, F., Liljas, L., and Hughes, D. 1994. Mutations to kirromycin resistance occur in the interface of domains I and III of EF-Tu.GTP. *FEBS Lett*. **352**:118–122.

Adamczyk, A.J. and Warshel, A. 2011. Converting structural information into an allosteric-energy-based picture for elongation factor Tu activation by the ribosome. *Proc. Natl. Acad. Sci. USA*. **108**:9827–9832.

Adams, J. M. 1968. On the release of the formyl group from nascent protein. *J. Mol. Biol*. **33**:571–589.

Adlagatta, A., Quillin, M.L., Omotoso, O., *et al*. 2005. Identification of an SH3-Binding Motif in a New Class of Methionine Aminopeptidases from Mycobacterium tuberculosis Suggests a Mode of Interaction with the Ribosome. *Biochemistry* **44**:7166–7174.

Agalarov, S.C., Sridhar Prasad, G., Funke, P.M., *et al*. 2000. Structure of the S15, S6, S18-rRNA complex: assembly of the 30S ribosome central domain. *Science* **288**:107–113.

Agirrezabala, X., Lei, J., Brunelle, J. L., *et al*. 2008. Visualization of the hybrid state of tRNA binding promoted by spontaneous ratcheting of the ribosome. *Mol. Cell* **32**:190–197.

Agirrezabala, X. and Frank, J. 2009. Elongation in translation as a dynamic interaction among the ribosome, tRNA, and elongation factors EF-G and EF-Tu. *Quart. Rev. Biophys.* **42**:159–200.

Agirrezabala, X., Schreiner, E., Trabuco, L.G., *et al*. 2011. Structural insights into cognate versus near-cognate discrimination during decoding. *EMBO J.* **30**:1497–1507.

Agmon, I., Auerbach, T., Baram, D., *et al.* 2003. On peptide bond formation, translocation, nascent protein progression and the regulatory properties of ribosomes. *Eur. J. Biochem.* **270**:2543–2556.

Agmon, I., Bashan, A., Zarivach, R., *et al*. 2005. Symmetry at the active site of the ribosome: Structural and functional implications. *Biol. Chem*. **386**:833–844.

Agrawal, R.K., Penczek, P., Grassucci, R.A., *et al.* 1996. Direct visualization of A-, P-, and E-site transfer RNAs in the *Escherichia coli* ribosome. *Science* **271**:1000–1002.

Agrawal, R.K., Penczek, P., Grassucci, R.A., and Frank, J. 1998. Visualization of elongation factor G on the *Escherichia coli* 70S ribosome: the mechanism of translocation. *Proc. Natl. Acad. Sci. USA.* **95**:6134–6138.

Agrawal, R.K., Heagle, A.B., Penczek, P., *et al*. 1999. EF-G-dependent GTP hydrolysis induces translocation accompanied by large conformational changes in the 70S ribosome. *Nat. Struct. Biol.* **6**:643–647.

Agrawal, V., and Kishan, K.V. 2003. OB-fold: growing bigger with functional consistency. *Curr. Prot. Pept. Sci.* **4**:195–206.

Agrawal, R.K., Sharma, M.R., Kiel, M.C., *et al*. 2004. Visualization of ribosome-recycling factor on the *Escherichia coli* ribosome: functional implications. *Proc. Natl. Acad. Sci. USA.* **101**:8900–8905.

Agrawal, R.K., Sharma, M.R., Yassin, A., *et al*. 2011. In: Ribosomes. Structure, function and dynamics. pp. 83–96. Editors MV Rodnina, W Wintermeyer, R Green. (ISBN 978-3-7091-0214-5). Springer Verlag.

Aitken, C.E. and Puglisi, J.D. 2010. Following the intersubunit conformation of the ribosome during translation in real time. *Nat. Struct. Mol. Biol.* **17**:793–800.

Aitken, C.E., Petrov, A., and Puglisi, J.D. 2010. Single ribosome dynamics and the mechanism of translation. *Annu. Rev. Biophys.* **39**:491–513.

Albanese, V. and Frydman, J. 2002. Where chaperones and nascent polypeptides meet. *Nat. Struct. Biol.* **9**:716–718.

Ali, I.K., Lancaster, L., Feinberg, J., *et al*. 2006. Deletion of a conserved, central ribosomal intersubunit RNA bridge. *Mol. Cell* **23**:865–874.

Aliprandi, P., Sizun, C., Perez, J., *et al*. 2008. S1 ribosomal protein functions in translation initiation and ribonuclease RegB activation are mediated by similar RNA-protein interactions. *An NMR and SAXS analysis. J. Biol. Chem.* **283**:13289–13301.

Al-Karadaghi, S., Ævarsson, A., Garber, M., *et al.* 1996. The structure of elongation factor G in complex with GDP: conformational flexibility and nucleotide exchange. *Structure* **4**:555–565.

Al-Karadaghi, S., Davydova, N., Eliseikina, I., *et al.* 2000a. Ribosomal proteins and their structural transitions on and off the ribosome. In *The Ribosome: Structure, Function, Antibiotics and Cellular Interactions,* Eds. R.A. Garrett, S.R. Douthwaite, *et al.,* pp. 65–72. ASM Press, American Society for Mocrobiology, Washington, D.C.

Al-Karadaghi, S., Kristensen, O., and Liljas, A. 2000b. A decade of progress in understanding the structural basis of protein synthesis. *Prog. Biophys. Mol. Biol.* **73**:167–193.

Allen, P.N., and Noller, H.F. 1989. Mutations in ribosomal proteins S4 and S12 influence the higher order structure of 16S ribosomal RNA. *J. Mol. Biol.* **208**:457–468.

Allen, G.S., Zavialov, A., Gursky, R., *et al*. 2005. The cryo-EM structure of a translation initiation complex from *Eschericia coli. Cell* **121**:703–712.

Allen, G.S. and Frank, J. 2007. Structural insights on the translation initiation complex: ghosts of a universal initiation complex. *Mol. Microbiol.* **63**: 941–950.

Almlöf, M., Andér, M., and Åqvist, J. 2007. Energetics of codon-anticodon recognition on the small ribosomal subunit. *Biochemistry* **46**:200–209.

Ambrogelly, A., Palioura, S., and Söll, D. 2007. Natural expansion of the genetic code. *Nature Chem. Biol.* **3**:29–35.

Andersen, G.R., Pedersen, L., Valente, L., *et al.* 2000. Structural basis for nucleotide exchange and competition with tRNA in the yeast elongation factor complex eEF1A:eEF1Balpha. *Mol. Cell* **6**:1261–1266.

Andersen, G.R., Nissen, P., and Nyborg, J. 2003. Elongation factors in protein biosynthesis. *Trends Biochem. Sci.* **28**:434–441.

Anderson, S., Bankier, A.T., Barrell, B.G., *et al*. 1981. Sequence and organization of the human mitochondrial genome. *Nature* **290**:457–465.

Andersson, S. and Kurland, C.G. 1987. Elongating ribosomes *in vivo* are refractory to erythromycin. *Biochemie* **69**:901–904.

Andersson, D.I., Andersson, S.G., and Kurland, C.G. 1986. Functional interactions between mutated forms of ribosomal proteins S4, S5 and S12. *Biochimie* **68**:705–713.

Angelini, S., Deitermann, S., and Koch, H.G. 2005. FtsY, the bacterial signal-recognition particle receptor, interacts functionally and physically with the SecYEG translocon. *EMBO Rep.* **5**:476–481.

Anton, B.P., Saleh, L., Benner, J.S., *et al*. 2008. RimO, a MiaB-like enzyme, methylthiolates the universally conserved Asp88 residue of ribosomal protein S12 in *Escherichia coli*. *Proc. Natl. Acad. Sci. USA.* **105**:1826–1831.

Antoun, A., Pavlov, M.Y., Andersson, K., *et al.* 2003. The roles of initiation factor IF2 and guanosine triphosphate in initiation of protein synthesis. *EMBO J.* **22**:5593–5601.

Antoun, A., Pavlov, M.Y., Lovmar, M., *et al*. 2006a. How initiation factors tune the rate of initiation of protein synthesis in bacteria. *EMBO J.* **25**:2539–2550.

Antoun, A., Pavlov, M.Y., Lovmar, M., *et al*. 2006b. How initiation factors maximize the accuracy of tRNA selection in initiation of bacterial protein synthesis. *Mol. Cell.* **23**:183–193.

Aoki, H., Dekany, K., Adams, S.L., *et al*. 1997. The gene encoding the elongation factor P protein is essential for viability and is required for protein synthesis. *J. Biol. Chem*. **272**:32254–32259.

Aoki, H., Xu, J., Emili, A., *et al*. 2008. Interactions of elongation factor EF-P with the *Escherichia coli* ribosome. *FEBS J*. **275**: 671–681.

Arai, K.I., Kawakita, M., and Kaziro, Y. 1972. Studies on polypeptide elongation factors from *Escherichia coli.* II. Purification of factors Tu-guanosine diphosphate, Ts, and Tu-Ts, and crystallization of Tu-guanosine diphosphate and Tu-Ts. *J. Biol. Chem.* **247**:7029–7037.

Arai, N., and Kaziro, Y. 1975. Mechanism of the ribosome-dependent uncoupled GTPase reaction catalyzed by polypeptide chain elongation factor G. *J. Biochem.* (Tokyo) **77**:439–447.

Aravind, L., and Koonin, E.V. 1998. The HD domain defines a new superfamily of metal-dependent phosphohydrolases. *Trends Biochem. Sci.* **23**:469–472.

Arevalo, M.A., Tejedor, F., Polo, F., and Ballesta, J.P. 1988. Protein components of the erythromycin binding site in bacterial ribosomes. *J. Biol. Chem.* **263**:58–63.

Arisue, N, Maki, Y, Yoshida, H, *et al*. 2004. Comparative analysis of the ribosomal components of the hydrogenosome-containing protist, *Trichomonas vaginalis*. *J. Mol. Evol*. **59**:59–71

Armache, J.-P., Jarasch, A., Anger, A.M., *et al*. 2010a. Cryo-EM structure and rRNA model of a translating eukaryotic 80S ribosome at 5.5-Å resolution. *Proc. Natl. Acad. Sci. USA*. **107**:19748–19753.

Armache, J.-P., Jarasch, A., Anger, A.M., *et al*. 2010b. Localization of eukaryotic-specific ribosomal proteins in a 5.5-Å cryo-EM map of the 80S eukaryotic ribosome. *Proc. Natl. Acad. Sci. USA*. **107**:19754–19759.

Artsimovitch, I., Patlan, V., Sekine, S., *et al*. 2004. Structural basis for transcription regulation by alarmone ppGpp. *Cell* **117**:299–310.

Åqvist, J., Warshel, A. 1993. Simulation of Enzyme Reactions Using Valence Bond Force Fields and Other Hybrid Quantum/Classical Approaches. *Chemical Reviews* **93**:2523–2544.

Åqvist, J., Luzhkov, V.B., and Brandsdal, B.O. 2002. Ligand Binding Affinities from MD Simulations. *Acc. Chem. Res*. **35**:358–365.

Åqvist, J., Lind, C., Sund, J., and Wallin, G. 2012. Bridging the gap between ribosome structure and biochemistry by mechanistic computations. *Curr. Op. Struct. Biol*. **22**:815–823.

Ataide, S.F., Schmitz, N., Shen, K., *et al*. 2011. The crystal structure of the signal recognition partile in complex with its receptor. *Science* **331**:881–886.

Atkins, J.F., and Gesteland, R.F. 2001. mRNA readout at 40. *Nature* **414**:693.

Auerbach, T., Bashan, A., and Yonath, A. 2004. Ribosomal antibiotics: structural basis for resistance, synergism and selectivity. *Trends Biotechnol*. **22**:570–576.

Ævarsson, A. 1995. Structure-based sequence alignment of elongation factors Tu and G with related GTPases involved in translation. *J. Mol. Evol.* **41**:1096–1104.

Ævarsson, A., Brashnikov, E., Garber, M., *et al.* 1994. Three-dimensional structure of the ribosomal translocase: elongation G from *Thermus thermophilus*. *EMBO J.* **13**: 3669–3677.

Baba, T., Ara, T., Hasegawa, M., *et al*. 2006. Construction or *Escherichia coli* K-12 in-frame, single-gene knockout mutants: the Keio collection. *Mol. Sys. Biol*. 1–11.

Baca, O.G., Rohrbach, M.S., and Bodley, J.W. 1976. Equilibrium measurements of the interactions of guanine nucleotides with *Escherichia coli* elongation factor G and the ribosome. *Biochemistry* **15**:4570–4574.

Bailey-Serres, J., Vangala, S., Szick, K., and Lee, C.-H.K. 1997. Acidic phosphoprotein complex of 60S ribosomal subunit of maize seedling roots. *Plant Physiol.* **114**: 1293–1305.

Baldwin, A.N. and Berg, P. 1966. Transfer ribonucleic acid-induced hydrolysis of valyladenylate bound to isoleucyl ribonucleic acid synthase. *J. Biol. Chem*. **241**:839–845.

Ball, L.A. and Kaesberg, P. 1973. Cleavage of the N-terminal formylmethionine residue from a bacteriophage coat protein *in vitro*. *J. Mol. Biol*. **79**:531–537.

Ballesta, J.P.G., and Remacha, M. 1996. The large ribosomal subunit stalk as a regulatory element of the eukaryotic translational machinery. *Prog. Nucl. Acid Res. Mol. Biol.* **55**:157–193.

Ballesta, J.P.G., Rodriguez-Gabriel, M.A., Bou, G., *et al.* 1999. Phosphorylation of the yeast ribosomal stalk. Functional effects and enzymes involved in the process. *FEMS Microbiol. Rev.* **23**:537–550.

Ballesta, J.P.G., Guarinos, E., Zurdo, J., *et al.* 2000. In *The Ribosome: Structure, Function, Antibiotics and Cellular Interactions,* Eds. R.A. Garrett, S.R. Douthwaite, A. Liljas, *et al.,* pp. 115–125. ASM Press, American Society for Mocrobiology, Washington, D.C.

Ban, N., Freeborn, B., Nissen, P., *et al*. 1998. A 9Å resolution X-ray crystallographic map of the large ribosomal subunit. *Cell* **93**:1105–1115.

Ban, N., Nissen, P., Hansen, J., *et al.* 1999. Placement of protein and RNA structures into a 5Å-resolution map of the 50S ribosomal subunit. *Nature* **400**:841–847.

Ban, N., Nissen, P., Hansen, J., *et al.* 2000. The complete atomic structure of the large ribosomal subunit at 2.4Å resolution. *Science* **289**:905–920.

Bang, H., Pecht, A., Raddatz, G., *et al*. 2000. Prolyl isomerases in a minimal cell. Catalysis of protein folding by trigger factor from *Mycoplasma genitalium*. *Eur. J. Biochem*. **267**:3270–3280.

Baram, D., Pyetan, E., Sittner, A., *et al*. 2005. Structure of trigger factor binding domain in biologically homologous complex with eubacterial ribosome reveals its chaperone action. *Proc. Natl. Acad. Sci. USA.* **102**:12017–12022.

Baranov, P.V., Sergiev, P.V., Dontsova, O.A., *et al.* 1998. The database of the *E. coli* ribosomal cross-links (DRC). *Nucl. Acids Res.* **26**:187–189.

Baranov, P.V., Kubarenko, A.V., Gurvich, O.L., *et al.* 1999. The database of the *E. coli* ribosomal cross-links: an update. *Nucl. Acids Res.* **27**:184–185.

Baranov, P.V., Gesteland, R.F., and Atkins, J.F. 2002a. Recoding: translational bifurcations in gene expression. *Gene* **286**:187–201.

Baranov, P.V., Gesteland, R.F., and Atkins, J.F. 2002b. Release factor 2 frameshifting sites in different bacteria. *EMBO Rep.* **3**:373–377.

Barbacid, M. and Vazquez, D. 1974. (^{3}H)anisomycin binding to eukaryotic ribosomes, *J. Mol. Biol.* **84**:91–102.

Bargis-Surgey, P., Lavergne, J.-P., Gonzalo, P., *et al.* 1999. Interaction of elongation factor eEF2 with ribosomal P proteins. *Eur. J. Biochem.* **262**:606–611.

Baron, C., Heider, J., and Böck, A. 1993. Interaction of translation factor SELB with the formate dehydrogenase H selenopolypeptide mRNA. *Proc. Natl. Acad. Sci. USA.* **90**: 4181–4185.

Barta, A., Steiner, G., Brosius, J., *et al.* 1984. Identification of a site on 23S ribosomal RNA located at the peptidyl transferase center. *Proc. Natl. Acad. Sci. USA.* **81**:3607–3611.

Bashan, A., Agmon, I., Zarivach, R., *et al.* 2003. Structural basis of the ribosomal machinery for peptide bond formation, translocation, and nascent chain progression. *Mol. Cell* **11**:91–102.

Batey, R.T., Rambo, R.P., Lucast, L., *et al.* 2000. Crystal structure of the ribonucleoprotein core of the signal recognition particle. *Science* **287**:1232–1239.

Battesti, A. and Bouveret, E. 2006. Acyl carrier protein/SpoT interaction, the switch linking SpoT-dependent stress response to fatty acid metabolism. *Mol. Microbiol.* **62**:1048–1063.

Battiste, J.L., Pestova, T.V., Hellen, C.U., and Wagner, G. 2000. The eIF1A solution structure reveals a large RNA-binding surface important for scanning function. *Mol. Cell* **5**:109–119.

Beauclerk, A.A.D., Cundliffe, E., and Dijk, J. 1984. The binding site for ribosomal protein complex L8 within 23S RNA of *Escherichia coli*. *J. Biol. Chem.* **259**: 6559–6563.

Beck, K., Wu, L.F., Brunner, J., and Muller, M. 2000. Discrimination between SRP- and SecA/SecB-dependent substrates involves selective recognition of nascent chains by SRP and trigger factor. *EMBO J.* **19**:134–143.

Becker, H.D., Min, B., Jacobi, C., *et al.* 2000. The heterotrimeric *Thermus thermophilus* Asp-tRNA(Asn) amidotransferase can also generate Gln-tRNA(Gln). *FEBS Lett.* **476**:140–144.

Beckmann, R., Bubeck, D., Grassucci, R., *et al.* 1997. Alignment of conduits for the nascent polypeptide chain in the ribosome-Sec61 complex. *Science* **278**:2123–2126.

Beckmann, R., Spahn, C.M., Eswar, N., *et al.* 2001. Architecture of the protein-conducting channel associated with the translating 80S ribosome. *Cell* **107**:361–372.

Beebe, K, Mock, M, Merriman, E, *et al*. 2008. Distinct domains of tRNA synthetase recognize the same base pair. *Nature* **451**:90–93.

Belitsina, N.V., Glukhova, M.A., and Spirin, A.S. 1975. Translocation in ribosomes by attachment-detachment of elongation factor G without GTP cleavage: evidence from a column-bound ribosome system. *FEBS Lett.* **54**:35–38.

Belousoff, M.J. Shapira, T., Bashan, A., *et al*. 2011. Crystal structure of the synergistic antibiotic pair, lankamycin and lankacidin, in complex with the large ribosomal subunit. *Proc. Natl. Acad. Sci. USA.* **108**:2717–2122.

Benjamin, D.R., Robinson, C.V., Hendrick, J.P., *et al.* 1998. Mass spectrometry of ribosomes and ribosomal subunits. *Proc. Natl. Acad. Sci. USA.* **95**:7391–7395.

Ben-Shem, A., Jenner, L., Yusupova, G., *et al*. 2010. Crystal structure of the eukaryotic ribosome. *Science* **330**:1203–1209.

Ben-Shem, A., Garreau de Luobresse, N., Melnikov, S., *et al.* 2011. The structure of the eukaryotic ribosome at 3.0Å resolution. *Science* **334**:1524–1529.

Berchtold, H., Reshetnikova, L., Reiser, C.O., *et al.* 1993. Crystal structure of active elongation factor Tu reveals major domain rearrangements. *Nature* **365**:126–132.

Berestowskaya, N.H., Vasiliev, V.D., Volkov, A.A., and Chetverin, A.B. 1988. Electron microscopy study of Q beta replicase. *FEBS Lett.* **228**:263–267.

Berg, P. 1961. Specificity in protein synthesis. *Ann. Rev. Biochem.* **30**:293–324.

Beribisky, A.V., Tavares, T.J., Amborski, A.N., *et al*. 2007. The three-dimensional structure of the *Moorella thermoacetica* selenocysteine insertion sequence RNA hairpin and its interaction with the elongation factor SelB. *RNA* **13**:1948–1956.

Beringer, M., Bruell, C., Xiong, L. *et al*. 2005. Essential mechanisms in the catalysis of peptide bond formation on the ribosome. *J. Biol. Chem.* **280**:36065–36072.

Berisio, R., Harms, J., Schluenzen, F., *et al.* 2003a. Structural insight into the antibiotic action of telithromycin against resistant mutants. *J. Bacteriol.* **185**:4276–4279.

Berisio, R., Schluenzen, F., Harms, J., *et al.* 2003b. Structural insight into the role of the ribosomal tunnel in cellular regulation. *Nat. Struct. Biol.* **10**:366–370.

Bernabeau, C., and Lake, J.A. 1982. Nascent polypeptide chains emerge from the exit domain of the large ribosomal subunit: immune mapping of the nascent chain. *Proc. Natl. Acad. Sci. USA.* **79**:3111–3115.

Bessho, Y., Shibata, R., Sekine, S., *et al*. 2007. Structural basis for functional mimicry of long-variable-arm tRNA by transfer-messenger RNA. *Proc. Natl. Acad. Sci. USA.* **104**:8293–8298.

Bhushan, S., Gartmann, M., Halic, M., *et al*. 2010. α-helical nascent polypeptide chains visualized within distinct regions of the ribosomal exit tunnel. *Nat. Struct. Mol. Biol.* **17**:313–318.

Bieling, P., Beringer, M., Adio, S., *et al*. 2006. Peptide bond formation does not involve acid-base catalysis by ribosomal residues. *Nat. Struct. Mol. Biol.* **13**:423–428.

Bilgin, N., Richter, A.A., Ehrenberg, M., *et al.* 1990. Ribosomal RNA and protein mutants resistant to spectinomycin. *EMBO J.* **9**:735–739.

Bilgin, N., Claesens, F., Pahverk, H., and Ehrenberg, M. 1992. Kinetic properties of *Escherichia coli* ribosomes with altered forms of S12. *J. Mol. Biol.* **224**: 1011–1027.

Bingel-Erlenmeyer, R., Kohler, R., Kramer, G., *et al*. 2008. A peptide deformylase-ribosome complex reveals mechanism of nascent chain processing. *Nature* **452**:108–111.

Biou, V., Shu, F., and Ramakrishnan, V. 1995. X-ray crystallography shows that translational initiation factor IF3 consists of two compact alpha/beta domains linked by an alpha-helix. *EMBO J.* **14**:4056–4064.

Bitto E. and McKay D.B. 2002. Crystallographic structure of SurA, a molecular chaperone that facilitates folding of outer membrane porins. *Structure* **10**:1489–1498.

Björk, G.R. 1995. Biosynthesis and function of modified nucleosides. In *tRNA: Structure, Biosynthesis, and Function*, Eds. D. Söll and U. RajBhandary, pp. 165–205.

Blaha, G., Wilson, D.N., Stroller, G., *et al.* 2003. Localization of the trigger factor binding site on the ribosomal 50S subunit. *J. Mol. Biol.* **326**:887–897.

Blaha, G., Gürel, G., Schroeder, S.J., *et al*. 2008. Mutations outside the anisomycin-binding site can make ribosomes drug-resistant. *J. Mol. Biol.* **379**:505–519.

Blaha, G., Stanley, R.E., and Steitz, T.A. 2009. Formation of the first peptide bond: The structure of EF-P bound to the 70S ribosome. *Science* **325**:966–970.

Blaha, G., Polikanov, Y.S., and Steitz, T.A. 2012. Elements of ribosomal drug resistance and specificity. *Curr. Op. Struct. Biol.* **22**:750–758.

Blanchard, S.C., Gonzalez, R.L., Kim, H.D., *et al*. 2004. tRNA selection and kinetic proofreading in translation. *Nat. Struct. Mol. Biol*. **11**:1008–1014.

Blanchard, SC. 2009. Single-molecule observations of ribosome function. *Curr. Op. Struct. Biol.* **19**:103–109.

Blobel, G., and Sabatini, D.D. 1970. Controlled proteolysis of nascent polypeptides in rat liver cell fractions. I. Location of the polypeptides within ribosomes. *J. Cell Biol.* **45**:130–145.

Bocharov, E.V., Gudkov, A.T., and Arseniev, A.S. 1996. Topology of the secondary structure elements of ribosomal protein L7/L12 from *E. coli* in solution. *FEBS Lett.* **379**:291–294.

Bocharov, E.V., Gudkov, A.T., Budovskaya, E.V., and Arseniev, A.S. 1998. Conformational independence of N- and C-domains in ribosomal protein L7/L12 and in the complex with protein L10. *FEBS Lett.* **423**:347–350.

Bocharov, E.V., Sobol, A.G., Pavlov, K.V., *et al.* 2004. From structure and dynamics of protein L7/L12 to molecular switching in ribosome. *J. Biol. Chem.* **279**:17697–17706.

Bodley, J.W., Zieve, F.J., Lin, L., and Zieve, S.T. 1969. Formation of the ribosome-G factor-GDP complex in the presence of fusidic acid. *Biochem. Biophys. Res. Commun.* **37**:437–443.

Bodley, J.W., Zieve, F.J., and Lin, L. 1970a. Studies on translocation. IV. The hydrolysis of a single round of guanosine triphosphate in the presence of fusidic acid. *J. Biol. Chem.* **245**:5662–5567.

Bodley, J.W., Zieve, F.J., Lin, L., and Zieve, S.T. 1970b. Studies on translocation. 3. Conditions necessary for the formation and detection of a stable ribosome-G factor guanosine diphosphate complex in the presence of fusidic acid. *J. Biol. Chem.* **245**:5656–5661.

Bodley, J.W., Lin, L., and Highland, J.H. 1970c. Studies on translocation. VI. Thiostrepton prevents the formation of a ribosome-G factor-guanine nucleotide complex. *Biochem. Biophys. Res. Commun.* **41**:1406–1411.

Boettcher, B., Wynne, S.A., and Crowther, R.A. 1997. Determination of the fold of the core protein of hepatitis B virus by electron cryomicroscopy. *Nature* **36**:88–91.

Bokov, K. and Steinberg, S.V. 2009. A hierarchial model for evolution of 23S ribosomal RNA. *Nature* **457**:977–980.

Boni, IV. 2006. Diverse molecular mechanisms of translational initiation in prokaryotes. *Mol. Biol.* **40**:658–668.

Borovinskaya, M.A., Shoji, S., Holton, J.M., *et al*. 2007. A steric block in translation caused by the antibiotic spectinomycin. *ACS Chem. Biol.* **2**:545–552.

Borovinskaya, M.A., Shoji, S., Fredrick, K., *et al*. 2008. Structural basis for hygromycin B inhibition of protein synthesis. *RNA* **14**:1590–1599.

Borowski, C., Rodnina, M.V., and Wintermeyer, W. 1996. Truncated elongation factor G lacking the G domain promotes translocation of the 3′-end but not of the anticodon domain of peptidyl-tRNA. *Proc. Natl. Acad. Sci. USA.* **93**:4202–4206.

Boublik, M., Hellmann, W., and Roth, H.E. 1976. Localization of ribosomal proteins L7/L12 in the 50S subunit of *Escherichia coli* ribosomes by electron microscopy. *J. Mol. Biol.* **107**:479–490.

Bourne, H.R., Sanders, D.A., and McCormick, F. 1990. The GTPase superfamily: a conserved switch for diverse cell functions. *Nature* **248**:125–132.

Bourne, H.R., Sanders, D.A., and McCormick, F. 1991. The GTPase superfamily: conserved structure and molecular mechanism. *Nature* **349**:117–127.

Branciamore, S. and Di Giulio, M. 2012. The origin of the 5S ribosomal RNA molecule could have been caused by a single inverse duplication: strong evidense from its sequence. *J. Mol. Evol.* **74**:170–186.

Brenner, S., Jacob, F., and Meselson, M. 1961. An unstable intermediate carrying information from genes to ribosomes for protein synthesis. *Nature* **190**:576–581.

Bretscher, M. 1968. Translocation in protein synthesis: a hybrid structure model. *Nature* **218**:675–677.

Bright, G.M., Nagel, A.A., Bordner, J., *et al.* 1988. Synthesis, *in vitro* and *in vivo* activity of a novel 9-deoxo-9a-AZA-9a-homoerythromycin A derivative — a new class of macrolide antibiotics, the azalides. *J. Antibiot.* **41**:1029–1047.

Britton, R.A. 2009. Role of GTPases in bacterial ribosome assembly. *Annu. Rev. Microbiol*. **63**:155–176.

Brodersen, D.E., Clemons, Jr, W.M. Carter, A.P., *et al*. 2000. The structural basis for the action of the antibiotics tetracycline, pactamycin, and hygomycin B on the 30S ribosomal subunit. *Cell* **103**: 1143–1154.

Brodersen, D.E., Clemons Jr., W.M., Carter, A.P., *et al*. 2002. Crystal structure of the 30S ribosomal subunit from *Thermus thermophilus*: structure of the proteins and their interactions with 16S RNA. *J. Mol. Biol*. **316**:725–768.

Brodersen, D.E., and Ramakrishnan, V. 2003. Shape can be seductive. *Nat. Struct. Biol*. **10**:78–80.

Brosius, J., Palmer, M.L., Kennedy, P.J., and Noller, H.F. 1978. Complete nucleotide sequence of a 16S ribosomal RNA gene from *Escherichia coli. Proc. Natl. Acad. Sci. USA.* **75**:4801–4805.

Brosius, J., Dull, T.J., and Noller, H.F. 1980. Complete nucleotide sequence of a 23S ribosomal RNA gene from *Escherichia coli. Proc. Natl. Acad. Sci. USA.* **77**:201–204.

Brown, C.M., McCaughan, K.K., and Tate, W.P. 1993. Two regions of the *Escherichia coli* 16S ribosomal RNA are important for decoding stop signals in polypeptide chain termination. *Nucl. Acids Res.* **21**:2109–2115.

Brown, C.M. and Tate, W.P. 1994. Direct recognition of mRNA stop signals by *Escherichia coli* polypeptide chain release factor two. *J. Biol. Chem.* **269**: 33164–33170.

Brune, M., Hunter, J.L., Corrie, J.E., and Webb, M.R. 1994. Direct, real-time measurement of rapid inorganic phosphate release using a novel fluorescent probe and its application to actinomycin subfragment 1 ATPase. *Biochemistry* **33**:8262–8271.

Bubunenko, M.G., and Gudkov, A.T. 1990. Elongation factors Tu and G change their conformation on interaction with ribosomes. *Biomed. Sci.* **1**:127–132.

Bubunenko, M.G., Chulkov, S.V., and Gudkov, A.T. 1992. The length of the interdomain region of the L7/L12 protein is important for its function. *FEBS Lett*. **313**: 232–234.

Bubunenko, M., Baker, T., and Court, D.L. 2007. Essentiality of ribosomal and transcription antitermination proteins analysed by systematic gene replacement in *Escherichia coli*. *J. Bact*. **189**: 2844–2853.

Buckingham, R.H., Grentzmann, G., and Kisselev, L. 1997. Polypeptide chain release factors. *Mol. Microbiol*. **24**:449–456.

Bukau, B., Deuerling, E., Pfund, C., and Craig, E.A. 2000. Getting newly synthesized proteins into shape. *Cell* **101**:119–122.

Bulkley, D., Innis, C.A., Blaha, G., *et al*. 2010. Revisiting the structures of several antibiotics bound to the bacterial ribosome. *Proc. Natl Acad. Sci. USA.* **107**:17158–17163.

Bult, C.J., White, O., Olsen, G.J., *et al.* 1996. Complete genome sequence of the methanogenic archaeon, *Methanococcus jannaschii*. *Science* **273**:1058–1073.

Burdett, V. 1991. Purification and characterization of Tet(M), a protein that renders ribosomes resistant to tetracycline. *J. Biol. Chem.* **266**:2872–2877.

Burdett, V. 1996. Tet(M)-promoted release of tetracycline from ribosomes is GTP dependent. *J. Bacteriol*. **178**:3246–3251.

Burma, D.P., Srivastava, A.K., Srivastava, S., and Dash, D. 1985. Interconversion of tight and loose couple 50S ribosomes and translocation in protein synthesis. *J. Biol. Chem.* **260**:10517–10525.

Bushuev, V.N., Gudkov, A.T., Liljas, A., and Sepetov, N.F. 1989. The flexible region of protein L12 from bacterial ribosomes studied by proton nuclear magnetic resonance. *J. Biol. Chem.* **264**:4498–4505.

Bycroft, M., Hubbard, T.J., Proctor, M., *et al.* 1997. The solution structure of the S1 RNA binding domain: a member of an ancient nucleic acid-binding fold. *Cell* **88**:235–242.

Byrne, R.T, Convega, A.L., Rodnina, M.V., *et al*. 2010. The crystal structure of unmodified $tRNA^{Phe}$ from *Eschericia coli*. *Nucleic Acids Res*. **38**:4154–4162.

Cabanas, M.J., Vazquez, D., and Modolell, J. 1978. Inhibition of ribosomal translocation by aminoglycoside antibiotics. *Biochim. Biophys. Res. Commun.* **83**:991–997.

Caetano-Anolles, G., Wang, M., Caetano-Anolles, D., *et al*. 2009. The origin, evolution and structure of the protein world. *Biochem. J*. **417**:621–637.

Caetano-Anolles, D., Kim, K.M., Mittenthal, J.E., *et al*. 2011. Proteome evolution and the metabolic origin of translation and cellular life, *J. Mol. Evol.* **72**:14–33.

Caldon, C.E., Yoong, P., and March, P.E. 2001. Evolution of a molecular switch: universal bacterial GTPases regulate ribosome function. *Mol. Microbiol*. **41**:289–297.

Calo, D. and Eichler, J. 2011. Crossing the membrane in Archaea, the third domain of life. *Biochim. Biophys. Acta* **1808**:885–891.

Calvin, K., and Li, H. 2008. RNA-splicing endonuclease structure and function. *Cell. Mol. Life Sci.* **65**:1176–1185.

Cameron, D.M., Thompson, J., March, P.E., and Dahlberg, A.E. 2002. Initiation factor IF2, thiostrepton and micrococcin prevent the binding of elongation factor G to the *Escherichia coli* ribosome. *J. Mol. Biol.* **319**:27–35.

Cameron, D., Thompson, J., Gregory, S., *et al*. 2004. Thiostrepton-resistant mutants of *Thermus thermophilus*. *Nucleic Acids Res*. **32**:3220–3227.

Capa, L., Mendoza, A., Lavandera, J.L., *et al*. 1998. Translation elongation factor 2 is part of the target for a new family of antifungals. *Antimicrob. Agents Chemother.* **42**:2694–2699.

Capecchi, M.R., and Klein, H.A. 1969. Characterization of three proteins involved in polypeptide chain termination. *Cold Spring Harb. Symp. Quant. Biol*. **34**:469–477.

Capel, M.S., Engelman, D.M., Freeborn, B.R., *et al*. 1987. A complete mapping of the proteins in the small ribosomal subunit of *Escherichia coli*. *Science* **238**: 1403–1406.

Carroll, A.J., Heazlewood, J.L., Ito, J. *et al*. 2008. Analysis of the arabidopsis cytosolic ribosome proteome provides detailed insights into its compontents and their post-translational modification. *Mol. Cell Proteom*. **7**:347–369.

Carter, A.P., Clemons, W.M., Brodersen, D.E., *et al*. 2000. Functional insights from the structure of the 30S ribosomal subunit and its interactions with antibiotics. *Nature* **407**:340–348.

Carter, A.P., Clemons Jr., W.M., Brodersen, D.E., *et al*. 2001. Crystal structure of an initiation factor bound to the 30S ribosomal subunit. *Science* **291**:498–501.

Carter, C.W. 1993. Cognition, mechanism and evolutionary relationships in aminoacyl-tRNA synthetases. *Annu. Rev. Blochem*. **62**: 715–745.

Caserta, E., Tomsic, J., Spurio, R., *et al*. 2006. Translation initiation factor IF2 interacts with the 30 S ribosomal subunit via two separate binding sites. *J. Mol. Biol*. **362**:787–799.

Cashel, M., Gentry, D.R., Hernandez, V.J., and Vinella, D. 1996. The stringent response. In *Escherichia coli and Salmonella thyphimurium: Cellular and Molecular Biology*, Eds. F.C. Neidhardt, *et al*., pp. 1458–1496, American Society for Microbiology, Washington, D.C.

Caskey, T., Scolnick, E., Tompkins, R., *et al*. 1969. Peptide chain termination, codon, protein factor, and ribosomal requirements. *Cold Spring Harb. Symp. Quant. Biol*. **34**:479–488.

Cate, J.H., Yusupov, M.M., Yusupova, G.Z., *et al*. 1999. X-ray crystal structures of 70S ribosome functional complexes. *Science* **285**:2095–2104.

Cathopoulis, T.J.T., Chuawong, P., and Hendrickson, T. 2008. Conserved discrimination against misacylated tRNAs by two mesophilic elongation factor Tu orthologs. *Biochemistry* **47**:7610–7616.

Cech, T.R., Zaug, A.J., and Grabowski, P.J. 1981. *In vitro* splicing of the ribosomal RNA precursor of tetrahymena: involvement of the guanosine nucleotide in the excision of the intervening sequence. *Cell* **27**:487–496.

Cetin, R., Krab, I.M., Anborgh, P., *et al*. 1996. Enacyloxin IIa, an inhibitor of protein biosynthesis that acts on EF-Tu and the ribosome. *EMBO J.* **15**:2604–2611.

Chamberlin, M. and Berg, P. 1962. Deoxyribonucleic acid-directed synthesis of ribonucleic acid by an enzyme from *Escherichia coli*. *Proc. Natl. Acad. Sci. USA.* **48**:81–94.

Chan, Y.L., Correll, C.C., and Wool, I.G. 2004. The location and the significance of a cross-link between the sarcin/ricin domain of ribosomal RNA and the elongation factor-G. *J. Mol. Biol.* **337**:263–272.

Chandrasekar, S., Chartron, J., Jaru-Ampornpan, P., *et al*. 2008. Structure of the chloroplast signal recognition particle (SRP) receptor: Domain arrangement modulates SRP-receptor interaction. *J. Mol. Biol.* **375**: 425–436.

Chao, F.C. and Schachman, H.K. 1956. The isolation and characterization of a macromolecular ribonucleoprotein from yeast. *Arch. Biochem. Biophys.* **61**:220–230.

Chen, X., Court, D.L., and Ji, X. 1999. Crystal structure of Era: a GTPase-dependent cell cycle regulator containing an RNA binding motif. *Proc. Natl. Acad. Sci. USA.* **96**:8396–8401.

Chen, Y., Koripell, R.K., Sanyal, S. *et al*. 2010. *Staphylococcus aureus* elongation factor G — structure and analysis of a target for fusidic acid. *FEBS J.* **277**: 3789–3803.

Cheng, K., Ivanova, N., Scheres, S.H.W., *et al*. 2010. tmRNA·SMpB complex mimics native aminoacyl-tRNAs in the A site of stalled ribosomes. *J. Struct. Biol.* **169**: 342.

Choi, S.K., Olsen, D.S., Roll-Mecak, A., *et al.* 2000. Physical and functional interaction between eukaryotic orthologs of prokaryotic translation initiation factors IF1 and IF2. *Mol. Cell. Biol.* **20**:7183–7191.

Choli, T., Franceschi, F., Yonath, A., and Wittmann-Liebold, B. 1993. Isolation of a new ribosomal protein from the *Thermophilic eubacteria*, *Thermus thermophilus*, *T. aquaticus* and *T. flavus*. *Biol. Chem. Hoppe Seyler.* **374**:377–383.

Chopra, I. 2000. New drugs for superbugs. *Microbiol. Today* **27**:4–6.

Chopra, I., Hawkey, P.M., and Hinton, M. 1992. Tetracyclines, molecular and clinical aspects. *J. Antimicrob. Chemother.* **29**:245–277.

Christensen, S.K., Mikkelsen, M., Pedersen, K., and Gerdes, K. 2001. RelE, a global inhibitor of translation, is activated during nutritional stress. *Proc. Natl. Acad. Sci. USA.* **98**:14328–14333.

Clemons, W.M. Jr., Davies, C., White, S.W., and Ramakrishnan, V. 1998. Conformational variability of the N-terminal helix in the structure of ribosomal protein S15. *Structure* **6**:429–438.

Clemons, W.M. Jr., May, J.L.C., Wimberly, B.T., *et al.* 1999. Structure of a bacterial 30S ribosomal subunit at 5.5Å resolution. *Nature* **400**:833–840.

Clemons, W.M. Jr., Brodersen, D.E., McCutcheon, J.P., *et al.* 2001. Crystal structure of the 30S ribosomal subunit from *Thermus thermophilus*: purification, crystallisation and structure determination. *J. Mol. Biol.* **310**:829–845.

Cochella, L. and Green, R. 2005. An active role for tRNA in decoding beyond codon: anticodon pairing. *Science* **308**:1178–1180.

Cohen, L.B., Goldberg, I.H., and Herner, A.E. 1969. Inhibition by pactamycin of the intiation of protein synthesis. Effect on the 30S ribosomal subunit. *Biochemistry* **8**:1327–1335.

Conn, G.L., Draper, D.E., Lattman, E.E., and Gittis, A.G. 1999. Crystal structure of a conserved ribosomal protein-RNA complex. *Science* **284**:1171–1174.

Connell, S.R., Trieber, C.A., Dinos, G.P., *et al.* 2003. Mechanism of Tet(O)-mediated tetracycline resistance. *EMBO J.* **22**:945–953.

Connell, S.R., Takemoto, C., Wilson, D.N., *et al*. 2007. Structural basis for interaction of the ribosome with the switch regions of GTP-bound elongation factors. *Mol. Cell* **25**:751–764.

Connell, A., Topf, M., Qin, Y., *et al*. 2008. A new tRNA intermediate revealed on the ribosome during EF4-mediated back-translocation. *Nat. Struct. Mol. Biol.* **15**:910–915.

Contreras, A. and Vazquez, D. 1977. Cooperative and antagonistic interactions of peptidyl-tRNA and antibiotics with bacterial ribosomes. *Eur. J. Biochem.* **74**:539–547.

Cool, R.H., and Parmeggiani, A. 1991. Substitution of histidine-84 and the GTPase mechanism of elongation factor Tu. *Biochemistry* **30**:362–366.

Copeland, P.R., Fletcher, J.E., Carlson, B.A., *et al*. 2000. A novel RNA binding protein, SBP2, is required for the translation of mammalian selenoprotein mRNAs. *EMBO J.* **19**:306–314.

Cornish, P.V., Ermolenko D.N., Noller, H.F., *et al*. 2008. Spontaneous subunit rotation in single ribosomes. *Cell* **30**:578–588.

Cowgill, C.A., Nichols, B.G., Kenny, J.W., *et al.* 1984. Mobile domains in ribosomes revealed by proton nuclear magnetic resonance. *J. Biol. Chem.* **259**:15257–15263.

Craigen, W.J., Cook, R.G., Tate, W.P., and Caskey, C.T. 1985. Bacterial peptide chain release factors: conserved primary structure and possible frameshift regulation of release factor 2. *Proc. Natl. Acad. Sci. USA.* **82**:3616–3620.

Cramer, P., Armache, K.-J., Baumli, S. *et al*. 2008. Structure of eukaryotic RNA polymerases. *Annu Rev Biophys* **37**:337–352.

Crick, F.H.C. 1958. On protein synthesis. *Symp. Soc. Exp. Biol*. **12**:138–163.

Crick, F.H.C. 1962. The genetic code. *Sci. Am.* **207**:66–74.

Crick, F.H.C. 1963. On the genetic code. *Science* **139**:461–464.

Crick, F.H.C. 1966a. The genetic code: Yesterday, today and tomorrow. *Cold Spring Harb. Symp. Quant. Biol.* **31**:1–9.

Crick, F.H.C. 1966b. Codon-anticodon pairing: the wobble hypothesis. *J. Mol. Biol.* **19**:548–555.

Crick, F.H.C. 1968. The origin of the genetic code. *J. Mol. Biol.* **38**:367–379.

Crick, F.H.C., Barnett, L., Brenner, S., and Watts-Tobin, R. 1961. General nature of the genetic code for proteins. *Nauchni Tr. Vissh. Med. Inst. Sofia Nat.* **192**:1227–1232.

Cross, R.A. 1997. A protein-making motor protein. *Nature* **385**:18–19.

Cross, B.C.S., Sinning, I., Luirink, J., *et al*. 2009. Delivering proteins for export from the cytosol. *Nat. Rev. Mol. Cell Biol.* **10**:255–264.

Culver, G.M., and Noller, H.F. 2000. Directed hydroxyl radical probing of RNA from iron(II) tethered to proteins in ribonucleoprotein complexes. *Methods Enzymol*. **318**:461–475.

Culver, G.M., Cate, J.H., Yusupova, G.Z., *et al.* 1999. Identification of an RNA-protein bridge spanning the ribosomal subunit interface. *Science* **285**:2133–2136.

Cundliffe, E. 1980. Antibiotics and prokaryotic ribosomes: action, interaction and resistance. In *Ribosomes: Structure Function and Genetics*, Eds. G. Chambliss, G.R. Craven, J. Davies, *et al.*, pp. 555–581. University Park Press, Baltimore.

Cundliffe, E. 1981. Antibiotic inhibitors of ribosome function. In *Antibiotic Inhibitors of Ribosome Function*, Eds. E.F. Gale, E. Cundliffe, P.E. Reynolds, *et al.*, Wiley, London, New York, Sydney, Toronto.

Cundliffe, E. 1987. On the nature of antibiotic binding sites in ribosomes. *Biochimie* **69**:863–869.

Cundliffe, E. 1990. Recognition sites for antibiotics within rRNA. In *The Ribosome: Structure, Function and Evolution*, Eds. W.E. Hill, A. Dahlberg, R.A. Garrett, *et al.*, pp. 479–490. ASM Press, Washington, DC.

Cundliffe, E., Dixon, P., Stark, M., *et al*. 1979. Ribosomes in thiostrepton-resistant mutants of B. megaterium lacking a single 50S subunit protein. *J. Mol. Biol*. **132**: 235–252.

Curnow, A.W., Ibba, M., and Söll, D. 1996. tRNA asparagine formation. *Nature* **382**: 589–590.

Curnow, A.W., Tumbula, D.L., Pelaschier, J.T., *et al*. 1998. Glutamyl-tRNA(Gln) amidotransferase in *Deinococcus radiodurans* may be confined to asparagine biosynthesis. *Proc. Natl. Acad. Sci. USA*. **95**:12838–12843.

Cusack, S. 1995. Eleven down and nine to go. *Nat. Struct. Biol.* **2**:824–831.

Cusack, S., Berthet-Colominas, C., Hartlein, M., *et al.* 1990. A second class of synthetase structure revealed by X-ray analysis of *Escherichia coli* seryl-tRNA synthetase at 2.5Å *Nature* **347**:347–255.

Czworkowski, J., Wang, J., Steitz, T.A., and Moore, P.B. 1994. The crystal structure of elongation factor G complexed with GDP, at 2.7Å resolution. *EMBO J.* **13**:3661–3668.

Dabbs, E. 1986. Mutant studies on the prokaryotic ribosome. In *Structure, Function, and Genetics of Ribosomes*, Eds. B. Hardesty and G. Kramer, pp. 733–748. Springer-Verlag, New York.

Dabbs, E.R. 1991. Mutants lacking individual ribosomal proteins as a tool to investigate ribosomal properties. *Biochimie* **73**:639–645.

Dabbs, E.R., Ehrlich, R., Hasenbank, R., *et al*. 1981. Mutants of *Escherichia coli* lacking ribosomal protein L1. *J. Mol. Biol*. **149**:553–578.

Dabbs, E.R., Hasenbank, R., Kastner, B., *et al.* 1983. Immunological studies of *Escherichia coli* mutants lacking one or two ribosomal proteins. *Mol. Gen. Genet*. **192**:301–308.

Dahlquist, K.D., and Puglisi, J.D. 2000. Interaction of translation initiation factor IF1 with the *E. coli* ribosomal A-site. *J. Mol. Biol.* **299**:1–15.

Dalbey, R.E. and Wickner, W. 1985. Leader peptidase catalyzes the release of exported proteins from the outer surface of the *Escherichia coli* plasma membrane. *J. Biol. Chem.* **260**:15925–15931.

Dallas, A., and Noller, H.F. 2001. Interaction of translation initiation factor 3 with the 30S ribosomal subunit. *Mol. Cell* **4**:855–864.

Dantley, K.A., Dannelly, H.K., and Burdett, V. 1998. Binding interaction between Tet(M) and the ribosome: requirements for binding. *J. Bacteriol.* **180**: 4089–4092.

Das, S., and Maitra, U. 2000. Mutational analysis of mammalian translation initiation factor 5 (eIF5): role of interaction between b subunit of 2IF2 and eIF5 in eIF5 function *in vitro* and *in vivo*. *Mol. Cell. Biol.* **20**:3942–3950.

Datta, P.P., Sharma, M.R., Qi, L. *et al*. 2005. Interaction of the G′ domain of elongation factor G and the C-terminal domain of ribosomal protein L7/L12 during translocation as revealed by cryo-EM. *Mol. Cell* **20**:723–731.

Davies, C., Gerstner, R.B., Draper, D.E., *et al.* 1998. The crystal structure of ribosomal protein S4 reveals a two-domain molecule with an extensive RNA-binding surface: one domain shows structural homology to the ETS DNA-binding motif. *EMBO J.* **17**:4545–4558.

Davies, C., Ramakrishnan, V., and White, S.W. 1996a. Structural evidence for specific S8-RNA and S8-protein interactions within the 30S ribosomal subunit: ribosomal protein S8 from *Bacillus stearothermophilus* at 1.9A resolution. *Structure* **4**:1093–1104.

Davies, C., White, S.W., and Ramakrishnan, V. 1996b. The crystal structure of ribosomal protein L14 reveals an important organizational component of the translational apparatus. *Structure* **4**:55–66.

Davies, J. 1990. What are antibiotics? Archaic functions for modern activities. *Mol. Microbiol.* **4**:1227–1232.

Davies, J., Gilbert, W., and Gorini, L. 1964. Streptomycin, suppression, and the code. *Proc. Natl. Acad. Sci. USA.* **51**:883–890.

Daviter, T., Wieden, H.J., and Rodnina, M. 2003. Essential role of histidine 84 in elongation factor Tu for the chemical step of GTP hydrolysis on the ribosome. *J. Mol. Biol.* **332**:689–699.

Davydov, I.I., Rozov, A.S., Tonevitsky, E.A., *et al*. 2008. The origin of eubacteria with three L7/L12 protein dimers in the ribosome. *Biochem. Biophys. Mol. Biol.* **422**:257–260.

Davydova, N., Streltsov, V., Wilce, M., *et al.* 2002. L22 ribosomal protein and effect of its mutation on ribosome resistance to erythromycin. *J. Mol. Biol.* **322**:635–644.

de Bruijn, M.H.L. and Klug, A. 1983. A model for the tertiary structure of mammalian mitochondrial transfer RNAs lacking the entire 'dihydrouridine' loop and stem. *EMBO J.* **2**:1309–1321.

Delage, L., Giege, P., Sakamoto, M., *et al*. 2007. Four paralogues are differently associated to ribosomes in plant mitochondria. *Biochimie* **89**:658–668.

deLivron, M., Makanji, H.S., Lane, M.C., *et al*. 2009. A novel domain in translational GTPase BipA mediates interaction with the 70S ribosome and influences GTP hydrolysis. *Biochemistry* **48**:10533–10541.

Demeshkina, N., Jenner, L., Yusupova, G., *et al*. 2010. Interactions of the ribosome with mRNA and tRNA. *Curr. Op. Struct. Biol.* **20**:325–332.

Demirci, H., Gregory, S., Dahlberg, A., *et al*. 2008a. Multiple-site trimethylation of ribosomal protein L11 by the PrmA methyltransferase. *Structure* **16**:1059–1066.

Demirci, H., Gregory, S., Dahlberg, A., *et al*. 2008b. Crystal structure of the *Thermus thermophilus* 16S rRNA methyltransferase RsmC in complex with cofactor and substrate guanosine. *J. Biol. Chem.* **283**:26548–26556.

Demirci, H., Murphy, F., Belardinelli, R., *et al*. 2010. Modification of 16S ribosomal RNA by the KsgA methyltransferase restructures the 30S subunit to optimize ribosome function. *RNA* **16**:2319–2324.

Dennis, P.P., Ehrenberg, M., and Bremer, H. 2004. Control of rRNA synthesis in *Escherichia coli*: a systems biology approach. *Microbiol. Mol. Biol. Rev*. **68**:639–668.

Dennis, P. and Nomura, M. 1974. Stringent control of ribvosomal gene expression in *Escherichia coli*. *Proc. Natl. Acad. Sci. USA*. **71**:3819–3823.

Desmond, E., Brochier-Armanet, C., Forterre, P. *et al*. 2011. On the last common ancestor and early evolution of eukaryotes reconstructing the history of mitochondrial ribosomes. *Res. Microbiol*. **162**:53–70.

Deuerling, E., Schulze-Specking, A., Tomoyasu, T., *et al*. 1999. Trigger factor and DnaK cooperate in folding of newly synthesized proteins. *Nature* **400**: 693–696.

Dey, D., Bochkariov, D.E., Jokhadze, G.G., and Traut, R.R. 1998. Cross-linking of selected residues in the N- and C-terminal *Escherichia coli* protein L7/L12 to other ribosomal proteins and the effect of elongation factor Tu. *J. Biol. Chem.* **273**: 1670–1676.

Diaconu, M., Kothe, U., Schlüntzen, F., *et al*. 2005. Structural basis for the function of the ribosomal L7/L12 stalk in factor binding and GTPase activation. *Cell* **121**:991–1004.

Di Guilio, M. 2009. A comparison among the models proposed to explain the origin of the tRNA molecule: A synthesis. *J. Mol. Evol*. **69**:1–9.

Dijk, J., Garrett, R.A., and Müller, R. 1979. Studies of the binding of the ribosomal protein complex L7/12-L10 and protein L11 to the 5′-one third of the 23S RNA: a functional center of the 50S subunit. *Nucl. Acids Res.* **6**:2717–2730.

Dijk, J., and Littlechild, J. 1979. Purification of ribosomal proteins from *Escherichia coli* under nondenaturing conditions. *Methods Enzymol.* **59**:481–502.

Dincbas-Renqvist, V., Engström, A., Mora, L., *et al*. 2000. A post-translational modification in the GGQ motif of RF2 from Escherichia coli stimulates termination of translation. *EMBO J.* **19**:6900–6907.

Dinos, G., Wilson, D.N., Teraoka, Y., *et al.* 2004. Dissecting the ribosomal inhibition mechanisms of edeine and pactamycin: the universally conserved residues G693 and C795 regulate P-site RNA binding. *Mol. Cell* **13**:113–124.

Dock-Bregeon, A.C., Sankaranarayanan, R., Romby, P., *et al.* 2000. Transfer RNA mediated editing in threonyl-tRNA synthetase: the class II solution to the double discrimination problem. *Cell* **103**:877–884.

Dock-Bregeon, AC, Rees, B, Torres-Larios, A, *et al*. 2004. Achieving Error-Free Translation: The Mechanism of Proofreading of Threonyl-tRNA Synthetase at Atomic Resolution. *Mol. Cell* **16**:375–387.

Dognin, M.J., and Wittmann-Liebold, B. 1980. Purification and primary structure determination of the N-terminal blocked protein, L11, from Escherichia coli ribosomes. *Eur. J. Biochem.* **112**:131–151.

Dominguez, J.M., Gomez-Lorenzo, M.G., and Martin, J.J. 1999. Sordarin inhibits fungal protein synthesis by blocking translocation differently to fusidic acid. *J. Biol. Chem.* **274**:22423–22427.

Dong, H., Nilsson, L., and Kurland, C. 1996. Co-variation of tRNA abundance and codon usage in *Escherichia coli* at different growth rates *J. Mol. Biol*. **260**:649.

Dorner, S., Panuschka, C., Schmid, W., *et al*. 2003. Mononucleotide derivatives as ribosomal P-site substrates reveal an important contribution of the 2'-OH to activity. *Nucleic Acids Res*. **31**:6536–6442.

Doudna, J.A., and Cech, T.R. 2002. The chemical repertoire of natural ribozymes. *Nature* **418**:222–228.

Draper, D.E., and von Hippel, P.H. 1978. Nucleic acid binding properties of *Escherichia coli* ribosomal protein S1. I. Structure and interactions of binding site I. *J. Mol. Biol.* **122**:321–338.

Draper, D.E., and Reynaldo, L.P. 1999. RNA binding strategies of ribosomal proteins. *Nucl. Acids Res.* **27**:381–388.

Driessen, A.J.M. and Nouwen, N. 2008. Protein translocation across the bacterial cytoplasmic membrane. *Annu. Rev. Biochem.* **77**:643–667.

Dubochet, J., Adrian, M., Chang, J.J., *et al*. 1988. Cryo-electron microscopy of vitrified specimens. *Quant. Rev. Biophys.* **21**:129–228.

Dudek, J., Dias de Escauriaza, M., Muller, A., *et al*. 2006. Signal recognition particle mediates arrest of translation involves competition with eEF2 on the ribosome. *J. Biol. Sci.* **6**:316–319.

Dunkle, J.A., Xiong, L., Mankin, A.S. *et al*. 2010. Structures of the *Escherichia coli* ribosome with antibiotics bound near the peptidyl transferase center explain spectra of drug action. *Proc. Natl. Acad. Sci. USA.* **107**:17152–17157.

Dunkle, J.A., Wang, L., Feldman, M.B., *et al*. 2011. Structures of the bacterial ribosome in classical and hybrid states of tRNA binding. *Science* **332**:981–984.

Eckerman, D.J., and Symons, R.H. 1978. Sequence at the site of attachment of an affinity-label derivative of puromycin on 23S ribosomal RNA of *E. coli* ribosomes. *Eur. J. Biochem.* **82**:225–234.

Egea, P.F., Shan, S.O., Napetschnig, J., *et al.* 2004. Substrate twinning activates the signal recognition particle and its receptor. *Nature* **427**:215–221.

Egea, P.F., Stroud, R.M., and Walter, P. 2005. Targeting proteins to membranes: Structure of the signal recognition particle. *Curr. Op. Struct. Biol.* **15**:213–220.

Egea, P.F., and Stroud, R.M. 2010. Lateral opening of a translocon upon entry of protein suggests the mechanism of insertion into membranes. *Proc. Natl. Acad. Sci. USA.* **107**:17182–17187.

Egebjerg, J., Douthwaite, S.R., Liljas, A., *et al.* 1990. Characterization of the binding sites of protein L11 and the L10·$(L12)^4$ pentameric complex in the GTPase domain of 23S ribosomal RNA from *Escherichia coli*. *J. Mol. Biol.* **213**:275–288.

Ehrenberg, M. and Blomberg, C. 1980. Thermodynamic constraints on kinetic proofreading in biosynthetic pathways. *Biophys. J.* **31**:333–358.

Ehrenberg, M., Rojas, A.-M., Weiser, J., and Kurland, C.G. 1990. How many EF-Tu molecules participate in aminoacyl-tRNA binding and peptide bond formation in *Escherichia coli* translation? *J. Mol. Biol.* **211**:739–749.

Eldred, E.W. and Schimmel, P.R. 1972. Rapid deacylation by isoleucyl transfer ribonucleic acid synthetase of isoleucine-specific transfer ribonucleic acid aminoacylated with valine. *J. Biol. Chem.* **247**:2961–2964.

Elf, J., Nilsson, D., Tenson, T., and Ehrenberg, M. 2003. Selective charging of tRNA isoacceptors explains patterns of codon usage. *Science* **300**:1718–1722.

Elkon, K.B., Parnassa, A.P., and Foster, C.L. 1985. Lupus autoantibodies target ribosomal P proteins. *J. Exp. Med.* **162**:459–471.

Endo, Y., Mitsui, K., Motizuki, M., and Tsurugi, K. 1987. The mechanism of action of ricin and related toxic lectins on eukaryotic ribosomes. The site and the characteristics of the modification in 28S ribosomal RNA caused by the toxins. *J. Biol. Chem.* **262**:5908–5912.

Engelman, D.M. and Moore, P.B. 1972. A new method for the determination of biological quaternary structure by neutron scattering. *Proc. Natl. Acad. Sci. USA.* **69**:1997–1999.

English, B.P., Hauryliuk, V., Sanamrad, A., *et al.* 2011. Single-molecule investigations of the stringent response machinery in living bacterial cells. *Proc. Natl. Acad. Sci. USA.* **108**:pE365–pE373.

Epe, B., Woolley, P., and Hornig, H. 1987. Competition between tetracycline and tRNA at both P- and A-sites of the ribosome of *Escherichia coli*. *FEBS Lett.* **213**: 443–447.

Eriani, G., Delarue, M., Poch, O., Gangloff, J., and Moras, D. 1990. Partition of tRNA synthetases into two classes based on mutually exclusive sets of sequence motifs. *Nature* **347**:203–206.

Ermolenko, D.N., Mjumdar, Z.K., Hickerson, R.P., *et al.* 2007. Observation of intersubunit movement of the ribosome in solution using FRET. *J. Mol. Biol.* **370**:530–540.

Ermolenko, D.N. and Noller, H.F. 2011. mRNA translocation occurs during the second step of ribosomal intersubunit rotation. *Nat. Struct. Mol. Biol.* **18**:457–462.

Escobar-Alvarez, S., Goldgur, Y., Yang, G., *et al*. 2009. *J. Mol. Biol.* **387**:1211–1228.

Estevez, A.M., and Simpson, L. 1999. Uridine insertion/deletion RNA editing in trypanosome mitochondria — a review. *Gene* **240**:247–260.

Estrozi, L.F., Boehringer, D., Shan, S., *et al*. 2011. Cryo-EM structure of the *E. coli* translating ribosome in complex with SRP and its receptor. *Nat. Struct, Mol. Biol.* **18**:88–90.

Eustice, D.C., and Wilhelm, J.M. 1984a. Fidelity on the eucaryotic codon-anticodon interaction: interference by aminoglycoside antibiotics. *Biochemistry* **23**: 1462–1467.

Eustice, D.C., and Wilhelm, J.M. 1984b. Mechanism of action of aminoglycoside antibiotics in eucaryotic protein synthesis. *Agents Chemother.* **26**:53–60.

Evans, R.N., Blaha, G., Bailey, S., *et al*. 2008. The structure of LepA, the ribosomal back translocase. *Proc. Natl. Acad. Sci. USA.* **105**:4673–4678.

Evguenieva-Hackenberg, E. 2005. Bacterial ribosomal RNA in pieces. *Mol. Microbiol*. **57**: 318–325.

Fabbretti, A., Pon, C.L., Hennelly, S.P., *et al*. 2007. The realtime path of translation factor IF3 onto and off the ribosome. *Mol Cell* **25**:285–296.

Fakunding, J.L., Traut, R.R., and Hershey, J.W. 1973. Dependence of initiation factor IF-2 activity on proteins L7 and L12 from *Escherichia coli* 50S ribosomes. *J. Biol. Chem*. **248**:8555–8559.

Farris, M., Grant, A., Richardson, T.B. *et al*. 1998. BipA: a tyrosine-phosphorylated GTPase that mediates interactions between enteropathogenic *Escherichia coli* (EPEC) and epithelial cells. *Mol. Microbiol*. **28**:265–279.

Fedorov, R., Nevskaya, N., Khairullina, A., *et al.* 1999. Structure of ribosomal protein L30 from *Thermus thermophilus* at 1.9Å resolution: conformational flexibility of the molecule. *Acta Cryst.* **D55**:1827–1833.

Fedorov, R., Meshcheryakov, V., Gongadze, G., *et al.* 2001. Structure of ribosomal protein TL5 complexed with RNA provides new insights into the CTC family of stress proteins. *Acta Cryst.* **D57**:968–976.

Ferbitz, L., Maier, T., Patzelt, H., *et al*. 2004. Trigger factor in complex with the ribosome forms a molecular cradle for nascent proteins. *Nature* **431**:590–596.

Fersht, A.R. 1977. Editing mechanisms in protein synthesis. Rejection of valine by the isoleucyl-tRNA synthetase. *Biochemistry* **16**:1025–1030.

Fersht, A.R. and Kaethner, M.M. 1976. Enzyme hyperspecificity. Rejection of threonine by the valyl-tRNA synthetase by misacylation and hydrolytic editing. *Biochemistry*: **15**:3342–3346.

Filipowics, W., Furuichi, Y., Sierra J.M., *et al*. 1976. A protein binding the methylated 5′-terminal sequence, m7GpppN, of eukaryotic messenger RNA. *Proc. Natl. Acad. Sci. USA.* **73**:1559–1563.

Focia, P.J., Shepotinovskaya, I.V., Seidler, J.A., and Freymann, D.M. 2004. Heterodimeric GTPase core of the SRP targeting complex. *Science* **303**:373–377.

Forchhammer, K., Leinfelder, W., and Böck, A. 1989. Identification of a novel translation factor necessary for the incorporation of selenocysteine into protein. *Nature* **342**:453–456.

Förster, T. 1948. Zwischenmoleculare energiwanderung und fluoreszenz. *Ann. Physik*, **2**:55–67.

Förster, T., 1965. Delocalized excitation and excitation transfer. In *Modern Quantum Chemistry; Istanbul Lectures*, ed. O. Sinanoglu (New York: Academic Press), section III-B, pp. 93–137. (Equation I, a corrected form of an earlier expression, is given in this reference.)

Fourmy, D., Recht, M.I., Blanchard, S.C., and Puglisi, J.D. 1996. Structure of the A-site of *Escherichia coli* 16S ribosomal RNA complexed with an aminoglycoside antibiotic. *Science* **274**:1367–1371.

Fourmy, D., Yoshizawa, S., and Puglisi, J.D. 1998. Paromomycin binding induces a local conformational change in the A-site of 16S rRNA. *J. Mol. Biol.* **277**:333–345.

Fox, G.E. and Ashinikumar, K.N. 2004. The evolutionary history of the translation machinery. In: de Pouplana LR, editor. *The genetic code and the origin of life.* New York: Kluwer Academic / Plenum. p. 92–105.

Franceschi, F. and Duffy, E.M. 2006. Structure-based drug design meets the ribosome. *Biochem. Pharmacol*. **7**:1016–1025.

Francuski, D. and Sænger, W. 2009. Crystal structure of the antitoxin-toxin protein complex RelB-RelE from *Metanococcus jannaschii. J. Mol. Biol*. **393**:898–908.

Frank, J. 2003. Electron microscopy of functional ribosome complexes. *Biopolymers* **68**:223–233.

Frank, J. 2009. Single-particle reconstruction of biological macromolecules in electron microscopy — 30 years. *Quart. Rev. Biophys*. **42**:139–158.

Frank, J. 2012. Intermediate states during mRNA-tRNA translocation. *Curr. Op. Struct. Biol*. **22**:778–785.

Frank, J. and Agrawal, R.K. 1998. The movement of tRNA through the ribosome. *Biophys. J.* **74**:589–594.

Frank, J. and Agrawal, R.K. 2000. A ratchet-like inter-subunit reorganization of the ribosome during translocation. *Nature* **406**:318–322.

Frank, J. and Agrawal, R.K. 2001. Ratchet-like movements between the two ribosomal subunits: their implications in elongation factor recognition and tRNA translocation. *Cold Spring Harb. Symp. Quant. Biol*. **66**:67–75.

Frank, J., Radermacher, M., Penczek, P., *et al.* 1996. SPIDER and WEB: processing and visualization of images in 3D electron microscopy and related fields. *J. Struct. Biol.* **116**:190–199.

Frank, J., Verschoor, A., and Boublik, M. 1981. Computer averaging of electron micrographs of 40S ribosomal subunits. *Science* **214**:1353–1355.

Frank, J., Verschoor, A., Li, Y., *et al*. 1995. A model of the translational apparatus based on a three-dimensional reconstruction of the *Escherichia coli* ribosome. *Biochem. Cell Biol*. **73**:757–765.

Frank, J., Verschoor, A., Li, Y., *et al*. 1995. A model of the translational apparatus based on a three-dimensional reconstruction of the *Escherichia coli* ribosome. *Biochem. Cell Biol*. **73**:757–765.

Frank, J., Verschoor, A., Wagenknecht, T., *et al*. 1988. A new non-crystallographic image-processing technique reveals the architecture or ribosomes, *Trends Biochem. Sci*. **13**:123–127.

Frank, J., Zhu, J., Penczek, P., *et al*. 1995. A model of protein synthesis based on cryo-electron microscopy of the *E. coli* ribosome. *Nature* **376**:441–444.

Frauenfeld, J., Gumbart, J., van der Sluis, E.O., *et al*. 2011. Cryo-EM structure of the ribosome-SecYE complex in the membrane environment. *Nat. Struct. Mol. Biol*. **18**:614–622.

Franzetti, B. Carol, P., and Mache, R. 1992. Characterization and RNA-binding properties of a chloroplast S1-like ribosomal protein. *J. Biol. Chem*. **267**:19075–19081.

Fredrick, K. and Noller, H.F. 2002. Accurate translocation of mRNA by the ribosome requires a peptidyl group or its analog on the tRNA moving into the 30S P-site. *Mol. Cell*. **9**:1125–1131.

Fredrick, K. and Noller, H.F. 2003. Catalysis of ribosomal translocation by sparsomycin. *Science* **300**:1159–1162.

Freistroffer, D.V., Pavlov, M.Y., MacDougall, J., *et al*. 1997. Release factor RF3 in *E. coli* accelerates the dissociation of release factors RF1 and RF2 from the ribosome in a GTP-dependent manner. *EMBO J*. **16**:4126–4133.

Freter, R.R. and Savageau, M.A. 1980. Proofreading systems of multiple stages for improved accuracy of biological discrimination. *J. Theor. Biol*. **85**:99–123.

Freymann, D.M., Keenan, R.J., Stroud, R.M., and Walter, P. 1997. Structure of the conserved GTPase domain of the signal recognition particle. *Nature* **385**:361–364.

Friesen, J.D., Fiil, N.P., Parker, J.M., and Haseltine, W.A. 1974. A new relaxed mutant of *Escherichia coli* with an altered 50S ribosomal subunit. *Proc. Natl. Acad. Sci. USA*. **71**:3465–3469.

Friesner, R. A., Banks, J. L., Murphy, L. B., *et al*. 2004. Glide: A new approach for rapid, accurate docking and scoring. 1. Method assessment of docking accuracy. *J. Med. Chem*. **47**:1739–1749.

Frolova, L., Seit-Nebi, A., and Kisselev, L. 2002. Highly conserved NIKS tetrapeptide is functionally essential in eukaryotic translation termination factor eRF1. *RNA* **8**:129–136.

Frolova, L.Y., Isivkovskii, R.Y., Sivolobva, G.F., *et al*. 1999. Mutations in the highly conserved GGQ motif of class 1 polypeptide release factors abolish ability of human eRF1 to trigger peptidyl-tRNA hydrolysis. *RNA*. **5**: 1014–1020.

Frydman, J. 2001. Folding of newly translated proteins *in vivo*: the role of molecular chaperones. *Ann. Rev. Biochem.* **70**:603–649.

Fuglsang, A. and Engberg, J. 2003. Non-randomness in Shine-Dalgarno regions: links to gene characteristics. *Biochem. Biophy. Res. Commun.* **302**:296–301.

Fujita, C., Maeda, M., Fujii, T., *et al.* 2002. Identification of an indispensable amino acid for ppGpp synthesis of *Escherichia coli* SpoT protein. *Biosci. Biotechnol. Biochem.* **66**:2735–2738.

Fujiwara, T., Ito, K., Nakayashiki, T., and Nakamura, Y. 1999. Amber mutaions in ribosome recycling factors of *Escherichia coli* and *Thermus thermophilus*: evidence for C-terminal modulator element. *FEBS Lett.* **447**:297–302.

Fukunaga, R. and Yokoyama, S. 2005. Crystal structure of Leucyl-tRNA synthetase from the archaeon *Pyrococcus horikosjii* reveals a novel editing domain orientation. *J. Mol. Biol.* **346**:57–71.

Fukunaga, R. and Yokoyama, S. 2007. Structure of the AlaX-M trans-editing enzyme from *Pyrococcus horikoshii*. *Acta Cryst. D* **63**:390–400.

Fulle, S. and Gohlke, H. 2009. Statics of the ribosomal exit tunnel: implications for cotranslational peptide folding, elongation regulation, and antibiotics binding. *J. Mol. Biol.* **387**:502–517.

Gabashvili, I.S., Agrawal, R.K., Grassuccl, R., *et al.* 1999. Structure and structural variations of the *Escherichia coli* 30S ribosomal subunit as revealed by three-dimensional cryo-electron microscopy. *J. Mol. Biol.* **286**:1285–1291.

Gabashvili, I.S., Agrawal, R.K., Spahn, C.M., *et al.* 2000. Solution structure of the *E. coli* 70S ribosome at 11.5 A resolution. *Cell* **100**:537–549.

Gabashvili, I.S., Gregory, S.T., Valle, M., *et al.* 2001. The polypeptide tunnel system in the ribosome and its gating in erythromycin resistance mutants of L4 and L22. *Mol. Cell* **8**:181–188.

Gagnon, M.G., Seetharaman, S.V., Bulkeley, D. *et al.* 2012. Structural basis for the rescue of stalled ribosomes: structure of YaeJ bound to the ribosome. Submitted.

Gallant, J., Bonthuis, P., and Lindsley, D. 2003. Evidence that the bypassing ribosome travels through the coding gap. *Proc. Natl. Acad. Sci. USA.* **100**: 13430–13435.

Galvani, C., Terry, J., and Ishiguro, E.E. 2001. Purification of the RelB and RelE proteins of *Escherichia coli*: RelE binds to RelB and to ribosomes. *J. Bacteriol.* **183**:2700–2703.

Ganichkin, O. and Wahl, M.C. 2007. Conformational switches in winged-helix domains 1 and 2 of bacterial translation factor SelB. *Acta Cryst. D* **63**:1075–1081.

Ganoza, M.C. 1966. Polypeptide chain termination in cell-free extracts of *E. coli*. *Cold Spring Harb. Symp. Quant. Biol.* **31**:273–278.

Gao, H., Sengupta, J., Valle, M., *et al.* 2003. Study of the structural dynamics of the *E. coli* 70S ribosome using real-space refinement. *Cell* **113**:789–801.

Gao, H., Zhou, Z., Rawat, U., *et al*. 2007a. RF3 induces ribosomal conformational changes responsible for dissociation of class I release factors. *Cell* **129**:929–941.

Gao, N., Zavialov, A., Li, W., *et al*. 2005. Mechanism for the disassembly of the post-termination complex inferred from cryo-EM studies. *Mol. Cell* **18**:663–674.

Gao, N., Zavialov, A.V., Ehrenberg, M., *et al*. 2007b. Specific interaction between EF-G and RRF and its implication for GTP-dependent ribosome splitting into subunits. *J. Mol. Biol.* **374**:1345–1358.

Gao, Y.G., Selmer, M., Dunham, C,M., *et al*. 2009. The structure of the ribosome with elongation Factor G trapped in the posttranslocational state. *Science* **326**:694–699.

Garcia, C., Fortier, P.L., Blanquet, S., *et al.* 1995a. Solution structure of the ribosome-binding domain of *E. coli* translation initiation factor IF3. Homology with the U1A protein of the eukaryotic spliceosome. *J. Mol. Biol.* **254**:247–259.

Garcia, C., Fortier, P.L., Blanquet, S., *et al.* 1995b. ^{1}H and ^{15}N resonance assignments and structure of the N-terminal domain of *Escherichia coli* initiation factor 3. *Eur. J. Biochem.* **228**:395–402.

Garrett, R.A., and Wittmann, H.G. 1973. Structure of bacterial ribosomes. *Adv. Prot. Chem.* **27**:277–347.

Gaur, R., Grasso, D., Datta, P.P., *et al*. 2008. A single mammalian mitochondrial translation initiation factor functionally replaces two bacterial factors. *Mol Cell* **29**:180–190.

Gavrilova, L.P., and Spirin, A.S. 1971. Stimulation of "non-enzymic" translocation in ribosomes by p-chloromercuribenzoate. *FEBS Lett.* **17**:324–326.

Gavrilova, L.P., and Spirin, A.S. 1972. A modification of the 30S ribosomal subparticle is responsible for stimulation of "non-enzymatic" translocation by p-chloromercuribenzoate. *FEBS Lett.* **22**:91–92.

Gavrilova, L.P., Koteliansky, V.E., and Spirin, A.S. 1974. Ribosomal protein S12 and "non-enzymatic" translocation. *FEBS Lett.* **45**:324–328.

Gavrilova, L.P., Kostiashkina, O.E., Koteliansky, V.E., *et al.* 1976. Factor-free ("non-enzymic") and factor-dependent systems of translation of polyuridylic acid by *Escherichia coli* ribosomes. *J. Mol. Biol.* **101**:537–552.

Geigenmuller, U., and Nierhaus, K.H. 1986. Tetracycline can inhibit tRNA binding to the ribosomal P-site as well as to the E-site. *Eur. J. Biochem.* **161**:723–726.

Genevaux, P., Keppel, F., Schwager, F., *et al*. 2004. *In vivo* analysis of the overlapping functions of DnaK and trigger factor. *EMBO Rep.* **5**:196–200.

Gentry, D.R. and Cashel, M. 1996. Mutational analysis of the *E. coli* spoT gene identifies distinct but overlapping regions involved in ppGpp synthesis and degradation. *Mol. Microbiol.* **19**:1373–1384.

Gerbi, S.A. 1996. Expansion segments: regions of variable size that interrupt the universal core secondary structure of ribosomal RNA. In *Ribosomal RNA. Structure, Evolution, Processing and Function in Protein Biosynthesis,* Eds. R.A. Dahlberg and A.E. Dahlberg, pp. 71–87. CRC Press, Boca Raton.

Gesteland, R.F., Cech, T.R., and Atkins, J.F. (Eds.) 1999. *The RNA World*, 2nd edition. Cold Spring Harbor Laboratory Press.

Gesteland, R.F., Cech, T.R., Atkins, J.F. 2006. The RNA world, 3rd edn. Cold Spring Harbor Laboratory Press, New York.

Giege, R., Sissler, M., and Florentz, C. 1998. Universal rules and idiosyncratic features in tRNA identity. *Nucl. Acids Res.* **26**:5017–5035.

Giglione, C., Fieulaine, S., and Meinnel, T. 2009. Cotranslational processing mechanisms: towards a dynamic 3D model. *Trends Biochem. Sci.* **34**:417–426.

Gilbert, W. 1963. Polypeptide synthesis in *Escherichia coli*. II. The polypeptide chain and S-RNA. *J.Mol. Biol.* **6**:389–403.

Gilbert, W. 1986. The RNA world. *Nature* **319**:618.

Gillet, R., Kaur, S., Hallier, M., *et al*. 2007. Scaffolding as an organizing principle in trans-translation. The roles of small protein B and ribosomal protein S1. *J. Biol. Chem*. **282**:6356–6363.

Giri, L. and Subramanian, A.R. 1977. Hydrodynamic properties of protein S1 from *Escherichia coli* ribosome. *FEBS Lett*. **81**:199–203.

Giri, L., Hill, W.E., Wittmann, H.G., and Wittmann-Liebold, B. 1984. Ribosomal proteins: their structure and spatial arrangement in prokaryotic ribosomes. *Adv. Prot. Chem.* **36**:1–78.

Girshovich, A.S., Bochkareva, E.S., and Ovchinnikov, Y.A. 1981. Elongation factor G and protein S12 are the nearest neighbors in the *Escherichia coli* ribosomes. *J. Mol. Biol*. **151**:229–243.

Glick, B.R., Chladek, S., and Ganoza, M.C. 1979. Peptide bond formation stimulated by protein synthesis factor EF-P depends on the aminoacyl moiety of the acceptor. *Eur. J. Biochem.* **97**:23–28.

Glotz, C. and Brimacombe, R. 1980. An experimentally-derived model for the secondary structure of the 16S ribosomal RNA from *Escherichia coli*. *Nucleic Acids Res*. **8**:2377–2395.

Glotz, C., Zwieb, C., Brimacombe, R., *et al.* 1981. Secondary structure of the large subunit ribosomal RNA from *Escherichia coli*, Zea mays chloroplast, and human and mouse mitochondrial ribosomes. *Nucl. Acids Res.* **9**: 3287–3306.

Glotz, C., Mussig, J., Gewitz, H.S., *et al.* 1987. Three-dimensional crystals of ribosomes and their subunits from eu- and archae-bacteria. *Biochem. Int.* **15**:953–960.

Gluehmann, M., Zarivach, R., Bashan, A., *et al.* 2001. Ribosomal crystallography: from poorly diffracting microcrystals to high-resolution structures. *Methods* **25**:292–302.

Goldberg, I.H., and Mitsugi, K. 1966. Sparsomycin, an inhibitor of aminoacyl transfer to polypeptide. *Biochem. Biophys. Res. Commun.* **23**:453–459.

Gomez-Lorenzo, M.G., and Garcia-Bustos, J.F. 1998. Ribosomal P-protein stalk function is targeted by sordarin antifungals. *J. Biol. Chem.* **273**: 25041–25044.

Gomez-Lorenzo, M.G., Spahn, C.M., Agrawal, R.K., *et al.* 2000. Three-dimensional cryo-electron microscopy localization of EF2 in the *Saccharomyces cerevisiae* 80S ribosome at 17.5Å resolution. *EMBO J.* **19**:2710–2718.

Gong, F., and Yanofsky, C. 2002. Instruction of translating ribosome by nascent peptide. *Science* **297**:1864–1867.

Gongadze, G.M., Meshcheryakov, V.A., Serganov, A.A., *et al.* 1999. N-terminal domain, residues 1–91, of ribosomal protein TL5 from *Thermus thermophilus* binds specifically and strongly to the region of 5S rRNA containing loop E. *FEBS Lett.* **451**:51–55.

Gongadze, G.M., Tischenko, S.V., Sedelnikova, S.E., and Garber, M.B. 1993. Ribosomal proteins, TL4 and TL5, from *Thermus thermophilus* form hybrid complexes with 5S ribosomal RNA from different microorganisms. *FEBS Lett.* **386**:46–48.

Gonzales, A., Jimenez, A., Vazquez, D., *et al.* 1978. Studies on the mode of action of hygromycin B, an inhibitor of translocation in eucaryotes. *Biochim. Biophys. Acta* **551**:459–469.

Gonzalo, P., Lavergne, J.P., and Reboud, J.-P. 2001. Pivotal role of the P1 N-terminal domain in mammalian ribosome stalk and in the proteosynthetic activity. *J. Biol. Chem.* **276**:19762–19769.

Gonzalo, P., and Reboud, J.-P. 2003. The puzzling lateral flexible stalk of the ribosome. *Biol. Cell* **95**:179–193.

Goody, R.S., Hofmann-Goody, W. 2002. Exchange factors, effectors, GAPs and motor proteins: common thermodynamic and kinetic principles for different functions. *Eur. Biophys. J.* **31**:268–274.

Gordon, J. 1969. Hydrolysis of guanosine 5′-triphosphate associated with binding of aminoacyl transfer ribonucleic acid to ribosomes. *J. Biol. Chem.* **24**:5680–5686.

Gornicki, P., Nurse, K., Hellmann, W., *et al.* 1984. High resolution localization of the tRNA anticodon interaction site on the *Escherichia coli* 30S ribosomal subunit. *J. Biol. Chem.* **259**:10493–10498.

Gotfredsen, M., and Gerdes, K. 1998. The *Escherichia coli* relBE genes belong to a new toxin-antitoxin gene family. *Mol. Microbiol.* **29**:1065–1076.

Gottesman, S. 2005. Micros for microbes: non-coding regulatory RNAs in bacteria. *Trends in Genetics* **21**:399–404.

Graille, M., Heurgue-Hamard, V., Champ, S. *et al.* 2005. Molecular basis for bacterial class I release factor methylation by PrmC. *Mol Cell* **20**:917–927.

Grajevskaja, R.A., Ivanov, Y.V. and Saminsky, E.M. (1982) 70-S ribosomes of Escherichia coli have an additional site for deacylated tRNA binding. *Eur. J. Biochem.* **128**:47–52.

Gravel, M., Melancon, P., and Brakier-Gringas, L. 1987. Cross-linking of streptomycin to the 16S ribosomal RNA of *Escherichia coli*. *Biochemistry* **26**:6227–6232.

Green, R. and Noller, HF. 1997. Ribosomes and translation. *Annu. Rev. Biochem.* **66**:679–717.

Green, R., Switzer, C., and Noller, H.F. 1998. Ribosome-catalyzed peptide-bond formation with an A-site substrate covalently linked to 23S ribosomal RNA. *Science* **280**:286–289.

Greenleaf, W.J., Woodside, M.T., and Block, S.M. 2007. High-resolution, single molecule measurements of biomolecular motion. *Annu. Rev. Biophys. Biomol. Struct.* **36**:171–190.

Gregory, S.T., Demirci, H., Belardinelli, R., *et al*. 2009. Structural and functional studies of the *Thermus thermophilus* 16S rRNA methyltransferase RsmG. *RNA* **15**:1693–1704.

Grela, P, Helgstrand, M, Krokowski, D, *et al*. 2007. Structural characterization of the ribosomal P1A-P2B protein dimer by small-angle X-ray scattering and NMR spectroscopy. *Biochemistry* **46**:1988–1998.

Griaznova, O. and Traut, R.R. 2000. Deletion of C-terminal residues of *E. coli* ribosomal protein L10 causes the loss of binding of one L7/L12 dimer: ribosomes with one L7/L12 dimer are active. *Biochemistry* **39**:4075–4081.

Grigoriadou, C., Marzi, S., Kirillov, S., *et al*. 2007. A quantitative kinetic scheme for 70 S translation initiation complex formation. *J. Mol. Biol.* **373**:562–572.

Gromadski, K.B. and Rodnina, M.V. 2004. Kinetic determinants of high-fidelity tRNA discrimination on the ribosome. *Mol. Cell.* **13**:191–200.

Grønlund, H., and Gerdes, K. 1999. Toxin-antitoxin systems homologous with relBE of *Escherichia coli* plasmid P307 are ubiquitous in prokaryotes. *J. Mol. Biol.* **285**: 1401–1415.

Gros, F., Gilbert, W., Hiatt, H., *et al.* 1961. Unstable ribonucleic acid revealed by pulse labelling of *Escherichia coli*. *Nature* **190**:581–585.

Grøsjean, H.J., de Henau, S., and Crothers, D.M. 1978. On the physical basis for ambiguity in genetic coding interactions. *Proc. Natl. Acad. Sci. USA.* **75**:610–614.

Grunberg-Manago, M., Dessen, P., Pantaloni, D., *et al.* 1975. Light-scattering studies showing the effect of initiation factors on the reversible dissociation of *Escherichia coli* ribosomes. *J. Mol. Biol.* **94**:461–478.

Gryaznova, O.I., Davydova, N.L., Gongadze, G.M., *et al.* 1996. A ribosomal protein from *Thermus thermophilus* is homologous to a general shock protein. *Biochimie* **78**:915–919.

Gu, S.Q., Peske, F., Wieden, H.J., *et al.* 2003. The signal recognition particle binds to protein L23 at the peptide exit of *Escherichia coli* ribosome. *RNA* **9**: 566–573.

Gualerzi, C.O. and Pon, C.L. 1990. Initiation of mRNA translation in prokaryotes. *Biochemistry* **29**:5881–5889.

Guarinos, E., Remacha, M., and Ballesta, J.P.G. 2001. Asymmetric interactions between the acidic P1 and P2 proteins in *Saccharomyces cerevisiae* ribosomal stalk. *J. Biol. Chem.* **276**:32474–32479.

Gudkov, A.T. 1997. The L7/L12 domain of the ribosome: structural and functional studies. *FEBS Lett.* **407**:253–256.

Gudkov, A.T. and Behlke, J. 1978. The N-terminal sequence protein of L7/L12 is responsible for its dimerization. *Eur. J. Biochem.* **90**:309–312.

Gudkov, A.T. and Bubunenko, M.G. 1989. Conformational changes in ribosomes upon interaction with elongation factors. *Biochimie* **71**:779–785.

Gudkov, A.T., Bubunenko, M., and Gryaznova, O. 1991. Overexpression of L7/L12 protein with mutations in its flexible region. *Biochimie* **73**:1387–1389.

Gudkov, A.T. and Gongadze, G.M. 1984. The L7/L12 proteins change their conformation upon interaction of EF-G with ribosomes. *FEBS Lett.* **176**:32–36.

Gudkov, A.T., Gongadze, G.M., Bushuev, V.N., and Okon, M.S. 1982. Proton nuclear magnetic resonance study of the ribosomal protein L7/L12 *in situ*. *FEBS Lett.* **138**:229–232.

Guerrier-Takada, C., Gardiner, K., Marsh, T., Pace, N., *et al*. 1983. The RNA moiety of ribonuclease P is the catalytically active subunit of the enzyme. *Cell* **35**:849–857.

Guilloteau, J.P., Mathieu, M., Giglione, C., *et al*. 2002. The crystal structures of four peptide deformylases bound to the antibiotic actinonin reveal two distinct types: a platform for the structurebased design of antibacterial agents. *J. Mol. Biol.* **320**:951–962.

Guo, M., Ignatov, M., Musier-Forsyth, K., *et al*. 2008. Crystal structure of tetrameric form of human lysyl-tRNA synthetase: Implications for multisynthetase complex formation. *Proc. Natl. Acad. Sci. USA.* **105**:2331–2336.

Guo, X., Peisker, K., Bäckbro, K., *et al*. 2012. Structure and function of FusB: an elongation factor G-binding fusidic acid protein active in ribosomal translocation and recycling. *Open Biol.* **2**:120016.

Gurel, G., Blaha, G., Moore, P.B., *et al*. 2009. U2504 determines the species specificity of the A-site cleft antibiotics: the structures of tiamulin, homoharringtonine, and bruceantin bound to the ribosome. *J. Mol. Biol.* **389**:146–156.

Gutgsell, N.S., Deutscher, M.P., and Ofengand, J. 2005. The pseudouridine synthase RluD is required for normal ribosome assembly and function in Escherichia coli. *RNA* **11**:1141–1152.

Gutmann, S., Haebel, P., Metzinger, L., *et al*. 2003. Crystal structure of the tRNA domain of transfer messenger RNA in complex with SmpB. *Nature* **424**:699–703.

Ha, T., Enderle, T., Ogletree, D.F., *et al*. 1996. Probing the interaction between two single molecules: fluorescence resonance energy transfer between a single donor and a single acceptor. *Proc Natl Acad Sci USA.* **93**:6264–6268.

Hahn, U., Palm, G.J., and Hinrichs, W. 2004. Old codons, new amino acids. *Angew. Chem. Int. Ed.* **43**:1190–1193.

Halic, M., Becker, T., Pool, M.R., *et al*. 2004. Structure of the signal recognition particle interacting with the elongation arrested ribosome, *Nature* **427**:808–814.

Halic, M., Blau, M., Becker, T., *et al*. 2006. Following the signal sequence from ribosomal tunnel exit to signal recognition particle. *Nature* **444**:507–511.

Hall, C.E. and Slayter, H.S. 1959. Electron microscopy of nucleoprotein particles from *E. coli*. *J. Mol. Biol.* **1**:329–332.

Hallier, M., Ivanova, N., Rametti, A., *et al*. 2004. Pre-binding of small protein B to a stalled ribosome triggers trans-translation. *J. Biol. Chem.* **279**: 25978–25985.

Hallier, M., Desreac, J., and Felden, B. 2006. Small protein B interacts with the large, the small subunits of a stalled ribosome during trans-translation. *Nucl. Acids Res.* **34**:1935–1943.

Hamel, E., Koka, M., and Nakamoto, T. 1972. Requirement of an *E. coli* 50S ribosomal protein component for effective interaction of the ribosome with T and G factors with guanosine triphosphate. *J. Biol. Chem.* **247**:805–814.

Hampl, H., Schulze, H., and Nierhaus, K.H. 1981. Ribosomal components from *Escherichia coli* 50S subunits involved in the reconstitution of peptidyltransferase activity. *J. Biol. Chem.* **256**:2284–2288.

Han, Q., Zhao, Q., Fish, S., *et al*. 2005. Molecular recognition by glycoside pseudo base pairs and triples in an apramycin-RNA complex. *Angew. Chem. Int. Ed*. **44**:2694–2700.

Han, M.-J., Cimen, H., Miller-Lee, J.L., *et al*. 2011. Purification of human mitochondrial ribosomal L7/L12 stalk proteins and reconstitution of functional hybrid ribosomes in *Escherichia coli*. *Prot. Express. Purif*. **78**:48–54.

Handa, Y., Hikawa, Y., Tochio, N., *et al*. 2010. Solution structure of the catalytic domain of the mitochondrial protein ICT1 that is essential for cell vitality. *J. Mol. Biol.* **404**:260–273.

Handa, Y., Inaho, N., and Nameki, N. 2011. YaeJ is a novel ribosome-associated protein in *Escherichia coli* that can hydrolyze peptidyl–tRNA on stalled ribosomes. *Nucl. Acids Res.* **39**:1739–1748.

Hansen, J.L., Ippolito, J.A., Ban, N., *et al*. 2002a. The structures of four macrolide antibiotics bound to the large ribosomal subunit. *Mol. Cell* **10**:117–128.

Hansen, J.L., Schmeing, T.M., Moore, P.B., and Steitz, T.A. 2002b. Structural insights into peptide bond formation. *Proc. Natl. Acad. Sci. USA.* **99**:11670–11675.

Hansen, J.L., Moore, P.B., and Steitz, T.A. 2003. Structures of five antibiotics bound at the peptidyl transferase center of the large ribosomal subunit. *J. Mol. Biol.* **330**:1061–1075.

Hanson, C.L., Fucini, P., Ilag, L.L., *et al*. 2003. Dissociation of intact *Escherichia coli* ribosomes is a mass spectrometer. *J. Biol. Chem.* **278**:1259–1267.

Hansson, S., Singh, R., Gudkov, A.T., *et al*. 2005. Structural insights into fusidic acid resistance and sensitivity in EF-G. *J. Mol. Biol.* **340**:939–949.

Hao, B., Gong, W., Ferguson, T.K., *et al*. 2002. A novel UAG encoded residue in the structure of a methanogen methyltransferase. *Science* **296**:1462–1466.

Hardesty, B., Culp, W., McKeehan, W. 1969. The sequence of reactions leading to the synthesis of a peptide bond on reticulocyte ribosomes. *Cold Spring Harbor Symp. Of Quant. Biol*. **34**:331–345.

Hardesty, B. and Kramer, G. 2001. Folding of a nascent peptide on the ribosome. *Prog. Nucl. Acid Res. Mol. Biol.* **66**:41–66.

Hardy, S.J.S. 1975. The stoichiometry of the ribosomal proteins of *Escherichia coli*. *Mol. Gen. Genet.* **140**:253–274.

Harms, J., Tocilj, A., Levin, I., *et al.* 1999. Elucidating the medium-resolution structure of ribosomal particles: an interplay between electron cryo-microscopy and X-ray crystallograhy. *Struct. Fold Des.* **7**:931–941.

Harms, J., Schlüenzen, F., Zarivach, R., *et al.* 2001. High resolution structure of the large ribosomal subunit from a mesophilic eubacterium. *Cell* **107**:679–688.

Harms, J., Schluenzen, F., Zarivach, R., *et al*. 2002. Protein structure: experimental and theoretical aspects. *FEBS Lett.* **525**:176–178.

Harms, J., Schlüntzen, F., Fucini, P., *et al*. 2004. Alterations at the peptidyl transferase centre of the ribosome induced by the synergistic action of the streptogramins dalfopristin and quinupristin. *BMC Biology* **2**:4.

Harms, J., Wilson, D.N., Schluenzen, F., *et al*. 2008. Translational regulation via L11: Molecular switches on the ribosome turned on and off by thiostrepton and micrococcin. *Mol. Cell* **30**:26–38.

Harris, J.K., Kelley, S.T., Spiegelman, G.B., and Pace, N. 2003. The genetic core of the universal ancestor. *Gen. Res.* **13**:407–412.

Harrison, C.J. 1997. La cage aux fold: asymmetry in the crystal structure of GroEL-GroES-(ADP)7. *Structure* **5**:1261–1264.

Hartl, F.U. and Hayer-Hartl, M. 2002. Molecular chaperones in the cytosol: from nascent chain to folded protein. *Science* **295**:1852–1858.

Haseltine, W.A., and Block, R. 1973. Synthesis of guanosine tetra- and pentaphosphate requires the presence of a codon-specific, uncharged transfer ribonucleic acid in the acceptor site of ribosomes. *Proc. Natl. Acad. Sci. USA.* **70**:1564–1568.

Haugland, R.P., Yguerabide, J., and Stryer, L. 1969. Dependence of the kinetics of singlet-singlet energy transfer on spectral overlap. *Proc Natl Acad Sci USA.* **63**:23–30.

Hauryliuk, V., Mitkevich, V., Draycheva, A., *et al*. 2009. Thermodynamics of GTP and GDP binding to bacterial initiation factor 2 suggests two types of structural transitions. *J. Mol. Biol.* **394**:621–626.

Hausmann, C.D. and Ibba, M. 2008. Aminoacyl-tRNA complexes: molecular multitasking revealed. *FEMS Microbiol. Rev.* **32**:705–721.

Hausner, T.P., Atmadja, J., and Nierhaus, K.H. 1987. Evidence that the G2661 region of 23S rRNA is located at the ribosomal binding sites of both elongation factors. *Biochimie* **69**:911–923.

Heffron, S.E. and Jurnak, F. 2000. Structure of an EF-Tu complex with a thiazol peptide antibiotic determined at 2.35Å resolution: atomic basis for GE2270A inhibition of EF-Tu. *Biochemistry* **39**:37–45.

Heimark, R.L., Hersehy, J.W., and Traut, R.R. 1976. Cross-linking of initiation factor IF2 to proteins L7/L12 in 70S ribosomes of *Escherichia coli. J. Biol. Chem.* **251**:779–784.

Heinemeyer, E.A., and Richter, D. 1977. *In vitro* degradation of guanosine tetraphosphate (ppGpp) by an enzyme associated with the ribosomal fraction from *Escherichia coli. FEBS Lett.* **84**:357–361.

Held, W.A., Ballou, B., Mizushima, S., and Nomura, M. 1974. Assembly mapping of 30S ribosomal proteins from *E. coli.* Further studies. *J. Biol. Chem.* **249**: 3103–3111.

Helgstrand, M., Rak, A.V., Allard, P., *et al.* 1999. Solution structure of the ribosomal protein S19 from *Thermus thermophilus. J. Mol. Biol.* **292**:1071–1081.

Helgstrand, M., Mandava, C.S., Mulder, F.A.A., *et al*. 2006. The ribosomal stalk binds to translation factors IF2, EF-Tu, EF-G and RF3 via a conserved region of the L12 C-terminal domain. *J. Mol. Biol.* **365**:468–479.

Helliwell, J.R. 1998. Synchrotron radiation facilities. *Nat. Struct. Biol.* **5**(Suppl): 614–617.

Helm, M., Brulé, H., Friede, D., Giegé, R. *et al*. 2000. Search for characteristic structural features of mammalian mitochondrial tRNAs. *RNA* **6**:1356–1379.

Helser, T.L., Davies, J.E., and Dahlberg, J.E. 1972. Mechanism of kasugamycin resistance in *Escherichia coli. Nat. New Biol.* **235**:6–9.

Hendrickson, W.A. 1991. Determination of macromolecular structures from anomalous diffraction of synchrotron radiation. *Science* **254**:51–58.

Herendeen, S.L., VanBogelen, R.A., and Neidhardt, F.C. 1979. Levels of major proteins of *Escherichia coli* during growth at different temperatures. *J. Bacteriol.* **139**:185–194.

Hermann, T. 2005. Drugs targeting the ribosome. *Curr. Op. Struct. Biol.* **15**:355–366.

Herr, A.J., Wills, N.M., Nelson, C.C., *et al.* 2001. Drop-off during ribosome hopping. *J. Mol. Biol.* **311**:445–452.

Herskovits, A.A. and Bibi, E. 2000. Association of *Escherichia coli* ribosomes with the inner membrane requires the signal recognition particle receptor but is independent of the signal recognition particle. *Proc. Natl. Acad. Sci. USA.* **97**:4621–4626.

Hesterkamp, T., Hauser, S., Lütcke, H., and Bukau, B. 1996. *Escherichia coli* trigger factor is a prolyl isomerase that associates with nascent polypeptide chains. *Proc. Natl. Acad. Sci. USA.* **93**:4437–4441.

Heurgué-Hamard, V., Champ, S., Egström, A. *et al*. 2002. The hemK gene in Escherichia coli encodes the N(5)-glutamine methyltransferase that modifies peptide release factors. *EMBO J.* **21**:769–778.

Heurgué-Hamard, V., Champ, S., Mora, L. *et al*. 2005. The glutamine residue of the conserved GGQ motif in Saccharomyces cerevisiae release factor eRF1 is methylated by the product of the YDR140w gene. *J. Biol. Chem.* **280**:2439–2445.

Highland, J.H., Howard, G.A., Ochsner, E., *et al.* 1975. Identification of a ribosomal protein necessary for thiostrepton binding to *E. coli* ribosomes. *J. Biol. Chem.* **250**:1141–1145.

Hinnebusch, A.G. 2000. Mechanism and regulation of initiator methionine tRNA binding to ribosomes. In *Translational Control of Gene Expression,* Eds. N. Sonnenberg, J.W. Hershey and M.B. Matthews, pp. 185–243. Cold Spring Harbor Laboratory Press.

Hirabayashi, N., Sato, N.S., and Suzuki, T. 2006. Conserved loop sequence of helix 69 in Escherichia coli 23S rRNA is involved in A-site tRNA binding and translational fidelity. *J. Biol. Chem.* **281**:17203–17211.

Hirashima, A., and Kaji, A. 1972. Factor-dependent release of ribosomes from messenger RNA. Requirement for two heat-stable factors. *J. Mol. Biol.* **65**:43–58.

Hirashima, A., and Kaji, A. 1973. Role of elongation factor G and a protein factor on the release of ribosomes from messenger ribonucleic acid. *J. Biol. Chem.* **248**:7580–7587.

Hirokawa, G., Kiel, M.C., Muto, A., *et al*. 2002. Post-termination complex disassembly by ribosome recycling factor, a functional tRNA mimic. *EMBO J.* **21**:2272–2281.

Hirokawa, G., Nijman, R.M., Raj, V.S., *et al*. 2005. The role of ribosome recycling factor in dissociation of 70S ribosomes into subunits. *RNA* **11**:1317–1328.

Hirsh, D. 1970. Tryptophan tRNA of Escherichia coli. *Nature* **228**:57.

Hoagland, M.B. 2003. Celebrating complementarity. *Ann. Intern. Med.* **138**:583–586.

Hoagland, M.B., Zamecnik, P., and Stephenson, M.L. 1957. Intermediate reactions in protein biosynthesis. *Biochim. Biophys. Acta* **24**:215–216.

Hoffmann, A. and Bukau, B. 2009. Trigger factor finds new jobs and contacts. *Nat. Struct. Mol. Biol.* **16**:1006–1008.

Hoffmann, A., Bukau, B., and Kramer, G. 2010. Structure and function of the molecular chaperone trigger factor. *Biochim. Biophys. Acta* **1803**:650–661.

Hoffmann, A., Merz, F., Rutkowska, A., *et al*. 2006. Trigger factor forms a protective shield for nascent polypeptides at the ribosome. *J. Biol. Chem.* **281**: 6539–6545.

Hoffman, D.W., Davies, C., Gerchman, S.E., *et al.* 1994. Crystal structure of prokaryotic ribosomal protein L9: a bi-lobed RNA- binding protein. *EMBO J.* **13**:205–212.

Hoffman, D.W., Cameron, C.S., Davies, C., *et al.* 1996. Ribosomal protein L9: a structure determination by the combined use of X-ray crystallography and NMR spectroscopy. *J. Mol. Biol.* **264**:1058–1071.

Hogg, T., Mechold, U., Malke, H., *et al.* 2004. The structural basis of (p)ppGpp metabolism and the stringent response: two conformations correspond to opposing activity states of a bifunctional RelA/SpoT homolog. Submitted.

Holley, R.W., Apgar, J., Everett, G.A., *et al.* 1965. Structure of a ribonucleic acid. *Science* **147**:1462–1465.

Hope, H., Frolow, F., von Böhlen, K., *et al.* 1989. Cryocrystallography of ribosomal particles. *Acta Cryst.* **B45**:190–199.

Hopfield, J.J. 1974. Kinetic proofreading: a new mechanism for reducing errors in biosynthetic processes requiring high specificity. *Proc. Natl. Acad. Sci. USA.* **71**: 4135–4139.

Hopfield, J.J. 1978. Origin of the genetic code: A testable hypothesis based on tRNA structure, sequence, and kinetic proofreading. *Proc. Natl. Acad. Sci. USA.* **75**:4334–4338.

Hsu, S.T.D., Fucini, P., Cabrita, L.D., *et al.* 2007. Structure and dynamics of a ribosome-bound nascent chain by NMR spectroscopy. *Proc. Natl. Acad. Sci. USA.* **104**:16516–16521.

Hsiao, C., Mohan, S., Kalahar, B.K., *et al.* 2009. Peeling the onion: Ribosomes are ancient molecular fossils. *Mol. Biol. Evol.* **26**:2415–2425.

Huai, Q., Wang, H., Sun, Y., *et al.* 2003. Three-dimensional structures of PDE4D in complex with rolipram and implication on inhibitor selectivity. *Structure* **11**:865–873.

Huang, C., Mandava, C.S., and Sanyal, S. 2010. The ribosomal stalk plays a key role in IF2-mediated association of the ribosomal subunits. *J. Mol. Biol.* **399**:145–153.

Huang, K.H., Fairclough, R.H., and Cantor, C.R. 1975. Singlet energy transfer studies of the arrangement of proteins in the 30S *Escherichia coli* ribosome. *J. Mol. Biol.* **97**:443–470.

Huang, Y.J., Swapna, G.V.T., Rajan, P.K., *et al.* 2003. Solution NMR structure of ribosome-binding factor A (RbfA), a cold-shock adaptation protein from *Escherichia coli. J. Mol.Biol.* **327**:521–536.

Hummel, H., and Böck, A. 1987. 23S ribosomal RNA mutations in halobacteria conferring resistance to the anti-80S ribosomal targeted antibiotic anisomycin. *Nucl. Acids Res.* **15**:2431–2443.

Hury, J., Nagaswami, U., Larioz-Sanz, M., *et al.* 2006. Ribosome origins: The relative age of 23S rRNA domains. *Orig. Life. Evol. Biosph.* **36**:421–429.

Huxley, H.E., and Zubay, G. 1960. Electron microscope observations on the structure of microsomal particles from *Escherichia coli. J. Mol. Biol.* **2**:10–18.

Ibba, M., Becker, H.D., Stathopoulos, C., *et al.* 2000. The adaptor hypothesis revisited. *Trends Biochem. Sci.* **25**:311–316.

Ibba, M., Morgan, S., Curnow, A.W., *et al.* 1997. A euryarchaeal lysyl-tRNA synthetase: resemblance to class I synthetases. *Science* **278**:1119–1122.

Ibba, M. and Söll, D. 2000. Aminoacyl-tRNA synthesis. *Annu. Rev. Biochem.* **69**:617–650.

Ibba, M., and Söll, D. 2001. The renaissance of aminoacyl-tRNA synthesis. *EMBO Rep.* **2**:382–387.

Ibba, M. and Söll, D. 2002. Genetic code: introducing pyrrolysine. *Curr. Biol.* **12**:R464–R466.

Ilag, L.L., Videler, H., McKay, A.R., *et al*. 2005. Heptameric $(L12)_6$/L10 rather than canonical pentameric complexes are found by tandem MS of intact ribosomes from thermophilic bacteria. *Proc. Natl. Acad. Sci. USA.* **102**:8192–8197.

Inge-Vechtomov, S., Zhouravleva, G., and Philippe, M. 2003. Eukaryotic release factors (eRFs) history. *Biol. Cell.* **95**:195–209.

Inoue, K., Alsina, J., Chen, J., and Inouye, M. 2003. Suppression of defective ribosome assembly in a rbfA deletion mutant by overexpression of Era, an essential GTPase in *Escherichia coli*. *Mol. Microbiol.* **48**:1005–1016.

Inoue-Yokosawa, N., Ishikawa, C., and Kaziro, Y. 1974. The role of guanosine triphosphate in translocation reaction catalyzed by elongation factor G. *J. Biol. Chem.* **249**:4321–4323.

Ioannou, M., Coutsogeorgopoulos, C., and Drainas, D. 1997. Determination of eukaryotic peptidyltransferase activity by pseudo-first-order kinetic analysis. *Anal. Biochem.* **247**:115–122.

Ippolito, J.A., Kanya, Z.F., Wang, D. *et al*. 2008. Crystal stucture of the oxazolidinone antibiotic Linezolid bound to the 50S ribosomal subunit. *J. Med. Chem.* **51**:3353–3356.

Ishigami, J., Fukuda, Y., and Hara, S. 1967. Clinical use of Kasugamycin for urinary tract infections due to *Pseudomonas aeruginosa*. *J. Antibiot. [B]* **20**:83–84.

Ishitani, R., Nureki, O., Nameki, N., *et al*. 2003. Alternative tertiary structure of a tRNA for recognition by a post-transcriptional modification enzyme. *Cell* **113**:383–394.

Ishitani, R., Yokoyama, S., and Nureki, O. 2008. Structure, dynamics, and function of RNA modification enzymes. *Curr. Op. Struct. Biol.* **18**:230–339.

Ishitsuka, H., Kuriki, Y., and Kaji, A. 1970. Release of transfer ribonucleic acid from ribosomes. A G factor and guanosine triphosphate-dependent reaction. *J. Biol. Chem.* **245**:3346–3351.

Ito, K., Fujiwara, T., Toyoda, T., and Nakamura, Y. 2002. Elongation factor G participates in ribosome disassembly by interacting with ribosome recycling factor at their tRNA-mimicry domains. *Mol. Cell* **9**:1263–1272.

Ito, K., Uno, M., and Nakamura, Y. 2000. A tripeptide "anticodon" deciphers stop codons in messenger RNA. *Nature* **403**:680–684.

Ito, T. and Yokoyama, S. 2010. Two enzymes bound to one transfer RNA assume alternative conformations for consequtive reactions. *Nature* **467**:612–616.

Izutsu, K., Wada, A., and Wada, C. 2001. Expression of ribosome modulation factor (RMF) in *Escherichia coli* requires ppGpp. *Genes Cells* **6**:665–676.

Jacquet, E. and Parmeggiani, A. 1988. Structure-function relationships in the GTP binding domain of EF-Tu: mutation of Val20, the residue homologous to position 12 in p21. *EMBO J.* **7**:2861–2867.

James, C.M., Ferguson, T.K., Leykam, J.F., and Krzycki, J.A. 2001. The amber codon in the gene encoding the monomethylamine methyltransferase isolated from *Methanosarcina barkeri* is translated as a sense codon. *J. Biol. Chem.* **276**: 34252–34258.

Janosi, L., Hara, H., Zhang, S., and Kaji, A. 1996. Ribosome recycling by ribosome recycling factor (RRF) — an important but overlooked step of protein biosynthesis. *Adv. Biophys.* **32**:121–201.

Janosi, L., Mottagui-Tabar, S., Isaksson, L.A., *et al.* 1998. Evidence for *in vivo* ribosome recycling, the fourth step in protein biosynthesis. *EMBO J.* **17**:1141–1151.

Jenner, L., Demeshkina, N., Yusupova, G., *et al*. 2010. Structural rearrangements of the ribosome at the tRNA proofreading step. *Nat. Struct. Mol. Biol.* **17**:1072–1079.

Jenner L., Romby P., Rees B., *et al*. 2005. Translational operator of mRNA on the ribosome: How repressor proteins exclude ribosome binding. *Science*. **308**:120–123.

Jenni, S. and Ban, N. 2003. The chemistry of protein synthesis and voyage through the ribosome tunnel. *Curr. Opin. Struct. Biol.* **13**:212–219.

Jenvert, R.-M. and Holmberg Schiavone, L. 2007. The flexible N-terminal domain of ribosomal protein L11 from *Escherichia coli* is necessary for the activation of stringent factor. *J. Mol. Biol*. **365**:764–772.

Jeppesen, M.G., Navratil, T., Spremulli, L.L., *et al*. 2005. Crystal structure of the bovine mitochondrial elongation factor Tu**-**Ts complex. *J. Biol. Chem.* **280**:5071–5081.

Jerinic, O. and Joseph, S. 2000. Conformational changes in the ribosome induced by translational miscoding agents. *J. Mol. Biol*. **304**:707–713.

Jiang, Y., Nock, S., Nesper, M., *et al*. 1996. Structure and importance of the dimerization domain in elongation factor Ts from *Thermus thermophilus*. *Biochemistry* **35**: 10269–10278.

Jin, H., Kelley, A.C., and Ramakrishnan, V. 2011. Crystal structure of the hybrid state of ribosome in complex with the guanosine triphosphate release factor 3. *Proc. Natl. Acad. Sci. USA.* **108**:15798–15803.

Johanson, U., and Hughes, D. 1994. Fusidic acid-resistant mutants define three regions in elongation factor G of *Salmonella typhimurium*. *Gene* **143**:55–59.

Johanson, U., Ævarsson, A., Liljas, A., and Hughes, D. 1996. The dynamic structure of EF-G studied by fusidic acid resistance and internal revertants. *J. Mol. Biol*. **258**: 420–432.

Johansson, M., Bouakaz, E., Lovmar, M., *et al*. 2008. The kinetics of ribosomal peptidyl transfer revisited. *Mol. Cell* **30**:589–598.

Johansson, M., Zhang, J., and Ehrenberg, M. 2012. Genetic code translation displays a linear trade-off between efficiency and accuray of tRNA selection. *Proc. Natl. Acad. Sci. USA.* **109**:131–136.

Johnson, C.H., Kruft, V., and Subramanian, A.R. 1990. Identification of a plastid-specific ribosomal protein in the 30S subunit of chloroplast ribosomes and

isolation of the cDNA clone encoding its cytoplasmic precursor. *J. Biol. Chem.* **265**: 12790–12795.

Jones, P.G. and Inouye, M. 1996. RbfA, a 30S ribosomal binding factor, is a cold-shock protein whose absence triggers the cold-shock response. *Mol. Microbiol.* **21**: 1207–1218.

Jones, P.G., Mitta, M., Kim, Y., *et al.* 1996. Cold shock induces a major ribosomal-associated protein that unwinds double-stranded RNA in *Escherichia coli*. *Proc. Natl. Acad. Sci. USA.* **93**:76–80.

Jørgensen, R., Ortiz, P.A., Carr-Schmid, A., *et al.* 2003. Two crystal structures demonstrate large conformational changes in the eukaryotic ribosomal translocase. *Nat. Struct. Biol.* **10**:379–385.

Joseph, S., and Noller, H.F. 2000. Directed hydroxyl radical probing using iron(II) tethered to RNA. *Methods Enzymol.* **318**:175–190.

Joyce, G.F. 2002. The antiquity of RNA-based evolution. *Nature* **418**:214–221.

Julian, P., Konevega, A.L., Scheres, S.H.W. *et al.* 2008. Structure of ratcheted ribosomes with tRNAs in hybri states. *Proc. Natl. Scad. Sci. USA.* **105**:16924–16927.

Julian., P., Milon, P., Agitezabal, X., *et al.* 2011. The Cryo-EM structure of a complete 30S translation initiation complex from *Escherichia coli*. *PLOS Biol.* **9**:7.

Justice, M.C., Hsu, M.J., Tse, B., *et al.* 1998. Elongation factor 2 as a novel target for selective inhibition of fungal protein synthesis. *J. Biol. Chem.* **273**:3148–3151.

Justice, M.C., Ku, T., Hsu, M.J., *et al.* 1999. Mutations in ribosomal protein L10e confer resistance to the fungal-specific eukaryotic elongation factor 2 inhibitor sordarin. *J. Biol. Chem.* **274**:4869–4875.

Kaempfer, R. 1972. Initiation factor IF-3: a specific inhibitor of ribosomal subunit association. *J. Mol. Biol.* **71**:583–598.

Kaji, A., Kiel, M.C., Hirokawa, G., *et al.* 2001. The fourth step of protein synthesis: disassembly of the posttermination complex is catalyzed by elongation factor G and ribosome recycling factor, a near-perfect mimic of tRNA. *Cold Spring Harb. Symp. Quant. Biol.* **66**:515–529.

Kaltschmidt, E., Dzionara, M., Donner, D., and Wittmann, H.G. 1967. Ribosomal proteins I. Isolation, amino acid composition, molecular weights and peptide mapping of proteins from *E. coli* ribosomes. *Mol. Gen. Genet.* **100**:364–373.

Kaltschmidt, E., and Wittmann, H.G. 1970. Ribosomal proteins. XII. Number of proteins in small and large ribosomal subunits of *Escherichia coli* as determined by two-dimensional gel electrophoresis. *Proc. Natl. Acad. Sci. USA.* **67**:1276–1282.

Kappen, L.S. and Goldberg, I.H. 1976. Analysis of the two steps in polypeptide chain initiation inhibited by pactamycin. *Biochemistry* **15**:811–818.

Karimi, R. and Ehrenberg, M. 1994. Dissociation rate of cognate peptidyl-tRNA from the A-site of hyperaccurate and error-prone ribosomes. *Eur. J. Biochem.* **226**:355–360.

Karimi, R. and Ehrenberg, M. 1996. Dissociation rate of peptidyl-tRNA from the P-site of *E. coli* ribosomes. *EMBO J.* **15**:1149–1154.

Karimi, R., Pavlov, M.Y., Buckingham, R.H., and Ehrenberg, M. 1999. Novel roles for classical factors at the interface between translation termination and initiation. *Mol. Cell* **3**:601–609.

Karzai, A.W., Susskind, M.M., and Sauer, R.T. 1999. SmpB, a unique RNAbinding protein essential for the peptide-tagging activity of SsrA (tmRNA). *EMBO J.* **18**:3793–3799.

Karzai, A.W., Roche, E.D., and Sauer, R.T. 2000. The SsrA-SmpB system for protein tagging, directed degradation and ribosome rescue. *Nat. Struct. Biol.* **7**:449–455.

Kasai, K., Kanno, T., Endo, Y., *et al*. 2004. Guanosine tetra and pentaphosphate synthase activity in chloroplasts of a higher plant: association with 70S ribosomes and inhibition by tetracycline. *Nucleic Acids Res.* **32**:5732–5741.

Kasai, K., Nishizawa, T., Takahashi, K. *et al*. 2006. Physiological analysis of the stringent response elicited in an extreme thermophilic bacterium, *Thermus thermophilus*. *J. Bact*. **188**:9–10.

Kastner, B., Stöffler-Meilicke, M., and Stöffler, G. 1981. Arrangement of the subunits in the ribosome of *Escherichia coli*: demonstration by immuno electron microscopy. *Proc. Natl. Acad. Sci. USA.* **78**:6652–6656.

Kato, T., Yoshida, H., Miyata, T., *et al*. 2010. Structure of the 100S ribosome in the hibernation stage revealed by electron microscopy. *Structure* **18**:719–724.

Katunin, V.I., Muth, G.W., Strobel, S., *et al*. 2002. Important contribution to catalysis of peptide bond formation by a single ionizing group within the ribosome. *Mol. Cell* **10**:339–346.

Kaur, S., Gillet, R., Li, W., *et al*. 2006. Cryo-EM visualization of transfer messenger RNA with two SmpBs in a stalled ribosome. *Proc. Natl. Acad. Sci. USA.* **109**:16484–16489.

Kavran, J.M. and Steitz, T.A. 2007. Structure of the base of the L7/L12 stalk of the *Haloarcula marismortui* large ribosomal subunit: Analysis of L11 movements. *J. Mol. Biol.* **371**:1047–1059.

Kawashima, T., Berthet-Colominas, C., Cusack, S., *et al*. 1996. The crystal structure of the *Escherichia coli* EF-Tu.EF-Ts complex at 2.5Å resolution: mechanism of GDP/GTP exchange. *Nature* **379**:511–518.

Kaziro, Y. 1978. The role of guanosine 5′-triphosphate in polypeptide chain elongation. *Biochim. Biophys. Acta* **505**:95–127.

Keasling, J.D., Bertsch, L., and Kornberg, A. 1993. Guanosine pentaphosphate phosphohydrolase of *Escherichia coli* is a long-chain exopolyphosphatase. *Proc. Natl. Acad. Sci. USA.* **90**:7029–7033.

Keeling, P.J. and Doolittle, W.F. 1995. An archaebacterial elF-1A: new grist for the mill. *Mol. Microbiol.* **17**:399–400.

Keeling, P.J., Fast, N.M., and McFadden, G.I. 1998. Evolutionary relationship between translation initiation factor eIF-2gamma and selenocysteine-specific elongation factor SELB: change of function in translation factors. *J. Mol. Evol.* **47**:649–655.

Keenan, R.J., Freymann, D.M., Walter, P., and Stroud, R.M. 1998. Crystal structure of the signal sequence binding subunit of the signal recognition particle. *Cell* **94**:181–191.

Keenan, R.J., Freymann, D.M., Stroud, R.M., and Walter, P. 2001. The signal recognition particle. *Ann. Rev. Biochem.* **70**:755–775.

Keiler, K.C., Waller, P.R., and Sauer, R.T. 1996. Role of a peptide tagging system in degradation of proteins synthesized from damaged messenger RNA. *Science* **271**:990–993.

Kelkar, D.A., Khushoo, A., Yang, Z., *et al*. 2012. Kinetic analysis of ribosome-bound fluorescent proteins reveals an early, stable, cotranslational folding intermediate. *J. Biol. Chem.* **287**:2568–2578.

Khorana, H.G., Büchi, H., Ghosh, H., *et al*. 1966. Polynucleotide synthesis and the genetic code. *Cold Spring Harb. Symp. Quant. Biol.* **31**:39–49.

Kidmose, R.T., Vasiliev, N.N., Chetverin, A.B., *et al*. 2010. Structure of the Qβ replicase, an RNA-dependent RNA polymerase consisting of viral and host proteins. *Proc. Natl. Acad. Sci. USA.* **107**:10884–10889.

Kihara, A., Akiyama, Y., Ito, K. 1995. FtsH is required for proteolytic elimination of uncomplexed forms of SecY, an essential protein translocase subunit. *Proc. Natl. Acad. Sci. USA.* **92**:4532–4536.

Kihira, K., Shimizu, Y., Shomura, Y., *et al*. 2012. Crystal structure analysis of the translation factor RF3 (release factor 3). *FEBS Lett*. **586**:3705–3709.

Kim, S.H., Suddath, F.L., Quigley, G.J., *et al*. 1974. Three-dimensional tertiary structure of yeast phenylalanine transfer RNA. *Science* **185**:435–440.

Kim, K.K., Hung, L.W., Yokota, H., *et al*. 1998. Crystal structures of eukaryotic translation initiation factor 5A from *Methanococcus jannaschii* at 1.8A resolution. *Proc. Natl. Acad. Sci. USA.* **95**:10419–10424.

Kim, D.F. and Green, R. 1999. Base-pairing between 23S rRNA and tRNA in the ribosomal A site. *Mol. Cell* **4**:859–864.

Kim, K.K., Min, K., and Suh, S.W. 2000. Crystal structure of the ribosome recycling factor from *Escherichia coli. EMBO J.* **19**:2362–2370.

Kim, H.D., Puglisi, J.D., Chu, S. 2007. Fluctuations of transfer TNAs between classical and hybrid states. *Biophys. J.* **93**:3573–3582.

Kingsbury, E.W. and Voelz, H. 1969. Induction of helical arrays of ribosomes by vinblastine sulphate in *Escherichia coli. Science* **166**:768–769.

Kirillov, S.V., Makarov, E.M., and Semenkov, Y.P. 1983. Quantitative study of interaction of deacylated tRNA with *Escherichia coli* ribosomes. Role of 50S subunits in formation of the E site. *FEBS Lett.* **157**:91–94.

Kirillov, S.V., Wower, J., Hixson, S.S., *et al*. 2002. Transit of tRNA through the *Escherichia coli* ribosome: cross-linking of the 30 end of tRNA to ribosomal proteins at the P and E sites. *FEBS Lett.* **514**:60–66.

Kirsebom, L.A. 2007. RNase P RNA mediated cleavage: Substrate recognition and catalysis. *Biochemie* **89**:1183–1194.

Kirsebom, L.A., Amons, R., and Isaksson, L.A. 1986. Primary structures of mutationally altered ribosomal protein L7/L12 and their effects on cellular growth and translational accuracy. *Eur. J. Biochem.* **156**:669–675.

Kischa, K., Möller, W., and Stöffler, G. 1971. Reconstitution of a GTPase activity by a 50S ribosomal protein from *E. coli*. *Nature New Biol.* **233**:62–63.

Kisselev, L.L., and Buckingham, R.H. 2000. Translational termination comes of age. *Trends Biochem. Sci.* **25**:561–566.

Kisselev, L., Ehrenberg, M., and Frolova, L. 2003. Termination of translation: interplay of mRNA, rRNAs and release factors? *EMBO J.* **22**:175–182.

Kjeldgaard, N.O., and Gaussing, K. 1974. Regulation of biosynthesis of ribosomes. In *Ribosomes,* Eds. M. Nomura *et al.,* pp. 369–392. Cold Spring Harbor Laboratory, Cold Spring Harbor, New York.

Kjeldgaard, M., Nissen, P., Thirup, S., and Nyborg, J. 1993. The crystal structure of elongation factor EF-Tu from *Thermus aquaticus* in the GTP conformation. *Structure* **1**:35–50.

Kjeldgaard, M., and Nyborg, J. 1992. Refined structure of elongation factor EF-Tu from *Escherichia coli*. *J. Mol. Biol.* **223**:721–742.

Kjeldgaard, M., Nyborg, J., and Clark, B.F.C. 1996. The GTP binding motif: variations on a theme. *FASEB J.* **10**:1347–1368.

Klaholz, B.P. 2011. Molecular recognition and catalysis in translation termination complexes. *Trends Biochem. Sci.* **36**:282–292.

Klaholz, B.P., Myasnikov, A.G., and van Heel, M. 2004. Visualization of release factor 3 on the ribosome during termination of protein synthesis. *Nature* **427**:862–865.

Klein, D.J., Schmeing, T.M., Moore, P.B., and Steitz, T.A. 2001. The kink-turn: a new RNA secondary structure motif. *EMBO J.* **20**:4214–4221.

Klein, D.J., Moore, P.B., and Steitz, T.A. 2004. The roles of ribosomal proteins in the structure, assembly, and evolution of the large ribosomal subunit. Submitted to *J. Mol. Biol.*

Klinge, S., Voights-Hoffmann, F., Leibundgut, M., *et al*. 2011. Crystal structure of the eukaryotic 60S ribosomal subunit in complex with initiation factor 6. *Science* **334**:941–948.

Klug, A. and Schwabe, J.W. 1995. Protein motifs 5. Zinc fingers. *FASEB J.* **9**:597–604.

Knight, R.D., Freeland, S.J., and Landweber, L.F. 2001. Rewiring the keyboard: evolvability of the genetic code. *Nat. Rev. Gen.* **2**:49–58.

Knowles, D.J.C., Foloppe, N., Matassova, N.B., and Murchie, A.I.H. 2002. The bacterial ribosome, a promising focus for structure based drug design. *Curr. Opin. Pharmacol.* **2**:501–506.

Knudsen, C.R., and Clark, B.F. 1995. Site-directed mutagenesis of Arg58 and Asp86 of elongation factor Tu from *Escherichia coli*: effects on the GTPase reaction and aminoacyl-tRNA binding. *Prot. Eng.* **8**:1267–1273.

Koc, E.C., Burkhart, W., Blackburn, K., *et al*. 2001a. The small subunit of the mammalian mitochondrial ribosome. Identification of the full complement of ribosomal proteins present. *J. Biol. Chem*. **276**:19363–19374.

Koc, E.C., Burkhart, W., Blackburn, K., *et al*. 2001b. The large subunit of the mammalian mitochondrial ribosome. Analysis of the complement of ribosomal proteins present.*J. Biol. Chem*. **276**:43958–43969.

Koc, E.C. and Spremulli L.L. 2002. Identification of mammalian mitochondrial translational initiation factor 3 and examination of its role in initiation complex formation with natural mRNAs. *J. Biol. Chem*. **277**:35541–35549.

Koc, E.C., Haque, M.E., and Spremulli, L.L. 2010. Current views of the structure of the mammalian mitochondrial ribosome. *Isr. J. Chem*. **50**:1–15.

Kolesnikov, A., and Gudkov, A. 2002. Elongation factor G with effector loop from elongation factor Tu is inactive in translocation. *FEBS Lett*. **514**:67–69.

Kolesnikov, A.V., and Gudkov, A.T. 2003. Mutation analysis of the role in ribosomal translocation for loops of domain IV of the elongation factor G. *Mol. Biol*. **37**:611–616.

Kolesnikov, I.V., Protasova, N.Y., and Gudkov, A.T. 1996. Tetracyclines induce changes in accessibility of ribosomal proteins to proteases. *Biochimie* **78**:868–873.

Kollman, P. 1993. Free-energy calculations — Applications to chemical and biochemical phenomena. *Chem Rev* **93**:2395–2417.

Komine, Y., Adachi, T. Inokuchi, H. *et al*. 1990. Genomic organization and physical mapping of the transfer RNA genes in *Escherichia coli* K-12. *J. Mol. Biol*. **212**:579–598.

Komoda, T., Sato, N., Phelps, S.S., *et al*. 2006. The A-site finger in 23S rRNA acts as a functional attenuator for translocation. *J. Biol. Chem*. **281**:32303–32309.

Konevega, A.L., Fischer, N., Semenkov, Y.P., 2007. Spontaneous reverse movement of mRNA-bound tRNA through the ribosome. *Nat. Struct. Mol. Biol*. **14**:318–324.

Kong, C., Ito, K., Walsh, M.A., *et al*. 2004. Crystal structure and functional analysis of the eukaryotic class II release factor eRF3 from *S. pombe. Mol. Cell*. **14**:233–245.

Koonin, E.V. and Novzhilov, A.S. 2009. Origin and evolution of the genetic code: the universal enigma. *IUBMB Life* **61**:99–111.

Korencic, D., Ahel, I., Schelert, J., *et al*. 2004. A freestanding proofreading domain is required for protein synthesis quality control in archaea. *Proc. Natl. Acad. Sci. USA*. **101**:10260–10265.

Korobeinikova, A.V., Gongadze, G.M., Korepanov, A.P., *et al*. 2008. 5S rRNA-recognition module of CTC family proteins and its evolution. *Biochemistry (Moscow)* **73**:156–163.

Korobeinikova, A.V., Garber, M.V., and Gongadze, G.M. 2012. Ribosomal proteins: Stucture, function and evolution. Biochemistry (Moscow) **77**:562–574.

Koripella, R.K., Chen, Y., Pelsker, K., *et al*. 2012. Mechanism of elongation factor-G-mediated fusidic acid resistance and fitness compensation in *Staphylococcus aureus*. *J. Biol. Chem*. **287**:30275–30267.

Korostelev, A. 2011. Structural aspects of translation termination on the ribosome. *RNA* **17**:1409–1421.

Korostelev, A., Asahara, H., Lancaster, L., *et al*. 2006. Crystal structure of a translation termination complex formed with release factor RF2. *Proc. Natl. Acad. Sci. USA.* **105**:19684–19689.

Korostelev, A. and Noller, H.F. 2007. The ribosome in focus: new structures bring new insights. *Trends Biochem. Sci.* **32**:434–441.

Korostelev, A., Ermolenko, D.N., and Noller, H.F. 2008. Structural dynamics of the ribosome. *Curr. Op. Chem. Biol.* **12**:674–683.

Korostelev, A., Zhu, J., Asahara, H., *et al*. 2010. Recognition of the amber UAG stop codon by release factor RF1. *EMBO J* **29**:2577–2585.

Kosolapov, A. and Deutsch, C. 2009. Tertiary interactions within the ribosomal exit tunnel. *Nat. Struct. Mol. Biol.* **16**:405–411.

Koteliansky, V.E., Domogatsky, S.P., and Gudkov, A.T. 1978. Dimer state of protein L7/L12 and EF-G dependent reactions on ribosomes. *Eur. J. Biochem.* **90**:319–323.

Kötting, C., Kallenbach, A., Suveyzdis, Y., *et al*. 2007. The GAP arginine finger movement into the catalytic of Ras increases the activation entropy. *Proc. Natl. Acad. Sci. USA.* **105**:6260–6265.

Kovtun, A.A., Minchenko, A.G. and Gudkov, A.T. 2006. Mutation analysis of the functional role of amino acid residues in domain IV of elongation factor G. *Mol. Biol.* **40**:764–769.

Kozak, M. 1986. Point mutations define a sequence flanking the AUG initiator codon that modulates translation by eukaryotic ribosomes. *Cell* **44**:283–292.

Kozak, M. 1987. At least six nucleotides preceding the AUG initiator codon enhance translation in mammalian cells. *J. Mol. Biol.* **196**:947–950.

Krab, I.M. and Parmeggiani, A. 1998. EF-Tu, a GTPase odyssey. *Biochim. Biophys. Acta* **1443**:1–22.

Krab, I.M. and Parmeggiani, A. 1999. Mutagenesis of three residues, isoleucine-60, threonine-61, and aspartic acid-80, implicated in the GTPase activity of *Escherichia coli* elongation factor Tu. *Biochemistry* **38**:13035–13041.

Krab, I.M. and Parmeggiani, A. 2002. Mechanisms of EF-Tu, a pioneer GTPase. *Prog. Nucleic Acids Res. Mol. Biol.* **71**:514–551.

Kramer, G., Ramachandiran, V., and Hardesty, B. 2001. Cotranslational folding — omnia mea mecum porto? *Int. J. Biochem. Cell Biol.* **33**:541–553.

Kramer, G., Boehringer, D., Ban, N., *et al*. 2009. The ribosome as a platform for co-translational processing, folding and targeting of newly synthesized proteins. *Nat. Struct. Mol. Biol.* **16**:389–397.

Kramer, G., Patzelt, H., Rauch, T., *et al*. 2004. Trigger factor peptidyl-prolyl cis/trans isomerase activity is not essential for the folding of cytosolic proteins in *Escherichia coli*. *J. Biol. Chem.* **279**:14165–14170.

Kramer, G., Ramachandiran, V., Horowitz, P.M., and Hardesty, B. 2002a. The molecular chaperone DnaK is not recruited to translating ribosomes that lack trigger factor. *Arch. Biochem. Biophys.* **403**:63–70.

Kramer, G., Rauch, T., Rist, W., *et al.* 2002b. L23 protein functions as a chaperone docking site on the ribosome. *Nature* **419**:171–174.

Kraulis, P. 1991. MOLSCRIPT: a program to produce both detailed and schematic plots of protein structures. *J. Appl. Cryst.* **24**:946–950.

Kravchenko, O., Mitroshin, I., Nikonov, S., *et al*. 2010. Structure of a two-domain N-terminal fragment of ribosomal protein L10 from *Metanococcus jannaschii* ribosomal stalk. *J. Mol. Biol*. **399**:214–220.

Kristensen, O. and Gajhede, M. 2003. Chaperone binding at the ribosome exit tunnel. *Structure* **11**:1547–1556.

Kristensen, O., Laurberg, M., Liljas, A., and Selmer, M. 2002. Is tRNA binding or tRNA mimicry mandatory for translation factors? *Curr. Prot. Pept. Sci*. **3**:133–141.

Kristensen, O., Laurberg, M., Liljas, A., *et al*. 2004. Structural characterization of the stringent response related exopolyphosphatase/guanosine pentaphosphate phosphohydrolase protein family. *Biochemistry* **43**:8894–8900.

Kristensen, O., Ross, B., and Gajhede, M. 2008. Structures of the PPX/GPPA phosphatase from Aquifex aeolicus in complex with the alarmone ppGpp. *J. Mol. Biol*. **375**:1469–1476.

Kromayer, M., Wilting, R., Tormay, P., and Böck, A. 1996. Domain structure of the prokaryotic selenocysteine-specific elongation factor SelB. *J. Mol. Biol.* **262**: 413–420.

Kromayer, M., Neuhierl, B., Friebel, A., and Böck, A. 1999. Genetic probing of the interaction between the translation factor SelB and its mRNA binding element in *Escherichia coli*. *Mol. Gen. Genet.* **262**:800–806.

Kubarenko, A.V., Sergiev, P.V., and Rodnina, M.V. 2005. GTPases of the translation apparatus. *Mol. Biol*. **39**:646.

Kumar, Y, Westram, R, Kipfer, P, *et al*. 2006. Evaluation of sequence alignments and oligonucleotide probes with respect to three-dimensional structure of ribosomal RNA using ARB software package. *BMC Bioinformatics* **7**: 240–251.

Kurland, C.G. 1960. Molecular characterization of ribonucleic acid from *E. coil* ribosomes, I. Isolation and molecular weights. *J. Mol. Biol*. **2**:83–91.

Kurland, C.G. 1972. Structure and function of the bacterial ribosome. *Ann. Rev. Biochem.* **41**:377–408.

Kurland, C.G. 1978. The role of guanine nucleotides in protein biosynthesis *Biophys. J*. **22**:373–392.

Kurland, C.G. 1992. Translational accuracy and the fitness of bacteria. *Ann. Rev. Genet*. **26**:29–50.

Kurland, C.G. 2010. The RNA dreamtime. Bioessays **32**:866–871.

Kurland, C.G., Hughes, D., and Ehrenberg, M. 1996. Limitations of translational accuracy. In *Escherichia coli and Salmonella typhimurium: Cellular and Molecular Biology,* Vol 1, Eds. F.C. Neidhardt, R. Curtis, III, J.L. Ingraham, pp. 979–1004. American Society for Microbiology Press.

Kuroda, A., Murphy, H., Cashel, M., *et al*. 1997. Guanosine tetra- and pentaphosphate promote accumulation of inorganic polyphosphate in *Escherichia coli*. *J. Biol. Chem.* **272**:21240–21243.

Kyrpides, N.C. and Woese, C.R. 1998a. Universally conserved translation initiation factors. *Proc. Natl. Acad. Sci. USA.* **95**:224–228.

Kyrpides, N.C., and Woese, C.R. 1998b. Archaeal translation initiation revisited: the initiation factor 2 and eucaryotic initiation factor 2B α-β-γ subunit families. *Proc. Natl. Acad. Sci. USA.* **95**:3726–3730.

Laffler, T., and Gallant, J. 1974. *spoT*, a new genetic locus involved in the stringent response in *Escherichia coli*. *Cell* **1**:27–30.

Lake, J.A. 1976. Ribosome structure determined by electron microscopy of *Escherichia coli* small subunits, large subunits and monomeric ribosomes. *J. Mol. Biol.* **105**:131–139.

Lake, J.A. 1977. Aminoacyl-tRNA binding at the recognition site is the first step of the elongation cycle of protein synthesis. *Proc. Natl. Acad. Sci. USA.* **74**:1903–1907.

Lake, J.A. 1982. Ribosomal subunit orientations determined in the monomeric ribosome by single- and double-labelling immune electron microscopy. *J. Mol. Biol.* **161**:89–106.

Lake, J.A. 1985. Evolving ribosome structure: domains in archaebacteria, eubacteria, eocytes and eucaryotes. *Ann. Rev. Biochem.* **54**:507–530.

Lake, J., Pendergast, M., Kahan, L., and Nomura, M. 1974. Localization of *Escherichia coli* ribosomal proteins S4 and S14 by electron microscopy of antibody-labelled subunits. *Proc. Natl. Acad. Sci. USA.* **71**:4688–4692.

Lake, J.A. and Strycharz, W.A. 1981. Ribosomal proteins L1, L17 and L27 from *Escherichia coli* localized at single sites on the large subunit by immune electron microscopy. *J. Mol. Biol.* **153**:979–992

Lancaster, L., Kiel, M.C., Kaji, A., and Noller, H.F. 2002. Orientation of ribosome recycling factor in the ribosome from directed hydroxyl radical probing. *Cell* **111**:129–140.

La Teana, A., Gualerzi, C.O., and Dahlberg, A.E. 2001. Initiation factor IF2 binds to the alpha-sarcin loop and helix 89 of *Escherichia coli* 23S ribosomal RNA. *RNA* **7**:1173–1179.

Laughrea, M. and Moore, P.B. 1977. Physical properties of ribosomal protein S1 and its interaction with the 30S ribosomal subunit of *Escherichia coli*. *J. Mol. Biol.* **112**:399–421.

Laurberg, M. 2002. Dynamics in protein synthesis. Structural studies of translation factors. Doctoral thesis from Lund University (ISBN 91-628-5088-1).

Laurberg, M., Asahara, H., Korostelev, A., *et al*. 2008. Structural basis for translation termination on the 70S ribosome. *Nature* **454**:852–857.

Laurberg, M., Kristensen, O., Martemyanov, K., *et al*. 2000. Structure of a mutant EF-G reveals domain III and possibly the fusidic acid binding site. *J. Mol. Biol.* **303**:593–603.

Laursen, R.A., L'Italien, J.J., Nagarkatti, S., and Miller, D.L. 1981. The amino acid sequence of elongation factor Tu of *Escherichia coli.* The complete sequence. *J. Biol. Chem.* **256**:8102–8109.

Laursen, B.S., Sorensen, H.P., Mortensen, K.K., *et al*. 2005. Initiation of protein synthesis in bacteria. *Microbiol. Mol. Biol. Rev.* **69**:101–123.

Lazzarini, R. and Dahlberg, A. 1971. The control of ribonucleic acid synthesis during amino acid depravation in *Escherichia coli. J. Biol. Chem.* **246**:420–429.

Lecompte, O., Ripp, R., Thierry, J.C., *et al.* 2002. Comparative analysis of ribosomal proteins in complete genomes: an example of reductive evolution at the domain scale. *Nucl. Acids Res.* **30**:5382–5390.

Lee, J.H., Choi, S.K., Roll-Mecak, A., *et al.* 1999. Universal conservation in translational initiation revealed by human and archaeal homologs of bacterial translation initiation factor IF2. *Proc. Natl. Acad. Sci. USA.* **96**:4342–4347.

Lee, J.H., Pestova, T.V., Shin, B.-S., *et al.* 2002. Initiation factor eIF5B catalyzes second GTP-dependent step in eukaryotic translation initiation. *Proc. Natl. Acad. Sci. USA.* **99**:16689–16694.

Lee, M.M., Jiang, R., Jain, R., *et al*. 2008. Structure of *Desulfitobacterium hafniense* PylSc, a pyrrolysyl-tRNA synthetase. *Biochem. Biophys. Res. Commun.* **374**:470–474.

Leffers, H., Kjems, J., Ostergaard, L., *et al*. 1987. Evolutionary relationships amongst archaebacteria — A comparative study of 23 S ribosomal RNAs of a sulphur-dependent extreme thermophile, an extreme halophile and a thermophilic methanogen. *J. Mol. Biol*. **195**:43–61.

Leibundgut, M., Frick, C., Thanbichler, M., *et al*. 2005. Selenocysteine tRNA-specific elongation factor SelB is a structural chimaera of elongation and initiation factors. *EMBO J.* **24**:11–22.

Leijonmarck, M., and Liljas, A. 1987. Structure of the C-terminal domain of the ribosomal protein L7/L12 from *Escherichia coli* at 1.7Å. *J. Mol. Biol.* **195**: 555–579.

Leijonmarck, M., Appelt, K., Badger, J., *et al.* 1988. Structural comparison of the procaryotic ribosomal protein L7/L12 and L30. *Proteins* **3**:243–248.

Leijonmarck, M., Eriksson, S., and Liljas, A. 1980. Crystal structure of a ribosomal component at 2.6A resolution. *Nature* **286**:824–826.

Leinfelder, W., Stadtman, T.C., and Böck, A. 1989. Occurrence *in vivo* of selenocysteyl-tRNA(SERUCA) in *Escherichia coli.* Effect of sel mutations. *J. Biol. Chem.* **264**: 9720–9723.

Leinfelder, W., Zehelein, E., Mandrand-Berthelot, M.A., *et al*. 1988. Gene for a novel tRNA species that accepts L-serine and cotranslationally inserts selenocysteine. *Nature* **331**:723–725.

Leipe, D.D., Wolf, Y.I., Koonin, E.V., and Aravind, L. 2002. Classification and evolution of P-loop GTPases and related ATPases. *J. Mol. Biol.* **317**:41–72.

Levitt, M. and Warshel, A. 1975. Computer simulation of protein folding. *Nature* **253**:694–698.

Levy, S.B. and Marshall, B. 2004. Antibacterial resistance worldwide: causes, challenges and responses. *Nature Medicine*, **10**:S122–S129.

Levy, S.B., McMurry, L.M., Barbosa, T.M., *et al.* 1999. Nomenclature for new tetracycline resistance determinants. *Antimicrob. Agents Chemother.* **43**:1523–1524.

Li, C., Reches, M., and Engelberg-Kulka, H. 2000. The bulged nucleotide in the *Escherichia coli* minimal selenocysteine insertion sequence participates in interaction with SelB: a genetic approach. *J. Bacteriol.* **182**:6302–6307.

Li, Z.Y., Liu, C.P., Zhu, L.Q., *et al.* 2001. The chaperone activity of trigger factor is distinct from its isomerase activity during co-expression with adenylate kinase in *Escherichia coli. FEBS Lett.* **506**:108–112.

Liang, S.-T., Xu, Y.-C., Dennis, P., *et al.* 2000. mRNA composition and control of bacterial gene expression. *J. Bact.* **182**:3037–3044.

Liljas, A. 1982. Structural studies of ribosomes. *Prog. Biophys. Mol. Biol.* **40**:161–228.

Liljas, L. 1986. The structure of spherical viruses. *Prog. Biophys. Mol. Biol.* **48**:1–36.

Liljas, A. 1990. Some structural aspects of elongation. In *The Structure, Function and Evolution of Ribosomes*, Eds. W. Hill, P.B. Moore, A. Dahlberg, *et al.,* pp. 309–317. ASM Press, American Society for Mocrobiology.

Liljas, A. 1991. Comparative biochemistry and biophysics of ribosomal proteins. *Int. Rev. Cytol.* **124**:103–136.

Liljas, A. 1996. Imprinting through molecular mimicry. Protein synthesis. *Curr. Biol.* **6**:247–249.

Liljas, A., and Al-Karadaghi, S. 1997. Structural aspects of protein synthesis. *Nat. Struct. Biol.* **4**:767–771.

Liljas, A. 2008. Getting close to termination. *Science* **322**:863–865.

Liljas, A., and Kurland, C.G. 1976. Crystallization of ribosomal protein L7/L12 from *Escherichia coli. FEBS lett.* **71**:130–132.

Liljas, A., Ehrenberg, M., and Åqvist, J. 2011. Comment on "The mechanism for activation of GTP hydrolysis on the ribosome". *Science*, **333**:37–a.

Liljas, A., Eriksson, S., Donner, D., and Kurland, C.G. 1978. Isolation and crystallization of stable domains of the protein L7/L12 from *Escherichia coli* ribosomes. *FEBS Lett.* **88**:300–304.

Liljas, A., Kirsebom, L.A., and Leijonmarck, M. 1986. Structural studies of the factor binding domain. In *Structure, Function and Genetics of Ribosomes,* Eds. B. Hardesty and G. Kramer, pp. 379–390. Springer-Verlag, New York.

Liljas, A., Kristensen, O., Laurberg, M., *et al.* 2000. The states, conformational dynamics and fusidic acid resistant mutants of EF-G. In *The Ribosome: Structure, Function, Antibiotics and Cellular Interactions,* Eds. R.A. Garrett, S.R. Douthwaite, A. Liljas, *et al.,* pp. 359–365. ASM Press, American Society for Mocrobiology, Washington, D.C.

Liljas, A, Liljas, L, Piskur, J, *et al*. 2009. *Textbook of structural biology*. World Scientific, Singapore.

Lill, R., Crooke, E., Guthrie, B., *et al*. 1988. The ''trigger factor cycle'' includes ribosomes, presecretory proteins, and the plasma membrane. *Cell* **54**:1013–1018.

Lill, R., Robertson, J.M., and Wintermeyer, W. 1986. Affinities of tRNA binding sites of ribosomes from *Escherichia coli*. *Biochemistry* **25**:3245–3255.

Lim, V., and Spirin, A.S. 1986. Stereochemical analysis of ribosomal transpeptidation. *J. Mol. Biol.* **188**:565–577.

Lipman, R.S., Sowers, K., and Hou, Y.M. 2000. Synthesis of cysteinyl-tRNA^{Cys} by a genome that lacks a normal cysteine-tRNA synthase. *Biochemistry* **39**:7792.

Lipmann, F. 1969. Polypeptide chain elongation in protein biosynthesis. *Science* **164**:1024–1031.

Liu, H., Chen, C., Zhang, H., *et al*. 2011. The conserved protein EF4 (LepA) modulates the elongation cycle of protein synthesis. *Proc. Natl. Acad. Sci. USA.* **108**:16223–16228.

Lodmell, J.S. and Dahlberg, A.E. 1997. A conformational switch in *Escherichia coli* 16S ribosomal RNA during decoding of messenger RNA. *Science* **277**:1262–1267.

Loerke, J., Giesebrecht, J., and Spahn, C.M. 2010. Multiparticle cryo-EM of ribosomes. *Meth. Enzymol.* **483**:161–177.

Loftfield, R.B., and Vanderjagt, D. 1972. The frequency of errors in protein biosynthesis. *Biochem. J.* **128**:1353–1356.

Longstaff, D.G., Blight, S. K., Zhang, L., *et al*. 2007. *In vivo* contextual requirements for UAG translation as pyrrolysine. *Mol. Microbiol.* **63**:229–241.

Lovmar, M., Vimberg, V., Lukk, E., *et al*. 2009. Cis-acting resistance peptides reveal dual ribosome inhibitory action of the macrolide josamycin. *Biochimie* **91**:989–995.

Lu, M. and Steitz, T.A. 2000. Structure of *Escherichia coli* ribosomal protein L25 complexed with a 5S rRNA fragment at 1.8-A resolution. *Proc. Natl. Aad. Sci. USA.* **97**:2023–2028.

Lubin, M. 1968. Observations on the shape of the 50S ribosomal subunit. *Proc. Natl. Acad. Sci. USA.* **61**:1454–1461.

Luger, K., and Richmond, T.J. 1998. The histone tails of the nucleosome. *Curr. Opin. Genet. Dev.* **8**:140–146.

Maguire, B.A., Benyaminov, A.D., Ramu, H., *et al*. 2005. A protein component at the heart of an RNA machine: The importance of protein L27 for the function of the bacterial ribosome. *Mol. Cell* **20**:427–435.

Maimets, T., Remme, J., and Villems, R. 1984. Ribosomal protein L16 binds to the 3′-end of transfer RNA. *FEBS Lett.* **166**:53–56.

Maivali, U. and Remme, J. (2004). Definition of bases in 23S rRNA essential for ribosomal subunit association. *RNA* **10**:600–604.

Maki, Y., Hashimoto, T., Zhou, M., *et al*. 2007. Three binding sites for stalk protein dimers are generally present in ribosomes from archaeal organism. *J. Biol. Chem*. **282**:32827–32833.

Maki, Y., Yoshida, H., and Wada, A. 2000. Two proteins, YfiA and YhbH, associated with resting ribosomes in stationary phase *Escherichia coli*. *Genes Cells* **5**:965–974.

Malkin, L.I. and Rich, A. 1967. Partial resistance to proteolytic digestion due to ribosomal shielding. *J. Mol. Biol.* **26**:329–346.

Mankin, A.S. 1997. Pactamycin resistance mutations in functional sites of 16S RNA. *J. Mol. Biol.* **274**:8–15.

Mankin, A.S. and Garrett, R.A. 1991. Chloramphenicol resistance mutations in the single 23S gene of the archaeon *H. halobium*. *J. Bacteriol*. **173**:3559–3563.

Mao, J.C.H. and Robishaw, E.E. 1971. Effects of macrolides on peptide-bond formation and translocation. *Biochemistry* **10**:2054–2061.

March, P.E. and Inouye, M. 1985. GTP-binding membrane protein of *Escherichia coli* with sequence homology to initiation factor 2 and elongation factors Tu and G. *Proc. Natl Acad. Sci. USA.* **82**:7500–7504.

Marck, C. and Grosjean, H. 2002. tRNomics: Analysis of tRNA genes from 50 genomes of Eukarya, Archaea, and Bacteria reveals anticodon-sparing strategies and domain-specific features. *RNA* **8**:1189–1232.

Margus, T., Remm, M., and Tenson, T. 2007. Phylogenetic distribution of translation GTPases in bacteria. *BMC Genomics* **8**:15.

Markus, M.A., Hinck, A.P., Huang, S., *et al.* 1997. High resolution solution structure of ribosomal protein L11-C76, a helical protein with a flexible loop that becomes structured upon binding to RNA. *Nat. Struct. Biol.* **4**:70–77.

Marshall, R.A., Dorywalska, M. and Puglisi, J.D. 2008. Irreversible chemical steps control intersubunit dynamics during translation. *Proc. Natl. Acad. Sci. USA.* **105**:15364–15369.

Martemyanov, K.A. and Gudkov, A.S. 1999. Domain IV of elongation factor G from *T. thermophilus* is strictly required for translation. *FEBS Lett.* **452**:155–159.

Martemyanov, K.A. and Gudkov, A.T. 2000. Domain III of elongation factor G from *Thermus thermophilus* is essential for induction of GTP hydrolysis on the ribosome. *J. Biol. Chem.* **275**:35820–35824.

Martemyanov, K.A., Yarunin, A.S., Liljas, A., and Gudkov, A.T. 1998. An intact conformation at the tip of elongation factor G domain IV is functionally important. *FEBS Lett.* **434**:205–208.

Martemyanov, K.A., Liljas, A., Yarunin, A.S., and Gudkov, A.T. 2001. Mutations in the G-domain of elongation factor G from *Thermus thermophilus* affect both its interaction with GTP and fusidic acid. *J. Biol. Chem.* **276**:28774–28778.

Martinez-Hackert, E. and Hendrickson, W.A. 2009. Promiscuous substrate recognition in folding and assembly activities of the trigger factor chaperone. *Cell* **138**:923–934.

Marzi, S., Myasnikov, A.G.,Serganov, A., *et al*. 2007. Structured mRNAs regulate translation initiation by binding to the platform of the ribosome. *Cell* **130**:1019–1031.

Mascarenhas, A.P., An, S., Rosen, A.E., *et al*. 2008. Fidelity mechanisms of the aminoacyl-tRNA synthetases. *Nucl. Acids. Mol. Biol*. **22**:155–203.

Maxwell, I.H. 1967. Partial removal of bound transfer RNA from polysomes engaged in protein synthesis *in vitro* after addition of tetracycline. *Biochim. Biophys. Acta* **138**:337–346.

May, R.P., Nowotny, V., Nowotny, P., *et al.* 1992. Inter-protein distances within the large subunit from *Escherichia coli* ribosomes. *EMBO J.* **11**:373–378.

McCaughan, K.K., Ward, C.D., Trotman, C.N.A., *et al*. 1984. The ribosomal binding domain for the bacterial release factors RF-l, RF-2 and RF-3. *FEBS Lett*. **175**:90–94.

McCloskey, J.A., and Crain, P.F. 1998. The RNA modification database. *Nucl. Acids Res*. **26**:196–197.

McCutcheon, J.P., Agrawal, R.K., Philips, S.M., *et al.* 1999. Location of translational initiation factor IF3 on the small ribosomal subunit. *Proc. Natl. Acad. Sci. USA.* **96**:4301–4306.

Mears, J.A., Cannone, J.J., Stagg, S.M., *et al*. 2002. Modelling a minimal ribosome based on comparative sequence analysis. *J. Mol. Biol*. **321**:215–234.

Meinnel, T., Sacerdot, C., Graffe, M., *et al.* 1999. Discrimination by *Escherichia coli* initiation factor IF3 against initiation on non-canonical codons relies on complementarity rules. *J. Mol. Biol.* **290**:825–837.

Melancon, P., Lemieux, C., and Brakier-Gringas, L. 1988. A mutation in the 530 loop of the *Escherichia coli* 16S ribosomal RNA causes resistance to streptomycin. *Nucl. Acids Res.* **16**:9631–9639.

Melnikov, S., Ben-Shem, A., Garreau de Loubresse, N., *et al*. 2012. One core, two shells: bacteria and eukaryotic ribosomes. *Nat. Struct. Mol. Biol.* **19**: 560–567.

Menetret, J.F., Neuhof, A., Morgan, D.G., *et al.* 2000. The structure of ribosome-channel complexes engaged in protein translocation. *Mol. Cell* **6**:1219–1232.

Mesters, J.R., Zeef, L.A., Hilgenfeld, R., *et al.* 1994. The structural and functional basis for the kirromycin resistance of mutant EF-Tu species in *Escherichia coli. EMBO J.* **13**: 4877–4885.

Miller, D.L., and Weissbach, H. 1977. Factors involved in the transfer of aminoacyl-tRNA to the ribosome. In *Molecular Mechanisms of Protein Biosynthesis*, Eds. H. Weissbach and S. Petska, pp. 323–373. Academic Press, New York.

Milligan, R.A., and Unwin, P.N.T. 1986. Location of exit channel for nascent protein in 80S ribosome. *Nature* **319**:693–695.

Milon, P., Carotti, M., Konevega, A.L., *et al*. 2010. The ribosome-bound initiation factor 2 recruits initiator tRNA to the 30S initiation complex. *EMBO Rep.* **11**:312–316.

Mitkevich, V.A., Shyp, V., Petrushanko, I,Y., *et al*. 2012. GTPases IF2 and EF-G bind GDP and the SRL RNA in a mutually exclusive manner. *Sci. Rep.* **2**:843.

Mitra, K., Schaffitzel, C., Shaikh, T., *et al* . 2005. Structure of the E. coli protein-conducting channel bound to a translating ribosome. *Nature* **438**:318–324.

Mittenhuber, G. 2001. Comparative genomics and evolution of genes encoding bacterial (p)ppGpp synthetases/hydrolases (the Rel, RelA and SpoT proteins). *J. Mol. Microbiol. Biotechnol.* **3**:585–600.

Mizushima, S., and Nomura, M. 1970. Assembly mapping of 30S ribosomal proteins from *E. coli*. *Nature* **226**:1214–1218.

Moazed, D., and Noller, H. 1986. Transfer RNA shields specific nucleotides in 16S ribosomal RNA from attack by chemical probes. *Cell* **47**:985–994.

Moazed, D. and Noller, H. 1987. Chloramphenicol, erythromycin, carbomycin and vernamycin B protect overlapping sites in the peptidyl transfer region of 23S RNA. *Biochimie* **69**:879–884.

Moazed, D., and Noller, H. 1987. Interaction of antibiotics with functional sites in 16S ribosomal RNA. *Nature* **327**:389–394.

Moazed, D., and Noller, H. 1989. Interaction of tRNA with 23S RNA in the ribosomal A-, P- and E-sites. *Cell* **57**:586–597.

Moazed, D., and Noller, H.F. 1990. Binding of tRNA to the ribosomal A- and P-sites protects two distinct sets of nucleotides in 16S rRNA. *J. Mol. Biol.* **211**:135–145.

Moazed, D., and Noller, H.F. 1991. Sites of interaction of the CCA-end of peptidyl-tRNA with 23S rRNA. *Proc. Natl. Acad. Sci. USA.* **88**:3725–3728.

Moazed, D., Robertson, J.M., and Noller, H.F. 1988. Interaction of elongation factors EF-G and EF-Tu with a conserved loop in 23S RNA. *Nature* **334**:362–364.

Moazed, D., Samaha, R.R., Gualerzi, C., and Noller, H.F. 1995. Specific protection of 16S rRNA by translation initiation factors. *J. Mol. Biol.* **248**:207–210.

Moazed, D., Stern, S., and Noller, H.F. 1986. Rapid chemical probing of conformation in 16 S ribosomal RNA and 30S ribosomal subunits using primer extension. *J. Mol. Biol.* **187**:399–416.

Modolell, J., Girbes, T., and Vazquez, D. 1975. Ribosomal translocation promoted by guanylylimido diphosphate and guanylyl-methylene diphosphonate. *FEBS Lett.* **60**:109–113.

Modolell, J. and Vasquez, D. 1977. Inhibition of ribosomal translocation oby viomycin. *Eur. J. Biochem.* **81**:491–497.

Mohr, D., Wintermeyer, W., and Rodnina, M.V. 2000. Arginines 29 and 59 of elongation factor G are important for GTP hydrolysis or translocation on the ribosome. *EMBO J.* **19**:3458–3464.

Mohr, D., Wintermeyer, W., and Rodnina, M.V. 2002. GTPase activation of elongation factors Tu and G on the ribosome. *Biochemistry* **41**:12520–12528.

Monro, R.E. 1967. Catalysis of peptide bond formation by 50S ribosomal subunits from *Escherichia coli*. *J. Mol. Biol.* **26**:147–151.

Monro, R.E., Cerna, J., and Marcker, K.A. 1968. Ribosome-catalyzed peptidyl transfer: substrate specificity at the P-site. *Proc. Natl. Acad. Sci. USA.* **61**:1042–1049.

Montandon, P.E., Wagner, R., and Stutz, E. 1986. *E. coli* ribosomes with a C912 to U base change in the 16S rRNA are streptomycin resistant. *EMBO J.* **5**:3705–3708.

Montesano-Roditis, L., Glitz, D.G., Traut, R.R., and Stewart, P.L. 2001. Cryo-electron microscopic localization of protein L7/L12 within the *Escherichia coli* 70S ribosome by difference mapping and Nanogold labeling. *J. Biol. Chem.* **276**: 14117–14123.

Montoya, G., Kaat, K., Moll, R., Schafer, G., and Sinning, I. 2000. The crystal structure of the conserved GTPase of SRP54 from the archaeon *Acidianus ambivalens* and its comparison with related structures suggests a model for the SRP-SRP receptor complex. *Struct. Fold. Des.* **8**:515–525.

Moore, P.B. 1999. Structural motifs in RNA. *Ann. Rev. Biochem.* **67**:287–300.

Moore, P.B. and Steitz, T.A. 2003a. After the ribosome structures: how does peptidyl transferase work? *RNA* **9**:155–159.

Moore, P.B. and Steitz, T.A. 2003b. The structural basis of large ribosomal subunit function. *Ann. Rev. Biochem.* **72**:813–850.

Moore, S.D. and Sauer, R.T. 2007. The tmRNA system for translational survillance and ribosome rescue. *Annu. Rev. Biochem.* **76**:101.

Moore, V.G., Atchison, R.E., Thomas, G., *et al*. 1975. Identification of a ribosomal protein essential for peptidyl transfer activity. *Proc. Natl. Acad. Sci. USA*. **72**:844–848.

Moras, D., Comarmond, M.B., Fischer, J., *et al.* 1980. Crystal structure of yeast $tRNA^{Asp}$. *Nature* **288**:669–674.

Moreno, J.M., Kildsgaard, J., Siwanowicz, I., *et al.* 1998. Binding of *Escherichia coli* initiation factor IF2 to 30S ribosomal subunits: a functional role for the N-terminus of the factor. *Biochem. Biophys. Res. Commun.* **252**:465–471.

Moreno, J.M.P., Dyrskjøtersen, L., Kristensen, J.E., *et al*. 1999. Characterization of the domains of *E. coli* initiation factor IF2 responsible for recognition of the ribosome. *FEBS Lett.* **455**:130–134.

Morgan, R.S. and Uzman, B.G. 1966. Nature of the packing of ribosomes within chromatoid bodies. *Science* **152**:214–216.

Mori, H. and Ito, K. 2001. The Sec protein-translocation pathway. *Trends Microbiol.* **9**:494–500.

Morrison, C.A., Bradbury, E.M., Littlechild, J., and Dijk, J. 1977. Proton magnetic resonance studies to compare *Escherichia coli* ribosomal proteins prepared by two different methods. *FEBS Lett.* **83**:348–352.

Montoya, G., Kaat, K., Moll, R., *et al*. 2000. The crystal structure of the conserved GTPase of SRP54 from the archaeon *Acidianus ambivalens* and its comparison with related structures suggests a model for the SRP–SRP receptor complex. *Struct. Fold. Des.* **8**:515–525.

Moura, G.R., Paredes, J.A., and Santos, M.A.S. 2010. Development of the genetic code: Insights from a fungal codon reassignment. *FEBS Lett.* **584**:334–341.

Mueller, F. and Brimacombe, R. 1997. A new model for the three-dimensional folding of *Escherichia coli* 16S ribosomal RNA. II. The RNA-protein interaction data. *J. Mol. Biol.* **271**:545–565.

Mueller, F., Stark, H., van Heel, M., *et al*. 1997. A new model for the three-dimensional folding of *Escherichia coli* 16S ribosomal RNA. III. The topography of the functional centre. *J. Mol. Biol.* **271**:566–587.

Mulder, F.A.A., Bauakaz, L., Lundell, A., *et al*. 2004. Conformation and dynamics of ribosomal stalk protein L12 in solution and on the ribosome. *Biochemistry* **43**:5930–5936.

Munishkin, A., and Wool, I.G. 1997. The ribosome-in-pieces: binding of elongation factor EF-G to oligoribonucleotides that mimic the sarcin/ricin and thiostrepton domains of 23S ribosomal RNA. *Proc. Natl. Acad. Sci. USA.* **94**:12280–12284.

Munro, J.B., Altman, R.B., O'Connor, N., *et al*. 2007. Identification of two distinct hybrid state intermediates on the ribosome. *Mol. Cell* **25**:505–517.

Murzin, A.G. 1993. OB (oligonucleotide/oligosaccharide binding)-fold: common structural and functional solution for non-homologous sequences. *EMBO J.* **12**:861–867.

Mushegian, A. 2005. Protein content of minimal and ancestral ribosome. *RNA* **11**:1400–1406.

Myasnikov, A.G., Marzi, S., Simonetti, A., *et al*. 2005. Conformational transition of initiation factor 2 from the GTP- to GDP-bound state visualized on the ribosome. *Nat. Struct. Mol. Biol.* **12**:1145–1149.

Myasnikov, A., Simonetti, A., Marzi, S., *et al*. 2009. Structure-function insights into prokaryotic and eukaryotic translation initiation. *Curr. Op. Struct. Biol.* **19**:300–309.

Myong, S. and Ha, T. 2009. Stepwise translocation of nucleic acid motors. *Curr. Op. Struct. Biol.* **20**:121–127.

Nagaev, I., Bjorkman, J., Andersson, D.I., and Hughes, D. 2001. Biological cost and compensatory evolution in fusidic acid-resistant *Staphylococcus aureus*. *Mol. Microbiol.* **40**:433–439.

Naganuma, T., Nomura, N., Yao, M., *et al*. 2010. Structural basis for translation factor recruitment to the eukaryotic/archaeal ribosomes. *J. Biol. Chem.* **285**: 4747–4756.

Nakamoto, T. 2009. Evolution and the universality of the mechanism of initiation of protein synthesis. *Gene* **432**:1–6.

Nakamura, Y. and Ito, K. 2002. A tripeptide discriminator for stop codon recognition. *FEBS Lett*. **514**:30–33.

Nakamura, Y. and Ito, K. 2003. Making sense of mimic in translation termination. *Trends Biochem. Sci*. **28**:99–105.

Nakatogawa, H. and Ito, K. 2001. Secretion monitor, SecM, undergoes selftranslation arrest in the cytosol. *Mol. Cell* **7**:185–192.

Nakatogawa, H. and Ito, K. 2002. The ribosomal exit tunnel functions as a discriminating gate. *Cell* **108**:629–636.

Nam, K.H., Kim, K.-H., Kim, E.E.K., *et al*. 2009. Crystal structure of an EfPDF complex with Met-Ala-Ser based on crystallographic packing. *Biochem. Biophys. Res. Commun.* **381**:630–633.

Navarre, W.W., Zou, S.B., Roy, H., *et al*. 2010. PoxA, YjeK, and elongation factor P coordinately modulate virulence and drug resistance in Salmonella enterica. *Mol. Cell* **39**:209–221.

Nechifor, R. and Wilson, K.S. 2007. Crosslinking of translation fqactor EF-G to proteins of the bacterial ribosome before and after translocation. *J. Mol. Biol.* **368**:1412–1425.

Nechifor, R., Murataliev, M., and Wilson, K.S. 2007. Functional interaction s between the G′ subdomain of bacterial translation factor EF-G and ribosomal protein L7/L12. *J. Biol. Chem*. **282**:36998–37005.

Neubauer, C., Gao, Y.-G., Andersen, K.R., *et al*., 2009. The structural basis for mRNA recognition and cleavage by the ribosome-dependent endonuclease RelE. *Cell* **139**:1084–1096.

Newbauer, C., Gillet, R., Kelley, A.C., *et al*. 2012. Decoding in the absence of a codon by tmRNA and SmpB in the ribosome. *Science* **335**:1366–1369.

Nevskaya, N., Tishchenko, S., Fedorov, R., *et al*. 2000. Archaeal ribosomal protein L1: the structure provides new insights into RNA binding of the L1 protein family. *Structure* **8**:363–371.

Newcomer, M.E. and Liljas, A. 1980. Purification and crystallization of a protein complex from Bacillus stearothermophilus ribosomes. *J. Mol. Biol.* **153**:393–398.

Nierhaus, K. 1990. Reconstitution of ribosomes. In *Ribosomes and Protein Synthesis*. pp. 161–189, IRL Press, Oxford, New York, Tokyo.

Nikonov, S., Nevskaya, N., Eliseikina, I. 1996. Crystal structure of the RNA binding ribosomal protein L1 from *Thermus thermophilus*. *EMBO J.* **15**:1350–1359.

Nikulin, A., Eliseikina, I., and Tishchenko, S. 2003. Structure of the L1 protuberance in the ribosome. *Nat. Struct. Biol.* **10**:104–108.

Ninio, J. 1974. A semi-quantitative treatment of missense and nonsense suppression in the strA and ram ribosomal mutants of *Escherichia coli*. Evaluation of some molecular parameters of translation *in vivo*. *J. Mol. Biol.* **84**:297–313.

Ninio, J. 1975. Kinetic amplification of enzyme discrimination. *Biochimie* **57**:587–595.

Nirenberg, M.W., Caskey, T., Marshall, R., *et al*. 1966. The RNA code and protein synthesis. *Cold Spring Harbor Symp. Quant. Biol.* **31**:11–24.

Nishimura, M., Kaminishi, T., Takemoto, C., *et al*. 2008. Crystal structure of human protein L10 core domain reveals eukaryote-specific motifs in addition to the conserved fold. *J. Mol. Biol.* **377**:421–430.

Nishimura, M., Yoshida, T., Shirouzu, M., *et al*. 2004. Solution structure of ribosomal protein L16 from Thermus thermophilus. *J. Mol. Biol.* **344**:1369–1383.

Nishizuka, Y. and Lipmann, F. 1966. Comparison of guanosine triphosphate split and polypeptide synthesis with a purified *E. coli* system. *Proc. Natl. Acad. Sci. USA.* **55**: 212–219.

Nissen, P., Kjeldgaard, M., and Thirup, S. 1995. Crystal structure of the ternary complex of Phe-tRNA^{Phe}, EF-Tu, and a GTP analog. *Science* **270**:1464–1472.

Nissen, P., Thirup, S., Kjeldgaard, M., and Nyborg, J. 1999. The crystal structure of Cys-tRNACys-EF-Tu-GDPNP reveals general and specific features in the ternary complex and in tRNA. *Struct. Fold Des.* **7**:143–156.

Nissen, P., Kjeldgaard, M., and Nyborg, J. 2000a. Macromolecular mimicry. *EMBO J.* **19**:489–495.

Nissen, P., Hansen, J., Ban, N., *et al.* 2000b. The structural basis of ribosome activity in peptide bond synthesis. *Science* **289**:920–930.

Nissen, P., Ippolito, J.A., Ban, N., *et al.* 2001. RNA tertiary interactions in the large ribosomal subunit: the A-minor motif. *Proc. Natl. Acad. Sci. USA.* **98**:4899–4903.

Noeske, J. and Cate, J.H.D. 2012. Structural basis for protein synthesis: snapshots of the ribosome in motion. *Curr Op. Struct. Biol.* **22**:743–749.

Noller, H.F. 1991. Ribosomal RNA and translation. *Ann. Rev. Biochem.* **60**:191–227.

Noller, H.F. 1993. Peptidyl transferase — protein, ribonucleoprotein, or RNA? *J. Bacteriol.* **175**:5297–5300.

Noller, H.F., and Chaires, J.B. 1972. Functional modification of 16S ribosomal RNA by kethoxal. *Proc. Natl. Acad. Sci. USA.* **69**:3115–3118.

Noller, H.F., Hoffarth, V., and Zimniak, L. 1992. Unusual resistance of peptidyl transferase to protein extraction procedures. *Science* **256**:1416–1419.

Noller, H.F., Kop, J., Wheaton, V., *et al.* 1981. Secondary structure model for 23S ribosomal RNA. *Nucl. Acids Res.* **9**:6167–6189.

Noller, H.F., and Woese, C.R. 1981. Secondary structure of 16S ribosomal RNA. *Science* **212**:403–411.

Nomura, M. 1973. Assembly of bacterial ribosomes. *Science* **179**:864–873.

Nomura, M. 1990. History of ribosome research: a personal account. In *The Ribosome. Structure, Function and Evolution.* Eds. W.E. Hill, A. Dahlberg, R.A. Garrett, *et al.,* pp. 3–55. ASM Press, Washington.

Nomura, M., Gourse, R., and Baughman, G. 1984. Regulation of the synthesis of ribosomes and ribosomal components. *Ann. Rev. Biochem.* **53**:75–117.

Nomura, M., Yates, J.L., Dean, D., and Post, L.E. 1980. Feedback regulation of ribosomal protein gene expression in *Escherichia coli*: structural homology of ribosomal RNA and ribosomal protein mRNA. *Proc. Natl. Acad. Sci. USA.* **77**:7084–7088.

Nomura, T, Nakatsuchi, M, Sugita, D., *et al.* 2008. Biochemical evidence for the heptameric complex L10(L12)$_6$ in the *Thermus thermophilus* ribosome: in vitro analysis of its molecular assembly and functional properties. *J. Biochem.* **144**:665–673.

Nozawa, K, O'Donoghue, P, Gundllapalli, S., *et al*. 2009. Pyrrolysyl-tRNA synthetase-tRNAPyl structure reveals the molecular basis of orthogonality. *Nature* **457**:1163–1167.

Nureki, O., Vassylev, D.G., Tateno, M., *et al.* 1998. Enzyme structure with two catalytic sites for double-sieve selection of substrate. *Science* **280**:578–582.

O'Connor, M., Gregory, S.T., Rajbhandary, U.L., and Dahlberg, A.E. 2001. Altered discrimination of start codons and initiator tRNAs by mutant initiation factor 3. *RNA* **7**:969–978.

Odom, O.W., Kramer, G., Henderson, A.B., *et al.* 1978. GTP hydrolysis during methionyl-tRNAf binding to 40S ribosomal subunits and the site of edeine inhibition. *J. Biol. Chem.* **253**:1807–1816.

Odom, O.W., Picking, W.D., Tsalkova, T., and Hardesty, B. 1991. The synthesis of polyphenylalanine on ribosomes to which erythromycin is bound. *Eur. J. Biochem.* **198**:713–722.

Ofengand, J. and Liou, R. 1980. Evidence for pyrimidine-pyrimidine cyclobutane dimmer formation in the covalent cross-linking between transfer ribonucleic acid and 16S ribonucleic aid at the ribosomal P site. *Biochemistry* **19**:4814–4822.

Ogle, J.M., Brodersen, D.E., Clemons, W.M. Jr., *et al.* 2001. Recognition of cognate transfer RNA by the 30S ribosomal subunit. *Science* **292**:897–902.

Ogle, J.M., Carter, A.P., and Ramakrishnan, V. 2003. Insights into the decoding mechanism from recent ribosome structures. *Trends Biochem. Sci.* **28**:259–266.

Ogle, J.M., Murphy, F.V., Tarry, M.J., and Ramakrishnan, V. 2002. Selection of tRNA by the ribosome requires a transition from an open to a closed form. *Cell* **111**:721–732.

Ogle, J.M. and Ramakrishnan, V. 2005. Structural insights into translational fidelity. *Annu. Rev. Biochem.* **74**:129–177.

Oh, E., Becker, A.H., Sandikci, A., *et al*. 2011. Selective ribosome profiling reveals the cotranslational chaperone action of trigger factor in *vivo*. *Cell* **147**:1295–1308.

Oleinikov, A.V., Jokhadze, G.G., and Traut, R.R. 1998. A single-headed dimer of *Escherichia coli* ribosomal protein L7/L12 supports protein synthesis. *Proc. Natl. Acad. Sci. USA.* **95**:4215–4218.

Okamoto, T., and Takanami, M. 1963. Interaction of ribosomes and natural polyribonucleotides. *Biochim. Biophys. Acta* **76**:266–274.

Okuyama, A., Machiyama, N., Kinoshita, T., *et al*. 1971. Inhibition by kasugamycin of initiation complex formation on 30S ribosomes. *Biochem. Biophys. Res. Commun.* **43**:196–199.

Orengo, C.A., and Thornton, J.M. 1993. Alpha plus beta folds revisited: some favoured motifs. *Structure* **1**:105–120.

Ose, T., Soler, N., Rasubala, L., *et al*. 2007. Structural basis for dynamic interdomain movement and RNA recognition of the selenocysteine-specific elongation factor SelB. *Structure* **15**:577–586.

Österberg, R., Sjöberg, B., Liljas, A., and Petterson, I. 1976. Small-angle X-ray scattering and crosslinking study of the protein L7/L12 from *E. coli* ribosomes. *FEBS Lett.* **66**:48–51.

Österberg, R., Sjöberg, B., Pettersson, I., *et al.* 1997. Small-angle scattering study of the protein complex of L7/L12 and L10 from *Escherichia coli* ribosomes. *FEBS Lett.* **73**:22–24.

Ovchinnikov, Yu. A., Alakhov, Yu. B., Bundulis, Yu. P., *et al.* 1982. The primary structure of elongation factor G from *Escherichia coli*: a complete amino acid sequence. *FEBS Lett.* **139**:130–135.

Pai, R.D., Zhang, W., Schuwirth, B.S., *et al.* 2008. Structural insights into ribosome recycling factor interactions with the 70S ribosome. *J. Mol. Biol.* **376**:1334–1347.

Palade, G.E. 1955. A small particulate component of the cytoplasm. *J. Biophys. Biochem. Cytol.* **1**:59–68.

Pallesen, J., Hashem, Y. Koripella, R.K., *et al.* 2013. RF3 is recruited to the ribosome by L7/L12, and its action cycle is regulated by coordinated interactions with class-I release factor and L7/L12. Submitted.

Pan, D., Kirillov, S.V., and Cooperman, B.S. 2007. Kinetically competent intermediates in the translocation step of protein synthesis. *Mol. Cell* **25**:619–529.

Pandit, S.B., and Srinivasan, N. 2003. Survey for g-proteins in the prokaryotic genomes: prediction of functional roles based on classification. *Proteins* **52**: 585–597.

Pape, T., Wintermeyer, W., and Rodnina, M.V. 1998. Complete kinetic mechanism of elongation factor Tu-dependent binding of aminoacyl-tRNA to the A-site of the *E. coli* ribosome. *EMBO J.* **17**:7490–7497.

Pape, T., Wintermeyer, W., and Rodnina, M. 1999. Induced fit in initial selection and proof-reading of aminoacyl-tRNA on the ribosome. *EMBO J.* **18**:3800–3807.

Pape, T., Wintermeyer, W., and Rodnina, M. 2000. Conformational switch in the decoding region of 16S rRNA during aminoacyl-tRNA selection on the ribosome. *Nat. Struct. Biol.* **7**:104–107.

Park, J.H., Johansson, H.E. Aoki, H., *et al.* 2012. Post-translational modification by β-lysylation is required for activity of *Escherichia coli* elongation factor P (EF-P). *J. Biol. Chem.* **287**:2579.

Park, M.H., Nishimura, K., Zanelli, C.F., *et al.* 2010. Functional significance of eIF5A and its hypusine modification in eukaryotes. *Amino Acids* **38**:491–500.

Parker, J., Watson, R.J., and Friesen, J.D. 1976. A relaxed mutant with an altered ribosomal protein L11. *Mol. Gen. Genet.* **144**:111–114.

Parmeggiani, A. and Nissen, P. 2006. Elongation factor Tu-targeted antibiotics: Four different structures, two mechanisms of action. *FEBS Lett.* **580**: 4576–4581.

Parmeggiani, A. and Swart, G.W. 1985. Mechanism of action of kirromycin-like antibiotics. *Ann. Rev. Microbiol.* **39**:557–577.

Parmeggiani, A., Krab, I.M., Watanabe, T., *et al*. 2006a. Enacyloxin IIa pinpoints a binding pocket of elongation factor Tu for development of novel antibiotics. *J. Biol. Chem.* **281**:2893–2900.

Parmeggiani, A., Krab, I.M., Okamura, S., *et al*. 2006b. Structural basis of the action of pulvomycin and GE2270A on elongation factor Tu. *Biochemistry* **45**:6846–6857.

Pasqualato, S. and Cherfils, J. 2005. Crystallographic evidence for substrate-assisted GTP hydrolysis by a small GTP binding protein. *Structure* **13**:533–540.

Patel, A.A. and Steitz, J.A. 2003. Splicing double: insights from the second spliceosome. *Nature Rev. Mol. Cell Biol.* **4**:960–970.

Patzelt, H., Rüdiger, S., Brehmer, D., *et al.* 2001. Binding specificity of *Escherichia coli* trigger factor. *Proc. Natl. Acad. Sci. USA.* **98**:14244–14249.

Pauling, L 1957. The probability of errors in the process of synthesis of protein molecules. In *Festschrift Arthur Stroll* (Basel, Switzerland; Birkhäuser-Verlag), pp. 597–602.

Pavlov, M.Y., Antoun, A., Lovmar, M., *et al*. 2008. Complementary roles of initiation factor 1 and ribosome recycling factor in 70S ribosome splitting. *EMBO J.* **27**:1706–1717.

Pavlov, M.Y., Zorzet, A., Andersson, D.I., *et al*. 2011. Activation of initiation factor 2 by ligands and mutations for rapid docking of ribosomal subunits. *EMBO J.* **30**:289–301.

Pech M, Karim, Z., Yamamota, H., *et al*. 2011. Elongation factor 4 (EF4/LepA) accelerates protein synthesis at increased Mg^{2+} concentrations. *Proc Natl. Acad. Sci. USA.* **108**:3199–3203.

Pedersen, K., Zavialov, A.V., Pavlov, M.Y., *et al*. 2003. The bacterial toxin RelE displays codon-specific cleavage of mRNAs in the ribosomal A site. *Cell* **112**:131–140.

Peil, L. Starosta, A.L. Virumäe, K. *et al*. 2012. Lys34 of translation elongation factor EF-P is hydroxylated by YfcM. *Nat. Chem. Biol.* **6**:695–697.

Peluso, P., Shan, S.O., Nock, S., *et al*. 2001. Role of SRP RNA in the GTPase cycles of Ffh and FtsY. *Biochemistry* **40**:15224–15233.

Penczek, P.A., Frank, J., and Spahn, C. 2006b. A method of focused classification, based on the bootstrap 3D variance analysis, and its application to EF-G-dependent translocation. *J. Struct. Biol.* **154**:184–194.

Penczek, P.A., Yang, C., Frank, J., *et al*. 2006a. Estimation of variance in single-particle reconstruction using the bootstrap technique. *J. Struct. Biol.* **154**:168–183.

Perdew, J.P., Ruzsinszky, A., Constatin, L.A., *et al*. 2009. Some fundamental issues in ground-state density functional theory: A guide for the perplexed. *J Chem Theor Comput* **5**:902–908.

Perutz, M.F. 1962. *Proteins and Nucleic Acids. Structure and Function,* Eighth Weizmann Memorial Lecture Series. Elsevier Publishing Company, Amsterdam.

Peske, F., Matassova, N.B., Savelsbergh, A., *et al.* 2000. Conformationally restricted elongation factor G retains GTPase activity but is inactive in translocation on the ribosome. *Mol. Cell* **6**:501–505.

Pestka, S. 1969. Studies on the formation of transfer ribonucleic acid-ribosome complexes. VI. Oligopeptide synthesis and translocation on ribosomes in the presence and absence of soluble transfer factors. *J. Biol. Chem.* **244**:1533–1539.

Pestka, S. 1972. Studies on transfer ribonucleic acid-ribosome complexes. Effects on antibiotics on peptidyl puromycin synthesis on polyribosomes from *Escherichia coli*. *J. Biol. Chem.* **247**:4669–4678.

Pestova, T.V. and Hellen, C.U. 2000. The structure and function of initiation factors in eucaryotic protein synthesis. *Cell. Mol. Life Sci.* **57**:651–674.

Pestova, T.V., Lomakin, I.B., Lee, J.H., *et al.* 2000. The joining of ribosomal subunits in eukaryotes requires eIF5B. *Nature* **403**:332–335.

Petermann, M.L. and Hamilton, M.G. 1952. An ultracenrifugal analysis of the macromolecular particles of normal and leukemic mouse spleen. *Cancer Res.* **12**:373–378.

Petoukhov, M.V. and Svergun, D.I. 2007. Analysis of X-ray and neutron scattering from biomacromolecular solutions. *Curr Opin Struct Biol.* **17**:562–571.

Petrelli, D., Garofalo, C., Lammi, M., *et al.* 2003. Mapping the active sites of bacterial translation initiation factor IF3. *J. Mol. Biol.* **331**:541–556.

Pettersson, I. and Kurland, C.G. 1980. Ribosomal protein L7/L12 is required for optimal translation. *Proc. Natl. Acad. Sci. USA.* **77**:4007–4010.

Pettersson, I., Hardy, S.J., and Liljas, A. 1976. The ribosomal protein L8 is a complex of L7/L12 and L10. *FEBS Lett.* **64**:135–138.

Phizicky, E.M. and Hopper, A.K. 2010. tRNA biology charges the front. Genes Dev. **24**:1832–1860.

Piekna-Przybylska, D., Decatur, W.A., and Fournier, M.J. 2008. The 3D rRNA modification maps database: with interactive tools for ribosome analysis. *Nucleic Acids Res.* **36**:D178–83.

Pinard, R., Peyant, C., Melancon, P., and Brakier-Gringas, L. 1993. The 5′ proximal helix of 16S rRNA is involved in the binding of streptomycin to the ribosome. *FASEB J.* **7**:173–176.

Pioletti, M., Schlünzen, F., Harms, J., *et al.* 2001. Crystal structures of complexes of the small ribosomal subunit with tetracycline, edeine and IF3. *EMBO J.* **20**:1829–1839.

Planta, R.J. and Mager, W.H. 1998. The list of cytoplasmic ribosomal proteins of *Saccharomyces cerevisiae*. *Yeast* **14**:471–477.

Plumbridge, J.A., Deville, F., Sacerdot, C., *et al.* 1985. Two translational initiation sites in the infB gene are used to express initiation factor IF2 alpha and IF2 beta in *Escherichia coli*. *EMBO J.* **4**:223–229.

Poehlsgaard, J. and Douthwaite, S. 2003. Macrolide antibiotic interaction and resistance on the bacterial ribosome. *Curr. Opin. Investig. Drugs* **4**:140–148.

Polacek, N. and Mankin, A.S. 2005. The ribosomal peptidyl transferase center: structure, function, evolution and inhibition. *Crit. Rev. Biochem. Mol. Biol.* **40**:285–311.

Polacek, N., Gaynor, M., Yassin, A., and Mankin, A.S. 2001. Ribosomal peptidyl transferase can withstand mutations at the putative catalytic nucleotide. *Nature* **411**:498–501.

Polacek, N., Gomez, M.J., Ito, K., *et al.* 2003. The critical role of the universally conserved A2602 of 23S RNA in the release of the nascent peptide during translation termination. *Mol. Cell* **11**:103–112.

Polekhina, G., Thirup, S., Kjeldgaard, M., *et al.* 1996. Helix unwinding in the effector region of elongation factor EF-Tu-GDP. *Structure* **4**:1141–1151.

Polewoda, B, and Sherman, F. 2007. Methylation of proteins involved in translation. *Mol. Microbiol.* **65**:590–606.

Polikanov, Y.S., Blaha, G.M., and Steitz, T.A. 2012. How hibernation factors RMF, HPF and YfiA turn off protein synthesis for storage of eubacterial ribosomes. *Science* **336**:915–918.

Pool, M.R., Stumm, J., Fulga, T.A., *et al.* 2002. Distinct modes of signal recognition particle interaction with the ribosome. *Science* **297**:1345–1348.

Poritz, M.A., Strub, K., and Walter, P. 1988. Human SRP RNA and *E. coli* 4.5S RNA contain a highly homologous structural domain. *Cell* **55**:4–6.

Porse, B.T., Kirillov, S.V., Awayez, M.J., *et al.* 1999. Direct crosslinking of the antitumor antibiotic sparsomycin, and its derivatives, to A2602 in the peptidyltransferase center of 23S like rRENA within ribosome-tRNA complexes. *Proc. Natl. Acad. Sci. USA.* **96**:9003–9008.

Porse, B.T., Leviev, I., Mankin, A.S., *et al.* 1998. The antibiotic thiostrepon inhibits a functional transition within protein L11 at the ribosomal GTPase centre. *J. Mol. Biol.* **276**:391–404.

Poulsen, S.M., Kofoed, C., and Vester, B. 2000. Inhibition of the ribosomal peptidyl-transferase reaction by the mycarose moiety of the antibiotics carbomycin, spiramycin and tylosin. *J. Mol. Biol.* **304**:471–481.

Powers, T., and Noller, H.F. 1990. Dominant lethal mutations in a conserved loop in 16S rRNA. *Proc. Natl. Acad. Sci. USA.* **87**:1042–1046.

Powers, T., and Noller, H.F. 1995. Hydroxyl radical footprinting of ribosomal proteins on 16S rRNA. *RNA* **1**:194–209.

Prince, J.B., Taylor, B.H., Thurlow, D.L., *et al.* 1982. Covalent crosslinking of tRNA1Val to 16S RNA at the ribosomal P-site: identification of crosslinked residues. *Proc. Natl. Acad. Sci. USA.* **79**:5450–5454.

Pyetan, E., Baram, D., Auerbach-Nevo, T., *et al.* 2007. Chemical parameters influencing fine-tuning in the binding of macrolide antibiotics to the ribosomal tunnel. *Pure Appl. Chem.* **79**:955–968.

Qin, Y., Polacek, N., Vesper, O., *et al.* 2006. The highly conserved LepA is a ribosomal elongation factor that backtranslocates the ribosome. *Cell* **127**:721–733.

Qu, X., Lancaster, L., Noller H.E., *et al*. 2012. Ribosomal protein S1 unwinds double-stranded RNA in multiple steps. *Proc. Natl. Acad. Sci. USA.* **109**:14458–14463.

Quiggle, K., Kumar, G., Ott, T.W., *et al*. 1981. Donor site of ribosomal peptidyltransferase: investigation of substrate specificity using 29(39)-O-(N-acyla-minoacyl)dinucleoside phosphates as models of the 39 terminus of N-acylaminoacyl transfer ribonucleic acid. *Biochemistry* **20**:3480–3485.

Rabl, J., Leibundgut, M., Ataide, S.F., *et al*. 2011. Crystal structure of the eukaryotic 40S ribosomal subunit in complex with initiation factor 1. *Science* **331**:730–736.

Ramagopal, S. 1976. Accumulation of free ribosomal proteins S1, L7 and L12 in *E. coli*. *Eur. J. Biochem.* **69**:289–297.

Ramakrishnan, V. 2002. Ribosome structure and the mechanism of translation. *Cell* **108**:557–572.

Ramakrishnan, V., and Moore, P.B. 2001. Atomic structure at last: the ribosome in 2000. *Curr. Opin. Struct. Biol.* **11**:144–154.

Ramakrishnan, V., and White, S.W. 1992. The structure of ribosomal protein S5 reveals sites of interaction with 16S rRNA. *Nature* **358**:768–771.

Ramakrishnan, V., and White, S.W. 1998. Ribosomal protein structures: insights into the architecture, machinery and evolution of the ribosome. *TIBS* **23**:208–212.

Ramrath, D.J., Yamamoto, H., Rother, K., *et al*. 2012. The complex of tmRNA-SmpB and EF-G on translocating ribosomes, *Nature* **485**:526–530.

Randau, L., Pearson, M., Söll, D. 2005. The complete set of tRNA species in *Nanoarchaeum equitans*. *FEBS Lett.* **579**:2945–2947.

Rangarajan, E.S., Nadeau, G., Li, Y., *et al*. 2006. The structure of the exopolyphosphatase (PPX) from *Escherichia coli* O**157**:H7 suggests a binding mode for long polyphosphate chains. *J. Mol. Biol.* **359**:1249–1260.

Rapoport, T.A., Jungnickel, B., and Kutay, U. 1996. Protein transport across eucaryoticendoplasmic reticulum and bacterial inner membrane. *Ann. Rev. Biochem.* **65**: 271–303.

Rao, A.R., and Varshney, U. 2001. Specific interactions between the ribosome recycling factor and the elongation factor G from *Mycobacterium tuberculosis* mediates peptidyl-tRNA release and ribosome recycling in *Escherichia coli*. *EMBO J.* **20**:2977–2986.

Ratje, A.H., Loerke, J., Mikolajka, A., *et al*. 2010. Head swiwel on the ribosome facilitates translocation by means of intra-subunit tRNA hybrid sites. *Nature* **468**:713–716.

Rawlings, N.D. and Barrett, A.J. 1994. Families of serine peptidases. *Meth. Enzymol.* **244**:19–61.

Remacha, M., Jimenez-Diaz, A., Bermejo, B., *et al*. 1995. Ribosomal acidic phosphoproteins P1 and P2 are not required for cell viability but regulate the pattern of protein expression in *Saccharomyces cerevisiae*. *Mol. Cell. Biol.* **15**:4754–4762.

Retsema, J., and Fu, W. 2001. Macrolides: structures and microbial targets. *Int. J. Antimicrob. Agents* **18**(suppl. 1):S3–S10.

Rheinberger, H.J. 2004. A history of protein biosynthesis and ribosome research. In Nierhaus, KH & Wilson, DN. *Protein synthesis and ribosome structure.* Wiley-VCH. Verlag GmbH & Co. KGaA Weinheim.

Rheinberger, H.J., Sternbach, H., and Nierhaus, K.H. 1981. Three tRNA binding sites on *Escherichia coli* ribosomes. *Proc. Natl. Acad. Sci. USA.* **78**: 5310–5314.

Ribas de Pouplana, L., and Schimmel, P. 2001. Aminoacyl-tRNA synthetases: potential markers of genetic code development. *TIBS* **26**:591–596.

Rich, A. 2001. RNA structure and the roots of protein synthesis. *Cold Spring Harb. Symp. Quant. Biol.* **66**:1–16.

Robbins, D. and Hardesty, B. 1983. Comparison of ribosomal entry and acceptor transfer ribonucleic acid binding sites on *Escherichia coli* 70S ribosomes. Fluorescence energy transfer measurements from Phe-tRNAPhe to the 3′ end of 16S ribonucleic acid. *Biochemistry* **22**:5675–5679.

Roberts, E., Luthey-Schulten, Z., Sethi, A., *et al*. 2008. Molecular signatures of ribosomal evolution. *Proc. Natl. Acad. Sci. USA.* **105**:13953–13958.

Robertus, J.D., Ladner, J.E., Finch, J.T., *et al.* 1974. Structure of yeast phenylalanine tRNA at 3Å resolution. *Nature* **250**:546–551.

Roderick, S.L. and Matthews, B.W. 1993. Structure of the cobalt-dependent methionine aminopeptidase from *Escherichia coli*: a new type of proteolytic enzyme, *Biochemistry* **32**:3907–3912.

Rodnina, M.V. and Wintermeyer, W. 1995. GTP consumption of elongation factor Tu during translation of heteropolymeric mRNAs. *Proc. Natl. Acad. Sci. USA.* **92**:1945–1949.

Rodnina, M. and Wintermeyer, W. 2003. peptide bond formation on the ribosome: structure and mechanism. *Curr. Opin. Struct. Biol.* **13**:334–340.

Rodnina, M.V., Fricke, R., and Wintermeyer, W. 1993. Kinetic fluorescence study on EF-Tu-dependent binding of Phe-tRNA^{Phe} to the ribosomal A-site. In *The Translational Apparatus: Structure, Function, Regulation and Evolution,* Eds. K.H. Nierhaus, F. Franceschi, A.R. Subramanian, *et al.,* pp. 317–326. Plenum Publishing Corp. New York.

Rodnina, M.V., Fricke, R., Kuhn, L., and Wintermeyer, W. 1995a. Codon-dependent conformational change of elongation factor Tu preceding GTP hydrolysis on the ribosome. *EMBO J.* **14**:2613–2619.

Rodnina, M.V., Pape, T., Fricke, R., and Wintermeyer, W. 1995b. Elongation factor Tu, a GTPase triggered by codon recognition on the ribosome: mechanism and GTP consumption. *Biochem. Cell Biol.* **73**:1221–1227.

Rodnina, M.V., Savelsbergh, A., Katunin, V.I., and Wintermeyer, W. 1997. Hydrolysis of GTP by elongation factor G drives tRNA movement on the ribosome. *Nature* **385**:37–41.

Rodnina, M.V., Savelsbergh, A., Matassova, N.B., *et al.* 1999. Thiostrepton inhibits the turnover but not the GTPase of elongation factor G on the ribosome. *Proc. Natl. Acad. Sci. USA.* **96**:9586–9590.

Rodnina, M.V., Stark, H., Savelsbergh, A., *et al.* 2000. GTPases mechanisms and functions of translation factors on the ribosome. *Biol. Chem.* **381**:377–387.

Rodnina, M.V., Daviter, T., Gromadski, K., *et al*. 2002. Structural dynamics of ribosomal RNA during decoding on the ribosome. *Biochimie* **84**:745–754.

Röhl, R. and Nierhaus, K.H. 1982. Assembly map of the large subunit (50S) of *Escherichia coli* ribosomes. *Proc. Natl. Acad. Sci. USA.* **79**:729–733.

Roll-Mecak, A., Cao, C., Dever, T.E., and Burley, S.K. 2000. X-ray structures of the universal translation initiation factor IF2/eIF5B: conformational changes on GDP and GTP binding. *Cell* **103**:781–792.

Roll-Mecak, A., Shin, B.S., Dever, T.E., and Burley, S.K. 2001. Engaging the ribosome: universal Ifs of translation. *Trends Biochem. Sci.* **26**:705–709.

Romby, P., and Springer, M. 2003. Bacterial translational control at atomic resolution. *Trends Genet*. **19**:155–161.

Rosendahl, G. and Douthwaite, S. 1994. The antibiotics micrococcin and thiostrepton interact directly with 23S rRNA nucleotides 1067A and 1095A. *Nucleic Acids Res.* **22**:357–363.

Ross, J.I., Eady, E.A., Cove, J.H., and Cunliffe, W.J. 1998. 16S rRNA mutation associated with tetracycline resistance in a gram-positive bacterium. *Antimicrob. Agents Chemother.* **42**:1702–1705.

Rossmann, M.G., and Blow, D.M. 1962. The detection of sub-units within the crystallographic asymmetric unit. *Acta Cryst*. **15**:24–31.

Rossmann, M.G., and Johnson, J.E. 1989. Icosahedral RNA virus structure. *Ann. Rev. Biochem.* **58**:533–573.

Rostom, A.A., Fucini, P., Benjamin, D.R., *et al.* 2000. *Proc. Natl. Acad. Sci. USA.* **97**:5185–5190.

Rudinger, J., Hillenbrandt, R., Sprinzl, M., and Giege, R. 1996. Antideterminants present in minihelix^{Sec} hinder its recognition by prokaryotic elongation factor Tu. *EMBO J.* **15**:650–657.

Rudner, R., Chevrestt, A., Buchholz, S.R., *et al*. 1993. Two tRNA gene clusters associated with rRNA operons rrnD and rrnE in *Bacillus subtilis*. *J. Bacteriol.* **175**:503–509.

Rutkowska, A., Mayer, M.P., Hoffmann, A., *et al*. 2008. Dynamics of trigger factor interaction with translating ribosomes. *J. Biol. Chem.* **283**:4124–4132.

Ruusala, T. and Kurland, C.G. 1984. Streptomycin preferentially perturbs ribosomal proofreading. *Mol.Gen.Genet*. **198**:100–104.

Ruusala, T., Andersson, D., Ehrenberg, M., *et al*. 1984. Hyper-accurate ribsomes inhibit growth. *EMBO J.* **3**:2575–2580.

Ruusala, T., Ehrenberg, M., and Kurland, C.G. 1982. Is there proofreading during polypeptide synthesis. *EMBO J.* **1**:741–745.

Sabatini, D.D., Tashiro, Y., and Palade, G.E. 1966. On the attachment of ribosomes to microsomal membranes. *J. Mol. Biol.* **19**:503–524.

Sacerdot, C., Vachon, G., Laalami, S., *et al.* 1992. Both forms of translational factor 2 (a and b) are required for maximal growth of *Escherichia coli.* Evidence for two translational initiation codons for IF2. *J. Mol. Biol.* **225**:67–80.

Saibil, H.R. and Ranson, N.A. (2002). The chaperonin folding machine. *Trends Biochem. Sci.* **27**:627–632.

Salyers, A.A., Speer, B.S., and Shoemacher, N.B. 1990. New perspectives in tetracycline resistance. *Mol. Microbiol.* **4**:151–156.

Samaha, R.R., Green, R., and Noller, H.F. 1995. A base pair between tRNA and 23S rRNA in the peptidyl transferase centre of the ribosome. *Nature* **377**:309–314. Erratum in: *Nature* **378**:419.

Sanchez-Pescador, R., Brown, J.T., Roberts, M., and Urdea, M.S. 1988. Homology of the TetM with translational elongation factors: implications for potential modes of tetM-conferred tetracycline resistance. *Nucl. Acids Res.* **16**:1218.

Sander, G. 1983. Ribosomal protein L1 from Escherichia coli. Its role in the binding of tRNA to the ribosome and in elongation factor G-dependent GTP hydrolysis. *J. Biol. Chem.* **258**:10098–10103.

Santos, C. and Ballesta, J.P.G. 1994. Ribosomal phosphoprotein P0, contrary to phosphoproteins P1 and P2, is required for *S. cerevisiae* viability and ribosome assembly. *J. Biol. Chem.* **269**:15689–15696.

Santos, C. and Ballesta, J.P.G. 1995. The highly conserved protein P0 carboxyl end is essential for ribosome activity only in the absence of proteins P1 and P2. *J. Biol. Chem.* **270**:20608–20614.

Sanyal, C.S. and Liljas, A. 2000. The end of the beginning: structural studies of ribosomal proteins. *Curr. Opin. Struct. Biol.* **10**:633–636.

Saraste, M., Sibbald, P.R., and Wittinghofer, A. 1990. The P-loop, a common motif in ATP- and GTP-binding proteins. *Trends Biochem. Sci.* **15**:430–434.

Sato, A., Watanabe, T., Maki, Y., *et al.* 2009. Solution structure of the E. coli ribosome hibernation promoting factor HPF: Implications for the relationship between structure and function. *Biochem. Biophys. Res. Commun.* **389**:580–585.

Sauerwald, A., Zhu, W., Major, T.A., *et al.* 2005. RNA-dependent cysteine biosynthesis in archaea. *Science,* **307**:1969–1972.

Savelsbergh, A., Katunin, V.I., Mohr, D., *et al.* 2002. An elongation factor G-induced ribosome rearrangement precedes tRNA-mRNA translocation. *Mol. Cell.* **11**: 1517–1523.

Savelsbergh, A., Matassova, N.B., Rodnina, M.V., and Wintermeyer, W. 2000a. Role of domains 4 and 5 in elongation factor G functions on the ribosome. *J. Mol. Biol.* **300**:951–961.

Savelsbergh, A., Mohr, D., Wilden, B., *et al.* 2000b. Stimulation of the GTPase activity of translation elongation factor G by ribosomal protein L7/12. *J. Biol. Chem.* **275**:890–894.

Savelsberg, A, Mohr, D, Kothe, U, *et al*. 2005. Control of phosphate release from elongation factor G by ribosomal protein L7/L12. *EMBO J*. **24**:4316–4323.

Savelsbergh, A., Rodnina, M.V., and Wintermeyer, W. 2009. Distinct functions of elongation factor G in ribosome recycling and translocation. *RNA* **15**: 772–780.

Sawaya, M.R., Prasad, R., Wilson, S.H., *et al*. 1997. Crystal structures of human DNA polymerase b complexed with gapped and nicked DNA: evidence for an induced fit mechanism. *Biochemistry* **36**:11205–11215.

Schaffitzel, C., Oswald, M., Berger, I., *et al*. 2006. Structure of the E. coli signal recognition particle bound to a translating ribosome. *Nature* **444**:503–506.

Schaffitzel, E., Rudiger, S., Bukau, B., and Deuerling, E. 2001. Functional dissection of trigger factor and DnaK: interactions with nascent polypeptides and thermally denatured proteins. *Biol. Chem*. **382**:1235–1243.

Schilling-Bartetzko, S., Franceschi, F., Sternbach, H., and Nierhaus, K.H. 1992. Apparent association constants of tRNAs for the ribosomal A-, P-, and E-sites. *J. Biol. Chem*. **267**:4693–4702.

Schimmel, P., and Ribas de Pouplana, L. 2001. Formation of two classes of tRNA synthetases in relation to editing functions and genetic code. *Cold Spring Harb. Symp. Quant. Biol*. **66**:161–166.

Schimmel, P., Giege, R., Moras, D., and Yokoyama, S. 1993. An operational RNA code for amino acids and possible relationship to the genetic code. *Proc. Natl. Acad. Sci. USA*. **90**:8763–8768.

Schlitter, J., Engels, M., Krüger, P., *et al*. 1993. Targetted molecular dynamics simulation of conformational change — application to the T<—>R transition in insulin. *Mol Sim* **10**:291–308.

Schlünzen, F., Tocilj, A., Zariwach, R., *et al*. 2000. Structure of functionally activated small ribosomal subunit at 3.3Å resolution. *Cell* **102**:615–623.

Schlünzen, F., Zariwach, R., Harms, J., *et al*. 2001. Structural basis for the interaction of antibiotics with the peptidyltransferase centre in eubacteria. *Nature* **413**:814–821.

Schlünzen, F., Harms, J.M., Franceschi, F., *et al*. 2003. Structural basis for the antibiotic activity of ketolides and azalides. *Structure* **11**:329–338.

Schlünzen, F., Takemoto, C., Wilson, D.N., *et al*. 2006. The antibiotic kasugamycin mimics mRNA nucleotides to destabilize tRNA binding and inhibit canonical translation inhibition. *Nat. Struct. Mol. Biol*. **13**:872–878.

Schmeing, M., Voorhees, R., Kelley, A.C., *et al*. 2009. The crystal structure of the ribosome bound to EF-Tu and aminoacyl-tRNA. *Science* **326**:688–694.

Schmeing, T.M., Seila, A.C., Hansen, J.L., *et al*. 2002. A pre-translocational intermediate in protein synthesis observed in crystals of enzymatically active 50S subunits. *Nat. Struct. Biol*. **9**:225–230.

Schmeing, T.M. and Ramakrishnan, V. 2009. What recent ribosome structures have revealed about the mechanism of translation. *Nature* **461**:1234–1242.

Schmeing, T.M., Moore, P.B., and Steitz, T.A. 2003. Structures of deacylated tRNA mimics bound to the A site of the large ribosomal subunit. *RNA* **9**: 1345–1352.

Schmeing, T.M., Huang, K.S., Strobel, S.A., *et al*. 2005. An induced-fit mechanism to promote peptide bond formation and exclude hydrolysis of peptidyl-tRNA. *Nature* **438**:520–524.

Schmeing, T.M., Voorhees, R.M., Kelley, A., *et al*. 2011. How mutations in tRNA distant from the anticodon affect fidelity of decoding. *Nat. Struct. Mol. Biol*. **18**:432–436.

Schmitt, E., Blanquet, S., and Mechulam, Y. 2002. The large subunit of initiation factor aIF2 is a close structural homologue of elongation factors. *EMBO J.* **21**:1821–1832.

Schuenemann, D., Gupta, S., Persello-Cartieaux, F., *et al*. 1998. A novel signal recognition particle targets light-harvesting proteins to the thylakoid membranes. *Proc. Natl. Acad. Sci. USA.* **95**:10312–10316

Schuette, J.C., Murphy, F.V., Kelley, A.C., *et al*. 2009. GTPase activation of elongation factor EF-Tu by the ribosome during decoding. *EMBO J*. **28**:755–765.

Schulze-Gahmen, U., Aono, S., Chen, S., *et al*. 2005. Structure of the hypothetical Mycoplasma protein MPN555 suggests a chaperone function, *Acta Cryst. D* **61**:1343–1347.

Schümmer, T., Gromadski, K.B., and Rodnina, M.V. 2007. Mechanism of EF-Ts-catalyzed guanine nucleotide exchange in EF-Tu: Contribution of interactions mediated by helix B of EF-Tu. *Biochemistry* **46**:4977–4984.

Schuwirth, B.S., Borovinskaya, M.A., Hau, C.W., *et al*. 2005. Structures of the bacterial ribosome at 3.5 Å resolution. *Science* **310**:827–834.

Schuwirth, B.S., Day, J.M., Hau, C.W., *et al*. 2006. Structural analysis of kasugamycin inhibition of translation. *Nat. Struct. Mol. Biol*. **13**:879–886.

Schürer, H., Schiffer, S., Marchfelder, A., and Mörl, M. 2001. This is the end: processing, editing and repair at the tRNA 39-terminus. *Biol. Chem.* **382**:1147–1156.

Schweins, T., Geyer, M., Scheffzek, K., *et al*. 1995. Substrate assisted catalysis as a mechanism for GTP hydrolysis of ras-p21 and other GTP-binding proteins. *Nat. Struct. Biol*. **2**:36–44.

Scolnick, E., Tompkins, R., Caskey, T., and Nirenberg, M. 1968. Release factors differing in specificity for terminator codons. *Proc. Natl. Acad. Sci. USA*. **61**:768–774.

Seit-Nebi, A., Frolova, L., Ivanova, N., *et al*. 2000. Mutation of a glutamine residue in the universal tripeptide GGQ in human eRF1 termination factor does not cause complete loss of its activity. Mol Biol. (Mosk) **34**:899–900.

Seit-Nebi, A., Frolova, L., Justesen, J., and Kisselev, L. 2001. Class-1 translation termination factors: invariant GGQ minidomain is essential for release activity and ribosome binding but not for stop codon recognition. *Nucl. Acids Res.* **29**:3982–3987.

Selivanova, O.M., Shiryaev, V.M., Tiktopulo, E.I., *et al.* 2003. Compact globular structure of *Thermus thermophilus* ribosomal protein S1 in solution. *J. Biol. Chem.* **278**:36311–36314.

Selmer, M. 2002. Protein-RNA interplay in translation. Structural studies of RRF, SelB and L1. Doctoral thesis from Lund University. (ISBN 91-7874-176-9).

Selmer, M. and Liljas, A. 2008. Exit biology: Battle for the nascent chain. *Structure* **16**:498–500.

Selmer, M. and Su, X.-D. 2002. Crystal structure of an mRNA binding fragment of *Moorella thermoacetica* elongation factor SelB. *EMBO J.* **21**:4145–4153.

Selmer, M., Al-Karadaghi, S., Hirokawa, G., *et al.* 1999. Crystal structure of *Thermatoga maritima* ribosome recycling factor: a tRNA mimic. *Science* **286**:2349–2352.

Sengupta, J., Agrawal, R.K., and Frank, J. 2001. Visualisation of protein S1 whithin the 30S ribosomal subunit and its interaction with mRNA. *Proc. Natl. Sci. Acad. USA.* **98**:11991–11996.

Seo, H.S., Abedin, S., Kamp, D., *et al*. 2006. EF-G-dependent GTPase on the ribosome. Conformational change and fusidic acid inhibition. *Biochemistry* **45**:2504–2514.

Seo, H.S., Kiel, M., Pan, D., *et al*. 2004. Kinetics and thermodynamics of RRF, EF-G, and thiostrepton interaction on the *Escherichia coli* ribosome. *Biochemistry* **43**:12728–12740.

Serdyuk, I.N., Smirnov, N.I., Ptitsyn, O.B. *et al*. 1970. On the presence of a dense internal region in the 50S subparticle of E. coli ribosomes. *FEBS Lett.* **2**:324–326.

Sergiev, P., Leonov. A., Dokudovskaya, S., *et al.* 2001. Correlating the X-ray structures for halo- and thermophilic ribosomal subunits with biochemical data for the *Escherichia coli* ribosome. *Cold Spring Harb. Symp. Quant. Biol.* **66**:87–100.

Sette, M., van Tilborg, P., Spurio, R., *et al.* 1997. The structure of the translational initiation factor IF1 from *E. coli* contains an oligomer-binding motif. *EMBO J.* **16**: 1436–1443.

Sharma, D., Southworth, D.R., and Green, R. 2004. EF-G-independent reactivity of a pre-translocation-state ribosome complex with the aminoacyl tRNA substrate puromycin supports an intermediate (hybrid) state of tRNA binding. *RNA* **10**:102–113.

Sharma, M.R., Booth, T.M., Simpson, L., *et al*. 2009. Structure of a mitochondrial ribosome with minimal RNA. *Proc. Natl. Acad. Sci. USA.* **106**:9637–9642.

Shatsky, I.N., Bakin, A.V., Bogdanov, A.A., and Vasiliev, V.D. 1991. How does the mRNA pass through the ribosome? *Biochimie* **73**:937–945.

Shaw, J.J. and Green, R. 2007. Two distinct components of release factor function uncovered by nucleophile partitioning analysis. *Mol. Cell* **28**: 458–467.

Shevack, A., Gewitz, H.S., Hennemann, B., *et al.* 1985. Characterization and crystallization of ribosomal particles from *Haloarcula marismortui. FEBS Lett.* **184**:68–71.

Shi, X., Khade, P.K., Sanbonmatsu, K.Y. *et al*. 2012. Functional role of the sarcin–ricin loop of the 23S rRNA in the elongation cycle of protein synthesis. *J. Mol. Biol*. **419**:125–138.

Shimizu, Y., and Ueda, T. 2006. SmpB triggers GTP hydrolysis of elongation factor Tu on ribosomes by compensating for the lack of codon-anticodon interaction during trans-translation initiation. *J. Biol. Chem.* **281**:15987–15996.

Shimmin, L.C., Ramirez, G., Matheson, A.T., and Dennis, P.P. 1989. Sequence alignment and evolutionary comparison of the L10 equivalent and L12 equivalent ribosomal proteins from archaebacteria, eubacteria, and eucaryotes. *J. Mol. Evol.* **29**:448–462.

Shin, B.-S., Maag, D., Roll-Mecak, A., *et al.* 2002. Uncoupling of initiation factor eIF5B/IF2 GTPase and translational activities by mutations that lower ribosome affinity. *Cell* **111**:1015–1025.

Shine, J. and Dalgarno, L. 1974. The 3′-terminal sequence of *Escherichia coli* 16S ribosomal RNA: complementarity to nonsense triplets and ribosome binding sites. *Proc. Natl. Acad. Sci. USA.* **71**:1342–1346.

Shoji, S., Walker, S.E. and Fredrick, K. 2006. Reverse translocation of tRNA in the ribosome. *Mol. Cell* **24**:931–942.

Sievers, A., Beringer, M., Rodnina, M.V., 2001. The ribosome as an entropy trap. *Proc. Natl. Acad. Sci*. **101**:7897–7901.

Silvian, L.F., Wang, J., and Steitz, T.A. 1999. Insights into editing from an Ile-tRNA synthetase structure with tRNAIle and mupirocin. *Science* **285**:1074–1077.

Simonetti, A., Marzi, S., Jenner, L. *et al*. 2009. A structural view of translation initiation in bacteria. *Cell. Mol. Life Sci.* **66**:423–436.

Simonetti, A., Marzi, S., Myasnikov, A., *et al*. 2009. Structure of the 30S translation initiation complex. *Nature* **455**:416–420.

Simonovic, M. and Steitz, T.A. 2009. A structural view on the mechanism of the ribosome-catalyzed peptide bond formation. *Biochim. Biophys. Acta* **1789**:612–623.

Singarapu, K.K., Xiao, R., Acton, T., *et al*. 2008. NMR structure of the peptidyl-tRNA hydrolase domain from Pseudomonas syringae expands the structural coverage of the hydrolysis domains of class 1 peptide chain release factors. *Proteins* **71**:1027–1031.

Skogerson, L. and Moldave, K. 1968. Characterization of the interaction of aminoacyltransferase II with ribosomes. Binding of transferase II and translocation of peptidyl transfer ribonucleic acid. *J. Biol. Chem.* **243**: 5354–5360.

Sköld, S.E. 1983. Chemical crosslinking of elongation factor G to the 23S RNA in 70S ribosomes from *Escherichia coli*. *Nucl. Acids Res.* **11**:4923–4932.

Skouloubris, S., Ribas de Pouplana, L., de Reuse, H., and Hendrickson, T.L. 2003. A noncognate aminoacyl-tRNA synthetase that may resolve a missing link in protein evolution. *Proc. Natl. Acad. Sci. USA.* **100**:11297–11302.

Skripkin, E., McConnell, T.S., DeVito, J., *et al*. 2008. Rc-01, a new family of oxazolidinones that overcome ribosome-based linezolid resistance. *Antimicrob. Agents Chemother*. **52**:3550–3557.

Sloof, P., Van den Burg, J., and Voogl, A. *et al*. 1985. Further characterization of the extremely small mitochondrial ribosomal RNAs from trypanosomes: a detailed comparison of 9S and 12S RNAs from Critidia fasciculataand Trypanosoma brucei with RNAs from other organisms. *Nucleic Acids Res*. **13**:4171–4190.

Smith, D. and Yarus, M. 1989. Transfer RNA structure and coding specificity. II. A D-arm tertiary interaction that restricts coding range. *J. Mol. Biol*. **206**:503–511.

Smith, D.R., Doucette-Stamm, L.A., Deloughery, C., *et al*. 1997. Complete genome sequence of *Methanobacterium thermoautotrophicum* deltaH: functional analysis and comparative genomics. *J. Bacteriol*. **179**:7135–7155.

Smith, T.F., Lee, J.C., Gutell, R.R., *et al*. 2008. The origin and evolution of the ribosome. *Biology Direct* **3**:1–13.

Smrt, J., Kemper, W., Caskey, T., and Nirenberg, M. 1970. Template activity of modified terminator codons. *J. Biol. Chem*. **245**:2753–2757.

Sokabe, M., Okada, A., Yao, M., *et al*. (2005). Molecular basis of alanine discrimination in editing site. *Proc. Nat. Acad. Sci. USA*. **102**:11669–11674.

Soler, N., Fourmy, D., and Yoshizawa, S. 2007. Structural insight into a molecular switch in tandem winged-helix motifs from elongation factor SelB. *J. Mol. Biol*. **370**:728–741.

Söll, D., Jones, D.S., Ohtsuka, E., *et al*. 1966. Specificity of sRNA for recognition of codons as studied by the ribosomal binding technique. *J. Mol. Biol*. **19**:556–573.

Sonenberg, N., Wilchek, M., and Zamir, A. 1975. Identification of a region in 23S rRNA located at the peptidyl transferase center. *Proc. Natl. Acad. Sci. USA*. **72**:4332–4336.

Song, H., Mugnier, P., Das, A.K., *et al*. 2000. The crystal structure of human eukaryotic release factor eRF1 — mechanism of stop codon recognition and peptidyl-tRNA hydrolysis. *Cell* **100**:311–321.

Sorensen M.A., Fricke J., and Pedersen S. 1998. Ribosomal protein S1 is required for translation of most, if not all, natural mRNAs in *Escherichia coli in vivo*. *J. Mol. Biol*. **280**:561–569.

Sorokin A., Serror P., Pujic P., *et al*. 1995. The *Bacillus subtilis* chromosome region encoding homologues of the *Escherichia coli mss*A and *rps*A gene products. *Microbiology*. **141**:311–319.

Soung, G.Y., Miller, J.L., Koc, H., *et al*. 2009. Comprehensive analysis of phosphorylated proteins of Escherichia coli ribosomes. *J. Proteome Res*. **8**:3390–3402.

Southworth, D.R., Brunelle, J.L., and Green, R. 2002. EFG-independent translocation of the mRNA:tRNA complex is promoted by modification of the ribosome with thiol-specific reagents. *J. Mol. Biol*. **324**:611–623.

Southworth, D.R. and Green, R. 2003. Ribosomal translocation: Sparsomycin pushes the button. *Curr. Biol*. **13**:R652–R654.

Spahn, C.M., Blaha, G., Agrawal, R.K., *et al.* 2001. Localization of the ribosomal protection protein Tet(O) on the ribosome and the mechanism of tetracycline resistance. *Mol. Cell.* **7**:1037–1045.

Spahn, C.M., Gomez-Lorenzo, M.G., Grassucci, R.A., *et al.* 2004. Domain movements of elongation factor eEf2 and the eukaryotic 80S ribosome facilitate tRNA translocation. *EMBO J.* **23**:1008–1019.

Shpanchenko, O.V., Zvereva, M.I., Ivanov, P.V., *et al.* 2005. Stepping transfer messenger RNA through the ribosome. *J. Biol. Chem.* **280**:18368–18374.

Spiegel, P.C., Ermolenko, D.N., and Noller, H.F. 2007. Elongation factor G stabilizes the hybrid-state conformation of the 70S ribosome. *RNA* **13**: 1473–1482.

Spirin, A.S. 1961. The 'temperature effect' and macromolecular structure of high-polymer ribonucleic acids of various origin. *Biochemistry* **26**:454–463.

Spirin, A.S. 1968. On the mechanism of ribosome function. The hypothesis of locking-unlocking of subparticles. *Dokl. Akad. Nauk SSSR* **179**:1467–1470.

Spirin, A.S. 1969. A model of the functioning ribosome: locking and unlocking of the ribosome particles. *Cold Spring Harb. Symp. Quant. Biol.* **34**:197–207.

Spirin, A.S. 1978. Energetics of the ribosome. *Prog. Nucl. Acid Res. Mol. Biol.* **21**:39–62.

Spirin, A.S. 1985. Ribosomal translocation: facts and models. *Prog. Nucl. Acid. Res. Mol. Biol.* **32**:75–114.

Spirin, A.S. 1999. In *Ribosomes*, Ed. P. Siekevitz. Kluwer Academic/Plenum Publishers, New York, Boston, Dordrecht, London, Moscow.

Spirin, A.S. 2002. Ribosome as a molecular machine. *FEBS Lett.* **514**:2–10.

Spirin, A.S., and Vasiliev, V.D. 1989. Localization of functional centers on the prokaryotic ribosome: immuno-electron microscopy approach. *Biol. Cell* **66**:215–223.

Spitnik-Elson, P. 1962. The solubilization of ribosomal protein from *Escherichia coli*. *Biochim. Biophys. Acta* **55**:741–747.

Srinivasan, G., James, C.M., and Krzycki, J.A. 2002. Pyrrolysine encoded by UAG in archaea: charging of a UAG-decoding specialized tRNA. *Science* **296**: 1459–1462.

Stanley, R.E., Blaha, G., Grodzicki, R.L., *et al.* 2010. The structures of the anti-tuberculosis antibiotics viomycin and capreomycin bound to the 70S ribosome. *Nat. Struct. Mol. Biol.* **17**:289–293.

Stanzel, M., Schon, A., and Sprinzl, M. 1994. Discrimination against misacylated tRNA by chloroplast elongation factor Tu. *Eur. J. Biochem.* **219**:435–439.

Stark, M.J.R. and Cundliffe, E. (1979). On the biological role of ribosomal protein BM-L11 of *Bacillus megaterium*, homologous with *Escherichia coli* ribosomal protein L11. *J. Mol. Biol.* **134**:767–779.

Stark, H., Rodnina, M.V., Rinke-Appel, J., *et al.* 1997. Visualization of elongation factor Tu on the *Escherichia coli* ribosome. *Nature* **389**:403–406.

Stark, H., Rodnina, M.V., Wieden, H.J., *et al.* 2000. Large scale movement of elongation factor G and extensive conformational change of the ribosome during translocation. *Cell* **100**:301–309.

Stark, H., Rodnina, M.V., Wieden, H.J., *et al.* 2002. Ribosome interactions of aminoacyl-tRNA and elongation factor Tu in the codon-recognition complex. *Nat. Struct. Biol.* **9**:849–854.

Stathopouplos, C., Li, T., Longman, R., *et al.* 2000. One polypeptide with two aminoacyl-tRNA synthetase activities, *Science* **287**:479–482.

Steinberg, S.V. and Bontorine, Y.I. 2007. G-ribo: A new structural motif in ribosomal RNA. *RNA* **13**:549–554.

Steitz, J.A. 1969. Polypeptide chain initiation: nucleotide sequences of the three ribosomal binding sites in bacteriophage R17 RNA. *Nature* **224**:957–964.

Stent, G.S., and Brenner, S. 1961. A genetic locus for the regulation of ribonucleic acid synthesis. *Proc. Natl. Acad. Sci. USA.* **47**:2005–2014.

Stern, S., Moazed, D., and Noller, H.F. 1988. Structural analysis of RNA using chemical and enzymatic probing monitored by primer extension. *Methods Enzymol.* **164**:481–489.

Stern, S., Powers, T., Changchien, L.M., and Noller, H.F. 1989. RNA-protein interactions in 30S ribosomal subunits: folding and function of 16S rRNA. *Science* **244**:783–790.

Stringer, E.A., Sarkar, P., and Maitra, U. 1977. Function of initiation factor 1 in the binding and release of initiation factor 2 from ribosomal initiation complexes in *Escherichia coli. J. Biol. Chem.* **252**:1739–1744.

Stöffler, G., and Stöffler-Meilicke, M. 1984. Immunoelectron microscopy of ribosomes. *Ann. Rev. Biophys. Bioeng.* **13**:303–330.

Stoller, G., Ruecknagel, K.P., Nierhaus, K.H., *et al.* 1995. A ribosome-associated peptidyl-prolyl cis/trans isomerase identified as the trigger factor. *EMBO J.* **14**:4939–4948.

Stout, C.D., Mizuno, H., Rubin, J., *et al.* 1976. Atomic coordinates and molecular conformation of yeast phenylalanyl tRNA. An independent investigation. *Nucl. Acids Res.* **3**:1111–1123.

Strychartz, W.A., Nomura, M., and Lake, J.A. 1978. Ribosomal protein L7/L12 localized at a single region of the large subunit by immune microscopy. *J. Mol. Biol.* **126**:123–140.

Subramanian, A.R. 1983. Structure and functions of ribosomal protein S1. *Prog. Nucl. Acid Res. Mol. Biol.* **28**:101–142.

Subramanian, A.R., and Davis, B.D. 1970. Activity of initiation factor F3 in dissociating *Escherichia coli* ribosomes. *Nature* **228**:1273–1275.

Subramanian, A.R., and van Duin, J. 1977. Exchange of individual ribosomal proteins between ribosomes as studied by heavy isotope-transfer experiments. *Mol. Gen. Genet.* **158**:1–9.

Subramanian, A.R. and Dabbs, E. 1980. Functional studies on ribosomes lacking protein L1 from mutant *E. coli. Eur. J. Biochem.* **112**:425–430.

Suh, W.C., Lu, C.Z., and Gross, C.A. 1999. Structural features required for the interaction of the Hsp70 molecular chaperone DnaK with its cochaperone DnaJ. *J. Biol. Chem.* **274**:30534–30539.

Sund, J., Andér, M., and Åqvist, J. 2010. Principles of stop-codon reading on the ribsome. *Nature* **465**:947–950.

Suppmann, S., Persson, B.C., and Böck, A. 1999. Dynamics and efficiency *in vivo* of UGA-directed selenocysteine insertion at the ribosome. *EMBO J.* **18**: 2284–2293.

Sutcliffe, J.A. 2005. Improving on nature: antibiotics that target the ribosome. *Curr. Op. Microbiol.* **8**:534–542.

Swairjo, M.A. and Schimmel, P.R. 2005. Breaking sieve for steric exclusion of a noncognate amino acid from active site of a tRNA synthetase. *Proc. Natl. Acad. Sci. USA.* **102**:988–993.

Sy, J. 1977. *In vitro* degradation of guanosine 59-diphosphate, 39-diphosphate. *Proc. Natl. Acad. Sci. USA.* **74**:5529–5533.

Sy, J., and Lipmann, F. 1973. Identification of the synthesis of guanosine tetraphosphate (MS I) as an insertion of a pyrophosphoryl group into the 3-position in guanosine 5-diphosphate. *Proc. Natl. Acad. Sci. USA.* **70**:306–309.

Takagi, H., Kakuta, Y., Okada, T., *et al*. 2005. Crystal structure of archaeal toxin–antitoxin RelE–RelB complex with implications for toxin activity and antitoxin effects. *Nat. Struct. Mol. Biol*. **12**:327–331.

Takanami, M. and Zubay, G. 1964. An estimate of the size of the ribosomal site for messenger RNA binding. *Proc. Natl. Acad. Sci. USA.* **51**:834–839.

Talkington, M.W.T., Siuzdak, G., and Williamson, J.R. 2005. An assebly landscape for the 30S subunit. *Nature* **438**:628–632.

Tan, J., Jakob, U., and Bardwell, J.C. 2002. Overexpression of two different GTPases rescues a null mutation in a heat-induced rRNA methyltransferase. *J. Bacteriol.* **184**:2692–2698.

Tarn, W.Y., Steitz, J.A. 1997. Pre-mRNA splicing: the discovery of a new spliceosome doubles the challenge. *Trends Biochem. Sci.* **22**:132–137.

Taylor, D.E. and Chau, A. 1996. Tetracycline resistance mediated by ribosomal protection. *Antimicrob. Agents Chemother.* **40**:1–5.

Taylor, D.E., Trieber, C.A., Trescher, G., and Bekkering, M. 1998. Host mutations (miaA and rpsL) reduce tetracycline resistance mediated by Tet(O) and Tet(M). *Antimicrob. Agents Chemother.* **42**:59–64.

Taylor, D.J., Devkota, B., Huang, A.D., *et al*. 2009. Comprehensive molecular structure of the eukaryotic ribosome. *Structure* **17**:1591–1604.

Tchorzewski, M. 2002. The acidic ribosomal P-proteins. *Int. J. Biochem. Cell Biol.* **1265**:1–5.

Tchorzewski, M., Boldyreff, B., Issinger, O.-G., and Grankowski, N. 2000a. Analysis of the protein-protein interactions between the human acidic ribosomal P-proteins: evaluation by the two hybrid system. *Int J. Biochem. Cell Biol.* **32**:737–746.

Tchorzewski, M., Boguszewska, A., Dukowski, P., and Grankowski, N. 2000b. Oligomeric properties of the acidic ribosomal P-proteins from *Saccharomyces*

cerevisiae: effect of P1A protein phosphorylation on the formation of the P1A-P2B hetero-complex. *Biochim. Biophys. Acta* **1499**:63–73.

Tchorzewski, M., Krokowski, D., Boguszewska, A., *et al.* 2003. Structural characterization of yeast acidic ribosomal P-proteins forming the hetero-complex P1A/P2B. *Biochemistry* **42**:3399–3408.

Tenson, T., Xiong, L., Kloss, P. *et al*. 1997. Erythromycin resistance peptides selected from random peptide libraries. *J. Biol. Chem*. **272**:17425–17430.

Tenson, T., and Ehrenberg, M. 2002. Regulatory nascent peptides in the ribosome tunnel. *Cell* **108**:591–594.

Terada, T, Nureki, O., Ishitani, R., *et al*. 2002. Functional convergence of two lysyl-tRNA synthetases with unrelated topologies. *Nat. Struct, Biol*. **9**:257–262.

Terhorst, C., Wittmann-Liebold, B., and Möller, W. 1972. 50S ribosomal proteins. Peptide studies on two acidic proteins, A1 and A2, isolated from 50S ribosomes of *Escherichia coli*. *Eur. J. Biochem.* **25**:13–19.

Teter, S.A., Houry, W.A., Ang, D., *et al.* 1999. Polypeptide flux through bacterial Hsp70: DnaK cooperates with trigger factor in chaperoning nascent chains. *Cell* **97**:755–765.

Thaker, M., Spanogiannopoulos, P., and Wright, G.D. 2010. The tetracycline resistome. *Cell. Mol. Life Sci.* **67**:419–431.

Thanbichler, M., Böck, A., and Goody, R.S. 2000. Kinetics of the interaction of translation factor SelB from *Escherichia coli* with guanosine nucleotides and selenocysteine insertion sequence RNA. *J. Biol. Chem.* **275**:20458–20466.

Thompson, J., Cundliffe, E. and Stark, M. 1979. Binding of thiostrepton to a complex of 23S rRNA with ribosomal protein L11. *Eur. J. Biochem*. **98**:261–265.

Thompson, J., Cundliffe, E., and Dahlberg, A.E. 1988. Site-directed mutagenesis of *Escherichia coli* 23S ribosomal RNA at position 1067 within the GTP hydrolysis center. *J. Mol. Biol*. **203**:457–465.

Thompson, J., Kim, D.F., O'Connor, M., *et al.* 2001. Analysis of mutations at residues A2451 and G2447 of 23S rRNA in the peptidyltransferase active site of the 50S ribosomal subunit. *Proc. Natl. Acad. Sci. USA.* **98**:9002–9007.

Thompson, J., Schmidt, F., and Cundliffe, E. 1982. Site of action of a ribosomal RNA methylase conferring resistance to thiostrepton. *J. Biol. Chem.* **257**: 7915–7917.

Ticu, C., Nechifor, R., Nguyen, B., *et al*. 2009. Conformational changes in switch I of EF-G drive its directional cycling on and off the ribosome. *EMBO J.* **28**:2053–2065.

Ticu, C., Murataliev, M., Nechifor, R., *et al*. 2011. A central cnterdomain protein joint in elongation factor G regulates antibiotic sensitivity, GTP hydrolysis, and ribosome translocation. *J. Biol. Chem.* **286**:21697–21705.

Tiennault-Desbordes, E., Cenatiempo, Y., and Laalami, S. 2001. Initiation factor 2 of *Myxococcus xanthus*, a large version of prokaryotic translation initiation factor 2. *J. Bacteriol*. **183**:207–213.

Tiller, N., Weingartner, M., Thiele, W., *et al*. 2012. The plastid-specific ribosomal proteins of Arabidopsis thaliana can be divided into non-essential proteins and genuine ribosomal proteins. *The Plant J*. **69**:302–316.

Tirion. M.M. 1996. Large amplitude elastic motions in proteins from a single-parameter, atomic analysis. *Phys. Rev. Lett*. **77**:1905–1908.

Tischendorf, G.W., Zeichhardt, H., and Stöffler, G. 1974. Location of proteins S5, S13, S14 on the surface of the 30S ribosomal subunit from *Escherichia coli* as determined by immune electron microscopy. *Mol. Gen. Genet*. **134**:209–223.

Tissieres A. and Watson J.D. 1958. Ribonucleoprotein particles from *Escherichia coli*. *Nature* **182**:778–780.

Tissieres, A., Schlessinger, D., and Gros, F. 1960. Amino acid incorporation into proteins by *Escherichia coli* ribosomes. *Proc. Natl. Acad. Sci. USA*. **46**:1450–1456.

Tissieres, A., Watson, J.D., Schlessinger, D. *et al*. 1959. Ribonucleoprotein particles from *Escherichia coli*. *J. Mol. Biol*. **1**:221–233.

Tobin, C., Mandawa, C.S., Ehrenberg, M., *et al*. 2010. Ribosomes lacking protein S20 are defective in mRNA binding and subunit association. *J. Mol. Biol*. **397**:767–776.

Tocilj, A., Schlünzen, F., Janell, D., *et al*. 1999. The small ribosomal subunit from *Thermus thermophilus* at 4.5 A resolution: pattern fittings and the identification of a functional site. *Proc. Natl. Acad. Sci. USA*. **96**:14252–14257.

Tomic, S., Johnson, A.E., Hartl, F.U., *et al*. 2006. Exploring the capacity of trigger factor to function as a shield for ribosome bound polypeptide chains. *FEBS Lett*. **580**:72–76.

Tomita, K., Ishitani, R., Fukai, S., *et al*. 2006. Complete crystallographic analysis of the dynamics of CCA sequence addition. *Nature* **443**:956–960.

Tourigny, D.S., Fernández, I.S., Kelley, A.C., *et al*. 2013. The crystal structure of elongation factor G trapped on a ribosome in an intermediate state of translocation. Science, In press.

Toyoda, T., Tin, O.F., Ito, K., *et al*. 2000. Crystal structure combined with genetic analysis of the *Thermus thermophilus* ribosome recycling factor shows that a flexible hinge may act as a functional switch. *RNA* **6**:1432–1444.

Trakhanov, S.D., Yusupov, M.M., Agalarov, S.C., *et al*. 1987. Crystallization of 70S ribosomes and 30S ribosomal subunits from *Thermus thermophilus*. *FEBS Lett*. **220**: 319–322.

Traut, R.R., and Monro, R.E. 1964. The puromycin reaction and its relation to protein synthesis. *J. Mol. Biol*. **10**:63–72.

Trieber, C.A., Burkhardt, N., Nierhaus, K.H., and Taylor, D.E. 1998. Ribosomal protection from tetracycline mediated by Tet(O): Tet(O) interaction with ribosomes is GTP-dependent. *Biol. Chem*. **379**:847–855.

Tritton, T.R. 1980. Proton NMR observation of the *Escherichia coli* ribosome. *FEBS Lett*. **120**:141–144.

Trobro, S. and Åqvist, J. 2006. Analysis of predictions for the catalytic mechanism of ribosomal peptidyl transfer. *Biochemistry* **45**:7049–7056.

Trobro, S. and Åqvist, J. 2007. A model for how ribosomal release factors induce peptidyl-tRNA cleavage in termination of protein synthesis. *Mol. Cell* **27**:758–766.

Trobro, S. and Åqvist, J. 2008. Role of ribosomal protein L27 in peptidyl transfer. *Biochemistry* **47**:4898–4906.

Trobro, S., and Åqvist, J. 2009. Mechanism of the translation termination reaction on the ribosome. *Biochemistry* **48**:11296–11303.

Tsalkova, T., Odom, O.W., Kramer, G., and Hardesty, B. 1998. Different conformations of nascent peptides on ribosomes. *J. Mol. Biol.* **278**:713–723.

Tumanova, L.G., Gongadze, G.M., Venyaminov, S. Yu., *et al.* 1983. Physical properties of ribosomal proteins isolated under different conditions from the *Escherichia coli* 50S subunit. *FEBS Lett.* **157**:85–90.

Tumbula, D.L., Becker, H.D., Chang, W.Z., and Söll, D. 2000. Domain-specific recruitment of amide amino acids for protein synthesis. *Nature* **407**:106–110.

Uchiumi, T., Wahba, A.J., and Traut, R.R. 1987. Topography and stoichiometry of acidic proteins in large ribosomal subunits from *Artemia salina* as determined by crosslinking. *Proc. Natl. Acad. Sci. USA.* **84**:5580–5584.

Ueta, M., Yoshida, H., Wada, C., *et al*. 2005. Ribosome binding proteins YhbH and YfiA have opposite functions during 100S formation in the stationary phase of *Escherichia coli*. *Genes Cells* **10**:1103–1112.

Ullers, R.S., Houben, E.N., Raine, A., *et al.* 2003. Interplay of signal recognition particle and trigger factor at L23 near the nascent chain exit site on the *Escherichia coli* ribosome. *J. Cell Biol.* **161**:679–684.

Umezawa, H., Hamada, M., Suhara, Y. *et al*. 1965. Kasugamycin, a new antibiotic. *Antimicrob. Agents Chemother*. **5**:753–757.

Unge, J., Al-Karadaghi, S., Liljas, A., *et al.* 1997. A mutant form of the ribosomal protein L1 reveals conformational flexibility. *FEBS Lett.* **411**:53–59.

Unge, J., Åberg, A., Al Karadaghi, S., *et al.* 1998. The crystal structure of ribosomal protein L22 from *Thermus thermophilus*: insights into the mechanism of erythromycin resistance. *Structure* **6**:1577–1586.

Urban, J.H. and Vogel, J. 2007. Translational control and target recognition by *Escherichia coli* small RNAs *in vivo*. *Nucl. Acids Res*. **35**:1018–1037.

Unwin, N. 1977. Three-dimensional model of membrane-bound ribosomes obtained by electron microscopy. *Nature* **269**:118–122.

Valentini, S.R., Casolari, J.M., Oliveira, C.C., *et al*. 2002. Genetic interactions of yeast eukaryotic translation initiation factor 5A (eIF5A) reveal connections to poly(A)-binding protein and protein kinase C signaling. *Genetics* **160**:393–405.

Valle, M., Sengupta, J., Swami, N.K., *et al*. 2002. Cryo-EM reveals an active role for aminoacyl-tRNA in the accommodation process. *EMBO J.* **21**:3557–3567.

Valle, M., Zavialov, A., Li, W., *et al.* 2003a. Incorporation of aminoacyl-tRNA into the ribosome as seen by cryo-electron microscopy. *Nat. Struct. Biol.* **10**:899–906.

Valle, M., Zavialov, A., Sengupta, J., *et al.* 2003b. Locking and unlocking of ribosomal motions. *Cell* **114**:123–134.

Valle, M., Gillet, R., Kaur, S., *et al.* 2003c. Visualizing tmRNA entry into a stalled ribosome. *Science* **300**:127–130.

van Agthoven, A., Maassen, J.A., Schrier, P.I., and Möller, W. 1975. Inhibition of EF-G dependent GTPase by an amino-terminal fragment of L7/L12. *Biochim. Biophys. Res. Commun.* **64**:1184–1191.

van Agthoven, A., Kriek, J., Amons, R., and Möller, W. 1978. Isolation and characterization of the acidic phosphoproteins of 60-S ribosomes from *Artemia salina* and rat liver. *Eur. J. Biochem.* **91**:553–565.

VanBogelen, R.A., and Neidhardt, F.C. 1990. Ribosomes are sensors of heat and cold shock in *Escherichia coli*. *Proc. Natl. Acad. Sci. USA.* **87**:5589–5593.

van den Berg, B., Clemons, W.M., Collinson, I., *et al.* 2004. X-ray structure of a protein conducting channel. *Nature* **427**:36–44.

van Doorn, L.J., Giesendorf, B.A., Bax, R., *et al.* 1997. Molecular discrimination between *Campylobacter jejuni, Campylobacter coli, Campylobacter lari* and *Campylobacter upsaliensis* by polymerase chain reaction based on a novel putative GTPase gene. *Mol. Cell Probes* **11**:177–185.

van Heel, M. 1987. Angular reconstruction: *a posteriori* assignment of projection direction for 3D reconstruction. *Ultramicroscopy* **21**:111–114.

VanLoock, M.S., Agrawal, R.K., Gabashvili, L.Q., *et al.* 2000. Movement of the decoding region of the 16S ribosomal RNA accompanies tRNA translocation. *J. Mol. Biol.* **304**:507–515.

Vasiliev, V.D. 1974. Morphology of the ribosomal 30S subparticle according to electron microscopic data. *Acta Biol. Med. Ger.* **33**:779–793.

Vasil'eva, I.A. and Moor, N.A. 2007. Interaction of aminoacyl-tRNA synthetases with tRNA: general principles and distuinguishing characteristics of the high-molecular-weight substrate recognition. *Biochemistry (Moscow)* **72**:306–324.

Vazquez, D. 1974. Inhibitors of protein synthesis. *FEBS Lett.* **40**(Suppl.):S63–S84.

Vazquez, D. 1979. Inhibitors of protein synthesis. *Mol. Biochem. Biochem. Biophys.* **30**:1–312.

Vesper, O. and Wilson, D.N. 2006. Ribosome recycling revisited. *Mol. Biol.* **40**:664–672.

Vester, B. and Douthwaite, S. 2001. Macrolide resistance conferred by base substitutions in 23S RNA. *Antimicrob. Agents Chemother.* **45**:1–12.

Vester, B. and Garrett, R.A. 1988. The importance of highly conserved nucleotides in the binding region of chloramphenicol at the peptidyl transfer center of *E. coli* 23S ribosomal RNA. *EMBO J.* **7**:3577–3588.

Vestergaard, B., Sanyal, S., Roessle, M., *et al.* 2005. The SAXS solution structure of RF1 differs from its crystal structure and is similar to its ribosome bound cryo-EM structure. *Mol. Cell* **20**:929–938.

Vestergaard, B., Van, L.B., Andersen, G.R., *et al.* 2001. Bacterial polypeptide release factor RF2 is structurally distinct from eucayotic eRF1. *Mol. Cell* **8**:1375–1382.

Vetter, I.R. and Wittinghofer, A. 2001. The guanine nucleotide-binding switch in three dimensions. *Science* **294**:1299–1304.

Vicens, Q. and Westhof, E. 2002. Crystal structure of a complex between the aminoglycoside tobramycin and an oligonucleotide containing the ribosomal decoding a site. *Chem. Biol.* **9**:747–755.

Vicens, Q. and Westhof, E. 2003. Crystal structure of geneticin bound to a bacterial 16S ribosomal RNA A site oligonucleotide. *J. Mol. Biol.* **326**:1175–1188.

Videler, H., Ilag, L.L., McKay, A.R.C., *et al*. 2005. Mass spectrometry of intact ribosomes. *FEBS lett.* **579**:943–947.

Vila-Sanjurjo, A., Squires, C.L., and Dahlberg, A.E. 1999. Isolation of kasugamycin resistant mutants in the 16 S ribosomal RNA of *Escherichia coli*. *J. Mol. Biol.* **293**:1–8.

Vila-Sanjurjo, A., Ridgeway, W.K., Seymaner, V., *et al.* 2003. X-ray crystal structures of the WT and a hyper-accurate ribosome from *Escherichia coli*. *Proc. Natl. Acad. Sci. USA.* **100**:8682–8687.

Vila-Sanjurjo, A., Schuwirth, B.-S., Hau, *et al*. 2004. Structural basis for the control of translation initiation during stress. *Nat. Struct. Mol. Biol*. **11**:1054–1059.

Villa, E., Sengupta, J., Trabuco, L.G., *et al*. 2009. Ribosome-induced changes in elongation factor Tu conformation control GTP hydrolysis. *Proc. Natl. Acad. Sci. USA*. **106**:1063–1068.

Vogel, J. and Wagner, E.G.H. 2007. Target identification of small decoding RNAs in bacteria. *Curr. Op. Microbiol.* **10**:262–270.

Vogeley, L., Palm, G.J., Mesters, J.R., and Hilgenfeld, R. 2001. Conformational change of elongation factor Tu (EF-Tu) induced by antibiotic binding. Crystal structure of the complex between ET-Tu.GDP and aurodox. *J. Biol. Chem.* **276**:17149–17155.

Voigts-Hoffmann, F., Klinge, S., and Ban, N, 2012. Structural insights into eukaryotic ribosomes and the initiation of translation. *Curr. Op. Struct. Biol*. **22**:768–777.

Völker, U., Engelmann, S., Maul, B., *et al*. 1994. Analysis of the induction of general stress proteins of *Bacillus subtilis*. *Microbiology* **140**:741–752.

von Bohlen, K., Makowski, I., Hansen, H.A., *et al.* 1991. Characterization and preliminary attempts for derivatization of crystals of large ribosomal subunits from *Haloarcula marismortui* diffracting to 3A resolution. *J. Mol. Biol.* **222**:11–15.

von Heijne, G. 1986. The distribution of positively charged residues in bacterial inner membrane proteins correlates with the trans-membrane topology. *EMBO J.* **5**:3021–3027.

von Heijne, G.1990. The signal peptide. *J. Membr. Biol*. **115**:195–201.

von Hippel, P.H. and Yager, T.D. 1992. The elongation-termination decision in transcription. *Science* **255**:809–812.

Voorhees, R.M., Weixlbaumer, A., Loakes, D., *et al*. 2009. Insights into substrate stabilization from snapshots of the peptidyl transferase center of the intact 70S ribosome. *Nature Struct. Mol. Biol*. **16**:528–533.

Voorhees, R.M., Schmeing, M., Kelley, A.C., *et al*. 2010. The mechanism for activation of GTP hydrolysis on the ribosome. *Science* 330. 835–838.

Voorhees, R.M., Schmeing, T.M., Kelley, A.C. *et al*. 2011. Response to comment on ''The mechanism for activation of GTP hydrolysis on the ribosome''. *Science* **333**:37.

Vorstenbosch, E., Pape, T., Rodnina, M.V., *et al*. 1996. The G222D mutation in elongation factor Tu inhibits the codon-induced conformational changes leading to GTPase activation on the ribosome. *EMBO J*. **15**:6766–6774.

Voss, N.R., Gerstein, M., Steitz, T.A., and Moore, P.B. 2006. The geometry of the ribosomal polypeptide exit tunnel. *J. Mol. Biol*. **360**:893–906.

Wabl, M.R. 1974. Electron microscopic location of two proteins on the surface of the 50S ribosomal subunit of *Escherichia coli* using specific antibody markers *J. Mol. Biol*. **84**:241–247.

Wada, A. 1998. Growth phase coupled modulation of *Escherichia coli* ribosomes. *Genes Cells* **3**:203–208.

Wada, A., Yamazaki, Y., Fujita, N., *et al*. 1990. Structure and probable genetic location of a 'ribosome modulation factor' associated with 100S ribosomes in stationary phase *Escherichia coli* cells. *Proc. Natl. Acad. Sci. USA*. **87**:2657–2661.

Wahl, M.C., Bourenkov, G.P., Bartunik, H.D., and Huber, R. 2000. Flexibility, conformational diversity and two dimerization modes in complexes of ribosomal protein L12. *EMBO J*. **19**:174–186.

Wahl, M.C., and Möller, W. 2002. Structure and function of the acid ribosomal stalk proteins. *Curr. Prot. Pept. Sci*. **3**:93–106.

Walker, J.E., Saraste, M., Runswick, M.J., and Gay, N.J. 1982. Distantly related sequences in the alpha- and beta-subunits of ATP synthase, myosin, kinases and other ATP-requiring enzymes and a common nucleotide binding fold. *EMBO J*. **1**:945–951.

Wallin, G. and Åqvist., J. 2010. The transition state for peptide bond formation reveals the ribosome as a water trap, *Proc. Natl. Acad. Sci. USA*. **107**:1888–1893.

Wallin, G., Kamerlin, S.C.L., and Åqvist, J. 2013. Energetics of activation of GTP hydrolysis on the ribosome. *Nat. Commun*. **4**:1733.

Walter, P. and Blobel, G. 1980. Purification of a membrane-associated protein complex required for protein translocation across the endoplasmic reticulum. *Proc. Natl. Acad. Sci. USA*. **77**:112–116.

Walter, P. and Blobel, G. 1982. Signal recognition particle contains a 7S RNA essential for protein translocation across the endoplasmic reticulum. *Nature* **299**:691–698.

Wang, D., Bushnell, D.A., Westover, K.D., *et al*. 2006. Structural basis of transcription: Role of the trigger loop in substrate specificity and catalysis. *Cell* **127**:941–954.

Wang, F., Zhong, N.-Q., Gao, P., *et al*. 2008. SsTypA1, a chloroplast-specific TypA/BipA-type GTPase from the halophytic plant Suaeda salsa, plays a role in oxidative stress tolerance. *Plant, Cell Envir.* **31**:982–994.

Wang, Y., Jiang, Y., Meyering-Voss, M., *et al*. 1997. Crystal structure of the EF-Tu. EF-Ts complex from *Thermus thermophilus*. *Nat. Struct. Biol.* **4**:650–656.

Warner, J.R., and Rich, A. 1964. The number of soluble RNA molecules on reticulocyte polyribosomes. *Proc. Natl. Acad. Sci. USA.* **51**:1134–1141.

Watson, J.D. 1964. The synthesis of proteins upon ribosomes. *Bull. Soc. Chim. Biol.* **46**:1399–1425.

Watson, J.D., and Crick, F. 1953. Molecular structure of nucleic acids. *Nature* **171**:737–738.

Wedekind, J.E., Dance, G.S., Sowden, M.P., and Smith, H.C. 2003. Messenger RNA editing in mammals: new members of the APOBEC family seeking roles in the family business. *Trends Genet.* **19**:207–216.

Weinger, J.S., Parnell, K.M., Dorner, S., *et al*. 2004. Substrate-assisted catalysis of peptide bond formation on the ribosome. *Nat. Struct. Mol. Biol.* **11**:1101–1106.

Weinstein, S., Jahn, W., Glotz, C., *et al*. 1999. Metal compounds as tools for the construction and the interpretation of medium-resolution maps of ribosomal particles. *J. Struct. Biol.* **127**:141–151.

Weixlbaumer, A., Petry, S., Dunham, C.M., *et al.* 2007. Crystal structure of the ribosome recycling factor bound to the ribosome. *Nat. Struct. Mol. Biol.* **14**:733–737.

Weixlbaumer, A., Hong, J., Neubauer, C., *et al*. 2008. Insights into translational termination from the structure of RF2 bound to the ribosome. *Science* **322**:953–957.

Welch, M., Chastang, J., and Yarus, M. 1995. An inhibitor of ribosomal peptidyltransferase using transition-state analogy. *Biochemistry* **34**:385–390.

Wendrich, T.M., and Marahiel, M.A. 1997. Cloning and characterization of a relA/spoT homologue from *Bacillus subtilis*. *Mol. Microbiol.* **26**:65–79.

Wendrich, T.M., Blaha, G., Wilson, D.N., *et al*. 2002. Dissection of the mechanism for the stringent factor RelA. *Mol. Cell* **10**:779–788.

Westhof, E., and Fritsch, V. 2000. RNA folding: beyond Watson-Crick pairs. *Struct. Fold. Des.* **8**:R55–R65.

Wettstein, F.O. and Noll, H. 1965. Binding of transfer ribonucleic acid to ribosomes engaged in protein synthesis: Number and properties of ribosomal binding sites. *J. Mol. Biol.* **11**:35–53.

Whirl-Carillo, M., Gabashvili, I., Bada, M., *et al*. 2002. Mining biochemical information: Lessons thaught by the ribosome. *RNA* **8**:279–289.

Wieden, H.J., Wintermeyer, W., and Rodnina, M.V. 2001. A common structural motif in elongation factor Ts and ribosomal protein L7/12 may be involved in the interaction with elongation factor Tu. *J. Mol. Evol.* **52**:129–136.

Wieden, H.J., Gromadski, K., Rodnin, D., and Rodnina, M.V. 2002. Mechanism of elongation factor (EF)-Ts-catalyzed nucleotide exchange in EF-Tu. Contribution of contacts at the guanine base. *J. Biol. Chem.* **277**:6032–6036.

Wienen, B., Ehlrich, R., Stöffler-Meilicke, M. *et al*. 1979. Ribosomal protein alterations in thiostrepton and micrococcin-resistant mutants of *Bacillus subtilis*. *J. Biol. Chem.* **254**:8031–8041.

Wilcox, M. 1969. Gamma-glutamyl phosphate attached to glutamine-specific tRNA. A precursor of glutaminyl-tRNA in *Bacillus subtilis*. *Eur. J. Biochem.* **11**:405–412.

Williamson, J.R. 2007. A postproteomic approach to study ribosome assembly. *FASEB J.* **21**:A45–2.

Willie, G.R., Richman, N., Godtfredsen, W.O., and Bodley, J.W. 1975. Some characteristics and structural requirements for the interaction of 24, 25-dihydrofusidic acid with ribosome elongation factor G complexes. *Biochemistry* **14**:1713–1718.

Willumeit, R., Diedrich, G., Forthmann, S., *et al.* 2001. Mapping proteins of the 50S subunit from *Escherichia coli* ribosomes. *Biochim. Biophys. Acta.* **1520**:7–20.

Wilson, D.N. 2004. Antibiotics and the inhibition of ribosome function, pp. 449–527. In: Nierhaus K, Wilson D, eds, *Protein Synthesis and Ribosome Structure*, Weinheim: Wiley-VCH.

Wilson, D.N. 2009. The A-Z of bacterial translation inhibitors. *Crit. Rev. Biochem. Mol. Biol*. **44**:393–433.

Wilson, D.N. 2011. On the specificity of antibiotics targetting the large ribosomal subunit. *Ann. N. Y. Acad. Sci.* **1241**:1–16.

Wilson, D.N. and Beckmann, R. 2011. The ribosomal tunnel as a functional environment for nascent polypeptide folding and translational stalling. *Curr. Op. Struct. Biol*. **21**:274–282.

Wilson, D.N., Schluenzen, F., Harms, J.M., *et al*. 2005. X-ray crystallography study on ribosome recycling: the mechanism of binding and action of RRF on the 50S ribosomal subunit. *EMBO J.* **24**:251–260.

Wilson, D.N., Schlünzen, F., Harms, J.M., *et al*. 2008. The oxazolidinone antibiotics perturb the ribosomal peptidyl-transferase center and affect tRNA positioning. *Proc. Natl. Acad. Sci. USA.* **105**:13339–13344.

Wilson, K.S. and Noller, H.F. 1998. Mapping the position of translational elongation factor EF-G in the ribosome by directed hydroxyl radical probing. *Cell* **92**:131–139.

Wilson, K.S., Appelt, K., Badger, J., *et al.* 1986. Crystal structure of a prokaryotic ribosomal protein. *Proc. Natl. Acad. Sci. USA.* **83**:7251–7255.

Wimberly, B.T., White, S.W., and Ramakrishnan, V. 1997. The structure of ribosomal protein S7 at 1.9Å resolution reveals a beta-hairpin motif that binds double-stranded nucleic acids. *Structure* **5**:1187–1198.

Wimberly, B.T., Guymon, R., McCutcheon, J.P., *et al.* 1999. A detailed view of a ribosomal active site: the structure of the L11-RNA complex. *Cell* **97**: 491–502.

Wimberly, B.T., Brodersen, D.F., Clemons, W.M. Jr., *et al.* 2000. Structure of the 30S ribosomal subunit. *Nature* **407**:327–339.

Wintermeyer, W., Savelsbergh, A., Semenkov, Y.P., *et al*. 2001. Mechanism of elongation factor G function in tRNA translocation on the ribosome. *Cold Spring Harb. Symp. Quant. Biol.* **66**:449–458.

Wittinghofer, A., 2005. Signalling via GTP-binding proteins of the Ras superfamily. *FEBS J.* **272**:5.

Wittinghofer, A. 2006. Phosphoryl transfer in Ras proteins, conclusive or elusive? *Trends. Biochem. Sci.* **31**:20–23.

Wittinghofer, A., and Pai, E.F. 1991. The structure of Ras protein: a model for a universal molecular switch. *Trends Biochem. Sci.* **16**:382–387.

Wittmann, H.G. 1982. Components of bacterial ribosomes. *Ann. Rev. Biochem.* **51**:155–183.

Wittmann-Liebold, B., and Greuer, B. 1978. The primary structure of protein S5 from the small subunit of the *Escherichia coli* ribosome. *FEBS Lett.* **95**:91–98.

Woese, C.R. 1965. On the evolution of the genetic code. *Proc. Natl. Acad. Sci. USA.* **54**:1546–1552.

Woese, C.R. 1970. Molecular mechanics of translation: a reciprocating ratchet mechanism. *Nature* **226**:817–820.

Woese, C.R. 1998. The universal ancestor. *Proc. Natl. Acad. Sci. USA.* **95**:6854–6859.

Woese, C.R. 2001. Translation: in retrospect and prospect. *RNA* **7**:1055–1067.

Woese, C.R. 2002. On the evolution of cells. *Proc. Natl. Acad. Sci. USA.* **99**:8742–8747.

Woese, C.R., and Fox, G.E. 1977. Phylogenetic structure of the procaryotic domain. The primary kingdoms. *Proc. Natl. Acad. Sci. USA.* **74**:5088–5090.

Woese, C.R., Kandler, O., and Wheelis, M.L. 1990. Towards a natural system of organisms: proposal for the domains archaea, bacteria and eucarya. *Proc. Natl. Acad. Sci. USA.* **84**:4576–4579.

Wolf, H., Chinali, G., and Parmeggiani, A. 1974. Kirromycin, an inhibitor of protein biosynthesis that acts on elongation factor Tu. *Proc. Natl. Acad. Sci. USA.* **71**: 4910–4914.

Wolf, H., Chinali, G., and Parmeggiani, A. 1977. Mechanism of the inhibition of protein synthesis by kirromycin. Role of elongation factor Tu and ribosomes. *Eur. J. Biochem.* **75**:67–75.

Wolstenholme, D.R., Macfarlane, J.L., Okimoto, R., *et al*. 1987. Bizarre tRNAs inferred from DNA sequences of mitochondrial genomes of nematode worms. *Proc. Natl. Acad. Sci. USA*. **84**:1324–1328.

Wong, J.T. 1991. Origin of genetically encoded protein synthesis a model based on selection for RNA peptidation. *Orig. Life Evol. Biosph*. **21**:165–176.

Wong, J.T. 2007. Coevolution theory of the genetic code: A proven theory. *Orig. Life Evol. Biosph*. **37**:403–408.

Wood, H., Luirink, J., and Tollervey, D. 1992. Evolutionarily conserved nucleotides within the *E. coli* 4.5S RNA are required for association with P48 *in vitro* and for optimal function in vivo. *Nucleic Acids Res.* **20**:5919–5925.

Woodcock, J., Moazed, D., Cannon, M., *et al*. 1991. Interaction of antibiotics with A-site specific and P-site specific bases in 16S ribosomal RNA. *EMBO J.* **10**:3099–3103.

Woodford, N., and Livermore, D.M. 2009. Infections caused by Gram-positive bacteria: a review of the global challenge. *J. Infect*. **59**:S4–S16.

Wool, I.G., Chan, Y.L., Gluck, A., and Suzuki, K. 1991. The primary structure of rat ribosomal proteins P0, P1 and P2 and a proposal for a uniform nomenclature for mammalian and yeast ribosomal proteins. *Biochemie* **73**:861–870.

Woolhead, C.A., McCormick, P.J., and Johnson, A.E. 2004. Nascent membrane and secretory proteins differ in FRET-detected folding far inside the ribosome and in their exposure to ribosomal proteins. *Cell* **116**:726–736.

Worbs, M., Huber, R., and Wahl, M.C. 2000. Crystal structure of ribosomal protein L4 shows RNA binding sites for ribosome incorporation and feedback control of the S10 operon. *EMBO J.* **19**:807–818.

Wower, I.K., Wower, J., and Zimmermann, R.A. 1998. Ribosomal protein L27 participates in both 50S subunit assembly and the peptidyltransferase reaction. *J. Biol. Chem.* **273**:19847–19852.

Wower, J., Kirillov, S.V., Wower, I.K., *et al*. 2000. Transit of tRNA through the *Escherichia coli* ribosome. Cross-linking of the 39-end of tRNA to specific nucleotides of the 23S ribosomal RNA at the A-, P- and E-sites. *J. Biol. Chem.* **275**:37887–37894.

Wu, B., Lukin, J., Yee, A., *et al*. 2008. Solution structure of ribosomal protein L40E a unique C4 finger protein encoded by archeaon *Sulolobus solfataricus*. *Protein Sci.* **17**:589–596.

Xiong, L., Polacek, N., Sander, P., *et al*. 2001. pKa of adenine 2451 in the ribosomal peptidyltransferase center remains elusive. *RNA* **7**:1365–1369.

Xiong, Y. and Steitz, T.A. 2004. Mechanism of transfer RNA maturation by CCA-adding enzyme without using an oligonucleotide template. *Nature* **430**:640–645.

Xu, R.X., Hassel, A.M., Vanderwall, D., *et al*. 2000. Atomic structure of PDE4: insights into phosphodiesterase mechanism and specificity. *Science* **288**:1822–1825.

Xu, Z., Horwich, A.L., and Sigler, P.B. 1997. The crystal structure of the asymmetric GroEL-GroES-(ADP)7 chaperonin complex. *Nature* **388**:741–750.

Yager, T.D. and von Hippel, P.H. 1991. A thermodynmic analysis of RNA transcript elongation and termination in *Escerichia coli*. *Biochemistry* **30**:1097–1118.

Yamada, T. and Nierhaus, N.H. 1978. Viomycin favours the formation of 70S ribosome couples. *Mol. Gen. Genet.* **161**:261–265.

Yamane, T. and Hopfield, J.J. 1977. Experimental evidence for kinetic proofreading in the aminoacylation of tRNA by synthetase. *Proc. Natl. Acad. Sci. USA.* **74**:2246–2250.

Yamaguchi, K. and Subramanian, A.R. 2000. The plastid ribosomal proteins. Identification of all the proteins in the 50S subunit of an organelle ribosome (chloroplast). *J. Biol. Chem.* **275**:28466–28482.

Yamaguchi, K., von Knoblauch, K., and Subramanian, A.R. 2000. The plastid ribosomal proteins. Identification of all the proteins in the 30S subunit of an organelle ribosome (chloroplast). *J. Biol. Chem.* **275**:28455–28465.

Yanigasawa, T., Sumida, T., Ishii, R., *et al*. 2010. A paralog of lysyl-tRNA synthetase aminoacylates a conserved lysine residue in translation elongation factor P. *Nat. Struct. Mol. Biol.* **17**:1136–1143.

Yarmolinsky, M.B., and de la Haba, G.L. 1959. Inhibition by puromycin of amino acid incorporation into protein. *Proc. Natl. Acad. Sci. USA.* **45**:1721–1729.

Ye, K., Serganov, A., Hu, W., *et al*. 2002. Ribosome-associated factor Y adopts a fold resembling a double-stranded RNA binding domain scaffold. *Eur. J. Biochem.* **269**:5182–5191.

Ye, Q.-Z., Xie, S.-X., Ma, Z.-Q., *et al*. 2006. Structural basis of catalysis by monometalated methionine aminopeptidase. *Proc. Natl. Acad. Sci. USA.* **103**:9470–9475.

Yegian, C.D., Stent, G.S., and Martin, E.M. 1966. Intracellular condition of *Escherichia coli* transfer RNA. *Proc. Natl. Acad. Sci. USA.* **55**:839–846.

Yokobori, S., Suzuki, T., and Watanabe, K. 2001. Genetic code variations in mitochondria: tRNA as a major determinant of genetic code plasticity. *J. Mol. Evol.* **53**:314–326.

Yokosawa, H., Kawakita, M., Arai, K., *et al*. 1975. Binding of aminoacyl-tRNA to ribosomes promoted by elongation factor Tu. Studies on the role of GTP hydrolysis. *J. Biochem.* (Tokyo). **77**:719–728.

Yonath, A. 2003. Structural insight into functional aspects of ribosomal RNA targeting. *Chem. Bio. Chem.* **4**:1008–1017.

Yonath, A., and Franceschi, F. 1998. Functional universality and evolutionary diversity: insights from the structure of the ribosome. *Structure* **6**:679–684.

Yonath, A., Mussig, J., Teshe, B., *et al*. 1980. Crystallization of the large ribosomal subunit from *B. stearothermophilus*. *Biochem. Int*. **1**:428–435.

Yonath, A., Mussig, J., and Wittmann, H.G. 1982. Parameters for crystal growth of ribosomal subunits. *J. Cell Biochem.* **19**:145–155.

Yonath, A., Leonard, K.R., and Wittmann, H.G.A. 1987. Tunnel in the large ribosomal subunit revealed by three-dimensional image reconstruction. *Science* **236**:813–816.

Yonath, A., Harms, J., Hansen, H.A.S., *et al*. 1998. Crystallographic studies on the ribosome, a large macromolecular assembly exhibiting severe nonisomorphism, extreme beam sensitivity and no internal symmetry. *Acta Cryst.* **A54**:945–955.

Yoshida, T., Uchiyama, S., Nakano, H., *et al*. 2001. Solution structure of the ribosome recycling factor from *Aquifex aeolicus*. *Biochemistry* **40**:2387–2396.

Yoshida, H., Maki, Y., Kato, H. *et al*. 2002. The ribosome modulation factor (RMF) binding site on the 100S ribosome of *Escherichia coli*. *J. Biochem*. **132**:983–989.

Yoshizawa, S., Fourmy, D., and Puglisi, J.D. 1998. Structural origins of of gentamin antibiotic interaction. *EMBO J.* **17**:6437–6448.

Yoshizawa, S., Fourmy, D., and Puglisi, J.D. 1999. Recognition of the codon-anticodon helix by ribosomal RNA. *Science* **285**:1722–1725.

Yoshizawa, S., Rasubala, L., Ose, T., *et al*. 2005. Structural basis for mRNA recognition by elongation factor SelB. *Nat. Struct. Mol. Biol*. **12**:198–203.

Youngman, E.M., Brunelle, J.L., *et al*. 2004. The active site of the ribosome is composed of two layers of conserved nucleotides with distinct roles in peptide bond formation and peptide release. *Cell* **117**:589–599.

Yusupov, M.M. and Spirin, A.S. 1986. Are there proteins between the ribosomal subunits? Hot tritium bombardment experiments. *FEBS Lett.* **197**:229–233.

Yusupov, M.M., Yusupova, G.Z., Baucom, A., *et al*. 2001. Crystal structure of the ribosome at 5.5Å resolution. *Science* **292**:883–896.

Yusupova, G.Z., Yusupov, M.M., Cate, J.H., and Noller, H.F. 2001. The path of messenger RNA through the ribosome. *Cell* **106**:233–241.

Yusupova, G., Jenner, L., Rees, B., *et al*. 2006. Structural basis for messenger RNA movement on the ribosome. *Nature* **444**:392–394.

Zaher, H.S. and Green, R. 2009. Fidelity at the molecular level: lessons from protein synthesis. *Cell* **136**:746–762.

Zantema, A., Maassen, J.A., Kriek, J., and Moller, W. 1982a. Fluorescence studies on the location of L7/L12 relative to L10 in the 50S ribosome of *Escherichia coli*. *Biochemistry* **21**:3077–3082.

Zantema, A., Maassen, J.A., Kriek, J., and Moller, W. 1982b. Preparation and characterization of fluorescent 50S ribosomes. Specific labeling of ribosomal proteins L7/L12 and L10 of *Escherichia coli*. *Biochemistry* **21**:3069–3076.

Zarrinpar, A., Bhattacharyya, R.P., and Lim, W.A. 2003. The structure and function of proline recognition domains, *Sci.* STKE, RE8.

Zavialov, A.V., Buckingham, R.H., and Ehrenberg, M. 2001. A post termination ribosomal complex is the guanine nucleotide exchange factor for peptide release factor RF3. *Cell* **107**:115–124.

Zavialov, A.V. and Ehrenberg, M. 2003. Peptidyl-tRNA regulates the GTPase activity of translation factors. *Cell* **114**: 113–122.

Zavialov, A.V., Mora, L., Buckingham, R.H., and Ehrenberg, M. 2002. Release of peptide promoted by the GGQ motif of class 1 release factors regulates the GTPase activity of RF3. *Mol. Cell* **10**:789–798.

Zeidler, W., Egle, C., Ribeiro, S., *et al.* 1995. Site-directed mutagenesis of *Thermus thermophilus* elongation factor Tu. Replacement of His85, Asp81 and Arg300. *Eur. J. Biochem.* **229**:596–604.

Zeidler, W., Schirmer, N.K., Egle, C., *et al.* 1996. Limited proteolysis and amino acid replacements in the effector region of *Thermus thermophilus* elongation factor Tu. *Eur. J. Biochem.* **239**:265–271.

Zhang, C.-M., Perona, J.J., Ryu K., *et al*. 2006. Distinct kinetic mechanisms of the two classes of aminoacyl-tRNA synthetases. *J. Mol. Biol*. **361**:300–311.

Zhang, W., Dunkle, J.A., and Cate, J.H.D. 2009. Structures of the ribosome in intermediate states of ratcheting. *Science* **325**:1014–1017.

Zhang, Y. and Gladyshev, V. N. 2007. High content of proteins containing 21st and 22nd amino acids, selenocysteine and pyrrolysine, in a symbiotic deltaproteobacterium of gutless worm *Olavius algarvensis*. *Nucl. Acids Res*. **35**:4952–4963.

Zhou, D.X. and Mache, R. 1989. Presence in the stroma of chloroplasts of a large pool of a ribosomal protein not structurally related to any *Escherichia coli* ribosomal protein. *Mol. Gen. Genet*. **219**:204–208.

Zhou, J., Lancaster, L., Trakhanov, S., *et al*. 2012. Crystal structure of release factor RF3 trapped in the GTP state on a rotated conformation of the ribosome. *RNA* **18**:230–240.

Zhou, Y.N. and Lin, D.J. 1998. The rpoB mutants destabilizing initiation complexes at stringently controlled promoters behave like "stringent" RNA polymerases in *Escherichia coli*. *Proc. Natl. Acad. Sci. USA*. **95**:2908–2913.

Zhu, J., Korostelev, A., Constantino, D.A., *et al*. 2011. Crystal structures of complexes containing domains from two viral internal ribosome entry sites (IRES) RNA bound to the 70S ribosome. *Proc. Natl. Acad. Sci. USA*. **108**:1839–1844.

Ziková, A., Panigrahi, A.K., Dalley, R.A., *et al*. 2008. *Trypanosoma brucei* mitochondrial ribosomes. *Mol. Cell. Proteomics* **7**:1286–1296.

Zimmer, J., Nam, Y. Rapoport, T.A. 2008. Structure of a complex of the ATPase SecA and the proteintranslocation channel. *Nature* **455**:936–943.

Zimmermann, R.A. 1980. Interactions among protein and RNA components of the ribosome. In *Ribosomes. Structure, Function and Genetics*, Eds. G. Chambliss, *et al.,* pp. 135–169. University Park Press, Baltimore.

Zinker, S. 1980. P5/P59, the acidic ribosomal phosphoprotein from *S. cerevisiae*. *Biochim. Biophys. Acta* **606**:76–82.

Zinker, S. and Warner, J.R. 1976. The ribosomal proteins of *Saccharomyces cerevisiae*. Phosphorylated and exchangeable proteins. *J. Biol. Chem*. **251**:1799–1807.

Ziv, G., Haran, G., and Thirumalai, D. 2005. Ribosome exit tunnel can entropically stabilize a-helices. *Proc. Natl. Acad, Sci. USA*. **102**:18956–18961.

Zurdo, J., Parada, P., van den Berg, A., *et al*. 2000. Assembly of *Saccharomyces cerevisiae* ribosome stalk: binding of P1 proteins is required for the interaction nof P2 proteins *Biochemistry* **39**:8929–8934.

Zuurmond, A.M., Olsthoom-Tielman, I.N., de Graaf, J.M., *et al*. 1999. Mutant EF-Tu species reveal novel features of the enacyloxin IIa inhibition on the ribosome. *J. Mol. Biol*. **294**:627–637.

This page intentionally left blank

Index

Note: Locators followed by '*f*' and '*t*' denote figures and tables.